Durability enhancement and prevention of damage in reinforced concrete structures using bacteria

A Thesis

Submitted in fulfillment of the requirements for the award of the degree of

DOCTOR OF PHILOSOPHY

IN

BIOTECHNOLOGY

By:

Sumit Joshi

(901500003)

Under the supervision of

Dr. M. Sudhakara Reddy

(Professor)

Dr. Shweta Goyal

(Associate Professor)

THAPAR INSTITUTE
OF ENGINEERING & TECHNOLOGY
(Deemed to be University)

Department of Biotechnology

Thapar Institute of Engineering & Technology, Patiala-147004

Punjab (India)

February, 2021

Certificate

Certified that the thesis "**Durability enhancement and prevention of damage in reinforced concrete structures using bacteria***"* which is submitted by **Mr. Sumit Joshi**, in fulfillment of the requirement for the award of the degree of **Doctor of Philosophy** in the Department of Biotechnology, Thapar Institute of Engineering & Technology, Patiala, is a record of the candidate's own independent and original research work carried out by him under my supervision and guidance. The matter embodied in this thesis has not been submitted in part or full to any other University or Institute for the award of any degree.

(Dr. Shweta Goyal)
Co-Supervisor
Associate Professor
Civil Engineering Department
Thapar Institute of Engineering & Technology
Patiala, Punjab, India

(Dr. M. Sudhakara Reddy)
Supervisor
Professor
Department of Biotechnology
Thapar Institute of Engineering & Technology
Patiala, Punjab, India

Declaration

I hereby declare that the work presented in the thesis entitled "**Durability enhancement and prevention of damage in reinforced concrete structures using bacteria"** in the fulfillment of the requirement for the award of the Degree of **Doctor of Philosophy** in the Department of Biotechnology, Thapar Institute of Engineering & Technology, Patiala, is an authentic record of my own work during the period June 2015 to June 2020, under the supervision of **Dr. M. Sudhakara Reddy**, Professor, Department of Biotechnology, Thapar Institute of Engineering & Technology, Patiala and **Dr. Shweta Goyal**, Associate professor, Civil Engineering Department, Thapar Institute of Engineering & Technology, Patiala. The material embodied in this thesis has not been submitted in parts or full in any other university or institute for the award of any degree in India or Abroad.

Sumit Joshi

Place: Patiala

Date: 18-02-2021

Sumit Joshi

Department of Biotechnology

Thapar Institute of Engineering & Technology

Patiala, Punjab, India

Acknowledgement

"A dream does not become reality through magic: it takes sweat, determination and hard work"

This thesis is the end of my journey in obtaining my PhD, probably the most stimulating activity of my life. It was a long and arduous yet very fulfilling journey that I completed. In pursuit of this academic endeavour, I feel that I have been exceptionally fortunate because inspiration, guidance, direction, cooperation, love and care - all came my way in abundance. I feel nostalgic when I look back into my journey and find it difficult to put into words the never ending support and encouragement of everyone throughout these years.

First and foremost, I would like to bow to Almighty for blessing me so abundantly, far beyond what I deserve. With a deep sense of gratitude, I acknowledge my PhD Supervisor, ***Prof. M. Sudhakara Reddy****, Department of Biotechnology, TIET, Patiala for giving me this wonderful opportunity of being a part of his vivacious research team. His pertinent guidance, patronage, motivation, enthusiasm, enormous knowledge and dedication for research rendered to me during my work, without which the present endeavour would not have achieved the same status. I thank his progressive, energizing and commendable guidance throughout my PhD programme. His intelligent ideas and thought provoking discussions helped me through this tedious journey. His comprehensive understanding, serendipitous observation and vision to convert ideas into scientific possibilities always kept me moving forward. His constructive criticism and spirit to strive for excellence is commendable. I am surely going to miss his gentle badgering about making tables correctly. It was his support and faith in my ability that made me strive for excellence and nothing less.*

I reckon this opportunity to express my regards and gratitude to my PhD co-supervisor, ***Assoc. Prof. Shweta Goyal*** *(Civil Engineering Department, TIET). Her valuable suggestions, proficient guidance and advice helped me to accomplish this difficult task with success. I could always rely on her for any support at the time of crisis during my study. I am forever indebted to her for constant motivation, constructive suggestions and meticulous approach towards science constantly encouraged me to perform better.*

I take this opportunity to express my gratitude for ***Prof. Prakash Gopalan****, Director, TIET, Patiala, for providing all the amenities and guidance for the completion of my research work. I extend my heartfelt*

*thanks to **Prof. Rafat Siddique**, Dean (Research and Sponsored Projects), TIET, Patiala, for providing motivating research environment during my stay in the Institute.*

*It is my privilege to thank **Assoc. Prof. Manoj Baranwal, Asst. Prof. Vikas Handa** Department of Biotechnology, TIET and **Prof. Amjad Ali,** School of Chemistry and Biochemistry, TIET, for their constant support and encouragement during the course of my study. I profoundly thank **Dr. M Vasundhara**, Department of Biotechnology for her valuable suggestions for the progress of my work and **Prof. Anil Kumar**, Coordinator, TIFAC-CORE in Agro and Industrial Biotechnology, TIET, for providing facilities, guidance and providing a brilliant environment which is very conducive for research work. My heartfelt gratitude goes to **Prof. Abhijit Mukherjee**, Department of Civil Engineering, Curtin University, Bentley, Australia, for his valuable suggestions for the progress of my research work. I extend my sincere word of thanks to **Prof. Rajesh kumar**, Department of Chemistry, Central University of Punjab, Bathinda, for encouraging me to join PhD under Dr. Reddy.*

I would take this opportunity to acknowledge all the faculty members of DBT, TIET, Patiala for their constant encouragement for my research work. I am thankful to the office and laboratory staff of Department of Biotechnology for their cooperation and help.

*I express my unfathomable regards to my colleagues **Mr. Arkadeep Mukherjee**, **Mrs. Bharti Thakur**, **Mrs. Shikha Khullar** and **Mrs. Tanveer Kaur** for their great support and treasured suggestions during need of the hour. I feel nostalgic about my delightful days spent with these wonderful people. I am surely going to cherish fond memories of conference at Jaipur which I attended with **Mrs. Bharti Thakur** and **Mr. Arkadeep Mukherjee** for many years to come. I would specially thank **Mr. Arkadeep Mukherjee** for his unconditional support throughout these years and many fruitful and refreshing discussions.*

*Here the time of special thanks and to acknowledge **Dr. Sandeep Bishnoi** (my friend from my graduation time), who supported me both academically and personally as well as stood by my side at every step of my life. As we were roommates during PhD (even in our graduation), I will always cherish those long late night discussions over with steaming hot food. Thanks for your absolute confidence in me.*

*I owe special thanks to my lab mates **Kamal, Navneet, Eetika, Fatima** and **Anu** for inspiring and stirring discussions and support. I would also like to thank all the project students who have worked in our Laboratory for their love and support. Most of the work would have been incomplete without the*

earnest support of Lab assistants. So, I owe a word of thanks to ***Mr. Soni Singh***, ***Mr. Ram Newal (Babbanji)*** *and* ***Lallanji****.*

I find it difficult to express in words, my sincere sense of indebtedness towards my parents, wife and sisters. A cabal of supremely positive individuals, who encouraged, pushed and supported me through the long years of this journey. My unquestionable gratitude is in order for the never-ending love and support of my father ***Mr. Satpal Joshi*** *and mother* ***Mrs. Lajjya Joshi.*** *My father is my backbone and mother is pillar of my strength. I consider myself lucky to have such supportive and loving parents.* ***Tammana****, my wife a rare combination of beauty, brain and spirit who assisted and advised me throughout my tenure of PhD. I extend my respect to my elder sisters* ***Mrs. Ridhima Vashisht*** *and* ***Mrs. Rimple Swami*** *for their unconditional love and support. I consider myself lucky to have such supportive siblings who always stood by my side and encouraged me during difficult times.*

Last but not the least, I wish to acknowledge all those, whose names have not figured here, but who helped me in any form during the period of my research work.

Date: 18-02-2021

Place: Patiala

Sumit Joshi

(Sumit Joshi)

List of Publications

The following publications in peer reviewed journals are the outcome of the present research work:

- **Joshi S**, Goyal S, Mukherjee A, Reddy MS (2017) Microbial healing of cracks in concrete: a review. Journal of Industrial Microbiology & Biotechnology, 44: 1511-1525.
- **Joshi S**, Goyal S, Reddy MS (2018) Influence of nutrient components of media on structural properties of concrete during biocementation. Construction and Building Materials, 158: 601-613.
- **Joshi S**, Goyal S, Reddy MS (2018) Corn steep liquor as a nutritional source for biocementation and its impact on concrete structural properties. Journal of Industrial Microbiology & Biotechnology, 45: 657-667.
- **Joshi S**, Goyal S, Mukherjee A, Reddy MS (2019) Protection of concrete structures under sulfate environments by using calcifying bacteria. Construction and Building Materials, 209: 156-166.
- **Joshi S**, Goyal S, Reddy MS (2020) Influence of biogenic treatment in improving the durability properties of waste amended concrete: A review. Construction and Building Materials, 263: 120170.
- Reddy MS, **Joshi S** (2018) Carbon dioxide sequestration on biocement-based composites. In Carbon dioxide sequestration in cementitious construction materials. Woodhead Publishing, (pp. 225-243).

International conferences

- **Joshi S**, Reddy MS (2017) Utilization of corn steep liquor in biogenic treatment of concrete structures. International Conference on "Emerging Trends in Biotechnology for Waste Conversion (ETBWC)" 2017, October 8-10, 2017, CSIR-National Environmental Engineering Research Institute, Nagpur, India.
- **Joshi S** (2018) A comparative analysis of nutrient selection in biocementation and its impact on the structural properties of concrete. International Conference on biotechnological research and innovation for sustainable development (BioSD), November 22-25, 2018, CSIR-Indian Institute of Chemical Technology, Hyderabad, India. (Participation in Young Scientist Presentation)

Table of Contents

List of Figures

List of Tables

List of Abbreviations

MICP	Microbial induced calcium carbonate precipitation
CSL	Corn steep liquor
NB	Nutrient broth
ASTM	American Society of Testing and Materials
IS	Indian standard
RCPT	Rapid chloride penetrability test
SEM	Scanning electron microscopy
EDX	Energy dispersive X-ray spectroscopy
XRD	X-ray diffraction
SCE	Saturated calomel electrode
I_{corr}	Corrosion current density
E_{corr}	Corrosion potential
FA	Fly ash

List of Symbols

%	Percentage
g	Gram
g/L	Gram/litre
v/v	Volume by volume
w/v	Weight by volume
mM	Millimolar
N	Normality
mm	Millimeter
cm	Centimeter
ml	Milliliter
sec	Second
min	Minute
h	Hour
°C	Degree Celsius
RH	Relative humidity
V	Voltage
mV	Millivolt
µA	Microampere
MPa	Megapascal

Abstract

Microbial induced calcium carbonate precipitation (MICP) has a potential to improve the durability properties and remediation of cracks in concrete. In this study, bacterial admixed treatment and bacterial spray treatment of concrete structures with ureolytic bacteria was carried out using different media components (especially nutrient media, urea and calcium source). In the first stage of investigation, influence on the addition of bacterial culture and organic components (carbon and nitrogen content) of bacterial growth media on the setting characteristics of cement, chemical and structural properties of microbial concrete was studied. In this study, main emphasis was placed upon replacing the commercially available laboratory grade nutrient broth (NB) with corn steep liquor (CSL), which is an industrial by-product. Addition of plain NB media without bacteria severely retarded the setting of cement paste as well as significant reduction in the compressive strength was observed in concrete specimens. In fact, the addition of plain CSL media without bacteria had no adverse effect on the setting characteristics of cement paste and strength properties of concrete. While, setting characteristics of cement paste remain unaffected on the addition of bacterial culture grown in NB/CSL media. In bacterial treated concrete, MICP as a result on the addition of bacterial culture grown in NB/CSL media significantly improved the compressive strength and permeation properties. Bacterial admixed treatment (that can be used for new structures) and bacterial spray treatment (that can be used as a repair procedure) were found to be effective in MICP treatment of concrete. In the comparative analysis of CSL and NB as a nutrient media, CSL would serve as a potential alternative nutrient source for bacterial cells in microbial treatment of concrete.

Further, durability of microbial treated concrete under aggressive environments was explored. This study aimed to assess the efficacy of bio-deposition as a barrier in microbial treated concrete against sulfate and chloride attack. Under sulfate exposure, bacterial admixed and bacterial spray treated mortar and concrete specimens performed well and no sign of surface scaling, strength loss and salt efflorescence was observed. During chloride exposure, microbial treatment in reinforced concrete structures significantly reduced the ingress of chloride ions in the concrete matrix and inhibition of rebar corrosion was observed. In both, bacterial admixed and bacterial spray treated reinforced concrete specimens, corrosion potential (E_{corr}) and corrosion current (I_{corr}) values were much below the range as compared to control and depicts

that corrosion is negligible. Overall, the application of MICP treatment improved the lifecycle performance of concrete under harsh sulfate environments as well as prevention of rebar from chloride induced corrosion.

In present study, a suitable fly ash amended bacterial grout with optimum flowability properties was developed for the remediation of cracks in concrete. Crack treatment in horizontal orientation with injectable bacterial grout shows maximum mechanical strength recovery and significant reduction in permeation as compared to untreated concrete specimen. In case of crack treatment in vertical orientation, strength gain was minimal however permeation was improved as compared to untreated concrete specimen. The developed 40% FA amended bacterial grout with optimum rheological properties will help as an economical and environment friendly MICP technology in injection based applications for the remediation of existing cracks in concrete structures which are in service.

The current work has conclusively established that MICP technique with bacterial admixed treatment and bacterial spray treatment would be effective in direct application on concrete structures. Direct incorporation of calcifying bacteria as an admixture can be used for new structures as well as bacterial spray treatment can be used as a repair procedure in concrete, respectively. From the results, it was concluded that CSL as growth media had not shown any modifications in the concrete chemical properties. On comparison with NB media, CSL may serve as a carbon and nitrogen supplement and replace yeast extract nutrient media. Utilization of biomineralization activity of calcifying bacteria in microbial treated concrete provides an innovative approach in achieving significant reduction of sulfate ingress under harsh sulfate environments and prevention of rebar from chloride induced corrosion under high chloride conditions, respectively. The developed fly ash amended biogrout will help as an economical and environment friendly MICP technology in injection based applications for the crack healing in concrete structures which are in service. The encouraging results in the current study will facilitate in upscaling this microbial based approach from lab scale to commercial scale.

INTRODUCTION

Chapter 1

Introduction

1.1 General Introduction

In the past decades, global society has witnessed the transition to more urbanization and infrastructure development processes. Meanwhile, development in infrastructure boosts economic growth of a country and plays a crucial factor in the global economic competitive index. With substantial growth in urbanization, demand for building (e.g. public housing, roads, bridges) infrastructure development has increased. In the large proportion of infrastructure categories delivered by construction sector, concrete and steel are the foremost materials which are used. Reinforced concrete with positive attributes like high durability, ability to mould into different shapes, low cost production and ease of use has made it attractive among other building materials. In a simplest form of definition, concrete is composed of a mixture of essential constituents like cement, aggregates and water. Production of concrete has experienced an increased demand to accompany innumerable infrastructure developments (Miller et al. 2018). With the ever-growing worldwide demands, yearly consumption of concrete approaches 30 billion tons (Monteiro et al. 2017). Consequently, high levels of concrete production results into high consumption of basic raw materials. To meet the demands of large volumes of concrete, global cement and aggregate consumption is escalated for construction projects. Apart from economic and social factors in construction industry, environmental concerns are also associated with it.

A number of lifecycle assessment reports of conventional concrete production indicate, extensive use of raw materials and high energy consumption (Sharma et al. 2011; Abd Rashid and Yusoff, 2015). The entire life cycle of concrete production process as a whole includes raw material extraction, production, distribution, use and final waste disposal (Vieira et al. 2016). The cement production and natural aggregate extraction are highly intensive energy consuming as well as a major CO_2 emitting process (Gursel et al. 2014). Production of conventional concrete contributes approximately 8-9% of the global anthropogenic CO_2 emissions as the cement processing units plays a significant contribution in it (Miller et al. 2016). The embodied energy and emission of conventional concrete is relatively high. The other aspect that is affecting the lifecycle performance of concrete is its premature deterioration. Although it was initially considered to be

a highly durable material but climate change, higher temperature and extreme weather events are severely affecting the lifecycle of concrete. Most of these threatening factors involve chemical attack on concrete or on the steel rebar embedded in it. Concrete being the most widely used construction material in the world and maintaining concrete structures from premature deterioration is proving to be a great challenge. Interconnected pore system and presence of microcracks in the concrete matrix acts as a favorable condition for the penetration of harmful agents like CO_2, SO_4^{2-} and Cl^- which causes the initiation of corrosion of steel rebar (Basheer et al. 2001). Early age deterioration of concrete structures severely affects its serviceability leading to high cost of maintenance. As nearly 80% of world's infrastructure is built in reinforced concrete, their maintenance needs a huge recurring investment for the restoration or replacement of deteriorated concrete structures that few countries in the world can afford.

To improve the durability properties and refinement of pores in concrete structures, use of different conventional treatment methods has been reported. Surface treatments with synthetic agents like epoxy coatings, silanes or siloxanes, acrylic coatings etc., are available for remediation of permeability of concrete as waterproof agents (Muhammad et al. 2015). Different chemical additives (e.g. methylmethacrylate, organo-modified montmorillonites, styrene butadiene polymer) are also used as an admixture to improve strength and permeability properties of concrete as well as corrosion inhibitors (e.g. calcium and sodium nitrate, polycarboxylate polymers, amino alcohol compounds) for remediation of rebar corrosions (Ann et al. 2006; Das and Pradhan, 2019). But these treatments with adhesive chemicals are subject to frequent controversy due to their limited long term performance, detachment with aging, need for constant maintenance, thermal expansion, cost, site accessibility and environmental impact (Pan et al. 2017b). Hence, to reduce the development cost as well as environmental burden contributed by construction industry, attention is given to develop a sustainable technology. For the durability enhancement of concrete structures and to protect the steel rebar in reinforced concrete from corrosion, a novel technique of microbial-based treatment has emerged as a promising technique. Introduction of applied biotechnology in the field of concrete has led to the development of a new type of concrete called "microbial concrete" or "bio-concrete". In this bio-inspired treatment, concrete structures are treated with calcifying bacteria to induce calcium carbonate precipitation to improve the durability properties of concrete and inhibit the rebar corrosion of reinforced concrete.

Microbial-induced calcium carbonate precipitation (MICP) is the capability of microorganism to form calcium carbonate extracellularly through a metabolic activity. The phenomenon of mineral formation by living organism due to reaction of its metabolic products with the surrounding environment is called biomineralization (Lowenstam, 1981). In natural environments, MICP by a variety of microorganisms is known, which contributes into cyanobacterial stromatolite, cave speleothems, hot spring travertine, marine reefs, lacustrine whitings (Riding, 2000). Biomineralization by different microbial species like photosynthetic organisms (cyanobacteria and algae), sulfate reducing bacteria (SRB) (dissimilatory reduction of sulfates), organisms utilizing organic acids and urea degrading bacteria in diverse environments under different pathways has been reported (Douglas and Beveridge, 1998). Four key factors which influence the biogenic precipitation of $CaCO_3$ includes calcium availability, dissolved inorganic carbon, pH and the bacterial cell surface as a nucleating site (Hammes and Verstraete, 2002). The occurrence of different calcifying microbial species in various geological settings with wide range of environmental conditions makes them the best option of engineering projects (Zhu and Dittrich, 2016). Inspired by the MICP potential of microbes, importance has been given to utilize these microbial strains in several applications.

During the last few years, MICP has been reported with immense potential in remediation of heavy metals, soil stabilization, restoration of ancient monuments, concrete crack healing and main emphasis on the improvement of concrete durability (Dhami et al. 2013b). Predominantly, $CaCO_3$ precipitation via urea hydrolysis by bacteria is an easily controlled mechanism, where high amounts of calcium carbonates are produced in a short time. Biogenic precipitation of different polymorphs of calcium carbonates (e.g. calcite, aragonite and vaterite) in the concrete structure acts as ideal pore filler and improves its mechanical strength and permeability. In MICP process, several genera of calcifying bacteria isolated from different environmental conditions such as calcareous, marine, karstic caves, hot springs and heavy metal contaminated landfill has been reported (Dhami et al. 2018; Sarkar et al. 2019; Rangamaran et al. 2019; Akiyama and Kawasaki, 2019). A decade of progress in microbial application on concrete, tremendous amount of studies has been published at lab scale experiments which reflect the importance of MICP technique.

1.2 Knowledge Gap

With all the positive attributes of using MICP in improving the durability properties of concrete, some challenges are also associated with it. Till date, studies revealed that different methodologies have been adopted to treat mortar or concrete structures with different bacterial strains. In majority of research studies, ureolytic bacterial strain with genus *Sporosarcina* has been used for the biomineralization. These bacteria hydrolyze urea by producing urease enzyme in large amount resulting into release of ammonia and carbon dioxide. The ammonia produced increases the pH in the surrounding of bacteria that leads to precipitation of calcium carbonate. In most of the MICP treatments, bacterial cultures are incorporated in concrete during casting and thereafter cured by submerging the bacterial admixed concrete in bacterial culture for surface treatment. In case of ureolytic bacterial strain, bacterial cells grown in nutrient medium are also supplemented with urea and calcium source. Apart from the surface application and incorporation of vegetative bacterial cells inside the concrete matrix, use of encapsulated bacteria as a self-healing agent is also evolved as new approach in improving the durability properties and remediation of cracks in concrete. In this approach, organic acids are used as supplement and admixed in concrete. The qualitative and quantitative evaluation of microbial concrete with positive outcomes is still reported in the lab scale.

However, till date, not many research studies are reported in which the changes in the chemical and structural properties of microbial concrete are evaluated on the addition of bacterial cells and organic substrate present in growth medium. Presence of organic admixtures has been reported to have an adverse effect on the hydration of cement which further affects the hardening of cement (Bolobova and Kondrashchenko, 2000). Furthermore, there is a need to evaluate the biodeposition pattern of calcium carbonate crystals after bacterial admixed treatment as well as bacterial surface treatment in concrete structures. pH is one of the most influential parameter in concrete durability and the alkaline condition of concrete with pH 12–13 keeps the steel rebar resistant to corrosion. Hence, a research work has to be carried out to evaluate the effect of alkaline nature of concrete on the $CaCO_3$ precipitation nature of viable bacterial cells admixed during bacterial treatment.

Some limitations which are necessary to be considered for the application of this technology at commercial scale have to be found. The operating cost of this technology at the commercial scale

has some economic limitations as in maximum studies use of laboratory grade bacterial growth medium is adopted. Implementation of MICP technique in newly constructed concrete structures at field scale with economical alternatives of growth medium with effective curing method is to be investigated. The comparative analysis of lab grade bacterial growth medium and alternate growth medium on the chemical and structural properties of microbial treated concrete is to be investigated.

In many research publications, the potential of MICP technique in improving mechanical and permeation properties of concrete under ideal conditions at lab scale are reported. While implementing MICP technique at field scale, the behavior of microbial concrete under aggressive environmental conditions, which affect the long term durability of concrete structures, has not been studied and reported so far. Interaction of concrete with external environment, the most threatening factor which influences its durability is chemical attack. The chlorides and sulfates belong to the aggressive chemicals that affect the long-term durability of concrete structures. However, the effect of harsh conditions such as sulfate environment on the microbial treated concrete is still unexplored. A detailed work is required to understand the performance of microbial concrete against external chloride exposure.

Different studies have been reported in which biogenic treatment of cracks with self healing mechanisms are adopted (Seifan et al. 2016; De Belie et al. 2018). While in self healing approach, bacterial encapsulation or protective carrier materials are used as admixture in concrete. However, limited studies are reported in which microbial healing to treat the existing cracks in concrete are investigated. A detailed work is required to develop an effective microbial healing material to repair the existing cracks in concrete structures.

Hence, a thorough research work is required to study the influence of organic substrates and $CaCO_3$ biodeposition on the structural properties of microbial concrete. The study of chemical attacks on microbial concrete will help in better understanding of long-term performance and its successful commercialization. Concrete crack repair with microbial healing material is to be investigated which will help in treating the existing cracks in concrete structures.

1.3 Aim and Objectives

The present work was aimed to develop better understanding in the application of calcifying bacteria in durability enhancement and prevention of damages in concrete structures under aggressive environments.

In the current research work, ureolytic bacterium with high efficiency of biocalcification was used to treat concrete structures. Two treatment methods; bacterial admixed treatment and bacterial spray treatment were adopted in MICP treatment of concrete. Influence of bacterial cells and organic substrates in the material mix on the durability properties of microbial concrete was investigated. To minimize the operating cost of MICP, corn steep liquor (CSL) as a bacterial growth medium was used and its impact on the chemical and structural properties of microbial concrete was examined. Further, long term performance of microbial concrete on the exposure to chemical and physical sulfate environment was investigated. Prevention of rebar corrosion due to external chloride exposure in microbial treated reinforced concrete was investigated. Crack remediation in concrete structures with microbial healing material was investigated. Accordingly, the above mentioned study was designed and carried out to investigate the following objectives:

1. The role of bacteria and material mix on the durability properties of reinforced concrete structures
2. The effectiveness of bacteria in biocalcification of concrete specimens at high and low pH and its impact on mechanical properties
3. The use of calcifying bacteria for prevention of damage in reinforced concrete structures (rebar corrosion and crack remediation)

REVIEW OF LITERATURE

Chapter 2

Review of Literature

2.1 Concrete as a building material

Concrete is the most widely used construction material of the world. With global industrialization and urbanization, demand for infrastructure expansion has increased (Doyle and Havlick, 2009). Understandably, an overwhelmingly large proportion of infrastructure is built with concrete. Production of concrete has experienced an increased demand to accompany innumerable infrastructure developments (Miller et al. 2018). The demographic change due to the gradual movement of population towards urban areas has increased the demand and the production of concrete which exceeded that of other building materials. Various factors are responsible for the popularity of concrete across the world which makes it the most widely used engineering material. Unlike wood and steel, concrete withstand the action of water to greater extent which makes it an ideal material for building structures. The other factor is formation of variety of shapes and sizes due to the plastic consistency of freshly made concrete. The plastic stage permits the fresh concrete material to flow into prefabricated formwork which attains defined shape after hardening. With the ever-growing worldwide demands, yearly consumption of concrete approaches 30 billion tons (Monteiro et al. 2017). Consequently, high levels of concrete production results into high consumption of basic raw materials (Miller et al. 2018). Concrete is a composite material which consists of water, a binder material and within which granular aggregates are embedded. Ordinary concrete consists of 12% cement and 80% aggregates by weight. To meet the demands of large volumes of concrete, ~3.8 Gt cement, ~17.5 Gt of aggregate and over ~2 Gt of water global consumption has been estimated (Miller et al. 2018). Concrete is composed of a mixture of essential constituents like cement, aggregates and water. In the modern development, built environment is unimaginable without cement-based materials. Cement is a finely pulverized hydraulic material which develops binding property as a result of hydration and forms stable hydration products in an aqueous environment. The portland cement on the hydration forms calcium silicate hydrates, which are primarily responsible for the adhesive characteristics. Globally, production of cement has been escalating to meet the growing need of construction projects. The global production of cement in the year 2019 was estimated to be 4.2 billion tons (Statista, 2020). Cement production increased almost 34-fold in the last 65

years was reported (Scrivener et al. 2018). It is reported that a constant increase in the global cement production is expected and a nation wise trend is shown in Figure 2.1.

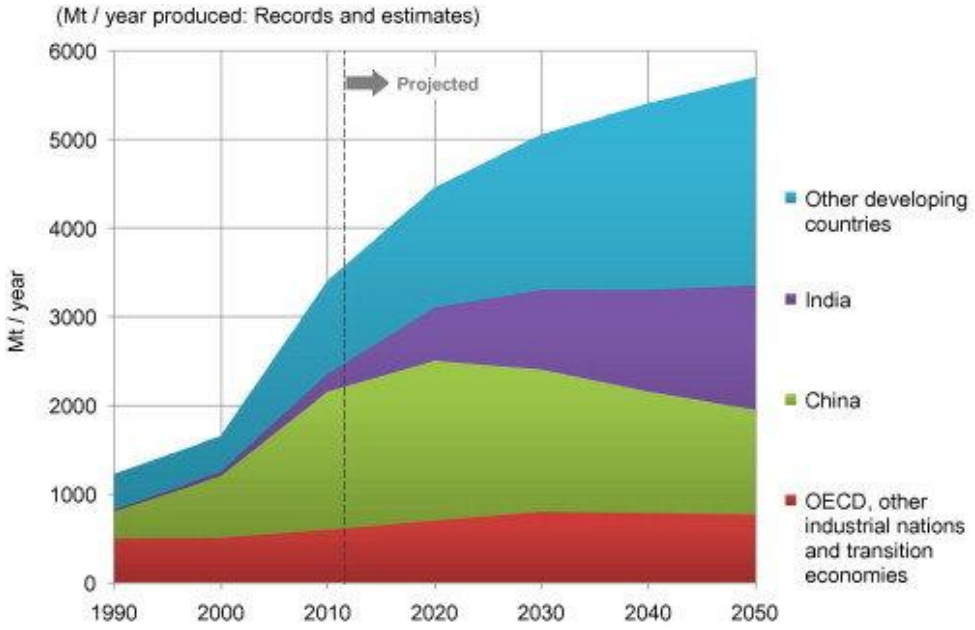

Figure 2.1 Estimated projection of worldwide cement production (Adapted from Imbabi et al. 2013)

In the database of Statisa portal the search of "Major countries in worldwide cement production" shows China and India are top cement producers globally followed by USA (Statista, 2019). Estimated production of cement in China and India was 2.4 billion metric tons and 290 million metric tons in year 2018 respectively. Natural aggregate (sand, gravel, and crushed stone) as construction material is the most valuable nonfuel commodity in the world. In volume, aggregates comprise about 85% of the concrete structures and the remaining 15% are made of steel and binders (Drew et al. 2002). The expected annual consumption of aggregates was estimated to increase till it reaches 66.3 billion tons by 2022 (Pedro et al. 2018). The aggregate phase is primarily responsible for elastic modulus and the dimensional stability of concrete structures. The aggregate is treated as inert filler, however, its significant characteristics such as grading, moisture absorption, shape, surface texture and crushing strength influence the durability properties of concrete. Concrete industry being one of the largest industrial consumer, its global water requirement is 1 trillion L per year (Mehta, 2001). The consumption of water in concrete industry is equivalent to approximately 18% of global annual industrial water consumption (Miller et al. 2018). A large amount of fresh water is used for concrete mixing and

curing in concrete industry. However, with the rapid urban construction and growing dependence, positive attributes of concrete like high durability, low cost production and ease of use has made it attractive among other building materials.

2.2 Lifecycle performance of concrete

In the current scenario, infrastructure of a country plays an important role in the global competitive index of economies. The improvement in infrastructure i.e. roads, bridges, dams, ports, public housing strengthen the economy of a nation. The economic growth and development of the modern society rely on excellent durable civil engineering structures and infrastructure facilities. In all the infrastructure categories, concrete and steel are the two most commonly used structural materials. Among them, reinforced concrete is the most versatile and potentially one of the most durable materials for almost any types of building structures. The incomparable durability property of concrete has made it attractive among other construction materials. Different definitions for 'durability' of concrete are reported by various researchers and presented it into different contexts. 'Durability' for a concrete structure means that concrete will continue to perform its intended functions, that is, to maintain its required strength and serviceability, during the specified or traditionally expected service life (Neville, 2001). In another report, durability was defined as the ability of the concrete structure to maintain serviceability when exposed to its intended service environment without spending a lot of expenditure to repair or rehabilitate (Gu et al. 2016). Durability of concrete was also defined as its ability in resistance against weathering action, chemical attack, abrasion, or any other process of deterioration to remain in its original form, quality and serviceability when exposed to its intended service environment (Tang et al. 2015). Concrete structures, owing to their inherent vulnerability, are at risk from aging, fatigue, and deterioration processes as the concrete structures are also not free from severe degradation problems. The factors that affect the lifecycle performance of concrete include climate change, higher temperature and extreme weather events which lead to its premature deterioration. Most of these threatening factors involve chemical attack on concrete or on the rebar embedded in reinforced concrete structures. The detrimental effect of these phenomenon leads over time into unsatisfactory structural performance of concrete under service loadings (Biondini and Frangopol, 2016). The economic impact of degradation of structural performance and deterioration processes on the serviceability of a

structure is exceptionally high. Early deterioration of infrastructure around the globe is a matter of concern. For the repair and rehabilitation of damaged concrete structures or to replace the deteriorated structures, countries are allocating considerable funds in their annual budget. As nearly 80% of world's infrastructure is built in reinforced concrete, their maintenance needs a huge recurring investment that few countries in the world can afford.

Durability problems usually appear and initiates from the materials i.e., either concrete or embedded steel at beginning, which progressively lead to structural damage and puts a potential danger to the structure. The cause of concrete deterioration is categorized as the combined effect of multi environmental attacks such as carbonation, sulfate attack, chloride induced steel rebar corrosion, freezing thawing (Tang et al. 2015). The transport movement of aggressive agents in the matrix of reinforced concrete is the cause of deterioration of concrete durability. The interconnected pore system and presence of micro-cracks also allow penetration of harmful agents like CO_2, SO_4^{2-} and Cl^- to cause corrosion of steel rebar (Basheer et al. 2001). The rate of deterioration of concrete structures mainly depends on two important factors: permeability of concrete matrix and development of micro-cracks (Basheer et al. 1996). The major durability problems in concrete including carbonation, sulfate attack, chloride attack and freeze–thaw are discussed in the following subsections.

2.2.1 Factors influencing concrete durability

2.2.1.1 Carbonation

Carbonation of concrete is a complex physiochemical process which means the progressive neutralization of the alkaline constituents of concrete by carbon dioxide in the environment forming mainly carbonates. Concrete neutralization refers to decrease in pH value of concrete to about 9-10 pH when CO_2 diffuses into concrete matrix (Gu et al. 2016). As the world's climate is undergoing considerable changes, increased level of CO_2 concentration in environment is a foremost result of global climate change. The primary source of increased level of CO_2 is anthropogenic emissions from fossil fuels in which cement production units play a significant contribution of 5% in global green house gas (GHG) emissions (Ekolu, 2016). With the increasing emissions, levels of global CO_2 concentration have surpassed the 400 ppm in 2018. Elevated level of CO_2 in atmosphere leads to increased rate of carbonation in reinforced concrete

(Ekolu, 2016). Natural carbonation of concrete as a result of climate change initiates carbonation induced corrosion in RC structures at a rather slow yet invasive rate. The process of carbonation in concrete is presented in the following chemical reactions (Zhou et al. 2015).

$$Ca(OH)_2 \rightarrow Ca^{+2}(aq) + 2OH^{-}(aq) \quad (2.1)$$

$$Ca^{+2}(aq) + 2OH^{-}(aq) + CO_2 \rightarrow CaCO_3 + H_2 \quad (2.2)$$

$$3CaO.\,2SiO_2.\,3H_2O + 3CO_2 \rightarrow 3CaCO_3.\,2SiO_2.\,3H_2O \quad (2.3)$$

$$3CaO.\,SiO_2 + \mu H_2O + 3CO_2 \rightarrow 3CaCO_3 + SiO_2.\,\mu H_2O \quad (2.4)$$

$$2CaO.\,SiO_2 + \mu H_2O + 3CO_2 \rightarrow 2CaCO_3 + SiO_2.\,\mu H_2O \quad (2.5)$$

During carbonation of concrete, chemical reaction of $Ca(OH_2)$ and $3CaO{\cdot}2SiO_2{\cdot}3H_2O$ (produced after sufficient hydration of cement) with diffused CO_2 gas in concrete matrix takes place results into calcium carbonate precipitation (as shown in Eq 2.1 – Eq 2.5). With continuous ingress into concrete matrix, CO_2 gas dissolves into pore solution to form carbonic acid (H_2CO_3) which reacts with $Ca(OH_2)$ and $3CaO{\cdot}2SiO_2{\cdot}3H_2O$ and precipitates mainly as calcium carbonate ($CaCO_3$). The cement concrete pore solutions are saturated $Ca(OH)_2$ and contains different auxiliary ions depending on the type of cement and supplementary cementing materials. Pore solution includes cations such as Ca^{2+}, Na^{+} and K^{+} and anions such as OH^{-} (Ghods et al. 2009). Due to carbonation, depletion of hydroxyl ions (OH^{-1}) lowers the pore water pH below 9.0 from strong alkaline pH value of 12–13 in non carbonated concrete matrix. At such low pH (9.0) value, the existing passive protection layer at steel rebar in RC structures becomes unstable allowing corrosion to occur in the sufficient presence of oxygen and water (Zhou et al. 2015). A variety of principal environmental factors which influence the carbonation process are relative humidity, CO_2 concentration, temperature (Ekolu, 2016). Apart from drop in pH values of carbonated concrete and making it vulnerable to corrosion, notable changes like reduced total porosity, improved mechanical strength and appearance of cracks are also reported due to precipitation of calcium carbonate in the pore network of concrete. In the last decade, several studies focusing on the carbonation of cement-based materials have been carried out. The performance of concrete under natural carbonation is very slow due to low CO_2 concentration in the atmosphere (400 ppm or 0.04%). Due to this, accelerated carbonation schemes are used at lab

scale to investigate the effects of carbonation on concrete (Ashraf, 2016). Wide range of variations (concentration of CO_2, relative humidity and temperature) in accelerated carbonation studies on concrete performance has been observed (Table 2.1).

Table 2.1 Overview of different conditions adopted for accelerated carbonation of concrete

Binder type	RH (%)	CO_2 concentration	Temprature (°C)	Duration	Refrences
OPC	70	20%	23	16 weeks	Chang and Chen (2006)
OPC	35, 55, 80	40%	-	3 days	Gonen and Yazicioglu (2007)
OPC	65	3%, 10%, 100%	22	103 days	Castellote et al. (2009)
OPC	65	50%	20	42 days	Turcry et al. (2014)
OPC + FA	62	10%	25	16 weeks	Morandeau et al. (2015)
OPC + FA	65	5%	20	3 months	Atiş (2003)
OPC + FA	55	4%	40	28 days	Khunthongkeaw et al. (2006)
OPC + FA/BFS	65	50%	20	123 days	Younsi et al. (2013)
OPC + BFS	60	10%	20	24 weeks	Gruyaert et al. (2013)
SCC	75	100%	24	240 days	Mohammed et al. (2014)
OPC+HVFA+ FA+ SF	60	1%, 10%	20	16 weeks	Van den Heede et al. (2019)
OPC+FA+BFS	60-70	5%	30	365 days	Hussain et al. (2018)

RH: Relative humidity; OPC: Ordinary Portland cement; FA: Fly ash; BFS: Blast furnace slag; HVFA: High volume fly ash; SF: Silica fume; SCC: Self compacting concrete

Carbonation is largely controlled by the diffusion rate of CO_2 through the microstructure of cementitious matrix and the most important factor which influences the rate of carbonation is relative humidity. Carbonation reaction rate is reported to be highest with RH within the range of 50–70% and which is commonly used in the previous studies. The effect of temperature is reported to have small change or no affect on carbonation. It is also reported that the concrete cover layer is the single 'line of defense' against the penetration of CO_2 in cementitious matrix, as the quality and the cover depth of this layer largely governs the service life of the concrete structures (Alexander and Beushausen, 2019). Schematic representation of cover layer of concrete is shown in Figure 2.2.

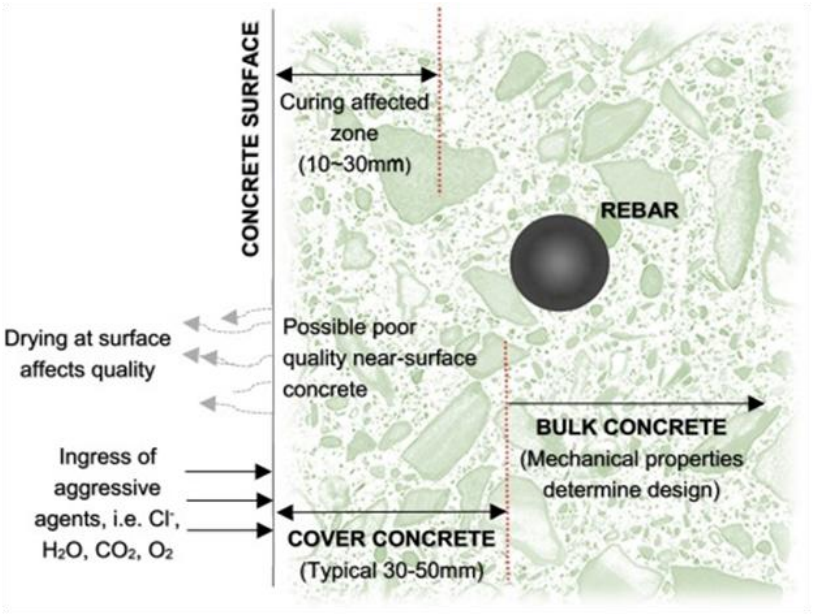

Figure 2.2 Schematic representation of concrete cover (Adapted from Alexander and Beushausen, 2019)

Various evaluation methods have been used to determine the carbonation profiles in concrete (Ashraf, 2016). The use of phenolphthalein pH indicator solution is the most well-known test method to measure the carbonation front in concrete. This indicator shows red (or pink) color in non carbonated concrete system where pH value is more than 9. During the carbonation reaction, the pH value of the carbonated region of concrete reduces to < 9.0 and as a result, phenolphthalein indicator stays colorless. This is the most frequently used carbonation test method which provides an approximate measurement of the carbonation depth. The second analytical method "thermogravimetric analysis (TGA)", provides quantitative information to obtain more precise carbonation profiles is also used. This test method determines the relative proportions of $Ca(OH)_2$ or $CaCO_3$ from which the degree of carbonation within the samples can be obtained. Fourier transformed infrared spectra and scanning electron microscopy (SEM) are mostly used to obtain qualitative information for the assessments of carbonated concrete. X-ray diffraction (XRD) is widely used to identify and quantify the changes at the microscopic phases of cement-based materials which are evolved during the carbonation reaction. Some recent studies has utilized gammadensimetry, nuclear magnetic resonance (NMR) spectra and nondestructive evaluation (NDE) methods such as nonlinear ultrasonic techniques to monitor

microstructural changes in cement-based materials due to the carbonation reaction (Villain et al. 2007; Kim et al. 2016).

2.2.1.2 Chloride Ingress

Reinforced concrete (RC) with properties such as strength and toughness makes it one of the most versatile and potential durable structural material around the world. The long-term durability of structures made from steel-reinforced concrete makes the construction of high-rise buildings as well as long span bridges. However, the service life and durability of RC structures is threatened when the steel rebar in the concrete structures is exposed to the chloride ions (Zhou et al. 2015). Ingress of aggressive Cl^- ions into the concrete matrix results into chloride induced corrosion of steel reinforcement. The source of chloride ions may be internal (contaminated aggregates in concrete mix) or external (de-icing salts and marine environments). Chloride-induced corrosion is a major deterioration problem and RC structures are under constant degradation due to aggressive chloride attack. A sound concrete normally provides a high degree of protection to reinforcing steel rebar with its non-aggressive environment by virtue of the high alkalinity. Concrete usually exhibits a pH value of 12.5-13.5 and under this high alkaline environment steel reinforcement remains passivated (Poursaee, 2016). After the hydration of cement in RC structures, a protective passive layer consisting of γ-Fe_2O_3 on the surface of steel rebar is formed with a thickness in the range of 10^{-3} to 10^{-1} μm (Goyal et al. 2018). This passive layer of oxides protects the steel by blocking the movement of ions in surrounding concrete cover thereby protect steel rebar from corrosion (Berrocal et al. 2016). The interconnected pore system and presence of micro-cracks in concrete matrix provides a continuous network through which chloride ions penetrates and initiate the steel depassivation. Chloride induced corrosion is an electrochemical process which requires anodic and cathode regions as well as ionic conduction path through an electrolyte (Figure 2.3). The steel surface activated by chloride ions becomes an anodic site and the passivated surface becomes a cathode site. Concrete pore solution acts as an electrolyte and allows the movement of ions (Neville, 1995).

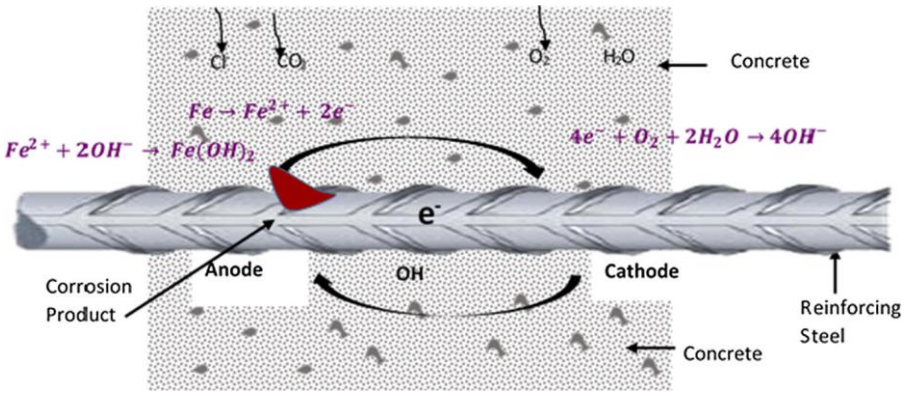

Figure 2.3 Schematic representation of chloride induced corrosion process in concrete (Adapted from Goyal et al. 2018)

The electrochemical reactions in chloride induced corrosions are as follow (Zhou et al. 2015):

$$Fe^{2+} + 2Cl^- \rightarrow FeCl_2 \qquad (2.6)$$

$$Fe \rightarrow Fe^{2+} + 2e^- \qquad (2.7)$$

$$O_2 + 2H_2O + 4e^- \rightarrow 4OH^- \qquad (2.8)$$

$$Fe^{2+} + 2OH^- \rightarrow Fe(OH)_2 \qquad (2.9)$$

$$4Fe(OH)_2 + 2H_2O + O_2 \rightarrow 4Fe(OH)_3 \qquad (2.10)$$

$$2Fe(OH)_3 \rightarrow Fe_2O_3.H_2O + 2H_2O \qquad (2.11)$$

As shown in Eq 2.6 – Eq 2.11, in presence of sufficient chloride ions, oxygen and water the passive layer on the surface is disrupted. The corrosion products (Hydrated ferric oxide i.e, rust) formed as result of electrochemical reactions are highly porous and voluminous (6–10 times of steel) in nature. The corrosion products directly affect the concrete properties, causing cracking and spalling. The progression of corrosion at the cross-sectional area of steel reduces its load-carrying capacity causing the failure of RC structures at later ages. Continuous process of the formation of corrosion products enhance the expansion, which ultimately leads to crack generation in concrete cover leading into delamination and then spalling. Different visual signs of damaged reinforced concrete buildings due to corrosion are shown in Figure 2.4.

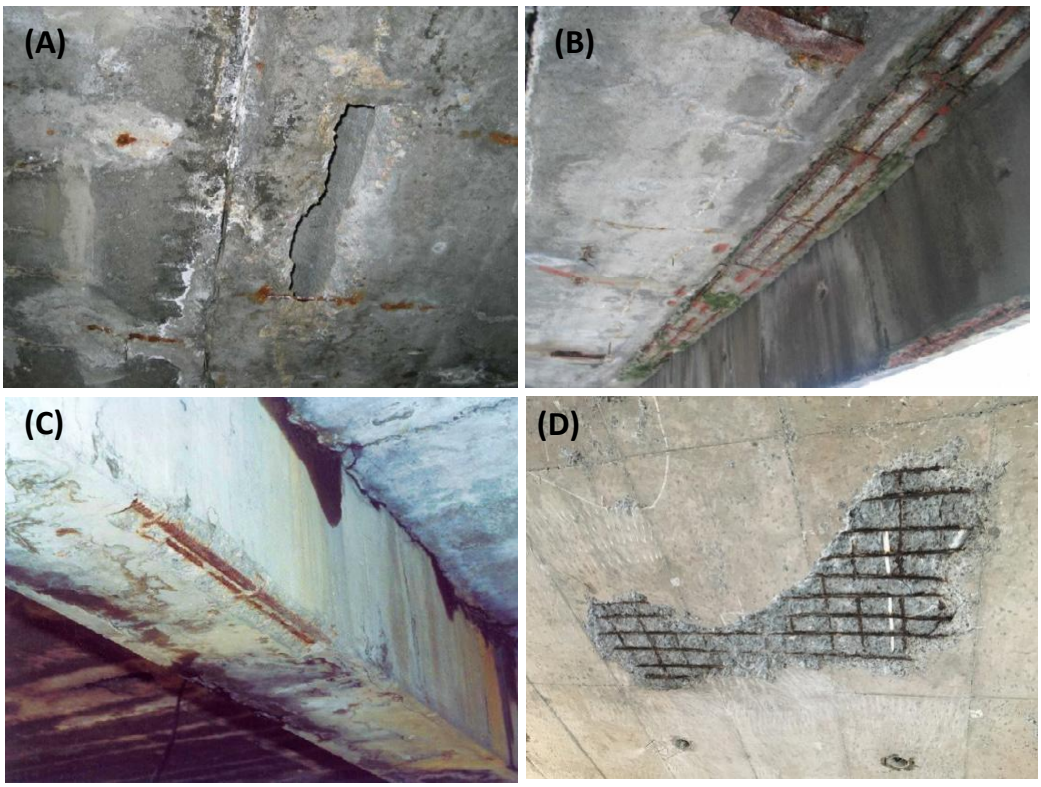

Figure 2.4 Typical damage of concrete during reinforcement corrosion (A) Floor precast slab (B and C) Beam in car parking structure (D) Slab in residential apartment (Adapted from Berkowski et al. 2013; Vijayalakshmi et al. 2017)

The reinforcement corrosion is reported to be dependent on different factors of RC structures. Corrosion initiation phase is the time required by the aggressive chloride ions to reach the rebar and initiate the corrosion. This phase depends upon the concrete cover depth and concentration or critical chloride content required for the depassivation of steel (Glass and Buenfeld, 2000). Other most important factor which influences the chloride ingress is the concrete porosity which affects the chloride transport mechanism. Water-binder ratio of concrete mix was reported to be the prime factor which significantly influences the capillary porosity of concrete matrix (Poursaee, 2016). Chloride binding capacity, curing conditions and age of concrete as well as ambient temperature and relative humidity were also reported to have a significant impact (Zhou et al. 2015).

In order to detect the transport movement of chloride ions in concrete, various test methods have been used. Rapid chloride permeability test (RCPT) which detects the diffusion rate is conducted to cover the determination of the electrical conductance of concrete to provide a rapid indication

of its resistance towards the penetration of chloride ions. A variety of nondestructive methods are used to determine corrosion rate for RC structures. These methods include half-cell potential, linear polarization resistance (LPR) measurement, electrochemical impedance spectroscopy (EIS), galvanostatic pulse technique, embeddable corrosion monitoring sensor, ultrasonic pulse velocity technique and infrared thermograph electrochemical method (Pradhan and Bhattacharjee, 2009; Zhou et al. 2015). Acoustic emission is a recent non-destructive method, which is used to follow the development of cracks in concrete cover due to the formation of corrosion products.

2.2.1.3 Sulfate attack

Sulfate attack is one of the most aggressive deterioration factors, which causes irremediable changes in concrete structures. Sulfate ingress had a significant impact on the durability of concrete structures constructed on sulfate rich soil or ground water (Leemann and Loser, 2011). Sulfate attack refers to the degradation process which comprises a series of chemical reactions triggered by sulfate ions and the cementitious components of hardened concrete. These reactions of sulfate ions with the hydrated products of cement results into the dissolution of calcium-bearing phases and formation of expansive products. These chemical reactions lead to cracking and progressive loss of strength causing overall failure of concrete structures (Van Tittelboom et al. 2013). Sulfate attack on concrete is categorized into external and internal attack. External sulfate attack occurs when sulfate ions penetrates from an external source (sulfate rich soil or water) into the cement matrix of concrete. Internal sulfate attack occurs with delayed expansive products formation in the post-hardened state of concrete due to the incorporation of aggregates with sulfide inclusions while casting (Menéndez et al. 2013). The phenomenon of external sulfate attack on the concrete structures is the most common alterations and well documented by researchers (Santhanam et al. 2001; Neville, 2004). When cement mortars and concrete during their service life comes in contact with the sulfate loaded environments, it causes the ingress of sulfate ions in cementitious matrix (Massaad et al. 2016). Transportation of the increased sulfate ions concentration from the surface into concrete bulk leads to its chemical interaction with hydrated products of cement (Rozière et al. 2009; Whittaker et al. 2015). Two stage mechanism of distress on concrete matrix in sulfate attack was reported to be the driving cause of deterioration. In the first stage, reaction of sulfate ions with portlandite (CH) forms gypsum,

which further reacts with tricalcium aluminate (C_3A) and results into ettringite precipitates in the pores of concrete, which is categorized as chemical sulfate attack (Nehdi and Hayek, 2005). Formation of gypsum results into the reduction of stiffness and strength of concrete structures. Ettringite precipitates formed during the continuous sulfate reactions have the ability to swell, which results into the densification of the microstructure of concrete. Ettringite crystals generate pressure followed by internal stresses in the pore matrix leads to cracking and destruction of the concrete (Maes and De Belie, 2014). During second stage, expansive forces associated with ettringite due to high crystallization pressure leads to swelling, cracking and spalling of concrete (Scherer, 2004).

This form of sulfate induced degradation is termed as physical sulfate attack (PSA), in which concrete is vulnerable to damage due to sulfate salt crystallization (Haynes and Bassuoni, 2011). Under this condition, process of capillary rise and evaporation of sulfate salts occurs during the contact of concrete surface with sulfate bearing solution (Najjar et al. 2017a). Generally, supersaturation of sulfate solution (conversion of anhydrous phase of sodium sulfate salt 'thenardite' into hydrous phase 'mirabilite') in concrete pore distribution results into increase in volume due to salt crystallization (Rodriguez-Navarro and Doehne, 1999). The developed crystallization is termed as salt weathering which damage the concrete by surface scaling, salt efflorescence and sub florescence (Aye and Oguchi, 2011). Different visual signs of damaged concrete structures due to sulfate ingress are shown in Figure 2.5.

Many parameters which influence the deterioration rate of sulfate attack on concrete structures are reported in the literature. The major factors which influence the sulfate attack mechanism are: type and concentration of sulfate ions, the possibility of diffusion of sulfate ions into the pore matrix of concrete structure, volume of C_3A content in the cement, pH of the sulfate solution and temperature. It has been reported that the sulfate solutions containing different cations acts differently with variation in the mechanism of damage on concrete. Different sulfate solutions have different solubility and the possibility of sulfate solutions to penetrate into the concrete structure is different. The rate of sulfate attack is affected by the strength of sulfate solutions, as it has been reported that higher the sulfate concentration results into highly aggressive environment.

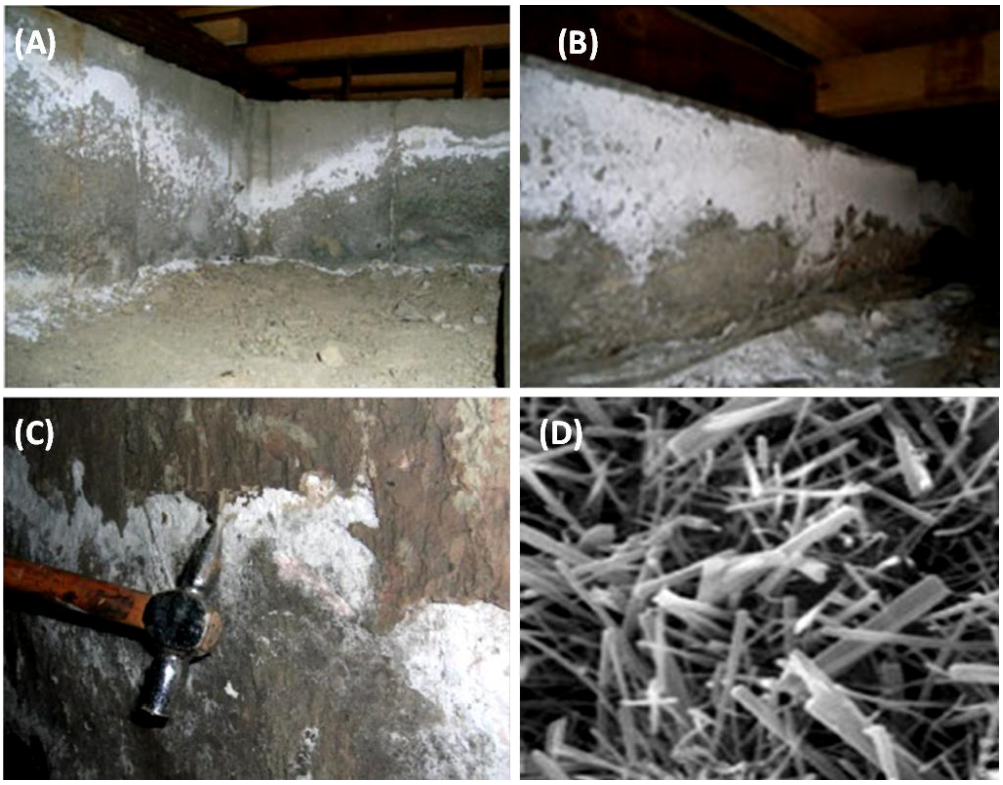

Figure 2.5 Typical appearance of deteriorated concrete foundation due to sulfate environment (A-C) Formation of salt efflorescence and spalling of concrete cover (D) Ettringite crystal formation in concrete matrix (Adapted from Yoshida, 2017; Liu et al. 2017)

The C_3A content of the cement plays a major role in the attack mechanism of sulfates as it was reported that the binding behavior of C_3A influence this multi-ion transport into the concrete matrix (Van Tittelboom et al. 2013). It was reported that presence of C_3A phase in cement clinker promotes the ettringite formation in sulfate environment. The lower availability of C_3A is recommended in cement clinkers to reduce the damage by sulfate attack due to reduced quantity of ettringite formation. Influence of high pore volume and high value of water/cement ratio in concrete is reported to be vulnerable to sulfate attack.

In order to evaluate the effect of sulfate attack on mortar and concrete, accelerated degradation mechanism with higher concentrations of sulfate solutions are adopted by researchers at lab scale experiments. To shorten the duration of sulfate tests, wet-dry cycle exposures are adopted. To evaluate the durability, standard test method for length change of mortars is the most widely accepted performance test. American Society of Testing and Materials (ASTM) standard is used

to evaluate the length expansion of mortar prisms under the exposure of sulfate solutions (ASTM C1012-04). Other analysis like visual observation, mass change in concrete, change in compressive strength and flexural strength are also conducted. XRD and SEM analysis are widely conducted for the microstructural evaluation of mortar and concrete specimens after sulfate exposure.

2.2.1.4 Microcrack formation

Presence of microcracks in cementitious matrix influences the stability by providing a preferential pathway for the ingress of aggressive elements by capillary action into structural elements of concrete structures. Formation of microcracks at cement paste–aggregate interfaces within concrete matrix has significant durability issues (Soroushian and Elzafraney, 2004). Shrinkage and volumetric expansion due to alkali aggregate reactions in concrete matrix are the major factors contributing the origin of microcrack formation (Wittmann et al. 2009; Noël et al. 2018). Cracking due to shrinkage in concrete takes place in two stages: (1) Plastic shrinkage (occurs at early ages) (2) Drying shrinkage (occurs at later ages). The early stage shrinkage occurs within the first few hours when concrete is in plastic stage and starting to harden. The principal cause of plastic shrinkage is generally been attributed to the excessive and rapid rate of water evaporation from the surface of concrete during exposure to the atmosphere (Combrinck and Boshoff, 2013). The drying shrinkage occurs in concrete due to volume reductions due to thermal changes caused by evaporation of internal water in hardened concrete. During the drying environments, drying front is developed from an exposed surface and the empty pores in cementitious matrix create tensile stress. When the developed tensile stress at the interfaces between aggregates and matrix exceeded the tensile strength of concrete, cracking initiates and growth of microcracks occurs (Hu et al. 2017). It is reported that cracks formed during plastic stage might further widened during the long term drying shrinkage in the hardened concrete structures. Early age formation of microcracks due to shrinkage and improper curing of concrete severely influence the serviceability of structures. Different thermal exposure on concrete due to cyclic temperature variation conditions propagates the formation of micro-cracks.

Alkali-Aggregate Reaction (AAR) is a chemical reaction between the alkali hydroxides in the concrete pore solution and some reactive mineral phases present on the aggregates. The formation of reaction products in AAR causes volumetric expansion and generates internal stress

in the concrete matrix which induces microcracks (Shayan, 2016). Three conditions which influence the initiation of AAR induced cracking in concrete are: (1) Presence of reactive aggregates, (2) high concentration of dissolved alkali hydroxides (K^+, $Na^+ – OH^-$) in the concrete pore fluid and (3) availability of sufficient moisture. Two major types of AAR depending upon the reactive minerals present in the aggregate are recognized: (1) alkali–silica reaction (ASR) and (2) alkali–carbonate reaction (ACR). In ASR, when the reactive microcrystalline silicas present within the aggregate particles reacts with the sodium and potassium alkali hydroxides dissolved in the concrete pore solution forms an unstable silica-alkaline gel. The ASR gel swells upon the uptake of water and various ionic species in the pore fluid induces expansive pressures within the reacting aggregate and the adjacent cement paste (Noël et al. 2018). Due to expansive ASR gel, tensile stresses build up and initiation of microcracking occurs in the cementitious matrix. The ACR is called desdolomitization reaction in which alkali hydroxides of the concrete pore fluid reacts with dolomite (a active minerals from dolomitic limestone aggregate) and precipitate brucite, calcite and alkaline carbonates. In ACR, no expansive gel is formed however expansion due to the generation of crystallized compounds results into crack initiation in the concrete matrix (Fournier and Bérubé, 2000).

Inevitable formation of microcracks promotes the penetration of water and ingress of deleterious substances (CO_2, SO_4^{2-} and Cl^-) as they provide an ideal pathway. In RC structures, initiation and propagation of microcracks expose the steel reinforcement to aggressive liquids and gases which endanger the durability of concrete structure. Microcracking in RC structures is one of the most harmful distress mechanisms, which severely affects the serviceability of infrastructure worldwide leading to its premature deterioration.

2.2.2 Environmental and economic impact in concrete construction

Concrete has become the highest manufactured and the consumed product (in terms of volume) on the Earth. The Indian construction industry is reported to currently consume about 400 Mt of concrete every year and further is estimated to reach 1000 Mt in less than a decade (Rana et al. 2015). Consequently, with such extensive levels of concrete production and consumption, on the basis of global environmental impact it is considered as a controversial and non-sustainable material (Turk et al. 2015). Production of conventional concrete is reported to contribute

approximately 8.6% of the global anthropogenic CO_2 emissions. High production of concrete worldwide means, high consumption of essential raw materials and large amount of energy for its production. Essential components of concrete, cement (a binding agent) and natural aggregates are the major mass resources that are used in the construction industry. The cement production and natural aggregate extraction are highly intensive energy consuming as well as a major CO_2 emitting process. However, the production of ordinary portland cement has been attributed as one of the major contributors to the anthropogenic carbon dioxide emission in the world. It is reported that cement production accounts for roughly 8% of global CO_2 emissions (Kajaste and Hurme, 2016). The production of traditional portland cement includes high relative emission processes (1) raw materials preparation (2) clinker production (process called calcinations) which requires large energy inputs and results in additional GHG emissions. It is reported that with the manufacture of 1 ton of cement, approximately 1 ton of CO_2 gas is released (Monteiro et al. 2017). The expected cement production in India is reported to grow from the current value of about 280 million tons and surpass 550 million tons by 2025, to meet the infrastructure requirements (Gettu et al. 2019). Globally, environmental impacts in cement manufacturing are responsible for 8-9% of the anthropogenic CO_2 emissions and 2-3% of energy demand.

Construction industry being a major consumer of natural resources, aggregates (sand, gravel, and crushed stone) which is an essential component represents 80% by mass of concrete. With the vast development projects around the world, global aggregate production was reported to be doubled from 21 billion tons to 40 billion tons in-between the time period of 2007-2014 (Tam et al. 2018). Aggregate extraction cause major environmental impacts as well as consume considerable amounts of energy. Aggregate production includes mining, processing, and transport operations which causes adverse changes in landscape and ecology of area of extraction, excessive noise and dust generation during mining process and degradation of groundwater and surface water (Mehta, 2001). Extraction of aggregates from mining and processing also contribute in environmental impacts including resource depletion, degradation of ground and surface water and global warming (Drew et al. 2002; Langer, 2016). Acceleration in infrastructure developments is escalating sand extraction which is putting more and more strain on limited sand deposits. Sand used in construction as a major portion is also extracted from rivers and beaches. Extensive sand mining induce erosion, degradation of ecosystem and

biological environments of river systems (Padmalal et al. 2008; Torres et al. 2017). A warning issued by United Nations Environment Programme (UNEP) that massive and unregulated sand mining from rivers by humans is rapidly using up its "sand budget", with damaging impacts (Cousins, 2019). The effect of a shortage of these construction materials is reported to have increased construction cost which results into transferring the burden to the end users (Ismail et al. 2013). Research efforts to reduce dependence on naturally occurring sand in construction sector and guarantee the sustainable development of concrete with reduced carbon footprints is going on.

The environmental impact of the construction industry especially that of its construction and demolition wastes (CDW) generated from early deterioration of existing infrastructure is a matter of concern around the globe. CDW are defined as a mixture of different material, including inert waste, non-inert non-hazardous and hazardous waste, generated from construction, renovation, repair and demolition works (Menegaki and Damigos, 2018). It was reported that the world produces around 7-10 billion metric tons of waste every year of which 36% consists of CDW (Duan et al. 2019). Jain et al. (2018) using material flow analysis (MFA) reported that estimated annual generation of CDW in India is approximately between 112 and 431 million tons. Generation of CDW is considered to be an unsustainable activity which causes progressive deterioration of the environment. Failure to adequately manage CDW leads to several major environmental impacts. Different factors such as toxicity hazards, severe air pollution and surface and ground water contamination are associated with CDW (Duan et al. 2019). Large landfill space for the disposal of incremental quantities of CDW creates land resource scarcity in the urban cities. The majority of CDW is disposed of in open landfill sites which on exposure to rainfall generate landfill leachate and this toxic pollutant contaminates surrounding surface and groundwater resources. Whether it is carbon emission from cement industries or the problem of solid waste generation on replacing the deteriorated concrete structures, environmental concerns are paramount.

Apart from environmental impact, economic concerns with extensive repair, rehabilitation and retrofitting of deteriorating concrete structures are also associated. Over a period of time, in concrete structures certain degradation or deterioration in the form of corrosion, cracking, spalling and delaminating affects the serviceability. For the repair and rehabilitation of damaged

concrete structures or to replace the deteriorated structures, many countries are forced to allocate considerable funds in their annual budget. Across the globe for repair and restoration of deteriorated concrete structures, annual expenditure of billions of dollars is reported (Bhattacharjee, 2018). Sidiq et al. (2019) reported that in USA, for the maintenance services and repairs of concrete infrastructures are estimated to be $5.2 billion annually. Indirect cost due to loss of productivity and traffic jams repair and retrofitting process makes the total cost 10 times the actual cost of maintenance. In 2006, a study reporting an estimated cost of $125 billion/year associated with the maintenance due to steel corrosion of reinforced concrete structures was published (Emmons and Sordyl, 2006). In another study reports, 45% of annual expenditure in UK on construction was estimated to be related to maintenance and repair costs of distressed concrete structures. In a recent study reported that, in UK an investment of £500 billion was dedicated for nation's infrastructure assets and approximately half of the construction budget of around £40 billion/year is spent on the repair and maintenance of concrete infrastructure (Al-Tabbaa et al. 2019). Similarly in case of Europe, approximately 50% of the annual construction budget was reported to be spent on maintenance and repair (Hilloulin et al. 2015). Due to the corrosion in reinforced concrete structures as well as concrete degradation, the cost of maintenance in China is reported to be nearly 250 billion RMB/year. As nearly 80% of world's infrastructure is built in reinforced concrete, their maintenance needs a huge recurring investment that few countries in the world can afford. There is a worldwide effort for sustainable technologies for maintenance of infrastructures that would offer economy without undue environmental or social costs.

2.3 Transport mechanism of deleterious substances in concrete

One of the most important and serious issue in reinforced concrete structures is the deterioration of durability properties when exposed to harsh environmental conditions. Most severe concerns in the drastic decrease of durability are reported to be associated with the transport properties of the concrete material. Ingress of gases, liquids and aggressive ions are the most important parameters which upon transportation through the low permeable concrete matrix lead to the premature deterioration (Long et al. 2001; Basheer et al. 2001). The deterioration of reinforced concrete structures is reported to be dependent on the permeation properties of cementitious matrix which influence the ingress of the aggressive ions. Transport mechanism of harmful

agents like CO_2, SO_4^{2-} and Cl^- from the service environment is influenced by pore spaces in the cement paste and paste-aggregate interfaces or microcracks of concrete (Zhu, 2020). It has been reported that microcracks facilitate the transport of aggressive agents and further impact on the severe deterioration of durability of concrete structures (Wu et al. 2015). Depending on the driving force of the process and the nature of the transported matter, different transport processes for deleterious substances within the hardened concrete are distinguished as diffusion, absorption and permeability (Lepech and Li, 2009). Recommended different codes of practice on the conditioning regime and sample dimensions required for measuring transport properties of cement-based materials are described in Table 2.2.

(1) **Diffusion**: Diffusion is a process in which aggressive agents penetrated within the concrete due to concentration gradient. In diffusion process, ions or molecules move from an area of higher concentrations to lower concentrations. Chloride ions, carbonation and sulfate ions transport in concrete is a primary example of diffusion mechanism where ions move from higher concentrations through pores, to internal zones where their concentration is lower. Transport of ions with diffusion mechanism are also accompanied by reactions such as physical and chemical binding with cement hydration products and other ions (e.g. Na^+, K^+, SO_4^{2-}) present in the concrete pore solution also affect the validity and accuracy of diffusivity. In general three diffusion tests are classified to determine the diffusion of aggressive ions (Bertolini et al. 2004):

- Steady state test
- Non-steady tests and
- Electric field migration tests

In the case of steady state tests, the rate of ionic transport is measured and diffusion coefficient is calculated using Fick's first law of diffusion. In this test, a thin slice of the test specimen is used as a barrier in between the ionic solution and control solution free from ions. Rate of diffusion due to a concentration gradient is obtained. This diffusion test typically requires six or more months to achieve a steady state of flow. However, in non-steady state tests, diffusion coefficient is obtained by calculating the depth of penetration of ions applying Fick's second law of diffusion. In this test, specimen is immersed in the solution or ponding the solution usually for 90 days containing specific ions (Basheer et al. 2001).

As the steady and non-steady tests take very long time, in electrical migration tests, transport of ions is accelerated with the application of electrical potential gradients. In this test, electrical field is applied across the specimen in a diffusion cell and ionic movement is examined across the test specimen by measuring the charge passed. The ion mobility under an electric field is directly related to the diffusion coefficient.

(2) **Absorption**: Transport of liquids in the capillary pores of concrete due to the surface tension forces acting in capillaries is called capillary absorption. Factors which influence the capillary transport are surface tension, viscosity and density of the liquid, angle of contact between the solid and liquid, the radius of capillary pore walls (Basheer, 2001). It is also reported that absorption is related to pore structure as well as the moisture condition of the concrete. Tests for the absorption characteristics of concrete are classified into three categories:

- Water absorption capacity
- Sorptivity test
- Absorptivity test

In water absorption capacity test, effective porosity of concrete is determined. When a dry specimen is immersed in a shallow depth of water, the increase in weight of specimen is referred to as the water absorption capacity. In this test, absorption takes place from all the surface of specimen, that's why the quantity of water absorbed is dependent both on the ratio of surface area to volume of the specimen and the duration of immersion.

Sorptivity defines the rate of inflow of water in a dry concrete when water is allowed to be absorbed unidirectionally under a negligible applied pressure. Sorptivity test is normally conducted to measure the capillary suction in concrete. The rate of absorption (sorptivity) of water by concrete is determined by measuring the increase in the mass of specimen resulting from the absorption of water as a function of time when only one surface of the specimen is exposed to water (Basheer, 2001; Bertolini et al. 2004).

Table 2.2 Recommended different codes of practice for measuring transport properties

Standard	Transport properties	Conditioning	Diameter (mm)	Thickness (mm)
CEMBUREAU:1989	Gas & water permeability	65% RH, 20 °C for 28 days; or 105 °C for 7 days, followed by 20 °C for 3 days	150	50
RILEM TC 116:1999	Gas permeability & capillary absorption	50 °C until pre-set weight loss is attained	150	50
BS EN 1015-19:1999	Water vapour permeability (mortar)	95% RH, 20 °C for 2–5 days, then 50% RH, 20 °C for 23–26 days	–	10–30
NT Build 369:1991	Water diffusion	40 °C for 7 days	100	20
ASTM C1202-12:2012	Chloride ion penetration	Vacuum saturated	100	50
DIN 1048:1978	Water impermeability (concrete)	–	150x150x150 concrete cube	
RILEM CPC 18:1988	Carbonation depth	65% RH, 20 °C	–	40–100
BS 1881-122:2011	Capillary absorption	105 °C for 3 days	75	32–150
ASTM C1585-04:2004	Sorptivity	Vacuum saturation, then conditioned in 50 ± 2 °C and RH of 80 ± 3 % for 3 days	100	50

RH: Relative humidity

In absorptivity tests, water movement into concrete is mainly achieved by capillary suction upon the application of low pressure. However, in this test there is no control over the direction of the water flow. The absorptivity test is further categorized into two tests: (1) Surface absorptivity tests (2) Drill hole absorptivity tests. The major difference between surface absorptivity tests and the drill hole absorptivity tests is source of water. In surface absorptivity test, the source of water is a reservoir mounted onto the surface of the concrete specimen however in drill hole absorptivity tests water is allowed to be absorbed from a hole drilled in the near surface region of concrete specimen. The initial surface absorption test (ISAT) is an example of surface absorptivity test in which the rate of flow of water into concrete per unit area after a stated interval is calculated at a constant applied head and temperature.

(3) **Permeability**: Permeability is defined as the measure of fluid medium which flow through the concrete with ease under the action of a pressure differential. The coefficient of permeability is a material characteristic describing the permeation of gases or liquids through the material. The permeability tests are broadly classified into (1) Liquid permeability tests and (2) Gas permeability tests (Basheer, 2001). Permeability is the most common performance properties used to represent concrete quality.

2.4 Improvement of concrete durability

In order to overcome the deterioration problem and to improve the durability properties of concrete structures, researchers associated with civil engineering has conducted extensive research work to develop variety of techniques for the protection of concrete quality. Basically protection techniques adopted are based on two mechanisms of treatment on concrete structures. First is the application of concrete protective agents as an external treatment source and second is the use of the protective agent as an internal mineral admixture in concrete during casting. Among the treatment methods, some techniques are based on the protection of concrete structures from the penetration of aggressive agents by external applications of organic and inorganic protection material. In terms of treatment approaches, protective materials are grouped into 4 types: (1) Surface treatment with organic and inorganic materials (2) Nanoparticle additive and (3) Crack healing agents.

2.4.1 Surface treatment

Concrete structures being prone to the penetration of aggressive agents, different varieties of surface treatment materials are investigated and reported to protect the concrete structures. Surface treatment method on concrete cover is reported to be a good barrier which protects the structures by resisting the ingress of aggressive substances. Surface treatment materials on the basis of chemical nature are broadly classified into two categories: (1) Organic and (2) Inorganic protective agents. The organic surface treatment materials are the protective agents which do not react with concrete substrate during the application and also are reported to have good barrier properties. The inorganic surface treatment materials are reported to be mainly aqueous solutions of sodium silicate which are more stable with better resistance to aging (Pan et al. 2017a). Surface treatments according to their function are further grouped into 4 categories: (1) Surface

coatings, which forms a continuous polymer layer which acts as a physical barrier to inhibit the ingress of the aggressive substances (2) Hydrophobic impregnation, forms a water-repellent pore surface (3) Poreblocking treatment material, reduces the porosity of surface layer by partially or completely filling the capillary pores and (4) Multifunctional surface treatment material, performs of at least two functions such as form hydrophobic layer as well as block the capillary pores (Pan et al. 2017b). Different types of protective agents for surface treatment of concrete structures with organic and inorganic nature classified into 4 categories are shown in Figure 2.6.

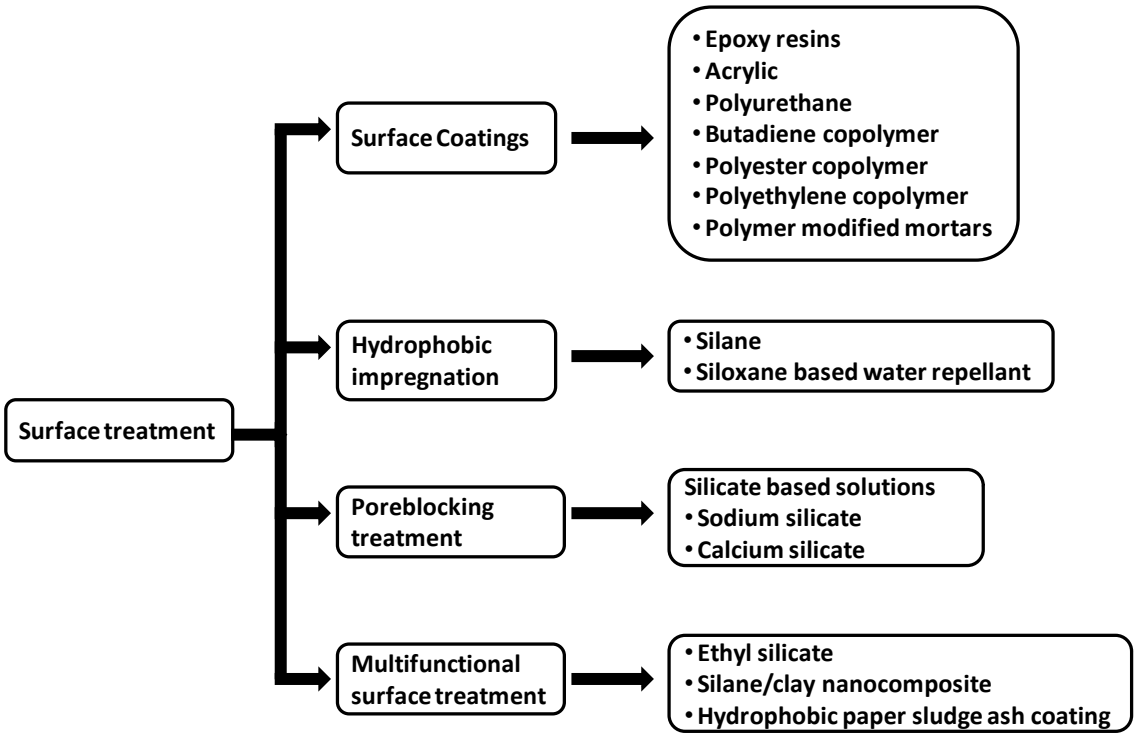

Figure 2.6 Overview of different surface treatment materials to protect concrete structures from aggressive agents

Various studies using these treatment materials have been reported with positive outcomes showing effective restriction of water ingress, chloride ingress and carbonation in treated concrete structures. Ibrahim et al. (1999) investigated the effect of 6 different sealants and coatings on the durability properties of concrete. It was reported that among sodium silicate, silicone resin solution, silane/siloxane, silane/siloxane with an acrylic topcoat, alkyl-alkoxy silane and two-component acrylic coating, the chloride diffusion and carbonation was most efficiently reduced in concretes coated with silane, silane/siloxane with an acrylic topcoat. Also

silane/siloxane with an acrylic topcoat was reported to be the most effective protective agent in minimizing the damage due to sulfate attack. Almusallam et al. (2003) also investigated the effectiveness of surface coatings with different concrete surface protective agents. It was reported that epoxy and polyurethane coatings were the most effective surface treatment materials instead of acrylic, polymer and chlorinated rubber coatings in reducing water absorption, chloride permeability and chloride diffusion after surface treatment of concrete.

Medeiros and Helene (2009) investigated the influence of surface treatment of RC structures in marine environment. In this study, hydrophobic agents as well as surface coatings were investigated to determine the chloride diffusion coefficient and absorption in treated RC structures. It was reported that all the surface protection treatments significantly reduced the sorptivity (> 70%) of concrete. However, chloride diffusion coefficient was significantly reduced (reduction rate of 86%) with polyurethane coating and reported it as the highly effective protective treatment. Use of ethyl silicate as a surface protection material on concrete structures was also reported (Franzoni et al. 2013). Ethyl silicate was reported to be the effective protection treatment for RC structures which provided the best performance in limiting the water ingress. Significant improvement in terms of chloride and carbonation resistance on the application of ethyl silicate was reported. Jia et al. (2016) reported the positive effects of inorganic surface treatment (fluosilicate and sodium silicate) on the water permeability of mortar and concrete specimens. It was reported that the application of both fluosilicate and sodium silicate surface treatments effectively reduces the permeability as well as porosity of surface layer of cement-based materials.

2.4.2 Nanoparticle additives

Over the past few years, inclusion of nano-materials in concrete as an effective application is making a great contribution to improve the durability properties. Nanotechnology is ranked as a most significant area of research application in the construction industry and is gaining momentum with immediate profitable return from high value products. Nano-engineering or nano-modifications in cementitious systems includes the following areas: (1) Incorporation of nanoscale materials (e.g., nano-SiO_2, TiO_2, Al_2O_3, Fe_2O_3 etc.) (2) Incorporation of carbon nanotubes/nanofibers as nanoreinforcements and (3) Nano-clay particles (Mukhopadhyay, 2011).

Nanoparticles are reported as an effective additive which improves the workability, mechanical strength, flexibility and durability of concrete. Addition of nano-materials and nanoreinforcements is reported to promote cement hydration and densify the microstructure and improve the interfacial transition zone (ITZ) of concrete structures (Sanchez and Sobolev, 2010). Different studies have been reported in which the improved durability properties of concrete on addition of various nanoscale materials. Jo et al. (2007) investigated the influence of addition of nano-SiO_2 particles with replacement of cement (3%, 6%, 10% and 12% by weight) in cement mortar. It was reported that, the addition of nano-SiO_2 to cement mortars improves the strength properties as the nano-SiO_2 content was increased from 3% to 12%. It was reported that, nano-scale SiO_2 behaves as filler which improved the mortar cement microstructure as well as promotes the pozzolanic reaction. In another study, cement was replaced with nano-SiO_2 (0%, 0.5%, 1%, 2% and 5% w/w) in cement pastes. It was reported that even in low concentrations of nanosilica, improved mechanical properties and dense microstructure was observed (Stefanidou and Papayianni, 2012). In the microstructural analysis, large crystal size of calcium silicate was observed in samples with 5% nanoparticles. Haruehansapong et al. (2014) reported the effect of optimum replacement of cement with nano-SiO_2 on the compressive strength of cement mortars. With the varying replacement contents (3%, 6%, 9% and 12%), the optimum replacement content of 9% nano-SiO_2 and independent of particle size was reported. It was reported that, pozzolanic activity and packing ability of nano-SiO_2 increased the compressive strength. Tobón et al. (2015) also reported the improvement in the durability properties of cement mortars on the inclusion of nano-silica by replacing cement (1%, 3%, 5%, and 10%). A significant refinement of pores with the decreased total pore volume was reported on incorporation of nano-silica. Replacement of cement with 10% nano-silica resulted into significantly improved compressive strength and reduced capillary porosity. Expansion in sulfate exposure was reported to be reduced by 90% and 95% with addition of 5% and 10% nano-silica in cement mortar.

Nano-TiO_2 is a common nano-material used in cementitious composites, which has the properties like photo catalysis, antibacterial and chemically stable. Different studies have also shown that nano-TiO_2 on incorporation in cement accelerates the hydration properties of Portland cement. Nano-TiO_2 also improved strength properties as well as abrasion resistance of concrete. Chen et al. (2012) reported that on addition of nano-TiO_2 (5% and 10%) in cement paste significantly enhanced the hydration rate of cement and compressive strength of mortars. It

was also reported that this nano-material acts as non-reactive fine filler with no pozzolanic activity. However, nano-TiO_2 had a catalytic effect during the cement hydration reaction. Ma et al. (2016) investigated the influence of addition of nano-TiO_2 in fly ash cement mortars. It was reported that nano-TiO_2 accelerates initial and final setting and decrease the fluidity. Introduction of nano-TiO_2 lead to a significant early age compressive strength increase but adverse effect at the later age strength. Similar effect of strength loss at later ages on addition of nano-TiO_2 was also reported in another study (Meng et al. 2012). However, positive effect of FA in late strength counter act the negative influence of nano-TiO_2 in cement mortar was reported (Ma et al. 2016).

Carbon nano-tubes/nano-fibers (CNT) are also becoming promising nanomaterials for their use as nano-reinforcements in cementitious materials. Carbon tubes are classified into two types: (1) Single wall CNT/SCNT (composed of single highly structured graphene sheet rolled into long hollow cylinders) (2) Multi-wall CNT/MCNT (consists of nested arrays of up to several tens of concentric graphene cylinders coaxially arranged around a hollow core). Liew et al., (2016) reported the four reinforcing mechanisms of CNTs: (1) crack-bridging (2) reduction of nanoporosity of cement pastes with the filling role of CNT (3) the modification of the microstructure and (4) nucleation effects.

Konsta-Gdoutos et al. (2010) reported the improved durability properties of carbon nanotube/cement nanocomposites on addition of short and long MCNT. Enhanced fracture resistance properties and high stiffness C–S–H and decreased porosity in cementitious matrix is reported. Rhee and Roh (2013) reported the significant increase in compressive strength (72%) of concrete cylinders as compared to control specimen on addition of well-dispersed (MCNT) in a dispersion solvent (sodium naphthalene sulfonate formaldehyde). Reduced permeability in concrete cylinders with MCNT was also reported.

2.4.3 Crack healing agents

In context of civil research, healing is the phenomenon of restoration of concrete structure from a state of damage. In case of crack healing, chemical and physical processes results into the introduction of secondary products which blocks or seals the cracks. According to the review of literature, terminology used for crack healing in cementitious material is based on the mechanism of healing process. First is self-healing or autogenous healing and second is engineered self-

healing. Autogenous healing is a natural process in which cementitious material has the ability to heal the crack. Engineered self-healing is a process in which new substitute is incorporated into the cement material, which is stimulated on crack propagation resulting into sealing of crack. While on searching the literature it was observed that over the last decade researchers are publishing their research articles based on engineered self-healing concrete (ESC) properties. The effective self-healing potential of engineered self-healing concrete to repair the cracks had made it attractive. From the last two decades, researchers are working extensively to develop a self-healing concrete to overcome the damage from concrete cracking. The application of supplementing concrete with healing agent, which stimulates its healing action on crack propagation, had shown promising results (Table 2.3). Three different approaches are used to incorporate self-healing material in concrete matrix and which activates its healing property when the crack appears in the structure. Based on the mechanisms, engineered self-healing concrete is classified as vascular based, capsule based and intrinsic based (Blaiszik et al. 2010).

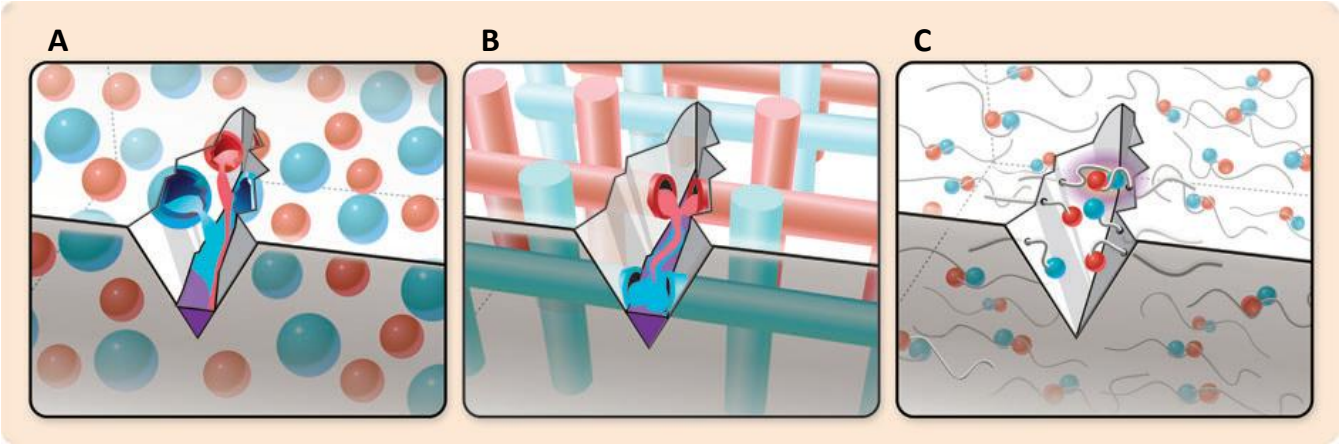

Figure 2.7 Different approaches in engineered self-healing concrete. (a) In vascular-based self-healing, hollow channels filled with healing agent ruptures on damage and releases healing material (b) In capsule-based self-healing, healing agent is released from ruptured capsules on damage (c) In intrinsic based approach, healing agent possess latent self-healing functionality which is triggered on damage or by external stimulus (Adapted from Blaiszik et al. 2010)

In vascular-based self-healing mechanism, healing material filled in hollow channels or fibers embedded in concrete matrix are released when damage ruptures the hollow channels or fibers (Figure 2.7a). The healing agent stored in capsules is triggered through the release of healing

material in concrete matrix when capsules are ruptured by damage (Figure 2.7b). Intrinsic self-healing materials embedded directly in concrete matrix possess a latent self-healing functionality which is triggered by damage or by external stimulus (Figure 2.7c). These materials rely on polymerizations, melting of thermoplastic phases or ionic interactions to initiate self healing.

Table 2.3 Overview of different healing agents and mechanism of healing action in cementitious matrix used in different research studies

Agent	Mechanism of application	Crack healing outcomes	References
Methyl methacrylate	Incorporation of hollow porous polypropylene fibers filled with healing agent in concrete structure	Reduction in permeability and enhancement in flexural toughening in active and passive mode respectively	Dry (1994)
Polymer admixtures	Polymer admixtures are used in mortar and concrete or as grout repairing material	Microcracks under stress in modified concrete are brigded by polymer films and prevent crack propagation	Ohama (1998)
Superglue (ethyl cyanoacrylate)	Hollow glass fibers filled with the healing agent was embedded in the concrete specimen	Microcracks generated on flexural loading were healed, validated by regaining flexural stiffness on reloading	Li et al. (1998)
Sikadur-52 (Epoxy adhesive)	Artificial cracks installed during casting in concrete cube were repaired with epoxy resin by gravity filling method	Increase in tensile and compressive strength across a crack in epoxy repair was observed	Issa and Debs (2007)
Low-lime fly ash	Fly ash in ratios of 35% and 55% by mass of binder was added. Load induced microcracks created in specimens were stored in lime water for 30 days.	Mechanical and permeation properties of cracked specimens recovered on self-healing action of fly ash	Şahmaran et al. (2008)
Expansive agent (C_4A_3S, $CaSO_4$, CaO) Chemical agent ($NaHCO_3$, Na_2CO_3) Geo-materials (Montmorillonite)	Healing agents were used as admixture substitute in concrete specimens with cracks created artificially.	Crack-width of 0.2 mm was completely healed at 33 day curing due to swelling effect, expansion effect and re-crystallization	Ahn and Kishi (2010)
Expansive additive (calcium sulfoaluminate)	10% additive by mass of total cementitious material was admixed	Surface crack introduced in specimen was submerged in water. $CaCO_3$ precipitation healed the surface crack in specimen	Sisomphon et al. (2012)

In the domain of engineered self-healing concrete, incorporation of hollow glass fibers filled with adhesive chemicals in cement matrices was reported in earliest studies (Dry, 1994). In the study, methyl methacrylate filled in hollow porous polypropylene fibers was embedded in cement beam. Specimens were subjected to loading, which causes the microcrack formation in the cement matrix and release of healing agent on the breakage of chemical filled fibers. To confirm the repair of microcracks with the released healing material, second load displacement test was conducted on the same specimen. It was reported an increase in flexural toughening for the samples containing the released adhesive agent for the second loading event than the control sample.

Use of polymer-based admixture was also reported to develop polymer modified concrete (PMC) or polymer modified mortar (PMM) (Ohama, 1998). Polymer admixtures were classified into four main types: polymer latex, redispersible polymer powders, water-soluble polymer and liquid polymer. Ohama (1998) reported that the microcracks in latex-modified mortar and concrete under stress were bridged by the polymer films preventing the crack propagation. Effectiveness in drying shrinkage reduction and its crack repairing property was also reported. Application of different polymer modifier like acrylic, styrene- butadiene latex, polyvinyl acetate and ethylene vinyl acetate in concrete crack sealing was reported (Fowler, 1999). Concept of release of chemicals to seal the tensile cracks by air curing was also studied (Li et al. 1998). In this study, thermoplastic superglue (ethyl cyanoacrylate) filled in hollow brittle glass fibers were used as a self-healing agent. The healing effect on the release of chemical in cracks generated in specimens during flexural testing was validated by regaining of flexural stiffness on reloading cycle. Binda et al. (1997) reported the injection of grouts to repair and strengthen stone masonry walls. Studies based on engineered self-healing concrete investigated by researchers were epoxy repairing of cracks by injection method and gravity filling method (Issa and Debs, 2007), incorporation of high volume fly-ash (Şahmaran et al. 2008), expansive healing material i.e. sodium aluminum silicate hydroxide containing swelling agent montmorillonite (Ahn and Kishi, 2010), crystalline additive and calcium sulfoaluminate based expansive additive (Sisomphon et al. 2012). In aforementioned investigations, promising results in crack closure based on self-healing action were observed.

2.5 Limitations in applications of synthetic materials on concrete

Although the evidence of using above mentioned methods in terms of durability enhancement of concrete is reported in previous studies, still many challenges are also associated with the synthesis, service life and cost of application at field scale implementation. In surface treatment of concrete structures, coatings of polymer based materials which are organic and inorganic in nature. Pan et al. (2017b) reported various failure patterns in polymer coatings, which reduces the surface life of protective materials. Blistering, cracking, holes and peeling in polymer coatings are reported which results from partial loss of adhesion due to osmotic pressure and shrinkage in coatings due to temperature change. It was reported that different thermal coefficients of concrete and polymer repair materials causes failure at the bond interface when significant temperature change undergo (Kosednar and Mailvaganam, 2005). In case of pore blocking surface treatments, formation of NaOH when sodium silicate and calcium hydroxide reacts in the cementitious matrix increases the possible risk of alkali-silicate reactions (Franzoni et al. 2013). It was also reported that micro-cracking on concrete surface and partial detachment on bricks applied with sodium silicate (Pan et al. 2017a; Navarro-Moreno et al. 2021).

Other major limitation associated with polymer materials is the cost of applications. Higher cost of polymer materials might makes its high volume applications impractical. Another problem associated with polymer materials is their poor fire resistance, which makes their inability to withstand high temperatures (Fowler, 1999). While the other limitations such as odorous smell, toxicity and flammability are also associated with polymer materials. Monomers and resins used to produce polymer materials are also reported to have safety issues such as skin allergy and fumes generated while applying (Fowler, 2009). Limited service life of surface treatment coatings is reported and the difficulty in removing the polymer coatings when its protective effects are weaken is also reported.

Use of nano-materials in concrete structures has shown promising results in its improving durability properties. Some limitations are also reported in the large scale applications of nano-materials. Synthesis of nano-materials at large production scale is an expensive process. It has been reported that in production of nano-materials, requirement of different types of expensive instruments makes it costly (Adesina, 2019). In case of graphene based CNTs, poor dispersion

property and weak bonding in cementitious matrix are the major limitation factors. For uniform dispersion of CNTs in cement matrix, different dispersion solvents are required to control the formation of agglomerates (Shamsaei et al. 2018). Incorporation of nanomaterials is also reported to reduce the setting time and workability of concrete. Apart from the negative effect of nanomaterials on the fresh properties of concrete, environmental threats are also associated with them. The very fine size of nano-materials such as nano-TiO_2 is reported to create air pollution while application and which on dispersion in air and cause health hazards.

2.6 Application of microorganisms in concrete

In order to develop sustainable concrete, a new biotechnological application has emerged in which microbes are used as bioagents to induce calcium carbonate deposition. This biobased approach called "Microbial induced calcium carbonate precipitation" (MICP) through biomineralization process has become an attractive topic of research in civil engineering. The potential of microbial induced biocementation has been widely studied in the fields of sand stabilization, bioremediation of heavy metals, restoration of lime stone monuments, durability properties of concrete structures and concrete crack remediation. In this review, metabolic pathways of biomineralization, different bacterial strains and their applications in concrete durability are discussed below.

2.6.1 Biomineralization

Biomineralization refers to a biological process of precipitation of mineral phases by living organism through its metabolic activity in the surrounding environment (Dhami et al. 2012). In nature, biomineralization leads to the formation of more than 60 different biominerals that exists as extracellularly or intracellularly (Anbu et al. 2016). These could be from biogenic origin involving bacteria, fungi, algae, and metazoan (Zhu and Dittrich, 2016). In the prokaryotic synthesis of biominerals, two different classes: Biological controlled mineralization (BCM) and Biological induced mineralization (BIM) are reported (Dhami et al. 2013b). BCM consists of cellular activities in which biominerals are directly synthesized at a specific location within or on the cell under certain conditions. It is reported that in most cases BCM happens intracellularly. BCM has been reported to be of three types (i) extracellular (BCMe) (ii) intracellular (BCMin) and (iii) intercellular (BCMint) (Castro-Alonso et al. 2019) as shown in Figure 2.8.

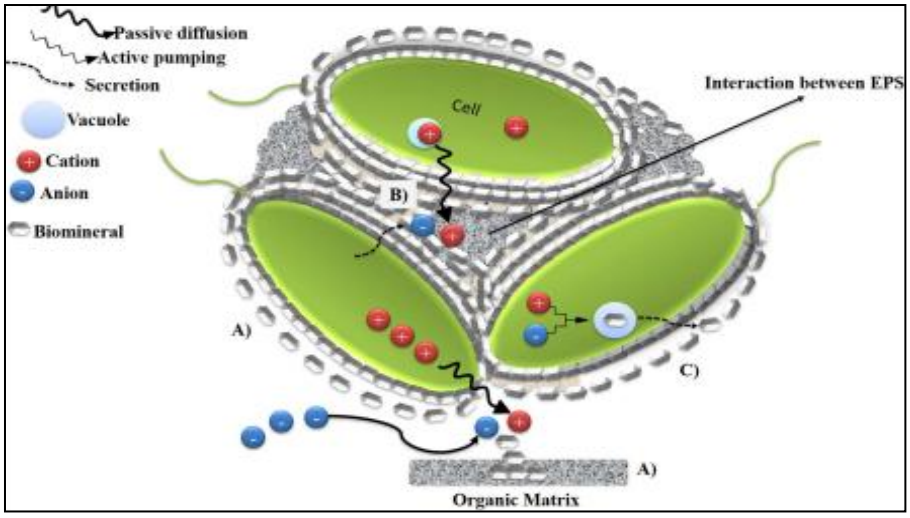

Figure 2.8 Graphical representation of biologically controlled mineralization (BCM) (A) BCMe showing mineral nucleation in organic matrix moving cations out of cell by passive diffusion (B) BCMin showing epithelial surface of cell as organic substrate for orientation and precipitation of minerals around the surface. (c) BCMint showing biominerals formed within the specialized vesicle of cell and secreted (Adapted from Castro-Alonso et al. 2019)

In BIM, biominerals generally nucleate and grow extracellularly as a result of metabolic activity of the organism (Castro-Alonso et al. 2019) as shown in Figure 2.9.

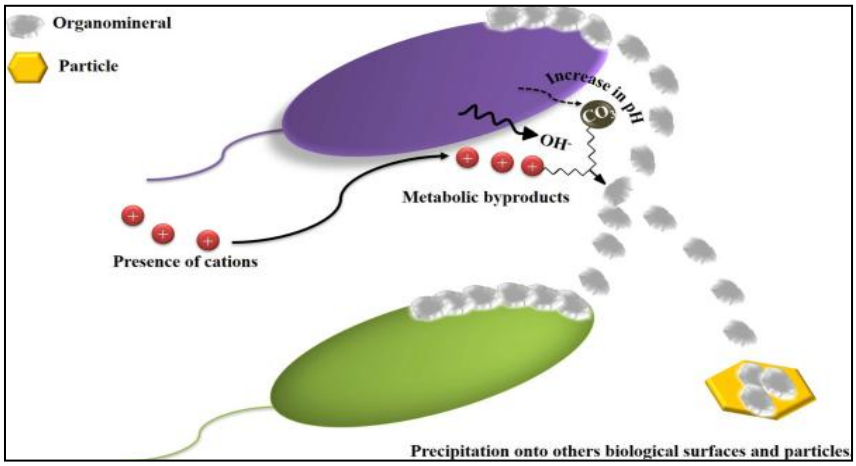

Figure 2.9 Graphical representation of BIM showing biomineral precipitation induced because of interaction between microbial metabolic products and inorganic compounds in the environment (Adapted from Castro-Alonso et al. 2019)

Calcium carbonate precipitation by bacteria is also associated with BIM and is the most widely studied branch of biomineralization. The phenomenon of deposition of calcium carbonate crystals by microbes is termed as microbial induced calcium carbonate precipitation (MICP).

2.6.2 Microbial induced calcium carbonate precipitation (MICP)

MICP is a process in which calcium carbonate crystals are precipitated through the reaction of metabolites generated by microorganism (CO_3^{2-}) and in the surrounding environment enriched with Ca^{2+}ions. Different bacterial species in natural habitats precipitate carbonates in alkaline environments rich in Ca^{2+} ions with various mechanisms (Ehrlich, 1998). It was reported by Boquet et al. (1973) that calcium carbonate formation under suitable conditions is a common phenomenon for almost all bacterial species. At neutral pH, presence of carboxyl, phosphoryl and amino groups at the bacterial cell surface results into heterogeneous electronegativity charge, which act as a nucleating site favoring the adsorption of positively charged cations (e.g. Ca^{2+}, Mg^{2+}). Presence of Ca^{2+} ions in the surroundings of bacterial cell wall results into the precipitation of calcium carbonate (Douglas and Beveridge, 1998). Biogenic precipitation of different polymorphs of calcium carbonates (e.g. calcite, aragonite and vaterite) is reported. Polymorphism in crystalline calcium carbonate is shown in Figure 2.10.

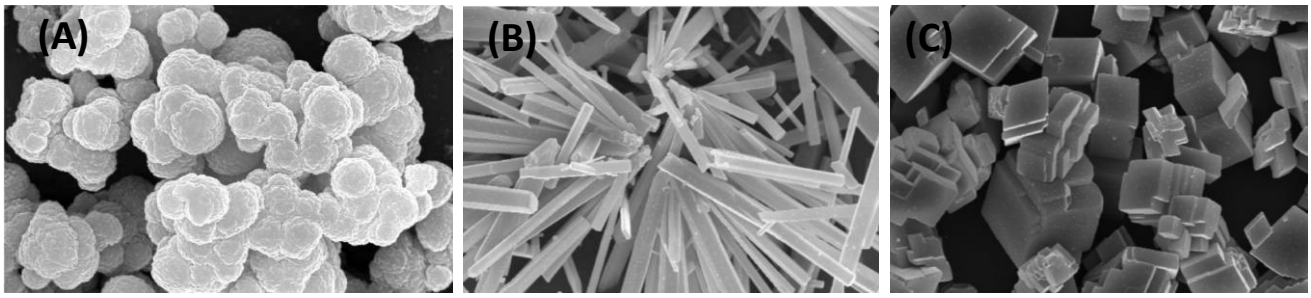

Figure 2.10 Scanning electron micrographs of (A) Vaterite (B) Aragonite (C) Calcite crystals (Adapted from Sarkar and Mahapatra, 2010)

Hammes and Verstraete (2002) reported four key factors such as (1) the calcium concentration; (2) the concentration of dissolved inorganic carbon (DIC); (3) the pH and (4) the availability of nucleation sites which influence the precipitation of $CaCO_3$. Four groups of microorganisms, such as photosynthetic organisms (cyanobacteria and algae), sulfate reducing bacteria (SRB) (dissimilatory reduction of sulfates), organisms utilizing organic acids and organisms involved in

the nitrogen cycle are reported to be involved in the process of biocementation (Mondal and Ghosh, 2019).

2.6.3 Routes of MICP

Broadly, there are two different metabolic pathways which are involved in the process of biomineralization associated with the microorganisms: (1) autotrophic pathway and (2) heterotrophic pathway.

2.6.3.1 Autotrophic mediated pathway

This is the conversion of CO_2 into calcium carbonate crystals by microbes in the presence of CO_2 and calcium source. Autotrophic precipitation of carbonates include oxygenic and anoxygenic photosynthesis and nonmethylotropic methanogenesis (Castanier et al. 1999). All of the three autotrophic pathways use CO_2 as a carbon source. Bacterial calcium carbonate precipitations with autotrophic pathways and their mechanisms are shown in Table 2.4. In nonmethylotrophic methanogenesis pathway, methanogenic archaebacteria utilizes CO_2 and H_2 to give methane in the absence of oxygen (Castanier et al. 1999). Anaerobic oxidation of methane results in the formation of bicarbonate by electron acceptor sulfate as shown in Eq. 2.13. Carbonate in the presence of calcium ions results into the precipitation of calcium carbonate as shown in Eq. 2.14.

Table 2.4 Different mechanisms of calcium carbonate precipitation by autotrophic bacteria

Metabolic pathway	Mediator	Mechanism	Eq. no.	References
Non-Methylotrophic methanogenesis	Methanogenic archaebacteria	$CO_2 + 4H_2 \rightarrow CH_4 + 2H_2O$	(2.12)	Castanier et al. (1999)
		$CH_4 + SO_4^{2-} \rightarrow HCO_3^- + HS^- + H_2O$	(2.13)	
		$Ca^{2+} + 2HCO_3^- \leftrightarrow CaCO_3 + CO_2 + H_2O$	(2.14)	
Anoxygenogenic photosynthesis	Sulphurous or non-sulphurous purple and green photosynthetic bacteria	$CO_2 + 2H_2S + H_2O \rightarrow CH_2O + 2S + 2H_2O$	(2.15)	Castanier et al. (2000)
		$2HCO_3^- \leftrightarrow CO_2 + CO_3^{2-} + H_2O$	(2.16)	
		$CO_3^{2-} + H_2O \leftrightarrow HCO_3^- + OH^-$	(2.17)	
		$Ca^{2+} + 2HCO_3^- \leftrightarrow CaCO_3 + CO_2 + H_2O$	(2.18)	
Oxygenogenic photosynthesis	Cyanobacteria	$CO_2 + H_2O \rightarrow CH_2O + O_2$	(2.19)	Ehrlich (1998)
		$2HCO_3^- \leftrightarrow CO_2 + CO_3^{2-} + H_2O$	(2.20)	
		$CO_3^{2-} + H_2O \leftrightarrow HCO_3^- + OH^-$	(2.20)	
		$Ca^{2+} + 2HCO_3^- \leftrightarrow CaCO_3 + CO_2 + H_2O$	(2.21)	

In anoxygenogenic photosynthesis, H_2S acts an electron donor in the formation of methanol carried out by purple and green photosynthetic bacteria as shown in Eq. 2.15 (Castanier et al. 2000). Oxygenogenic photosynthesis is carried out by cyanobacteria using visible light (680-685 nm) as a source of energy leading into the production of oxygen. In this process, water acts as an electron donor as shown in Eq. 2.19 (Ehrlich, 1998). Oxygenic photosynthetic pathway associated with cyanobacteria in marine and fresh water is one of the major contributors of the production of carbonates. Cyanobacterial calcification is an extracellular process and occurs on extrapolysaccharide sheath (EPS) or proteinaceous hydrophobic surface layer (S-layer), which possesses negatively charged sites surrounding the cell (Schultze-Lam and Beveridge, 1994). Generation of alkaline pH at the EPS or S-layer due to carbonic anhydrase (CA) activity promotes the increased CO_3^{2-} concentration at the cell exterior and acts as nucleation site for $CaCO_3$ precipitation (Jansson and Northen, 2010).

2.6.3.2 Heterotrophic mediated pathway

In heterotrophic mediated pathway, two mechanism of calcium carbonate precipitation through sulphur and nitrogen cycle are reported. First heterotrophic pathway involving sulfur cycle is carried out by sulfate reducing bacteria (SRB) via dissimilatory reduction of sulfate (Muyzer and Stams, 2008). In this process, calcium carbonate is produced in anoxic environment when the medium is rich in organic matter, calcium source and sulfate (Seifan et al. 2016). As the organic matter is degraded by SRB, bicarbonate ions and hydrogen sulfide by reducing sulfates are produced. Elevation of pH in the surrounding environment due to H_2S and in the presence of Ca^{2+}, the precipitation of calcium carbonate occurs.

Second heterotrophic pathway in calcium carbonate precipitation involves nitrogen cycle and is further categorized into three different mechanisms: (1) ammonification of amino acids (presence of organic matter and calcium in aerobic conditions) (2) dissimilatory reduction of nitrate (presence of organic matter, calcium, and nitrate in anaerobic conditions) and (3) urea degradation (presence of organic matter, calcium, and urea in aerobic conditions) (Castanier et al. 2000). In all these three mechanisms, carbonate and bicarbonate ions as well as ammonia (NH_3) are produced as a metabolic end product. Generation of ammonia creates high alkaline pH in the microenvironment of the bacterial cell and decreased H^+ concentration, affecting the

carbonate-bicarbonate equilibria shift towards the production of CO_3^{2-} ions. Presence of calcium ions in the surrounding of bacterial cell results in the precipitation of calcium carbonate. Among the aforementioned mechanisms in heterotrophic pathway, microbially induced calcium carbonate precipitation via urea hydrolysis is widely used in various applications.

2.6.4 MICP via urea hydrolysis

Microbially induced precipitation of calcium carbonates via urea hydrolysis is an easily controlled mechanism in which high amounts of carbonates are produced by the ureolytic bacteria in short time period. In this mechanism, degradation of urea is catalyzed by microbial urease enzyme into carbonate and ammonium (Stocks-Fischer et al. 1999). One mole of urea is hydrolyzed intracellularly to one mole of ammonia and one mole of carbamate which spontaneously hydrolyses to form one mole of ammonia and carbonic acid as shown in Eq. 2.22 – Eq. 2.23.

$$CO(NH_2)_2 + H_2O \xrightarrow{Bacteria} NH_2COOH + NH_3 \qquad 2.22$$

$$NH_2COOH + H_2O \rightarrow NH_3 + H_2CO_3 \qquad 2.23$$

These products further equilibrate in water to form bicarbonate and two moles of ammonium and hydroxide ions Eq. 2.24 – Eq. 2.25.

$$2NH_3 + 2H_2O \rightarrow 2NH_4^+ + 2OH^- \qquad 2.24$$

$$2OH^- + H_2CO_3 \rightarrow CO_3^{2-} + 2H_2O \qquad 2.25$$

Generation of ammonia on the hydrolysis of urea results in the increased pH creating an alkaline condition in the microenvironment around the bacterial cell (Stocks-Fischer et al. 1999). Presence of calcium ions in the surroundings of bacterial cell wall results into the precipitation of calcium carbonate as the super-saturation is reached as shown in Eq. 2.26.

$$CO_3^{2-} + Ca^{2+} \leftrightarrow CaCO_3 \qquad 2.26$$

The heterogeneous electronegatively charged bacterial cell wall acts as a nucleating site favoring the adsorption of positively charged cations (e.g. Ca^{2+}, Mg^{2+}) on the cell surface. Presence of

different negatively charged groups at neutral pH, anionic charge dominates the bacterial cell surface results into deposition of divalent positively charged metal ions on interaction (Beveridge, 1981; Douglas and Beveridge, 1998). Bacterial cell surface plays an important role in precipitation of calcium carbonate as nucleation site.

To utilize the biomineralization process in autotrophic mediated and heterotrophic mediated pathways, different calcium sources such as calcium chloride, calcium nitrate and calcium acetate has been used by researchers. In biomineralization with ureolytic bacterial strains, urea and calcium chloride medium for the precipitation of calcium carbonate has been preferred by researchers as shown in Eq. 2.27 – Eq. 2.29.

$$Ca^{2+} + Cell \rightarrow Cell\text{-}Ca^{2+} \qquad 2.27$$

$$Cl^{-} + HCO_3^{-} + NH_3 \rightarrow NH_4Cl + CO_3^{2-} \qquad 2.28$$

$$Cell\text{-}Ca^{2+} + CO_3^{2-} \rightarrow Cell\text{-}CaCO_3 \qquad 2.29$$

2.6.5 Urease enzyme

Urease (urea amidohydrolase; EC 3.5.1.5) enzyme is one of the important factor which plays a major role in ureolytic activity during MICP application. Urease was first isolated enzyme which was crystallized from the plant source *Canavalia ensiformis* (jack bean) and shown as the protein nature of enzymes. Urease was the first example of nickel (II) metalloenzyme and was the first protein reported which shown the nickel in the active site (Dixon et al. 1975). The presence of thiol groups in a protein was also first described by titrating crystalline urease from jack beans with nitroprusside (Qin and Cabral, 2002). Urease activity is found in a wide range of plants, algae, fungi and several microorganisms, some of which produce the enzyme in large quantities (Ciurli et al. 1999). Urease catalyzes the hydrolysis of urea to yield ammonia and carbamate. This process is reported to occur 10^{14} times faster than the noncatalyzed reaction with a half-time in the order of microseconds. The carbamate compound spontaneously decomposes to yield another molecule of ammonia and carbonic acid (Mobley et al. 1995). The reaction products from urea hydrolysis cause an abrupt overall pH increase.

The significant highlights of the urease enzyme reported are: (1) Primary role of urease enzyme is that it allows the organism to use urea (generated external or internally) as a nitrogen source. (2) Its importance in environmental transformations of nitrogenous compounds, including urea based fertilizers as the resulting product ammonia can be taken up and utilized by soil microbes and plants. (3) In plants, urease enzyme participates in systemic nitrogen transport pathways which possibly acts as a toxic defense protein. (4) Role in recycling the nitrogenous wastes in the rumens of domestic livestock and (5) Urease serves as a virulence factor in infections of the urinary and gastrointestinal tracts in human and animal causing the formation of infection-induced urinary stones (Ciurli et al. 1999).

The urease expression in microorganisms is based on two regulation modes influenced by environmental conditions. In one mode, urease synthesis is activated in some microorganisms when conditions such as the presence of poor nitrogen sources are available. This control is dependent on the nitrogen regulatory system (NTR) and ultimately the action of the positive regulator NAC (nitrogen assimilation control) at the level of urease transcription. The microorganisms in this category belong to the genus *Klebsiella* (Mobley et al. 1995). It was reported that, when the cells of *K. aerogenes* bacterial strain are grown in presence of high-quality nitrogen sources such as ammonia, urease is not synthesized. However, urease synthesis is activated when conditions of nitrogen starvation are present or when the cultures are grown in minimal medium containing a poor nitrogen source such as proline, arginine, or histidine. Nitrogen regulation of the cloned *Klebsiella* urease genes occurs in a number of host backgrounds (e.g., *Escherichia, Salmonella, and Klebsiella* sp.) in which low enzyme levels are present during growth on nitrogen-rich medium. In second mode, nitrogen control plays no role in regulation of the urease gene expression. Urease enzyme is induced by the presence of the substrate urea. Rather, urease of *Sporosarcina pasteurii* (formerly known as *Bacillus pasteurii*), *Proteus vulgaris* and *Helicobacter pylori* species is induced by the substrate urea to levels 5 to 25 fold over those in uninduced cultures (Jones and Mobley, 1987). During the urea hydrolysis in the presence of high concentration of urea substrate, ammonium ions formed as a reaction product is reported to be a limiting factor by suppressing the urease activity of microbes. In the presence of ammonium ion in the surrounding microenvironment of microbes such as *Pseudomonas aeruginosa*, *Klebsiella aerogenes*, urease activity is repressed (Friedrich and Magasanik, 1977). Urease from bacterial strain *Sporosarcina ureae* closely related to

Sporosarcina pasteurii was reported to be highly alkaline stable (pH 7.75-12.5) (McCoy et al. 1992). Similar observations of optimal growth of *S. pasteurii* bacterial strain because of the high urease activity in alkaline medium with urea substrate and high concentrations of ammonium is reported (Jahns, 1996). From the above considerations, bacterial species for biocementation application in construction materials is to have high urea hydrolyzing activity. As well as the urease enzyme production should remain unaffected or unsuppressed under the high urea substrate, ammonium environment and high pH conditions.

2.6.6 Applications of MICP

MICP has developed as a novel and sustainable technique in improving the strength and durability of construction materials. The potential and effectiveness of MICP application in various fields such as heavy metal remediation, soil stabilization, restoration of monuments and durability enhancement of concrete structures are discussed below and shown in Table 2.5.

2.6.6.1 Microbial precipitation of metals

Now a days, MICP has become a hot topic of research in bioremediation of water and soils contaminated with heavy metals. Discharge of waste waters contaminated with large amounts from industries is introduced in soils through leaching and further accumulates in plants which at later stages critically impact the human health. Different conventional methods have been adopted to treat the heavy metal contaminated soils and water such as adsorption, chemical precipitation, ion exchange and electrochemical treatments (Vullo et al. 2008; Wang and Chen, 2009). In recent years, MICP has been reported with immense potential in removing significant quantities of heavy metals from contaminated water, soils and mine waste (Jain and Arnepalli, 2019). In this bioremediation process, different ureolytic bacterial and fungal strains are isolated by researchers and there potential in immobilizing the metals through the formation of metallic carbonates are reported (Tamayo-Figueroa et al. 2019). Achal et al. (2011d) reported the removal of 95% of copper from contaminated soil with calcifying bacterial strain *Kocuria flava* CR1 treatment. This copper tolerant bacterial strain was isolated from copper contaminated mining area and was reported to be of high urease enzyme activity.

Table 2.5 Overview of different applications of biocementation with different calcifying bacterial strains

Microorganism	Isolation/ Culture repository	Application	Evaluation	References
Kocuria flava CR1	Copper mine	Bioremediation of Cu	95% removal of Copper	Achal et al. (2011d)
Pararhodobacter sp.	Beach rock	Bioremediation of Pb	Complete removal of 1036 mg/L Pb^{2+} during 6 h of incubation	Mwandira et al. (2017)
Aspergillus sp. UF3, *Fusarium oxysporum* UF8	karstic caves	Bioremediation of lead and Strontium	34% to 54% Pb and 48% to 31% Sr removal, respectively	Dhami et al.(2017)
Staphylococcus epidermidis HJ2	Industrial area	Bioremediation of lead and Chromium	86% Pb and 76.8% Cr removal	He et al. (2019)
Serratia marcescens and *Enterobacter cloacae*	NCIM MTCC	Bioremediation of Cd	96% and 98% removal of Cd, respectively	Bhattacharya et al. (2018)
Sporoscarcina pasteurii	-	Sand consolidation	Increased shear stiffness of sand with shear wave velocity of 140 m/s to 600 m/s	Martinez et al. (2013)
Bacillus sp. MCP11	Activated sludge and soil	Sand consolidation	Improved strength and packing of sand grains in column	Al-Thawadi et al. (2012)
Bacillus sp.	Mine tailing soil	Desert sand stabilization	High resistance to wind erosion	Chen et al. (2016)
Oceanobacillus profundus KBZ 1–3, *Oceanobacillus profundus* KBZ 2–5	Lead mine waste	Sand consolidation	Capping of mine waste prevented wind erosion	Mwandira et al. (2019)
Myxococcus xanthus	STCC	Archaeological gypsum plaster	Efficient consolidation, both at the surface and in-depth due to biocementation	Jroundi et al. (2014)
B. pumilus	Karst cave	Marble restoration	Vaterite thin film formation and stone loss rate reduced	Daskalakis et al. (2015)

NCIM: National collection of industrial microorganisms; MTCC: Microbial type culture collection and gene bank; STCC: Spanish type culture collection

Table 2.5 Cont. Overview of different applications of biocementation with different calcifying bacterial strains

Microorganism	Isolation/ Culture repository	Application	Evaluation	References
Pseudomonas sp., *B. cereus*, *Lysinibacillus sphaericus*	Historical white marble	Marble restoration	Calcite and vaterite precipitation	Li et al. (2018)
B. pasteurii	ATCC	Cement mortar	Increased compressive strength	Ramachandran et al. (2001)
B. sphaericus LMG 22557	BCCM	Cement mortar and concrete	Decrease in uptake of water and gas permeability	De Muynck et al. (2008)
B. megaterium	ATCC	Cement mortar and concrete	Enhanced compressive strength in mortar and improved water resistance in concrete	Achal et al. (2011c)
S. pasteurii, *B. sphaericus*	ATCC	Concrete	Denser calcium carbonate precipitation and decrease in water absorption	Kim et al. (2013)
S. pasteurii	ATCC	Cement mortar	Increased compressive strength	Bundur et al. (2015)
B. subtilis	ATCC	Shotcrete	Increased compressive strength and decreased water absorption	Kalhori and Bagherpour (2017)
Exiguobacterium mexicanum (MSR1)	Sea water	Concrete	Increased compressive strength and reduced water absorption under 5% salt stress	Bansal et al. (2016)

ATCC: American type culture collection; BCCM: Belgian coordinated collections of microorganisms

In another research work, a ureolytic bacteria *Pararhodobacter* sp. was reported to efficiently removed Pb^{2+} ions from lead contaminated mine waste (Mwandira et al. 2017). Transformation of free Pb^{2+} ions into stable bioprecipitation together with calcite was reported. Dhami et al. (2017) reported the potential of two ureolytic calcifying fungal strains *Aspergillus* sp. UF3 and *Fusarium oxysporum* UF8 isolated from karstic caves, in co-precipitation of lead and strontium carbonates through biomineralization. In a recent research work, ureolytic *Staphylococcus epidermidis* HJ2 strain isolated from contaminated soil of industrial area was reported in significantly immobilizing lead and chromium ions (He et al. 2019). Removal of 86% of Pb(II) and 76.8% of Cr(VI) from initial concentration through MICP was reported. In another research work, urease positive *Serratia marcescens* and *Enterobacter cloacae* EMB19 were used to remediate cadmium contamination through ureolysis induced calcium carbonate precipitation (Bhattacharya et al. 2018). Co-precipitation of Cd(II) and Ca(II) carbonates results in 96 and 98% of initial concentration of cadmium by ureolytic *Serratia marcescens* and *Enterobacter cloacae* EMB19 strains respectively. MICP has been reported to be an economical method to remediate metal contaminated sites.

2.6.6.2 Sand and soil stabilization

The potential application of MICP in stabilization of sand and soil through biodeposition has been reported by various researchers (Mujah et al. 2017; Jiang et al. 2020). In this technique, bacterial cells along with cementation solution (Nutrient supplement, calcium source and urea) are injected vertically in soil/sand columns. To reduce the permeability and increase the shear strength of soil, MICP was performed by using *Bacillus* sp. VS1 with urea and calcium solution by Chu et al. (2012). Increase in stiffness of MICP treated sand and permeability reduction on six sequential treatments was observed. In laboratory experiment, the bacterial strain *S.pasteurii* with biological solution was introduced in half-meter sand column in one-dimensional flow by injection (Martinez et al. 2013). Change in shear wave velocity from 140 m/s to an average of 600 m/s was observed due to calcium carbonate precipitation resulting into increased shear stiffness of sand. Stocks-Fischer et al. (1999) reported the urease activity of alkaliphilic bacteria *Bacillus pasteurii* to hydrolyze urea and high pH being the favorable condition for calcite precipitation in porous sand media. Sand column supplemented with live bacterial cells, nutrient broth and urea-$CaCl_2$ constituted 30% calcite of total weight of column. To study MICP as a soil

strengthening process, a sand column of 5 meter dimension was treated with urease positive *Sporosarcina pasteurii* (DSMZ 33) (Whiffin et al. 2007). Reduced pore volume due to increased calcium carbonate precipitation was reported. Soil strength was reported to increase due to microbial carbonate precipitation. In another study, sand column with sand grain size (90–400 µm) was treated by four volumes of up-flushings of *Bacillus* sp. MCP11 strain and cementing solution (Al-Thawadi et al. 2012). Calcite precipitation by microbial treatment results in strength gain and improved packing of sand grains.

In another research work, biostabilization of desert sand with MICP to prevent wind erosion of soil during sand storm was reported (Chen et al. 2016). Sand collected from the Gurbantinggut desert, China was treated with ureolytic *Bacillus* sp. along with cementation solution by spraying. Biostabilized sand was reported to have high resistance to strong wind erosion even after 12 days of exposure to freeze-thaw cycles. In another research work, researchers reported effective resistance against wind erosion when sandy soil collected from sand Yazd Desert, Iran was treated with ureolytic *Sporsarcina pasteurii* strain (Maleki et al. 2016). It was reported that, MICP provide sand dune fixation for dust control and future re-vegetation. In a recent research article, researchers reported the solidification of sand by capping lead mine waste dump with ureolytic *Oceanobacillus profundus* KBZ 1–3 and *Oceanobacillus profundus* KBZ 2–5 strains (Mwandira et al. 2019). It was reported that both the strains were Pb tolerant and biocemented the sand particles by precipitating $CaCO_3$ crystals. It was reported that dust erosion and leaching of heavy metal was retarded. In a recent research work, application of non-ureolytic bacteria on desert sand – cement bricks with increased compressive strength as well as reduced water absorption was reported (Bisht et al. 2020). Treatment of bricks with non-ureolytic bacteria (*B. cohnii*) was reported to be a better bio-cementation application with excellent densification in desert sand bricks.

2.6.6.3 Stone monument restoration

Concept of ancient monument restoration with the help of calcifying bacterial strains through MICP application has been reported by various researchers. Different approaches of MICP treatment in conservation of stones at laboratory scale are reported (Dhami et al. 2014a; Rodrigues and Pinto, 2019). Le Metayer-Levrel et al. (1999) treated limestone samples first with

carbonatogenic bacteria by spraying and then fed the bacterial cells attached on limestone with successive spraying of nutrient medium. Reduction in water absorption of treated limestone samples due to effective biocalcin coating was reported. Tiano et al. (1999) reported the bacterial treatment of limestone samples with *Micrococcus* sp. and *Bacillus subtilis* by brushing and shown the reduction of about 60% in water absorption. Rodriguez-Navarro et al. (2003) found that deposition of calcite and vaterite crystals in porous limestone on treatment with *Myxococcus xanthus* strain resulted into efficient protection and consolidation. Jroundi et al. (2014) reported effective consolidation of archaeological gypsum plaster due to biotreatment based on the spray application of *Myxococcus xanthus* on the upper surface for 6 days. Bacterial treatment was reported to precipitate vaterite ($CaCO_3$), which produces a good level of consolidation, both at the surface and in-depth. Daskalakis et al. (2015) also reported the effective biomineral (vaterite) precipitation on the marble sample treated with *Bacillus pumilus* strain isolated from a cave stone. Stone loss rate was reduced when the bacterial treated samples were subjected to sonication. In another research work, deteriorated globigerina limestone treatment by spraying with *Bacillus subtilis* strain was reported to have uniform bioconsolidation up to a depth of 30 mm (Micallef et al. 2016). The improved surface drilling resistance and reduction in water absorption was reported. In recent research work, isolation of calcifying bacterial strains from white plaques present on white marble in an ancient monument site in China was reported (Li et al. 2018). Four bacterial strains *Pseudomonas* sp., *Bacillus cereus*, *Lysinibacillus sphaericus* and *Bacillus* sp. were reported to have ability to induce $CaCO_3$ precipitations.

2.6.6.4 Concrete durability enhancement

The potential of MICP application in cementitious materials to enhance the mechanical properties as well as permeability properties has been reported by various researchers. Precipitation of calcium carbonate by bacteria inside the cement matrix leads into pore refinement resulting in reduced permeability and increased compressive strength of concrete structure. Ramachandran et al. (2001) reported increased compressive strength of cement mortar cubes on direct incorporation of live bacterial cells of *S. pasteurii* strain inside the cement matrix. De Muynck et al. (2008) reported the effectiveness of pure and mixed ureolytic cultures in biodeposition on surface treatment of concrete. Specimens were immersed in pure bacterial culture of *B. sphaericus* for 24 hours and the submerged in nutrient solution for successive six

days. In case of mixed ureoltic culture treatment, a paste of thickness 0.5-1 mm from centrifuged ureolytic sludge was applied on the surface of specimens. They observed that the use of pure culture of *B. sphaericus* resulted in more pronounced decrease in uptake of water and gas permeability than the use of mixed ureolytic culture. Achal et al. (2011c) reported the fly ash-amended mortar and concrete specimens on treatment with ureolytic bacterial strain *B. megaterium* showed improvement in strength and permeability properties. Deposition of microbial calcite on treated mortar cubes results into three times less water absorption than control specimen. Dhami et al. (2013a) reported an increase in compressive strength of cement mortar specimen and energy-efficient green building materials by treating with bacteria. Blocks of cement and sand were cured by spraying treatment with NBU medium and bacterial strain *B. megaterium* SS3 for 28 days. Reduction of 40% in water absorption and 31% in the porosity was reported in the biogenic surface treated specimens on comparison with control specimens. Kim et al. (2013) investigated the distribution of calcium carbonate precipitation and capillary water absorption of concrete specimens after surface treatment with two bacterial strains, *B. sphaericus* and *S. pasteurii* individually. Denser calcium carbonate crystals and lowest weight increase was reported in specimens treated with *B. sphaericus* strain than the specimens treated with *S. pasteurii* strain. Bundur et al. (2015) reported increased compressive strength of mortar specimen prepared with incorporation of vegetative bacterial cells than the control specimen. Application of halophilic bacteria *Exiguobacterium mexicanum* isolated from sea water showed 23.5% increase in compressive strength and 5 times reduction in water absorption on concrete specimens under 5% salt stress condition (Bansal et al. 2016). Kumari et al. (2017) reported 49% increase in compressive strength by using non-ureolytic bacteria *Bacillus cohnii*. Achal et al. (2012) in a study showed that *Bacillus* sp. CT-5-treated reinforced concrete (RC) specimens reduced the corrosion rate, reduction in mass loss and increase in pullout strength than the control specimens. Kalhori and Bagherpour (2017) studied the effect of $CaCO_3$ precipitating bacteria *Bacillus subtilis* on healing and mechanical properties of shotcrete. Their results showed 30% increase in the compressive strength of bacteria-exposed shotcrete specimens compared to control specimens. The presence of bacteria in the mix design and curing solution enhanced the tensile strength, decreased the water absorption and porosity of shotcrete.

2.6.6.5 Bio-inspired applications in crack healing

Formation of crack is a commonly observed phenomenon in concrete structures. Though micro-crack formation may hardly affect the structural properties of constructions, increased permeability due to micro-crack networking substantially reduce the durability of concrete structures due to risk of ingress of aggressive substances particularly in moist environments. In order to increase the often observed autogenous crack-healing potential of concrete, specific healing agents are incorporated into the concrete matrix. Apart from the surface application and incorporation of live bacterial cells inside the cement matrix, use of bacteria as a self-healing agent is also evolved as new approach. Different methodologies have been adopted by researchers to test the compatibility of calcifying bacterial strains to heal the cracks autonomously (Table 2.6). Initially, the application of bacteria to remediate the cracks in cement mortar specimens was investigated by Ramachandran et al. (2001). Cracks in cement mortar beams and cubes were simulated artificially with constant width 3.175 mm and different depths. It was reported that calcite precipitated during MICP application enhanced the compressive strength of cracked mortar cubes. The mineralization process was effective in shallow cracks than in deeper ones because the bacteria grow more actively in presence of oxygen. To enhance the effectiveness of MICP in remediation of deep cracks, polyurethane-immobilized *B. pasteurii* cells were used in cement matrices (Bang et al. 2001). In cement mortar cubes (50.8 x 50.8 x 50.8 mm) with simulated cracks of width 3.18 mm and 25.4 mm crack depth, polyurethane strip encapsulating bacterial cells was placed in the cracks. Precipitation of calcite throughout of the crack matrices was reported as the PU matrix provides protection to bacterial cells from extreme alkaline nature of concrete. Jonkers and Schlangen (2007) used the spores of *Bacillus pseudofirmus* than vegetative cells as self-healing agent in concrete matrix to seal the cracks. The healing effect in freshly formed cracks appears on revival of immobilized spores by entering water and growth nutrients.

To augment the potential of bacteria as a self-healing agent in crack filling, immobilization of bacterial cells with different carriers had been studied. To protect the bacteria from strong alkaline environment of concrete, bacteria (*B. sphaericus*) immobilized in silica gel was investigated by Van Tittelboom et al. (2010).

Table 2.6 Overview of crack remediation in concrete using bacteria as crack healing agent

Microorganism	Carrier material	Incubation treatment	Crack healing	References
B. pasteurii	Polyurethane immobilized cells	Incubated in urea-$CaCl_2$ medium for 28 days	Crack width of 3.18 mm and depth of 25.4 mm	Bang et al. (2001)
B. sphaericus	Cells immobilized in silica gel	Immersed in solution of urea and calcium source for 3 days	Crack width of 0.3 mm and depths of 10.0 mm and 20.0 mm	Van Tittelboom et al. (2010)
B. alkalinitrilicus	Spores embedded in expanded clay with calcium lactate	Immersed in water for 100 days	Crack width ranging from 0.05 mm to 1.0 mm	Wiktor and Jonkers (2011)
Bacillus sp. CT-5	Cells mixed with sand	Immersed in urea and $CaCl_2$ medium for 28 days	Crack width of 3.0 mm and depths of 13.4 mm, 18.8 mm and 27.2 mm	Achal et al. (2013)
B. sphaericus	Hydrogel encapsulated spores with nutrient and calcium source	Submerged in water for 4 weeks with wet-dry cycle	Crack width of 0.5 mm	Wang et al. (2014)
B. cohnii	Treated externally	Submerged in medium containing bacterial spores, yeast extract and calcium source	Crack width ranging 0.1 mm to 0.4 mm	Xu and Yao (2014)
B. sphaericus	Spores encapsulated in microcapsule	Immersed in water for 8 weeks with wet-dry cycle	Maximum crack width healed is 0.97 mm	Wang et al. (2014)
Non-axenic ureolytic spores	Cyclic enriched ureolytic powder	Immersed in urea and de-mineralized water for 4 weeks	Crack healing of width 0.45 mm	Da Silva et al. (2015)
B. sphaericus	Spores encapsulated in modified alginate hydrogel	Fully immersed in water	N.A	Wang et al. (2015)
S. pasteurii	Bacterial spores loaded on ceramsite particles	4 wet-dry cycles for 4 weeks	Crack healing up to 273 μm	Xu et al. (2018)
Bacillus pseudofirmus	Spores and nutrients encapsulated in perlite	Exposed to 100% relative humidity conditions at 30° C for 165 days	Crack width of 350 μm	Alazhari et al. (2018)
S. pasteurii	Bacterial culture and urea	10 cycles of bacterial treatment followed by air curing for 24hours	Crack width of > 150 μm	Ruan et al. (2019)

Standard cracks of width 0.3 mm with two depths of 10 mm and 20 mm were prepared in concrete samples by introducing thin copper plate in cement paste while casting. Realistic cracks with width range from 0.05 mm to 0.87 mm were also created in concrete cylinders of diameter 80 mm and height 75 mm by subjecting to splitting test and used for water permeability test. Specimens treated with silica gel immobilized bacteria showed promising results in crack filling and low water permeability similar to epoxy treated specimens. Wiktor and Jonkers (2011) incorporated a mixture of bacterial spores (*Bacillus alkalinitrilicus*) and calcium lactate embedded in expanded clay particles as self-healing agent in concrete. Multiple cracks of widths ranging from 0.05 to 1.0 mm were created in specimen on stretching embedded steel by applying tensile force. Cracked bacterial embedded specimens and control specimens were immersed in water to investigate the self-healing properties. It was reported that after 100 days of immersion in water, bacterial based specimen showed crack-healing of up to 0.46 mm while in control it was only up to 0.18 mm.

Xu and Yao (2014) investigated non-ureolytic bacterially-induced $CaCO_3$ precipitation as a self-healing strategy for concrete cracking by using *Bacillus cohnii* spores. They suggested that incorporation of bacteria and calcium source nutrients as a two-component healing agent in concrete matrix induces $CaCO_3$ precipitation upon crack formation. Crack width in range of 0.1-0.4 mm was sealed completely as well as a layer of precipitates on the surface of specimen was reported in externally applied healing. They also reported that self-healing efficiency in specimens with incorporated bacterial spores and nutritional agents was higher than the control specimens. Higher efficiency of calcium carbonate precipitation in crack healing on external treatment and self-healing application was observed in calcium glutamate precursor than calcium lactate. Achal et al. (2013) investigated the remediation of simulated cracks in mortar specimens (width 3 mm and depths of 13.4 mm, 18.8 mm, and 27.2 mm) by using bacterial strain *Bacillus* sp. CT-5. Their results showed an increase of 40% and 37% in compressive strength in bacterial treated specimen with crack depth of 13.4 mm and 27.2 mm, respectively as compared to control. Successful healing of deepest crack of depth 27.2 mm was reported in bacterial treated specimen. Wang et al. (2014) encapsulated bacterial spores into hydrogel and then incorporated into specimens to investigate their healing efficiency. Hydrogel was used because of its water retention properties and providing favorable microenvironment to bacterial spores with moisture

and nutrients for activation. $CaCO_3$ precipitation by hydrogel-encapsulated spores was demonstrated by Thermogravimetric analysis (TGA). Their findings suggest that sufficient amount of water is essential for the bacterial spores to achieve the realistic self-healing mechanism to seal the cracks. The mortar specimens with hydrogel-encapsulated spores healed crack width of about 0.5 mm and the water permeability was decreased by 68% compared to control where maximum healed crack width was 0–0.3 mm and the average water permeability was decreased only by 15–55%.

Application of microcapsules as self-healing agent carrier in crack remediation was investigated by Wang et al. (2014). The spores of *B. sphaericus* were encapsulated in melamine based microcapsules. They reported that the crack healing ratio was much higher for specimens treated with bacteria compared to the ones without bacteria where 18% to 50% of crack area healed in control while it was 48% to 80% in the bacteria treated specimens. The maximum crack width healed in the bacterial treated specimens was 970 μm which was about 4 times wider than control (250 μm). Wang et al. (2015) tested modified-alginate based hydrogel as encapsulating agent for application of *B. sphaericus* spores in concrete. Their results indicated efficient protection of the hydrogel for spores in concrete and great potential to be used for crack self-healing in concrete applications.

To reduce the operational cost of bio-based self-healing action in concrete, a new powderous material containing an efficient ureolytic microbial community (Cyclic EnRiched Ureolytic Powder or CERUP) has been developed (Da Silva et al. 2015). CERUP was produced from a sub-stream of a vegetable treatment plant containing non-axenic bacterial culture with the ability to sporulate. After drying, it was ground to a particle size below 500 μm in diameter. Highest capacity of crack healing was observed in CERUP admixed specimen with complete crack closing up to 0.45 mm crack width after 4 weeks. In specimen without CERUP, autogenous crack healing was observed with closing of crack with 0.25 mm crack width.

Xu et al. (2018) investigated the bacteria-based self-healing with the developed healing agents loaded on ceramsite carriers. Bacterial spores of *S. pasteurii* and urea–$Ca(NO_3)_2$ medium were used in the study. Porous ceramsite particles with the same size of sand were selected as protective carrier material. Mortar cubes (50 × 50 × 50 mm) with crack were subjected to wet-

dry cycles for 4 weeks. It was reported that, the cracks up to 273 μm was healed with a 86% closure ratio in 28 days. Regain of compressive strength and decrease in water absorption coefficient was reported to be 24% and 27% as compared to the reference.

Alazhari et al. (2018) investigated the self healing of cracks in mortar specimen by using bacterial spores encapsulated in expanded perlite. In this investigation, encapsulated *Bacillus pseudofirmus* strain and encapsulated nutrients containing calcium acetate and yeast extract were used. Encapsulated particles were coated with a dual layer of sodium silicate solution and cement powder to prevent leaching of the spores and nutrients into the mortar. In mortar specimen, sand was replaced with 20% mix of encapsulated bacterial spores and nutrients and crack of 350 μm width was generated. It was reported that, complete crack filling was observed in mortar in which 8 x 10^9 spores per g of calcium acetate was used when placed under the condition of 100% humidity at 30° C for 165 days.

Ruan et al. (2019) investigated the crack healing efficiency of *S. pasteurii* strain in reactive magnesia cement (RMC) based dog bone shaped samples. It was reported that, MICP mechanism of ureolytic bacteria in RMC blend samples lead to the formation of hydrated magnesium carbonates (HMCs) during crack sealing. Samples were subjected to bacteria-urea solution treatment for 24 hours followed by air curing for 24 hours. This treatment was repeated for 10 cycles till the crack healing. It was reported that the production of HMCs was an effective method for healing cracks (> 150 μm) in RMC-based samples. Their findings identified that the major healing products within the cracks of samples subjected to bacteria-urea solution were two HMCs, nesquehonite and hydromagnesite.

2.6.6.6 Field based application of MICP

The field-based potential of MICP in sealing of sandstone fractures below the ground surface in wellbore using ureolytic bacteria was demonstrated by Phillips et al. (2016). Horizontally fractured sandstone 340.8 meters below the ground surface was sealed with ureolytic bacterial strain *S. pasteurii* using conventional oil field delivery technology. In the field test, bacterial culture was injected into the fracture by using an 11.4 litre wireline dump bailer for 4 days. Microbial suspensions after injection in fracture was allowed to attach for 1 hour and later on the inoculum was amended with calcium containing growth solution (urea and nutrient broth) to

promote the growth. In this treatment, 24 urea/calcium solution and 6 microbial suspensions were injected into the fracture zone for 4 days. They reported that the flow rate decreased from 1.9 to 0.47 L/min and in-well pressure falloff from >30% before to 7% after treatment. Their findings suggest that MICP is a promising tool for sealing subsurface fractures in the near wellbore environment. To monitor the applications of MICP nondestructively in time and space, Kirkland et al. (2017) used a low-field Nuclear magnetic resonance (NMR) well-logging probe in a sand-filled bioreactor by inoculating *S. pasteurii* and pulsed injections of urea and calcium substrate. NMR signal amplitude and T_2 relaxation were measured after the experiments. They reported that the water content in the reactor decreased to 76% of its initial value and changes in T_2 relaxation distributions due to changes in pore volume and surface mineralogy. Their results indicate the low-field NMR well-logging probe is sensitive to the physical and chemical changes caused by MICP in a laboratory bioreactor. Wiktor and Jonkers (2015) studied field performance of bacteria-based repair system of a two storey parking garage suffering from cracking and damaged concrete pavement due to freeze/thaw. Denitrifying bacteria supplemented with two solutions i) Solution A (sodium silicate, sodium gluconate) and ii) Solution B (calcium nitrate) were treated by spraying manually until saturation of concrete. Crack-sealing efficiency was evaluated after two months of bacteria-based application in treated area of parking garage by means of water permeability test. Concrete pavement was also evaluated in resistance to freeze/thaw conditions and deicing salts by drilling cores from treated area. They reported that cracks that had not been treated with the bacteria-based repair system were still heavily leaking and freeze/thaw resistance of concrete was higher with the bio-based repair system than the untreated concrete.

2.6.6.7 Reinforcement corrosion resistance with MICP

The application of MICP in improving the resistance towards the chloride induced corrosion of reinforcement in mortar and concrete has also been reported. The positive outcome of microbial induced biocementation in resisting the chloride ingress and rebar corrosion is investigated by researchers. Achal et al. (2012) reported the efficient chloride resistance in bacterial treated reinforced concrete specimen as compared to control. In this study, accelerated corrosion process was adopted in which constant anodic potential of 40 V was applied to rebar with a constant drip of 3.5% NaCl solution on the concrete specimens. After 7 days of exposure, corrosion current

density (I_{corr}) for bacterial treated specimen was reported to be reduced by 4 folds as compare to control specimen. At the end of accelerated corrosion process, enhanced pullout strength and reduced mass loss was reported in bacterial treated reinforced concrete specimens. Ling and Qian (2017) also reported the protective effects of microbial treated reinforced mortar in the resistance towards the accelerated transmission of chloride. Microbial treated mortar was reported to the exposed of 3.5% NaCl solution with 15 V voltage as a DC current source. Current density (I_{corr}) and corrosion potential (E_{corr}) was reported to be lower than control specimen at the end of accelerated chloride exposure. Erşan et al. (2018) reported a significant improvement in inhibiting the rebar corrosion by using nitrate (NO_{3-}) reducing bacteria along with crack healing application in reinforced mortar prism. In this study, microbe based self-healing composites (0.5% w/w cement), $Ca(NO_3)_2$ (3% w/w cement) and $Ca(HCOO)_2$ (2% w/w cement) were added in mortar. Artificial cracks were developed in the mortar with a depth of 20mm and a width of ~300 µm. For corrosion testing, capillary sorption was used and cracked surface of mortar was exposed to 0.5 M NaCl solution. It was reported that anodic corrosion was inhibited by nitrate reducing bacterial granules with the production of nitrite inhibitor. After 28 days, crack of width 300 µm was reported to be healed as well as after 120 days of chloride exposure, corrosion potential (E_{corr}) was reported to be above the critical potential value of -250 mV.

2.6.6.8 MICP in waste amended concrete

The positive outcome of MICP in enhancing durability properties of mortar and concrete has encouraged the researchers to further make this technique more eco-friendly. To improve this biogenic process, efforts have been made to utilize waste by-products as a replacement for cement and aggregates (Table 2.7). Achal et al. (2011c) proposed the improvement in strength and permeability of fly ash (FA) amended mortar (10%, 20% and 40% dosage) after treatment with bacterial strain *Bacillus megaterium*. It was reported that viability of bacterial cells in FA amended mortar was also higher. Even in mortar specimen with higher FA dosage (40%), involvement of calcite precipitation improved strength properties. Farmani et al. (2015) reported increased compressive strength and weight gain in silica fume (SF) amended mortar (20% dosage) due to biodeposition of calcite and aragonite precipitation. Bacterial treatment of SF amended mortar was reported to significantly reduce the water absorption.

Table 2.7 Overview of different waste utilization along with MICP application

Industrial waste	Replacement	Bacterial strain	Evaluation	References
Fly ash	Cement	*Bacillus megaterium*	Higher bacterial cell viability, improved strength of mortar with 40% FA dosage	Achal et al. (2011c)
Silica fume	Cement	*Sporoscarcina pasteurii*	Biocementation increases strength and reduces water absorption in mortar, 20% SF dosage recommended	Farmani et al. (2015)
Silica fume	Cement	*B. aerius*	Improved mechanical and permeation properties of concrete, 10% SF dosage recommended	Siddique et al. (2017)
Rice husk ash	Cement	*B. aerius*	Improved compressive strength and permeability properties of concrete, 10% SF dosage recommended	Siddique et al. (2016)
Cement kiln dust	Cement	*B. halodurans*	Increased compressive and tensile strength, decreased permeation, 10% CKD dosage suggested	Kunal et al. (2016)
Metakaolin	Cement	*B. cereus*	Improved compressive strength by 26% in metakaolin modified mortar, 50% metakaolin dosage recommended	Li et al. (2017)
Recycled concrete aggregate	Normal aggregate	*B. sphaericus*	Bio-deposition decreased water absorption of RCA, compressive strength increased by 40% in concrete	Wang et al. (2017)
Recycled concrete aggregate	Natural aggregate	*B. pseudofirmus*	Reduction in water absorption and crushing values, adherence of $CaCO_3$ crystals on to the surface of RCA	Wu et al. (2018)
Recycled fine aggregates	Fine aggregate	*S. pasteurii*	Increment in compressive strength (32%) of mortar with 100% treated RFA	Zhan et al. (2019)

Siddique et al. (2017) reported the significant improvement of durability properties of SF amended concrete (5%, 10% and 20% dosage) with bacterial treatment. It was reported that, 12% strength gain in SF concrete (10% dosage) was achieved after treatment with calcifying bacteria. Due to biodeposition of calcite, water absorption, porosity, capillary water rise and chloride permeability was reported to be decreased.

In another research work, Siddique et al. (2016) proposed the usage of rice husk ash (RHA) as cement replacement (5%, 10%, 15% and 20%) in concrete along with bacterial treatment. It was reported that 10% RHA is the optimum dosage and strength gain by 9% and 11.8% was achieved at the age of 28 and 56 days respectively as compare to control. Inclusion of RHA and bacterial treatment reduced chloride ion ingress and calcite precipitation improved the durability of RHA amended concrete. Kunal et al. (2016) reported the decrease of alkalinity by 67.3% on treatment of highly alkaline cement kiln dust (CKD) with *Bacillus halodurans* strain. Further, the bacterial treated CKD was used as cement replacement (10%, 20% and 30%). Inclusion of 10% bacterial treated CKD in concrete was reported to increase compressive and tensile strength. Permeation properties were also reported to be decreased by 10% as compared to control. In another study, researchers proposed the improved durability properties of bacterial treated metakaolin (MK) modified cement mortars (Li et al. 2017). In this research work, cement was replaced by 25% and 50% MK in mortar cubes. MK modified mortars were treated with *Bacillus cereus* NS4 strain. It was reported that, biomineralization activity of bacterial strain enhanced the compressive strength of MK modified mortars. Strength gain of 27% was reported for MK modified mortar with 50% replacement dosage as compare to control.

Utilization of recycled concrete aggregates (RCA) along with MICP treatment has been extensively studied by many researchers. Qiu et al. (2014) reported the significant reduction of water absorption in MICP treated RCA with *S. pasteurii* strain. After 72 hrs of bacterial surface treatment, weight increase of RCA was reported due to the surface modification through biogenic $CaCO_3$ precipitation. In another research work, RCA was treated with *Bacillus sphaericus* by immersion and spraying method (Wang et al. 2017). It was reported that, immersion method results into high weight increase (2%) and decreased water absorption rate due to biogenic $CaCO_3$ precipitation. Increase by 40% of compressive strength was reported in bacterial treated RCA concrete.

Enhancement in performance of recycled aggregate was also proposed on treatment with non-ureolytic and ureolytic bacteria (Singh et al. 2018). Improvement in recycled aggregate such as reduction in water absorption as well as increased specific gravity was reported after treatment with non- ureolytic and ureolytic bacteria. Reduction in water absorption of recycled aggregate after treatment with non- ureolytic bacteria as well as ureolytic bacteria was reported to be 43% and 64%, respectively. Increase in specific gravity of recycled aggregate on treatment with non-ureolytic (29%) and ureolytic bacteria (30%) was reported. Wu et al. (2018) proposed a new biodeposition approach based on bacterially induced $CaCO_3$ precipitation through respiration to improve RCA properties. Bio-deposition treatment of RCA was done by pouring *B. pseudofirmus* culture on RCA and soaked it for 20 days. In this process, calcium chloride as external calcium source and adhered mortar as internal calcium source was adopted to induce $CaCO_3$ precipitation. Reduction in water absorption (23%) and crushing values (12%) was reported for 5 mm bacterial treated particles. Zhan et al. (2019) reported the increment of 32% in compressive strength of mortar containing 100% bacterial treated recycled fine aggregates. Authors also suggested the use of calcium chloride as calcium source for better $CaCO_3$ precipitation in bacterial treated recycled fine aggregates instead of calcium nitrate.

2.6.7 Biocementation based on CO_2 capture

Biomineralization of CO_2 by $CaCO_3$ precipitation is a common phenomenon in marine, freshwater, and terrestrial ecosystems. Photosynthetic microbes, such as cyanobacteria and microalgae, play a prominent role in carbon sequestration by simultaneously capturing CO_2 (Zhu and Dittrich, 2016). Employment of cyanobacteria in biomineralization offers a novel and self-sustaining strategy carbon capture and sequestration (CCS). Novel models for point-source CCS based on biomineralization are emerging (Jansson and Northen, 2010). Microalgae have a great potential to be developed as media for biocement production through photosynthetic metabolism (Ariyanti et al. 2012). Carbonic anhydrase (CA) is a first discovered zinc-containing metalloenzyme that is widespread in animals, plants and microorganisms which catalyses the conversion of carbon dioxide and water into bicarbonate (Smith and Ferry, 1999). The CA is widespread in metabolically diverse species of bacteria indicating that this enzyme plays a significant role in concentrating CO_2 (Dhami et al. 2014b). In natural process of photosynthetic assimilation of CO_2, carbonic anhydrase enzyme acts as biocatalyst (Jansson and Northen, 2010).

Potential role of CA enzyme in addressing environmental issues like reducing carbon emissions through CO_2 sequestration has gained considerable attention. Carbonic anhydrase enzyme is reported to be a potential tool to sequester carbon dioxide from emission sources (Bose and Satyanarayana, 2017). Some authors had reported the potential of bacteria and microalgae in bio-cementation of sand stabilization, fugitive dust and concrete restoration based on CO_2 capture and utilization. Okyay et al. (2016) evaluated the potential of ureolytic consortia in CO_2 sequestration through MICP. In this study, ureolytic consortia were obtained from the 'Cave without a name' and 'Pamukkale travertines' using 13 different growth media for ureolytic microorganisms. Consortia containing larger abundances of *Sporosarcina, Sphingobacterium, Stenotrophomonas, Acinetobacter* and *Elizabethkingia* genera were reported for higher CO_2 sequestration and $CaCO_3$ precipitations. It was suggested that combination of CA enzyme activity with MICP in the consortia might have resulted in a greater rate of CO_2 sequestration. Dhami et al. (2014b) also reported the synergistic role of urease (UA) and CA enzyme in biomineralization of calcium carbonate. Calcite precipitation was reported to be significantly reduced when both the enzymes were inhibited in comparison with those of the individual enzyme inhibitions. It was suggested that UA and CA enzyme are important for efficient biomineralization in urea hydrolyzing bacteria. It was reported that carbonic anhydrase plays a role in hydrating carbon dioxide to bicarbonate whereas UA activity maintained the alkaline pH promoting calcification process. CO_2 sequestering capability of *B. megaterium SS3* in biocementation was also reported (Kaur et al. 2016). In this study, urea was replaced with CO_2 flux and under accelerated carbonation in bacterial treated concrete specimen improved compressive strength (117%) as compared to control specimen. Significant reduction in the water absorption was also reported in bacterial treated carbonated specimens. Calcite as well as aragonite crystals were observed in association with the bacterial cells. CO_2 as an alternate was suggested instead of urea in calcium carbonate precipitation paving a way to develop green building structures. Zhan et al. (2016) reported microbial induced mineralization and cementation of fugitive dust under the action of *Paenibacillus mucilaginosus*. Cementitious material of biological carbonates was prepared by mixing *P. mucilaginosus* bacterial powder and calcium nitrate with water and sprinkled. It was reported that carbon dioxide was absorbed, transformed and produced carbonate ions under the enzymatic action of *P. mucilaginosus* resulting into cementation of fugitive dust due to calcite consolidation layer. Zhan and Qian

(2017) investigated the stabilization of sand particles using bio-cementation process based on CO_2 capture and utilization. Bacteria powder of *Paenibacillus* strain and calcium nitrate dissolved in deionized water was sprayed evenly on the surface of sand particles. It was reported that average porosity of samples was reduced from 18.3% to 13.3%. Calcite precipitation due to the enzymatic activity of bacteria and carbonate ion formation due to CO_2 absorption was also reported. Feasibility of application of using cyanobacteria *Synechococcus* PCC8806 in concrete restoration through biomineralization process was reported by Zhu et al. (2015). In this study, concrete cubes with a size of 3 x 3 x 1.5 cm were immersed in 50 mM calcium chloride solution with 1.5×10^8 cells/mL under shaking condition for 45 days. Thick calcite-cell layer adhering to the treated concrete specimen decreased the water absorption twice as compared to control specimen. Zhu et al. (2017) reported the calcification by cyanobacteria *Gloeocapsa* PCC73106 in mortars. Mortar cubes of a size 50 x 50 x 50 mm were treated abiotically, with live *Gloeocapsa* PCC73106 cells under illumination, with live cells under darkness and with UV-killed cells immersed in the cell solution (with a concentration of 3.5×10^7 cells/mL). Largest amount of precipitates was reported in treatment with live cells under illumination while highest compressive strength, the least water absorption and the lowest porosity was reported in UV-killed cells. In treatment with live cells, a thin layer of EPS around cells helped in the attachment to the surface of the mortar. After being exposed to UV light, the UV-killed cells produced more EPS resulting into larger coverage than live cells. It was reported that UV-killed cells were not metabolically active and EPS enhanced biofilm formation triggering calcium carbonate precipitation on the mortar surface.

2.7 Summary of literature review

With the advancement in concrete research, application of biotechnology in the field of civil engineering led to the development of a new domain called ‘‘microbial concrete”. The innovative MICP application has attracted the researchers from all over the world for its positive benefits in enhancing the durability properties of concrete structures. A decade of progress in microbial application on concrete, tremendous amount of studies has been published at lab scale experiments which reflect the importance of MICP technique. However, till now qualitative and quantitative evaluation of microbial concrete is confined to lab scale under ideal conditions. The study on the performance of microbial treated concrete on interaction with external

environmental conditions, which varies from place to place, is quite limited. Concrete is vulnerable to the ingress of reactive agents such as sulfates and chlorides which on interaction with hydration products of concrete causes severe degradation problems. To implement MICP technique at field scale, further studies on the long term durability properties of microbial concrete under extreme conditions are to be done. In various research publications, incorporation of bacterial culture along with the addition of organic nutrient media in concrete structures is carried out during microbial treatment. In these studies, evaluation of microbial concrete is carried out on the basis of strength and permeation properties. However, the influence of organic substrates in the material mix on the durability properties of microbial concrete is not investigated in detail. A thorough research work is to be carried out to study the influence of organic substrate on the chemical and structural properties of microbial treated concrete. Along with this, a suitable curing mechanism for microbial treatment of concrete structures is to be developed which could be implemented at field scale applications. The operating cost of MICP technology at the commercial scale might have economic limitations as in majority of previous studies the use of laboratory grade nutrient was adopted. Implementation of MICP technique in newly constructed concrete structures at field scale would not be possible because of its expensive cost. Hence, further studies should be carried out with the use of an inexpensive, alternative nutrient source to minimize the overall operating cost of MICP. Different research groups have worked on the repair of concrete cracks with self-healing mechanism, however limited studies are reported in which microbial healing to treat the existing cracks in concrete are investigated. A detailed work is required to develop an effective and low cost microbial healing material to repair the existing cracks in concrete structures. The goal of present work is to develop a better understanding in MICP technique, which will facilitate the practical implementation of microbial concrete in construction sector in the near future.

MATERIALS AND METHODS

Chapter 3

Materials and Methods

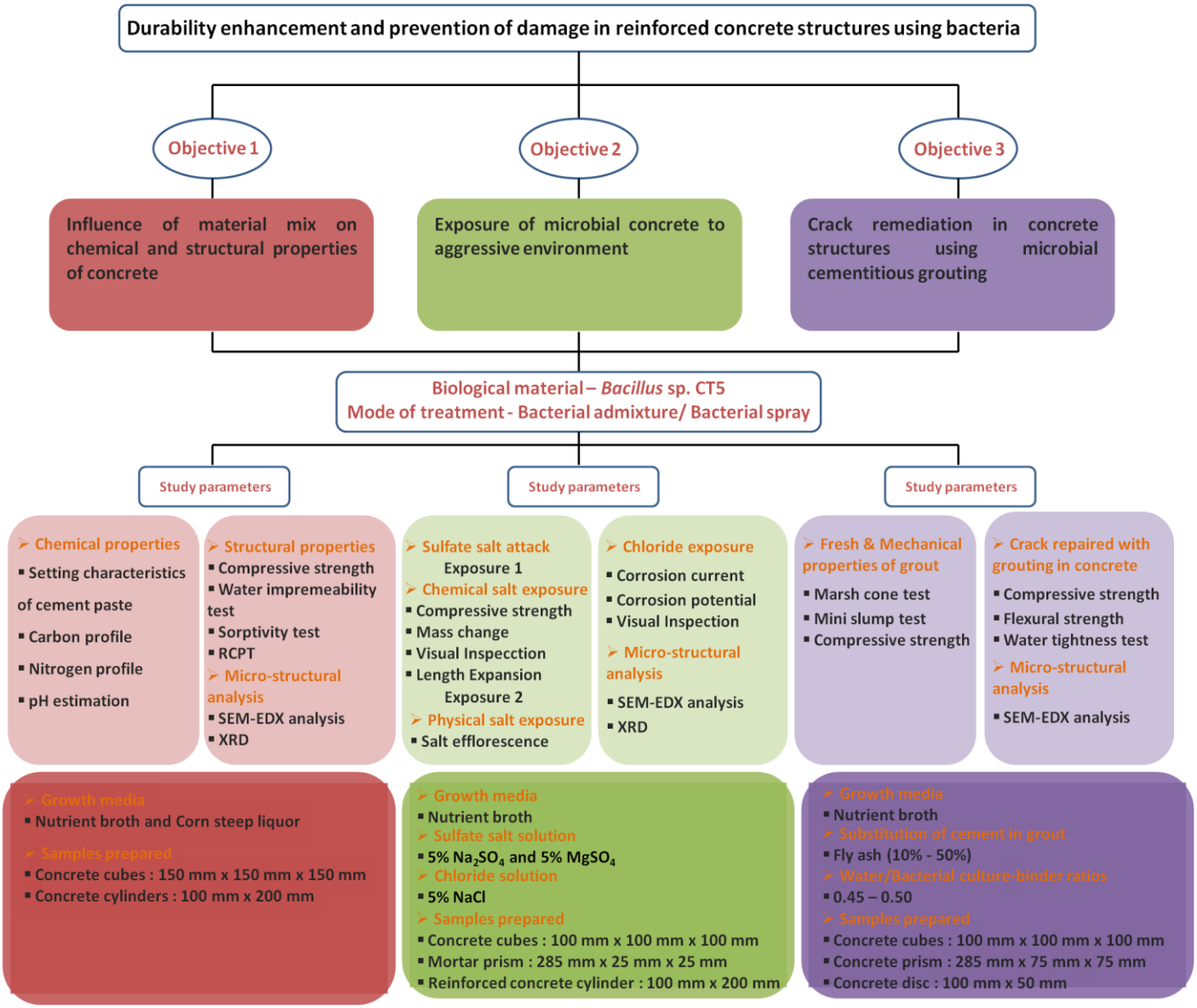

Figure 3.1 Overview of methodology adopted to address the objectives of the study

3.1 Materials

3.1.1 Biological material and culture conditions

The biological material used throughout the study was calcifying bacterial strain, *Bacillus* sp. CT5. The glycerol stock of this strain was maintained at -80°C in the TIFAC-CORE laboratory of TIET campus, Patiala (Punjab, India). This bacterial strain was isolated from the commercially available cement sample (Achal et al. 2011b). This alkaliphilic strain was selected because of its high urease producing activity with high efficiency to precipitate $CaCO_3$ crystals (Achal et al. 2010b). Details of physiological characteristics and enzymatic properties of bacterial stain, *Bacillus* sp. CT5 used in study are provided in Table 3.1.

Table 3.1 Characteristics of bacterial strain used in the study (Achal et al. 2010b)

Characteristics	***Bacillus* sp. CT5**
Gram stain	Positive
Shape	Rod
Temperature tolerance (°C)	25-55
Alkalinity (pH tolerance)	5-12.9
NaCl tolerance (%)	0-10
Urease production	High (670.71 U/ml at 120 h)
Extracellular Polymeric Substances	High (46 nmol/ml)

Based on the characteristics, such as tolerance to extreme environment as well as high calcium carbonate precipitation activity this bacterial strain was selected for the study.

3.1.2 Growth media

For the growth and propagation of bacterial strain, two growth media were used in the study. First, a laboratory grade Nutrient broth (NB) was procured from Himedia laboratories (Mumbai, India). NB media are basic culture media used for general cultivation of microorganisms. The chemical composition of NB media is as follows: Peptone 10 g/L, Yeast extract 10 g/L, Sodium chloride 5 g/L. The pH of the NB media was maintained at 7.5 before autoclaving.

Secondly, Corn steep liquor (CSL), a by-product from the starch industry was used as a low-cost nutrient medium. The positive attribute of CSL as growth media in biocalcification activity of ureolytic bacteria has been well reported (Achal et al. 2010a). Corn steep liquor was collected from Sukhjit Starch & Chemicals Limited, Phagwara, Punjab (India). Nutrient profile of CSL was analyzed by HPLC method. The chemical composition of the CSL is as follows: total carbohydrates 5.8%; proteins 24%; fats 1.0%; minerals 8.2%. The initial pH of CSL was recorded to be in the range of 4.0-4.5. For the bacterial growth and experimental purposes, 1.5% CSL (v/v) was used throughout the study. The pH of the CSL media was adjusted to 7.5 with 1 N NaOH before autoclaving.

To carry out microbial calcium carbonate precipitation, the bacterial culture was grown in autoclaved NB media (1.3% w/v) and CSL media (1.5% v/v) at 37 °C under shaking condition (120 rpm). The optimized concentration of 2% urea (w/v) and 25 mM $CaCl_2$ solution was supplemented in the grown bacterial culture as described in Achal et al. (2010b). Laboratory grade urea and calcium chloride were procured from Himedia laboratories (Mumbai, India).

3.1.3 Construction materials

An ordinary portland cement (43 Grade) confirming to Indian standards (IS: 8112-2013) was used in the present study. The physiochemical properties of ordinary portland cement and sand are presented in Table 3.2.

Table 3.2 Physicochemical properties of ordinary portland cement and sand

Parameters	Cement	Sand
Physical Analysis		
pH	12.5-12.8	-
Fineness (m^2/kg)	307	-
Specific gravity	3.13	2.70
Chemical composition (%)		
Calcium oxide (CaO)	65.1	5.73
Silicon dioxide (SiO_2)	22.3	77.39
Aluminum oxide (Al_2O_3)	5.9	8.38
Iron oxide (Fe_2O_3)	2.8	2.39
Sulfur trioxide (SO_3)	1.3	-
Magnesium oxide (MgO)	0.8	0.70
Sodium oxide (Na_2O)	0.4	0.005
Potassium oxide (K_2O)	0.8	0.02

Clean, dry and well graded natural river sand confirming to Zone II was used as fine aggregate. The values of specific gravity and water absorption of fine aggregates were 2.70 and 1.8%, respectively. The coarse aggregate used was crushed gravel with nominal particle size of 20 mm and 10 mm. The specific gravity and water absorption of 20 mm aggregates was 2.63 and 1.38% and for 10 mm aggregates, it was 2.65 and 1.4%, respectively. Both fine aggregate and coarse aggregate confirming to Indian standards (IS: 383-1970).

3.2 Influence of material mix on setting properties of cement

The change in the setting characteristics of cement paste upon addition of plain nutrients (NB and CSL) as well as bacterial culture grown in NB, CSL media supplemented with urea and $CaCl_2$ was investigated. Initial setting time and final setting time of cement pastes was determined by using vicat apparatus as per Indian standard (IS 4031: 1988) (Part 5). For conducting setting time test, water required to produce standard cement paste, i.e., standard consistency was first determined by IS 4031: 1988 (Part 4).

In this experiment, five sets of cement pastes were prepared. The composition and nomenclature of the pastes is presented in Table 3.3. Control paste was made by mixing cement and water. CSL paste was prepared by adding 1.5% of corn steep liquor, 2% urea and 25 mM $CaCl_2$ to cement, while NB paste was made by adding 1.3% of nutrient broth, 2% urea and 25 mM $CaCl_2$ to cement. CSL-CT5 paste and NB-CT5 paste were prepared by mixing cement with bacterial culture grown in CSL medium and NB medium supplemented with 2% urea and 25 mM $CaCl_2$, respectively. The consistency of all cement pastes were kept same.

Table 3.3 Composition of cement pastes with standard consistency using NB, CSL and bacterial culture

Cement mixes	Cement (g)	Water (g)	NB media (g)	CSL media (g)	Bacterial culture (g)
Control paste	400	100.3	–	–	–
CSL paste	400	–	–	100.3	–
NB paste	400	–	100.3	–	–
CSL-CT5 paste	400	–	–	–	100.3
NB-CT5 paste	400	–	–	–	100.3

CSL: Corn steep liquor, NB: Nutrient broth, CSL-CT5 bacterial paste in CSL, NB-CT5 bacterial paste in NB

To determine the standard consistency of cement paste, 400 g of cement along with a weighed quantity of distilled water was taken. Cement paste was prepared by mixing cement with the weighed quantity of water and gauging was completed within 3 minutes to 5 minutes. As specified in the standard, cement paste was filled in the vicat mould within the gauging time. After completely filling the mould, cement paste surface was smoothen with trowel and making its level with the top of the mould. After resting the mould on the resting plate, vicat plunger (IS: 5513- l996) was allowed to touch the top surface of mould and was quickly released to sink into the paste. The standard consistency of a cement paste is defined as that consistency which will permit the vicat plunger to penetrate to a point 5 to 7 mm from the bottom of the vicat mould.

Then a neat cement paste was prepared by gauging the cement with 0.85 times the water required to give a paste of standard consistency. The vicat mould was filled with a cement paste gauged as above and the mould was allowed to rest in moist room. To determine the initial setting time, rod bearing the needle in vicat apparatus was lowered gently until it comes in contact with the top surface of mould filled with cement paste. The needle is quickly released repeatedly until it fails to pierce the cement paste beyond 5.0 ± 0.5 mm measured from the bottom of the mould. The time when water is added to the cement and the time at which the needle fails to pierce the cement paste to a point of 5.0 ± 0.5 mm measured from the bottom of the mould is the initial setting time.

To determine the final setting time, needle of the vicat apparatus was replaced with an annular attachment. The cement is considered as finally set when, upon applying the needle gently to the surface of the paste, the needle makes an impression thereon, while the attachment fails to do so. The time when water is added to the cement and the time at which the needle makes an impression on the surface of cement paste while the attachment fails to do so is the final setting time.

3.3 Influence of bacteria and material mix on durability properties of concrete

For performing the various experimental studies on the role of bacteria as well as material mix on the durability properties of concrete structures, different sets of concrete and mortar specimens were cast. Fabrication of concrete and mortar specimens prepared according to different mixes is described in section 3.3.1 and section 3.3.2.

3.3.1 Preparation of concrete mixes

Control concrete mix was prepared by using cement: sand: coarse aggregate in the ratio of 1: 1.82: 3.24 (by weight) and water to cement ratio (w/c) of 0.5. For casting of media treated concrete mix, NB media (1.3% w/v) and CSL media (1.5% v/v) supplemented with 2% urea (w/v) and 25 mM calcium chloride solution (w/v) were used instead of water. For casting of bacterial treated specimens, bacterial culture (4×10^8 cells/ml) grown in CSL media (1.5% v/v) and NB media (1.3% w/v) supplemented with 2% urea (w/v) and 25 mM calcium chloride solution (w/v) were used instead of water. The bacterial culture was prepared by growing the cells in CSL and NB medium till it attained the $O.D_{600}$, of 0.5 (exponential phase). Then this culture was admixed with the concrete. The bacterial culture to cement ratio was also maintained at 0.5.

For the bacterial spray treatment, casting of concrete mix was done using water similar to control mix. During curing, the bacterial culture was grown in CSL as well as in NB medium till it reached the $O.D_{600}$, of 0.5 (4×10^8 cells/ml) and used as spray treatment. Cement, sand and aggregates were thoroughly mixed for 2 min in the concrete mixture before adding water, CSL medium, NB medium and bacterial culture. The ingredients were mixed properly and the fresh mix in the plastic stage was immediately transferred to iron moulds. After casting, all the specimens were allowed to remain in the iron moulds and kept in a casting room at room temperature of 27 ± 2 °C for 24 h. Thereafter, the specimens were demoulded and cured till the testing age. Different curing regimes were adopted in this study as mentioned in Table 3.4

3.3.2 Preparation of mortar specimen

Three different sets of mortar prism were also prepared according to ASTM standard (ASTM C1012-04). Control mortar prism was prepared by using cement: sand in the ratio of 1: 3 (by weight) with water to cement ratio (w/c) of 0.47. For casting of bacterial admixed mortar prism, instead of water, bacterial culture ($O.D_{600}$ 0.5) was grown in NB medium supplemented with 2% urea and 25 mM calcium chloride solution (w/v) and was admixed with the cement and sand mixture. The cement: sand ratio was kept constant and bacterial culture to cement ratio was also maintained at 0.47. For the bacterial spray treated mortar, control mortar mix was used and cured by spraying with bacterial culture ($O.D_{600}$ 0.5) grown in NB medium supplemented with 2% urea and 25 mM calcium chloride solution (w/v) for 28 days. After casting, three different curing regimes for the mortar specimens are specified in Table 3.5 were adopted.

Table 3.4 Outline of different sets of concrete specimen and mechanism of curing treatments

Specimens	**Material used**	**Mechanism of curing**
Control	Cement: sand: coarse aggregate Water/Cement = 0.5	Water Curing for 28 days
CSL treated (CT)	Cement: sand: coarse aggregate CSL media/Cement = 0.5	Submersion in CSL media with urea and $CaCl_2$ without bacteria for 28 days
NB treated (NT)	Cement: sand: coarse aggregate NB media/Cement = 0.5	Submersion in NB media with urea and $CaCl_2$ without bacteria for 28 days
CSL-Bacterial admixed treated (CBAT)	Cement: sand: coarse aggregate Bacterial culture/Cement = 0.5	Submersion in CSL media, urea, $CaCl_2$ and bacterial culture for 28 days
NB-Bacterial admixed treated (NBAT)	Cement: sand: coarse aggregate Bacterial culture/Cement = 0.5	Submersion in NB media, urea, $CaCl_2$ and bacterial culture for 28 days
CSL-Bacterial spray treated (CBST)	Cement: sand: coarse aggregate Water/Cement = 0.5	Bacterial spray on specimens twice a day till 28 days
NB-Bacterial spray treated (NBST)	Cement: sand: coarse aggregate Water/Cement = 0.5	Bacterial spray on specimens twice a day till 28 days

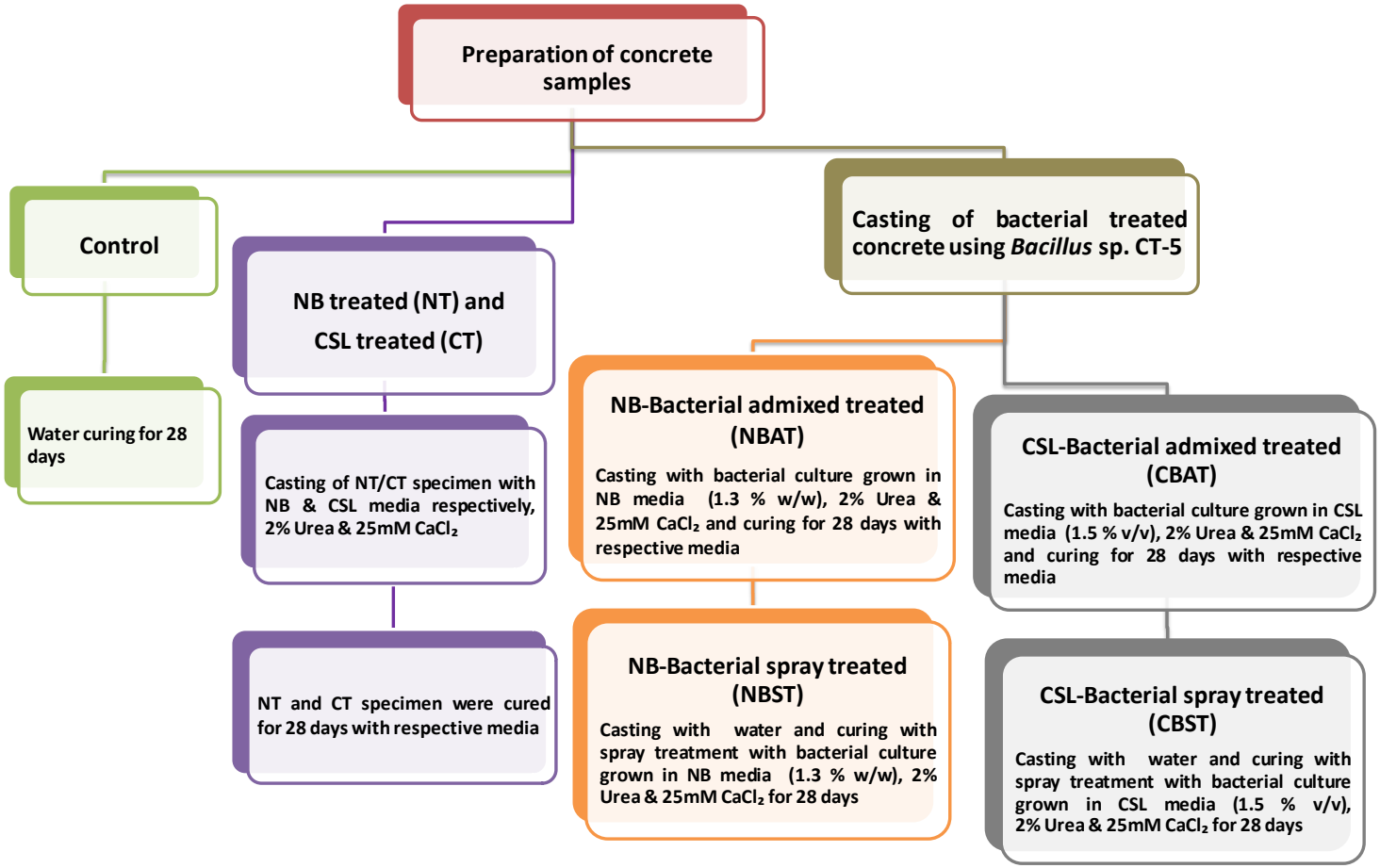

Figure 3.2 Schematic illustration of fabrication of different concrete specimens with respective curing regime

Table 3.5 Outline of different sets of mortar specimen and mechanism of curing treatments

Specimens	Material used	Mechanism of curing
Control	Cement: sand Water/cement = 0.47	Water Curing for 28 days
NB-bacterial admixed mortar (NBAM)	Cement: sand Bacterial culture/cement = 0.47	Submersion in NB media, urea $CaCl_2$ and bacterial culture for 28 days
NB-bacterial spray treated mortar (NBSM)	Cement: sand Water/cement = 0.47	Bacterial spray on specimens twice a day till 28 days

NB medium, urea and calcium chloride had the following concentrations: NB medium (1.3% w/v), 2% urea (w/v) and 25 mM calcium chloride (w/v).

Different concrete and mortar specimens prepared according to different mixes as described in Table 3.4 and Table 3.5 were used to evaluate various study parameters. Overview of concrete and mortar specimens with different shapes and dimensions used according to study parameters are presented in the Table 3.6.

Table 3.6 Overview of different concrete and mortar samples prepared for the study

Study parameters	Samples	Dimensions (mm)	Growth media	Concrete mixes
Chemical and structural properties	Concrete cubes Concrete cylinders	150 x 150 x 150 100 x 200	NB and CSL medium	Control NT and CT NBAT and CBAT NBST and CBST
Sulfate salt exposure	Concrete cubes Mortar prisms	100 x 100 x 100 285 x 25 x 25	NB medium	Control NBAT and NBST NBAM and NBSM
Rebar corrosion	Reinforced concrete cylinders	100 x 200	NB medium	Control NBAT NBST
Crack remediation	Concrete cubes Concrete cylinder disc Concrete prism	100 x 100 x 100 100 x 50 285 x 75 x 75	-	Control

NT: NB treated concrete; CT: CSL treated concrete; NBAT: NB-bacterial admixed treated concrete; CBAT: CSL-bacterial admixed treated concrete; NBST: NB-bacterial spray treated concrete; CBST: CSL-bacterial spray treated concrete; NBAM: NB-bacterial admixed mortar; NBSM: NB-bacterial spray treated mortar

3.4 Influence of material mix on chemical and structural properties of concrete

During the microbial treatment of concrete, NB and CSL media along with urea and $CaCl_2$ were used in the form of bacterial growth medium. Effect of incorporation of vegetative bacterial cells and the associated nutrient medium (both organic and inorganic in nature) on the chemical and structural properties of different microbial treated concrete mixes was analyzed.

3.4.1 Carbon and nitrogen profile in concrete specimens

To analyze the change in the chemical properties while using vegetative bacterial cells and organic nutrients in microbial concrete, presence of carbon and nitrogen as organic content was determined at different depths.

Sample collection

Different sets of concrete cubes were used in this study after respective curing regimes as mentioned in Table 3.4 and Table 3.6. Different sets of concrete cubes were drilled using a rotary hammer drilling machine to collect the concrete powder for analyses. The cubes were drilled up to the depth of 50 mm from two opposite sides as shown in Figure 3.3A. Concrete powder was separately collected from each depth. The sample was collected by drilling at 12 points on one surface of the cube as shown in Figure 3.3B. Homogenous samples were prepared by collecting the samples of each depth of concrete specimen.

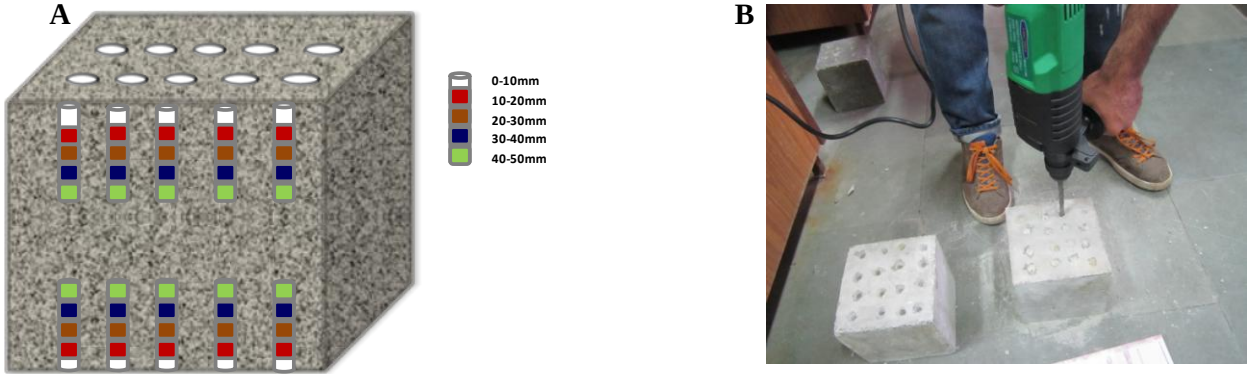

Figure 3.3 Layout of the drilling pattern (A) and collection of concrete powder (B) from different depths

The powder samples obtained were analyzed to calculate carbon and nitrogen content at various depths. To calculate the amount of organic carbon in concrete powder, Walkley–Black procedure was followed (Walkley and Black, 1934). Kjeldahl method was used to determine the ammonia producing nitrogen in the concrete powder as per Indian standard (IS: 5194- 1969).

3.4.1.1 Carbon estimation

Reagents

- Potassium dichromate solution: 49.035 g of potassium dichromate was dissolved in 1 litre of distilled water.
- Ferrous sulfate solution (0.5 N): 140 g of ferrous sulfate was dissolved in 0.5 N sulfuric acid to make one litre of the solution.
- Concentrated sulfuric acid
- Orthophosphoric acid (85 %)
- Indicator: 0.25 g of sodium diphenylamine sulphonate was dissolved in 100 ml of distilled water.

Standardization of ferrous sulfate solution

10 ml of potassium dichromate solution was added to 20 ml of concentrated sulfuric acid. The mixture was swirled carefully to mix and allowed to cool for some time. 200 ml of distilled water was added to the mixture followed by 10 ml of phosphoric acid and 1 ml of indicator. The mixture was shaken vigorously. Then, ferrous sulfate solution was added from a burette in 0.5 ml increments, the contents of the flash swirled to mix until the color of the solution changed from blue to green. A further 0.5 ml of potassium dichromate solution was added to change back the color to blue. Ferrous sulfate solution was then added drop by drop with continued swirling until the color of the solution changed from blue to green after the addition of a single drop. The total volume of ferrous sulfate solution used (B) was noted.

Test procedure

- 2 g of concrete powder was weighed and transferred to a 500 ml dry conical flask.
- Measured volume of 10 ml potassium dichromate solution and 20 ml of concentrated sulfuric acid was added to the flask containing powder sample.
- The mixture was thoroughly mixed by swirling for about 1 minute and the mixture was allowed to stand for 30 minutes for the oxidation of organic matter.
- 200 ml of distilled water was added to the mixture followed with the addition of 10 ml of orthophosphoric acid and 1 ml of the indicator. The mixture was shaken vigorously.
- Ferrous sulfate solution was added from the second burette in 0.5 ml increments, with constant mixing, until the color of the solution changes from blue to green.

- An additional 0.5 ml of potassium dichromate solution was added to change the color from green to blue
- The mixture was titrated with ferrous sulfate solution and added drop wise till the color change from blue to green.

Calculations

Organic carbon, percent by weight = $\frac{10 \times (B - S) \times 0.003 \times 100}{B \times wt.of\ sample\ (g)}$

Where:

B = total volume of ferrous sulfate used in standardized test

S = total volume of ferrous sulfate used with sample

3.4.1.2 Nitrogen estimation

The Kjeldahl method for the determination of nitrogen content is convenient for determining ammonia producing nitrogen, especially in organic compounds. The principle of the determining nitrogen in sample is begin with the digestion of sample with concentrated sulfuric acid in the presence of a catalyst to convert the organic nitrogen into ammonium sulfate. The ammonia is liberated by distillation with concentrated alkali solution and then the ammonia evolved is absorbed in boric acid and titrated against standard acid.

Reagents

- Potassium sulfate or Anhydrous sodium sulfate
- Copper sulfate as a catalyst
- Concentrated sulfuric acid
- Sodium hydroxide solution: 450 g of sodium hydroxide pellets are dissolved in 1000 ml of water.
- Standard Sulfuric Acid (0.5 N)
- Boric acid solution: 60 g of boric acid was dissolved in 1 litre of hot water and allowed to mature for 3 days before decanting the clear liquid.
- Mixed indicator solution: Prepared by using methyl red and methyl blue

Apparatus

- Kjeldahl flask: 500 ml capacity.
- Distillation assembly

- Fume hood

Test procedure

- 2 g of concrete powder was weighed and transferred into a dry kjeldahl digestion flask.
- 10 g of potassium sulfate or anhydrous sodium sulfate, 0.5 to 1 g of the catalyst and 30 ml of concentrated sulfuric acid was added into the flask.
- Digestion flask is placed in an inclined position in a fume cupboard for boiling the liquid mixture.
- The liquid mixture is heated till the boiling point until the liquid mixture becomes clear.
- The content of the digestion flask is completely transferred into the round bottom flask of the distillation assembly. 100 to 150 ml of distil water was added to mixture.
- Excess of sodium hydroxide solution was added separating funnel to make the solution alkaline.
- The round bottom flask containing sample was connected to steam trap and condenser.
- Dip tube of condenser was arranged to dip properly in a beaker containing 50 ml of boric acid.
- About one third of the total volume of the solution in the flask was distilled.
- After distillation, 2 to 3 drops of mixed indicator was added in the distillate collected in the beaker containing boric acid.
- The ammonia present in the distillate was titrated with standard sulfuric acid until the grass green color changes to steel grey, a further drop then giving the purple color.

Calculations

$$\text{Nitrogen, percent by weight} = \frac{1.4 \times V \times N}{W}$$

Where:

V = volume in ml of standard sulfuric acid used in titration

N = normality of standard sulfuric acid

W = weight in g of the sample taken

3.4.2 Estimation of pH

One of the most influential parameter in concrete durability is the pH value of concrete structure. pH was measured by ex-situ leaching method, which is based on using a given amount of powder suspension of a ground concrete with water. In order to investigate the effect of microbes

as well as nutrient medium onto the alkaline nature of concrete, pH of the resultant concrete mixes as described in section 3.3.1 was measured by using concrete powder collected from various depths as shown in Figure 3.3. Different sets of concrete cubes as mentioned in Table 3.6 were used in this study to collect the concrete powder samples. pH value at various depths was measured potentiometrically by immersing pH glass electrode in the suspension of a 1:5 concrete powder (g):water (ml) after stirring for 1 h (Behnood et al. 2016).

3.4.3 Compressive strength of concrete specimens

To study the compressive strength, seven different sets of concrete cubes were used in this study after respective curing regimes as mentioned in Table 3.4 and Table 3.6. Effect of incorporation of vegetative bacterial cells and the associated nutrient medium (NB and CSL medium supplemented with urea and $CaCl_2$) on the mechanical strength properties of different microbial treated concrete mixes were studied at the age of 28 days of curing as per Indian standard (IS 516: 1959). Compression test was performed with automatic compression testing machine, COMPTEST 3000 (AIMIL India Ltd, New Delhi). The average of three specimens was taken as the compressive strength of the mix.

3.4.4 Permeation properties of concrete specimens

The efficiency in resistance towards water penetration was investigated for the different concrete mixes as described in section 3.3.1 and Table 3.4 at the age of 28 days. To determine the permeation properties of concrete specimens, different water absorption tests such as water impermeability, sorptivity and Rapid chloride penetration test were conducted.

3.4.4.1 Water impermeability test

The water impermeability test was carried in seven different sets of concrete cubes as mentioned in Table 3.6 after 28 days of curing. After air drying, concrete cubes were firmly kept in position in the test apparatus (AIMIL India Ltd, New Delhi) and water penetration test was carried out as per German standard (DIN 1048: 1978). The concrete specimens were exposed to a water pressure of 0.5 N/mm^2 for 72 hours through water nozzles connected onto the exposed surface of concrete. To prevent any water leakage when specimens were subjected to water pressures, gaskets were properly fixed and checked at regular interval. After completion of test, specimens were removed and split into two halves to determine the vertical penetration depth of water into concrete. Water ingress in the concrete specimens was measured and marked with black marker.

3.4.4.2 Sorptivity test

The rate of uni-directional absorption of water by concrete sample due to capillary rise is defined as sorptivity test. It correlates the transport of water with the pore system of specimen. Sorptivity of concrete specimens was determined according to ASTM standard (ASTM C1585). This test method is used to determine the rate of absorption of water by hydraulic cement concrete by measuring the increase in the mass of a specimen resulting from absorption of water as a function of time when only one surface of the specimen is exposed to water. Seven concrete mixes as specified in section 3.3.1 were used for the casting of concrete cylinders and curing in a similar manner as mentioned in Table 3.4. The standard test sample, concrete discs with diameter 100 mm and 50 mm thickness were obtained from the cured concrete cylinders (Table 3.6). The test setup is illustrated in Figure 3.4. The concrete disc sample was then saturated by placing in vacuum dedicator and vacuum is maintained for 3 hours. After saturating, samples are placed in the environmental chamber at a temperature of 50 ± 2 °C and RH of 80 ± 3 % for 3 days. After the 3 days, samples were placed inside a sealable container and stored at 23 ±2 °C for at least 15 days before the start of the absorption procedure.

Figure 3.4 Arrangement of the sorptivity test

Test Procedure

- After conditioning, mass of the conditioned sample to the nearest 0.01 g before sealing of side surfaces was recorded.
- Average diameter of sample with its exposed surface to water was calculated.
- Side surfaces of each sample which are not exposed to water were sealed with a suitable sealing material (e.g. epoxy sealant).

- Mass of the sealed sample to the nearest 0.01 g was measured and recorded as its initial mass for water absorption calculations.
- A pan with support device at its bottom was filled with tap water was used for water absorption mass measurement of specimens.
- For each mass determination, the test sample was removed from the pan and excess water was blot off with a dampened paper towel or cloth. After blotting, mass to nearest 0.01 g of specimen was recorded with the balance pan.
- Immediately the specimen was replaced on the support device of water filled pan.
- The mass change was recorded at the intervals of 60 s, 5 min, 10 min, 20 min, 30 min, 60 min and every hour up to 6 hours.
- From the value of mass change, volume of water absorbed per unit cross sectional area was evaluated for each time interval.
- A plot between the square root of time and volume of water absorbed was plotted.

Calculations

The absorption, *I*, is the change in mass divided by the product of the cross-sectional area of the test specimen and the density of water. For the purpose of this test, the temperature dependence of the density of water is neglected and a value of 0.001 g/mm^3 is used. The units of *I* are mm.

$$I = \frac{m_t}{a * d}$$

Where:

I = the absorption by specimen, (mm)

m_t = change in mass of specimen in grams (g) at time interval (t)

a = cross-sectional area of specimen, (mm^2)

d = density of water, (g/mm^3)

The rate of water absorption (mm/s$^{1/2}$) is defined as the slope of the line that is the best fit to *I* plotted against the square root of time (s$^{1/2}$). This slope is obtained by using least squares, linear regression analysis of the plot of *I* versus time$^{1/2}$.

3.4.4.3 Rapid chloride penetration test

This test was conducted to cover the determination of the electrical conductance of concrete to provide a rapid indication of its resistance towards the penetration of chloride ions. Rapid chloride penetrability test (RCPT) was conducted as per ASTM standard (ASTM C1202-12).

The standard test sample, a concrete discs with diameter 100 mm and 50 mm thickness were obtained from the cured concrete cylinders. Seven different sets of concrete cylinder disc as mentioned in Table 3.6 were used in this experiment. In this test method, amount of electrical current passed through concrete disc sample was monitored during a period of 6 hours. A potential difference of 60 V dc was maintained across the ends of the specimen, one of which is immersed in a sodium chloride solution, the other in a sodium hydroxide solution. Total charge passed (in terms of coulombs) is a measure of the electrical conductance of the concrete and directly proportional to the chloride penetrability.

Apparatus

- Vacuum Saturation Apparatus
- Vacuum Desiccator with Vacuum Gage
- Vacuum Pump
- Voltage Application and Data Readout Apparatus
- Applied Voltage Cell
- Voltmeter
- Constant Voltage Power Supply

Reagents

- Sodium Chloride Solution: 3.0 % by mass (AR grade) in distilled water.
- Sodium Hydroxide Solution: 0.3 N (AR grade) in distilled water.
- Specimen-Cell Sealant: Capable of sealing concrete to rubber gasket

Conditioning of concrete specimen

De-aerated water was prepared by vigorously boiling tap water in a large sealable container and allowed to cool at ambient temperature. Rapid setting sealant was prepared and coated by brush onto the side surfaces of concrete disc samples. After coating with sealant, samples were allowed to cure until the sealant is no longer sticky to the touch. Thereafter, coated samples were placed in vacuum desiccator in such a way that both end faces of samples must be exposed. Desiccator was filled with de-aerated as prepared earlier and sealed with cover. Vacuum pump was started and pressure was decreased to less than 50 mm Hg within a few minutes. Vacuum was maintained for 3 hours. Then vacuum line stopcock was closed and vacuum pump was turned off. Then the test samples were soaked under water in the beaker for 18 hours.

Test Procedure

- Conditioned samples were removed from water and excess water was blot off with dampened paper towel.
- Sample was installed into the voltage cell by applying sealant around cell and sample boundary.
- Rubber gaskets were used to make it water tight.
- Two halves of the test cell was sealed together and one side of the cell containing the one exposed surface of the samples was completely filled with 3.0 % NaCl solution (This side of the cell was connected to the negative terminal of the power supply).
- Second side of the cell containing other exposed surface of sample was completely filled with 0.3 N NaOH solution (This side of the cell was connected to the positive terminal of the power supply).
- Wires were attached to make electrical connections to the voltage application and data readout apparatus.
- Power supply was turned on and concrete disc sample inside the voltage test cell was subjected to a potential difference of 60 V for 6 hours.
- During the test, voltage apparatus was monitored at every 30 minutes of interval as the current was recorded automatically by data acquisition device.
- Test was terminated after 6 hours and concrete samples were removed.
- Automatic data processing equipment performed the integration during the test and displays the coulomb value. The total charge passed is a measure of the electrical conductance of the concrete during the 6 hour period of the test.

Table 3.7 provides a qualitative relationship between the results of the test and the chloride ion penetrability of concrete.

Table 3.7 Chloride ion penetrability based on charge passed (ASTM C1202-12 standard)

Charge passed (coulombs)	**Chloride ion penetrability**
>4,000	High
2,000–4,000	Moderate
1,000–2,000	Low
100–1,000	Very Low
<100	Negligible

3.4.5 Micro-structural analysis

Scanning Electron Microscopy (SEM) (ZEISS EVO 50) analysis was done on the concrete specimens at the age of 28 days. The elemental composition of micro-structural crystals was identified with Energy Dispersive X-ray spectroscopy (EDX). For conducting SEM and EDX analyses, small pieces of samples from different depths were collected. Samples were finely polished and gold coated with a sputter coating. To disperse excess charge from the sample, a thin coating of carbon was applied on the polished surface.

X-ray diffraction (XRD) was done on the powdered samples obtained from various depths and sieved through 90 µm sieve. XRD spectrum was obtained using Bruker D8 X-ray diffractometer with a Cu anode (40 kV and 30 mA) and scanning from 10° to 80° 2θ. $CaCO_3$ crystals present in concrete powder were identified with standards established by the International Center for Diffraction data.

3.5 Exposure of microbial concrete to external sulfate attack

External sulfate attack is one of the most aggressive deterioration factors, which causes irremediable changes in concrete structures. This section aimed to assess the efficacy of bio-deposition as a barrier in microbial treated concrete against the penetration of aggressive agents. The performance of microbial treated concrete specimens on chemical and physical sulfate exposure was evaluated.

3.5.1 Testing methods

The performance of control and microbial treated specimens under sulfate environment was determined by subjecting to chemical and physical salt exposures. In all the tests, mixture of 5% Na_2SO_4 and 5% $MgSO_4$ were used as sulfate salt solution. The pH value of the produced sulfate salt solution was maintained in the range of 7.0-8.0. Two exposure regimes adopted in this experiment are specified below.

Exposure 1: Chemical sulfate attack

Different sets of concrete cubes (control, NBAT and NBST) and mortar prisms (control, NBAM and NBSM) specified in Table 3.6 were subjected to chemical sulfate attack. Concrete and mortar specimens were fully submerged in sulfate solution for 12 months in plastic container and room temperature was maintained at 27 ± 2 ℃. To accelerate the chemical attack, all specimens were exposed to wet-dry cycle in sulfate solution. Wet cycle and dry cycle was kept for 5 days and 2 days respectively throughout experiment of 12 months. Sulfate solution in container was

renewed every month. The performance of control and microbial treated concrete specimens on exposure to chemical sulfate attack were evaluated by different test procedures.

- Compressive strength

  The performance of control and microbial treated concrete specimens in context to mechanical property under exposure of sulfate attack was monitored for 1 year. Prior to sulfate exposure, the initial compressive strength of different concrete cube specimens at the age of 28 days of curing was recorded in order to monitor any change over the investigation period. The strength properties of concrete cubes were studied at different time intervals of exposure as per Indian standard (IS 516: 1959) using automatic compression testing machine, COMPTEST 3000.

- Mass change

  In addition to mechanical strength, mass changes of the concrete cube samples during the exposure to Na_2SO_4 and $MgSO_4$ solutions have also been measured. As the reaction of sulfate ions with portlandite (CH) and tricalcium aluminate (C_3A) forms ettringite precipitates which yields an increase in volume of the reactant materials. To investigate any mass variations in concrete samples due sulfate ions ingress under chemical sulfate exposure, change in mass of concrete sample was monitored at different time intervals throughout the experiment.

  Calculations:

  $$\text{Mass change at time (t)} = \frac{Mt - Mi}{Mi} \times 100$$

  Where:

  Mi is the initial mass of cube and *Mt* is the mass of cube at time (t)

- Visual Inspection

  Sulfate induced degradation such as cracking and spalling due to harsh conditions of sulfate attack are associated with concrete structures. Visual observations of concrete specimens under chemical sulfate exposure were recorded till the 12 months of the experiment. Severity of surface scaling in concrete specimens was rated as specified in ASTM standard (ASTM C672/C672M – 12).

- Length expansion

  In different set of mortar prisms (as mentioned in Table 3.5), length change due to expansion or shrinkage after chemical sulfate exposure was monitored by using length comparator according to ASTM standard (ASTM C1012-04). This test method was adopted to observe the sulfate resistance based on length change measurements of mortar prisms immersed in sulfate solution. The initial lengths of all the mortar prisms were recorded prior to submersion in sulfate solutions.

  Calculations:

  $$\text{Length change at time (t)} = \frac{Lt - Li}{Li} \times 100$$

  Where:

  Li is the initial length of prism and *Lt* is the length of prism at time (t)

Exposure 2: Physical sulfate attack

In physical sulfate attack, contact of concrete surface with sulfate solution makes it vulnerable to damage due to sulfate salt crystallization in the pore structure of cementitious matrix. To investigate the performance of cement mortar samples, three different sets of mortar prismatic specimens specified in Table 3.5 were subjected to physical sulfate attack. All the prismatic specimens were subjected to partial immersion, in which one third length base of all the specimens was rested against the container of sulfate solution. Similar wet-dry cycle was adopted for the mortar prisms as mentioned in exposure I. Sulfate solution was renewed every month during the experimental period. Appearance of salt efflorescence due to rise of sulfate solution in all the specimens was monitored and recorded throughout the experiment.

3.5.2 Micro-structural analysis

SEM-EDX analysis was performed to investigate the presence of reaction products at micro-structural changes after sulfate exposure. The elemental composition of micro-structural crystals was identified with SEM-EDX. For conducting SEM and EDX analyses, small pieces of concrete were collected from different sets of concrete cubes within the range of 5–10 mm depth. Samples were finely polished and gold coated with a sputter coating. To disperse excess charge from the sample, a thin coating of carbon was applied on the polished surface.

X-ray diffraction (XRD) was done on the powdered samples obtained from concrete samples and sieved through 90 μm sieve. XRD spectrum was obtained using Bruker D8 X-ray diffractometer with a Cu anode (40 kV and 30 mA) and scanning from 10° to 80° 2θ. Different crystal structure

of $CaCO_3$ and secondary products like gypsum and ettringite present in concrete powder were identified with standards established by the International Center for Diffraction data.

3.6 Prevention of chloride induced corrosion in reinforced concrete

Chloride attack is a mechanism of deterioration of reinforced concrete, which occurs due to the ingress of chloride ions in the well-connected pore matrix of concrete leading to corrosion of steel rebar. This section aimed to assess the performance of microbial treated reinforced concrete in prevention of damages against chloride induced corrosion.

3.6.1 Preparation and preconditioning of steel specimens

Before casting of reinforced concrete samples, steel specimen was drilled and threaded on its one end to fix a stainless steel screw and nut. Then, the prepared steel specimen was preconditioned before used in concrete casting. Steel specimen was rubbed with wire brush to remove any rust present on it. Thereafter, steel specimen was cleaned with AR grade hexane and was kept for air drying. On the one end of steel rebar with threaded portion, insulating tape was wrapped up to 40mm length so that 180 mm length of rebar remained exposed. Then, epoxy was applied over insulated portion carefully as this is the protruded portion of steel specimen during casting.

3.6.2 Preparation of concrete cylinders

In this experiment, reinforced concrete cylinders (100 mm diameter and 200 mm in height) were used as described in Table 3.6. A standard steel rebar with 12 mm diameter and 220 mm length of Fe 415 grade as specified in Indian standards (IS:1786-2008) was used. During casting, steel rebar was embedded axially in the concrete cylinder accurately with a clear cover of 44 mm. Exposed length of 180 mm of steel rebar was kept inclined in concrete cylinder for monitoring chloride induced corrosion during the experiment as shown in Figure 3.5.

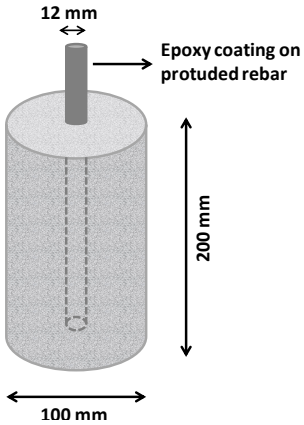

Figure 3.5 Pictorial representation of the reinforced concrete cylinders used for monitoring chloride induced corrosion

Three different sets of reinforced concrete cylinders control, NB-Bacterial admixed treated (NBAT) and NB-Bacterial spray treated (NBST) were cast and cured as mentioned in section 3.3.1.

3.6.3 Exposure conditions

After 28 days of curing, concrete cylinders were air-dried for 2 days and kept at ambient temperature. After that, epoxy resin was applied on the lower horizontal surface of all the concrete cylinders. After coating with epoxy, samples were allowed to cure until the sealant was no longer sticky to the touch. Then the specimens were kept immersed in 5% sodium chloride (NaCl) solution so that the vertical surface of cylinders up to the height of 190 mm is exposed to the solution. The purpose of keeping the NaCl solution below the upper surface of cylinder specimen is to protect the protruded rebar from atmospheric corrosion. Specimens exposed to chloride solutions are shown in Figure 3.6.

Figure 3.6 Reinforced cylinders exposed to 5% NaCl solution

To accelerate the chloride ion ingress in reinforced concrete specimens, wet-dry cycle of 7 days immersion in NaCl solution and 3 days air drying was adopted. This wetting and drying cycle of chloride exposure was adopted so that the specimens remain partially saturated as well as sufficient oxygen is also available in abundance. With the availability of oxygen, corrosion can proceed unhindered in steel reinforcement when initiated. The corrosive solution of 5% NaCl was renewed after every 10 days.

3.6.4 Corrosion monitoring

The performance of control and microbial treated concrete specimens under chloride exposure were studied by corrosion monitoring device ACM corrosion analyzer. This field machine is capable of performing various non-destructive electrochemical tests to analyze the corrosion initiation in reinforcement. The corrosion of the rebar was monitored at every 10^{th} day of exposure and electrochemical test such as linear polarization resistance (LPR) was conducted. Experimental arrangement is shown in Figure 3.7.

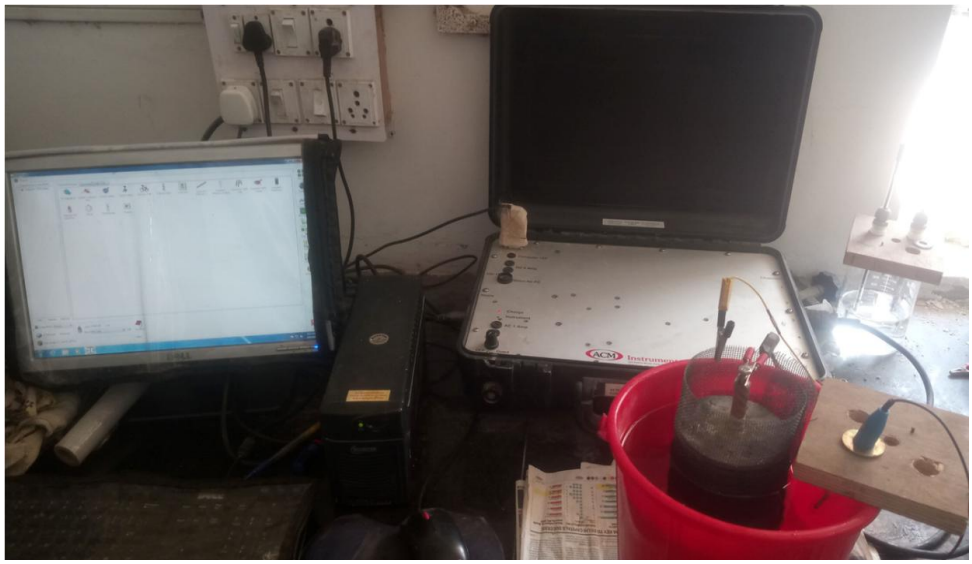

Figure 3.7 Experimental arrangement of corrosion analyzer to monitor rebar corrosion

Test procedure

- For conducting linear polarization resistance measurement, a stainless steel mesh rolled around reinforced cylinders was used as the counter electrode. Concrete specimen with steel mesh as a cathode were placed in a bucket containing 5% NaCl solution.
- The steel reinforcement inside the concrete cylinder as a working electrode with screw was connected with wire using alligator clip with corrosion analyzer.
- A saturated calomel electrode (SCE) connected to corrosion analyzer was dipped in NaCl solution and was used as a reference electrode.
- For LPR measurement, steel rebar as working electrode was polarized to ± 25mV from the equilibrium potential at a scan rate of 0.2 mV per second.

- The polarization resistance (Rp) values obtained were converted into corrosion current by using the Stern-Geary equation (Stern and Geary, 1957)

Calculations $I_{corr} = \frac{B}{R_p}$

Where:

I_{corr} = Corrosion current

B = Stern-Geary constant

R_p is the polarization resistance

$$B = \frac{\beta_a \times \beta_c}{2.30\ (\beta_a + \beta_c)}$$

βa and βc are anodic and cathodic Tafel constants respectively.

Table 3.8 provides a qualitative and quantitative relationship between the corrosion potential (E_{corr}) and corrosion current density (I_{corr}) results of the specimens respectively with the ASTM guidelines (ASTM C 876-09).

Table 3.8 Indication of severity of rebar corrosion conditions based on corrosion potential (E_{corr}) and corrosion current (I_{corr})

E_{corr} (mV) vs SCE	**Corrosion condition**	**I_{corr} (µA/cm^2)**	**Corrosion severity**
> -125	Low (10% risk of corrosion)	<0.1	Passive condition
-126 to -275	Increased likehood	0.1–0.5	Low to moderate corrosion risk
< -276	High (<90% risk of corrosion)	0.5–1	Moderate to high corrosion risk
< -426	Severe corrosion	>1	High corrosion condition

3.7 Crack remediation in concrete structures using microbial cementitious grouting

Early age formation of cracking in concrete structure severely affects the serviceability leading to high cost of maintenance. Apart from conventional methods of repairing cracks, a microbial crack-healing approach has shown promising results. Main emphasis in this section has been laid on crack repair in concrete structures by using bacteria-based cementitious grouts.

3.7.1 Preparation of grout mixture

In this experiment, bacterial based cementitious grout was prepared for crack repair in the concrete structures. For cementitious grout, an ordinary Portland cement (43 Grade) confiirming to Indian standards (IS: 8112-2013) was used. In this study, binary combination of cementitious

grout was used for crack repair. In cement grout, cement was substituted with different ratios of fly ash (10% to 50%) by total mass of cement. The influence on the incorporation of fly ash with different substitution ratios as well as different water/bacterial culture-binder ratios (0.45 and 0.50) on the fresh properties of grout mixtures was investigated. Grout mix prepared with plain cement is denoted as control grout. Different cement grout mixes prepared with water are denoted as neat grouts and the cement grout mixes prepared with bacterial culture are denoted as bacterial grouts. To prepare bacterial based cementitious grout, bacterial culture was prepared by growing the cells in NB medium till it attained the $O.D_{600}$, of 0.5 (4×10^8 cells/ml).

For the preparation of grout, hobart-type laboratory mixer (AIMIL India Ltd, New Delhi) was used to mix cement and fly ash as shown in Figure 3.8.

Figure 3.8 Hobart-type laboratory mixer to prepare fly ash amended cemetitious grout

A standard procedure was followed in which cement and fly ash was dry mixed for 1 minute in the mixer operating at slow speed (140±5 rpm). Then the water was added into the mixer with dry composite of cement and fly ash material and the mixer was operated for next 1 minute at slow speed and thereafter the speed of mixer was increased immediately for next 30 seconds. In case of bacterial based cementitious grout, bacterial culture was added into the mixer instead of water. The mixer was stopped for 90 seconds and the cementitious grout was hand mixed properly in the mean time. Further, the mixer was operated for the last 1 minute at high speed

(285±5 rpm). Twenty four grout mixtures were prepared to study the fresh properties with marsh cone test and mini slump. All the tests were conducted within 10 to 12 minutes after the preparation of grout.

3.7.2 Fresh properties of cementitious grout

3.7.2.1 Marsh cone test

Marsh cone test is a workability test through which the flow characteristic of a grout is evaluated. Marsh cone test was conducted as per ASTM standard (ASTM C 939-10) on a metallic funnel that has a capacity of 1,500 cm^3 with a fixed orifice at the end of the funnel, which is 50mm long by 4.7 mm in diameter (Figure 3.9).

Figure 3.9 Marsh cone apparatus to study the flowability of grout

The prepared grout mix was poured in the marsh cone which is attached to a stand and the bottom orifice of cone is closed. 1000 ml of grout filled in marsh cone was allowed to pass through the bottom outlet and collected in the beaker placed underneath the marsh cone apparatus. The efflux time needed for 800 ml of grout mix to flow out through the orifice was noted as the flow time.

3.7.2.2 Mini slump test

It is a miniature slump test devise to evaluate the workability of fresh cementitious paste in which small size cone is used and spread diameter of paste on lifting the cone is calculated. Mini slump test was done on mini slump cone with dimensions of top diameter 19 mm, bottom

diameter 38 mm and height 57 mm. This mini slump cone dimensions are in the same proportions as that are of slump cone of concrete (ASTM C-143) and was proposed by kantro, (1980). In this experiment, freshly prepared cementitious grout was poured in mini cone resting over a glass. The mini slump cone was filled completely and a small spatula was moved laterally and vertically to remove the entrapped air bubbles. Then the slump cone was lifted and the grout mix was allowed to spread. The mini slump area was calculated as the total spread area minus the initial area at the bottom of the mini slump cone. Several spread diameters of grout were noted and the average flow diameter was calculated.

3.7.2.3 Compressive strength of hardened grout mixes

The compressive strength development in the various FA amended cementitious grout mixes was monitored, using cubic specimens with 50 mm x 50 mm x 50 mm dimensions at the age of 28 day curing according to ASTM standard (ASTM C942-15). For the preparation of different grout mixes, similar procedure was adopted as mentioned in section 3.3.1. For bacterial grouts mixes, bacterial culture supplemented with 2% urea (w/v) and 25 mM $CaCl_2$ (w/v) was used instead of water. After casting, all specimens were allowed to remain in iron moulds and were kept in casting room at room temperature of 27 ± 2 °C for 24 h. Thereafter, the specimens were demoulded and were cured till the testing age. Cube specimens prepared with neat grout mixes were cured in water and cubes prepared with bacterial grout mixes were cured in bacterial culture supplemented with 2% urea (w/v) and 25 mM $CaCl_2$ (w/v).

3.7.3 Artificial crack generation in concrete

Control concrete cubes (100 mm x 100 mm x 100 mm), concrete prisms (285 mm x 75 mm x 75 mm) and concrete cylinder disc (100 mm diameter x 50 mm height) were prepared by using cement: sand: coarse aggregate in the ratio of 1:1.82:3.24 (w/w) and water to cement ratio (w/c) of 0.5. Artificial cracks were generated in all the concrete specimens while casting. When the fresh concrete mix in plastic stage was transferred to iron moulds, a steel plate was inserted in the mix. Steel plate of 0.8 mm width was inserted in the concrete mix up to the depth of 20 mm. To keep the crack depth in the range of 20 mm, steel plates were marked accordingly prior the insertion. After insertion of steel plates, specimens were monitored properly till the final setting of concrete mix was initiated. Then the steel plates were removed carefully from the concrete mix so that the concrete around the crack remain intact. After casting, all specimens were

allowed to remain in iron moulds and were kept in casting room at room temperature of 27 ± 2 °C for 24 h. Thereafter, the specimens were demoulded and were cured till the testing age.

3.7.4 Crack repair with grouting

To repair the concrete crack, 100 ml of bacterial based cementitious grout supplemented with 2% urea (w/v) and 25 mM calcium chloride solution (w/v) was prepared and all the cracked concrete specimens were repaired with injectable grouts using a 20 ml capacity syringe. In the crack repair experiment, two methods to heal the crack with bacterial cementitious grout were adopted. In first approach, cracked concrete specimens were placed in horizontal position and the prepared grout was injected into the crack. In second approach, concrete specimens were placed in vertical position and the grout was injected into the crack. Before injecting the concrete specimens with the bacterial cementitious grout, 20 ml of water was injected in each crack, using the 20 ml capacity syringe. This procedure was intended to mitigate the water sorption by the internal cracked concrete surface. After injecting the bacterial incorporated grout, specimens were left for 24 hours till the hardening of grout. Thereafter, different sets of repaired concrete specimens as specified in Table 3.9 were subjected to curing for two weeks.

Table 3.9 Outline of different sets of concrete specimen and mechanism of curing treatment

Specimens	**Grouting material**	**Curing regime**
Untreated concrete (UTC)	Without grouting	-
Fly ash-cement grout (FCG)	FA - Cement grout Water/Binder ratio = 0.5	Water curing of cracked area for 14 days
Bacterial grout with spray treatment (BGS)	FA - Cement grout Bacterial culture/Binder ratio = 0.5	Bacterial spray on repaired crack area twice a day till 14 days
Bacterial grout with ponding treatment (BGP)	FA - Cement grout Bacterial culture/Binder ratio = 0.5	Ponding with bacterial culture supplemented with 2% urea and 25 mM $CaCl_2$ till 14 days

The schematic representation of bacterial treatment of crack in concrete specimens is shown in Figure 3.10.

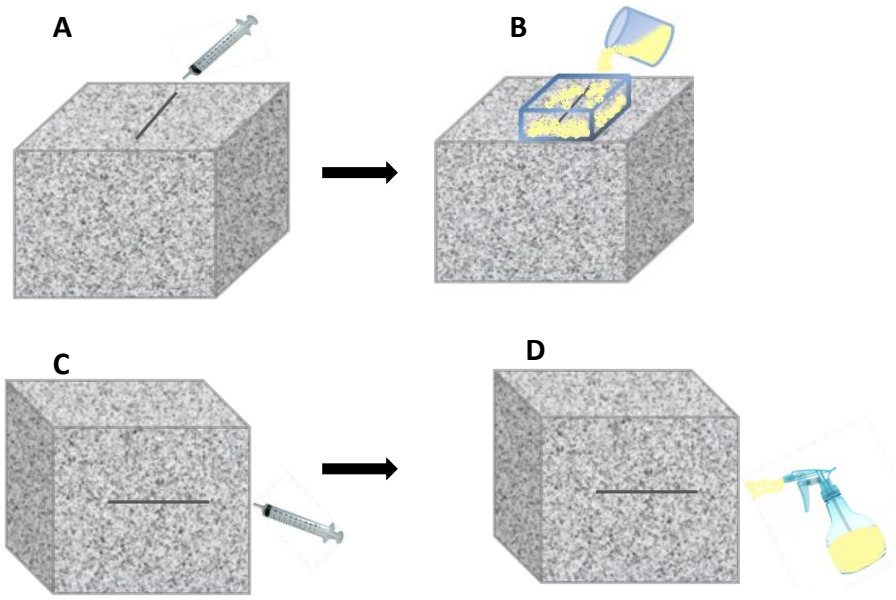

Figure 3.10 Schematic illustration of remediation of cracks with injectable bacterial grout and curing with bacterial culture (A-B) Bacterial grout with ponding treatment (C-D) Bacterial grout with spray treatment

In repaired concrete specimens placed in horizontal position, ponding of acrylic fibers surrounding the cracked area was created. However, in repaired concrete specimens placed in vertical position, curing was done by bacterial culture spray. Before this curing method, only repaired crack surface was exposed for bacterial spray and rest the surface of concrete was wrapped with parafilm tape. For the curing of treated crack, bacterial culture supplemented with 2% urea and 25 mM $CaCl_2$ was poured over the pond area as well as spray shown in Figure 3.11.

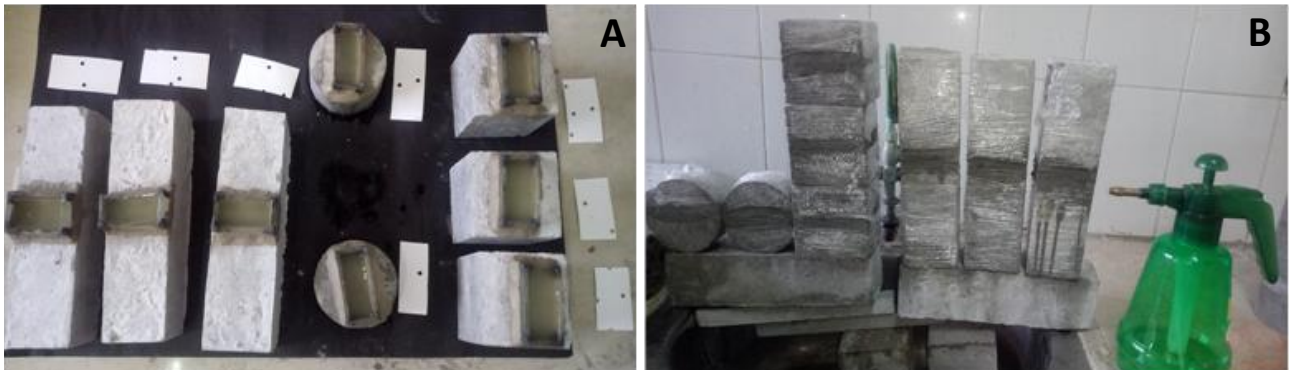

Figure 3.11 Curing of treated cracks with bacterial culture (a) Ponding method (b) Spray treatment

3.7.5 Testing methods

3.7.5.1 Compressive strength

To study the compressive strength, untreated and bacterial grout repaired concrete cubes were used. The effect of crack repair with bacterial grouts and curing with ponding and spraying methods with bacterial cells grown in NB medium supplemented with 2% urea and 25 mM $CaCl_2$ on the mechanical properties of concrete cubes was studied at the age of 14 days of curing as per Indian standard (IS 516: 1959) using automatic compression testing machine, COMPTEST 3000. The average of three specimens was taken as the compressive strength of the mix.

3.7.5.2 Flexural strength

To study the efficiency of bacterial treatment in flexural strength recovery, untreated and bacterial grout repaired concrete prisms were used. Flexural strength test of all concrete prisms was carried out using the flexural testing machine (AIMIL India Ltd, New Delhi) according to Indian standard (IS: 516-1959) as shown in Figure 3.12. In order to perform flexural strength test, concrete prism were placed on the supporting rollers of testing machine and uniform loading was applied to uppermost surface of specimen until the failure.

Figure 3.12 Flexural testing machine with arrangement of concrete prism in between supporting and loading rollers

The flexural strength of specimen is expressed as the modules of rupture f_b, which is calculated as:

$$f_b = \frac{3 \text{ x } p \text{ x } a}{b \text{ x } d^2}$$

Where

a = distance between the line of fracture and nearer support (mm)

b = width of specimen (mm)

d = depth of specimen at the point of failure (mm)

p = maximum load in kilo Newton (KN)

3.7.5.3 Water tightness of repaired crack

The efficiency of bacterial grouting in resistance towards water penetration was investigated. To determine the water tightness property of healed concrete specimens, sorptivity test was conducted on a crack repaired concrete cylinder disc. Sorptivity test was conducted according to ASTM standard (ASTM C1585) following the same procedure as described earlier. However, a modification was done in the exposed surface area of concrete disc. Apart from the choosing entire circular surface area of disc, only localized water ingress around the repaired crack area was selected by covering the entire concrete disc area with epoxy sealant (Figure 3.13).

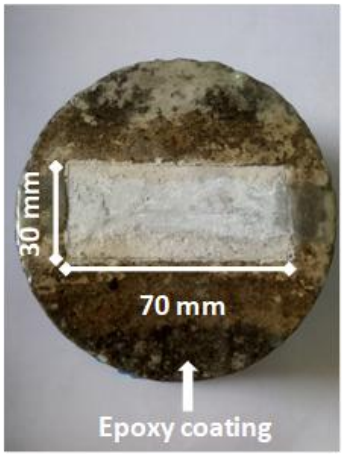

Figure 3.13 Exposed crack repaired area in concrete disc for water tightness analysis

Therefore, only the area (70 mm x 30 mm) surrounding the crack repaired with grouting was in contact with the water throughout the test. The mass change due to the absorbed water was monitored at the regular intervals of 60 s, 5 min, 10 min, 20 min, 30 min, 60 min and every hour up to 6 hours.

3.7.6 Micro-structural analysis

For analyzing the microbial induced calcium carbonate crystals in grouting material after the curing age of 14 days, scanning electron microscopy (SEM) (ZEISS EVO 50) was done. The elemental composition of micro-structural crystals was identified with energy dispersive X-ray spectroscopy (EDX). For conducting SEM and EDX analyses, small pieces of grouting samples were collected. Samples were finely polished and gold-coated with a sputter coating. To disperse excess charge from the sample, a thin coating of carbon was applied on the polished surface. X-ray diffraction (XRD) was done on the powdered grout samples, obtained while drilling and sieved through 90 μm sieve. XRD spectrum was obtained using Bruker D8 X-ray diffractometer with a Cu anode (40 kV and 30 mA) and scanning from 10° to 80° 2θ.

3.8 Statistical analysis

All the experiments were performed in triplicates. One-way analysis of variance was performed and the means were compared with Tukey's test at $P < 0.05$. All the analyses were performed by using Graph Pad Prism 5.1 software.

RESULTS AND DISCUSSION

Chapter 4

Results and Discussion

4.1 The role of bacteria and material mix on the durability properties of reinforced concrete structures

Microbially induced calcium carbonate precipitation (MICP) using calcifying bacteria have emerged as a promising technique in the field of concrete research. In this microbial treatment of concrete structures, different media components (especially nutrient media, urea and calcium source) were mixed along with ureolytic bacterial culture during the formation of microbial concrete. In the present investigation, influence on the addition of bacterial culture and organic components (carbon and nitrogen content) of bacterial growth media on the setting characteristics of cement, chemical and structural properties of microbial concrete was studied. In this objective two bacterial growth media were used: (1) Commercially available laboratory grade nutrient broth (NB) and (2) corn steep liquor (CSL), an industrial effluent generated as a by-product from the starch industry. On comparison, laboratory grade NB is a culture media with well defined growth components containing all the elements needed for the bacterial growth. Besides, production of bacterial culture using NB media is relatively an expensive process due to its high cost as compared to CSL media. However, CSL is a very low-cost, easily available and high protein containing industrial effluent which can be used as an alternative nutritional source for bacterial growth. To minimize the operating cost of MICP and to examine the chemical and structural properties of microbial concrete, addition of CSL as a bacterial growth media was investigated in this study.

4.1.1 Initial and final setting times of cement mixes

In preliminary investigation, a comparative study was conducted to figure out the influence of bacterial culture grown in nutrient broth (NB) and corn steep liquor (CSL) on the setting property of cement. Setting of cement is an early-age development in concrete mix while casting. It is described as the stiffening of cement through percolation process, which consists of two fundamental steps: (1) the coagulation of isolated cement grains during water mixing and (2) rigidification of cement hydrates formed during coagulation process (Zhang et al. 2010). Setting of fresh portland cement concrete is a process of transformation from loss of workability in to early hardening of cement paste or concrete (Hu et al. 2014). The specific change on initial and

final set times due to the addition of microbial cells along with the associated nutrients on the resultant cement pastes is presented in Table 4.1.

Table 4.1 Effect of NB, CSL media and bacterial cells on cement setting properties

Cement Mixes	Initial setting time (min)	Final setting time (min)
Control paste	118±5.1a	230±7.7a
CSL paste	132±12.2a	255±10.2b
NB paste	215±9.4b	480±14.2c
CSL - CT5 paste	140±8.2a	270±8.1b
NB - CT5 paste	160±9.2c	290±12.4d

Values sharing a common letter within the treatment are not significant at $P < 0.05$. Values are mean ± standard deviation (n = 3)

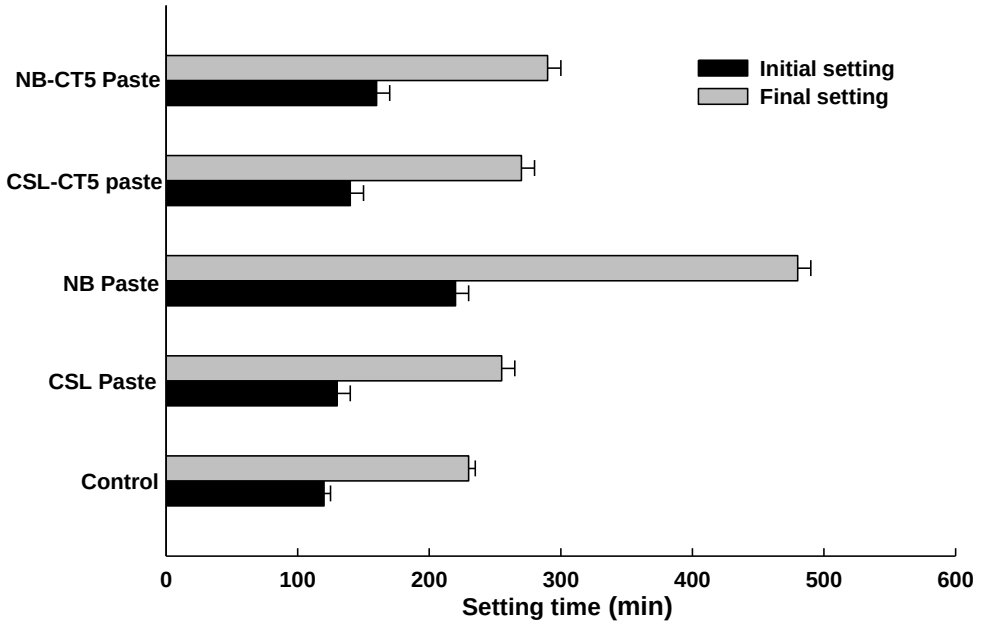

Figure 4.1 Initial and final setting times of different cement paste mixes. Error bars represent standard deviation (n = 3)

The initial and final setting time of control paste mix was 120 and 240 min, respectively as shown in Figure 4.1. On comparison with control paste mix, no delay in initial and final setting was observed in CSL paste mix. However, a significant delay in both initial and final setting time was observed in NB paste mix. Initial setting time was increased by 100 minutes and the final setting time by 250 minutes in NB paste mix when compared to control paste mix. In CSL-CT5 paste mix, an increase of 20 min in initial setting and 30 min in final setting time was recorded as compared to control paste. In case of NB-CT5 paste mix, the initial setting time was increased by 40 min and final setting time by 50 min when compared to control paste. On comparison with control paste, negative effect on initial and final setting time of NB paste was observed with introduction of plain NB media in cement paste. But in NB-CT5 paste, incorporation of bacterial cells grown in NB media had minor influence on the retardation of setting property of cement. On comparison of NB-CT5 paste with NB paste, delayed cement setting might had been compensated with the utilization of fresh NB media during growth of bacterial cells and calcium carbonate precipitation. Addition of plain CSL media had no influence on the initial and final setting time of cement paste. In CSL-CT5 cement paste, addition of bacterial cells showed no retardation in setting characteristics of cement. In fact, the presence of organic admixtures (carbohydrates and amino acids) has been reported to have an adverse effect on the chemical properties of cement resulting into retardation of initial hydration of cement (Young, 1972; Neville, 1995). Clare and Sherwood (1954) reported that the retardation in setting of cement due to organic admixture prevents the cement hardening. Retardation of setting process of soil-cement mixtures due to organic matter have also been reported. It has been reported that the presence of organic matter in soil-cement mixtures delay the hydration process of cement, thus affecting the cementing process (Tremblay et al. 2002). Organic compounds with hydroxyl and carboxyl groups may retard the hardening of cement. In NB cement paste, nutrient media contains yeast extract and it has been reported that yeast extract acts as a retardation substance and influence the degree of hydration of cement (Williams et al. 2016). Presence of different fractions of carbohydrates in yeast extract might be the effective chemical retarders (Thomas and Birchall, 1983; Bundur et al. 2015). Amiri and Bundur (2018) also reported the delay in initial setting in urea-yeast extract media as compared to CSL and control samples. It was reported that carbohydrate strongly affects the silicate component and retards the hardening of portland cement (Bolobova and Kondrashchenko, 2000). Presence of 4 times higher carbohydrate content

in NB media as that of CSL media acts as a retarding component in cement hardening. However, low carbohydrate content in CSL might have not affected the cement hydration. All these observations indicate that the addition of plain CSL media had no influence on the setting characteristics of cement. Whereas the addition of plain NB media severely influenced the setting characteristics of cement. Incorporation of bacterial cells with CSL media showed an inconsequential effect on the setting characteristics. Addition of bacterial cells grown in NB media causes not as much of delay in setting of cement as it was observed in NB paste. In fact, in NB-CT5 paste, addition of bacterial cells grown in NB media accelerated the cement setting time as compared to the NB paste.

4.1.2 Influence of bacteria and material mix on chemical properties of concrete

The effect of addition of microbes and nutrient components on chemical and mechanical properties of resultant concrete was investigated. To induce $CaCO_3$ precipitation in microbial treated concrete, nutrient ingredients along with bacterial cells were added to concrete mixes while casting or during curing treatment. Addition of CSL and NB media might alter the chemical composition of concrete matrix as in both the media; carbon and nitrogen components are present. For the vegetative growth of bacteria, nutrient media are required to be added along with bacteria. The components required for ureolytic bacterial strain are growth media, urea and calcium source. The incorporation of bacteria along with the associated nutrients can cause modifications in the concrete matrix, and hence affects the properties of the mixes.

4.1.2.1 Carbon and nitrogen profile

Different organic components (especially carbon, nitrogen sources) of NB and CSL media are mixed along with bacteria during the formation of microbial concrete. These components might influence the structural properties of concrete. The presence of high carbon content is known to have adverse effects on the workability, air entrainment mechanism, compressive strength etc. (Neville, 1996). Therefore carbon and nitrogen content at 28 days of casting with respective curing was obtained at different depths in concrete specimens. The results of carbon and nitrogen content in concrete specimens with depth-wise profiling are presented in Table 4.2 and Table 4.3 respectively.

Table 4.2 Depth wise representation of carbon content (% by mass) in concrete specimens on addition of CSL media, NB media and bacterial culture

Depth (mm)	Control	NT	CT	NBAT	CBAT	NBST	CBST
0-10	0.08±0.002b	0.22±0.03a	0.13±0.01a	0.29±0.06a	0.18±0.03a	0.23±0.02a	0.10±0.01a
10-20	0.07±0.001c	0.18±0.02b	0.13±0.02a	0.23±0.04b	0.14±0.01b	0.19±0.01b	0.07±0.01c
20-30	0.09±0.002a	0.17±0.02c	0.12±0.01b	0.20±0.04b	0.13±0.01c	0.17±0.02c	0.07±0.01c
30-40	0.09±0.002a	0.17±0.01c	0.12±0.01b	0.17±0.03c	0.14±0.01b	0.17±0.02c	0.08±0.01b
40-50	0.09±0.001a	0.17±0.01c	0.11±0.01c	0.17±0.04c	0.12±0.01c	0.17±0.01c	0.08±0.01b

Values sharing a common letter within the column are not significant at $P < 0.05$ respectively. Values are mean ± standard deviation (n = 3)

Table 4.3 Depth wise representation of nitrogen content (% by mass) in concrete specimens on addition of CSL media, NB media and bacterial culture

Depth (mm)	Control	NT	CT	NBAT	CBAT	NBST	CBST
0-10	0.02±0.001a	0.12±0.03a	0.09±0.002a	0.15±0.02a	0.12±0.01a	0.06±0.01a	0.06±0.01a
10-20	0.02±0.001a	0.10±0.02b	0.09±0.002a	0.12±0.01b	0.09±0.02b	0.05±0.01b	0.03±0.01b
20-30	0.02±0.002a	0.11±0.02b	0.09±0.001a	0.11±0.001c	0.09±0.01b	0.03±0.01c	0.03±0.01b
30-40	0.02±0.002a	0.08±0.01c	0.09±0.001a	0.10±0.001c	0.09±0.01b	0.03±0.01c	0.03±0.01b
40-50	0.02±0.001a	0.08±0.01c	0.09±0.001a	0.10±0.001c	0.09±0.01b	0.02±0.01c	0.02±0.01c

Values sharing a common letter within the column are not significant at $P < 0.05$ respectively. Values are mean ± standard deviation (n = 3)

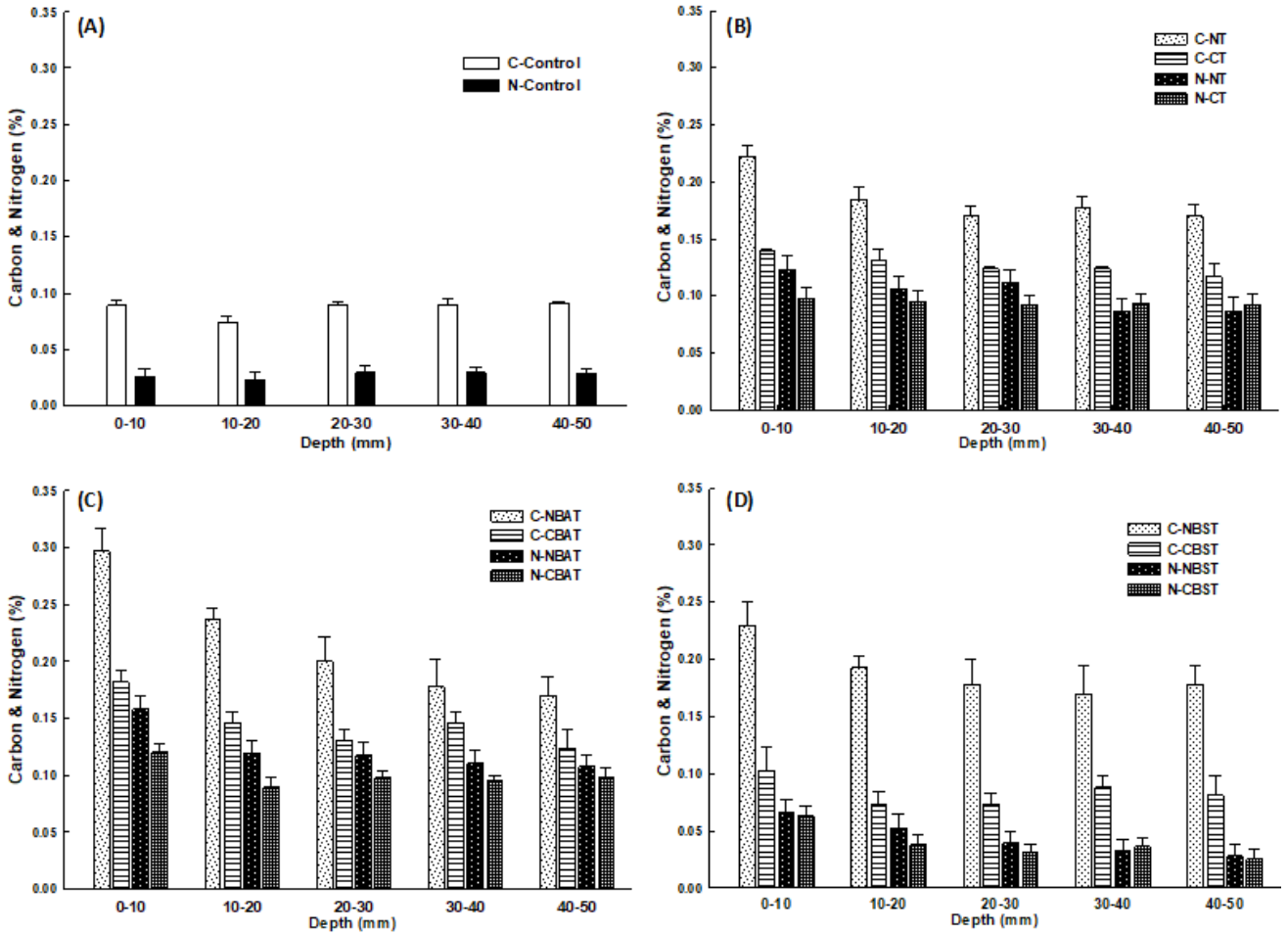

Figure 4.2 Carbon and nitrogen content (% by mass) of concrete specimens at different depths in various treatments. C: Carbon content; N: Nitrogen content (A) Control (B) NT: NB treated; CT: CSL treated (C) NBAT: NB-Bacterial admixed treated; CBAT: CSL-Bacterial admixed treated (D) NBST: NB-Bacterial spray treated; CBST: CSL-Bacterial spray treated. Error bars represents standard deviation (n = 3)

Comparative analysis of organic matter present in the form of carbon and nitrogen content in all the concrete specimens treated with CSL and NB media was done (Figure 4.2). It was observed that the percentage of carbon and nitrogen content remains same at all depths for the control specimen (Figure 4.2A). The percentage of carbon and nitrogen content was lowest for the control specimen at all depths. CSL-Bacterial admixed treated (CBAT) and NB-Bacterial admixed treated (NBAT) specimens registered maximum carbon and nitrogen content at all depths. The carbon and nitrogen content in CSL-Bacterial spray treated (CBST) and NB-Bacterial spray treated (NBST) specimens was maximum in the upper depths (0–20 mm) followed by almost same at all depths (Figure 4.2D). However, overall carbon and nitrogen content in NBAT and NBST specimens was observed to be much higher than CBAT and CBST specimens at all depths. Similar trend of overall carbon and nitrogen content was observed to be higher in NB treated (NT) specimen on comparison with CSL treated (CT) specimen at all depths (Figure 4.2B).

Both carbon and nitrogen contents in NT and CT specimens were higher than the corresponding values of the control mix (Figure 4.2B). During bacterial treatment, highest amount of carbon and nitrogen content was observed in NBAT and NBST specimens as compared to CBAT and CBST specimens in all the depths respectively (Figure 4.2C and 4.2D). In bacterial admixed (NBAT and CBAT) as well as bacterial spray treated (NBST and CBST) specimens, higher contents of both carbon and nitrogen in upper depths (0-10 mm and 10-20 mm) were observed. This might be due to the additional accumulation of curing material and bacterial cells on the outer surface. In case of NT specimen, similar trend of higher amount of carbon and nitrogen content was observed than in CT specimen.

4.1.2.2 pH profile

The introduction of microbes into concrete leads to changes in its chemical composition and hence, might affect the alkaline nature of concrete pore solution. In microbial precipitation of calcium carbonate, there might be fluctuation in pH value in concrete because of the generation of carbon dioxide due to microbial respiration and ammonia due to enzymatic hydrolysis of urea (Stocks-Fischer et al. 1999). Therefore, in order to investigate effect of addition of microbes into concrete on alkaline nature, pH of the resultant mixes were measured at various depths, starting from the surface of concrete as shown in Table 4.4.

Table 4.4 Effect of bacterial and material mix on the depth wise pH profile in different samples

Depth (mm)	Control	NT	CT	NBAT	CBAT	NBST	CBST
0-10	12.19±0.002c	12.31±0.002a	12.30±0.002a	12.15±0.002b	12.20±0.002a	12.27±0.003a	12.14±0.001b
10-20	12.24±0.002b	12.16±0.002c	12.35±0.002a	12.06±0.001c	12.20±0.001b	12.25±0.002b	12.14±0.002b
20-30	12.27±0.001b	12.16±0.001c	12.32±0.003a	12.11±0.002b	12.22±0.002b	12.24±0.002c	12.26±0.002a
30-40	12.25±0.003b	12.28±0.001b	12.32±0.003a	12.26±0.002a	12.40±0.002b	12.24±0.003c	12.28±0.003a
40-50	12.30±0.002a	12.25±0.003b	12.38±0.001a	12.23±0.002a	12.36±0.002b	12.20±0.003c	12.30±0.003a

Values sharing a common letter within the column are not significant at $P < 0.05$ respectively. Values are mean ± standard deviation (n = 3)

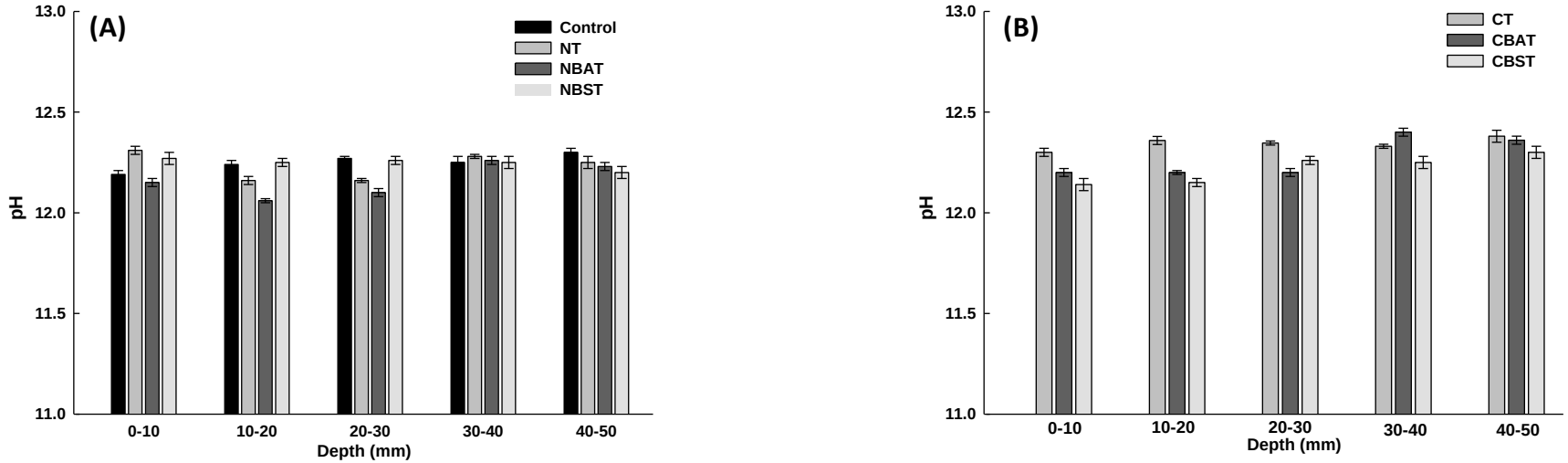

Figure 4.3 Depth wise estimation of pH for different concrete specimens. (A) Control; NT: NB treated; NBAT: NB-Bacterial admixed treated; NBST: NB-Bacterial spray treated (B) CT: CSL treated; CBAT: CSL-Bacterial admixed treated; CBST: CSL-Bacterial spray treated. Error bars represents standard deviation (n = 3)

pH is one of the most influential parameters in concrete durability and the alkaline condition of concrete with pH 12–13 keeps the reinforced steel resistant to corrosion (Behnood et al. 2016). The drop of pH of concrete destabilizes the passive state of steel which results into rebar corrosion and hence leads to premature deterioration of reinforced concrete (Huet et al. 2005). Alkaline environment of concrete was not influenced with addition of bacterial cells supplemented with either NB or CSL in this study (Figure 4.3). No significant variation in pH was observed in NT and CT specimens as compared to control specimens in this study and the pH was maintained above 12. In NBAT and NBST specimens, no fluctuation in pH value occurred due to microbial precipitation of calcium carbonate and pH was maintained above 12 (Figure 4.3A). Even in CBAT and CBAT specimens, no significant effect on pH value was observed (Figure 4.3B).

4.1.3 Influence of bacteria and material mix on mechanical and permeation properties of concrete

4.1.3.1 Compressive strength

The influence of microbial treatment on the strength properties of concrete cubes with bacterial culture as admixture and bacterial culture as a spray treatment was investigated. Microbial treatment and effect of NB/CSL media on the strength properties of concrete after 28 days of curing is presented in Table 4.5.

Table 4.5 Compressive strength of concrete specimens at the 28 days age of curing

Specimen	Compressive strength (MPa)
Control	36.2±1.2d
CT	34.0±1.1e
NT	29.4±1.6f
CBAT	45.2±0.8a
NBAT	46.6±2.2a
CBST	41.6±1.8b
NBST	39.2±2.4c

Values sharing a common letter within the treatment are not significant at $P < 0.05$.
Values are mean ± standard deviation (n = 3)

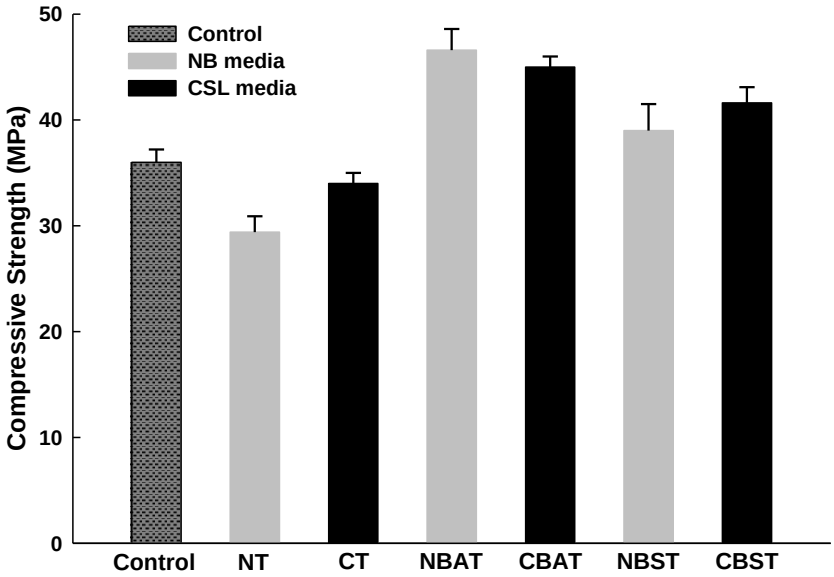

Figure 4.4 Influence of CSL media, NB media and bacterial culture on compressive strength (MPa) of concrete specimens at the age of 28 days curing. Error bars represent standard deviation (n = 3)

Compressive strength of control specimens was 36 MPa after 28 days of curing. Addition of bacterial culture grown in CSL/NB media along with urea-$CaCl_2$ in concrete specimen and curing with respective media for 28 days significantly increased the compressive strength compared to control specimen (Figure 4.4). The CBAT specimens showed an increase of 25% in compressive strength as compared to the control specimens. The CBST specimens in which bacteria were introduced into concrete after casting in the form of spray during curing also increased 16% in compressive strength compared to the control specimens. The NBAT specimens showed an average increase of 29% in compressive strength as compared to the control specimens. After 28 days of bacterial spray curing, slight increase in compressive strength (8%) as compared to the control mix was registered in NBST specimen (39 MPa). However, the compressive strength of NT specimen registered a drastic decrease by 19% compared to the control mix. It indicates that the addition of plain NB media of organic nature and urea-$CaCl_2$ into concrete leads to retardation in compressive strength development. In case of CT specimen, no significant effect on the compressive strength as compared to control specimen was observed. In case of mechanical properties of concrete, NT specimens casted with plain NB media showed drastic reduction in the compressive strength (Figure 4.4). The results of setting time and compressive strength indicates that the addition of organic matter (i.e., yeast

extract) alone has a retardation effect on hydration. The negative effect of introducing organic nutrients on the initial and final setting times of NB cement paste mix was also observed. Ersan et al. (2015) also reported a decrease in the compressive strength of a mortar specimen due to the presence of yeast extract. In bacterial admixed and bacterial spray treatment of concrete specimen with NB/CSL as bacterial growth media had shown effective compressive strength increase in both the curing regimes. The results indicated that the incorporation of bacterial cells along with nutrient media in concrete specimens lead to significant improvement in compressive strength of the mix. The increase of 29% in compressive strength was observed in NBAT; while in NBST specimens, marginal increase in compressive strength by 8% was observed. Therefore, it indicates that the adverse effect of introducing yeast extract into NBAT and NBST concrete specimens on hydration can be overcome by the calcium carbonate precipitation done by bacteria. In case of CBAT and CBST specimens, increase in compressive strength on comparision with control was obserevd to be 25% and 16% respectively. However, use of CSL as growth media had not shown any deleterious modifications in the concrete properties. Addition of CSL media had not altered the chemical and mechanical properties of concrete in this study. In previous studies, increase in compressive strength in specimens treated with bacteria grown in CSL as compared to control specimens was reported (Achal et al. 2010a). As the CSL is a nutritional supplement, it comprised rich, free amino acids and vitamins, which act as excellent growth stimulants for bacterial cells (Sharma et al. 2013). On comparing the effect of bacterial curing treatments on mechanical properties of concrete, it was observed that spray treatment by bacteria after casting of concrete leads to only marginal increase in compressive strength. It can be due to the fact that spray treatment is a surface treatment and may not alter the bulk concrete properties to a large extent. However, significant increase was registered in the bacterial admixed concrete (NBAT/CBST) and curing by submerging the concrete specimen in bacterial culture with supplementation of urea and $CaCl_2$ for biocementation. Another parameter that is altered by the addition of bacterial cells and the associated nutrients into concrete is its chemical composition. Both the carbon and nitrogen contents of all bacterial treated specimens were higher than the corresponding values of the control mix. It is obviously due to addition of organic matter and urea in the mixes as nutrient sources for bacteria. The highest amount of carbon content was observed in NBAT/CBAT specimens. It is reported that high carbon content due to addition of yeast extract and peptones present in growth media adversely affect the

compressive strength of the concrete mix (Jonkers et al. 2010). However, the highest compressive strength of NBAT/CBAT specimens indicates that the correlation between carbon content and compressive strength might not be true for bacterially treated concrete. The observed improvement in compressive strength despite of higher carbon content is due to successful calcium carbonate precipitation that helped in densifying the concrete matrix. Even, the high nitrogen content of NBAT and CBAT specimens, which is due to inclusion of urea in material mix at the time of casting had not influenced the compresive strength. The similar observation was reported in which urea addition had no statistically significant effect on the compressive strength of concrete (Pei et al. 2013). However, in NBST/CBST specimens, carbon and nitrogen content was observed to be quite low in the inner depths as compare to NBAT/CBAT specimens. It is due to the fact that the bacterial cells grown in NB/CSL media and supplementation of urea and $CaCl_2$ were sprayed regularly on the surface of concrete during curing process in NBST/CBST specimens. Due to this, the calcium carbonate precipitation at the upper surface blocked the pores of concrete, hence reducing the ingress of nutrients further inside the concrete matrix. The nutrient content has no significant effect on the compressive strength of the bacterial admixed or bacterial spray concrete mixes.

4.1.3.2 Permeation properties

Apart from strength improvement, emphasis was also given to analyze the impact of two different curing processes on permeation properties using NB and CSL as bacterial growth media. The permeation characteristics of bacterial treated specimens were studied with respect to three properties; sorptivity coefficient, RCPT and water impermeability after 28 days of curing and presented in Table 4.6. Among all the tested concrete mixes, control mix registered the highest sorptivity coefficient (0.02). The specimens treated with bacterial cultures grown in CSL media (CBAT and CBST) registered significantly lowest sorptivity coefficient followed by the specimens treated with bacteria grown in NB media (NBAT and NBST) as compared to control or media treated (NT and CT) specimens (Table 4.6). In both NT and CT specimens, sorptivity coefficients were recorded to be in the similar range of 0.014. In case of NBAT and NBST specimens, sorptivity coefficients were observed to be 0.008 and 0.007, which shows that bacterial precipitation of calcium carbonates significantly reduced the ingress of water. However, both CBAT and CBST specimens registered the lowest sorptivity coefficients (0.005). Sorptivity

test shows the water ingress into an unsaturated concrete, which is dominated by capillary suction and is an important parameter that can be correlated to the ingress of deteriorating substances (chlorides or sulfates) into concrete (McCarter et al. 1992). Sorptivity is a good measure of the quality of near surface concrete, which governs durability parameters related to rebar corrosion (Dias, 1995). The results from sorptivity test indicate that the transport mechanism of water in specimens through capillary rise was altered effectively in both the microbial treatment methods (bacterial admixed and bacterial spray).

Resistance of concrete to chloride ion penetration can be indirectly measured by RCPT. In RCPT, resistance to chloride ions penetration by all specimens was evaluated. Results from all specimens were compared with the control specimen shown in Table 4.6. In control specimen, the charge passed was 3180 coulombs and its permeability characteristics falls under moderate type. In NT and CT specimens, the charge passed was 2942 and 2838 coulombs respectively with moderate permeability type. Control specimens and media treated specimen's registered almost similar charge transfer resistance and falls in the category of moderate penetration type. While in NBAT specimen the total charge passed was 1204 coulombs and NBST specimens registered charge of 1340 coulombs. However, in CBAT specimen the total charge passed was 1228 coulombs and in CBST specimen it was 1310 coulombs. The charge transfer was significantly reduced in all specimens treated with bacteria and the penetration values fall in low penetration range (Table 4.6). In RCPT, similar trend of significant reduction to chloride ion penetration was observed in both curing treatments, as NBAT/CBAT and NBST/CBST specimens showed low permeability type (Table 4.6). Resistance to chloride ions penetration indicates the effectiveness of both curing treatments in concrete specimens. The movement of aggressive chemical ions with pore water present in the well-connected pore matrix of concrete leads to corrosion of rebar. The transport mechanism of deleterious substances is influenced by the pore distribution, pore number and pore size in the concrete (Basheer et al. 2001). In RCPT, results indicate the improvement in concrete permeability properties in both microbial treatment methods adopted, bacterial admixed treated (NBAT and CBAT) and the surface treated concrete with bacterial spray (NBST and CBST) which showed a significant resistance of chloride movement.

Table 4.6 Permeation properties of media and bacterial treated concrete specimens

Specimen	Sorptivity coefficient '*k*'[a]	RCPT		Water penetration (mm)[a]
		Mean charge passed (in coulombs)[a]	Penetration type[b]	
Control	0.020 ± 0.0[a]	3180 ± 127[a]	Moderate	30.2 ± 2.1[b]
CT	0.014 ± 0.0[b]	2838 ± 141[b]	Moderate	28.2 ± 3.2[b]
NT	0.014 ± 0.0[b]	2942 ± 148[b]	Moderate	31.2 ± 1.7[a]
CBAT	0.005 ± 0.0[d]	1228 ± 79[c]	Low	12.5 ± 1.5[c]
NBAT	0.008 ± 0.0[c]	1204 ± 95[c]	Low	14.2 ± 2.1[c]
CBST	0.005 ± 0.0[d]	1310 ± 58[c]	Low	13.9 ± 1.3[c]
NBST	0.007 ± 0.0[c]	1340 ± 62[c]	Low	13.6 ± 1.4 [c]

[a] Mean values sharing a common letter within the column are not significant at $P < 0.05$

[b] The range of charge for high (> 4000), moderate (2000–4000), low (1000–2000) and very low (100–1000) as per the ASTM C1202-12 standard

The water penetration depth defines the ease with which water can flow through concrete under a pressure differential. In this case also, the governing feature of ingress is capillary pores of concrete. Effect of calcium carbonate precipitation in bacterial mixed specimen and bacterial spray treated specimen indicated efficient resistance to water penetration. In water impermeability test, maximum vertical penetration of water was found in control specimen (30.2 mm) and NT specimen (31.2), while minimum penetration depth of 12.5 mm and 13.9 mm was measured in CBAT and CBST specimens. NBAT and NBST specimens also registered very low water penetration depth of 14.2 mm and 13.6 mm respectively. The water penetration in concrete matrix was effectively altered by microbial calcium carbonate precipitation. The reduction in pore number and pore size due to carbonate precipitation leads into reduced movement of water. It was observed in water permeability test that, the penetration of water into the pore matrix of concrete was significantly prevented due to the precipitation of calcium carbonate by bacteria. Biodeposition of calcite crystals acts as pore blocker which results into reduced pore number and pore size; leading into reduced movement of water in bacterial treated concrete specimens. It was observed that the application of bacterial spray treatment can effectively restrict the damage from the penetration of aggressive agents and can be used as natural water repellant. At field-scale application, curing with bacterial spray treatment will also help in the implementation of MICP technology as a repair procedure on existing structures to improve the surface permeability properties of concrete.

4.1.3.3 Micro-structural analysis

SEM and XRD analysis of all the concrete specimens was performed to characterize the calcium carbonate crystals. SEM analysis of all the concrete specimens was done by collecting samples from three different depths at the age of 28 days of curing. The SEM images of both NBAT and NBST specimens taken from the upper depth of 0–10 mm clearly shows the presence of calcium carbonate crystals associated with bacterial cells (Figure 4.5). In case of NBAT specimen, presence of different crystal lattice of calcium carbonate was found. Rhombohedral calcite crystal and needle shaped aragonite crystals were observed (Figure 4.5A and 4.5B). The EDX analysis also confirmed the elemental composition of crystals with peaks showing high amount of calcium and carbon.

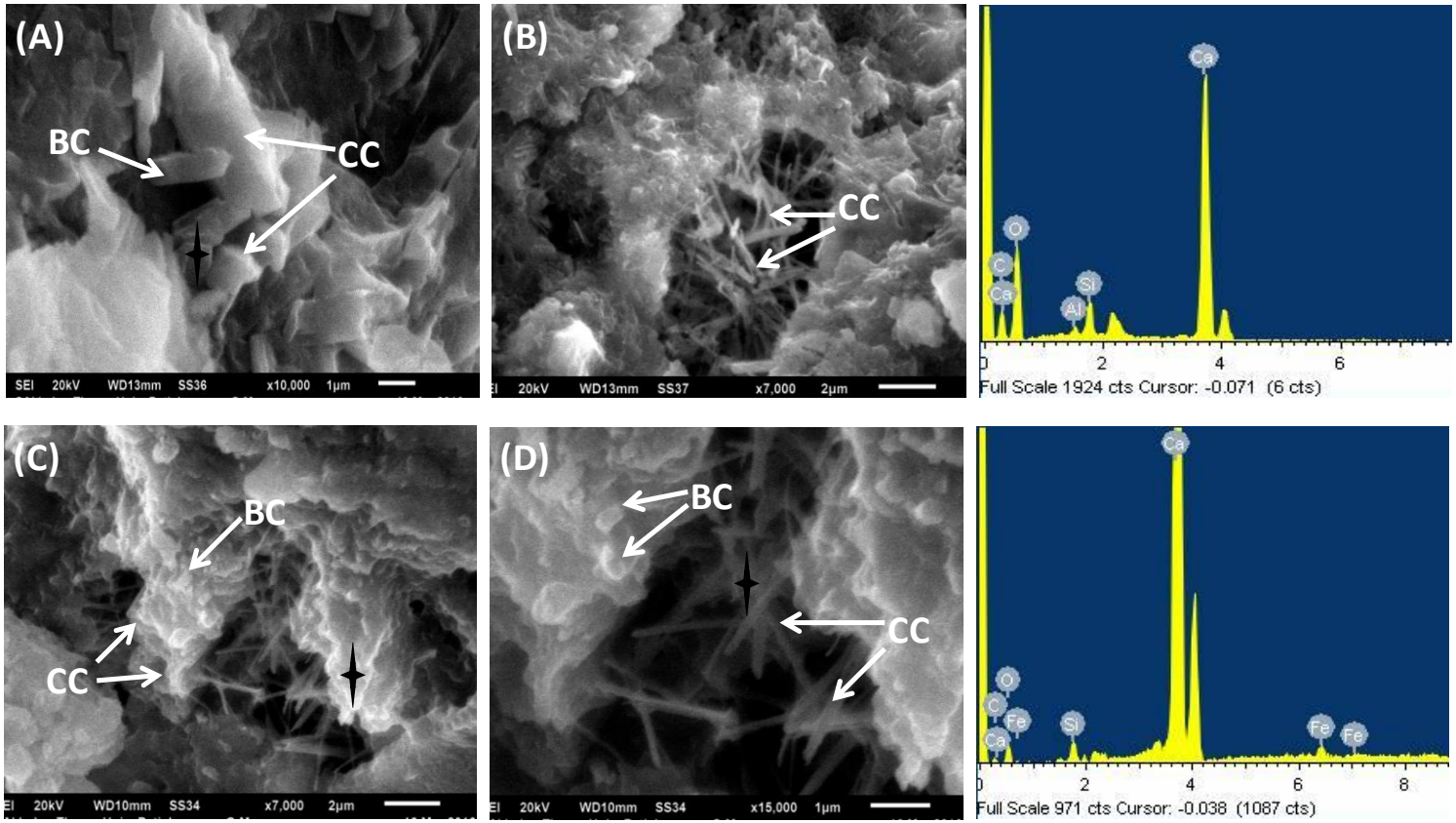

Figure 4.5 SEM images represent the $CaCO_3$ crystal (CC) associated with rod shaped bacterial cells (BC) at upper depth (0-10mm) in NB-Bacterial admixed treated (NBAT) specimen (A-B) and NB-bacterial spray treated (NBST) specimen (C-D). Arrows show calcium carbonate crystals and bacterial cells. '✦' shows the spots of EDX analysis

In NBST specimen, high biodeposition of calcium carbonate precipitation was observed. Morphology of rhombohedral calcite and aragonite crystals in association with bacterial cells was also identified (Figure 4.5C and 4.5D). The high peak of calcium on EDX analysis further confirmed the presence of calcium carbonate crystals. XRD analysis of NBAT and NBST specimens was performed by collecting the powder sample from the upper depth. XRD analysis of NBAT and NBST specimens is presented in Figure 4.6.

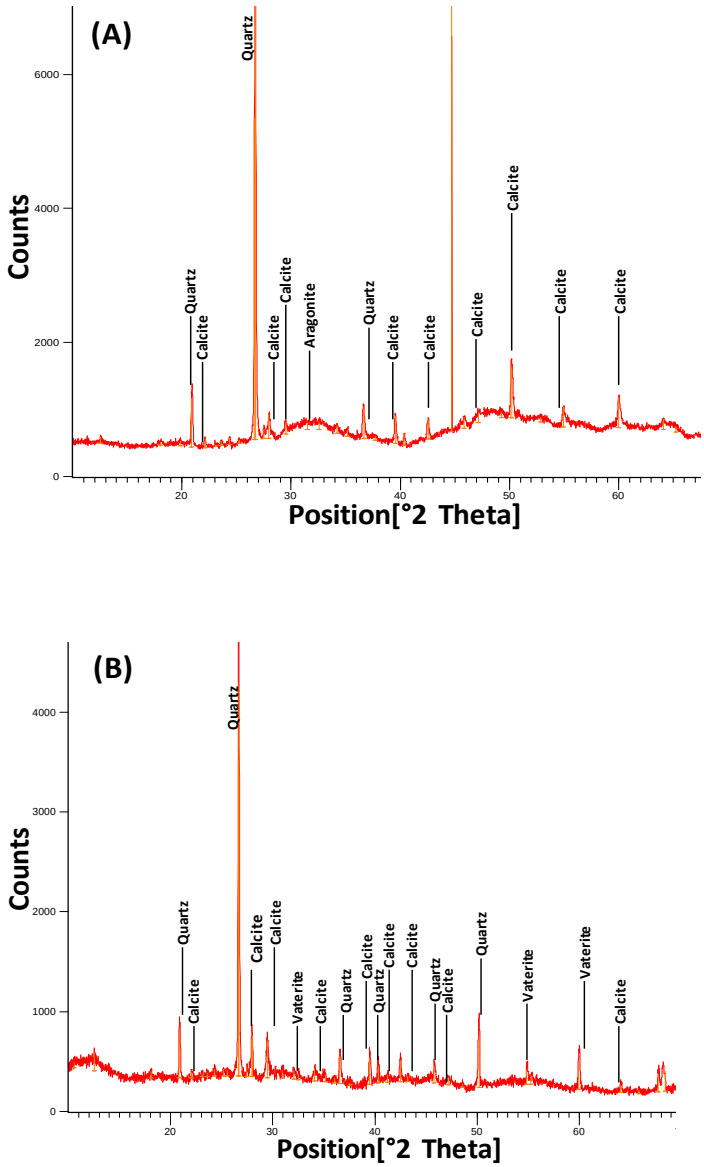

Figure 4.6 XRD patterns of NB-Bacterial admixed treated (NBAT) specimen (A) and NB-bacterial spray treated (NBST) specimen (B) depicts calcite ($CaCO_3$) as predominat crystalline phase. Crystalline phases of argonite and vaterite (polymorphs of $CaCO_3$) were also observed

Presence of calcite crystals in upper depth of NBAT and NBST specimens were confirmed with predominant peaks as shown in Figure 4.6A and Figure 4.6B respectively. Apart from calcite, argonite and vaterite polymorphs of calcium carbonate crystals were also confirmed. In the upper depth (0-10 mm) of NBAT specimen, apart from thick deposition of calcite and needle shaped aragonite crystals, different morphology of calcium carbonate crystals with multinodular structure having micro needles was also observed (Figure 4.5A and 4.5B). On EDX analysis, the peak of calcium, carbon and oxygen was observed. The micro needles morphology might be due to presence of some magnesium impurities in the tap water used while curing. Similar calcium carbonate crystal formation was reported on addition of magnesium (Xie et al. 2005). Formation of micrite calcite with mirconeedles due the distortion of sideward growth of calcite under the influence of magnesium ions has also been reported (Folk, 1974). In NBST specimens, presence of mucous matrix on the closely attached rhombohedral calcite and aragonite carbonate crystals along with bacterial cells due to exopolymeric substances (EPS) was observed in the upper depth (Figure 4.5C and 4.5D). Important role of EPS in cell adhesion and calcium carbonate precipitation was reported (Bains et al. 2015).

SEM images of both CBAT and CBST specimens taken from the upper depth (0–10 mm) are presented in Figure 4.7. SEM–EDX analysis of bacterial treated specimens showed the presence of dense deposition of bacterial mediated precipitation of calcium carbonate. In case of CBAT specimen, presence of different crystal lattice of calcium carbonate was found. Rhombohedral calcite crystal and spheroid vaterite crystals were observed (Figure 4.7A and 4.7B). The EDX analysis also confirmed the elemental composition of crystals with peaks showing high amount of calcium and carbon. Formation of different kind of morphology of calcium carbonate crystals depends on composition and minerology of the substrate. Calcitic substrate promotes the growth of bacterial calcite while silicate substrate promotes the formation of spherulitic vaterite (Rodriguez-Navarro et al. 2012). In CBST specimen, presence of dense biodeposition of closely attached rhombohedral calcite crystals was observed (Figure 4.7C and 4.7D). The high peak of calcium and carbon on EDX analysis further confirmed the presence of calcium carbonate crystals.

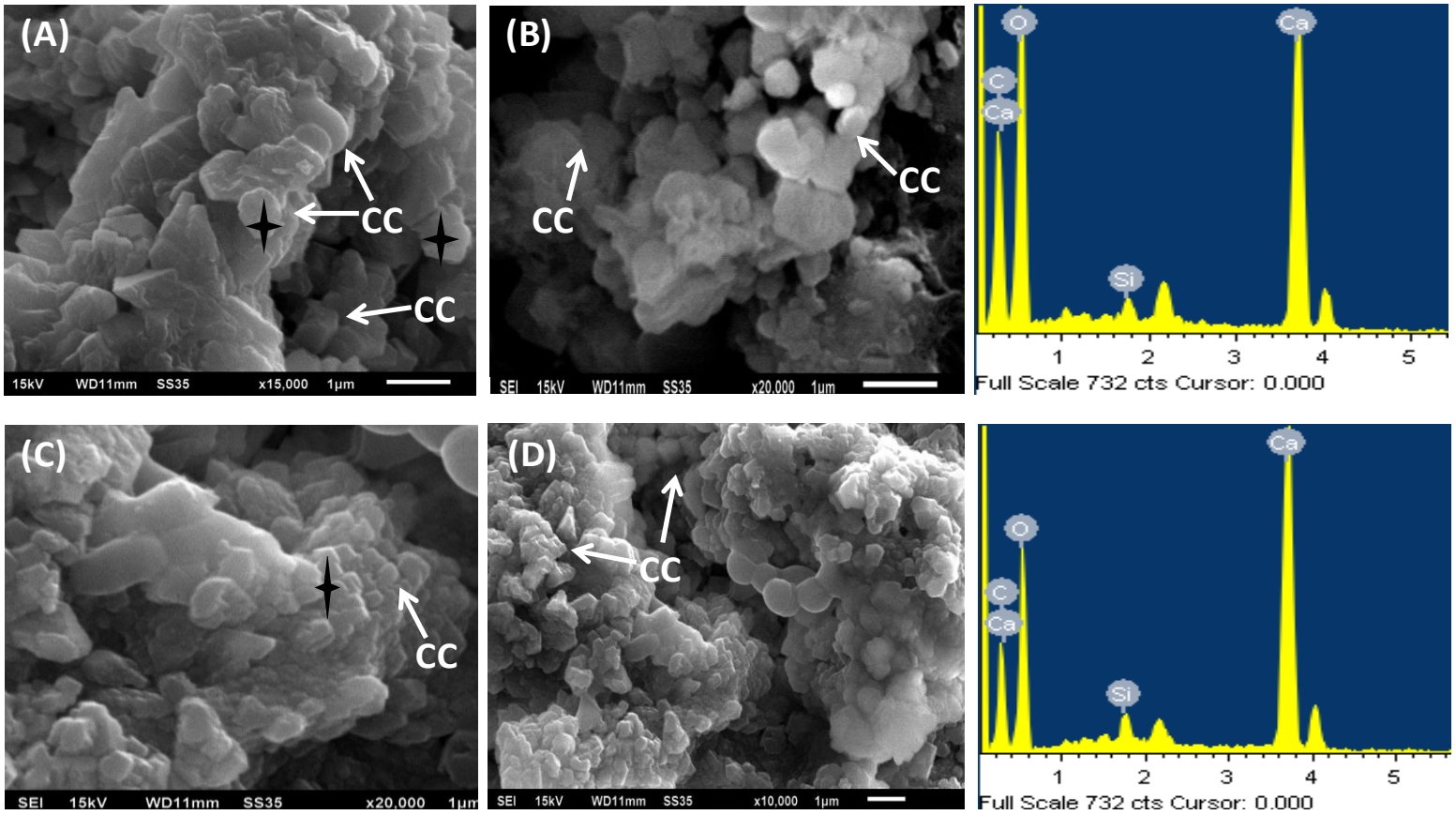

Figure 4.7 SEM images represent the $CaCO_3$ crystals (CC) at upper depth (0-10 mm) in CSL-bacterial admixed treated (CBAT) specimen (A-B) and CSL-bacterial spray treated (CBST) specimen (C-D). Arrows show calcium carbonate crystals. '✦' shows the spots of EDX analysis

XRD analysis of CBAT and CBST specimens is presented in Figure 4.8. XRD analysis of CBAT and CBST specimen showed that majority of the calcium carbonate deposits were calcite and vaterite (Figure 4.8A and 4.8B).

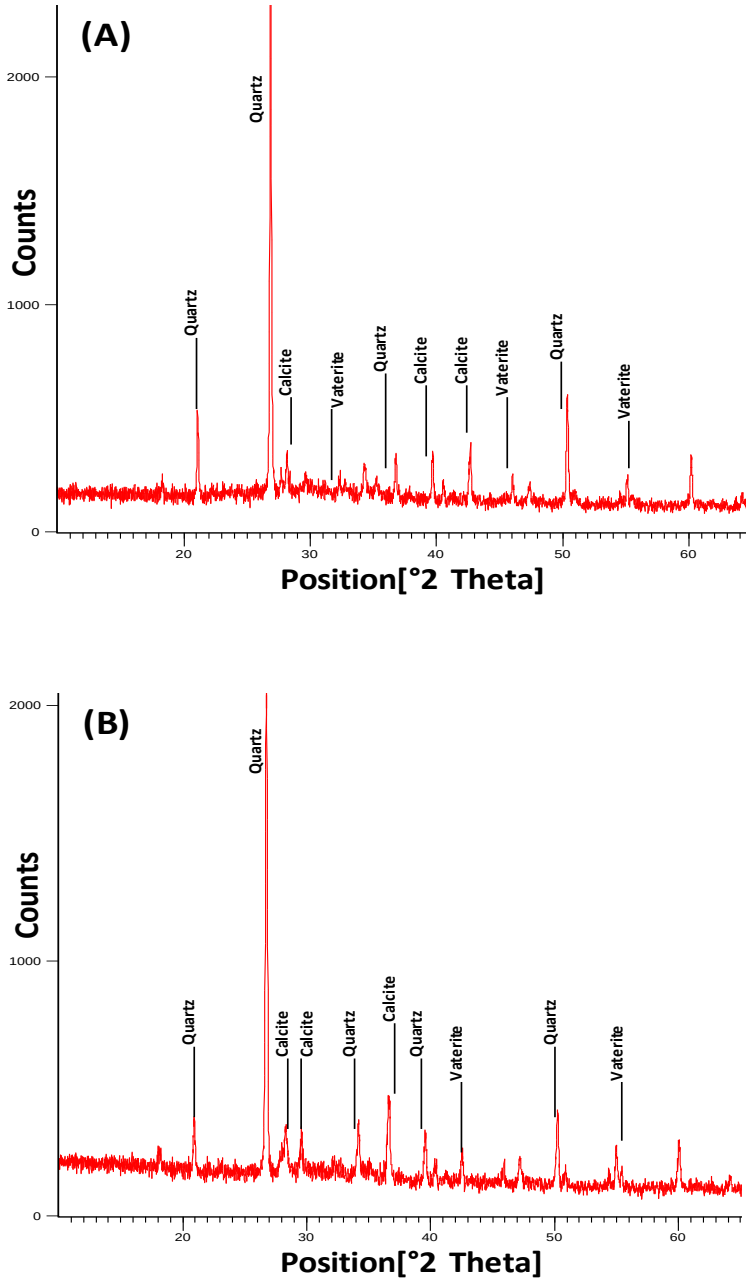

Figure 4.8 XRD patterns of CSL-bacterial admixed treated (CBAT) specimen (A) CSL-bacterial spray treated (CBST) specimen (B) depicts calcite ($CaCO_3$) as predominat crystalline phase. Crystalline phases of vaterite (polymorphs of $CaCO_3$) were also observed

The SEM images of NBAT specimen (Figure 4.9A) and NBST specimen (Figure 4.9C) at the middle depth (20–30 mm) shows the presence of bacterial cells only. However, in the proximity of bacterial cells, no precipitation of calcium carbonate crystals was observed. A SEM image in the samples taken from inner depth (40–50 mm) shows the presence of bacterial cells without any calcium carbonate precipitation in NBAT specimen (Figure 4.9B). In case of NBST specimen (Figure 4.9D), no precipitation and the bacterial cells were detected. The EDX analysis also identified high silicon peaks in both the specimens. The SEM images of CBAT specimen (Figure 4.10A) and CBST specimen (Figure 4.10C) at the middle depth (20–30 mm) shows the presence of bacterial cells. However, in the proximity of bacterial cells, no precipitation of calcium carbonate crystals was observed. SEM image from the inner depth (40–50 mm) shows only calcium silicate hydrate (CSH) without any calcium carbonate precipitation in the concrete matrix of CBAT specimen (Figure 4.10B). In case of CBST specimen (Figure 4.10D), absence of calcium carbonate precipitation and the bacterial cells was observed in the inner depth. The EDX analysis also identified high silicon peaks in both the specimens. In middle depths (20-30 mm) of NBAT/CBAT specimens, presence of bacterial cells without calcium carbonate precipitation was noticed. Bacterial cells in inner depths remains incorporated in the concrete matrix without precipitation activity (Figure 4.9 and Figure 4.10). In case of NBST and CBST specimens, bacterial cells without calcum carbonate precipitation activity were observed in the middle depth (Figure 4.9 and Figure 4.10). But in the inner most depth (40-50 mm), presence of bacterials cells without precipitation was observed in NBAT and CBAT specimens, while in NBST and CBST specimens presence of bacterial cells was not observed (Figure 4.9 and Figure 4.10).

The capability of bacterial cells to hydrolyse urea and nutrient media might be hindered by the harsh alkaline pH of concrete matrix and low oxygen availability. These factors might had effected the ureolytic activity of bacterial cells inside the concrete matrix. The absence of calcite precipitation in the inner depth of concrete can be due to blocking of upper pore matrix of concrete by calcium carbonate precipitation during initial days of spray curing. This might had inhibited the ingress of curing media during spray treatment, and hence this treatment could not improve the compressive strength of concrete substantially.

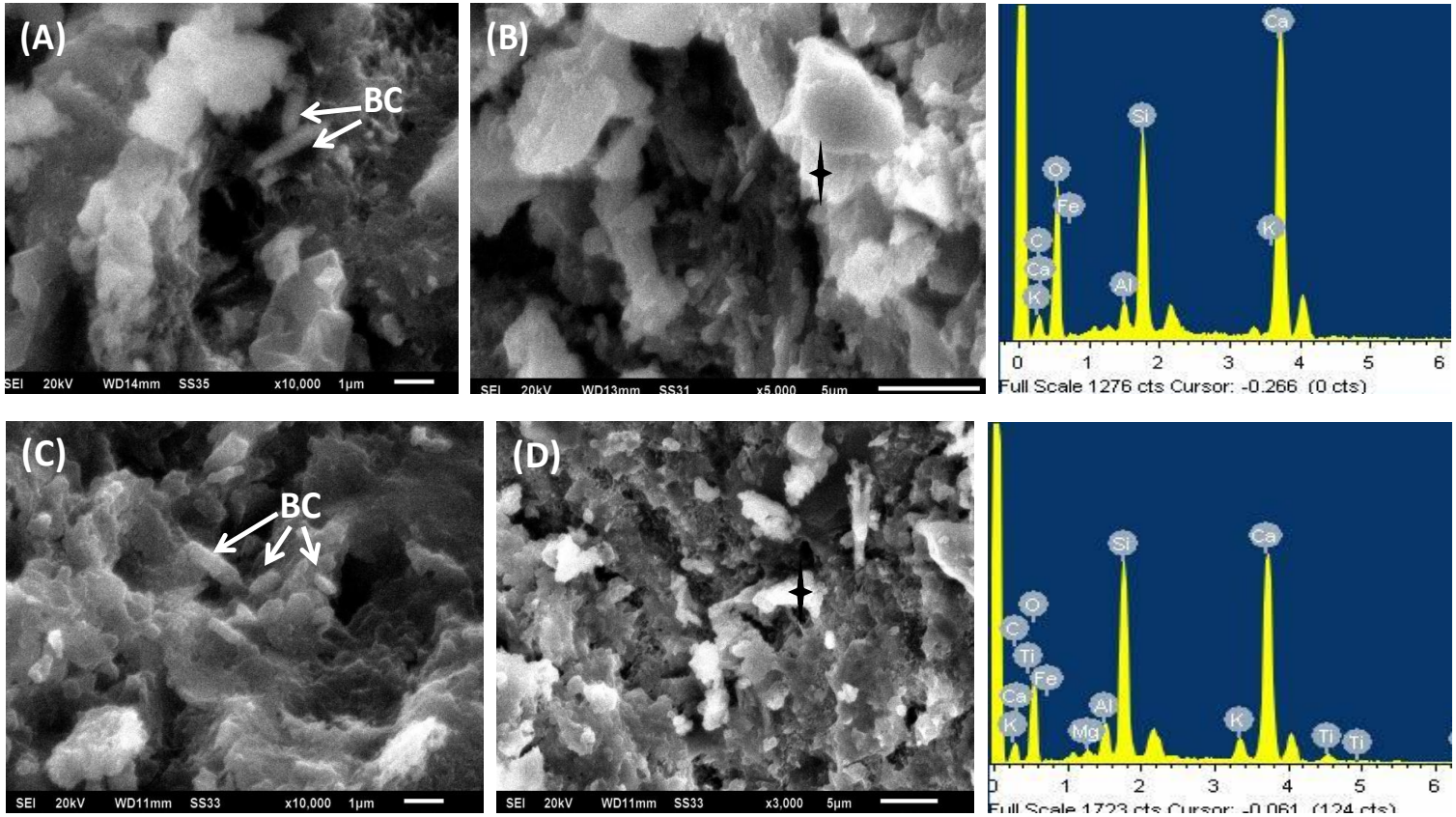

Figure 4.9 SEM images of NB-bacterial admixed treated (NBAT) specimen (A-B) and NB-bacterial spray treated (NBST) specimen (C-D) at middle depth (20-30) and inner depth (40-50 mm). '✦' shows the spots of EDX analysis

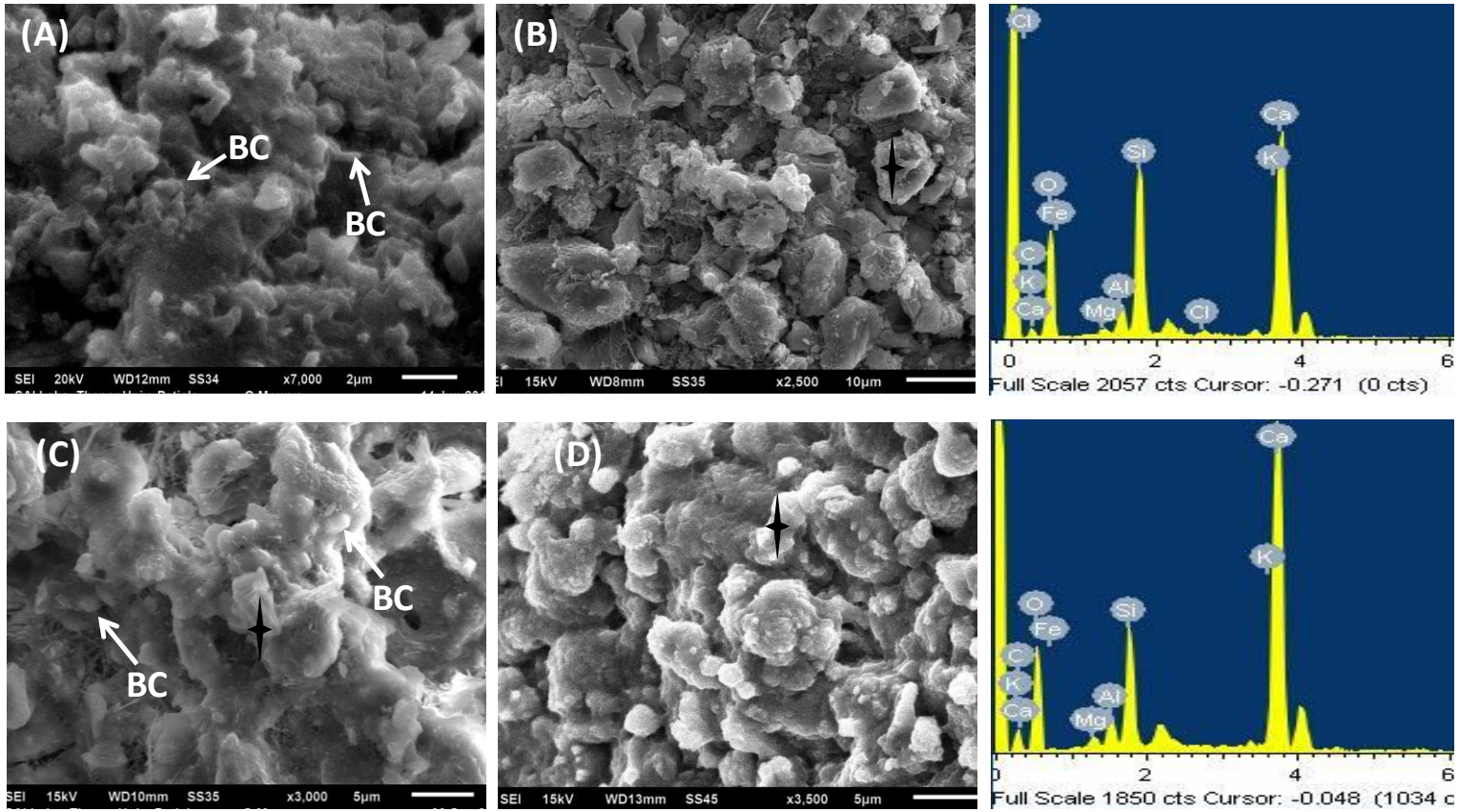

Figure 4.10 SEM images of CSL-bacterial admixed (CBAT) specimen (A-B) and CSL-bacterial spray treated (CBST) specimen (C-D) at middle depth (20-30) and inner depth (40-50 mm). '✦' shows the spots of EDX analysis

The bacterial admixed treatment was observed to be highly efficient in improving the compressive strength of concrete. However, even in this treatment in the inner depth of concrete matrix, bacterial cells are visible but no calcite precipitation was identified. Furthermore, the viability of bacterial cells in the interior of concrete structure due to highly alkaline pH and very restricted oxygen availability is a matter of concern. Some researchers had reported that the live bacterial cells might form spores or die in these harsh conditions of concrete (Wang et al. 2014; Ersan et al. 2015).

In SEM analysis of NT specimen (Figure 4.11A - 4.11B) and CT specimen (Figure 4.11C - 4.11D) at different depths, absence of calcium carbonate precipitation was observed. EDX analysis further confirmed the absence of calcium carbonate crystals.

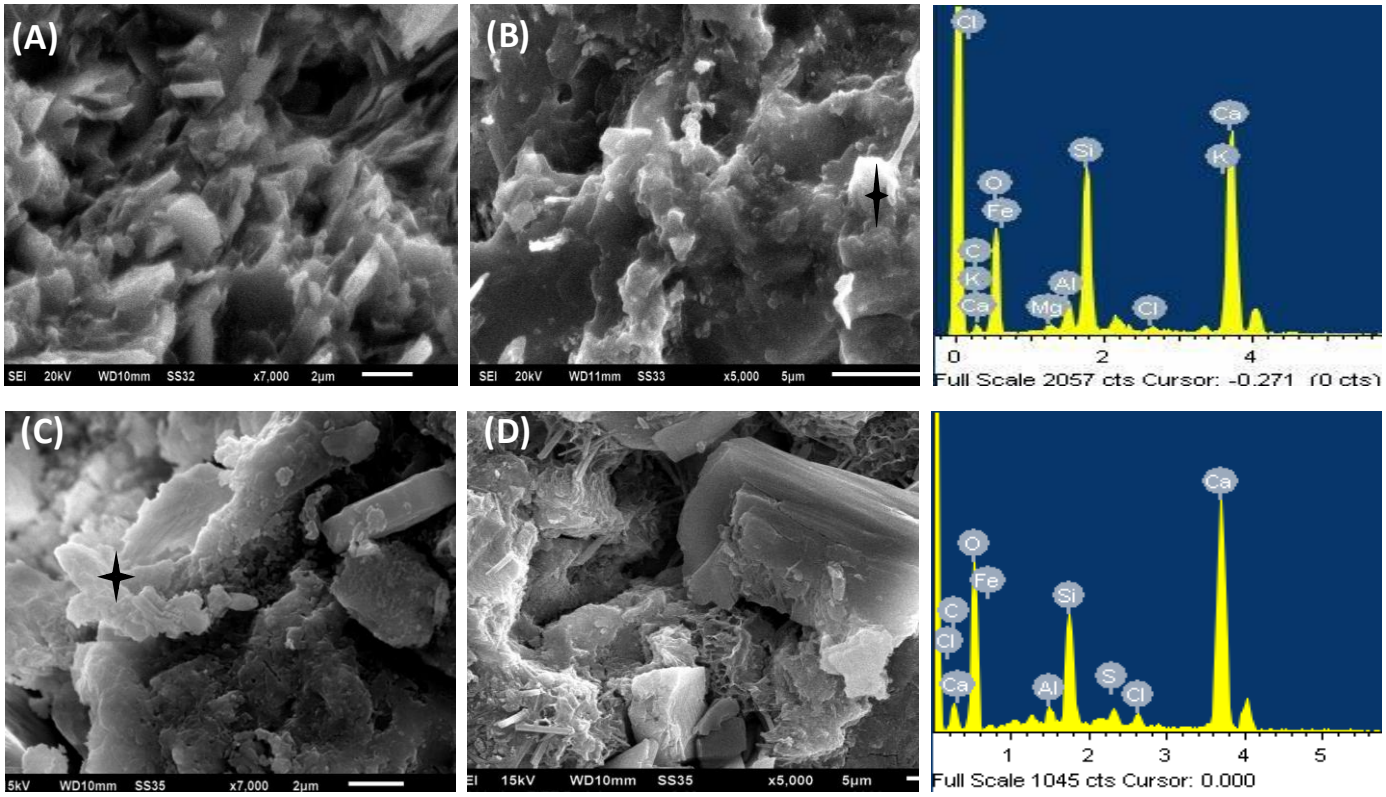

Figure 4.11 SEM images of NB treated (NT) specimen (A-B) and CSL treated (CT) specimen (C-D) from different depths. ✦ shows the spots of EDX analysis

In case of NT and CT specimen, XRD spectrum revealed that the major phases present are quartz, coesite, calcium aluminium silicate and vaterite (Figure 4.12A and 4.12B).

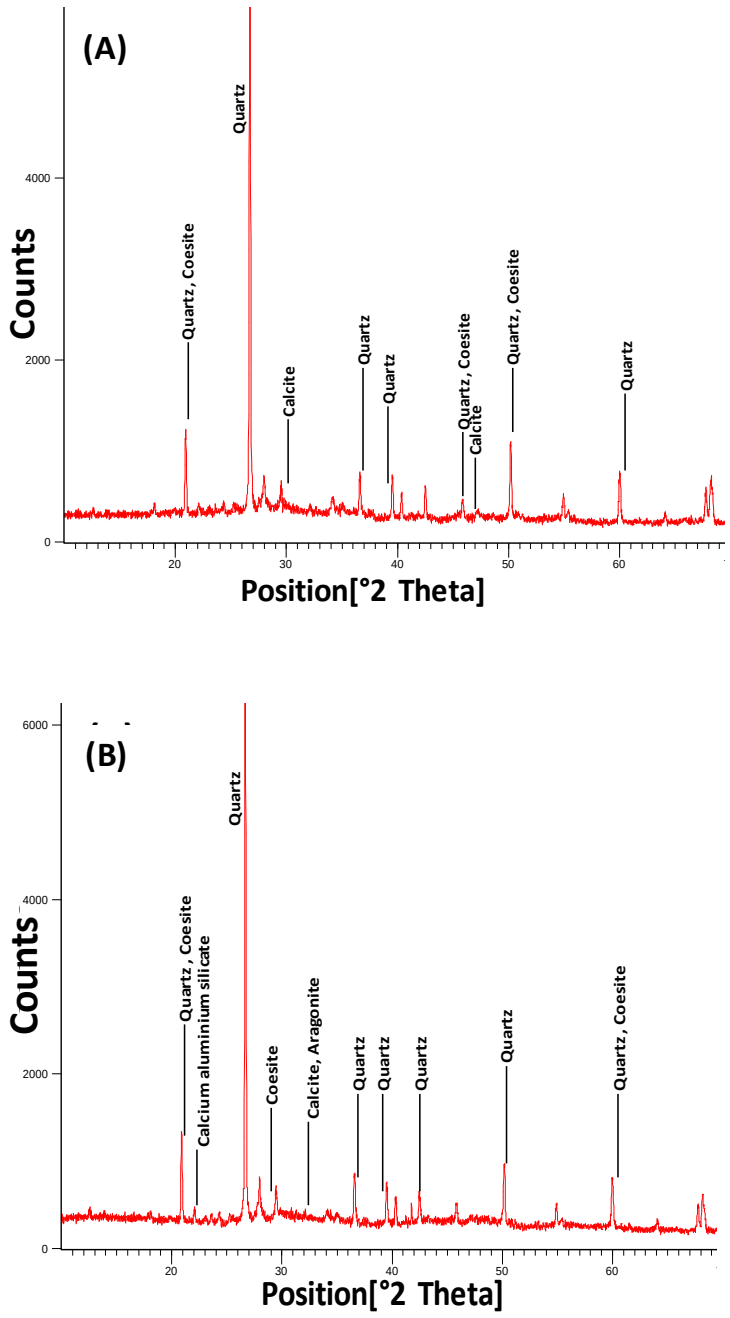

Figure 4.12 XRD patterns of NB treated (NT) specimen (A) CSL treated (CT) specimen (B) depicts the presence of quartz as predominat crystalline phase

In case of control specimen, SEM images from different depths also showed the absence of calcium carbonate crystals (Figure 4.13). EDX analysis further confirmed the absence of calcium carbonate crystals. XRD spectrum of control specimens also confirmed that the major phases present are quartz, calcium hydrate and coesite (Figure 4.14).

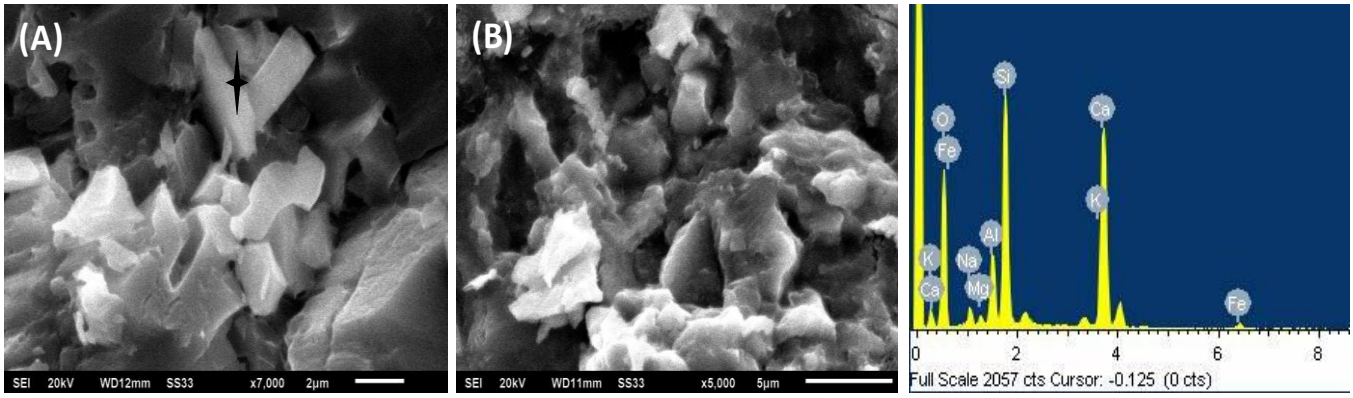

Figure 4.13 SEM images of control specimen (A-B) from different depths shows the formation of calcium silicate hydrate. '✦' shows the spots of EDX analysis

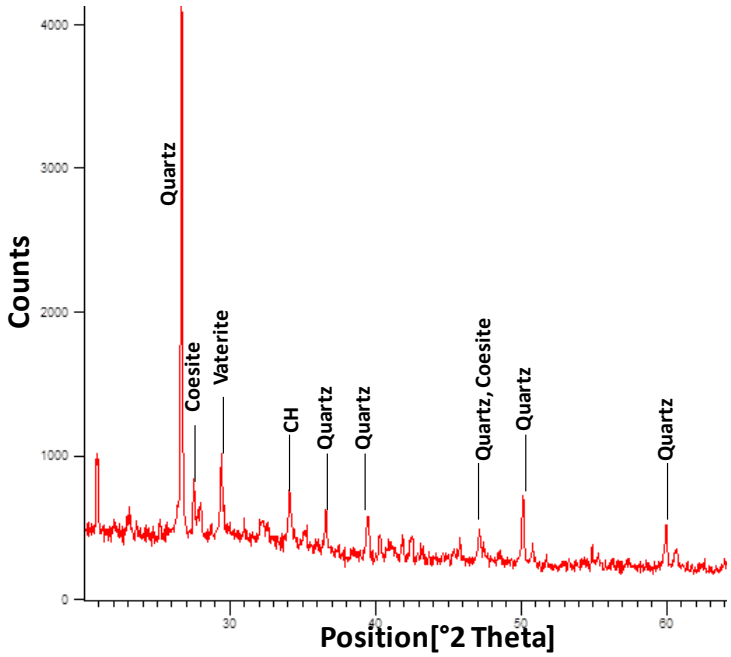

Figure 4.14 XRD patterns of control specimen depicts the presence of quartz as predominat crystalline phase

However, results of the present study indicate that the incorporation of vegetative bacterial cells grown in NB/CSL media as an admixture along with urea and $CaCl_2$ enhanced the mechanical strength as well as improved reistance towards the water ingress of concrete. On the other side, bacterial spray treatment of concrete strutucres significantly improves the permeation properties by providing efficent resistance to water ingress.

4.1.4 Conclusions

In the present investigation, effect of nutrient components of media such as carbon and nitrogen content of organic nutrients and bacterial cells on the chemical and structural properties of concrete was studied. Apart from the laboratory grade nutrient broth (NB), corn steep liquor (CSL), an industrial by-product as an alternate growth media was used during biocementation. Addition of plain CSL media without bacteria had no adverse effect on the setting characteristics of cement paste, while severe retardation was noticed in cement setting with NB media due to its yeast extract component. Retarding nature of organic matter of yeast extract causes significant reduction of strength in concrete specimens treated with NB media only. Setting character of cement was not affected on addition of bacterial culture grown in NB/CSL media. Use of NB media in bacterial admixed and bacterial spray treated specimen's results into higher carbon and nitrogen content than CSL media. Significant improvement in compressive strength and permeation properties as a result of using NB and CSL in bacterial treatment of concrete was observed. The biogenic precipitations of $CaCO_3$ by bacterial cells counteract the retarding effect of organic nutrients of concrete and enhance the durability properties. Use of bacterial admixture, media only (CSL and NB) and surface treatment with bacterial spray did not affect the alkaline nature of concrete. Both bacterial admixed treatment (that can be used for new structures) and bacterial spray treatment (that can be used as a repair procedure) using NB/CSL as bacterial growth media were found to be effective in improving the properties of concrete. Bacterial spray treatment of concrete will help in future application of MICP technology at field scale. From these results it was concluded that CSL (an industrial by-product of the starch industry), an inexpensive nutrient media as compared to yeast extract and peptone in NB media, would serve as a potential nutrient source for bacterial cells in microbial treatment of concrete and thus enhance the durability properties of concrete. CSL will also help in developing low-cost and environment-friendly MICP technology in future on a field scale.

4.2 Durability properties of microbial concrete under aggressive environments

Application of microbial induced calcium carbonate precipitation (MICP) via biomineralization process has been considered as a novel method in improving durability properties of concrete. This bio-based treatment had been extensively targeted to improve the overall performance of concrete at lab scale experiments. The qualitative and quantitative evaluation of MICP in improving mechanical and permeation properties of concrete are still reported under ideal conditions at lab scale. Durability of microbial treated concrete under aggressive environments is still unexplored. The current study aimed to assess the efficacy of bio-deposition as a barrier in microbial treated concrete against the penetration of sulfate ions in external sulfate attack. Along with sulfate exposure, prevention with microbial treatment against chloride induced corrosion of rebar was also investigated.

4.2.1 Exposure to chemical sulphate attack

4.2.1.1 Compressive strength

Compressive strength results of control and microbial treated concrete specimens during sulfate exposure are presented in Table 4.7. The performance of concrete specimens under exposure of sulfate attack was monitored for 1 year. Prior to sulfate exposure, NB-Bacterial admixed treated (NBAT) and NB-Bacterial spray treated (NBST) specimen's registered significant increase in compressive strength as compared to control specimens due to biocementation at the age of 28 days curing. The NBAT and NBST specimens showed an increase of 35% and 16% in compressive strength as compared to the control specimen, respectively as shown in Figure 4.15. Severe strength loss was observed in control specimen after 12 months of sulfate exposure. After the sulfate exposure, compressive strength of control specimen registered a drastic decrease of 30% as compared to its initial strength value before exposure. However in NBAT and NBST specimen, minor variations in compressive strength were observed after sulfate exposure. No major sign of strength loss was registered in NBAT and NBST specimens throughout the sulfate exposure.

Table 4.7 Effect of sulfate exposure on compressive strength properties of different concrete specimens

Specimen	Compressive strength (MPa)							
	Before exposure	**30 days**	**60 days**	**120 days**	**180 days**	**240 days**	**300 days**	**365 days**
Control	31.2±1.9c	32.7±1.4c	33.5±2.2c	35.3±1.1b	33.4±2.0a	29.9±1.4b	26.2±1.5b	22.1±0.8c
NBST	36.5±1.8b	35.8±1.4b	37.8±0.5b	36.2±0.5b	37.8±1.2b	40.4±1.2a	39.3±1.3a	38.1±0.7b
NBAT	42.1±0.8a	41.8±1.1a	43.3±1.1a	42.6±1.2a	40.8±1.4c	41.5±1.4a	40.8±1.1a	41.1±0.5a

Values sharing a common letter within the column are not significant at $P < 0.05$. Values are mean ± standard deviation (n = 3)

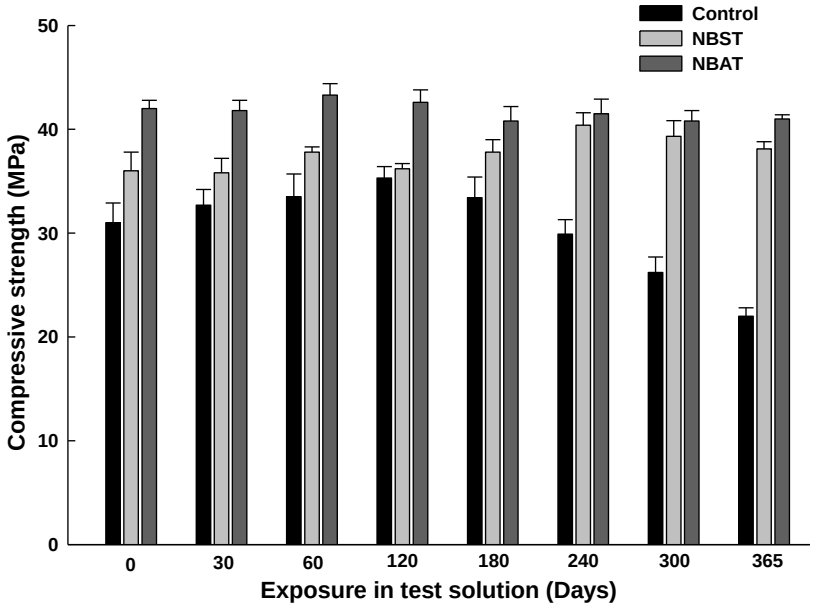

Figure 4.15 Influence of sulfate exposure on compressive strength of control and microbial treated concrete specimens till the age of 365 days. Error bars represent standard deviation (n = 3)

4.2.1.2 Mass change

The mass variations were monitored for all the concrete specimens under chemical sulfate exposure are shown in Figure 4.16. Control concrete specimens gained the higher mass with respect of NBAT and NBST specimens. Mass gain in control specimens was registered till the immersion age of 270 days but thereafter loss in mass was observed. During the sulfate exposure, maximum mass gain in control was measured to be 0.78% from its initial mass till the age of 270 days. In case of NBAT and NBST specimens, marginal mass gain was observed. In NBAT and NBST specimens, mass gain observed at the end of sulfate exposure was 0.28% and 0.4% from their initial mass. Effective resistance towards the ingress of sulfate ions was observed in NBAT and NBST specimens.

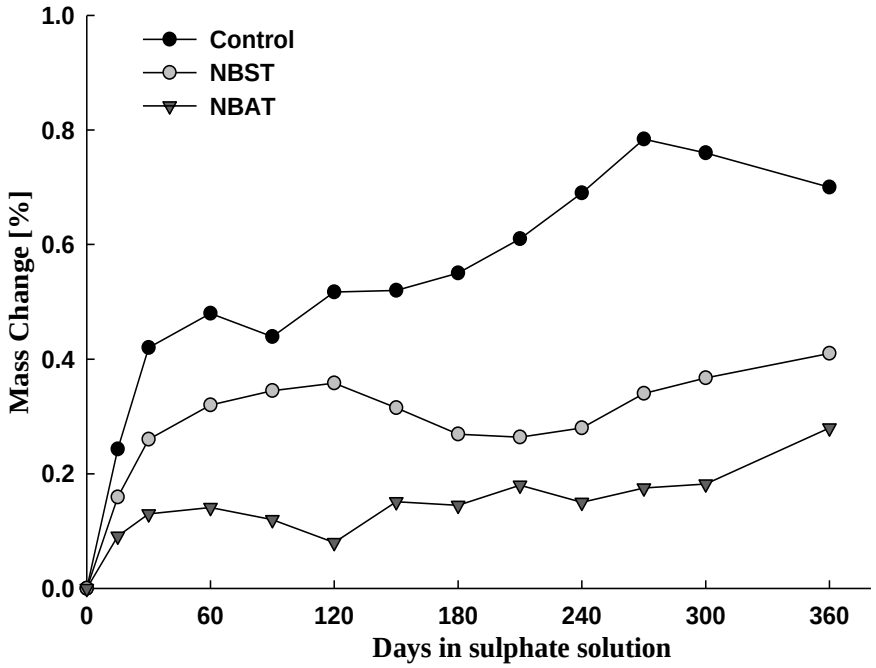

Figure 4.16 Influence of chemical sulfate exposure on mass variations of control, NB-bacterial admixed treated (NBAT) and NB-bacterial spray treated (NBST) specimens till the age of 365 days

4.2.1.3 Visual appearance

Visual observations of control specimens under chemical sulfate exposure for 12 months are presented in Figure 4.17. Clear sign of surface degradation was observed in control specimens during 12 months of immersion in sulfate solution. The first sign of surface cracks in control specimen was visualized at the exposure time of 180 days. The damaging process in control specimen continued with loss of cohesion less particles on the edges due to spalling. Maximum surface deterioration was noted in control specimen during the sulfate exposure. However, no sign of deterioration such as cracking and spalling were visualized in NBAT and NBST specimens and these microbial treated specimens remained intact (Figure 4.18 and Figure 4.19). Severity of surface scaling in concrete specimens is rated as specified in ASTM standard and presented in Table 4.8. On the basis of severity of surface scaling, control specimen after the end of sulfate exposure period falls under the category of moderate to severe scaling. However, NBAT and NBST specimens after the end of sulfate exposure fall under the category of no scaling.

Table 4.8 Surface scaling visual rating adapted from ASTM C672/C672M – 12

Specimens	**Exposure time (months)**				
	1	**3**	**6**	**9**	**12**
Control	0	1	2	3	4
NBAT	0	0	0	0	0
NBST	0	0	0	0	0

0: No scaling; 1: Very slight scaling; 2: Slight to moderate scaling; 3: Moderate scaling; 4: Moderate to severe scaling; 5: Severe scaling

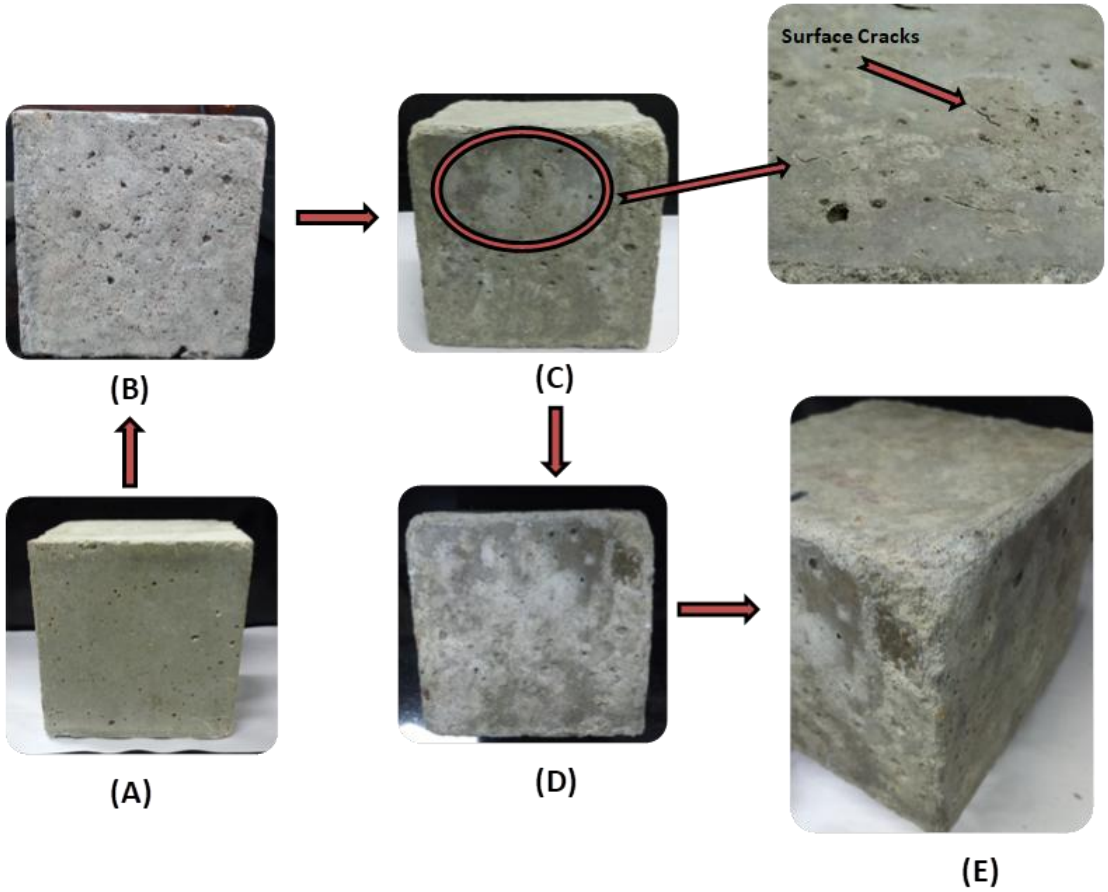

Figure 4.17 Visual appearance of control specimen after chemical sulfate exposure at the age of (A) 30 Days (B) 90 Days (C) 180 Days (D) 270 Days (E) 365 Days. Surface deterioration with the formation of surface cracks and spalling was visualized in control specimen during sulfate exposure

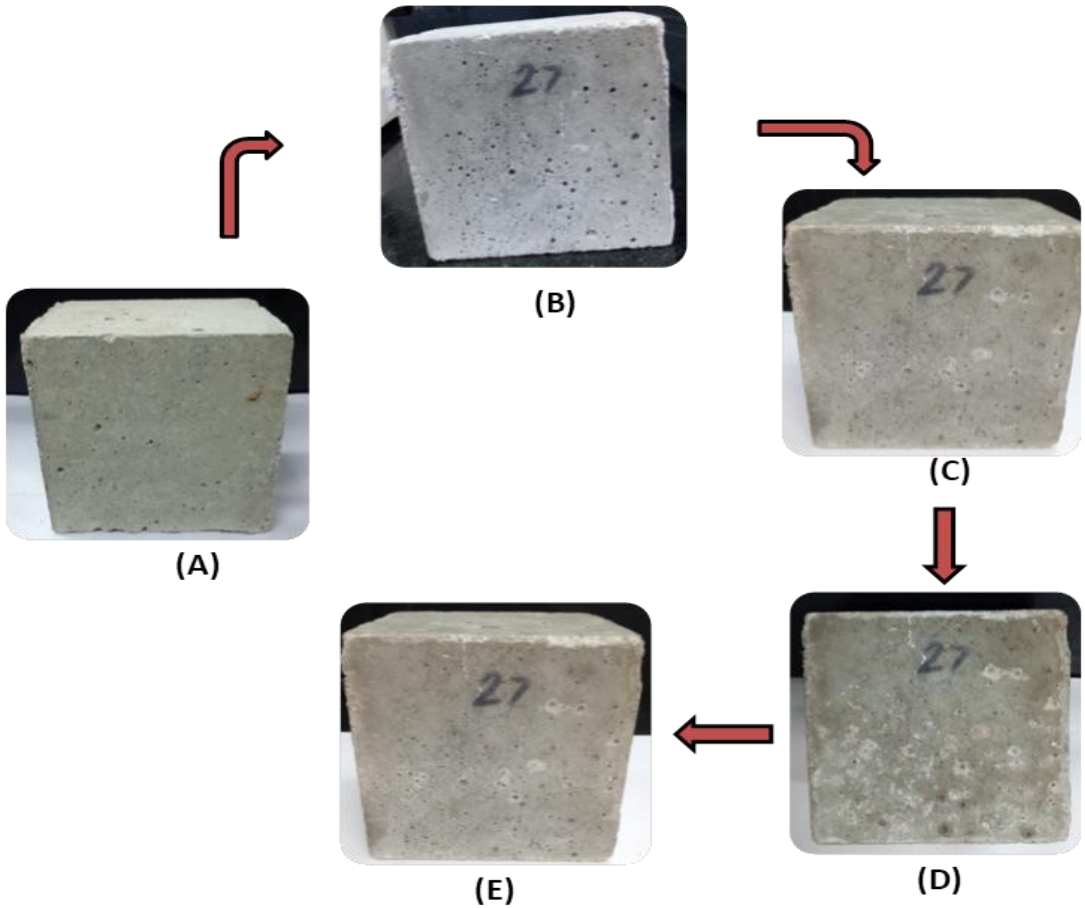

Figure 4.18 Visual appearance of NB-bacterial admixed treated (NBAT) specimen at regular intervals of chemical sulfate exposure (A) 30 Days (B) 90 Days (C) 180 Days (D) 270 Days (E) 365 Days. No sign of surface deterioration was observed throughout the sulfate exposure

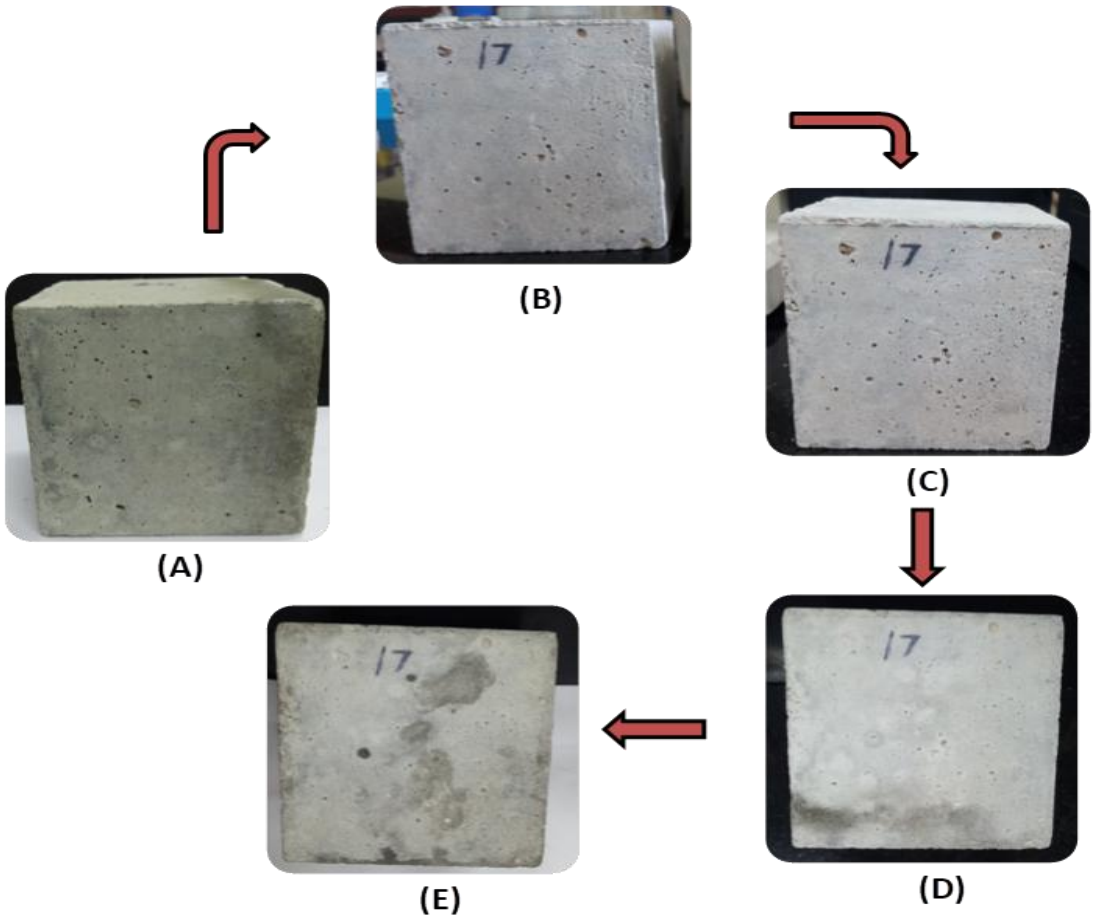

Figure 4.19 Visual appearance of NB-bacterial spray treated (NBST) specimen at regular intervals of chemical sulfate exposure (A) 30 Days (B) 90 Days (C) 180 Days (D) 270 Days (E) 365 Days. No sign of surface cracking and spalling was observed during the sulfate exposure

4.2.1.4 Mortar length change

The length expansion results for all the mortar prismatic specimens are shown in Figure 4.20. After 12 months of full immersion, maximum length expansion was observed in control prismatic specimens.

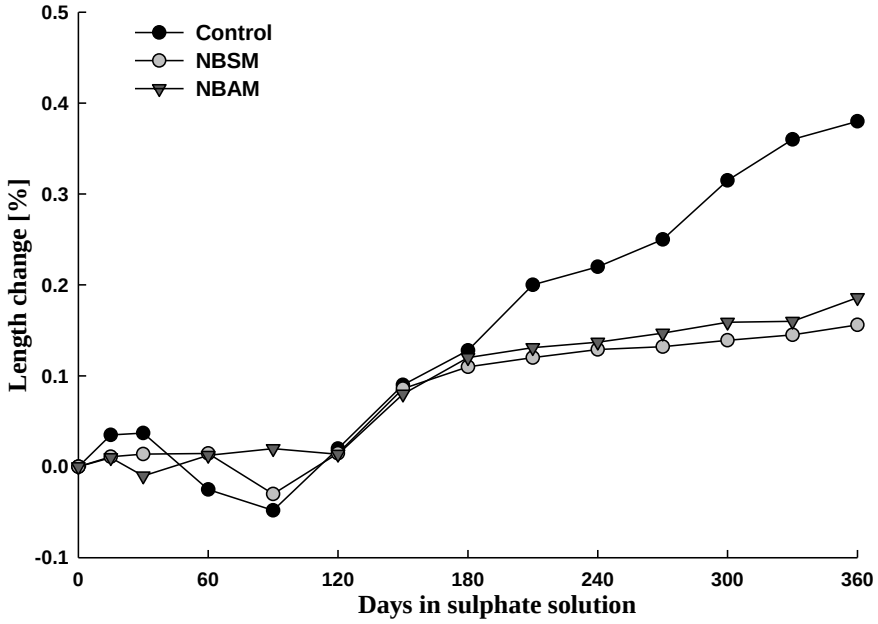

Figure 4.20 Influence of chemical sulfate exposure on length expansion of control, NB-bacterial admixed mortar (NBAM) and NB-bacterial spray treated mortar (NBSM) specimens till the age of 365 days

The control prism yielded the maximum expansion of about 0.38% after the complete cycle of sulfate exposure. However, bacterial treated prismatic specimens indicate the higher resistance against sulfate attack towards expansion. In NB-bacterial admixed mortar (NBAM) and NB-bacterial spray treated mortar (NBSM) prisms no evident effect on length was observed as compared to control prism, with maximum expansion reaching 0.18% and 0.15% respectively. Results indicates that NBAM and NBSM prism showed 52% and 60% lower expansion than control prism, respectively.

4.2.1.5 Micro-structural evaluation

SEM analysis of all concrete specimens was performed at different ages of sulfate exposure. In control concrete specimens, deposition of different secondary products like gypsum and ettringite crystals were observed (Figure 4.21). Presence of needle shaped crystals was observed in the pore matrix of control specimen at the immersion age of 90 days (Figure 4.21A). With the increasing sulfate immersion age, precipitation rate of ettringite crystals were also escalated. Intense deposition of ettringite crystals with long needle shape and elongated rectangular prism faced column shape in control specimens were observed at the age of 365 days (Figure 4.21C). The EDX analysis also confirmed the elemental composition of crystals with peaks showing high amount of calcium, sulphur and aluminum (Figure 4.21D). XRD analyses of concrete specimens were performed to identify the presence of different crystalline phases during chemical sulfate exposure. In control specimen, XRD profile indicates the peak for quartz as well as ettringite and gypsum as the main secondary reaction products (Figure 4.22).

In NBAT and NBST specimen, on the sulfate exposure till the age of 180 days, secondary products due to sulfate ingress were not observed (Figure 4.23 and Figure 4.25). Biogenic calcium carbonate precipitation due to bacterial curing adopted for NBAT and NBST specimens, results into an efficient resistance towards the sulfate ingress. However after 365 days of severe sulfate attack, development of micro needle crystals of gypsum and ettringite were observed in NBAT and NBST specimen (Figure 4.23C and Figure 4.25C). EDX analysis confirmed the formation of gypsum and ettringite crystals showing the peaks of calcium, sulphur, aluminum and oxygen. XRD analyses of NBAT and NBST specimens were performed to identify the presence of different crystalline phases during chemical sulfate exposure (Figure 4.24 – Figure 4.26).

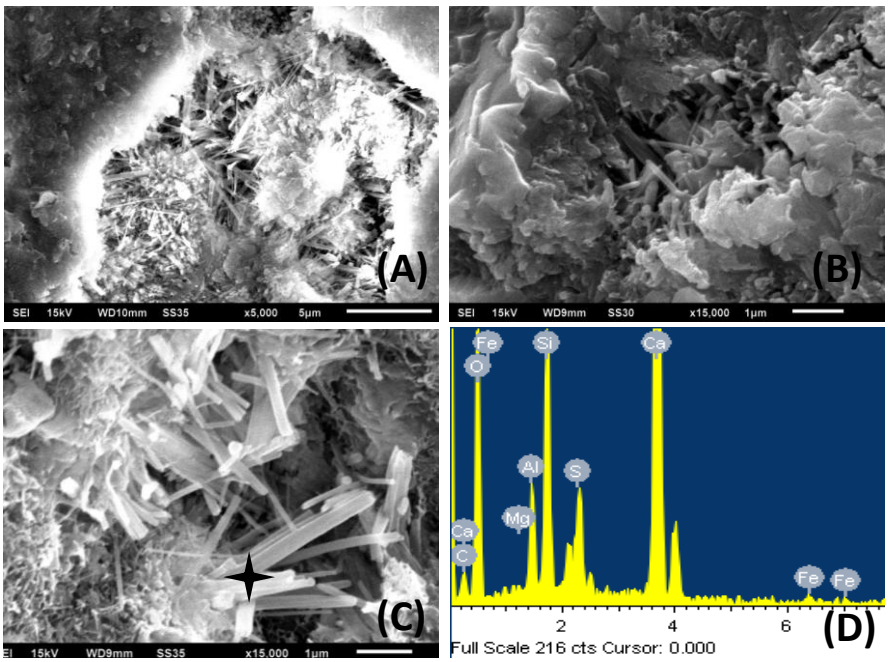

Figure 4.21 SEM images of control specimen after (A) 90 days (B) 180 days (C) 365 days of chemical sulfate exposure. (D) EDX analysis represents formation of reaction products. '✦' shows the spot of EDX analysis

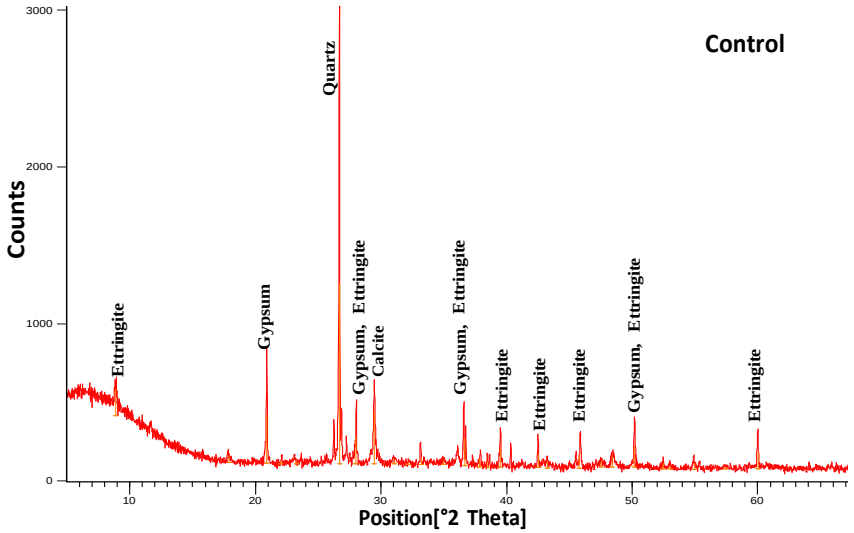

Figure 4.22 XRD patterns of control specimen after the 12 months of chemical sulfate exposure depicts ettringite as predominat crystalline phase. Crystalline phases of gypsum were also observed

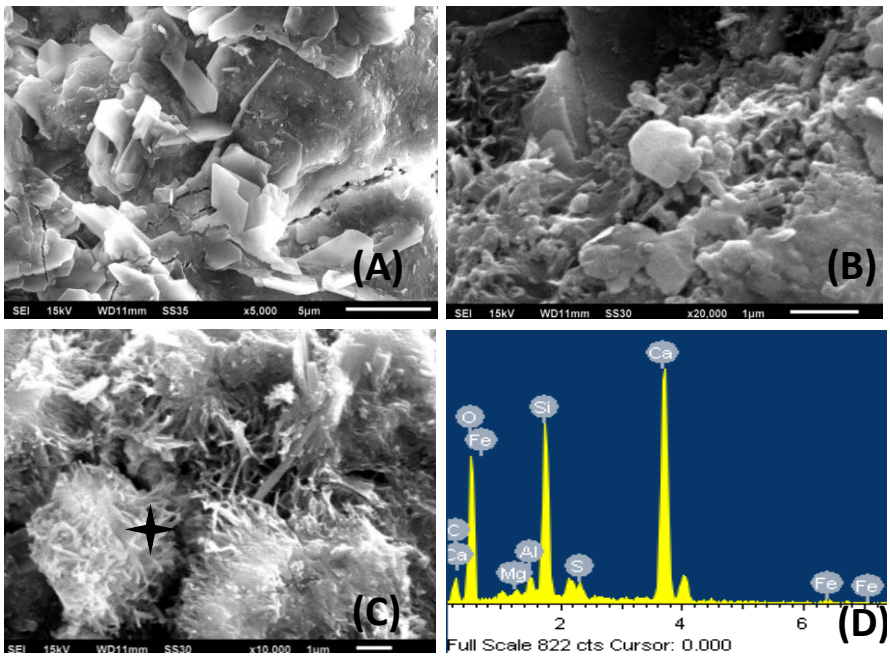

Figure 4.23 SEM images of NBAT specimen after (A) 90 days (B) 180 days (C) 365 days of sulfate exposure. (D) EDX analysis represents formation of reaction products. '✦' shows the spot of EDX analysis

XRD analyses of NBAT specimen performed at the end of chemical sulfate exposure revealed the presence of calcite as the major phase as well as some peaks of gypsum and thaumasite as shown in Figure 4.24.

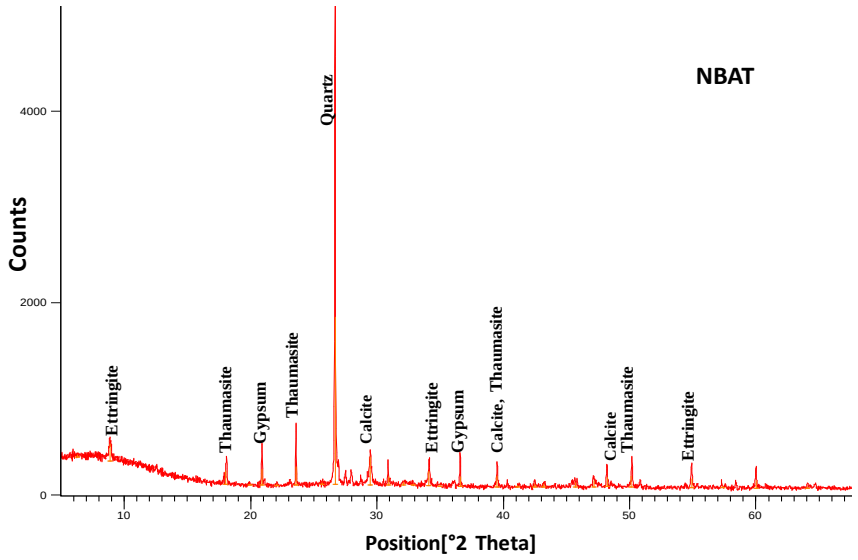

Figure 4.24 XRD patterns of NB-bacterial admixed treated (NBAT) specimen at the end of chemical sulfate exposure depicts calcite, gypsum and ettringite as predominat crystalline phases

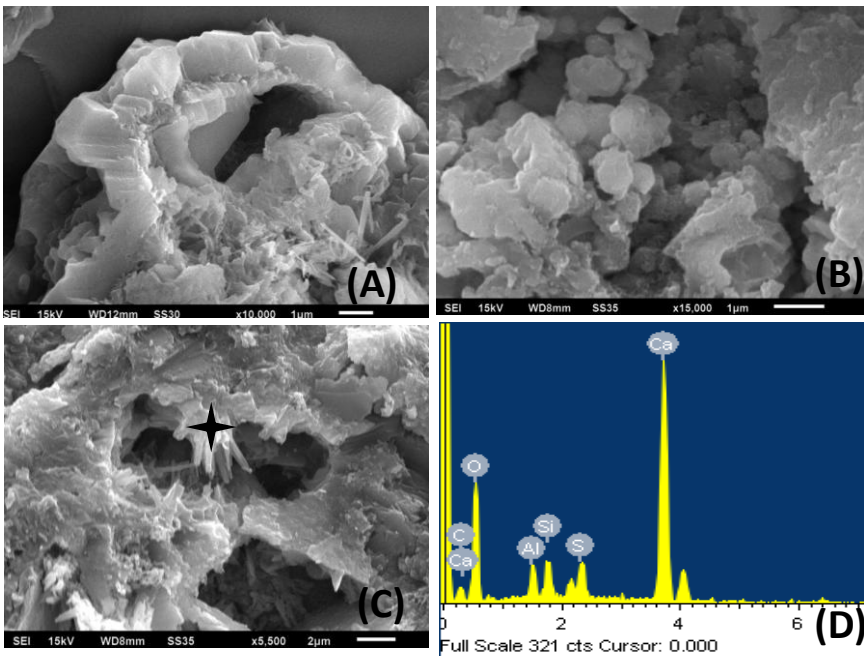

Figure 4.25 SEM images of NBST specimen after (A) 90 days (B) 180 days (C) 365 days of sulfate exposure. (D) EDX analysis represents formation of reaction products. '✦' shows the spot of EDX analysis

XRD analyses of NBST specimen performed to identify the presence of different crystalline phases during chemical sulfate exposure. In NBST specimen, XRD profile indicates the peak of calcite as the major phase as well as some peaks of ettringite and thaumasite as secondary products formed during the sulfate ingress (Figure 4.26).

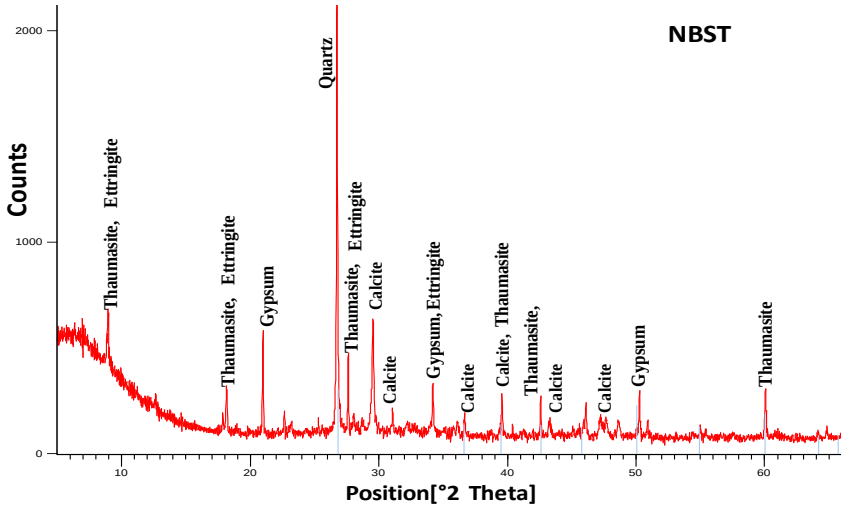

Figure 4.26 XRD patterns of NB-bacterial spray treated (NBST) specimen at the end of chemical sulfate exposure depicts calcite, ettringite and thaumasite as major crystalline phases

Performance and evaluation of control concrete specimens, monitored under chemical sulfate attack through the durability factors like compressive strength change and mass change revealed that during the initial 120 days of exposure, improvement in compressive strength was observed (Figure 4.15). This behavior of the initial improvement in mechanical strength reflects the densification of cementitious matrix at microstructural level (Mittermayr et al. 2015). It was also reported that due to continuous ingress of sulfate ions into the cementitious matrix progresses the development of expansive products such as gypsum and ettringite was observed. The quantity of expansive products fills the pores and voids causing the microstructure denser during the initial period of sulfate exposure (Najjar et al. 2017a). With the long time exposure, the severity of chemical sulfate attack intensified and results into significant strength loss in control specimen. Gradual loss in strength observed after 180 days of immersion may be due to increased penetration of sulfate salts causing higher accumulation of expansive products in the pores of control specimens. Formation of ettringite crystals led to the factors like reduction in the quantity of CH and C_3A content of cementitious matrix (Aye and Oguchi, 2011) and salt crystallization pressure within the pores of concrete (Lee and Kurtis, 2017). It was reported that quantity of CH and C_3A content favored the attack of Na_2SO_4 salt and calcium silicate hydrate (CSH) favored the $MgSO_4$ attack (Aye and Oguchi, 2011). Deterioration in the form of spalling and cracking on the concrete surface was observed in control specimens.

As indicated in Figure 4.17, surface cracks were observed in control specimens at the immersion age of 180 days which further accelerated with the exposure time. In SEM analysis, association of gypsum and ettringite crystals accumulation in the pores of concrete supported the possible reason of damage (Figure 4.21). Presence of elongated column shaped ettringite crystals generated a significant stress in the pores which causes damage to pore walls resulting into cracking. On the other hand, influence of sulfate ingress in the pores of control specimen on the mass change was also observed. As shown in Figure 4.16, it was observed that control specimen undergo mass gain of 0.8% till the immersion age of 270 days. It seems that mass variation may be due to the formation of expansive products during the reaction of hydration products of cement with sulfate ions which leads to compaction of microstructure (Maes and De Belie, 2014). Concrete with high porosity was reported to gain mass because of higher ingress of sulfate absorption (Nehdi et al. 2014). Higher pore volume was reported to be the main reason, responsible for the transportation of sulfate ions and consequently filling the concrete pores with

expansive products (Najjar et al. 2017a). However, in the later ages of immersion, trend of mass loss was observed in control specimens as the sulfate exposure progressed (Figure 4.16). Development of stress due to enhanced growth of expansive products causes surface scaling and loss of cohesion less particles on the edges (Figure 4.17). Existence of gypsum and ettringite crystals in concrete pores was claimed to be the deterioration factors (Maes and De Belie, 2014). Expansive behavior of reaction products will be the factors responsible for cracking and spalling on the outermost layer of concrete. In SEM and XRD analysis (Figure 4.21 and Figure 4.22), presence of gypsum and ettringite confirmed the deterioration of control specimens, which is further responsible for mass loss. In addition, trends of length increase in control prism due to expansive product formation were also observed. As shown in Figure 4.20, rate of expansion was much higher in control prism as compared to microbial treated prisms. Length expansion of control mortar prism indicates higher ingress of sulfate ions and filling its pore volume with reaction products. Moreover, during the sulfate exposure a longitudinal crack along the whole length of control prism was observed. Similar observation of crack generation along the length of mortar prism was also reported (Maes and De Belie, 2014). Appearance of cracks confirms the formation of ettringite and gypsum crystals as responsible factors for deterioration.

Ettringite and gypsum were also reported as the cause of expansion in mortar specimens subjected to sulfate environment (Tian and Cohen, 2000; Rozière et al. 2009). It has also been reported that leaching of $Ca(OH)_2$ plays an important role in the degradation of mortar specimen immersed in sodium sulfate solution (El-Hachem et al. 2012). Dissolution of $Ca(OH)_2$ together with external sulfate attack increased the porosity and making the diffusivity of sulfate ions easier for the formation of gypsum. This mechanism was reported for triggering the overall expansion and cracking of mortar prism. In contrast, overall performance of microbial treated specimens against sulfate resistance was excellent. Application of both microbial treatments (bacterial admixture and bacterial spray) improved the mechanical and permeation properties of concrete structures. Due to biogenic precipitation of $CaCO_3$ crystals, ingress of sulfate ions was extensively reduced inside the cementitious matrix. Efficient resistance towards sulfate ingress results into marginal variations in compressive strength and mass of NBAT and NBST specimens (Figure 4.15 and Figure 4.16). Low ingress of sulfate ions further reduces the deterioration of concrete leading from the formation of expansive reaction products like ettringite and gypsum (Figure 4.23 and Figure 4.25). However, some researchers also reported that the

presence of carbonate in cementitious matrix will favor the thaumasite form of sulfate attack (Irassar, 2009). It was reported that limestone fillers were used as admixture with different replacement levels in concrete mixes (Rahman and Bassuoni, 2014). Contrary to the reports of deterioration of concrete structures incorporated with limestone on exposure to sulfate solutions, improvement in resistance against the sulfate attack was reported (Mittermayr et al. 2015; Skaropoulou et al. 2013). In XRD analysis, presence of calcite as well as thaumasite phases at the end of exposure was observed (Figure 4.24 and Figure 4.26). On the whole, NBAT and NBST specimens remain unaffected as compared to control specimens and performed well in the chemical sulfate attack.

4.2.2 Exposure to physical sulfate attack

4.2.2.1 Salt efflorescence

A typical appearance of white efflorescence was developed in the mortar prisms during physical sulfate exposure. Thick deposition of salt efflorescence was developed in the upper portion of the control prism during immersion period (Figure 4.27).

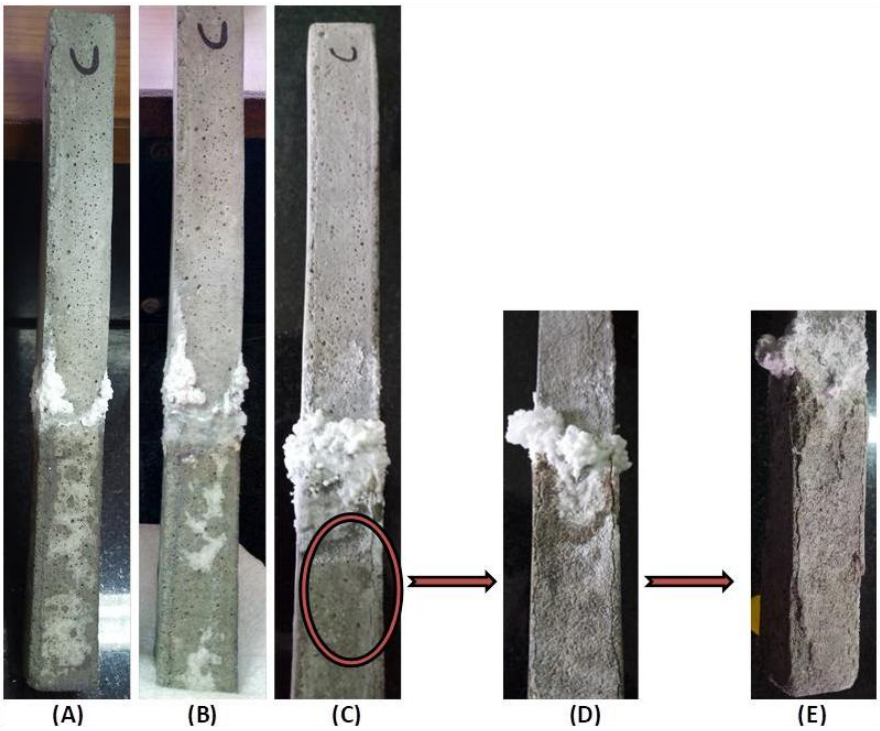

Figure 4.27 Typical salt efflorescence development in upper portion of control prism during successive intervals of physical sulfate exposure (a) 30 days (b) 90 days (c) 180 days (d) 270 days (e) 365 days. Longitudinal cracks were also observed in the submerged portion of prism

After 30 days of immersion, salt precipitation above the sulfate solution level was developed in control specimens. After 90 days of exposure, crack formation along the edges of control specimen was observed. At a later age, higher surface scaling and increase in longitudinal cracks in submerged portion was observed. XRD analysis performed for the control prism at the end of the sulfate exposure is shown in Figure 4.28. XRD patterns from submerged portion revealed the presence of ettringite and gypsum as the major sulfate reaction phases (Figure 4.28A). In case of salt efflorescence developed above the sulfate solution level, XRD patterns revealed the formation of thenardite and epsomite as the major phases with minor peaks of mirabilite (Figure 4.28B).

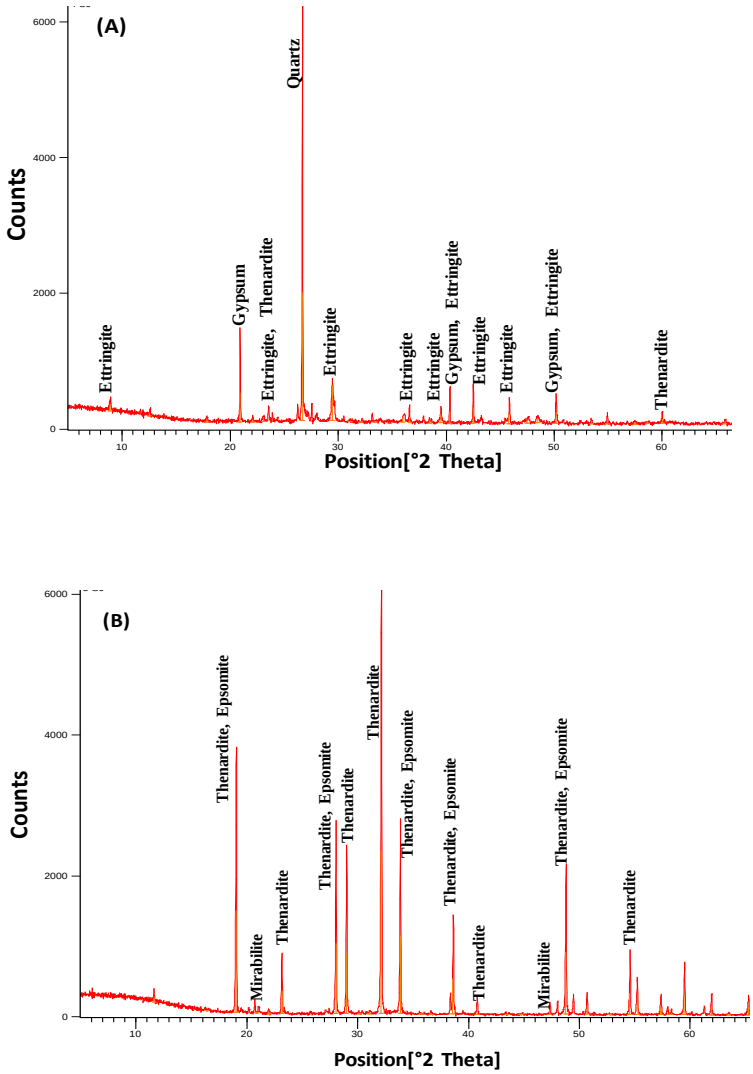

Figure 4.28 XRD patterns of submerged portion of control prism (A) depicts ettringite and gypsum as major crystalline phases and salt efflorescence (B) depicts thenardite and epsomite as the major phases

During the physical sulfate exposure, a thick white efflorescence was developed in control prism on the drying mortar surface which is just above the submerged portion. With the exposure time, thickness of efflorescence continued to increase in control prism (Figure 4.27). However, longitudinal crack formation after 90 days of sulfate exposure in submerged portion and severe surface scaling at later ages was observed. This behavior of efflorescence deposition on the upper portion and surface scaling on the submerged portion of mortar prism were reported to be a dual action of physical and chemical sulfate attack respectively (Nehdi et al. 2014). It is reported that in physical sulfate attack, stress development due to salt crystallization pressure in pore structure is the deterioration mechanism. Sulfate ions penetrate from sulfate rich surroundings into concrete pores by capillary suction and are transported to the evaporation surfaces (Liu et al. 2014). At the upper dry surface, rate of evaporation exceeds the rate of capillary rise due to which salt solution becomes supersaturated causing the salt crystallization on the surface (Haynes and Bassuoni, 2011). Salt solution uptake into the pores by capillary pressure is dependent on the pore distribution of porous body as well as its wetting behavior (Scherer, 2004). It was also reported that increased porosity and permeability further increases the flux of salt solutions causing more accumulation of salts (Lee and Kurtis, 2017). In control mortar prism, dual effect of physical sulfate attack on the upper portion and chemical sulfate attack on the submerged portion was observed. However above the efflorescence region no sign of damage like cracking and spalling were observed. It is reported that the growth of mirabilite crystals inside the pore wall generates high crystallization stress developing subflorescence region (above the efflorescence region) where damage occurs (Lee and Kurtis, 2017). In XRD analysis, presence of anhydrous thenardite deposits on the evaporative surface of control prism shows that the hydrous mirabilite phase dried out on the surface during the exposure (Figure 4.28B). This thick efflorescence on upper surface indicates higher concentration of sulfate salt ingress in control specimen. However, in XRD analysis, presence of ettringite and gypsum crystals in the damaged submerged region also mimics the chemical sulfate attack (Figure 4.28A). In the submerged portion, instead of salt efflorescence, crack formation along the edges due to expansion was observed. Similar to chemical sulfate attack, this typical crack formation and spalling in the submerged portion causes severe surface damage.

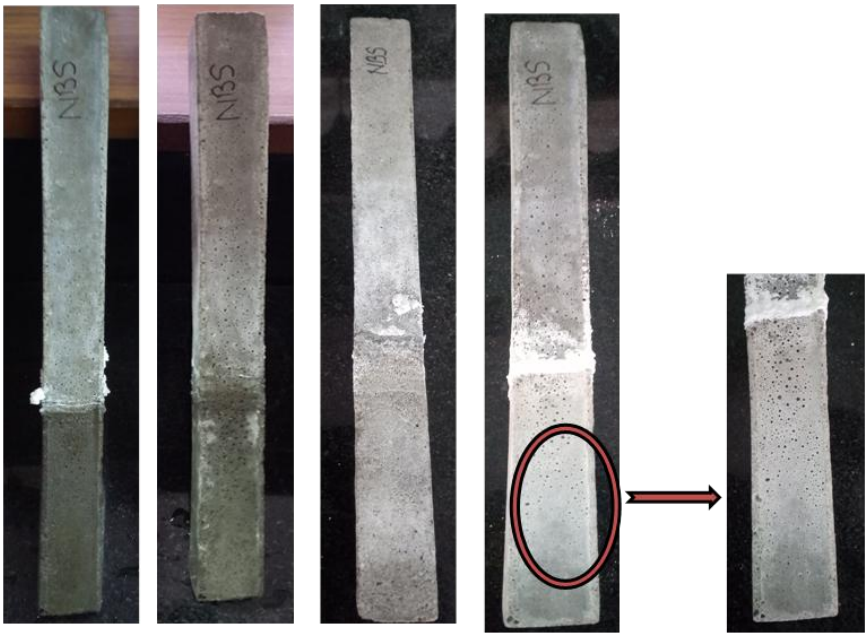

Figure 4.29 NB-bacterial spray treated mortar (NBSM) during successive intervals of physical sulfate exposure (a) 30 days (b) 90 days (c) 180 days (d) 270 days (e) 365 days. No sign of surface cracks was observed till the end of sulfate exposure

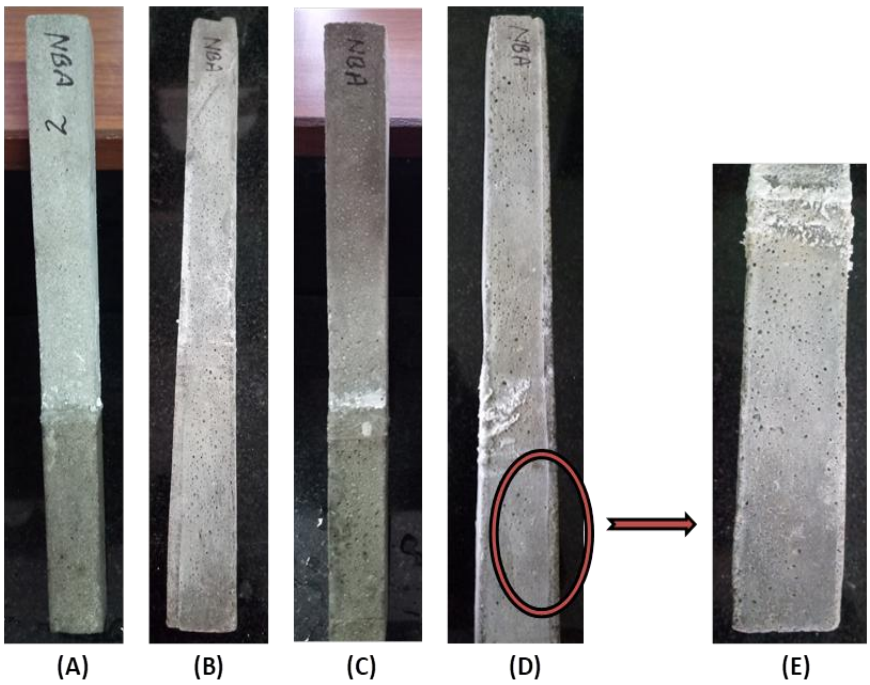

Figure 4.30 NB-bacterial admixed mortar (NBAM) during successive intervals of physical sulfate exposure at the age of (a) 30 days (b) 90 days (c) 180 days (d) 270 days (e) 365 days. No sign of surface scaling and salt efflorescence was observed till the end of sulfate exposure

However, NBSM and NBAM prism shows better resistance against the physical sulfate attack. No visible deterioration such as surface scaling or crack formation observed in NBSM and NBAM throughout the exposure (Figure 4.29 and Figure 4.30). Slight formation of salt efflorescence above the sulfate solution level was observed in NBSM and NBAM at later ages. In case of NBAM and NBSM prisms, resistance to capillary rise of sulfate salts was adequately achieved due to microbial treatment. Throughout the exposure, there was no sign of surface scaling in the submerged portion of NBAM and NBSM prisms were observed (Figure 4.29 and Figure 4.30). Precipitation of calcium carbonate during microbial treatment might have densify the cementitious pore matrix and acts as a pore blocker. It is reported that permeation properties of concrete structures are significantly improved by bacterial calcium carbonate precipitation. Further, the transport mechanism of salt contaminated water through capillary rise in pore matrix is effectively altered by bacterial treated concrete (Bansal et al. 2016). NBAM and NBSM prisms exhibited excellent resistance to sulfate ingress and leading to protection from physical and chemical form of sulfate attacks.

4.2.3 Exposure of reinforced concrete to chloride attack

Chloride induced corrosion in reinforced concrete structures is a widespread deterioration factor which causes premature loss in the serviceability of concrete structures. Reinforcement in concrete structures is prone to corrosion when chloride ingress into the concrete matrix from the surrounding environment. In this study, performance of reinforced concrete specimens under chloride induced corrosion was studied. Resistance towards chloride ingress in microbial treated specimens was monitored and compared with control specimen. During the chloride exposure, corrosion potential and corrosion current density of rebar embedded in concrete cylinders was measured. The corrosion potential and corrosion current density values were recorded after wet-dry cycle of 7 days immersion in NaCl solution and 3 days air drying.

4.2.3.1 Corrosion potential

Corrosion potential (E_{corr}) values of all the reinforced concrete cylinders exposed to aggressive chloride solution is shown in Table 4.9. Corrosion potential values of all concrete specimens were measured at regular interval of time up to 130 days of exposure. Initial corrosion potential values in control, NB-bacterial spray treated (NBST) and NB-bacterial admixed treated (NBAT) specimens before the exposure of chlorides were 121.7 mV/SCE, 115.9 mV/SCE and 111.8

mV/SCE respectively (Figure 4.31). Among all specimens, maximum decrease in corrosion potential was observed in control specimen.

Table 4.9 Corrosion potential 'E_{corr}' (mV/SCE) measurements at different chloride exposure time

Specimens	Exposure time				
	Before exposure	**3rd cycle**	**6th cycle**	**9th cycle**	**12th cycle**
Control	121.76	-329.28	-432.48	-431.71	-522.23
NBAT	111.80	-14.28	-153.83	-130.56	-220.40
NBST	115.90	-14.28	-356.54	-437.59	-382.62

SCE: Saturated calomel electrode; NBAT: NB-bacterial admixed treated; NBST: NB-bacterial spray treated

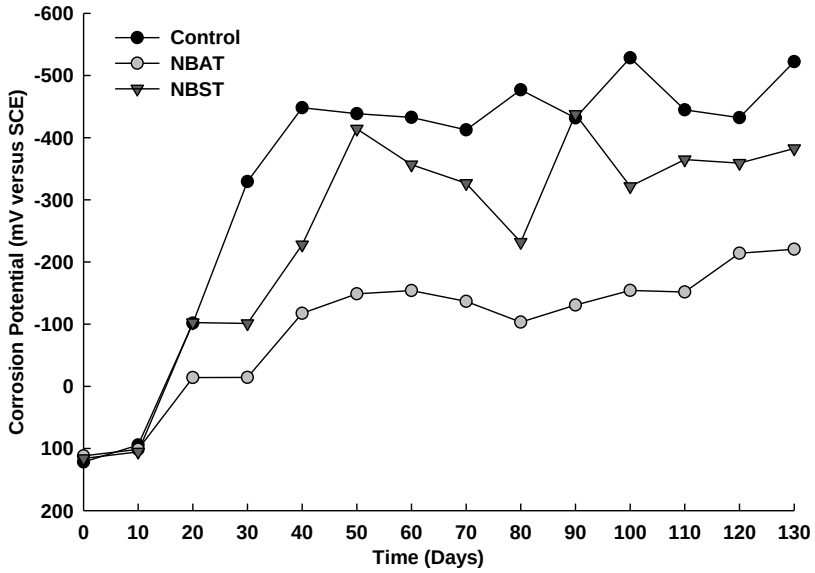

Figure 4.31 Corrosion potential 'E_{corr}' (mV/SCE) values of control, NB-bacterial admixed treated (NBAT) and NB-bacterial spray treated (NBST) reinforced concrete specimens during the chloride exposure

After the first 4 cycle of chloride exposure, corrosion potential in control specimen was decreased to the value of -448.01 mV/SCE. Then the corrosion potential further dropped to more electronegative value (-522.30 mV/SCE) in control specimen at the end of 12th cycle of chloride exposure. In NBST specimens, corrosion potential values till the 6th exposure cycle remains within the range of -321.4 mV/SCE and - 414.07 mV/SCE. At the end of chloride exposure,

potential value in NBST specimen was observed to be - 382.6 mV/SCE. However in NBAT specimen, corrosion potential value at the end of chloride exposure was observed to be - 220.4 mV/SCE. Among all reinforced concrete specimens, lowest drop in the potential value on the chloride exposure was observed in NBAT specimen.

4.2.3.2 Corrosion current (I_{corr})

To monitor the degree of corrosion rate in rebar, corrosion current density (I_{corr}) for all specimens were measured. During the chloride exposure, I_{corr} values were recorded in all specimens till the stage of corrosion was initiated and are presented in Table 4.10 and Figure 4.32.

Table 4.10 Corrosion current 'I_{corr}' ($\mu A/cm^2$) measurements at different chloride exposure time

Specimens	Exposure time		
	Before exposure	6^{th} cycle	12^{th} cycle
Control	$7.200e^{-3}$	0.04	0.34
NBAT	$1.900e^{-3}$	$6.900e^{-3}$	0.02
NBST	$4.300e^{-3}$	0.001	0.03

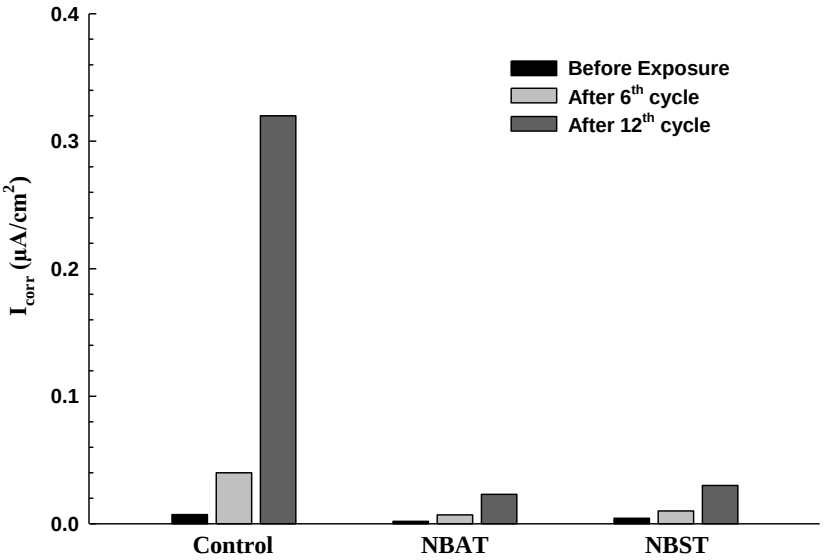

Figure 4.32 Corrosion current 'I_{corr}' ($\mu A/cm^2$) values of control, NB-bacterial admixed treated (NBAT) and NB-bacterial spray treated (NBST) reinforced concrete specimens during the chloride exposure

Among all specimens, control specimen recorded the maximum I_{corr} value at the end of 12^{th} wet-dry cycle. At the end of chloride exposure, I_{corr} value in control specimen recorded was 0.34 $\mu A/cm^2$ which illustrates the start of depassivation process on the rebar surface. However, in NBST and NBAT specimens, I_{corr} values of 0.02 $\mu A/cm^2$ and 0.03 $\mu A/cm^2$ were recorded at the end of chloride exposure. The values of I_{corr} recorded in NBST and NBAT were quite low representing the negligible rate of corrosion.

During the chloride exposure, in control specimen an increased trend of corrosion potential with successive cyclic chloride exposure was observed. At the end of 6^{th} cycle, corrosion potential in control specimen dropped to more electronegative value (-432 mV/SCE) which depicts the corrosion susceptibility of rebar is above 90% and a sign of active corrosion. According to ASTM standard (ASTM C876-09), the probability of reinforcement corrosion initiation on steel surface is above 90% when the potential value drops below -426 mV/SCE. However, the corrosion current density of control specimen after the same exposure interval of 6 wet-dry cycles was observed to be very low (0.04 $\mu A/cm^2$) as shown in Figure 4.32. The observed corrosion current value of control specimen indicates the passive state of rebar with no sign of corrosion. This trend of corrosion potential while monitoring shows that more negative values do not necessarily indicate an increase in corrosion of reinforcement.

It was also reported that, more negative corrosion potential drops might reflects the lack of oxygen concentration at the boundary of the steel rebar and cementitious matrix (Kupwade-Patil and Allouche, 2013). Further, the corrosion potential in control specimen remains steady till the successive 5 wet-dry cycles and the values lies between -431.7 mV/SCE to -476.84 mV/SCE. Corrosion potential followed an ascending trend and the highest value in control specimen was recorded to be -522 mV/SCE after the 12^{th} wet-dry cycle, which indicates the probability of corrosion initiation on the steel rebar surface. In control specimen, this trend in corrosion potential might be attributed to the de-passivation of the passive layer on the rebar. With the accelerated effect due to wet-dry cycle of chloride exposure, jump in corrosion current value of control specimen was observed. At the end of 12^{th} cycle, corrosion current density in control specimen reached to the value of 0.34 $\mu A/cm^2$. It is reported that, the corrosion current density more than the value of 0.1 $\mu A/cm^2$ is the sign of the initiation of de-passivation process of steel rebar (Niu et al. 2020). The value of corrosion current in the range of 0.1 μAcm^2 to 0.5 μAcm^2 is

an indication of weak to moderate susceptibility of corrosion on the rebar surface (Broomfield, 1997). On comparison with control, NBAT specimen registered significant resistance against the ingress of chloride ions due to the microbial treatment. In NBAT specimen, biodeposition of calcium carbonate after bacterial curing effectively blocks the pore matrix of concrete and permitted low chloride ion penetrability. At the end of 6^{th} wet-dry cycle, NBAT specimen shows the lowest drop in the corrosion potential (-148 mV/SCE) which indicates the passive condition of rebar. At the end of chloride exposure, corrosion potential value (-220 mV/SCE) and corrosion current density in NBAT specimen was lowest. In comparison with NBAT, NBST specimen after 6^{th} cycle exhibited further drop in the corrosion potential (-414 mV/SCE). As with the further chloride exposure, at the end of 12^{th} cycle, corrosion potential of NBST lies at -382 mV/SCE and the corrosion current value was observed to be 0.03 μAcm^2. On the basis of corrosion current value, chloride induced corrosion on the reinforcement of NBST specimen had not significant detrimental effect and condition of steel rebar falls under passive state. Among all reinforced concrete specimens, maximum resistance against the chloride ingress was observed in NBAT specimen. The electrochemical analysis indicates that microbial $CaCO_3$ precipitation effectively reduced the porosity of cementitious matrix.

Reports on the prevention of reinforcement corrosion in cementitious materials with different applications of MICP are still limited. Achal et al. (2012) reported significant reduction in MICP treated reinforced concrete structures as compared to control specimen during accelerated chloride induced corrosion. It was reported that calcite precipitation in microbial treated specimens, reduced the corrosion rate by four times than the control specimens. Biogenic precipitation of calcium carbonate was reported to act as a barrier in the ingress of chloride ions which prevented the initiation of corrosion in reinforcement. Ling and Qian (2017) also reported the protective effects of microbial treated reinforced mortar in the resistance towards the accelerated transmission of chloride. However, in the above mentioned studies, accelerated corrosion tests were used by applying impressed current on concrete and mortar specimens to study corrosion phenomenon. In another study, Erşan et al. (2018) reported the prevention of rebar corrosion in concrete structures treated with nitrite producing bacteria. In this study, nitrate reducing bacteria was used for bio-calcification as well as inhibition of rebar corrosion in mortar prism. In this study, bacterial culture was used for biomineralization process by supplementing the culture with calcium nitrate. It was reported that apart from biomineralization process, nitrite

ions (NO_2^-) (intermediate product) were produced, which act as an anodic corrosion inhibitor. Different MICP applications on mortar and concrete specimens have reported the positive outcomes to protect the structures from chloride induced corrosion damages.

4.2.3.3 Visual observation

After monitoring the performance of all the specimens during chloride exposure, control and NBAT specimens were placed in compression testing machine to split the concrete cylinders along the rebar to visualize the corrosion products. In control specimen, formation of corrosion products in rebar-concrete interfaces at different positions throughout the rebar length was observed (Figure 4.33). Presence of corrosion products at rebar-concrete interface supports the beginning of depassivation process on the rebar surface at different points. For the microstructural analysis of corrosion products, powder sample was collected from the rebar/binder interface.

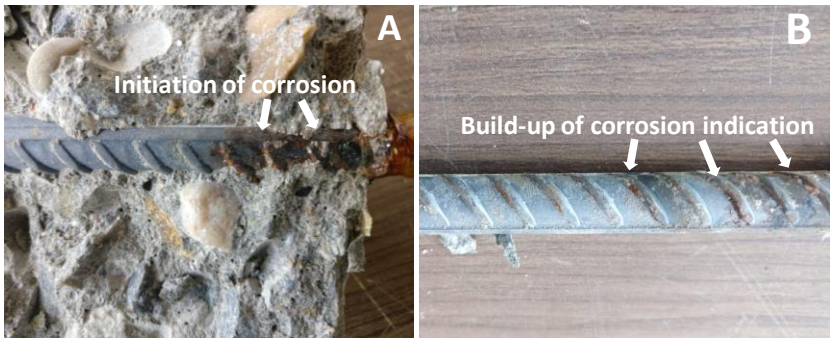

Figure 4.33 Rebar-concrete interface of control specimen (a) rebar with corrosion products (b) after 130 days of chloride exposure

XRD analysis was performed for the samples collected from control specimen at the rebar-concrete interface. As shown in Figure 4.34, peaks of quartz, magnetite along with the some peaks of akanegite a corrosion product was observed. However, in bacterial treated concrete specimens, no sign of corrosive product was observed. As shown in Figure 4.35, rebar-concrete interface in NBAT specimen remained free from chloride induced corrosion after the exposure of 130 days. This observation shows that the passivation layer on the reinforcement was unaffected from the ingress of chloride ions.

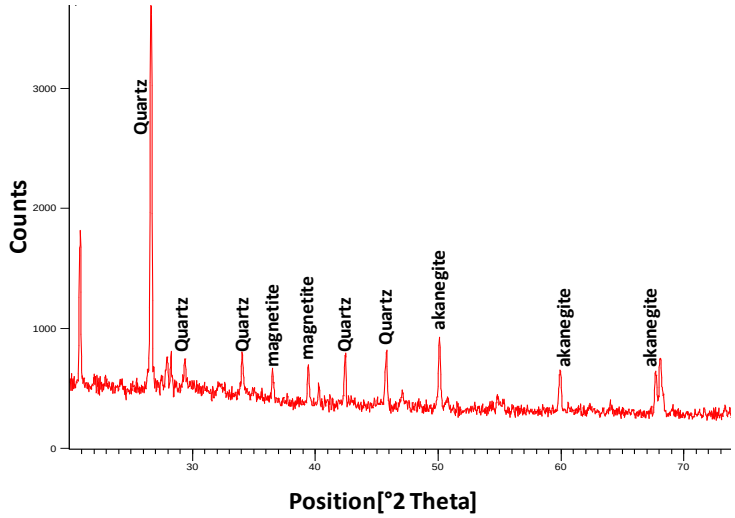

Figure 4.34 XRD analysis of control specimen at rebar-concrete interface revealed the initiation of rebar corrosion with presence of akanegite crystalline phase

Figure 4.35 Rebar-concrete interface of NBAT specimen after 130 days of chloride exposure depicts no sign of corrosion initiation

Unaffected rebar surface from corrosion in NBAT specimen shows the significant reduction in diffusion of chloride ions inside concrete matrix. This study on the basis of corrosion monitoring obtained throughout chloride exposure, highlight the potential of MICP applications in resisting the ingress of chloride ions. On the basis of I_{corr} and E_{corr} trends obtained, NBAT and NBST specimen performed effectively under the aggressive chloride environment. From the observed results in the present study, it is concluded that the utilization of biomineralization activity of calcifying bacteria provides an innovative approach in the prevention of rebar corrosion.

4.2.4 Conclusions

In this study, resistance of bacterial treated concrete against the sulfate and chloride attack was investigated. Two different sulfate exposure regimes were adopted and the performance of bacterial treated concrete as compare to control concrete was monitored for 12 months. In case of chloride attack, bacterial treated reinforced concrete specimens were exposed to 5% NaCl solution and resistance against rebar corrosion was monitored. On the basis of experimental outcomes, following conclusions were drawn:

- During the chemical and physical sulfate exposure, significant reduction of sulfate ions ingress was observed in microbial treated concrete and mortars.
- Throughout the chemical sulfate exposure, NBAT and NBST concrete specimens exhibited no surface deterioration or strength loss. Both specimens were remained intact and no sign of damage due to expansion was observed until the end of experimental study.
- Under physical sulfate exposure, NBAM and NBSM specimen performed well and no sign of surface scaling and salt efflorescence on the upper drying front was observed.
- During the experiment, untreated concrete specimens performed relatively poor. Deterioration due to expansive products causes surface scaling in both exposure regimes. Thick efflorescence as well as severe surface scaling was observed during physical sulfate attack.
- During chloride exposure, microbial treatment in reinforced concrete structures significantly reduced the ingress of chloride ions in the concrete matrix.
- After complete chloride exposure with wet-dry cycles, NBAT and NBST registered the corrosion current (I_{corr}) values much below the 0.1 $\mu A/cm^2$, which depicts that the corrosion was negligible in both the microbial treated specimens
- In control specimen, I_{corr} value was recorded above the range of 0.3$\mu A/cm^2$ which depicts the initiation of corrosion. After splitting the control specimen along the rebar, corrosion product formation at the rebar-concrete interface was observed.
- In microbial treated specimen, no sign of corrosion initiation was observed at the rebar-concrete interface.
- Overall, the application of MICP treatment improved the lifecycle performance of concrete under harsh sulfate environments as well as prevention of rebar from chloride induced corrosion.

4.3 Crack remediation in concrete structures using microbial cementitious grout

Concrete is the most widely used construction material of the world and maintaining concrete structures from premature deterioration is proving to be a great challenge. Early age formation of cracks in concrete structure severely affects the serviceability leading to high cost of maintenance. Apart from conventional methods of repairing cracks with sealants or treating the concrete with adhesive chemicals to prevent the cracks from widening, development of a new domain called a microbial crack-healing has shown promising results. In this study, the objective was to develop a fly ash (FA) amended cementitious grout with optimized flowability to repair crack in concrete. The repaired crack with grouting in concrete was cured with bacterial ponding and bacterial spray. Improvement in water tightness and mechanical strength recovery after crack repairing in concrete was analyzed.

4.3.1 Fresh and mechanical properties of cementitious grout

4.3.1.1 Marsh cone test

Flowability is an important parameter of a grouting material which ensures its efficient pumping or injectability in repairing the concrete crack. In this study, flowability of grout was evaluated by using marsh cone test. Marsh cone belongs to the family of orifice tests in which fresh properties of grout such as workability as well as quality control of grouts are evaluated. This test was conducted to investigate the influence of addition of fly ash and bacterial cells on the fluidity of cementitious grout. The flow time of all the grout mixes is shown in Table 4.11. In marsh cone test, flow time of all twenty four grout mixes was reduced with increase in water/bacterial culture-binder ratios as shown in Figure 4.36. In control grout mixes, flow time was higher among all grout mixtures at both water/binder and bacterial culture/binder ratios (0.45 and 0.5). However, with the addition of FA as well as bacterial culture in control grout mix, reduction in flow time was observed. In neat grouts, subsequent addition of FA at all the replacement levels significantly reduces the flow time as compare to control grout. In neat grouts with 0.5 water/binder ratio and subsequent FA replacements, notable reduction in flow time was observed which varies from as high for control (96 seconds) to as low for 50% FA grout mix (61 seconds). In bacterial grouts, when bacterial culture/binder ratio was increased from 0.45 to 0.5 significant reduction in flow time was observed on comparison of all the grout mixes.

Table 4.11 Results of flow time (FT_{800} in seconds) for different combinations of FA cement grouts

	w/b ratio	**Control**	**10%FA**	**20%FA**	**30%FA**	**40%FA**	**50%FA**
Neat grout	0.45	105±2.1a	86±2.2b	82±1.5b	81±1.6c	72±3.1d	79±2.4c
	0.5	96±3.4a	76±3.1b	78±1.6b	64±2.2c	64±2.1c	61±1.6d
	bc/b ratio						
Bacterial grout	0.45	98±1.8a	82±2.4b	80±2.4c	73±1.8d	61±2.2f	67±3.1e
	0.5	91±2.4a	71±3.2b	68±3.2b	60±2.2c	53±2.1d	58±2.1c

Values sharing a common letter within the row are not significant at $P < 0.05$. Values are mean ± standard deviation (n = 3); FA: Fly ash; w/b ratio: water/binder ratio; bc/b ratio: bacterial culture/binder ratio; FT_{800}: flow time for 800 ml

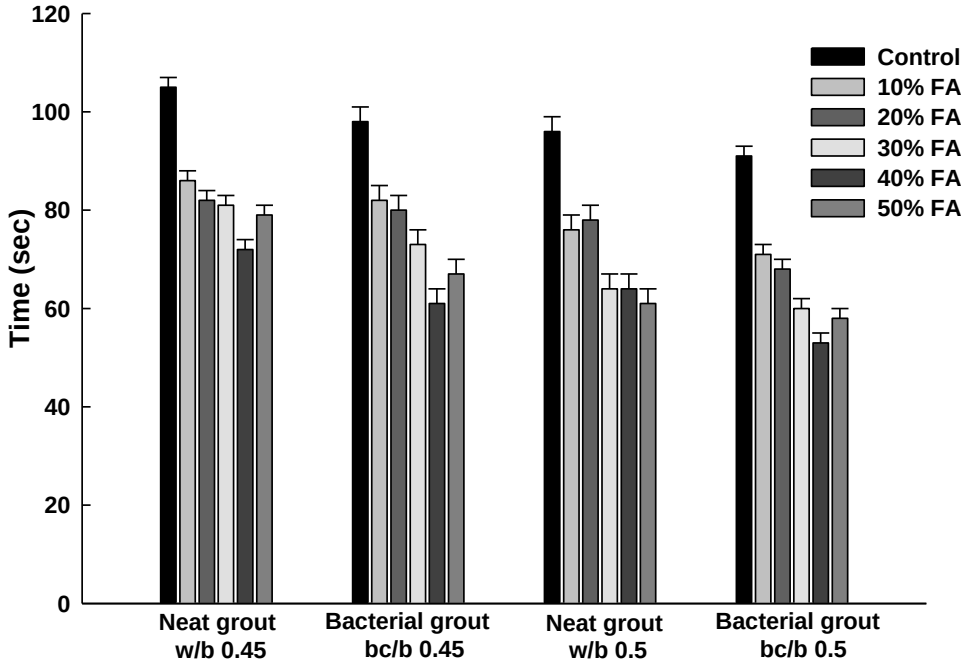

Figure 4.36 Marsh cone test analysis of fluidity of grout mixtures amended with different dosages of FA. w/b ratio: water/binder ratio; bc/b ratio: bacterial culture/binder ratio

Flow time in bacterial grouts varies from 91 seconds for control to as low as 53 seconds for 40% FA grout mix. Incorporation of 40% FA with higher bacterial culture-binder ratio (0.5), reduces the flow time as compared to control bacterial grout by 74%. It was observed that, at higher bacterial culture-binder ratio and higher FA incorporation results into higher grout flowability.

4.3.1.2 Mini slump test

Mini slump test was conducted for comparing the addition of FA and bacterial culture on the plastic viscosities of various combinations of grout mixes. The spread flow of grout mixes with different water/bacterial culture-binder ratios and FA replacements is shown in Table 4.12. In general, gradual increase in spread diameters of neat grouts and bacterial grouts was observed when water/bacterial culture-binder ratios were increased from 0.45 to 0.5. Further, flowability and spreading ability of grouts was enhanced with addition of FA resulting into increased mini slump diameters. As shown in Figure 4.37, mini slump diameter in control mix (neat grout) was observed to increase up to 10% when water/binder ratio was increased from 0.45 to 0.5. In a similar fashion, spread diameter of control mix (bacterial grout) was increased up to 24% when bacterial culture/binder ratio was increased from 0.45 to 0.5.

Table 4.12 Results of grout spread flow (mm) for different combinations of FA cement grouts

	w/b ratio	**Control**	**10%FA**	**20%FA**	**30%FA**	**40%FA**	**50%FA**
Neat grout	0.45	80±2.1a	77±2.2b	72±1.5b	81±1.6c	87±3.1d	79±2.4c
	0.5	92±3.4a	82±3.1b	86±1.6b	92±2.2c	97±2.1c	97±1.6d
	bc/b ratio						
Bacterial grout	0.45	84±1.8a	76±2.4b	79±2.4c	87±1.8d	92±2.2f	84±3.1e
	0.5	97±2.4a	84±3.2b	82±3.2b	94±2.2c	102±2.1d	92±2.1c

Values sharing a common letter within the row are not significant at $P < 0.05$. Values are mean ± standard deviation (n = 3); FA: Fly ash; w/b ratio: water/binder ratio; bc/b ratio: bacterial culture/binder ratio

Incorporation of FA with increased dosages showed a general trend of substantial increase of mini slump diameter in all the grout mixes reflecting an increase in fluidity property. In FA amended cement grouts, higher replacements of cement with FA significantly increased the mini slump diameter showing better workability. Among the bacterial grouts, maximum spread diameter was observed in 40% FA amended grout (bc/b 0.5) with 43% increment as compared to control grout (bc/b 0.45) and 16% increment as compared to control grout (bc/b 0.5). In Figure 4.37, a notable decrease in plastic viscosity was observed when water/bacterial culture content

was increased from 0.45 to 0.5. From the results, it can be predicted that addition of higher dosage (40%) of FA along with combination of bacterial culture significantly enhanced the dispersion ability of grout.

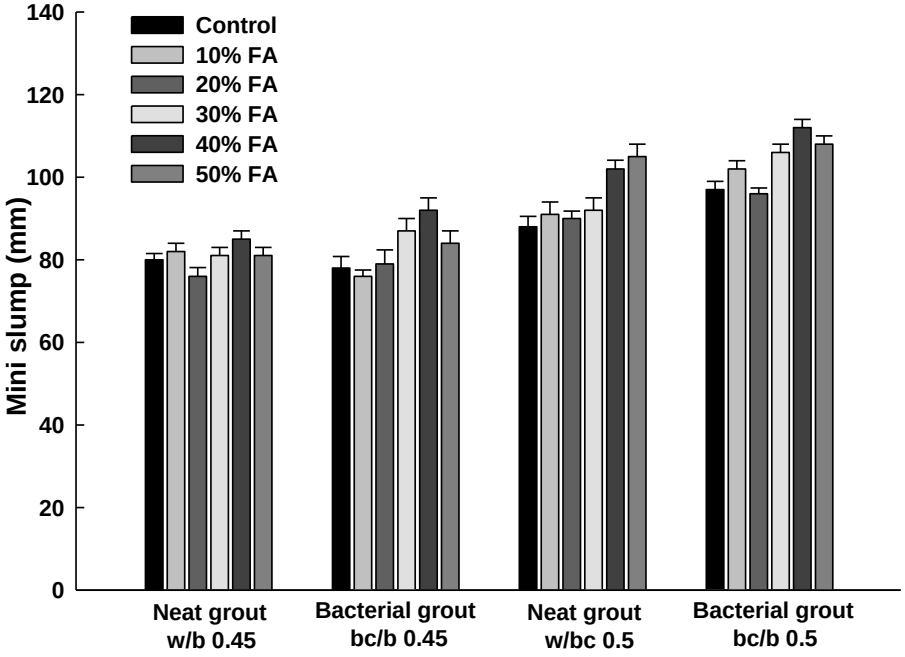

Figure 4.37 Mini slump diameters of different combinations of FA cement grout mixtures. w/b ratio: water/binder ratio; bc/b ratio: bacterial culture/binder ratio

4.3.1.3 Strength properties of grouts

The compressive strength results of neat grout and bacterial grout are presented in Table 4.13. Effect of addition of FA with different dosage and effect of incorporation of bacterial culture was investigated. During the casting of grout mixes, water/binder ratio as well as bacterial culture/binder ratio of 0.5 was maintained. Compressive strength of control neat grout and bacterial grout was observed to be 16.2 MPa and 18.2 MPa. On the addition of FA in neat grout mixes, maximum strength gain was observed in 20% FA amended grout (18.2 Mpa) and with successive increase of FA dosage in neat grouts, reduction in strength as compared to control was observed (Figure 4.38). Among all the neat grout mixes, 50% FA amended grout showed the significant decrease in compressive strength (15.8 MPa) as shown in Figure 4.38.

Table 4.13 Compressive strength (MPa) of neat and bacterial grout mixes amended with different dosages of FA at 28 days age of curing

		Control	10%FA	20%FA	30%FA	40%FA	50%FA
Neat grout	***w/b ratio* (0.5)**	16.2±0.8d	17.6±1.3b	18.8±1.2a	17.9±1.4b	16.8±1.6c	15.8±1.8e
Bacterial grout	***bc/b ratio* (0.5)**	18.2±1.4d	18.8±0.9d	20.1±0.8b	19.8±0.7c	21.2±1.2a	16.8±1.9e

Values sharing a common letter within the row are not significant at $P < 0.05$. Values are mean ± standard deviation (n = 3). w/b ratio: water/binder ratio; bc/b ratio: bacterial culture/binder ratio

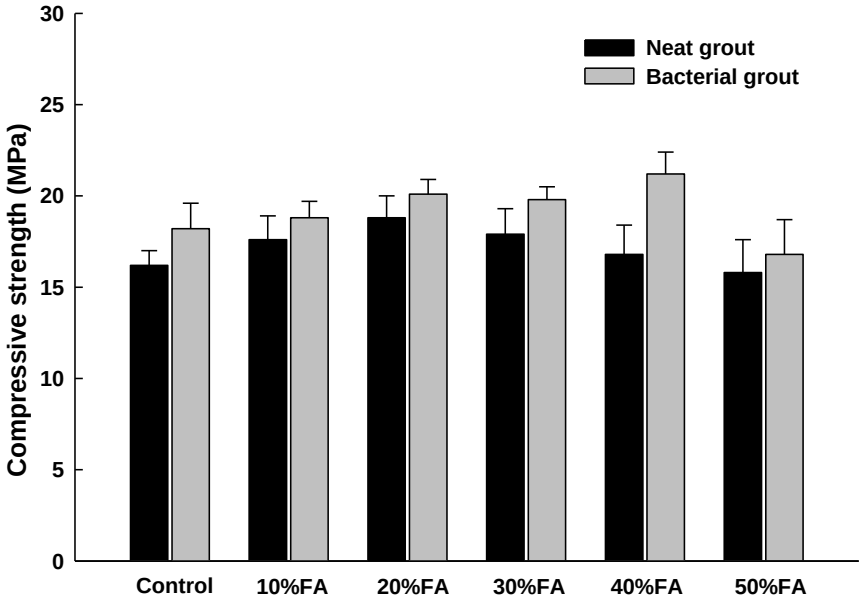

Figure 4.38 Compressive strength of neat and bacterial grout mixes amended with different dosages of FA and water/bacterial culture-binder ratio of 0.5 at 28 days age of curing

In case of bacterial grout mixes, effect of incorporation of bacterial cells as well as curing with bacterial treatment results into strength gain. Bacterial treatment enhances the strength in almost all the bacterial grout mixes on comparison to control neat mix. Maximum strength gain was observed in 40% FA amended bacterial grout (21.4 MPa) however slight decrease was observed in 50% FA amended bacterial grout. The results indicate that due to bacterial treatment, overall strength improvement was observed among all the bacterial grout mixes.

Cement based grouts has been widely used as a repair material for cracks which are generated in concrete structures due to distress during their service life. For repair and rehabilitation of cracked concrete structures, cement based grouts are applied by injection method for filling cracks. Cement grouts are essentially fluid mixtures which contain cement, water and might be with or without admixtures which can be injected into cracks using gravity flow or pressure-assisted pumping. For penetrability and pumpability of cement grouts in cracks, factors like high flowability, good workability, strength and durability plays an important role in successful operations of grouting.

In this study, substitution of cement with FA as well as bacterial culture was introduced in the cement grout to seal the cracks in concrete structures. To achieve a suitable grouting material, different replacement dosages of FA (10% to 50%) in cement and two water-binder ratios (0.45 and 0.5) were studied. First, flow properties of different mixes were investigated by conducting marsh cone and mini slump test (Figure 4.36 - 4.37). It was observed that subsequent addition of fly ash in neat grout mixes reduces the efflux flow time on comparison of control mix. Maximum reduction in flow time was observed in neat cement grout mix with 40% FA and 50% FA on comparison to control when water-binder ratio was kept low at 0.45 (Figure 4.36). In a similar trend, when water-binder ratio was increased to the value of 0.5, reduction in efflux flow time was observed and neat grout with 40% FA and 50% FA showed lowest efflux flow time. The results indicate that, FA incorporation at higher levels in cement grout increase the flowability of suspension and significantly reduce the flow time. In previous studies, the addition of FA as cement substitution with various dosages has also been reported the increased flowability of cement paste (Mirza et al. 2002). Najjar et al. (2017b) also reported the decreased efflux time when FA dosage was increased from 10% to 50% in two stage concrete grout.

Apart from the increased fluidity, spread diameter in mini slump test also showed an enhanced flowability when FA dosage was increased. In neat grout with high water-binder ratio (0.5), maximum spread diameter was observed in 40% FA and 50% FA amended grout (Figure 4.37). The results obtained in marsh cone test and mini slump test indicated that fly ash particles play an important role in influencing the fresh properties of grout mixes (Figure 4.36 - 4.37). It has been reported in previous studies that, fly ash as compared to cement particle has spherical shape as well as smooth surface texture, which results into ball bearing effect in the suspension causing the reduction in the internal frictional forces (Bras et al. 2010; Najjar et al. 2017b). This property

of fly ash in the suspension further leads to lubricating effect, thus facilitating mobility and better pumpability of grout (Manz, 1999). Wang et al. (2013) also reported that more percentage of fly ash dosage have significant effect of linear decrease on the plastic viscosity.

In cement grouts, water-binder ratio also plays an important role. It was observed that when water/binder ratio in neat grouts was increased from 0.45 to 0.5, efflux flow time in marsh cone was decreased and spread diameter in mini slump was increased at all the replacement levels of FA (Figure 4.36 – 4.37). The flow property of a grout is inversely proportional to water content, which can also be stated that higher the water-binder ratio in grout mix, lower is the viscosity of grout mix. It is reported that fresh properties like yield stress and plastic viscosity of a grout composition decreased with increase in percentage of water (Bras et al. 2010). Yield stress in a grout is a limit stress value which means that when yield stress is lower than resistance in the grout to start flow is less. So when the water content is sufficient in a grout, its yield stress property will be less and which results into the penetrability of grout mixture into cracks and voids (Celik and Canakci, 2015). The range of water-binder ratios for the consolidation and repair of masonry structures is reported between 0.5 and 1.5. Based upon the previous reports as well as the observed results in this study, the higher water - binder ratio (0.5) was opted for the further studies.

Apart from neat grout mixes, incorporation of bacterial culture instead of water in the various grout compositions was also investigated. On the addition of bacterial culture in grout mixes, efflux flow time in marsh cone and mini slump flowability was almost similar with the trends of neat grout mixes. However, when bacterial culture-binder ratio was higher (0.5), minimum flow time was observed in 40% FA amended bacterial grout and mini slump spread diameter of 40% FA and 50% FA grout remained almost similar with minimal difference (Figure 4.37). In some previous studies, use of microorganisms as viscosity modifying admixtures was reported. Pei et al. (2015) reported the use of bacterial cell walls of *Bacillus subtilis* as viscosity enhancing admixture in the cement paste. Increase in viscosity of all the cement pastes was reported, however the viscosity was reported to be decreased when the shear rate was increased and w/c ratio was kept higher. Bacterial cell wall is a peptidoglycan, a polysaccharide and functions as a viscosity modifying admixtures. In high water-binder ratio, the attractive forces between adjacent polysaccharide chains are weakened in the presence of more water and the increase in

the viscosity of cement paste diminished (Pei et al. 2015). In a recent study, influence of *Sporasarcina pasteurii* cells on the viscosity of cement-based materials was reported (Azima and Bundur, 2019). It was reported that addition of bacterial cells (which are broadly polysaccharides and peptidoglycans) at lower w/c ratio in cement paste increased the viscosity and lowers the flowability properties. However at higher w/c ratios, influence of bacterial cells as viscosity modifying admixture was less pronounced and high water content limits the attractive forces between polysaccharide chains leading to high fluidity in cement paste.

Based on the flow time and mini slump results, water/bacterial culture – binder ratio (0.5) in FA amended grouts was opted for the further studies. After fresh properties, compressive strength of hardened grout with water/bacterial culture - binder ratio (0.5) was investigated after 28 days age of curing. It was observed that when FA dosage was increased in neat grout mixes after 20% FA replacement, decrease in the strength properties was registered in successive cement grout specimens with higher FA. On maximum replacement levels with FA, compressive strength in 50% FA amended grout specimen was registered to be the lowest. The observed results of decreased strength with higher FA dosage might be due to the decreased concentration of hydration products such as C_3S. It was also reported in a previous study that, when 50% cement was replaced in grout mix with FA, then the calcium ions (Ca^{2+}) adsorb on the surface of FA particles which causes a depression of the calcium concentration in the pore solution (Najjar et al. 2017b). This phenomenon further delay the CH and calcium silicate hydrate (CSH) nucleation and crystallization. Chindaprasirt et al. (2005) also reported the strength loss in cement paste when FA with the replacement level of 40% was used. It was reported that blended cement pastes with original fly ash leads into higher total porosity and capillary porosity resulting into lower compressive strength than portland cement paste.

However in bacterial grouts, overall strength properties among all the mixes were improved as compare to neat grouts. Among bacterial grout mixes, 40% FA amended grout specimen showed maximum strength. The results indicated that addition of bacterial cells improve the strength properties as compared to neat grout specimens. As the bacterial culture was supplemented with urea and calcium chloride which results into calcium carbonate precipitation in the cement matrix compensating the reduction in strength due to FA incorporation. From the observation,

40% FA amended grout mix and (0.5) bacterial culture – binder ratio was selected to further implement the resulting grout in concrete crack repairing.

4.3.2 Influence of bacterial grouting on mechanical strength and permeation properties

In this section, effect of crack repairing with 40% FA amended bacterial grout on strength recovery and water tightness of concrete specimens was presented. In bacterial grouting process, cracks in horizontal orientation and vertical orientation were treated with bacterial curing. Micro structural analysis of bacterial grouting was performed after the end of 14 days of curing. The graphical representation of bacterial treatment of cracks is shown in Figure 4.39.

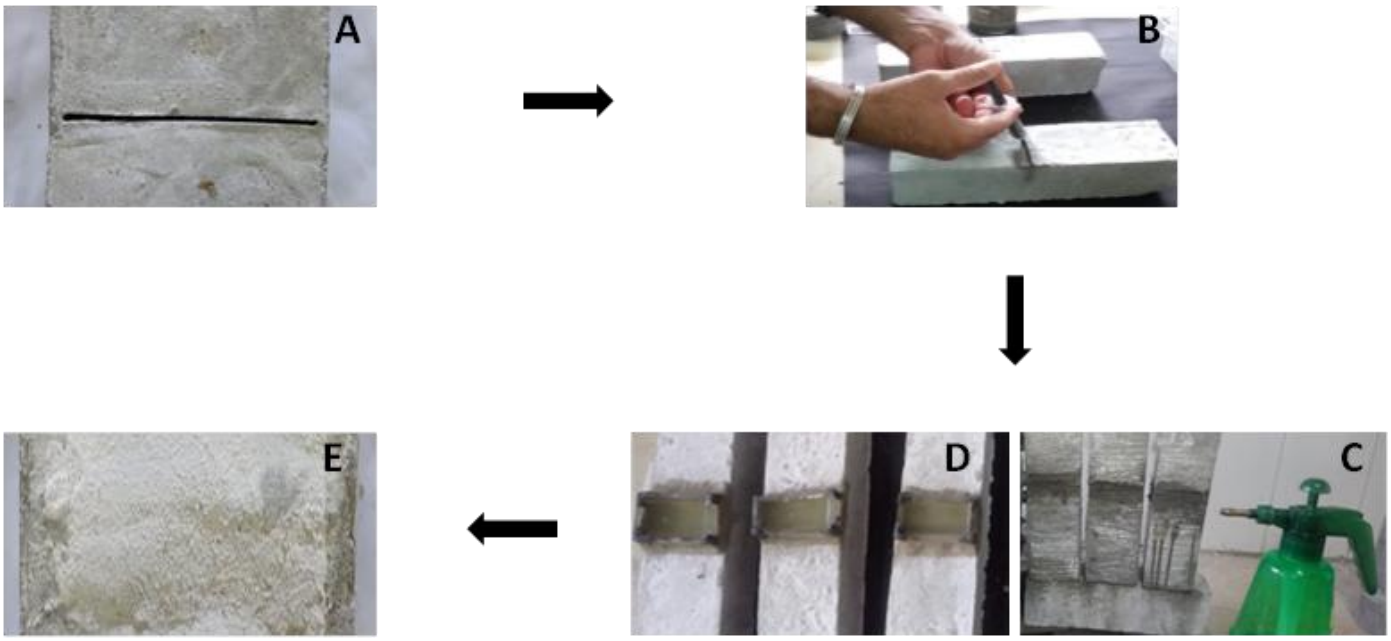

Figure 4.39 Treatment of artificially generated cracks with injectable 40% FA amended bacterial grout (A) Crack generated in concrete (B) Crack repairing with bacterial grout (C and D) Curing with bacterial ponding and bacterial spray (E) Repaired crack after bacterial curing

4.3.2.1 Compressive strength

Effect of crack repair on the strength properties of concrete cube specimens with bacterial cementitious grouting as well as bacterial curing was investigated. Compressive strength of all the different sets of concrete specimens is shown in Figure 4.40. Compressive strength of UTC (untreated concrete) without grout repairing was observed to be 32.5 MPa. Compressive strength

in FCG (FA - cement grout) specimen after crack repair with 40% FA amended cement grout was observed to be 35.8 MPa resulting into strength gain of up to 11% on comparison with UTC.

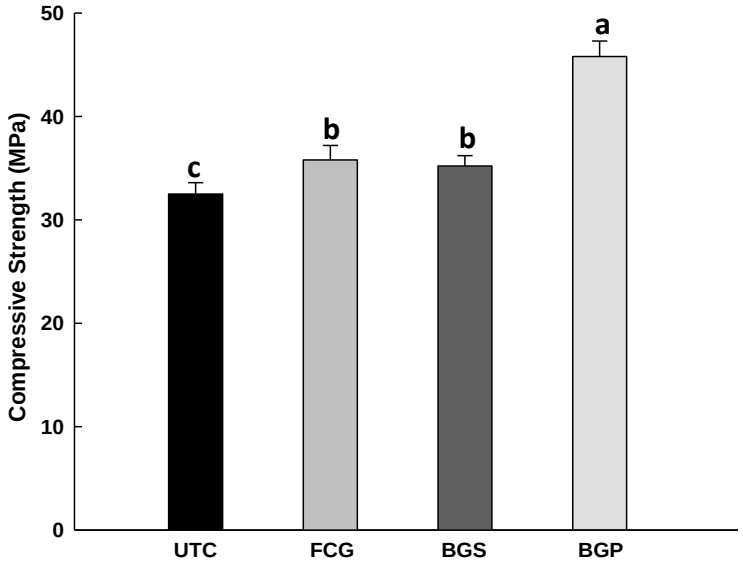

Figure 4.40 Compressive strength of concrete specimen after crack treatment with grouting. UTC: Untreated concrete; FCG: FA-cement grout; BGS: Bacterial grout with spray treatment; BGP: Bacterial grout with ponding treatment. Bars sharing a common letter within the treatment are not significant at $P < 0.05$. Error bars represents standard deviation (n = 3)

In BGS (bacterial grout with spray treatment) specimen, crack repaired with 40% FA amended bacterial grout as well as curing with spray treatment using bacterial culture grown in NB supplemented with urea and $CaCl_2$ for 14 days showed a compressive strength of 35.2 MPa. As compared to UTC specimen, compressive strength with an increase of 11% was observed in BGS specimen. However, in BGS and FCG specimens no major difference in strength gain was observed. In BGP (bacterial grout with ponding treatment) specimens, after crack repair with 40% FA amended bacterial grout and curing with bacterial culture using ponding method showed a significant increase of compressive strength (45.8 MPa). As compare to UTC, BGP registered a strength recovery of up to 40% due to biocementation. In an overall trend, highest mechanical strength recovery was observed in BGP specimen among all the concrete specimens.

4.3.2.2 Flexural strength

The effect of crack repair with FA amended bacterial grout on the flexural strength of concrete prisms was investigated after 14 days of bacterial curing. Flexural strength of all concrete prisms is shown in Figure 4.41.

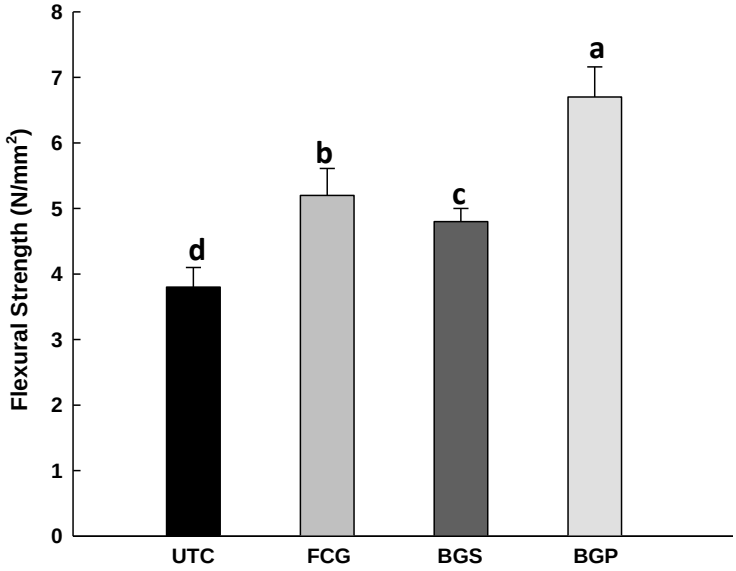

Figure 4.41 Flexural strength of concrete prisms after crack treatment with grouting. UTC: Untreated concrete; FCG: FA-cement grout; BGS: Bacterial grout with spray treatment; BGP: Bacterial grout with ponding treatment. Bars sharing a common letter within the treatment are not significant at $P < 0.05$. Error bars represents standard deviation (n = 3)

Flexural strength of UTC (untreated concrete) without grout repairing was observed to be 3.8 N/mm^2. Flexural strength in FCG (FA - cement grout) specimen after crack repair with 40% FA amended cement grout was observed to be 4.8 N/mm^2 resulting into gain of up to 26% on comparison with UTC. In BGS specimen, crack repaired with 40% FA amended bacterial grout as well as curing with spray treatment using bacterial culture grown in NB supplemented with urea and $CaCl_2$ for 14 days showed a flexural strength of 4.2 N/mm^2. As compared to UTC specimen, flexural strength with an increase of 10% was observed in BGS specimen. In BGP specimens, after crack repair with 40% FA amended bacterial grout and curing with bacterial culture using ponding method showed a significant increase of flexural strength (6.7 N/mm^2). As compare to UTC, BGP specimen exhibited highest flexural strength recovery due to bacterial grouting and the respective curing regime.

4.3.2.3 Water tightness

Upon crack repair with FA amended bacterial grout, capillary water absorption test was conducted for all concrete specimens after 14 days of the respective curing regimes and results are presented in Table 4.14 and Figure 4.42. Among all the concrete specimens, UTC registered the highest sorptivity coefficient (0.03). In case of FCG specimen, sorptivity coefficient (0.01) less than UTC specimen was observed and registered less water absorption than UTC.

Table 4.14 Sorptivity analysis of concrete specimens after crack treatment with grouting

Specimen	Sorptivity coefficient 'k'
UTC	0.03 ± 0.0^{a}
FCG	0.01 ± 0.0^{b}
BGS	0.005 ± 0.0^{c}
BGP	0.002 ± 0.0^{d}

Mean values sharing a common letter within the column are not significant at $P < 0.05$

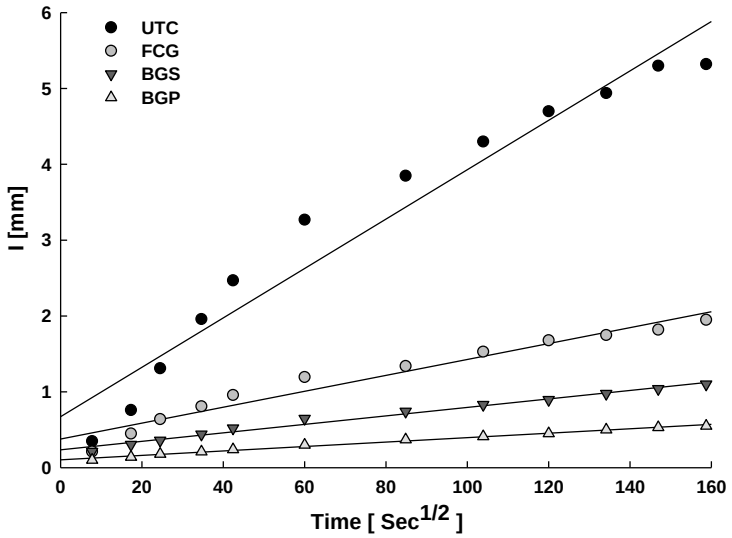

Figure 4.42 Sorptivity analysis of untreated concrete (UTC), FA-cement grout treated (FCG), Bacterial grout with spray treatment (BGS) and Bacterial grout with ponding treatment (BGP)

However, lowest water absorption was registered in BGP specimen and sorptivity coefficient of 0.002 was noted in. As compared to BGP, slight increase in water absorption was observed in BGS specimen. On the basis of water absorption rate, significant restriction of water ingress in BGP specimen showed the efficient curing method of ponding with bacterial culture.

4.3.3 Micro-structural analysis

SEM analysis of all the cracks repaired concrete specimens was done to characterize the calcium carbonate crystals. The SEM images of both BGP and BGS specimen is presented in Figure 4.43. The SEM images of both BGP and BGS specimens taken from the upper depth of 0–10 mm clearly identified the presence of calcium carbonate crystals.

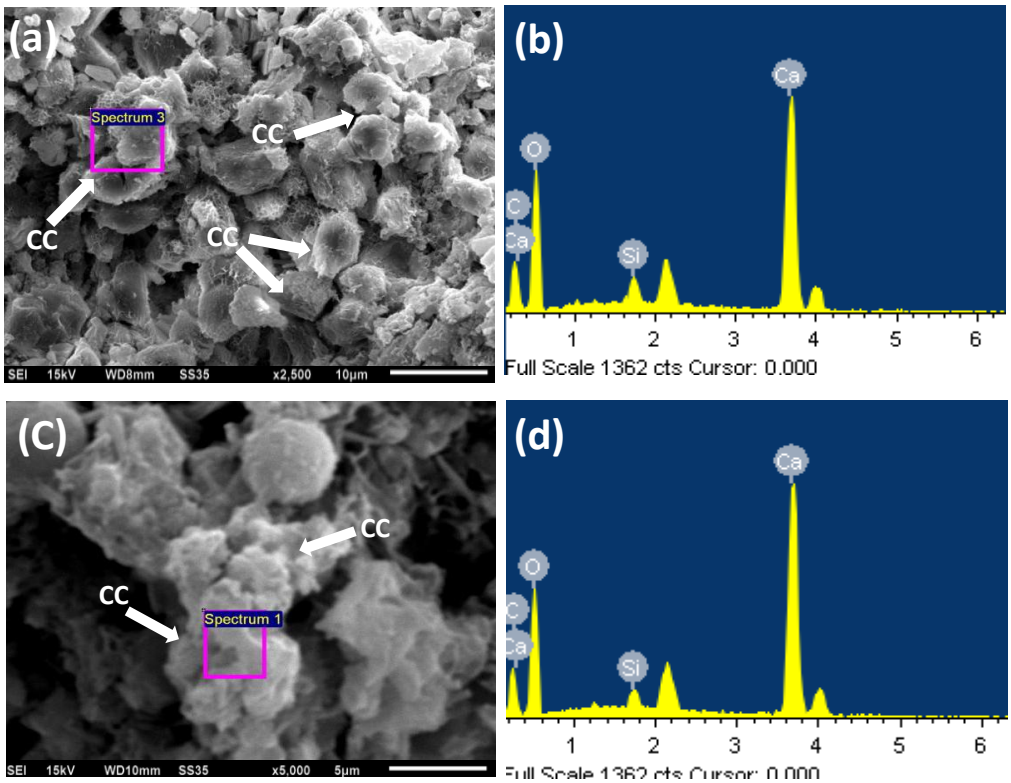

Figure 4.43 SEM-EDX images represent the $CaCO_3$ crystals (CC) in BGP specimen (a, b) and BGS specimen (c, d). Square sign '□' indicate the spot of spectrum for EDX analysis

In case of BGP specimen, presence of thick biodeposition of calcium carbonate crystals was observed. Dense formation of rhombohedral calcite crystals were observed in grout repaired cracks as shown in Figure 4.43a. The EDX analysis also confirmed the elemental composition of crystals with peaks showing high amount of calcium and carbon (Figure 4.43b). In BGS specimen, presence of dense biodeposition of closely attached calcite crystals in association with bacterial cells was observed (Figure 4.43 c). The EDX analysis also confirmed the elemental composition of crystals with peaks showing high amount of calcium and carbon (Figure 4.43d).

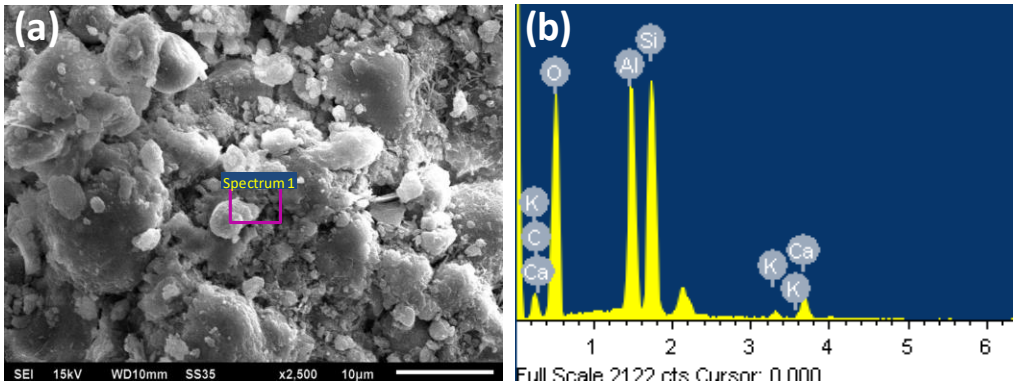

Figure 4.44 SEM-EDX images of FCG specimen. Square sign '□' indicate the spot of spectrum for EDX analysis

In case of FCG specimen, calcium silicate hydrate (CSH) gel was observed in SEM analysis in the presence of fly ash particles (Figure 4.44a). In EDX analysis, high silica peaks along with aluminum peaks was observed (Figure 4.44b). In comparison of BGS and BGP specimens, absence of calcium carbonate crystals was noticed in FCG specimen during SEM analysis.

In this study, repair of concrete cracks with bacterial grouting and its effect on the mechanical strength recovery as well as water tightness of repaired concrete structures was investigated. As discussed in the previous section, 40% FA amended bacterial grout composition and the optimum bacterial culture - binder ratio of 0.5 was selected to use as a crack repairing material. As to repair the artificially generated cracks in concrete, two repairing methods were adopted. In the first approach, cracked surface of concrete structures was kept in horizontal position so as to create a replica of concrete slab crack. In second approach, cracked surface was kept in vertical position so as to create similar conditions of crack in a wall. In both the repair approaches, 40% FA amended bacterial grout was injected in the cracks by using 20 ml capacity syringe. After the grouting process was completed, curing of repaired cracks was done after the grout was hardened. The effect of grouting treatment of cracks on the strength properties of concrete structures was investigated. The compressive strength of UTC and FCG specimen was observed to be 32.5 MPa and 35.8 MPa respectively. In this study, UTC was considered as a reference specimen in which crack was kept untreated. Among all the treated specimens, maximum strength recovery was registered in BGP specimens with 40% increase as that of UTC. However in BGS specimen, compressive strength was slightly improved by 8% as compared to UTC specimen. Similar pattern of flexural strength recovery after bacterial grouting was observed.

Among all concrete prisms, maximum flexural strength recovery was observed in BGP specimen as compared to UTC specimen. Bacterial treatment of crack with 40% FA amended bacterial grout as well as curing with bacterial culture using ponding leads to significant flexural strength gain as compared to untreated concrete specimen. Notable flexural strength gain in BGP specimen indicates that biomineralization during bacterial grouting effectively resist the bending failure. From the observed trend of compressive and flexural strength, it was noted that the crack surface in horizontal position recovered the strength significantly on treatment with 40% FA bacterial grout. Further, curing of hardened grout material with bacterial culture using ponding method efficiently improved the compressive as well as flexural strength. However, crack treatment placed in the vertical position results into less strength gain, which might be due to improper or partially injected bacterial grout material.

Apart from strength recovery, effect of bacterial grouting on the permeation properties of crack repaired concrete was also analyzed. Ingress of water and other aggressive agents through cracks in concrete further accelerates the deterioration of structures. Ingress of chlorides and sulfates through the pathway of cracks enhances the rebar corrosion or the formation of expansive products which influence the serviceability of concrete structures. Sorptivity studies were conducted in all the concrete specimens. Sorptivity test measures the water ingress into an unsaturated concrete, which is dominated by capillary suction and is an important parameter that can be correlated to the ingress of deteriorating substances (chlorides or sulfates) into concrete (McCarter et al. 1992). The results of sorptivity test shows that maximum water ingress was observed in UTC specimen with 0.03 sorptivity coefficient (Figure 4.42). In the FCG specimen, water ingress was less than UTC and its sorptivity coefficient was 0.01. The results showed that 40% FA amended neat grout provides better resistance to water ingress in the crack. However, the transport mechanism of water in BGS and BGP specimens through capillary rise was altered effectively in after bacterial grout treatments. Sorptivity coefficient in BGS specimen was observed to be 0.005, which indicates that water penetration inside the treated cracks was efficiently altered by bacterial spray curing. In fact the maximum reduction in water transport was observed in BGP specimen with lowest sorptivity coefficient value (0.002). From the results of sorptivity test, it can be concluded that bacterial grout treatment is an effective way to heal the cracks, which significantly alter the water ingress. In the two treatment methods with two

different crack orientations, improved strength and permeation properties were observed in the horizontal concrete crack treated with 40% FA amended bacterial grout.

The notable mechanical strength recovery and reduction in water ingress due to capillary suction in BGP specimen is achieved due to bacterial induced calcium carbonate precipitation. The approach of using bacterial grout helps in intruding the ureolytic bacterial cells inside the crack depth in a homogenous fashion. Thereafter, curing of hardened bacterial grout with bacterial culture supplemented with urea and $CaCl_2$ enhances the ureolytic activity of bacterial cells. At the end of curing using ponding method, thick biodeposition of calcium carbonate precipitation layer was observed on the treated crack surface. In SEM-EDX analysis of BGP specimen, presence of closely packed rhombohedral calcite crystals provides an evidence of enhanced mechanical properties as well as pore clogging in the grouting material (Figure 4.43a). In the EDX spectrum, high peaks of calcium, carbon and oxygen supports the crystal morphology in the grouting material (Figure 4.43b). In the SEM-EDX analysis of BGS, calcium carbonate crystals in a stacked arrangement were also observed. In BGS specimen, bacterial cells present in grout material were provided with nutrient media, urea and $CaCl_2$ to induce calcium carbonate by surface treatment. Due to repeated cycle of spray treatment, porosity of grout material in the outer depth of cracks might have blocked due to thick biodeposition of calcium carbonate crystals. The $CaCO_3$ precipitation along with exopolymeric substances on the outer portion of grout of crack depth might have affected the movement of nutrient media to pass inside the crack depth. However in BGP specimen, grouting material sufficiently ingresses deeper inside the crack depth and flows under gravity. Due to easy flow of grouting material as well as effective curing with ponding method, bacterial grout repaired the crack in the horizontal position very effectively.

4.3.4 Conclusions

This study investigated the efficiency of bio-based FA amended cementitious grout in the remediation of crack in concrete. Among different FA amended bacterial grouts, maximum fluidity and workability (as fresh properties) and compressive strength (as hardened grout property) were observed in 40% FA amended bacterial grout. Crack treatment in horizontal orientation with injectable bacterial grout and curing method of ponding with bacterial culture showed maximum mechanical strength recovery and significant reduction in permeation as

compared to untreated concrete specimen. In case of crack treatment in vertical orientation and curing method of spraying with bacterial culture showed that the strength gain was nominal however permeation was significantly improved as compared to untreated concrete specimen. In curing approach, ponding of bacterial culture supplemented with urea – $CaCl_2$ showed significant improvement in the overall performance of concrete with repaired crack. The developed bacterial grout with optimum rheological properties will help as an economical and environment friendly MICP technology in injection based applications for the remediation of cracks in concrete. From the results it was concluded that crack repair with 40% FA amended bacterial grout would serve as a potential healing product.

SUMMARY

Chapter 5

Summary

Microbial induced calcium carbonate precipitation (MICP) has a potential to improve the durability properties and remediation of cracks in concrete. The present work was aimed to develop better understanding in the application of calcifying bacteria in durability enhancement and prevention of damages in concrete structures under aggressive environments. The calcifying bacterial strain *Bacillus* sp. CT5 (an alkaliphilic strain), was used in this study because of its high urease producing activity with high efficiency to precipitate $CaCO_3$ crystals. The outcome of research study designed into three objectives is summarized below into three sections.

In the first section of research work, influence on the addition of bacterial culture and organic nutrients (carbon and nitrogen content) of NB and CSL growth media on the setting characteristics of cement, chemical and structural properties of microbial concrete was studied. The setting characteristics of cement paste upon addition of plain nutrients (NB and CSL) as well as bacterial culture grown in NB, CSL media and supplemented with urea and $CaCl_2$ was investigated. Five sets of cement pastes, control paste, NB paste (1.3% of NB, 2% urea and 25 mM $CaCl_2$), CSL paste (1.5% of CSL, 2% urea and 25 mM $CaCl_2$), NB-CT5 paste and CSL-CT5 paste were prepared by mixing cement with bacterial culture grown in NB media and CSL media supplemented with 2% urea and 25 mM $CaCl_2$, respectively. In comparison with control paste mix, it was observed that the addition of plain NB media severely influenced the setting characteristics of cement. Initial setting time was delayed by 100 min and the final setting time by 250 min in NB paste mix when compared to control paste mix. However, addition of plain CSL media had no influence on the setting characteristics of cement. Incorporation of CSL-CT5 showed an inconsequential effect on the setting characteristics. However, addition of NB-CT5 causes not as much of delay in setting of cement as it was observed in NB paste. Introduction of organic components of plain NB (Yeast extract) has a retarding nature, which severely affected the chemical properties of cement resulting into retardation of initial hydration of cement.

To analyze the change in the chemical and structural properties, seven mixes for concrete cubes (150 x150 x 150 mm) and concrete cylinder disc (100 x 50 mm) were prepared with mix design as cement: sand: coarse aggregate in the ratio of 1:1.82:3.24 (w/w) and water to cement ratio (w/c) of 0.5. Control, CSL treated (CT), NB treated (NT), CSL-bacterial admixed treated (CBAT), NB-bacterial admixed treated (NBAT), CSL-bacterial spray treated (CBST) and NB-

bacterial spray treated (NBST) concrete specimens were prepared. The carbon and nitrogen content in concrete cubes with depth-wise profiling (up to 50 mm) was done by collecting powder samples with drilling at regular interval.

In control specimen lower levels of carbon and nitrogen was observed at all depths. Maximum carbon and nitrogen content was observed in NBAT and NBST specimens followed by NT at all the depths. On comparison, CBAT and CT specimens followed by CBST registered minimum carbon and nitrogen content. Overall, carbon and nitrogen content in NBAT and NBST specimens was observed to be higher than CBAT and CBST specimens at all depths. Similar trend of overall carbon and nitrogen content was observed to be higher in NT specimen on comparison with CT specimen at all depths. Alkaline environment of concrete was not influenced with addition of bacterial cells or with the carbon and nitrogenous material. The pH values in all specimens was found to be in the range of 12.0–12.4, which indicates that bacteria and addition of NB and CSL media does not have a significant effect on the alkaline environment of concrete.

Compressive strength of control specimens was 36 Mpa after 28 days of curing. On comparison with control, NBAT and NBST specimens showed an average increase of 29% and 8% in compressive strength. Whereas, NT specimens registered a drastic decrease by 19%. CBAT and CBST specimens showed an increase of 25% and 16% in compressive strength as compared to control specimen. In case of CT specimen, no significant effect on the compressive strength as compared to control specimen was observed.

Among concrete mixes, control registered the highest sorptivity coefficient (0.02). Both CBAT and CBST registered significantly lowest sorptivity coefficient (0.005) followed by NBAT and NBST (0.008 and 0.007) respectively. In both NT and CT specimens, sorptivity coefficients were recorded to be in the similar range of 0.014. In RCPT, charge passed in control was 3180 coulombs and its permeability characteristics falls under moderate type. In NT and CT specimens, the charge passed was 2942 and 2838 coulombs respectively with moderate permeability type. While NBAT and NBST falls in low penetration range, with total charge passed were 1204 coulombs and 1340 coulombs respectively. In case of CBAT and CBST, charge passed was 1228 and 1310 coulombs respectively and falls in low penetration range. In water impermeability test, maximum penetration of water was found in control specimen (30.2 mm) and NT specimen (31.2). While minimum penetration depth of 12.5 mm and 13.9 mm was

measured in CBAT and CBST specimens. NBAT and NBST specimens also registered very low water penetration depth of 14.2 mm and 13.6 mm respectively.

In case of NBAT and NBST specimens, presence of different crystal lattice of calcium carbonate such as rhombohedral calcite crystal and needle shaped aragonite crystals in the upper depth were observed in SEM-EDX analysis. In case of NT, CT and control specimens, no calcium carbonate precipitation was observed in SEM-EDX analysis. In SEM and XRD analysis of CBAT and CBST specimen, presence of dense biodeposition of closely attached rhombohedral calcite crystals as well as spheroid vaterite crystals were observed.

From the results, it was concluded that CSL as growth media had not shown any modifications in the concrete chemical properties. On comparison with NB media, CSL may serve as a carbon and nitrogen supplement and replace yeast extract nutrient media.

In second section, the efficacy of bio-deposition as a barrier in microbial treated concrete against the penetration of aggressive agents was investigated. Three different sets of concrete cubes (Control, NBAT and NBST) of 100 x 100 x 100 mm dimensions and mortar prism (Control, NBAM and NBSM) of dimensions 285 mm x 25 mm x 25 mm were used. Performance of control and microbial treated concrete and mortar prisms on chemical and physical sulfate salt environments under wet-dry cycles was evaluated. Throughout the exposure, mixture of 5% Na_2SO_4 and 5% $MgSO_4$ were used as sulfate salt solution. Prior to sulfate exposure, NBAT and NBST specimens registered significant increase in compressive strength (35% and 16%) as compare to control specimens due to microbial treatment at the age of 28 days curing. After 12 months of chemical sulfate exposure, compressive strength of control concrete specimen registered a drastic decrease of 30% as compared to its value before exposure. Also during the chemical sulfate exposure, mass gain (0.8%) in control concrete specimen was registered till the immersion age of 270 days but thereafter loss in mass was observed. Visual observations of control concrete specimen also showed a clear sign of surface degradation during 12 months of sulfate exposure. The damaging process in control specimen continued from surface cracks and with loss of cohesion less particles on the edges due to spalling at the end of exposure. After 12 months of chemical sulfate exposure, control prismatic specimen yielded the maximum length expansion of about 0.38%. However in NBAT and NBST specimen, no major sign of strength loss as well as mass gain was observed after chemical sulfate exposure. Throughout the chemical

sulfate exposure, NBAT and NBST concrete specimens exhibited no surface deterioration. Both specimens were remained intact and no sign of damage due to expansion was observed until the end of sulfate exposure. In SEM-EDX analysis, intense deposition of ettringite crystals with long needle shape and elongated rectangular prism faced column shape in control specimens were observed at the age of 365 days. In control specimen, XRD profile indicates the peak for quartz as well as ettringite and gypsum as the main secondary reaction products. In contrast, calcium carbonate crystals in NBAT and NBST specimen were present and till the exposure age of 180 days, secondary products due to sulfate ingress were not observed. Development of micro needle crystals of gypsum and ettringite were observed in NBAT and NBST specimen at the exposure of 365 days.

During the physical sulfate exposure, thick deposition of salt efflorescence was developed in the upper portion and crack formation along the edges of the control prism. At the end of exposure, higher surface scaling and increase in longitudinal cracks in submerged portion was observed. XRD patterns from submerged portion revealed the formation of ettringite and gypsum products and XRD patterns in the salt efflorescence, revealed the formation of thenardite and epsomite as the major phases with minor peaks of mirabilite. Under physical sulfate exposure, NBAM and NBSM specimens performed well and no sign of surface scaling and salt efflorescence on the upper drying front was observed. During the experiment, control specimens performed relatively poor and deterioration due to expansive products results into surface scaling in both exposure regimes. Overall, in chemical and physical sulfate exposures, significant reduction of sulfate ions ingress was observed in microbial treated concrete and mortar specimens.

Further in this section, performance of microbial treated reinforced concrete specimens under chloride induced corrosion was studied. Three different sets of concrete cylinders (100 mm diameter and 200 mm in height) embedded with a steel rebar of 12 mm diameter and 220 mm length were prepared. Control, NBAT and NBST reinforced concrete specimens were prepared. To accelerate the chloride ion ingress in reinforced concrete specimens, wet-dry cycle of 7 days immersion in 5% NaCl solution and 3 days air drying was adopted. Initial corrosion potential values in control, NBST and NBAT specimens before the exposure of chlorides were 121.7 mV/SCE, 115.9 mV/SCE and 111.8 mV/SCE respectively. At the end of 5^{th} wet-dry cycle, corrosion potential in control specimen dropped to more electronegative value (-438 mV/SCE). Corrosion potential followed an ascending trend and the highest value in control specimen was

recorded to be -522 mV/SCE after the 12th wet-dry cycle. Corrosion current of control specimen was also observed to be higher and reaches the value of 0.34 μA/cm^2 which illustrate the start of depassivation process on the rebar surface. In NBST specimen, corrosion potential at the end of 12th wet-dry cycle of chloride, corrosion potential of NBST lies at -382 mV/SCE and corrosion current value was observed to be 0.03 μAcm^2. Among all the reinforced concrete specimens, maximum resistance against the chloride ingress was observed in NBAT specimen. At the end of chloride exposure, corrosion potential value was measured as -220 mV/SCE and corrosion current was recorded as 0.023 μAcm^2. In the visual observation of rebar surface in control specimen, formation of corrosion products in rebar/concrete interfaces at different positions throughout the rebar length was observed. In XRD analysis of control specimen at the rebar/concrete interface, peaks of quartz, magnetite and akanegite a corrosion product was observed. However, in bacterial treated concrete specimens, no sign of corrosive product was observed. From these results, it was concluded that the utilization of biomineralization activity of calcifying bacteria provides an innovative approach in the prevention of rebar corrosion.

In third section, main emphasis has been laid on crack repair in concrete structures by using bacteria-based cementitious grouts. Concrete cubes of 100 x 100 x 100 mm dimensions and concrete cylinder disc of 100 mm diameter x 50 mm height dimensions were prepared. Artificial cracks (0.8 mm width and 20 mm depth) were generated in all the concrete specimens while casting procedure by inserting steel plates. Cementitious grout was prepared with binary combination of cement and fly ash with different substitution ratios (10% to 50%) as well as different water-binder ratios (w/b 0.45 and 0.50) and termed as neat grout. To prepare bacterial based cementitious grout, instead of water bacterial culture (bc/b 0.45 and 0.5) was used and prepared in NB media till it attained the $O.D_{600}$, of 0.5 (4×10^8 cells/ml) and termed as bacterial grout. In marsh cone test, flow time of all the combinations of 24 grout mixes was reduced with the increase in water/bacterial culture - binder ratios (0.45 to 0.5). Flow time in bacterial grout mixes varies from 91 seconds for control to as low as 53 seconds for 40% FA grout mix. Incorporation of 40% FA with higher bacterial culture-binder ratio (0.5), reduces the flow time as compared to control bacterial grout by 74%. In mini slump cone test, among the bacterial grout mixes, maximum spread diameter was observed in 40% FA amended grout (bc/b 0.5) with 16% increment as compared to control grout (bc/b 0.5). In the strength properties of hardened grout mixes, maximum strength gain (21.4 MPa) was observed in 40% FA amended bacterial

grout. 40% FA amended bacterial grout (bacterial culture-binder ratio 0.5) was injected into the concrete cracks with horizontal and vertical orientation. Compressive strength of untreated crack (UTC) without microbial grout repairing was observed to be 32.5 MPa. In FA-cement grout treated specimen (FCG), crack was repaired with 40% FA amended cement grout and water curing was done. Compressive strength in FCG specimen was observed to be 35.8 MPa resulting into strength gain of up to 11% on comparison with UTC. In BGS specimen, crack in vertical orientation was repaired with 40% FA amended bacterial grout and cured with spray treatment of bacterial culture supplemented with 2% urea and 25 mM $CaCl_2$ for 14 days. In BGS, compressive strength of 35.2 MPa with increment of 11% as compared to UTC was observed. In BGP specimens, crack in horizontal orientation was repaired with 40% FA amended bacterial grout and cured with bacterial culture using ponding method. BGP showed a significant increase of compressive strength (45.8 MPa) which registered a strength recovery of up to 40% as that of UTC. From the results of sorptivity test, it was noticed that bacterial grout treatment is an effective way to heal the cracks which significantly alter the water ingress. Maximum water ingress was observed in UTC specimen with 0.03 sorptivity coefficient. In the FCG specimen, water ingress was less than UTC and its sorptivity coefficient was 0.01. In BGS, capillary rise of water was altered effectively and sorptivity coefficient was 0.005. However, BGP registered significantly lowest sorptivity which was observed to be 0.002. SEM analysis of both BGP and BGS specimens taken from the upper depth of 0–10 mm clearly identified the presence of calcium carbonate crystals. Dense formation of rhombohedral calcite crystals were observed in grout repaired cracks.

Final conclusion and future perspectives

Application of microbial induced calcium carbonate precipitation (MICP) in cement-based materials has become substantially popular. The approach of MICP application using calcifying bacteria offers the positive benefits in the enhancement of mechanical strength and adequate impermeability of concrete structures. This study has conclusively established that MICP technique with bacterial admixed treatment and bacterial spray treatment would be effective in direct application on concrete structures. Direct incorporation of calcifying bacteria as an admixture can be used for new structures as well as bacterial spray treatment can be used as a repair procedure in concrete, respectively. The results of the study suggested that, biogenic

precipitations of $CaCO_3$ by bacterial cells counteract the retarding effect of organic nutrient media (particularly carbon content due to yeast extract and peptones) on setting property of cement paste and decrease in compressive strength of concrete. It was concluded that CSL (an industrial by-product of the starch industry), an inexpensive nutrient media as compared to yeast extract and peptone in NB media, would serve as a potential nutritional source for bacterial cells in microbial treatment of concrete and help in developing low-cost and environment-friendly MICP technology in future on a field scale. This is the first published study, to achieve significant reduction of sulfate ingress in microbial treated concrete under harsh sulfate environments and prevention of rebar from chloride induced corrosion under high chloride conditions, respectively. A suitable fly ash amended bacterial grout with optimum flowability properties was developed for the remediation of cracks in concrete. The developed fly ash amended biogrout will help as an economical and environment friendly MICP technology in injection based applications for the remediation of existing cracks in the concrete structures which are in service.

The encouraging results in the current study will facilitate in upscaling this microbial based approach from lab scale to commercial scale. Despite the positive outcomes, upscaling of this microbial approach from lab scale to commercial scale is the major challenge. Economical limitations such as cost of nutrient media for bacterial growth, optimum bacterial dosage and efficiency of treatment in real-life concrete structures is still needs to be further proven. Some challenges are associated with microbial treatment of concrete which are necessary to be addressed for the development of this technique for commercial scale applications. Performance of MICP treated concrete under different environmental conditions such as repeated freeze thaw conditions, cyclic loadings and cyclic carbonation conditions is still to be reported. In addition, there is a need for more investigations of long-term performance and durability properties of microbial treated concrete. In future studies, MICP application on crack repair and monitoring with non-destructive techniques will help in more practical implementation in real life concrete structures at field scale. In previous studies, it is reported that ureolytic pathway for MICP process is predominantly preferred on the performance basis. Apart from ureolytic pathway, biomineralization of CO_2 with the employment of cyanobacteria can also offers an innovative and self-sustaining strategy in calcium carbonate precipitation. Biocementation with the employment of cyanobacteria with carbon sequestration strategy will provides a cost-effective

and environment friendly mechanism that can be implemented in construction material. Application of cyanobacteria on concrete structures to enhance durability properties is still limited. This biocementation approach could be used for precast products such as concrete blocks and bricks. The economic limitations such as use of expensive nutrient media for bacterial growth, aseptic conditions to produce axenic pure bacterial cultures has been reported for the high production cost of microbial concrete at industrial scale. Some potential alternative nutrients for bacterial growth and economically suitable substitute for urea have been suggested for cheap and affordable implementation of MICP application at field scale. More studies with the consideration of abovementioned concerns will facilitate the practical implementation of microbial treated concrete in construction sector in the near future.

REFERENCES

References

Abd Rashid AF, Yusoff S (2015) A review of life cycle assessment method for building industry. Renewable and Sustainable Energy Reviews, 45: 244-248.

Achal V, Mukherjee A, Goyal S, Reddy MS (2012) Corrosion prevention of reinforced concrete with microbial calcite precipitation. ACI Materials Journal, 109: 157-164.

Achal V, Mukherjee A, Reddy MS (2010a) Biocalcification by *Sporosarcina pasteurii* using corn steep liquor as the nutrient source. Industrial Biotechnology, 6: 170-174.

Achal V, Mukherjee A, Reddy MS (2011a) Effect of calcifying bacteria on permeation properties of concrete structures. Journal of Industrial Microbiology & Biotechnology, 38: 1229-1234.

Achal V, Mukherjee A, Reddy MS (2011b) Microbial concrete: way to enhance the durability of building structures. Journal of Materials in Civil Engineering 23: 730-734.

Achal V, Mukherjee A, Reddy MS (2013) Biogenic treatment improves the durability and remediates the cracks of concrete structures. Construction and Building Materials, 48: 1-5.

Achal V, Mukherjee A, Reddy, MS (2010b) Characterization of two urease-producing and calcifying *Bacillus* sp. isolated from cement. Journal of Microbiology and Biotechnology, 20: 1571-1576.

Achal V, Pan X, Özyurt N (2011c) Improved strength and durability of fly ash-amended concrete by microbial calcite precipitation. Ecological Engineering, 37: 554-559.

Achal V, Pan X, Zhang D (2011d) Remediation of copper-contaminated soil by *Kocuria flava* CR1, based on microbially induced calcite precipitation. Ecological Engineering, 37: 1601-1605.

Adesina A (2019) Durability enhancement of concrete using nanomaterials: An overview. Materials Science Forum, 967: 221–227.

Ahn TH, Kishi T (2010) Crack self-healing behavior of cementitious composites incorporating various mineral admixtures. Journal of Advanced Concrete Technology, 8: 171-186.

Akiyama M, Kawasaki S (2019) Biogeochemical simulation of microbially induced calcite precipitation with *Pararhodobacter* sp. strain SO1. Acta Geotechnica, 14: 685-696.

Alazhari M, Sharma T, Heath A, Cooper R, Paine K (2018) Application of expanded perlite encapsulated bacteria and growth media for self-healing concrete. Construction and Building Materials, 160: 610-619.

Alexander M, Beushausen H (2019) Durability, service life prediction, and modelling for reinforced concrete structures–review and critique. Cement and Concrete Research, 122: 17-29.

Almusallam AA, Khan FM, Dulaijan SU, Al-Amoudi OSB (2003) Effectiveness of surface coatings in improving concrete durability. Cement and Concrete Composites, 25: 473-481.

Al-Tabbaa A, Litina C, Giannaros P, Kanellopoulos A, Souza L (2019) First UK field application and performance of microcapsule-based self-healing concrete. Construction and Building Materials, 208: 669-685.

Al-Thawadi S, Cord-Ruwisch R, Bououdina M (2012) Consolidation of sand particles by nanoparticles of calcite after concentrating ureolytic bacteria in situ. International Journal of Green Nanotechnology, 4: 28-36.

Amiri A, Bundur ZB (2018) Use of corn-steep liquor as an alternative carbon source for biomineralization in cement-based materials and its impact on performance. Construction and Building Materials, 165: 655-662.

Anbu P, Kang CH, Shin YJ, So JS (2016) Formations of calcium carbonate minerals by bacteria and its multiple applications. Springerplus, 5: 1-26.

Ann KY, Jung HS, Kim HS, Kim SS, Moon, HY (2006) Effect of calcium nitrite-based corrosion inhibitor in preventing corrosion of embedded steel in concrete. Cement and Concrete Research, 36: 530-535.

Ariyanti D, Handayani NA, Hadiyanto (2012) Feasibility of using microalgae for biocement production through biocementation. Journal Bioprocessing & Biotechniques, 2: 1-4.

Ashraf W (2016) Carbonation of cement-based materials: challenges and opportunities. Construction and Building Materials, 120: 558-570.

ASTM C1012-04 (2004) Standard test method for length change of hydraulic-cement mortars exposed to a sulfate solution. ASTM International, West Conshohocken, PA. http://www.astm.org/

ASTM C1202-12 (2012) Standard test method for electrical indication of concrete's ability to resist chloride ion penetration, ASTM International, West Conshohocken, PA. http://www.astm.org/

ASTM C1585-04 (2004) Standard test method for measurement of rate of absorption of water by hydraulic-cement concretes. ASTM International, West Conshohocken, PA. http://www.astm.org/

ASTM C672 / C672M-12 (2012) Standard test method for scaling resistance of concrete surfaces exposed to deicing chemicals. ASTM International, West Conshohocken, PA. http://www.astm.org/

ASTM C876-09 (2009) Standard test method for corrosion potentials of uncoated reinforcing steel in concrete. ASTM International, West Conshohocken, PA. http://www.astm.org/

ASTM C939-10 (2010) Standard test method for flow of grout for preplaced-aggregate concrete (Flow cone method). ASTM International, West Conshohocken, PA. www.astm.org

ASTM C942-15 (2015) Standard test method for compressive strength of grouts for preplaced-aggregate concrete in the laboratory, ASTM International, West Conshohocken, PA. www.astm.org

Atiş CD (2003) Accelerated carbonation and testing of concrete made with fly ash. Construction and Building Materials, 17: 147-152.

Aye T, Oguchi CT (2011) Resistance of plain and blended cement mortars exposed to severe sulfate attacks. Construction and Building Materials, 25: 2988-2996.

Azima M, Bundur ZB (2019) Influence of *Sporasarcina pasteurii* cells on rheological properties of cement paste. Construction and Building Materials, 225: 1086-1097.

Bains A, Dhami NK, Mukherjee A, Reddy MS (2015) Influence of exopolymeric materials on bacterially induced mineralization of carbonates. Applied Biochemistry and Biotechnology, 175: 3531-3541.

Bang SS, Galinat JK, Ramakrishnan V (2001) Calcite precipitation induced by polyurethane-immobilized *Bacillus pasteurii*. Enzyme and Microbial Technology, 28: 404-409.

Bansal R, Dhami NK, Mukherjee A, Reddy MS (2016) Biocalcification by halophilic bacteria for remediation of concrete structures in marine environment. Journal of Industrial Microbiology & Biotechnology, 43: 1497-1505.

Basheer L, Kropp J, Cleland DJ (2001) Assessment of the durability of concrete from its permeation properties: a review. Construction and Building Materials, 15: 93-103.

Basheer PAM, Chidiact SE, Long AE (1996) Predictive models for deterioration of concrete structures. Construction and Building Materials, 10: 27–37.

Behnood A, Van Tittelboom K, De Belie N (2016) Methods for measuring pH in concrete: A review. Construction and Building Materials, 105: 176-188.

Berkowski P, Dmochowski G, Kosior-Kazberuk M (2013) Analysis of structural and material degradation of a car-park's RC bearing structure due to city environmental influences. Procedia Engineering, 57: 183-192.

Berrocal CG, Lundgren K, Löfgren I (2016) Corrosion of steel bars embedded in fibre reinforced concrete under chloride attack: state of the art. Cement and Concrete Research, 80: 69-85.

Bertolini L, Elsener B, Pedeferri P, Polder RP (2004) Transport processes in concrete. In Corrosion of steel in concrete: Prevention, diagnosis, repair, Wiley, Weinheim, Germany, (pp. 21–48).

Beveridge TJ (1981) Ultrastructure, chemistry, and function of the bacterial wall. International Review of Cytology Volume, 72: 229–317.

Bhattacharjee J (2018) Deterioration of concrete structures along with case studies in India. Proceedings of the Institution of Civil Engineers-Forensic Engineering, 171: 80-90.

Bhattacharya A, Naik SN, Khare SK (2018) Harnessing the bio-mineralization ability of urease producing *Serratia marcescens* and *Enterobacter cloacae* EMB19 for remediation of heavy metal cadmium (II). Journal of Environmental Management, 215: 143-152.

Binda L, Modena C, Baronio G, Abbaneo S (1997) Repair and investigation techniques for stone masonry walls. Construction and Building Materials, 11: 133-142.

Biondini F, Frangopol DM (2016) Life-cycle performance of deteriorating structural systems under uncertainty. Journal of Structural Engineering, 142: F4016001.

Bisht V, Chaurasia L, Singh LP, Gupta S (2020) Bacterially Stabilized Desert-Sand Bricks: Sustainable Building Material. Journal of Materials in Civil Engineering, 32: 04020131.

Blaiszik BJ, Kramer SL, Olugebefola SC, Moore JS, Sottos NR, White SR (2010) Self-healing polymers and composites. Annual Review of Materials Research, 40: 179-211.

Bolobova AV, Kondrashchenko VI (2000) Use of yeast fermentation waste as a biomodifier of concrete. Applied Biochemistry and Microbiology, 36: 205-214.

Boquet E, Boronat A, Ramos-Cormenzana A (1973) Production of calcite (calcium carbonate) crystals by soil bacteria is a general phenomenon. Nature, 246: 527-529.

Bose H, Satyanarayana T (2017) Microbial carbonic anhydrases in biomimetic carbon sequestration for mitigating global warming: prospects and perspectives. Frontiers in Microbiology, 8: 1615.

Bras A, Henriques FM, Cidade MT (2010) Effect of environmental temperature and fly ash addition in hydraulic lime grout behaviour. Construction and Building Materials, 24: 1511-1517.

Broomfield JP (1997) Corrosion of steel in concrete, E&FN Spon, London.

BS 1881-122:2011 (2011) Testing Concrete, Part 122: Method for determination of water absorption, British Standards Institution.

BS EN 1015-19:1999 (1999) Determination of water vapour permeability of hardened rendering and plastering mortars, British Standards Institution.

Bundur ZB, Kirisits MJ, Ferron RD (2015) Biomineralized cement-based materials: Impact of inoculating vegetative bacterial cells on hydration and strength. Cement and Concrete Research, 67: 237-245.

Castanier S, Le Métayer-Levrel G, Perthuisot JP (1999) Ca-carbonates precipitation and limestone genesis—the microbiogeologist point of view. Sedimentary Geology, 126: 9-23.

Castanier S, Le Metayer-Levrel G, Perthuisot JP (2000) Bacterial roles in the precipitation of carbonate minerals. In Microbial sediments. Springer, Berlin, Heidelberg, (pp. 32-39).

Castellote M, Fernandez L, Andrade C, Alonso C (2009) Chemical changes and phase analysis of OPC pastes carbonated at different CO_2 concentrations. Materials and Structures, 42: 515-525.

Castro-Alonso MJ, Montañez-Hernandez LE, Sanchez-Muñoz MA, Macias Franco MR, Narayanasamy R, Balagurusamy N (2019) Microbially Induced Calcium carbonate Precipitation (MICP) and its potential in Bioconcrete: Microbiological and molecular concepts. Frontiers in Materials, 6: 126.

Celik F, Canakci H (2015) An investigation of rheological properties of cement-based grout mixed with rice husk ash (RHA). Construction and Building Materials, 91: 187-194.

Chang CF, Chen JW (2006) The experimental investigation of concrete carbonation depth. Cement and Concrete Research, 36: 1760-1767.

Chen F, Deng C, Song W, Zhang D, Al-Misned FA, Mortuza MG, Gadd MG, Pan X (2016) Biostabilization of desert sands using bacterially induced calcite precipitation. Geomicrobiology Journal, 33: 243-249.

Chen J, Kou SC, Poon CS (2012) Hydration and properties of nano-TiO_2 blended cement composites. Cement and Concrete Composites, 34: 642-649.

Chindaprasirt P, Jaturapitakkul C, Sinsiri T (2005) Effect of fly ash fineness on compressive strength and pore size of blended cement paste. Cement and Concrete Composites, 27: 425-428.

Chu J, Stabnikov V, Ivanov V (2012) Microbially induced calcium carbonate precipitation on surface or in the bulk of soil. Geomicrobiology Journal, 29: 544-549.

Ciurli S, Benini S, Rypniewski WR, Wilson KS, Miletti S, Mangani S (1999) Structural properties of the nickel ions in urease: novel insights into the catalytic and inhibition mechanisms. Coordination Chemistry Reviews, 190: 331-355.

Clare KE, Sherwood PT (1954) The effect of organic matter on the setting of soil-cement mixtures. Journal of Applied Chemistry, 4: 625-630.

Combrinck R, Boshoff WP (2013) Typical plastic shrinkage cracking behaviour of concrete. Magazine of Concrete Research, 65: 486-493.

Cousins S (2019) Shifting sand: Why we're running out of aggregate. Construction Research and Innovation, 10: 69-71.

Da Silva FB, De Belie N, Boon N, Verstraete W (2015) Production of non-axenic ureolytic spores for self-healing concrete applications. Construction and Building Materials, 93: 1034-1041.

Das JK, Pradhan B (2019) Effect of cation type of chloride salts on corrosion behaviour of steel in concrete powder electrolyte solution in the presence of corrosion inhibitors. Construction and Building Materials, 208: 175-191.

Daskalakis MI, Rigas F, Bakolas A, Magoulas A, Kotoulas G, Katsikis I, Karageorgis AP, Mavridou A (2015) Vaterite bio-precipitation induced by *Bacillus pumilus* isolated from a solutional cave in Paiania, Athens, Greece. International Biodeterioration & Biodegradation, 99: 73-84.

De Belie N, Gruyaert E, Al-Tabbaa A, Antonaci P, Baera C, Bajare D, Darquennes A, Davies R, Ferrara L, Jefferson T, Litina C, Miljevic B, Otlewska A, Ranogajec J, Roig-Flores M, Paine K, Lukowski P, Serna P, Tulliani JM, Vucetic S, Wang J, Jonkers HM (2018) A review of self-healing concrete for damage management of structures. Advanced Materials Interfaces, 5: 1800074.

De Muynck W, Cox K, De Belie N, Verstraete W (2008) Bacterial carbonate precipitation as an alternative surface treatment for concrete. Construction and Building Materials, 22: 875-885.

Dhami NK, Mukherjee A, Watkin EL (2018) Microbial diversity and mineralogical-mechanical properties of calcitic cave speleothems in natural and in vitro biomineralization conditions. Frontiers in Microbiology, 9: 40.

Dhami NK, Quirin MEC, Mukherjee A (2017) Carbonate biomineralization and heavy metal remediation by calcifying fungi isolated from karstic caves. Ecological Engineering, 103: 106-117.

Dhami NK, Reddy MS, Mukherjee A (2012) Biofilm and microbial applications in biomineralized concrete. In Advanced topics in biomineralization. IntechOpen, (pp. 137-164).

Dhami NK, Reddy MS, Mukherjee A (2013a) *Bacillus megaterium* mediated mineralization of calcium carbonate as biogenic surface treatment of green building materials. World Journal of Microbiology and Biotechnology, 29: 2397-2406.

Dhami NK, Reddy MS, Mukherjee A (2013b) Biomineralization of calcium carbonates and their engineered applications: a review. Frontiers in Microbiology 4: 314.

Dhami NK, Reddy MS, Mukherjee A (2014a) Application of calcifying bacteria for remediation of stones and cultural heritages. Frontiers in Microbiology, 5: 304.

Dhami NK, Reddy MS, Mukherjee A (2014b) Synergistic role of bacterial urease and carbonic anhydrase in carbonate mineralization. Applied Biochemistry and Biotechnology, 172: 2552-2561.

Dias WPS (1995) Sorptivity testing for assessing concrete quality. In proceedings of international conference on concrete under severe exposure conditions (CONSEC'95), Spon, London, (pp. 433-442).

DIN 1048 (1978) Test methods of concrete impermeability to water: part 2. Deutscher Institute Fur Normung, Germany

Dixon NE, Gazzola C, Blakeley RL, Zerner B (1975) Jack bean urease (EC 3.5. 1.5) metalloenzyme. Simple biological role for nickel. Journal of the American Chemical Society, 97: 4131-4133.

Douglas S, Beveridge TJ (1998) Mineral formation by bacteria in natural microbial communities. FEMS Microbiology Ecology, 26: 79-88.

Doyle MW, Havlick DG (2009) Infrastructure and the environment. Annual Review of Environment and Resources, 34: 349-373.

Drew LJ, Langer WH, Sachs JS (2002) Environmentalism and natural aggregate mining. Natural Resources Research, 11: 19-28.

Dry C (1994) Matrix cracking repair and filling using active and passive modes for smart timed release of chemicals from fibers into cement matrices. Smart Materials and Structures, 3: 118.

Duan H, Miller TR, Liu G, Tam VW (2019) Construction debris becomes growing concern of growing cities. Waste Management, 83: 1-5.

Ehrlich HL (1998) Geomicrobiology: its significance for geology. Earth-Science Reviews, 45: 45-60.

Ekolu SO (2016) A review on effects of curing, sheltering, and CO_2 concentration upon natural carbonation of concrete. Construction and Building Materials, 127: 306-320.

El-Hachem R, Rozière E, Grondin F, Loukili A (2012) Multi-criteria analysis of the mechanism of degradation of Portland cement based mortars exposed to external sulphate attack. Cement and Concrete Research, 42: 1327-1335.

Emmons PH, Sordyl DJ (2006) The state of the concrete repair industry, and a vision for its future. Concrete Repair Bulletin, 19: 7-14.

Erşan YÇ, Da Silva FB, Boon N, Verstraete W, De Belie N (2015) Screening of bacteria and concrete compatible protection materials. Construction and Building Materials, 88: 196-203.

Erşan YÇ, Van Tittelboom K, Boon N, De Belie N (2018) Nitrite producing bacteria inhibit reinforcement bar corrosion in cementitious materials. Scientific Reports, 8: 1-10.

Farmani F, Bonakdarpour B, Ramezanianpour AA (2015) pH reduction through amendment of cement mortar with silica fume enhances its biological treatment using bacterial carbonate precipitation. Materials and Structures, 48: 3205-3215.

Folk RL (1974) The natural history of crystalline calcium carbonate; effect of magnesium content and salinity. Journal of Sedimentary Research, 44: 40-53.

Fournier B, Bérubé MA (2000) Alkali-aggregate reaction in concrete: a review of basic concepts and engineering implications. Canadian Journal of Civil Engineering, 27: 167–191.

Fowler DW (1999) Polymers in concrete: a vision for the 21st century. Cement and Concrete Composites, 21: 449-452.

Fowler DW (2009) Repair materials for concrete structures. In Failure, distress and repair of concrete structures. Woodhead Publishing, (pp. 194-207).

Franzoni E, Pigino B, Pistolesi C (2013) Ethyl silicate for surface protection of concrete: performance in comparison with other inorganic surface treatments. Cement and Concrete Composites, 44: 69-76.

Friedrich B, Magasanik B (1977) Urease of *Klebsiella aerogenes*: control of its synthesis by glutamine synthetase. Journal of Bacteriology, 131: 446-452.

Gettu R, Patel A, Rathi V, Prakasan S, Basavaraj AS, Palaniappan S, Maity S (2019) Influence of supplementary cementitious materials on the sustainability parameters of cements and concretes in the Indian context. Materials and Structures, 52: 10.

Ghods P, Isgor OB, McRae G, Miller T (2009) The effect of concrete pore solution composition on the quality of passive oxide films on black steel reinforcement. Cement and Concrete Composites, 31: 2-11.

Glass GK, Buenfeld NR (2000) Chloride-induced corrosion of steel in concrete. Progress in Structural Engineering and Materials, 2: 448–458.

Gonen T, Yazicioglu S (2007) The influence of compaction pores on sorptivity and carbonation of concrete. Construction and building materials, 21: 1040-1045.

Goyal A, Pouya HS, Ganjian E, Claisse P (2018) A review of corrosion and protection of steel in concrete. Arabian Journal for Science and Engineering, 43: 5035-5055.

Gruyaert E, Van den Heede P, De Belie N (2013) Carbonation of slag concrete: Effect of the cement replacement level and curing on the carbonation coefficient–Effect of carbonation on the pore structure. Cement and Concrete Composites, 35: 39-48.

Gu X, Jin X, Zhou Y (2016) Durability of concrete structures. In Basic principles of concrete structures. Springer, Berlin, Heidelberg (pp. 553-597).

Gursel AP, Masanet E, Horvath A, Stadel A (2014) Life-cycle inventory analysis of concrete production: A critical review. Cement and Concrete Composites, 51: 38-48.

Hammes F, Verstraete W (2002) Key roles of pH and calcium metabolism in microbial carbonate precipitation. Reviews in Environmental Science and Biotechnology, 1:3-7.

Haruehansapong S, Pulngern T, Chucheepsakul S (2014) Effect of the particle size of nanosilica on the compressive strength and the optimum replacement content of cement mortar containing nano-SiO_2. Construction and Building Materials, 50: 471-477.

Haynes H, Bassuoni MT (2011) Physical salt attack on concrete. Concrete International 33: 38-42.

He J, Chen X, Zhang Q, Achal V (2019) More effective immobilization of divalent lead than hexavalent chromium through carbonate mineralization by *Staphylococcus epidermidis* HJ2. International Biodeterioration & Biodegradation, 140: 67-71.

Hilloulin B, Van Tittelboom K, Gruyaert E, De Belie N, Loukili A (2015) Design of polymeric capsules for self-healing concrete. Cement and Concrete Composites, 55: 298-307.

Hu J, Ge Z, Wang K (2014) Influence of cement fineness and water-to-cement ratio on mortar early-age heat of hydration and set times. Construction and Building Materials, 50: 657-663.

Hu X, Shi Z, Shi C, Wu Z, Tong B, Ou Z, De Schutter G (2017) Drying shrinkage and cracking resistance of concrete made with ternary cementitious components. Construction and Building Materials, 149: 406-415.

Huet B, L'Hostis V, Miserque F, Idrissi H (2005) Electrochemical behavior of mild steel in concrete: Influence of pH and carbonate content of concrete pore solution. Electrochimica Acta, 51: 172-180.

Hussain S, Bhunia D, Singh SB, Aggrawal M (2018) Mechanical strength and durability of mineral admixture concrete subjected to accelerated carbonation. Journal of Structural Integrity and Maintenance, 3: 44-51.

Ibrahim M, Al-Gahtani AS, Maslehuddin M, Dakhil FH (1999) Use of surface treatment materials to improve concrete durability. Journal of Materials in Civil Engineering, 11: 36-40.

Imbabi MS, Carrigan C, McKenna S (2012) Trends and developments in green cement and concrete technology. International Journal of Sustainable Built Environment, 1: 194-216.

Irassar EF (2009) Sulfate attack on cementitious materials containing limestone filler—A review. Cement and Concrete Research, 39: 241-254.

IS: 1786-2008 (2008) Indian standard high strength steel bars and wires for concrete reinforcement-specification. Bureau of Indian Standards, New Delhi-110002.

IS: 383-1970 (1970) Indian standard specifcation for coarse and fne aggregates from natural sources for concrete. Bureau of Indian Standards, New Delhi-110002.

IS: 4031 (Part 4)-1988 (1988) Indian standard methods of physical tests for hydraulic cement. Part 4: Determination of consistency of standard cement paste. Bureau of Indian Standards, New Delhi-110002.

IS: 4031 (Part 5)-1988 (1988) Indian standard methods of physical tests for hydraulic cement. Part 5: Determination of initial and final setting times. Bureau of Indian Standards, New Delhi-110002.

IS: 516-1959 (1959) Indian Standard code of practice – Methods of test for strength of concrete. Bureau of Indian Standards, New Delhi-110002.

IS: 5194-1969 (1969) Indian standard method for determination of nitrogen-Kjeldahl method. Bureau of Indian Standards, New Delhi-110002.

IS: 5513-1996 (1996) Indian standards for vicat apparatus specification. Bureau of Indian Standards, New Delhi-110002.

IS: 8112-2013 (2013) Indian standard specifcation for 43 grade ordinary portland cement. Bureau of Indian Standards, New Delhi-110002.

Ismail S, Hoe KW, Ramli M (2013) Sustainable aggregates: The potential and challenge for natural resources conservation. Procedia-Social and Behavioral Sciences, 101: 100-109.

Issa CA, Debs P (2007) Experimental study of epoxy repairing of cracks in concrete. Construction and Building Materials, 21: 157-163.

Jahns T (1996) Ammonium/urea-dependent generation of a proton electrochemical potential and synthesis of ATP in *Bacillus pasteurii*. Journal of Bacteriology, 178: 403-409.

Jain S, Arnepalli DN (2019) Biominerlisation as a remediation technique: a critical review. In Geotechnical characterisation and geoenvironmental engineering. Springer, Singapore, (pp. 155-162).

Jansson C, Northen T (2010) Calcifying cyanobacteria—the potential of biomineralization for carbon capture and storage. Current Opinion in Biotechnology, 21: 365-371.

Jia L, Shi C, Pan X, Zhang J, Wu L (2016) Effects of inorganic surface treatment on water permeability of cement-based materials. Cement and Concrete Composites, 67: 85-92.

Jiang NJ, Tang CS, Hata T, Courcelles B, Dawoud O, Singh DN (2020) Bio-mediated soil improvement: The way forward. Soil Use and Management, 36: 185-188.

Jo BW, Kim CH, Tae GH, Park JB (2007) Characteristics of cement mortar with nano-SiO_2 particles. Construction and Building Materials, 21: 1351-1355.

Jones BD, Mobley HL (1987) Genetic and biochemical diversity of ureases of *Proteus*, *Providencia*, and *Morganella* species isolated from urinary tract infection. Infection and Immunity, 55: 2198-2203.

Jonkers HM, Schlangen E (2007) Crack repair by concrete-immobilized bacteria. In Proceedings of the first international conference on self healing materials (Vol. 18, p. 20).

Jonkers HM, Thijssen A, Muyzer G, Copuroglu O, Schlangen E (2010) Application of bacteria as self-healing agent for the development of sustainable concrete. Ecological Engineering 36: 230-235.

Jroundi F, Gonzalez-Muñoz MT, Garcia-Bueno A, Rodriguez-Navarro C (2014) Consolidation of archaeological gypsum plaster by bacterial biomineralization of calcium carbonate. Acta Biomaterialia, 10: 3844–3854.

Kajaste R, Hurme M (2016) Cement industry greenhouse gas emissions–management options and abatement cost. Journal of Cleaner Production, 112: 4041-4052.

Kalhori H, Bagherpour R (2017) Application of carbonate precipitating bacteria for improving properties and repairing cracks of shotcrete. Construction and Building Materials, 148: 249-260.

Kantro DL (1980) Influence of water-reducing admixtures on properties of cement paste—a miniature slump test. Cement, Concrete and Aggregates, 2: 95-102.

Kaur G, Dhami NK, Goyal S, Mukherjee A, Reddy MS (2016) Utilization of carbon dioxide as an alternative to urea in biocementation. Construction and Building Materials, 123: 527-533.

Khunthongkeaw J, Tangtermsirikul S, Leelawat T (2006) A study on carbonation depth prediction for fly ash concrete. Construction and Building Materials 20: 744-753.

Kim G, Kim JY, Kurtis KE, Jacobs LJ, Le Pape Y, Guimaraes M (2016) Quantitative evaluation of carbonation in concrete using nonlinear ultrasound. Materials and Structures, 49: 399-409.

Kim HK, Park SJ, Han JI, Lee HK (2013) Microbially mediated calcium carbonate precipitation on normal and lightweight concrete. Construction and Building Materials, 38: 1073-1082.

Kirkland CM, Zanetti S, Grunewald E, Walsh DO, Codd SL, Phillips AJ (2017) Detecting microbially induced calcite precipitation in a model well-bore using downhole low-field NMR. Environmental Science & Technology, 51: 1537-1543.

Kollek JJ (1989) The determination of the permeability of concrete to oxygen by the Cembureau method—a recommendation. Materials and Structures, 22: 225-230.

Konsta-Gdoutos MS, Metaxa ZS, Shah SP (2010) Multi-scale mechanical and fracture characteristics and early-age strain capacity of high performance carbon nanotube/cement nanocomposites. Cement and Concrete Composites, 32: 110-115.

Kosednar J, Mailvaganam NP (2005) Selection and use of polymer-based materials in the repair of concrete structures. Journal of Performance of Constructed Facilities, 19: 229-233.

Kumari C, Das B, Jayabalan R, Davis R, Sarkar P (2017) Effect of nonureolytic bacteria on engineering properties of cement mortar. Journal of Materials in Civil Engineering, 29: 06016024.

Kunal, Siddique R, Rajor A, Singh M (2016) Influence of bacterial-treated cement kiln dust on strength and permeability of concrete. Journal of Materials in Civil Engineering, 28: 04016088.

Kupwade-Patil K, Allouche EN (2013) Examination of chloride-induced corrosion in reinforced geopolymer concretes. Journal of Materials in Civil Engineering, 25: 1465-1476.

Langer W (2016) Sustainability of aggregates in construction. In Sustainability of construction materials. Woodhead Publishing, (pp. 181-207).

Le Metayer-Levrel G, Castanier S, Orial G, Loubiere JF, Perthuisot JP (1999) Applications of bacterial carbonatogenesis to the protection and regeneration of limestones in buildings and historic patrimony. Sedimentary Geology, 126: 25-34.

Lee BY, Kurtis KE (2017) Effect of pore structure on salt crystallization damage of cement-based materials: Consideration of w/b and nanoparticle use. Cement and Concrete Research, 98: 61-70.

Leemann A, Loser R (2011) Analysis of concrete in a vertical ventilation shaft exposed to sulfate-containing groundwater for 45 years. Cement and Concrete Composites, 33: 74-83.

Lepech MD, Li VC (2009) Water permeability of engineered cementitious composites. Cement and Concrete Composites, 31: 744-753.

Li M, Zhu X, Mukherjee A, Huang M, Achal V (2017) Biomineralization in metakaolin modified cement mortar to improve its strength with lowered cement content. Journal of Hazardous Materials, 329: 178-184.

Li Q, Zhang B, Ge Q, Yang X (2018) Calcium carbonate precipitation induced by calcifying bacteria in culture experiments: Influence of the medium on morphology and mineralogy. International Biodeterioration & Biodegradation, 134: 83-92.

Li VC, Lim YM, Chan YW (1998) Feasibility study of a passive smart self-healing cementitious composite. Composites Part B: Engineering, 29: 819-827.

Liew KM, Kai MF, Zhang LW (2016) Carbon nanotube reinforced cementitious composites: An overview. Composites Part A: Applied Science and Manufacturing, 91: 301-323.

Ling H, Qian C (2017) Effects of self-healing cracks in bacterial concrete on the transmission of chloride during electromigration. Construction and Building Materials, 144: 406–411.

Liu Z, Deng D, De Schutter G (2014) Does concrete suffer sulfate salt weathering?. Construction and Building Materials, 66: 692-701.

Liu Z, Zhang F, Deng D, Xie Y, Long G, Tang X (2017) Physical sulfate attack on concrete lining–A field case analysis. Case Studies in Construction Materials, 6: 206-212.

Long AE, Henderson GD, Montgomery FR (2001) Why assess the properties of near-surface concrete? Construction and Building Materials, 15: 65-79.

Lowenstam HA (1981) Minerals formed by organisms. Science, 211: 1126-1131.

Ma B, Li H, Li X, Mei J, Lv Y (2016) Influence of nano-TiO_2 on physical and hydration characteristics of fly ash–cement systems. Construction and Building Materials, 122, 242-253.

Maes M, De Belie N (2014) Resistance of concrete and mortar against combined attack of chloride and sodium sulphate. Cement and Concrete Composites, 53: 59-72.

Maleki M, Ebrahimi S, Asadzadeh F, Tabrizi ME (2016) Performance of microbial-induced carbonate precipitation on wind erosion control of sandy soil. International Journal of Environmental Science and Technology, 13: 937-944.

Manz OE (1999) Coal fly ash: a retrospective and future look. Fuel, 78: 133-136.

Martinez BC, DeJong JT, Ginn TR, Montoya BM, Barkouki TH, Hunt C, Tanyu B, Major D (2013) Experimental optimization of microbial induced carbonate precipitation for soil improvement. Journal of Geotechnical and Geoenvironmental Engineering, 139: 587-598.

Massaad G, Rozière E, Loukili A, Izoret L (2016) Advanced testing and performance specifications for the cementitious materials under external sulfate attacks. Construction and Building Materials, 127: 918-931.

McCarter WJ, Ezirim H, Emerson M (1992) Absorption of water and chloride into concrete. Magazine of Concrete Research, 44: 31-37.

McCoy DD, Cetin A, Hausinger RP (1992) Characterization of urease from *Sporosarcina ureae*. Archives of Microbiology, 157: 411-416.

Medeiros MHF, Helene P (2009) Surface treatment of reinforced concrete in marine environment: Influence on chloride diffusion coefficient and capillary water absorption. Construction and Building Materials, 23: 1476-1484.

Mehta PK (2001) Reducing the environmental impact of concrete. Concrete International 23: 61-66.

Menegaki M, Damigos D (2018) A review on current situation and challenges of construction and demolition waste management. Current Opinion in Green and Sustainable Chemistry, 13: 8-15.

Menéndez E, Matschei T, Glasser FP (2013) Sulfate attack of concrete. In Performance of cement-based materials in aggressive aqueous environments. Springer, Dordrecht, (pp. 7-74).

Meng T, Yu Y, Qian X, Zhan S, Qian K (2012) Effect of nano-TiO_2 on the mechanical properties of cement mortar. Construction and Building Materials, 29: 241-245.

Micallef R, Vella D, Sinagra E, Zammit G (2016) Biocalcifying *Bacillus subtilis* cells effectively consolidate deteriorated Globigerina limestone. Journal of Industrial Microbiology & Biotechnology, 43: 941-952.

Miller SA, Horvath A, Monteiro PJ (2016) Readily implementable techniques can cut annual CO_2 emissions from the production of concrete by over 20%. Environmental Research Letters, 11: 074029.

Miller SA, Horvath A, Monteiro PJ (2018) Impacts of booming concrete production on water resources worldwide. Nature Sustainability, 1: 69-76.

Miller SA, John VM, Pacca SA, Horvath A (2018) Carbon dioxide reduction potential in the global cement industry by 2050. Cement and Concrete Research, 114: 115-124.

Mirza J, Mirza MS, Roy V, Saleh K (2002) Basic rheological and mechanical properties of high-volume fly ash grouts. Construction and Building Materials, 16: 353-363.

Mittermayr F, Rezvani M, Baldermann A, Hainer S, Breitenbücher P, Juhart J, Graubner CA, Proske T (2015) Sulfate resistance of cement-reduced eco-friendly concretes. Cement and Concrete Composites, 55: 364-373.

Mobley, HL, Island MD, Hausinger RP (1995) Molecular biology of microbial ureases. Microbiological Reviews, 59: 451-480.

Mohammed MK, Dawson AR, Thom NH (2014) Carbonation of filler typed self-compacting concrete and its impact on the microstructure by utilization of 100% CO_2 accelerating techniques. Construction and Building Materials, 50: 508-516.

Mondal, S, Ghosh AD (2019) Review on microbial induced calcite precipitation mechanisms leading to bacterial selection for microbial concrete. Construction and Building Materials, 225: 67-75.

Monteiro PJ, Miller SA, Horvath A (2017) Towards sustainable concrete. Nature Materials 16: 698-699.

Morandeau A, Thiéry M, Dangla P (2015) Impact of accelerated carbonation on OPC cement paste blended with fly ash. Cement and Concrete Research, 67: 226-236.

Muhammad NZ, Keyvanfar A, Majid MZA, Shafaghat A, Mirza J (2015) Waterproof performance of concrete: A critical review on implemented approaches. Construction and Building Materials, 101: 80-90.

Mujah D, Shahin MA, Cheng L (2017) State-of-the-art review of biocementation by microbially induced calcite precipitation (MICP) for soil stabilization. Geomicrobiology Journal, 34: 524-537.

Mukhopadhyay AK (2011) Next-generation nano-based concrete construction products: a review. In Nanotechnology in civil infrastructure. Springer, Berlin, Heidelberg, (pp. 207-223).

Muyzer G, Stams AJ (2008) The ecology and biotechnology of sulphate-reducing bacteria. Nature Reviews Microbiology, 6: 441-454.

Mwandira W, Nakashima K, Kawasaki S (2017) Bioremediation of lead-contaminated mine waste by *Pararhodobacter* sp. based on the microbially induced calcium carbonate precipitation technique and its effects on strength of coarse and fine grained sand. Ecological Engineering, 109: 57-64.

Mwandira W, Nakashima K, Kawasaki S, Ito M, Sato T, Igarashi T, Chirwa M, Banda K, Nyambe I, Nakayama S, Nakata H, Ishizuka M (2019) Solidification of sand by Pb (II)-tolerant bacteria for capping mine waste to control metallic dust: Case of the abandoned Kabwe Mine, Zambia. Chemosphere, 228: 17-25.

Najjar MF, Nehdi ML, Soliman AM, Azabi TM (2017a) Damage mechanisms of two-stage concrete exposed to chemical and physical sulfate attack. Construction and Building Materials, 137: 141-152.

Najjar MF, Soliman AM, Nehdi ML (2017b) Grouts incorporating supplementary cementitious materials for two-stage concrete. Journal of Materials in Civil Engineering, 29: 04016298.

Navarro-Moreno D, Martínez-Arredondo A, García-Vera VE, Gutiérrez-Carrillo ML, Madrid JA, Lanzón M (2021) Nanolime, ethyl silicate and sodium silicate: Advantages and inconveniences in consolidating ancient bricks (XII-XIII century). Construction and Building Materials, 277: 122240.

Nehdi M, Hayek M (2005) Behavior of blended cement mortars exposed to sulfate solutions cycling in relative humidity. Cement and Concrete Research, 35: 731-742.

Nehdi ML, Suleiman AR, Soliman AM (2014) Investigation of concrete exposed to dual sulfate attack. Cement and Concrete Research, 64: 42-53.

Neville A (1995) Chloride attack of reinforced concrete: an overview. Materials and Structures, 28: 63.

Neville A (2001) Consideration of durability of concrete structures: Past, present, and future. Materials and Structures, 34: 114-118.

Neville A (2004) The confused world of sulfate attack on concrete. Cement and Concrete Research, 34: 1275-1296.

Neville AM (1996) Properties of concrete. Pearson Higher Education, 4th edition. Prentice Hall, New Jersey.

Niu D, Zhang L, Fu Q, Wen B, Luo D (2020) Critical conditions and life prediction of reinforcement corrosion in coral aggregate concrete. Construction and Building Materials, 238: 117685.

Noël M, Sanchez L, Tawil D (2018) Structural implications of internal swelling reactions in concrete: review and research needs. Magazine of Concrete Research, 70: 1052-1063.

NT Build 506 (2006) Water permeability of water-saturated concrete, Nordtest Method.

Ohama Y (1998) Polymer-based admixtures. Cement and Concrete Composites, 20: 189-212.

Okyay TO, Nguyen HN, Castro SL, Rodrigues DF (2016) CO_2 sequestration by ureolytic microbial consortia through microbially induced calcite precipitation. Science of the Total Environment, 572: 671-680.

Padmalal D, Maya K, Sreebha S, Sreeja R (2008) Environmental effects of river sand mining: a case from the river catchments of Vembanad lake, Southwest coast of India. Environmental Geology, 54: 879-889.

Pan X, Shi Z, Shi C, Ling TC, Li N (2017a) A review on concrete surface treatment Part I: Types and mechanisms. Construction and Building Materials, 132: 578-590.

Pan X, Shi Z, Shi C, Ling TC, Li N (2017b) A review on surface treatment for concrete–Part 2: Performance. Construction and Building Materials, 133: 81-90.

Pedro D, De Brito J, Evangelista L, Bravo M (2018) Technical specification proposal for use of high-performance recycled concrete aggregates in high-performance concrete production. Journal of Materials in Civil Engineering, 30: 04018324.

Pei R, Liu J, Wang S (2015) Use of bacterial cell walls as a viscosity-modifying admixture of concrete. Cement and Concrete Composites, 55: 186-195.

Pei R, Liu J, Wang S, Yang M (2013) Use of bacterial cell walls to improve the mechanical performance of concrete. Cement and Concrete Composites, 39: 122–130.

Phillips AJ, Cunningham AB, Gerlach R, Hiebert R, Hwang C, Lomans BP, Westrich J, Mantilla C, Kirksey J, Esposito R, Spangler L (2016) Fracture sealing with microbially induced calcium carbonate precipitation: A field study. Environmental Science & Technology, 50: 4111-4117.

Poursaee A (2016) Corrosion of steel in concrete structures. In Corrosion of steel in concrete structures. Woodhead Publishing, (pp. 19-33).

Pradhan B, Bhattacharjee B (2009) Performance evaluation of rebar in chloride contaminated concrete by corrosion rate. Construction and Building Materials, 23: 2346-2356.

Qin Y, Cabral JM (2002) Review properties and applications of urease. Biocatalysis and Biotransformation, 20: 1-14.

Qiu J, Tng DQS, Yang EH (2014) Surface treatment of recycled concrete aggregates through microbial carbonate precipitation. Construction and Building Materials, 57, 144-150.

Rahman MM, Bassuoni MT (2014) Thaumasite sulfate attack on concrete: Mechanisms, influential factors and mitigation. Construction and Building Materials, 73: 652-662.

Ramachandran SK, Ramakrishnan V, Bang SS (2001) Remediation of concrete using micro-organisms. ACI Materials Journal, 98: 3-9.

Ramachandran VS, Beaudoin JJ (2000) Handbook of analytical techniques in concrete science and technology: principles, techniques and applications. Elsevier.

Rana A, Kalla P, Csetenyi LJ (2015) Sustainable use of marble slurry in concrete. Journal of Cleaner Production 94: 304-311.

Rangamaran VR, Shanmugam VK (2019) Biocalcification by piezotolerant *bacillus* sp. NIOTVJ5 isolated from deep sea sediment and its influence on the strength of concrete specimens. Marine Biotechnology, 21: 161-170.

Rhee I, Roh YS (2013) Properties of normal-strength concrete and mortar with multi-walled carbon nanotubes. Magazine of Concrete Research, 65: 951-961.

Riding R (2000) Microbial carbonates: the geological record of calcified bacterial–algal mats and biofilms. Sedimentology, 47: 179-214.

RILEM CPC 18 (1988), Measurement of hardened concrete carbonation depth, RILEM Recommendations for the Testing and Use of Constructions Materials, E & FN SPON, 56–58.

RILEM TC 116-PCD (1999) Permeability of concrete as a criterion of its durability. Material and Structures, 32: 174–179.

Rodrigues JD, Pinto APF (2019) Stone consolidation by biomineralisation. Contribution for a new conceptual and practical approach to consolidate soft decayed limestones. Journal of Cultural Heritage, 39: 82-92.

Rodriguez-Navarro C, Doehne E (1999) Salt weathering: influence of evaporation rate, supersaturation and crystallization pattern. Earth Surface Processes and Landforms: The Journal of the British Geomorphological Research Group, 24: 191-209.

Rodriguez-Navarro C, Jroundi F, Schiro M, Ruiz-Agudo E, González –Muñoz MT (2012) Influence of substrate mineralogy on bacterial mineralization of calcium carbonate: implications for stone conservation. Applied and Environment Microbiology, 78: 4017–4029.

Rodriguez-Navarro C, Rodriguez-Gallego M, Chekroun KB, Gonzalez-Munoz MT (2003) Conservation of ornamental stone by *Myxococcus Xanthus* induced carbonate biomineralization. Applied and Environmental Microbiology, 69: 2182-2193.

Rozière E, Loukili A, El Hachem R, Grondin F (2009) Durability of concrete exposed to leaching and external sulphate attacks. Cement and Concrete Research, 39: 1188-1198.

Ruan S, Qiu J, Weng Y, Yang Y, Yang EH, Chu J, Unluer C (2019) The use of microbial induced carbonate precipitation in healing cracks within reactive magnesia cement-based blends. Cement and Concrete Research, 115: 176-188.

Şahmaran M, Keskin SB, Ozerkan G, Yaman IO (2008) Self-healing of mechanically-loaded self consolidating concretes with high volumes of fly ash. Cement and Concrete Composites, 30: 872-879.

Sanchez F, Sobolev K (2010) Nanotechnology in concrete–a review. Construction and Building Materials, 24: 2060-2071.

Santhanam M, Cohen MD, Olek J (2001) Sulfate attack research—whither now? Cement and Concrete Research, 31: 845-851.

Sarkar A, Chatterjee A, Mandal S, Chattopadhyay B (2019) An alkaliphilic bacterium BKH 4 of Bakreshwar hot spring pertinent to bioconcrete technology. Journal of Applied Microbiology 126: 1742-1750.

Sarkar A, Mahapatra S (2010) Synthesis of all crystalline phases of anhydrous calcium carbonate. Crystal Growth & Design, 10: 2129-2135.

Scherer GW (2004) Stress from crystallization of salt. Cement and Concrete Research 34: 1613-1624.

Schultze-Lam S, Beveridge TJ (1994) Physicochemical characteristics of the mineral forming S-layer from the cyanobacterium *Synechococcus* strain GL24. Canadian Journal of Microbiology, 40: 216-223.

Scrivener KL, John VM, Gartner EM (2018) Eco-efficient cements: Potential economically viable solutions for a low-CO_2 cement-based materials industry. Cement and Concrete Research, 114: 2-26.

Seifan M, Samani AK, Berenjian A (2016) Bioconcrete: next generation of self-healing concrete. Applied Microbiology and Biotechnology, 100: 2591–2602.

Shamsaei E, de Souza FB, Yao X, Benhelal E, Akbari A, Duan W (2018) Graphene-based nanosheets for stronger and more durable concrete: A review. Construction and Building Materials, 183: 642-660.

Sharma A, Saxena A, Sethi M, Shree V (2011) Life cycle assessment of buildings: a review. Renewable and Sustainable Energy Reviews, 15: 871-875.

Sharma N, Prasad GS, Choudhury AR (2013) Utilization of corn steep liquor for biosynthesis of pullulan, an important exopolysaccharide. Carbohydrate Polymers, 93: 95-101.

Shayan A (2016) Effects of alkali–aggregate reaction on concrete and structures. Proceedings of the Institution of Civil Engineers-Construction Materials, 169: 145-153.

Siddique R, Jameel A, Singh M, Barnat-Hunek D, Aït-Mokhtar A, Belarbi R, Rajor A (2017) Effect of bacteria on strength, permeation characteristics and micro-structure of silica fume concrete. Construction and Building Materials, 142: 92-100.

Siddique R, Singh K, Singh M, Corinaldesi V, Rajor A (2016) Properties of bacterial rice husk ash concrete. Construction and Building Materials, 121: 112-119.

Sidiq A, Gravina R, Giustozzi F (2019) Is concrete healing really efficient? A review. Construction and Building Materials, 205: 257-273.

Singh LP, Bisht V, Aswathy MS, Chaurasia L, Gupta S (2018) Studies on performance enhancement of recycled aggregate by incorporating bio and nano materials. Construction and Building Materials, 181: 217-226.

Sisomphon K, Copuroglu O, Koenders EAB (2012) Self-healing of surface cracks in mortars with expansive additive and crystalline additive. Cement and Concrete Composites, 34: 566-574.

Skaropoulou A, Sotiriadis K, Kakali G, Tsivilis S (2013) Use of mineral admixtures to improve the resistance of limestone cement concrete against thaumasite form of sulfate attack. Cement and Concrete Composites, 37: 267-275.

Smith KS, Ferry JG (1999) A plant-type (β-class) carbonic anhydrase in the thermophilic methanoarchaeon *Methanobacterium thermoautotrophicum*. Journal of Bacteriology, 181: 6247-6253.

Soroushian P, Elzafraney M (2004) Damage effects on concrete performance and microstructure. Cement and Concrete Composites, 26: 853-859.

Statista, 2019. Major countries in worldwide cement production 2014-2018. https://www.statista.com/statistics/267364/world-cement-production-by-country/ (accessed 12 May 2020)

Statista, 2020. Cement production worldwide from 1995 to 2019. https://www.statista.com/statistics/1087115/global-cement-production-volume/ (accessed 12 May 2020)

Stefanidou M, Papayianni I (2012) Influence of nano-SiO_2 on the portland cement pastes. Composites Part B: Engineering, 43: 2706-2710.

Stern M, Geary AL (1957) Electrochemical polarization: I. A theoretical analysis of the shape of polarization curves. Journal of the Electrochemical Society, 104: 56.

Stocks-Fischer S, Galinat JK, Bang SS (1999) Microbiological precipitation of $CaCO_3$. Soil Biology and Biochemistry, 31: 1563-1571.

Tam VW, Soomro M, Evangelista ACJ (2018) A review of recycled aggregate in concrete applications (2000–2017). Construction and Building Materials, 172: 272-292.

Tamayo-Figueroa DP, Castillo E, Brandão PF (2019) Metal and metalloid immobilization by microbiologically induced carbonates precipitation. World Journal of Microbiology and Biotechnology, 35: 58.

Tang SW, Yao Y, Andrade C, Li ZJ (2015) Recent durability studies on concrete structure. Cement and Concrete Research, 78: 143-154.

Taylor HF, Mohan K, Moir GK (1985) Analytical study of pure and extended portland cement pastes: I, pure portland cement pastes. Journal of the American Ceramic Society, 68: 680-685.

Thomas NL, Birchall JD (1983) The retarding action of sugars on cement hydration. Cement and Concrete Research, 13: 830-842.

Tian B, Cohen MD (2000) Does gypsum formation during sulfate attack on concrete lead to expansion?. Cement and Concrete Research, 30: 117-123.

Tiano P, Biagiotti L, Mastromei G (1999) Bacterial bio-mediated calcite precipitation for monumental stones conservation: methods of evaluation. Journal of Microbiological Methods, 36: 139-145.

Tobon JI, Payá J, Restrepo OJ (2015) Study of durability of Portland cement mortars blended with silica nanoparticles. Construction and Building Materials, 80: 92-97.

Tobon JI, Payá J, Restrepo OJ (2015) Study of durability of Portland cement mortars blended with silica nanoparticles. Construction and Building Materials, 80: 92-97.

Torres A, Brandt J, Lear K, Liu J (2017) A looming tragedy of the sand commons. Science, 357: 970-971.

Tremblay H, Duchesne J, Locat J, Leroueil S (2002) Influence of the nature of organic compounds on fine soil stabilization with cement. Canadian Geotechnical Journal 39: 535-546.

Turcry P, Oksri-Nelfia L, Younsi A, Aît-Mokhtar A (2014) Analysis of an accelerated carbonation test with severe preconditioning. Cement and Concrete Research, 57: 70-78.

Turk J, Cotič Z, Mladenovič A, Šajna A (2015) Environmental evaluation of green concretes versus conventional concrete by means of LCA. Waste Management, 45: 194-205.

Van den Heede P, De Schepper M, De Belie N (2019) Accelerated and natural carbonation of concrete with high volumes of fly ash: chemical, mineralogical and microstructural effects. Royal Society Open Science, 6: 181665.

Van Tittelboom K, De Belie N, De Muynck W, Verstraete W (2010) Use of bacteria to repair cracks in concrete. Cement and Concrete Research, 40: 157-166.

Van Tittelboom K, De Belie N, Hooton RD (2013) Test methods for resistance of concrete to sulfate attack–a critical review. In Performance of cement-based materials in aggressive aqueous environments. Springer, Dordrecht, (pp. 251-288).

Vieira DR, Calmon JL, Coelho FZ (2016) Life cycle assessment (LCA) applied to the manufacturing of common and ecological concrete: A review. Construction and Building Materials, 124: 656-666.

Vijayalakshmi R, Ramanagopal S, Sathia R, Raj RA (2017) Case study on the repair and rehablitation of G+3 residential appartment located near sea shore, Tamil nadu, India. Indian Journal of Science and Technology, 10: 26.

Villain G, Thiery M, Platret G (2007) Measurement methods of carbonation profiles in concrete: Thermogravimetry, chemical analysis and gammadensimetry. Cement and Concrete Research, 37: 1182-1192.

Vullo DL, Ceretti HM, Daniel MA, Ramírez SA, Zalts A (2008) Cadmium, zinc and copper biosorption mediated by *Pseudomonas veronii* 2E. Bioresource Technology, 99: 5574-5581.

Walkley A, Black IA (1934) An examination of the Degtjaref method for determining soil organic matter and a proposed modifcation of the chromic acid titration method. Soil Science, 37: 29–38.

Wang HY, Kuo WT, Lin CC, Po-Yo C (2013) Study of the material properties of fly ash added to oyster cement mortar. Construction and Building Materials, 41: 532-537.

Wang J, Chen C (2009) Biosorbents for heavy metals removal and their future. Biotechnology Advances, 27: 195-226.

Wang J, Mignon A, Snoeck D, Wiktor V, Van Vliergerghe S, Boon N, De Belie N (2015) Application of modified alginate encapsulated carbonate producing bacteria in concrete: a promising strategy for crack self-healing. Frontiers in Microbiology, 6: 1088.

Wang J, Vandevyvere B, Vanhessche S, Schoon J, Boon N, De Belie N (2017) Microbial carbonate precipitation for the improvement of quality of recycled aggregates. Journal of Cleaner Production, 156: 355-366.

Wang JY, Snoeck D, Van Vlierberghe S, Verstraete W, De Belie N (2014) Application of hydrogel encapsulated carbonate precipitating bacteria for approaching a realistic self-healing in concrete. Construction and Building Materials, 68: 110-119.

Wang JY, Soens H, Verstraete W, De Belie N (2014) Self-healing concrete by use of microencapsulated bacterial spores. Cement and Concrete Research, 56: 139-152.

Whiffin VS, Van Paassen LA, Harkes MP (2007) Microbial carbonate precipitation as a soil improvement technique. Geomicrobiology Journal, 24: 417-423.

Whittaker M, Black L (2015) Current knowledge of external sulfate attack. Advances in Cement Research, 27: 532-545.

Wiktor V, Jonkers HM (2011) Quantification of crack-healing in novel bacteria-based self-healing concrete. Cement and Concrete Composites, 33: 763-770.

Wiktor V, Jonkers HM (2015) Field performance of bacteria-based repair system: Pilot study in a parking garage. Case Studies in Construction Materials, 2: 11-17.

Williams SL, Kirisits MJ, Ferron RD (2016) Optimization of growth medium for S*porosarcina pasteurii* in bio-based cement pastes to mitigate delay in hydration kinetics. Journal of Industrial Microbiology & Biotechnology, 43: 567-575.

Wittmann FH, Beltzung F, Zhao TJ (2009) Shrinkage mechanisms, crack formation and service life of reinforced concrete structures. International Journal of Structural Engineering, 1: 13-28.

Wu CR, Zhu YG, Zhang XT, Kou SC (2018) Improving the properties of recycled concrete aggregate with bio-deposition approach. Cement and Concrete Composites, 94: 248-254.

Wu Z, Wong HS, Buenfeld NR (2015) Influence of drying-induced microcracking and related size effects on mass transport properties of concrete. Cement and Concrete Research, 68: 35-48.

Xie AJ, Shen YH, Zhang CY, Yuan ZW, Zhu XM, Yang YM (2005) Crystal growth of calcium carbonate with various morphologies in different amino acid systems. Journal of Crystal Growth, 285: 436-443.

Xu J, Wang X, Wang B (2018) Biochemical process of ureolysis-based microbial $CaCO_3$ precipitation and its application in self-healing concrete. Applied microbiology and biotechnology, 102: 3121-3132.

Xu J, Yao W (2014) Multiscale mechanical quantification of self-healing concrete incorporating non-ureolytic bacteria-based healing agent. Cement and Concrete Research, 64: 1-10.

Yoshida N (2019) Sulfate attack on residential concrete foundations in Japan. Journal of Sustainable Cement-Based Materials, 8: 327-336.

Young JF (1972) A review of the mechanisms of set-retardation in portland cement pastes containing organic admixtures. Cement and Concrete Research, 2: 415-433.

Younsi A, Turcry P, Aït-Mokhtar A, Staquet S (2013) Accelerated carbonation of concrete with high content of mineral additions: effect of interactions between hydration and drying. Cement and Concrete Research, 43: 25-33.

Zhan M, Pan G, Wang Y, Fu M, Lu X (2020) Recycled aggregate mortar enhanced by microbial calcite precipitation. Magazine of Concrete Research, 72: 622-633.

Zhan Q, Qian C (2017) Stabilization of sand particles by bio-cement based on CO_2 capture and utilization: Process, mechanical properties and microstructure. Construction and Building Materials, 133: 73-80.

Zhan Q, Qian C, Yi H (2016) Microbial-induced mineralization and cementation of fugitive dust and engineering application. Construction and Building Materials, 121: 437-444.

Zhang MH, Sisomphon K, Ng TS, Sun DJ (2010) Effect of superplasticizers on workability retention and initial setting time of cement pastes. Construction and Building Materials, 24: 1700-1707.

Zhou Y, Gencturk B, Willam K, Attar A (2015) Carbonation-induced and chloride-induced corrosion in reinforced concrete structures. Journal of Materials in Civil Engineering, 27: 04014245.

Zhu T, Dittrich M (2016) Carbonate precipitation through microbial activities in natural environment, and their potential in biotechnology: a review. Frontiers in Bioengineering and Biotechnology, 4:4.

Zhu T, Lu X, Dittrich M (2017) Calcification on mortar by live and UV-killed biofilm-forming cyanobacterial *Gloeocapsa* PCC73106. Construction and Building Materials, 146: 43-53.

Zhu T, Paulo C, Merroun ML, Dittrich M (2015) Potential application of biomineralization by *Synechococcus* PCC8806 for concrete restoration. Ecological Engineering, 82: 459-468.

Zhu W (2020) Permeation properties of self-compaction concrete. In Self-compacting concrete: materials, properties and applications. Woodhead Publishing, (pp. 117-130).

PUBLICATION

Construction and Building Materials 158 (2018) 601–613

Contents lists available at ScienceDirect

Construction and Building Materials

journal homepage: www.elsevier.com/locate/conbuildmat

Influence of nutrient components of media on structural properties of concrete during biocementation

Sumit Joshi [a], Shweta Goyal [b], M. Sudhakara Reddy [a,*]

[a] Department of Biotechnology, Thapar University, Patiala 147004, Punjab, India
[b] Department of Civil Engineering, Thapar University, Patiala 147004, Punjab, India

HIGHLIGHTS

- Nutrients retarded setting property of cement paste and decreased compressive strength of concrete.
- No impact on setting property of cement paste when admixed with bacterial culture.
- Compressive strength increased and permeability reduced with bacterial treated concrete.
- No significant variation in pH from bacterial treated and control specimens.
- Biogenic precipitation of $CaCO_3$ by bacteria counteract the retarding effect of organic nutrients.

ARTICLE INFO

Article history:
Received 7 August 2017
Accepted 10 October 2017
Available online 17 October 2017

Keywords:
Biomineralization
Curing
Organic admixture
Durability
Carbon
Nitrogen

ABSTRACT

Application of microbial induced carbonate precipitation in cement-based materials has become substantially popular. In the present investigation, effect of nutrient components of media such as carbon and nitrogen content of organic nutrients and bacterial cells on the chemical and structural properties of concrete were studied. The retarding effect of organic nutrient medium on setting property of cement paste and decrease in compressive strength of concrete was observed. However, no impact on setting property of cement paste admixed with bacterial culture was observed. Significant increase in compressive strength and reduction in permeability was observed with bacterial admixed and surface treated concrete specimens. Carbon and nitrogen content were significantly increased in bacterial treated specimens compared to control. No significant variation in pH was observed from the samples collected from different depths of the concrete specimens both in bacterial treated and control specimens. Present study results suggested that biogenic precipitations of $CaCO_3$ by bacterial cells counteract the retarding effect of organic nutrients of concrete and enhance the durability properties.

1. Introduction

Concrete is the most important element of infrastructure development across the globe. Rapid growth in infrastructure has resulted into enhanced use of concrete as a construction material. With the increasing population, the demand for residential buildings, transport connectivity and industrial units has been escalated. After the start of industrial era, concrete has become the most widely used construction material. The incomparable property of concrete like high compressive strength, durability under aggressive environments, ability to be moulded into different shapes etc. has made it attractive among other construction materials. However, concrete is not free from severe degradation problems. The external attacks on concrete like chloride ingress, sulfate ingress and carbonation of concrete due to increasing level of carbon dioxide around its surrounding environment are matter of concern [1]. These external environmental attacks on the concrete structures are causing irreversible changes in its serviceability. The ingress of aggressive agents into concrete indicates the importance of permeation properties of surface layer of concrete [2,3]. Researchers had investigated the use of different treatments to refine the pore structure of concrete and to prevent the premature deterioration of concrete structures from the aggressive environment. Surface treatments like epoxy coatings, pore blockers, silanes, acrylic coatings etc., are available but these treatments are subject to frequent controversy due to their limited long-term performance, need for constant maintenance, cost, site accessibility and environmental impact [4].

* Corresponding author.
E-mail address: msreddy@thapar.edu (M.S. Reddy).

https://doi.org/10.1016/j.conbuildmat.2017.10.055
0950-0618/

With time, microbially induced calcium carbonate precipitation (MICP) using calcifying bacteria has emerged as a promising technique in the field of concrete research. Initial applications of MICP include archeological stone restoration [5–7], soil strengthening [8] etc. During the last decade, the potential of calcifying bacteria in concrete has also been explored by researchers. The use of MICP in enhancing both strength and durability of concrete is investigated by various researchers [9–12]. The combined effect of precipitation of calcium carbonate by ureolytic bacteria in increasing compressive strength and reducing porosity of concrete has given the edge to biogeotechnology over other conventional techniques. Lab-scale experiments to remediate cracks in concrete had also shown promising results in which polyurethane embedded bacteria [9], silica gel immobilized bacteria [13], hydrogel encapsulated bacteria [14] were used to remediate cracks in concrete. Calcium carbonate crystals precipitated by bacteria resulted as a crack healing material which results into decreased water permeability.

The civil oriented research with microbial precipitation has focused on the use of ureolytic bacteria. These bacteria hydrolyze urea by producing urease enzyme in large amount resulting into release of ammonia and carbon dioxide. The ammonia produced increases the pH in the surrounding of bacteria that leads to precipitation of calcium carbonate [15]. Bacteria were supplemented with calcium source (i.e. calcium chloride) along with urea which results into the formation of calcium carbonate crystals with different morphologies like calcite, aragonite and vaterite. The biochemical reaction resulting from urea and $CaCl_2$ medium on the negatively charged cell surface of bacteria and leading to calcium carbonate precipitation was proposed as follow [15,16]:

$$Ca^{2+} + Cell \rightarrow Cell - Ca^{2+} \quad (1)$$

$$Cl^- + HCO_3^- + NH_3 \rightleftarrows NH_4Cl + CO_3^- \quad (2)$$

$$Cell - Ca^{2+} + CO_3^{2-} \rightarrow Cell - CaCO_3 \downarrow \quad (3)$$

Along with all these positive attributes of using bacteria in concrete, the disadvantage of use of organic matter on the retardation of setting process of soil-cement mixtures have also been reported by many researchers [17–19]. It has been reported that the presence of organic matter in soil-cement mixtures delay the hydration process of cement, thus affecting the cementing process. Organic compounds with hydroxyl and carboxyl groups may retard the hardening of cement and resulting into no strength gain [18]. During the process of microbial induced carbonate precipitation, different nutrients (both organic and inorganic) are used. The use of these organic nutrients might affect some properties of concrete.

The present study was aimed to test the efficacy of nutrient medium and urea on the structural properties of concrete. The ureolytic bacteria *Bacillus* sp. CT-5 strain isolated from cement sample was used to induce the calcium carbonate precipitation. To evaluate the presence of organic content and nitrogenous material in concrete specimens, carbon and nitrogen content was determined at different depths of the concrete specimens. Furthermore, the concrete specimens were analyzed for compressive strength, sorptivity test, water permeability test, rapid chloride permeability test (RCPT), SEM-EDX and XRD.

2. Materials and methods

2.1. Bacterial strain

Bacillus sp. CT-5 strain isolated from the cement sample was used because of its high urease (UA) producing activity with high efficiency to precipitate $CaCO_3$ crystals [20]. The strain was grown in autoclaved Nutrient broth medium (Peptone 10 g/L, Yeast extract 10 g/L, Sodium chloride 5 g/L). For *in vitro* calcium carbonate precipitation, the culture was grown in Nutrient broth (Himedia, India) supplemented with filter sterilized 2% urea (w/v) (NBU) and 25 mM $CaCl_2$ solution at 37 °C under shaking condition (120 rpm).

2.2. Materials

An ordinary Portland cement (43 Grade) confirming to BIS 8112-2013 [21] was used in the present study. Clean, dry and well graded natural river sand confirming to Zone II was used as fine aggregate (natural river sand). The values of specific gravity and water absorption of fine aggregates was 2.70 and 1.8%, respectively The coarse aggregate used was crushed gravel with nominal particle size of 20 mm and 10 mm. The specific gravity and water absorption of 20 mm aggregates was 2.63 and 1.38% and for 10 mm aggregates, it was 2.65 and 1.4%, respectively. Both fine aggregate and coarse aggregate conformed to BIS: 383-1970 [22].

2.3. Cement paste composition

The change in setting characteristics of cement paste upon addition of bacteria and associated nutrients at the casting stage was investigated by performing initial setting time and final setting time tests on cement pastes. Three types of cement pastes were prepared. One cement paste was made by adding water and termed as control paste mix. Second mix was prepared by mixing cement with 1.3% nutrient broth supplemented with 2% urea (NBU medium) and 25 mM $CaCl_2$. The third cement paste was prepared by mixing bacterial culture grown in NBU medium and 25 mM $CaCl_2$. The consistency of all the mixes was kept same. The composition and nomenclature of the pastes is presented in Table 1.

2.4. Concrete mix proportions

Concrete mix was prepared by using cement: sand: coarse aggregate in the ratio of 1:1.82:3.24 (w/w) and water to cement ratio (w/c) of 0.5. For casting of bacterial treated specimens, nutrient broth with bacterial culture (OD_{600} 0.5) supplemented with 2% urea (w/v) and 25 mM $CaCl_2$ solution (w/v) were used instead of water. The bacterial culture to cement ratio was maintained at 0.5. During casting, the raw material was dry mixed for 2 min in concrete mixer before adding water. After adding water/NBU, the ingredients were mixed for another 2 min. The fresh mix in the plastic stage was immediately transferred to iron moulds. After casting, all specimens were allowed to remain in iron moulds and were kept in casting room at room temperature of 27 ± 2 °C for 24 h. Thereafter, the specimens were demoulded and were cured till the testing age. Four different curing regimes as specified in Table 2 were adopted in this study.

2.5. Test procedures

2.5.1. Compressive strength

Concrete cubes of 150 mm dimension were casted for compressive strength measurements. The effect of incorporating bacterial cells grown in NBU-$CaCl_2$ medium during casting and spraying of bacterial cells suspended in NBU-$CaCl_2$ medium on the mechanical properties of concrete cubes was studied at the age of 7 and 28 days of curing as per BIS 516: 1959 [23] using automatic compression testing machine, COMPTEST 3000. The average of three specimens was taken as the compressive strength of the mix.

Table 1
Preparation of cement paste and their composition.

Cement Mixes	Cement (g)	Water (g)	Nutrient broth	Bacterial culture
Control paste	400 g	78.2 g	–	–
Media paste	400 g	–	78.2 g	–
Bacterial paste	400 g	–	–	78.2 g

NBU medium and calcium chloride had the following concentration: Nutrient broth (Peptone 10 g/L, Yeast extract 10 g/L, Sodium chloride 5 g/L), 2% Urea (w/v) and 25 mM $CaCl_2$ (w/v).

Table 2
Outline of different sets of concrete specimen and mechanism of curing treatments.

Specimens	Material used	Mechanism of curing
Control	Cement: sand: coarse aggregate Water/cement = 0.5	Water Curing for 28 days
Media treated (MT)	Cement: sand: coarse aggregate Media/ Cement = 0.5	Submersion in NBU medium with urea and $CaCl_2$ without bacteria for 28 days
Bacterial admixed treatment (BAT)	Cement: sand: coarse aggregate Bacterial culture/cement = 0.5	Submersion in NBU medium, with urea, $CaCl_2$ and bacterial culture for 28 days
Bacterial spray treatment (BST)	Cement: sand: coarse aggregate Water/cement = 0.5	Bacterial spray on specimens twice a day till 28 days

NBU medium and calcium chloride had the following concentration: Nutrient broth (Peptone 10 g/L, Yeast extract 10 g/L, Sodium chloride 5 g/L), 2% Urea (w/v) and 25 mM Calcium chloride (w/v).
All specimens were prepared in triplicate.

2.5.2. Permeation properties

Permeation properties of various mixes were measured at 28 days of casting, taking the average of three specimens as the representative value. Sorptivity was determined according to ASTM C1585 [24]. The test is based on the rate of uni-directional absorption of water by concrete sample due to capillary rise. It correlates the transport of water with the pore system of specimen [25]. To conduct sorptivity test, the concrete cylinders with diameter 100 mm and 50 mm thickness were prepared. Before conducting the test, side surface of specimen was sealed with epoxy sealing material and initial mass was noted. One surface of specimen was exposed to water and mass increase of specimen by absorption was monitored by weighing it at different time intervals. The test setup is illustrated in Fig. 1. The mass change was recorded at the intervals of 60 s, 5, 10, 20, 30, 60 min and every hour up to 6 h. From the value of mass change, volume of water absorbed per unit cross sectional area was evaluated for each time interval. A plot between the square root of time and volume of water absorbed was plotted. Slope of the graph is taken as the value of sorptivity for that specimen.

Rapid chloride penetrability test (RCPT) was conducted as per ASTM C 1202-97 [26]. Concrete cylinders with diameter 100 mm and 50 mm thickness were prepared for conducting RCPT test. Cylindrical specimens were subjected to a potential difference of 60 V for 6 h by placing it inside the test cell. The solution of sodium chloride 3% (by mass) was kept in one side of test cell connected to the negative terminal of power supply and sodium hydroxide solution (0.3 N) was kept in other side of test cell connected to the positive terminal of power supply. Total charge passed (in terms of coulombs) is a measure of the electrical conductance of the concrete and directly proportional to the chloride penetrability.

The water permeability test was carried out as per DIN 1048 at the age of 28 days [27]. The concrete specimens were exposed to a water pressure of 0.5 N/mm^2 for 72 h and the vertical penetration depth of water into concrete was then measured after breaking the concrete specimen.

2.5.3. Analysis of concrete specimens for carbon, nitrogen, pH and $CaCO_3$ precipitates

Apart from the standard tests on concrete, powdered samples of concrete were taken from various depths and were analyzed for $CaCO_3$ precipitation, carbon content and nitrogen content. Along with this, pH of concrete was also measured at various depths. Concrete cubes after respective curing were drilled using rotary hammer drilling machine to collect the concrete powder for analysis. The cubes were drilled up to the depth of 50 mm from two opposite sides (Fig. 2). Concrete powder was separately collected from each depth. The sample was collected by drilling at 12 points on one surface of the cube as shown in Fig. 3. Homogenous samples were prepared by collecting the samples of each depth of concrete specimen.

Carbon in concrete powder was determined according to the method described in Walkley-Black [28]. Kjeldahl method was used to determine the ammonia producing nitrogen in the concrete powder as per BIS: 5194-1969 [29]. pH value at various depths was measured potentiometrically by immersing pH glass electrode in the suspension of a 1:5 concrete powder: water after stirring for 1 h.

Fig. 1. Arrangement of the sorptivity test.

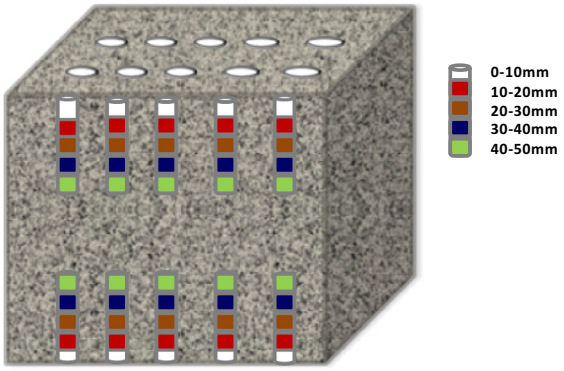

Fig. 2. Layout of the drilling pattern.

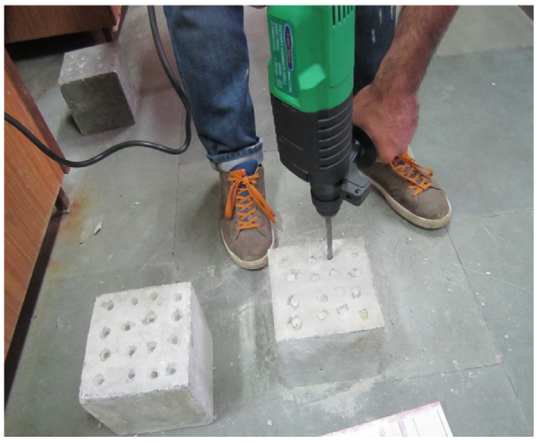

Fig. 3. Collection of concrete powder from different depths.

Calcium carbonate precipitation in concrete specimens was determined by thermogravimetric analysis (TGA). Briefly, 20 mg of concrete powder was placed in TGA holder and temperature was increased constantly from room temperature up to 1000 °C at heating rate of 10 °C/min. Nitrogen was used as purge gas at 10 ml/min. The graphical representation for the loss of weight (%) of sample during heating was shown against temperature (°C). The weight loss in the temperature range of 550–750 °C corresponds to $CaCO_3$ decomposition.

2.6. Micro-structural analysis

Scanning Electron Microscopy (SEM) (ZEISS EVO 50) analysis was done on the concrete specimens at the age of 28 days. The elemental composition of micro-structural crystals was identified with Energy Dispersive X-ray spectroscopy (EDX). For conducting SEM and EDX analyses, small pieces of samples from different depths were collected. Samples were finely polished and gold coated with a sputter coating. To disperse excess charge from the sample, a thin coating of carbon was applied on the polished surface. X-ray diffraction was done on the powdered samples obtained from various depths and sieved through 90 μm sieve. XRD spectrum was obtained using Bruker D8 X-ray diffractometer with a Cu anode (40 kV and 30 mA) and scanning from 10° to 80° 2θ.

All the experiments were performed in triplicates. The data are presented as mean ± standard deviation. All the analyses were performed using Sigma plot (v.9) software.

3. Results

3.1. Initial and final setting times of cement mixes

The initial and final setting time of various cement paste mixes is presented in Fig. 4. The initial and final setting time of control cement mix was 120 min and 260 min respectively. The delay in both initial setting time and final setting time was observed in cement paste mixed with media only. Initial setting time increased by 60 min while the final setting time registered an increase of 240 min in media cement paste as compared to control cement paste. However, cement paste admixed with bacterial culture had no influence on initial setting while an increase of 30 min in final setting was observed. These observations indicate that the setting characteristics of the mix incorporating bacterial culture is similar to the control mix. However, addition of nutrient broth without bacteria delayed in setting of cement.

3.2. Compressive strength

Addition of *Bacillus* sp. along with NBU – $CaCl_2$ media in concrete specimen and curing with respective medium significantly increased the compressive strength compared to control specimen (Fig. 5). The bacterial admixed treated (BAT) specimens showed an average increase of 29% in compressive strength as compared to the control specimens. The bacterial sprayed (BST) specimens in which bacteria were introduced into concrete after casting in the form of spray treatment with bacterial culture during curing also registered slight increase in compressive strength (8%) as compared to the control mix. However, the compressive strength of media treated (MT) specimens casted with nutrient medium only registered a drastic decrease by 15.5% as compared to the control mix (Fig. 5).

3.3. Permeation properties

Among all the tested mixes, control mix has highest sorptivity coefficient. When compared to control mix, both BAT and BST specimens showed lowest sorptivity coefficient (Table 3). In RCPT, resistance to chloride ions penetration by all specimens was evaluated. Both control specimens and MT specimens had similar charge transfer resistance and falls in the category of moderate penetration type. With bacterial treatment, the charge transfer is reduced drastically, and the penetration values fall in low penetration range. While in BAT specimen the total charge passed was

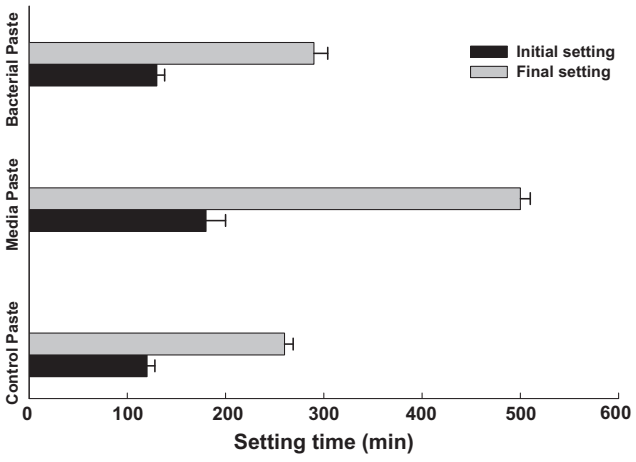

Fig. 4. Initial and final setting times of different cement paste mixes.

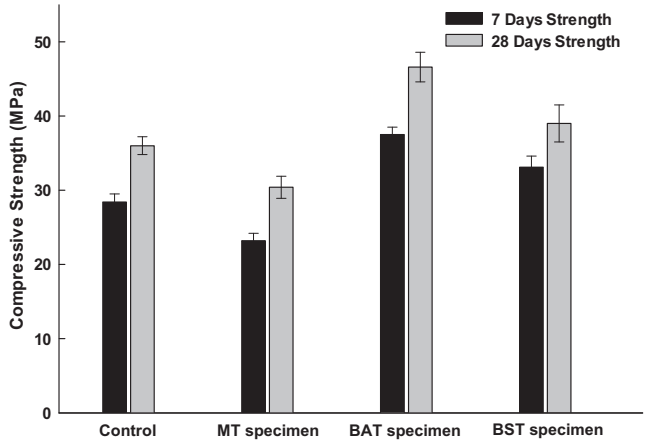

Fig. 5. Compressive strength (Mpa) of all specimens after 7 days and 28 days curing.

1128 coulombs and BST specimens registered charge of 1340 coulombs (Table 3).

In water impermeability test, maximum vertical penetration of water was found in control specimen (35.3 mm), while minimum penetration depth of 13.6 mm was measured in BST specimens. A nominal difference between penetration depth values were observed in BAT (14.2 mm) and BST specimens. MT specimen prepared by using nutrient medium had the water penetration depth of 31.2 mm, which is nearly similar to the penetration depth obtained for control specimen (Table 3).

3.4. Chemical analysis of specimens

3.4.1. Carbon and nitrogen profile

Different medium components (especially carbon, nitrogen sources) are mixed along with bacteria during the formation of microbial concrete. These components might influence the structural properties of concrete. The presence of high carbon content is known to have adverse effects on the workability, air entrainment mechanism, compressive strength etc. [30]. Therefore carbon and nitrogen content at 28 days of casting with respective curing was obtained at different depths in concrete specimens. The results so obtained were then correlated with the mechanical properties of the respective mixes. The results of carbon and nitrogen content in concrete specimens with depth-wise profiling are presented in Fig. 6.

The percentage of carbon and nitrogen remains same at all depths for the control specimen while BAT specimen showed maximum carbon and nitrogen content at all depths (Fig. 6). The carbon content in BST and MT specimen was almost same at all depths. The amount of carbon content in all the treatments was maximum at the surface, and decreased with the increase in depth of concrete. The carbon content at 30 mm depth becomes almost similar to the corresponding value obtained for the control mix (Fig. 6a). The percentage of nitrogen content was minimum for the control specimen at all depths; while BAT specimen registered maximum nitrogen content at all depths, followed by MT specimen. In BST specimen, nitrogen contents become almost same as control specimen after initial 20–30 mm depth (Fig. 6b).

3.4.2. pH profile

The introduction of microbes into concrete leads to changes in its chemical composition and hence, might affect the alkaline nature of concrete pore solution. Therefore, in order to investigate effect of addition of microbes into concrete on alkaline layer, pH of the resultant mixes were measured at various depths, starting from the surface of concrete. The pH values in all specimens was found to be in the range of 12.0–12.4, which indicates that bacteria and various ingredients added in the process does not have significant effect on pH and on alkaline environment of concrete (Fig. 7).

3.5. Micro-structural analysis

SEM analysis of all concrete specimens was done from three different depths. The SEM images of both BAT and BST specimens taken from the upper depth of 0–10 mm clearly identified the presence of calcium carbonate crystals associated with bacterial cells (Fig. 8). In case of BAT specimen, presence of different crystal lattice of calcium carbonate was found. Rhombohedral calcite crystal and needle shaped aragonite crystals were observed (Fig. 8A and B). The EDX analysis also confirmed the elemental composition of crystals with peaks showing high amount of calcium and carbon. In BST specimen, higher biodeposition of calcium carbonate precipitation was observed. Morphology of rhombohedral calcite and aragonite crystals in association with bacterial cells was also identified (Fig. 8D–F). The high peak of calcium on EDX analysis further confirmed the presence of calcium carbonate crystals.

The SEM images of BAT (Fig. 9A and B) and BST (Fig. 9D–F) specimens at the middle depth shows the presence of bacterial cells. However, in the proximity of bacterial cells, no precipitation of calcium carbonate crystals was observed. EDX analysis confirmed the absence of any carbonate crystals with high silicon peak in the graph. In the presence of rod shaped bacterial cells indicates the ingress of bacterial cells through pores during the spray curing treatment (Fig. 9D–F).

Fig. 10 shows the SEM images of the specimens taken at inner depth of 40–50 mm. Presence of bacterial cells without any calcium carbonate precipitation was observed in BAT specimen (Fig. 10A). In case of BST specimen (Fig. 10B), no precipitation and the associated bacterial cells were detected. The EDX analysis also identified high silicon peaks in both the specimens. In SEM analysis of control specimen (Fig. 10C–E) and MT specimen (Fig. 11A–C) at different depths, absence of calcium carbonate precipitation was observed. EDX analysis further confirmed the absence of calcium carbonate crystals.

XRD analysis of all concrete specimens at the top surface was also performed along with SEM morphology analysis. The XRD analysis of all mixes is presented in Figs. 12 and 13. Presence of cal-

Table 3
Sorptivity coefficient, RCPT and water impermeability of various mixes measured at 28 days.

Specimen	Sorptivity Coefficient 'k'	RCPT		Water penetration
		Average charge passed	Penetration type	
Control	0.0191	2930 Coulombs	Moderate	35.5 mm
MT specimen	0.0110	2638 Coulombs	Moderate	31.2 mm
BAT specimen	0.0071	1128 Coulombs	Low	14.2 mm
BST specimen	0.0075	1340 Coulombs	Low	13.6 mm

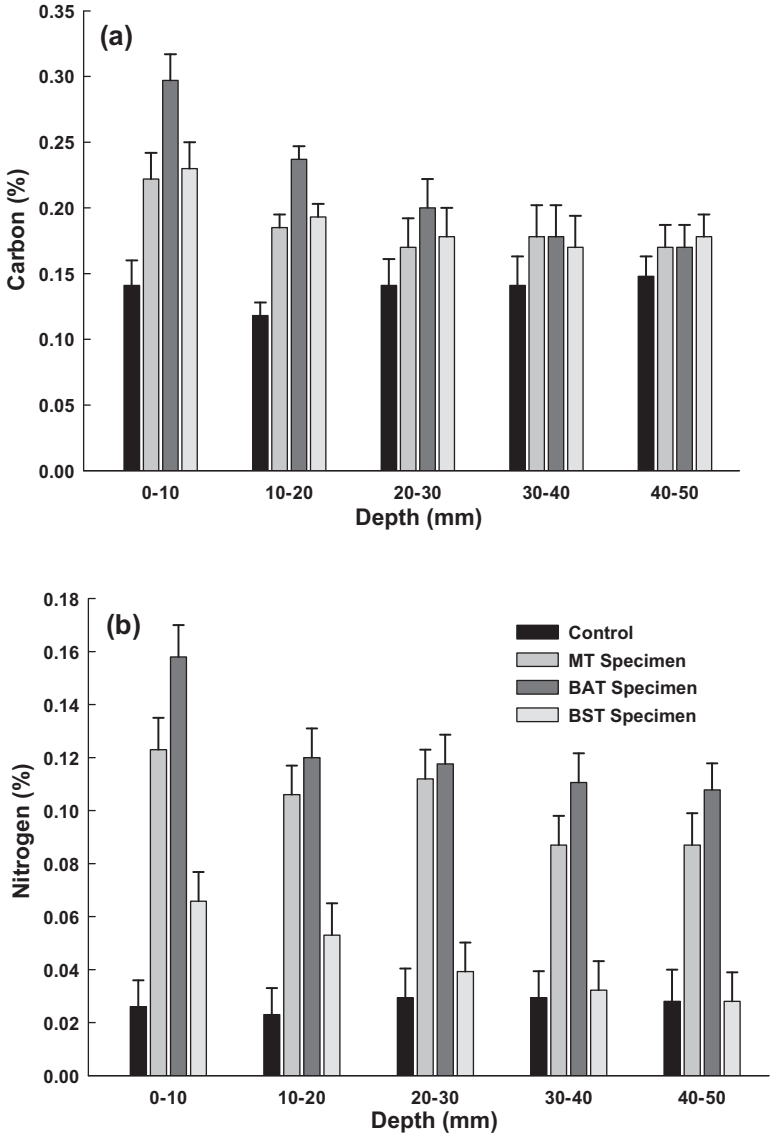

Fig. 6. Carbon (a) content and nitrogen (b) content (% by mass) of concrete specimens at different depths in various treatments. Error bars represents standard deviation (n = 3).

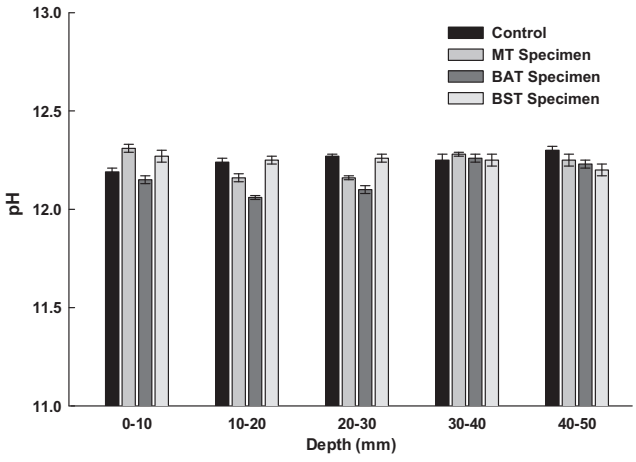

Fig. 7. Depth wise estimation of pH for different specimens.

cite crystals in upper depth of BAT and BST specimen were confirmed with the XRD analysis as shown in Fig. 12. In case of MT and control specimens, no calcium carbonate precipitation was observed in XRD analysis as shown in Fig. 13. XRD spectrum of media and control specimens revealed that the major phases present are quartz, calcium aluminium silicate and coesite.

To verify $CaCO_3$ precipitation by bacteria in the upper layer, TGA was conducted for all mixes at 28 days of casting. TGA results demonstrated the presence of $CaCO_3$ precipitation in BAT specimen as well as in BST specimen. As shown in Fig. 14, weight of bacterially treated samples decreased continuously from room temperature till about 800 °C. As it can be seen in Fig. 14, between 550 and 750 °C sharp weight loss of about 9% and 11% occurred in BAT and BST specimens from the initial sample weight. This weight loss indicates decomposition of $CaCO_3$ into CaO and CO_2 in the temperature range 600–750 °C [31]. While in control and MT specimens no weight loss occurred between 550–750 °C showing no $CaCO_3$ precipitations.

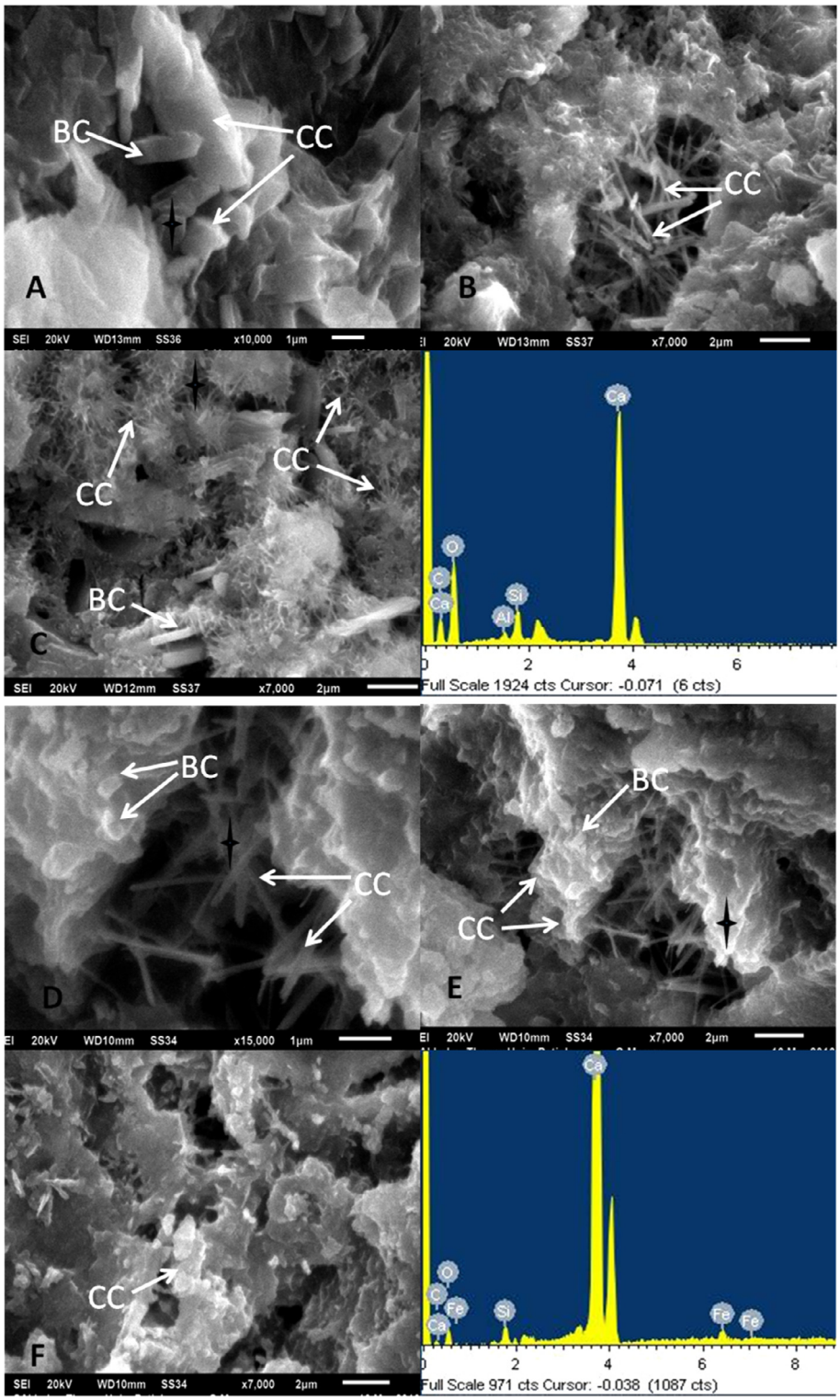

Fig. 8. SEM images represent the $CaCO_3$ crystal (CC) associated with rod shaped bacterial cells (BC) at upper depth (0–10 mm) in BAT specimens (A-C) and BST specimens (D-F). Arrows show carbonate crystals and bacterial cells. '✦' shows the spots of EDX analysis.

4. Discussion

4.1. Effects of bacterial cells and organic matter on the properties of concrete

The effect of addition of microbes on the properties of resultant concrete was investigated in the present study. The bacteria were added to concrete either during the casting stage or spray treatment after casting in different mixes. For the vegetative growth of bacteria, nutrients are required to be added along with bacteria. The two main nutrient components required for *Bacillus* sp. CT-5 strain are urea and nutrient broth medium containing yeast extract. The incorporation of bacteria along with the associated nutrient can cause modifications in

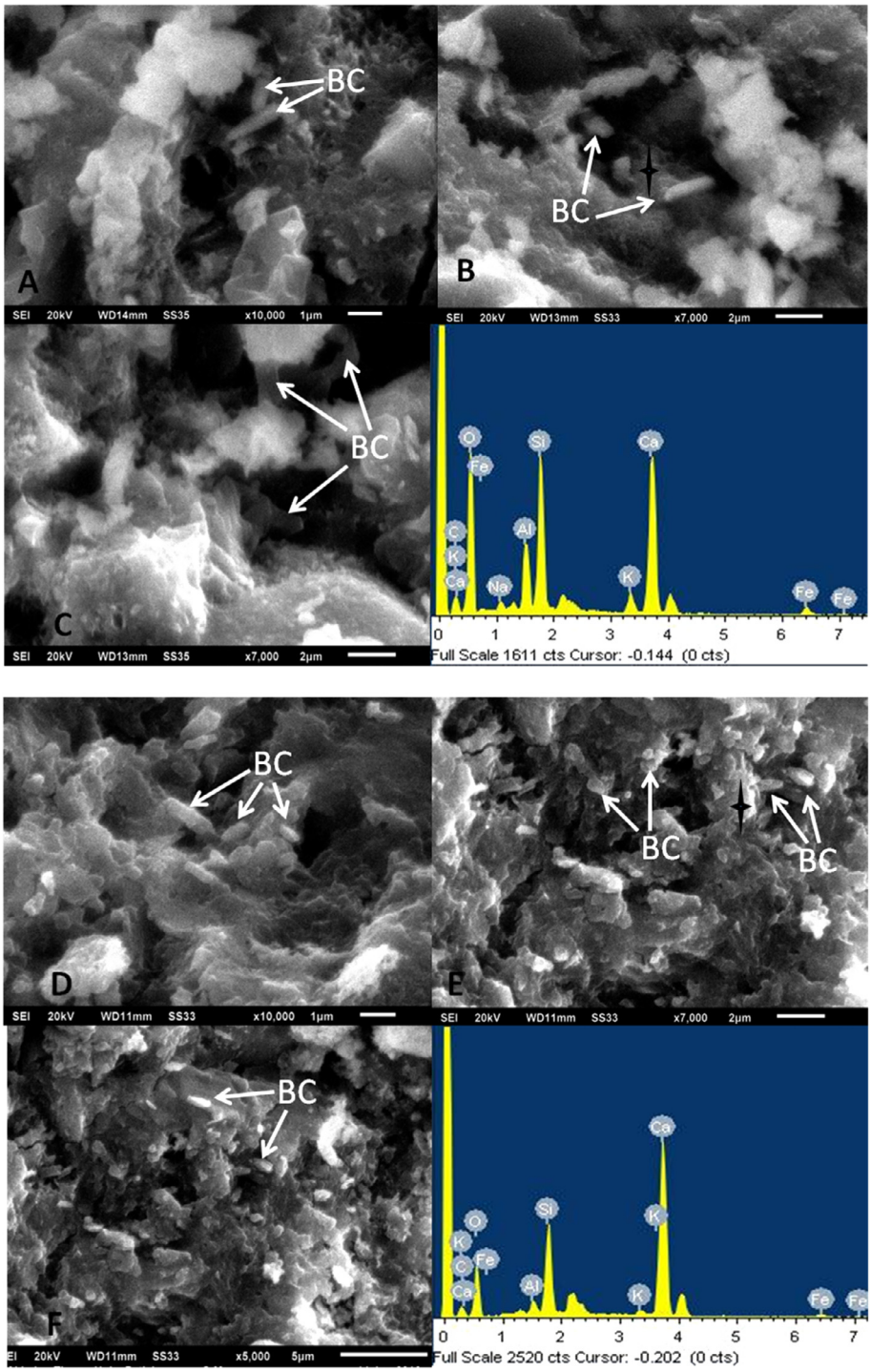

Fig. 9. SEM images from the middle depth (20–30 mm) of BAT specimen (A-C) and BST specimen (D-F). Arrows show bacterial cells (BC). '✦' shows the spots of EDX analysis.

the concrete matrix, and hence affects the properties of the mixes.

The results indicated that the incorporation of bacterial cells along with nutrient medium in concrete specimens lead to significant improvement in compressive strength of the mix. The increase of 29% in compressive strength was observed in the mix in which bacterial cells along with nutrient medium was introduced during casting (BAT specimens); while in BST specimens, marginal increase in compressive strength by 8% was observed. Addition of plain nutrient medium without bacterial cells in concrete specimens showed distinctive decrease in compressive strength on comparison with control specimens at 7 and 28 days curing age (Fig. 5). It indicates that the addition of organic matter in the form of yeast extract and urea into concrete leads to retardation in compressive strength development. The phenomenon of retardation in compressive strength due to the addition of organic nutrients in concrete has also been reported by Ersan et al. [32].

The negative effect of introducing organic nutrients on the initial and final setting times of cement paste mixes was also observed (Fig. 4). In media only mix having organic yeast extract and urea, noticeable delay in initial and final setting times of cement paste mix was observed. But in case of bacterial admixed

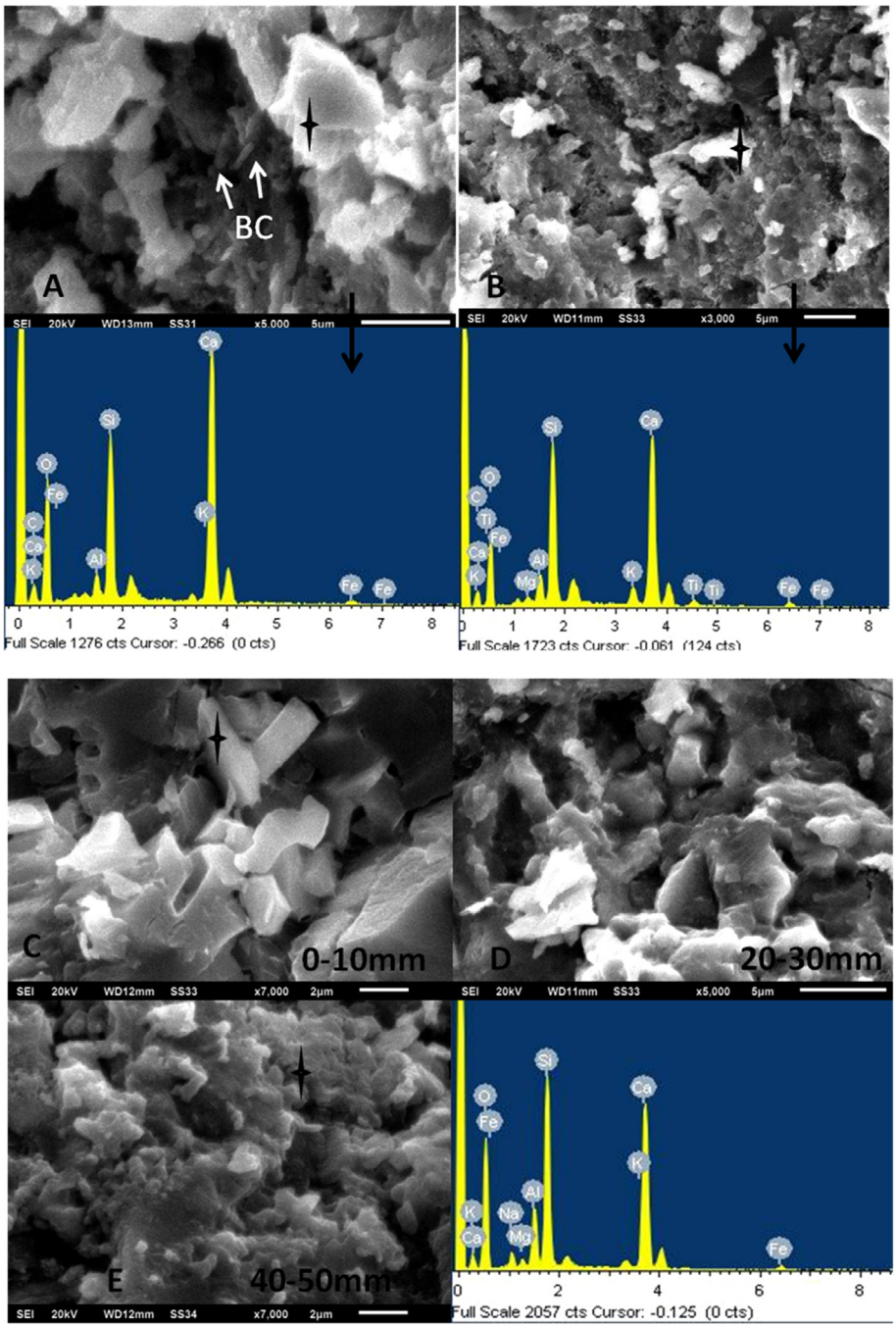

Fig. 10. SEM images represent BAT specimens (A) with bacterial cells and BST specimens (B) without bacterial cells at the inner depth (40–50 mm). SEM images of control specimen (C-E) from different depths. '✦' shows the spots of EDX analysis.

pastes, no delay in initial setting was observed while a minor delay in final setting time was noticed. The results of setting time and compressive strength together indicate that the addition of organic matter/urea alone has retardation effect on hydration and hence on setting of the mix, which further influence later age mechanical properties. Actually, the organic nutrient added in the concrete mix while casting to fulfill essential chemical requirements of bacteria for the microbial growth is a yeast extract and is used as a carbon source by bacteria. The adverse effect of yeast extract on hydration of cement was reported earlier by Williams et al. [33]. It was also reported by Bundur et al. [34] that the addition of organic substance in concrete influences the degree of hydration and yeast extract act as a retardation substance. Ersan et al. [32] also reported that the compressive strength of mortar mix can decrease by up to 25% when yeast extract and urea are added to the mix. Presence of higher percentage of carbon and nitrogen content in MT specimen than control specimen was also observed (Fig. 6).

However, this negative effect of addition of organic matter into concrete was not visible when it is added along with bacteria. In BAT specimen, casting of the mix was carried out by the bacteria culture consisting of bacterial cells, nutrient broth and urea. Its addition into cement paste has not delayed the setting time of cement. Also, the compressive strength of the resultant mix registered a significant increase of 29% as compared to the control mix. Therefore, it indicates that the adverse effect of introducing yeast

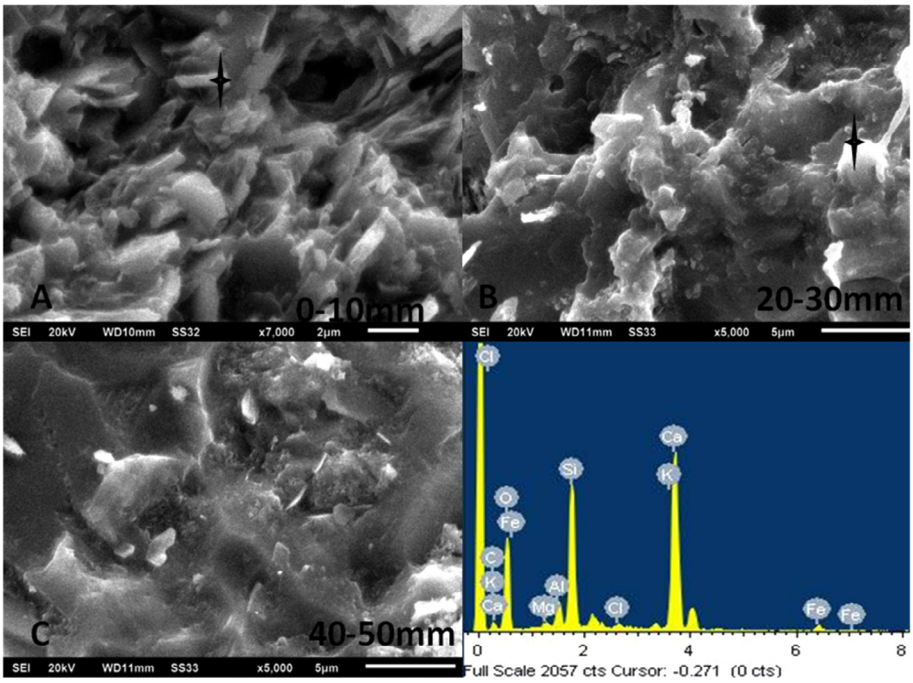

Fig. 11. SEM images of MT specimen (A-C) from different depths. '✦' shows the spots of EDX analysis.

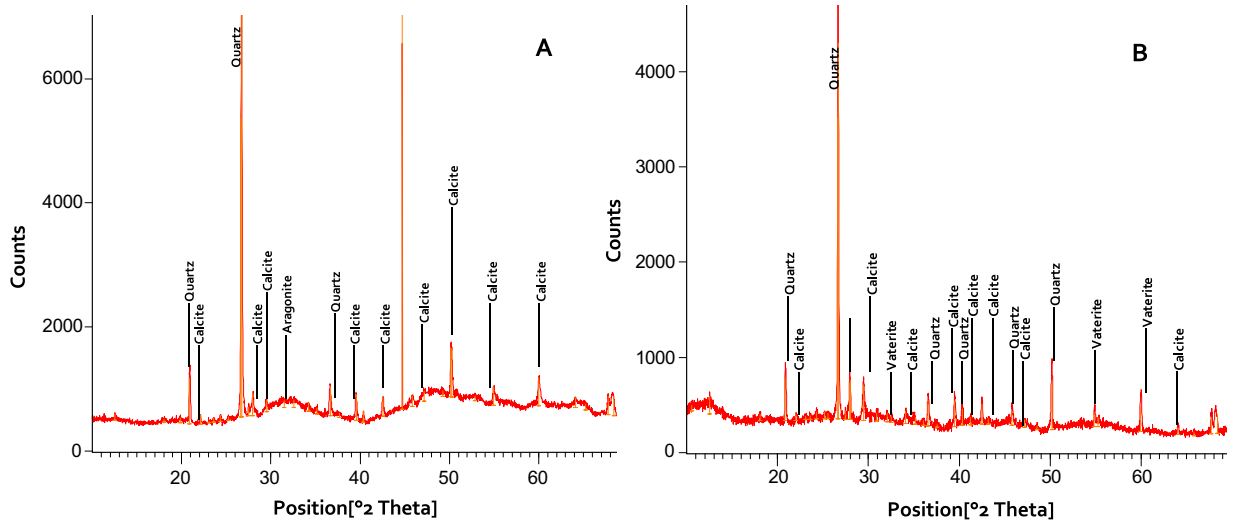

Fig. 12. XRD patterns of $CaCO_3$ crystals obtained: (A) BAT specimen (B) BST specimen.

extract into concrete on hydration can be overcome by the calcium carbonate precipitation done by bacteria. This precipitation starts as soon as the culture is mixed with cement, as is clear from the setting characteristics of the cement paste.

On comparing the effect of type of bacterial treatment on mechanical properties of concrete, it can be observed that spray treatment by bacteria after casting of concrete leads to only marginal increase in compressive strength, as against large increase registered in the alternate treatment in which bacteria was introduced at the time of casting. It can be due to the fact that spray treatment is a surface treatment and may not alter the bulk concrete properties to a large extent. It is confirmed by the SEM images of the mixes taken at three depths. While at the upper surface, SEM images of both the treatments are similar with dense biodeposition of calcium carbonate precipitation and associated bacterial cell (Fig. 8). Large numbers of bacterial cells were visible in the middle depth of 20–30 mm, while no calcium carbonate precipitation associated with bacteria cells was observed (Fig. 9). The absence of calcite precipitation in the inner depth of concrete can be due to blocking of upper pore matrix of concrete by calcium carbonate precipitation during initial days of spray curing. This might inhibited the ingress of curing medium during spray treatment, and hence this treatment could not improve the compressive strength of concrete substantially.

The bacterial admixed treatment is observed to be highly efficient in improving the compressive strength of concrete. However, even in this treatment in the inner depth of concrete matrix, bacterial cells are visible but no calcite precipitation is identified. As the precipitation of calcium carbonate occurs on the cell surface of bacteria, the cells might have died due to limited nutrient and oxygen availability. Furthermore, the viability of bacterial cells in the interior of concrete structure due to highly alkaline pH and

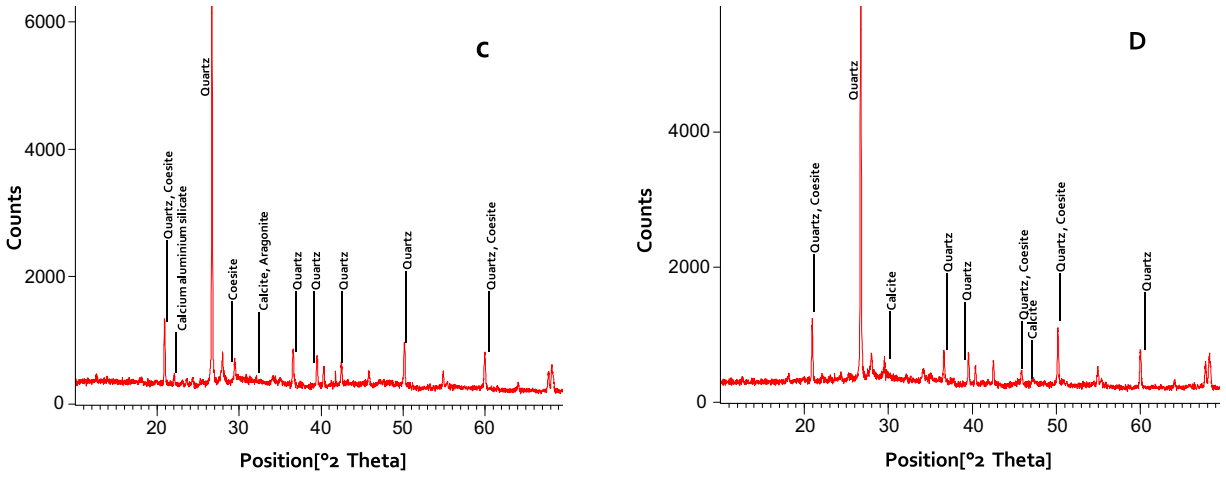

Fig. 13. XRD patterns of $CaCO_3$ crystals obtained: (C) Control specimen (D) MT specimen.

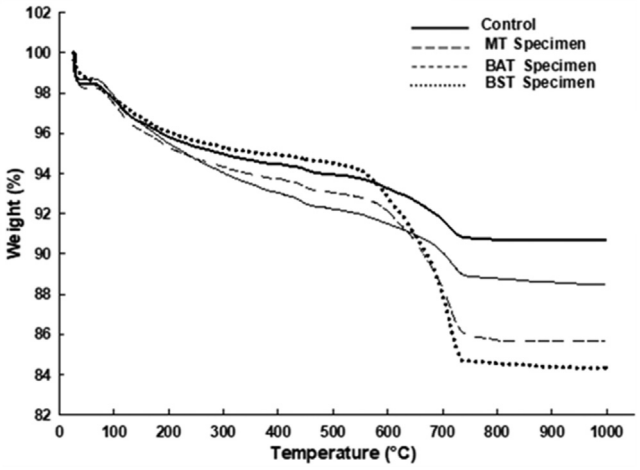

Fig. 14. Thermogravimetric analysis graph of different specimens.

very restricted oxygen availability is a matter of concern. Some researchers had reported that the live bacterial cells might form spores or die in these harsh conditions of concrete. Da silva et al. [35] reported the use of non-axenic ureolytic spores in the form of cyclic enriched ureolytic powder as a self-healing admixture. They observed no negative effect of this self-healing material on the mechanical strength of mortar specimen when added as 0.5–1% of the weight of cement. However, results of the present study indicate that the incorporation of live bacterial cells along with NBU-$CaCl_2$ medium enhance the mechanical strength of concrete.

Another parameter that is altered by the addition of bacterial cells and the associated nutrients into concrete is its chemical composition. Both the carbon and nitrogen contents of all three treated specimens were higher than the corresponding values of the control mix. It is obviously due to addition of organic matter and urea in the mixes as nutrient sources for bacteria. The highest amount of carbon content is observed in BAT specimens. It is believed that high carbon content adversely affect compressive strength of the mix [36]. However, the highest compressive strength of BAT specimens indicates that the correlation between carbon content and compressive strength might not be true for bacterially treated concrete. The observed improvement in compressive strength despite of higher carbon content is due to successful carbonate precipitation that helped in densifying the concrete matrix. The higher nitrogen content of BAT and MT specimens is due to incorporation of urea at the time of casting of concrete. The BST specimens do not have large nitrogen content in the inner depths. It is due to the fact that urea was introduced into concrete after casting of specimens. The bacterial cells along with nutrient were sprayed regularly on the surface of concrete during curing in BST specimens. Due to this, the carbonate precipitation occurred at the concrete surface, which blocked the pores of surface concrete, hence reducing the ingress of nutrients further inside the concrete matrix. The nutrient content has no significant effect on the compressive strength of the resultant mix.

One of the most influential parameter in concrete durability is pH value of cover concrete. The alkaline condition of concrete with pH 12–13 keeps the reinforced steel immune from corrosion [37]. The passive state of steel can be destabilized with the drop of pH of concrete which results into rebar corrosion and hence leads to premature deterioration of reinforced concrete [38]. Alkaline environment of concrete was not influenced with addition of bacterial cells supplemented with organic content and nitrogenous material. In BAT and BST specimens, no fluctuation in pH value occurred due to microbial precipitation of calcium carbonate and pH was maintained above 12. Even in MT specimen, no significant effect on pH value was observed.

4.2. Effects of curing treatments on permeation properties

Along with strength, it was important to analyze the effect of microbial treatment on permeation properties of concrete. The major focus of the study is to investigate the change in permeation characteristics of concrete undergoing two different curing processes; bacterial admixed treatment and bacteria spray treatment. Along with this, the effect of addition of only nutrient broth was also investigated. The permeation characteristics were studied with respect to three properties; sorptivity, RCPT and water impermeability.

Sorptivity studies the water ingress into an unsaturated concrete, which is dominated by capillary suction and is an important parameter that can be correlated to the ingress of deteriorating substances (chlorides or sulfates) into concrete [39]. It is a good measure of the quality of near surface concrete, which governs durability parameters related to rebar corrosion [40]. The water penetration depth defines the ease with which water can flow through concrete under a pressure differential. In this case also, the governing feature of ingress is capillary pores of concrete. Resistance of concrete to chloride ion penetration can be indirectly

measurement by RCPT. The three tests help in better understanding of permeation properties of resultant concrete. The results from sorptivity test indicated that the transport mechanism of water in specimens through capillary rise was altered effectively in both bacterial treatments. However, the results in sorptivity test showed that surface treatment of concrete significantly influence the permeation properties and restrict the ingress movement of aggressive agents (Table 3). The low '*k*' values of BST specimens indicated that the permeation properties can be significantly improved by spray treatment. In RCPT, similar trend of significant reduction to chloride ion penetration was observed. In both curing treatments, BAT and BST specimens showed low permeability type (Table 3). Resistance to chloride ions penetration indicates the effectiveness of both curing treatments in concrete specimens. The movement of aggressive chemical ions with pore water present in the well-connected pore matrix of concrete leads to corrosion of rebar. The transport mechanism of deleterious substances is influenced by the pore distribution, pore number and pore size in the concrete [3]. It was observed in water permeability test that, the penetration of water into the pore matrix of concrete was significantly prevented due to the precipitation of calcium carbonate by bacteria. Biodeposition of calcite crystals acts as pore blocker which results into reduced pore number and pore size; leading into reduced movement of water in treated concrete specimens. It was observed that the application of bacterial spray treatment can effectively restrict the damage from the penetration of aggressive agents and can be used as natural water repellant. At field-scale application, curing with bacterial spray treatment will also help in the implementation of MICP technology as a repair procedure on existing structures to improve the surface permeability properties of concrete.

4.3. Quantitative and qualitative analysis of $CaCO_3$ precipitation in concrete matrix

The results from SEM/EDX and XRD analysis indicated dense deposition of bacterial mediated precipitation of calcium carbonate in bacterially treated specimens. Presence of $CaCO_3$ crystals in association with bacterial cells had given an evidence of the enhanced mechanical properties and pore clogging of bacterially treated concrete specimens. In BAT specimen, apart from calcite and needle shaped aragonite crystals different morphology of calcium carbonate crystals with multinodular structure having micro needles was also observed (Fig. 8C). On EDX analysis, the peak of high calcium content and carbon was observed. This kind of morphology might be due to the presence of some magnesium impurities in the tap water used while curing. Similar calcium carbonate crystal formation was reported by Xie et al. [41] on addition of magnesium. Formation of micrite calcite with mirconeedles due the distortion of sideward growth of calcite under the influence of magnesium ions has also been reported by Folk [42]. In BST specimens, presence of mucous matrix on the closely attached carbonate crystals along with bacterial cells due to exopolymeric substances (EPS) was observed. Important role of EPS in cell adhesion and calcium carbonate precipitation was reported by Dhami et al. [43]. While in inner depths of treated specimens, presence of bacterial cells without calcium carbonate precipitation was noticed. Bacterial cells in inner depths remains incorporated in the concrete matrix without precipitation activity. The capability of bacterial cells to hydrolyse urea and nutrient media might be hindered by the harsh alkaline pH of concrete matrix and low oxygen availability. As the pores on upper surface were clogged by bacterial precipitated carbonate crystals which restricted the movement of media and oxygen. These factors might had effected the ureolytic activity of bacterial cells inside the concrete matrix. Apart from the majority of calcite crystals, XRD analysis of bacterially treated specimens showed different polymorphs of calcium carbonate like aragonite and vaterite. TGA results further strengthen the evidence of the precipitation of calcium carbonate crystals.

5. Conclusions

The current study investigated the efficiency of curing treatments in improvement of mechanical properties and permeation properties of concrete using ureolytic bacterial strain *Bacillus* sp. CT-5. Compressive strength was significantly improved and drastic reduction in permeability properties was observed in bacterially treated specimens. Both bacterial admixed treatment (that can be used for new structures) and bacterial spray treatment (that can be used as a repair procedure) were found to be effective in improving the properties of concrete. The admixed treatment improves both strength and permeation characteristics efficiently while the spray treatment drastically reduced the permeability properties of concrete due to effective sealant of biodeposition by bacteria. Retarding nature of organic matter of yeast extract severely affect the setting property of cement paste as well as significant reduction of strength in concrete specimens treated with medium only. Use of bacterial admixture, medium only and surface treatment with bacterial spray did not affect the alkaline nature of concrete. Surface treatment of concrete with bacterial spray showed the potential to improve the resistance against the aggressive agents. Bacterial spray treatment of concrete will help in future application of MICP technology at field-scale.

Acknowledgement

Authors are thankful to Science and Engineering Research Board, Department of Science & Technology, Government of India, India for sponsoring the research project SB/S3/CEE/0063/2013.

Conflicts of interest

None.

References

[1] A.E. Long, G.D. Henderso, F.R. Montgomery, Why access the properties of near-surface concrete?, Constr Build. Mater. 15 (2001) 65–79.
[2] A. Neville, Consideration of durability of concrete structures: past, present, and future, Mater. Struct. 34 (2001) 114–118.
[3] L. Basheer, J. Kropp, D.J. Cleland, Assessment of the durability of concrete from its permeation properties: a review, Constr. Build. Mater. 15 (2001) 93–103.
[4] X. Pan, Z. Shi, C. Shi, T.C. Ling, N. Li, A review on surface treatment for concrete – Part 2: performance, Constr. Build. Mater. 132 (2016) 578–590.
[5] G. Le Metayer-Levrel, S. Castanier, G. Orial, J.F. Loubière, J.P. Perthuisot, Applications of bacterial carbonatogenesis to the protection and regeneration of limestones in buildings and historic patrimony, Sediment. Geol. 126 (1999) 25–34.
[6] P. Tiano, L. Biagiotti, G. Mastromei, Bacterial bio-mediated calcite precipitation for monumental stones conservation: methods of evaluation, J. Microbiol. Methods 36 (1999) 139–145.
[7] F. Jroundia, M.T. Gonzalez-Muñoza, A. Garcia-Buenob, C. Rodriguez-Navarro, Consolidation of archaeological gypsum plaster by bacterial biomineralization of calcium carbonate, Acta. Biomaterialia. 10 (2014) 3844–3854.
[8] W. De Muynck, N. De Belie, W. Verstraete, Microbial carbonate precipitation in construction materials: a review, Ecol. Eng. 36 (2010) 118–136.
[9] S.S. Bang, J.K. Galinat, V. Ramakrishnan, Calcite precipitation induced by polyurethane-immobilized Bacillus pasteurii, Enz. Microbial. Technol. 28 (2001) 404–409.
[10] W. De Muynck, D. Debrouwer, N. De Belie, W. Verstraete, Bacterial carbonate precipitation improves the durability of cementitious materials, Cement. Concrete. Res. 38 (2008) 1005–1014.
[11] V. Achal, A. Mukerjee, M.S. Reddy, Biogenic treatment improves the durability and remediates the cracks of concrete structures, Constr. Build. Mater. 48 (2013) 1–5.
[12] N.K. Dhami, M.S. Reddy, A. Mukherjee, Bacillus megaterium mediated mineralization of calcium carbonate as biogenic surface treatment of green building materials, World J. Microbiol. Biotechnol. 29 (2013) 2397–2406.

[13] J. Wang, K. Van Tittelboom, N. De Belie, W. Verstraete, Use of silica gel or polyurethane immobilized bacteria for self-healing concrete, Constr. Build. Mater. 26 (2012) 532–540.
[14] J.Y. Wang, D. Snoeck, S. Van Vlierberghe, W. Verstraete, N. De Belie, Application of hydrogel encapsulated carbonate precipitating bacteria for approaching a realistic self-healing in concrete, Constr. Build. Mater. 68 (2014) 110–119.
[15] S. Stocks-Fischer, J.K. Galinat, S.S. Bang, Microbiological precipitation of $CaCO_3$, Soil. Biol. Biochem. 31 (1999) 1563–1571.
[16] S. Douglas, T.J. Beveridge, Mineral formation by bacteria in natural microbial communities, FEMS Microbiol. Ecol. 26 (1998) 79–88.
[17] K.E. Clare, P.T. Sherwood, The effect of organic matter on the setting of soil-cement mixtures, J. Appl. Chem. 4 (1954) 625–630.
[18] K.E. Clare, P.T. Sherwood, Further studies on the effect of organic matter on the setting of soil-cement mixtures, J. Appl. Chem. 6 (1956) 317–324.
[19] H. Tremblay, J. Duchesne, J. Locat, S. Leroueil, Influence of the nature of organic compounds on fine soil stabilization with cement, Can. Geotech. J. 39 (2002) 535–546.
[20] V. Achal, A. Mukerjee, M.S. Reddy, Microbial concrete: way to enhance the durability of building structures, J. Mater. Civil. Eng. 23 (2011) 730–734.
[21] BIS: 8112, Specification for 43 grade ordinary Portland cement by Bureau of Indian Standards, 2013.
[22] BIS: 383-1970, Specifications for coarse and fine aggregates from natural sources for concrete. Bureau of Indian standards, New Delhi, India.
[23] BIS: 516, Bureau of Indian Standards – Methods of tests for strength of concrete, New Delhi-2004, 1959 (Reaffirmed 2004).
[24] ASTM International, ASTM C1585, Standard test method for measurement of rate of absorption of water by hydraulic-cement concretes, 2004.
[25] B.B. Sabir, S. Wild, M. O'farrell, A water sorptivity test for martar and concrete, Mater. Struct. 31 (1998) 568–574.
[26] ASTM C1202-97, Standard test method for electrical indication of concrete's ability to resist chloride ion penetration Annual book of ASTM standards vol. 04.02, Philadelphia, 2001, pp. 646–651.
[27] German Standard, DIN 1048––Test Methods of Concrete Impermeability to Water: Part 2, Deutscher Institute Fur Normung, Germany, 1978.
[28] A. Walkley, I.A. Black, An examination of the Degtjareff method for determining soil organic matter and a proposed modification of the chromic acid titration method, Soil. Sci. 37 (1934) 29–38.
[29] BIS 5194, Bureau of Indian Standards – Method for determination of nitrogen-kjeldahl method, 1969 (Reaffirmed 2002).
[30] A.M. Neville, Properties of Concrete, Longman, London, 1995.
[31] H.F.W. Taylor, K. Mohan, G.K. Moir, Analytical study of pure and extended portland cement pastes: I, pure portland cement pastes, J. Am. Ceram. Soc. 68 (1985) 680–685.
[32] Y.C. Erşana, F.B. Da Silva, N. Boon, W. Verstraete, N. De Belie, Screening of bacteria and concrete compatible protection materials, Constr. Build. Mater. 88 (2015) 196–203.
[33] S.L. Williams, M.J. Kirisits, R.D. Ferron, Optimization of growth medium for *Sporosarcina pasteurii* in bio–based cement pastes to mitigate delay in hydration kinetics, J. Ind. Microbiol. Biotechnol. 43 (2016) 567–575.
[34] Z.B. Bundur, M.J. Kirisits, R.D. Ferron, Biomineralized cement-based materials: impact of inoculating vegetative bacterial cells on hydration and strength, Cem. Concrete. Res. 67 (2015) 237–245.
[35] F.B. da Silva, N. De Belie, N. Boon, W. Verstraete, Production of non-axenic ureolytic spores for self-healing concrete applications, Constr. Build. Mater. 93 (2015) 1034–1041.
[36] H.M. Jonkers, A. Thijssen, G. Muyzer, O. Copuroglu, E. Schlangen, Application of bacteria as self-healing agent for the development of sustainable concrete, Ecol. Eng. 36 (2010) 230–235.
[37] A. Behnood, K. Van Tittelboom, N. De Belie, Methods for measuring pH in concrete: a review, Constr. Build. Mater. 105 (2016) 176–188.
[38] B. Huet, V. L'Hostis, F. Miserque, H. Idrissi, Electrochemical behavior of mild steel in concrete: influence of pH and carbonate content of concrete pore solution, Electrochimica. Acta. 51 (2005) 172–180.
[39] W.J. McCarter, H. Ezirim, M. Emerson, Absorption of water and chloride into concrete, Mag. Concr. Res. 44 (1992) 31–37.
[40] W.P.S. Dias, Sorptivity testing for assessing concrete quality, in: Proc. Int. Conf. on Concrete under Severe Exposure Conditions (CONSEC '95), Spon, London, 1995, pp. 433-442
[41] A.J. Xie, Y.H. Shen, C.Y. Zhang, Z.W. Yuan, X.M. Zhu, Y.M. Yang, Crystal growth of calcium carbonate with various morphologies in different amino acid systems, J. Cryst. Growth. 285 (2005) 436–443.
[42] R.L. Folk, The natural history of crystalline calcium carbonate: effect of magnesium content and salinity, J. Sediment. Petrol. 44 (1974) 40–53.
[43] A. Bains, N.K. Dhami, A. Mukherjee, M.S. Reddy, Influence of exopolymeric materials on bacterially induced mineralization of carbonates, Appl. Biochem. Biotechnol. 175 (2015) 3531–3541.

Journal of Industrial Microbiology & Biotechnology (2018) 45:657–667
https://doi.org/10.1007/s10295-018-2050-4

SIMB
Society for Industrial Microbiology and Biotechnology

ENVIRONMENTAL MICROBIOLOGY - ORIGINAL PAPER

Corn steep liquor as a nutritional source for biocementation and its impact on concrete structural properties

Sumit Joshi[1] · **Shweta Goyal**[2] · **M. Sudhakara Reddy**[1]

Received: 17 January 2018 / Accepted: 21 May 2018 / Published online: 28 May 2018

Abstract

Microbial-induced carbonate precipitation (MICP) has a potential to improve the durability properties and remediate cracks in concrete. In the present study, the main emphasis is placed upon replacing the expensive laboratory nutrient broth (NB) with corn steep liquor (CSL), an industrial by-product, as an alternate nutrient medium during biocementation. The influence of organic nutrients (carbon and nitrogen content) of CSL and NB on the chemical and structural properties of concrete structures is studied. It has been observed that cement-setting properties were unaffected by CSL organic content, while NB medium influenced it. Carbon and nitrogen content in concrete structures was significantly lower in CSL-treated specimens than in NB-treated specimens. Decreased permeability and increased compressive strength were reported when NB is replaced with CSL in bacteria-treated specimens. The present study results suggest that CSL can be used as a replacement growth medium for MICP technology at commercial scale.

Keywords Biomineralization · Curing · Organic admixture · Concrete · Corn steep liquor · Carbon and nitrogen content

Introduction

Concrete is one of the most widely used structural building materials in the world. The incomparable and excellent properties of concrete, such as strength and durability, have made it an attractive construction material. An escalating demand for urban infrastructure has become a great challenge with the increasing world population. Annually, 10 billion tons of concrete production was estimated to meet the increasing demands of all urban infrastructures like residential buildings, transport connectivity and industrial units [7]. With growing dependence, sustainable design of concrete structures is also a prime concern in the world. Studies conducted by the Organization for Economic Cooperation and Development (OECD) have reported that approximately 30% of greenhouse gases are emitted from the residential and commercial building sectors [45]. Energy requirements, water resources, natural resources consumption and demolition waste have left an enormous environmental footprint on earth [36].

Factors like climate change, temperature variations and external chemical attacks affect the lifecycle performance of concrete leading to its durability problems [28]. Ingress of aggressive agents like CO_2, SO_4^{2-} and Cl^- ions into the matrix of concrete leads to premature deterioration causing irreversible changes in its serviceability. Permeation due to the interconnected pore system in the near surface concrete matrix directly influences the rate of deterioration [10]. Early deterioration of infrastructures around the globe is a matter of concern. Intensive research has been done to protect the concrete structures suffering from the penetration of aggressive agents. Use of different organic and inorganic surface pore-blocking agents has been reported by researchers to protect the concrete structures from the ingress of aggressive substances. Varity of concrete surface treatments with silanes, siloxanes sodium silicate, polyurethane, ethyl silicate and nano-SiO_2 has been investigated [28, 38]. Drawbacks like detachment with aging in outdoor exposure are also associated with

Electronic supplementary material The online version of this article (https://doi.org/10.1007/s10295-018-2050-4) contains supplementary material, which is available to authorized users.

✉ M. Sudhakara Reddy
msreddy@thapar.edu

[1] Department of Biotechnology, Thapar Institute of Engineering & Technology, Patiala, Punjab 147004, India

[2] Department of Civil Engineering, Thapar Institute of Engineering & Technology, Patiala, Punjab 147004, India

the surface coaters, which did not promise the long-term performance.

Recently, application of biotechnology in concrete research led to a bio-inspired treatment method to enhance the durability properties of concrete. Microbial-induced calcium carbonate precipitation (MICP) by using calcifying bacteria in construction material via biomineralization process has become substantially popular. MICP technology has become an innovative and promising technique for improving the durability properties of concrete structures [5, 21, 23, 30, 32, 37]. Improved mechanical strength and effective reduction in porosity of concrete with MICP are positive attributes. The challenges associated with the use of MICP for improving concrete durability include the potential negative impacts of the organic substrates in the growth medium on the concrete setting process and the cost associated with supplying the bacterial growth medium. Disadvantages in the use of organic matter (i.e., yeast extract) on the retardation of setting process of cement paste have been reported by many researchers [20, 42, 44]. The operating cost of this technology at the commercial scale might have economic limitations [22, 30]. The use of laboratory grade nutrient broth, i.e., yeast extract cost is as high as 60% of the total operating cost [33]. Implementation of MICP technique in newly constructed concrete structures at field scale would not be possible because of its expensive cost. Hence, it is essential to use an inexpensive, high-protein-containing alternative nutrient source to reduce the overall production cost of this technology. Previously, we reported the use of lactose mother liquor, collected from the dairy industry, as a nutrient source for biomineralization [1]. Later, we used corn steep liquor (CSL), a by-product from the starch industry, as a low-cost nutrient medium for the MICP technology [3]. We have extended these studies further to study the durability properties of building materials, such as compressive strength, permeability and prevention of corrosion and compared the results with the commercially available nutrient medium [2, 4]. Eryuruk et al. [27] demonstrated that the hydraulic conductivity of a paddy field decreased through a biocalcification process using CSL as a source of nutrients. Recently, Amiri and Bundur [6] used CSL as an alternative carbon source for biomineralization in cement-based materials and studied its impact on initial setting of cement paste and mortar mixes and compressive strength. Though CSL served as an alternative to nutrient medium or yeast extract medium in biomineralization and improved the permeability, compressive strength and initial setting of cement-based materials, no reports are available about the nutrient components, such as carbon and nitrogen content, bacterial cells and change in pH on the chemical and structural properties of concrete.

The present study was aimed to test the efficacy of nutrient components present in the CSL on the structural properties of concrete. To evaluate the presence of organic matter in concrete specimens, carbon and nitrogen content was determined at different depths of the concrete specimens. The change in pH at different depths of the concrete specimens was also monitored. A comparative study was conducted to figure out the influence of nutrient broth and CSL on setting property of cement and compressive strength of concrete. Further, the CSL-treated concrete specimens were analyzed for sorptivity test, water permeability test, rapid chloride permeability test (RCPT), scanning electron microscopy/energy-dispersive X-ray spectroscopy (SEM–EDX), and X-ray diffraction (XRD).

Materials and methods

Microbial strains and culture conditions

The bacterial strain, *Bacillus* sp. CT5, isolated by us from the cement sample [1] was used in this study. Corn steep liquor was collected from Sukhjit Starch & Chemicals Limited, Phagwara, Punjab, India. The chemical composition of the CSL is as follows: pH 4.0; total carbohydrates 5.8%; proteins 24%; fats 1.0%; minerals 8. 2%. For the growth and experimental purposes, 1.5% CSL was used throughout the study. Nutrient broth (NB) (Peptone 10 g/L, yeast extract 10 g/L, sodium chloride 5 g/L) procured from Himedia (Himedia, India) was also used to grow the bacteria. To carry out microbial calcium carbonate precipitation in concrete specimens, the culture was grown in autoclaved CSL medium (1.5% v/v) and nutrient broth supplemented with filter-sterilized 2% urea (w/v) and 25 mM $CaCl_2$ solution at 37 °C under shaking condition (120 rpm). The pH of the CSL and NB media was adjusted to 7.5 with 1 N NaOH prior to autoclave without urea and $CaCl_2$.

Materials

Ordinary Portland cement (43 Grade) conforming to IS 8112-2013 standards [14] was used in the present study. Locally available, clean, dry and well-graded natural river sand conforming to Zone II was used as fine aggregate. The specific gravity of fine aggregates was 2.70. The coarse aggregate used was crushed gravel with nominal particle size of 20 and 10 mm. The specific gravity for 20 mm aggregates and 10 mm aggregates was 2.63 and 2.65, respectively. Both fine aggregate and coarse aggregate conform to IS: 383-1970 standards [15].

Preparation of cement paste

This experimental program was conducted to study the influence of addition of the bacterial culture and plain nutrient ingredients on the initial and final setting properties of cement. The change in initial setting characteristic of cement paste upon incorporation of bacterial cells and the associated nutrients at the casting stage was investigated by using Vicat Apparatus as per IS 4031: 1988 (Part 5) [17]. Briefly, for conducting setting time test, water required to produce standard cement paste, i.e., standard consistency was first determined by IS 4031: 1988 (Part 4) [16]. Then the paste for measuring setting time was prepared by using 0.85 times the water required to give a paste of standard consistency. In the present study, the standard consistency was determined to be 29.5%. Accordingly, 25.1% water was added for measuring setting time of cement.

Five types of cement pastes were prepared. The composition and nomenclature of the pastes is presented in Table 1. Control paste was made by mixing cement and water. Corn steep liquor paste was prepared by adding 1.5% of corn steep liquor, 2% urea and 25 mM $CaCl_2$ to cement, while NB paste was made by adding 1.3% of nutrient broth, 2% urea and 25 mM $CaCl_2$ to cement. CSL-CT5 paste and NB-CT5 paste were prepared by mixing cement with bacterial cells grown in CSL medium and NB medium supplemented with 2% urea and 25 mM $CaCl_2$, respectively. The consistency of all the mixes was kept the same.

Preparation of concrete specimens

Concrete mix was prepared by using cement: sand: coarse aggregate in the ratio 1: 1.82: 3.24 (by weight) and water to cement ratio (w/c) of 0.5. For casting of bacterial-treated specimens, CSL medium and NB medium with bacterial culture (4×10^8 cells/ml) supplemented with 2% urea (w/v) and 25 mM calcium chloride solution (w/v) were used instead of water. The bacterial culture was prepared by growing the cells in CSL and NB medium till it attained the $O.D_{600}$, of 0.5 (exponential phase). Then this culture was admixed with the concrete. The bacterial culture to cement ratio was also maintained at 0.5. For the bacterial spray treatment, the culture was grown in CSL as well as in NB medium till it reached the $O.D_{600}$, of 0.5 (4×10^8 cells/ml). Cement, sand and aggregates were thoroughly mixed for 2 min in the concrete mixture before adding water, CSL medium and NB medium. The ingredients were mixed properly and the fresh mix in the plastic stage was immediately transferred to iron moulds (150 mm × 150 mm × 150 mm). After casting, all the specimens were allowed to remain in the iron moulds and kept in a casting room at room temperature of 27 ± 2 °C for 24 h. Thereafter, the specimens were demoulded and cured till the testing age. Four different curing regimes as specified in Table 2 were adopted in this study.

Table 1 Mixing ingredients of cement paste mixes

Cement mixes	Cement (g)	Water (g)	NB media (g)	CSL media (g)	Bacterial culture (g)
Control	400	100.3	–	–	–
CSL	400	–	–	100.3	–
NB	400	–	100.3	–	–
CSL-CT5	400	–	–	–	100.3
NB-CT5	400	–	–	–	100.3

CSL corn steep liquor medium, *NB* nutrient broth medium, *CSL-CT5* bacterial paste in CSL, *NB-CT5* bacterial paste in NB

Compressive strength, carbon and nitrogen and pH profile

To study the compressive strength, concrete cubes of 150 mm dimension were casted. The specimens were cured in bacterial culture grown in CSL and NB medium along with their respective controls. After 28 days of curing, the compressive strength was measured as per IS 516: 1959 standards [13] using an automatic compression testing machine, COMPTEST 3000.

Concrete cubes after respective curing were drilled using a rotary hammer drilling machine to collect the concrete powder for analyses. Concrete cubes were drilled up to the depth of 50 mm from two opposite sides as reported earlier by us [31]. Concrete powder was separately collected from each depth. Different points were drilled from each side of the cube to get a homogenous sample of concrete powder. The powder samples obtained were analyzed to calculate carbon and nitrogen content at various depths. To calculate the amount of organic carbon in concrete powder, Walkley–Black procedure was followed [43]. Kjeldahl method was used to determine the ammonia producing nitrogen in the concrete powder as per IS: 5194-1969 standards [18]. For the quantitative determination of carbohydrate content in NB and CSL media, anthrone method was used [34]. Briefly, 4 ml of anthrone reagent (200 mg anthrone in 100 ml of 95% H_2SO_4) was added in 1 ml of NB/CSL media and the test tube was heated in boiling water bath for 10 min. After cooling, absorbance was measured at 620 nm by the UV–Vis spectrophotometer. Concentration of the sugar in the sample was calculated from the glucose calibration curve. The pH variations at various depths were investigated potentiometrically in concrete specimens treated microbially with CSL media. The pH glass electrode was immersed in the suspension of a 1:5 concrete powder: water after stirring for 1 h.

Table 2 Outline of different sets of concrete specimens and method of curing treatments

Specimens	Material used	Method of curing
Control	Cement: sand: coarse aggregate water/cement = 0.5	Water curing for 28 days
CSL treated (CT)	Cement: sand: coarse aggregate CSL media/cement = 0.5	Submersion in CSL media with urea and $CaCl_2$ without bacteria for 28 days
NB treated (NT)	Cement: sand: coarse aggregate NB media/cement = 0.5	Submersion in NB media with urea and $CaCl_2$ without bacteria for 28 days
CSL-bacterial admixed treatment (CBAT)	Cement: sand: coarse aggregate bacterial culture/cement = 0.5	Submersion in CSL media, urea, $CaCl_2$ and bacterial culture for 28 days
NB-bacterial admixed treatment (NBAT)	Cement: sand: coarse aggregate bacterial culture/cement = 0.5	Submersion in NB media, urea, $CaCl_2$ and bacterial culture for 28 days
CSL-bacterial spray treatment (CBST)	Cement: sand: coarse aggregate bacterial culture/cement = 0.5	Bacterial spray on specimens twice a day till 28 days
NB-bacterial spray treatment (NBST)	Cement: sand: coarse aggregate bacterial culture/cement = 0.5	Bacterial spray on specimens twice a day till 28 days

CSL media, NB media, urea and calcium chloride had the following concentrations: CSL (1.5% v/v), NB media (1.3% w/v), 2% urea (w/v) and 25 mM calcium chloride (w/v). All specimens were prepared in triplicate

Permeation properties

The efficiency in resistance towards water penetration was investigated for the different mixes as described in Table 2 at the age of 28 days. Sorptivity was determined according to ASTM C1585 [9]. The cylindrical test specimen of diameter 100 mm and thickness 50 mm was prepared to conduct the sorptivity test. Before conducting the test, a side surface of the specimen was sealed by sealing material (i.e., epoxy) and the initial mass was noted. One surface of the specimen was exposed to water and the mass increase of the specimen by absorption was monitored by weighing it at different time intervals. The mass change was recorded at the intervals of 60 s, 5, 10, 20, 30, 60 min and every hour up to 6 h. From the value of mass change, the volume of water absorbed per unit of cross-sectional area was evaluated at each time interval. A plot between the square root of time and volume of water absorbed was plotted. The slope of the graph is taken as the value of sorptivity for that specimen.

To determine the penetration of chloride ions in concrete through electrical conductance, a rapid chloride penetration test (RCPT) was conducted as per ASTM C1202-97 [8]. Cylindrical specimens were subjected to a potential difference of 60 V for 6 h by placing them inside the test cell. The solution of sodium chloride 3% (by mass) was kept in one side of the test cell connected to the negative terminal of power supply, and the sodium hydroxide solution (0.3 N) was kept in the other side of the test cell connected to the positive terminal of power supply. Total charge passed (in terms of coulombs) is a measure of the electrical conductance of the concrete and directly proportional to the chloride penetrability.

The water permeability test was carried out as per DIN 1048 standards [25] at the age of 28 days. The concrete specimens were exposed to a water pressure of 0.5 N/mm^2 for 72 h and the vertical penetration depth of water into concrete was then measured after breaking the concrete specimen.

Micro-structural analysis

For analyzing the calcium carbonate crystals in concrete specimens at the age of 28 days, scanning electron microscopy (SEM) (ZEISS EVO 50) was done. The elemental composition of micro-structural crystals was identified with energy-dispersive X-ray spectroscopy (EDX). For conducting SEM and EDX analyses, small pieces of concrete samples were collected. Samples were finely polished and gold-coated with a sputter coating. To disperse excess charge from the sample, a thin coating of carbon was applied on the polished surface. X-ray diffraction (XRD) was done on the powdered samples, obtained while drilling and sieved through 90 µm sieve. XRD spectrum was obtained using Bruker D8 X-ray diffractometer with a Cu anode (40 kV and 30 mA) and scanning from 10° to 80° 2θ.

Statistical analysis

All the experiments were performed in triplicates. One-way analysis of variance was performed and the means were compared with Tukey's test at $P < 0.05$. Results of compressive strength were analysed by using unpaired t test. All the analyses were performed by using Graph Pad Prism 5.1 software.

Results and discussion

Initial setting time cement mixes

The initial and final setting time of control paste mix was 120 and 240 min, respectively. On comparison with control paste mix, no delay in initial and final setting was observed in CSL paste mix. However, a significant delay in both initial and final setting time was observed in NB paste mix. Initial setting time increased by 100 min and the final setting time by 250 min in NB paste mix when compared to control paste mix (Fig. 1). In CSL-CT5 paste mix, an increase of 20 min in initial setting and 30 min in final setting time was recorded as compared to control paste. The initial setting time was increased by 40 min and final setting time by 50 min when compared to control paste in the case of NB-CT5 paste mix (Fig. 1). All these observations indicate that the addition of plain CSL medium had no influence on the setting characteristics of cement. Whereas the addition of plain NB medium severely influenced the setting characteristics of cement. Incorporation of bacterial cells with CSL medium showed inconsequential effect on the setting characteristics. However, addition of bacterial cells grown in NB media causes not as much of delay in setting of cement as it was observed in NB paste.

The presence of organic admixtures has been reported to have an adverse effect on the chemical properties of cement resulting in retardation of initial hydration of cement [46]. In NB cement paste, nutrient media contains yeast extract, and it has been reported that yeast extract acts as a retardation substance and influences the degree of hydration of cement [44]. The presence of different fractions of carbohydrates in the yeast extract acts as an effective chemical retardant [20, 41]. It was reported that carbohydrate strongly affects the silicate component and retards the hardening of Portland cement [19]. Amiri and Bundur [6] also reported the delay in initial setting in urea yeast extract medium as compared to CSL and control samples. Higher carbohydrate content in NB medium (fourfold) as compared to CSL medium might have affected the retarding characteristics in cement hardening.

Compressive strength

Addition of *Bacillus* sp. (CT-5) along with CSL/NB media and urea-$CaCl_2$ in concrete specimen and curing with respective medium for 28 days significantly increased the compressive strength as compared to control specimen (Fig. 2). The CBAT specimens showed an increase of 25% in compressive strength as compared to the control specimens. The CBST specimens in which bacteria were introduced into concrete after casting in the form of spray during curing also increased 16% in compressive strength as compared to the control specimens. The concrete specimens with bacterial admixture in NB medium supplemented with urea-$CaCl_2$ during casting and spraying with respective medium showed an increase of 29 and 8% in compressive strength, respectively. However, the compressive strength of specimens treated with NB only registered a drastic decrease by 19% as compared to the control mix.

Specimens casted with nutrient medium alone showed drastic reduction in the compressive strength. The results of setting time and compressive strength together indicate that the addition of organic matter (i.e., yeast extract) alone has a retardation effect on hydration. Ersan et al. [26] also reported a decrease in the compressive strength of a mortar specimen due to the presence of yeast extract. Contrary to this, Amiri and Bundur [6] reported that the compressive strength of mortar increased when the specimens

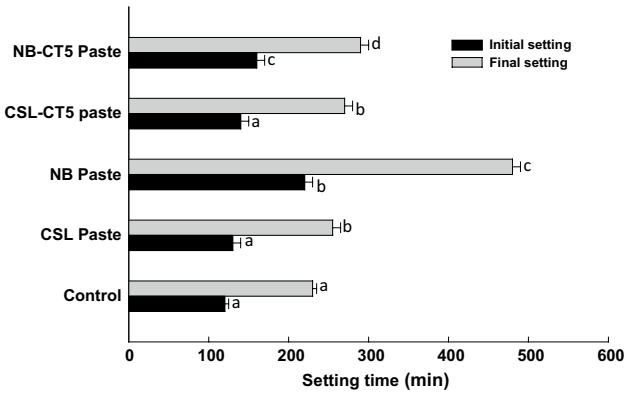

Fig. 1 Initial and final setting times of different cement paste mixes. Bars sharing a common letter within the treatment are not significant at $P < 0.05$. Error bars represent standard deviation ($n = 3$)

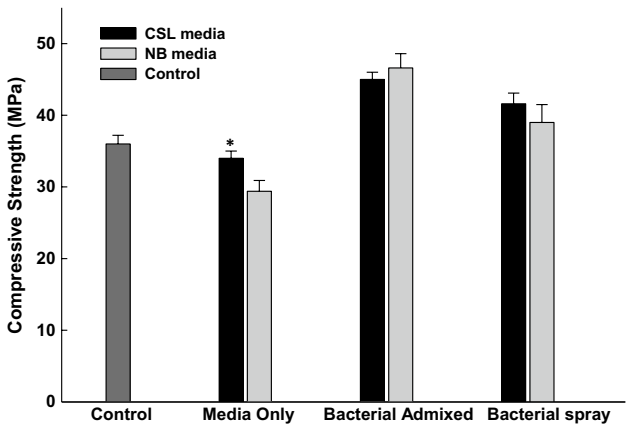

Fig. 2 Influence of CSL media, NB media and bacterial culture on compressive strength (MPa) of concrete specimens at the age of 28 days curing. Error bars represent standard deviation ($n = 3$). *$P < 0.05$

were treated with yeast extract and CSL as compared to control specimens as well as the specimens treated with bacteria grown in yeast extract and in CSL. Addition of CSL media had not altered the chemical and mechanical properties of concrete in this study. Our previous results also showed an increase in compressive strength in specimens treated with bacteria grown in CSL as compared to control specimens [2–4]. As the CSL is a nutritional supplement, it comprised rich, free amino acids and vitamins, which act as excellent growth stimulants for bacterial cells [40]. In bacterial admixed and bacterial spray treatment of concrete specimen with NB/CSL media had shown effective compressive strength gain in both the curing regimes. However, use of CSL as growth medium had not shown any modifications in the concrete chemical properties. On comparison with NB media, CSL may serve as a carbon and nitrogen supplement and replace yeast extract nutrient medium.

Carbon, nitrogen and pH profile

Carbon and nitrogen content in concrete specimens with depth-wise profile was determined. It was observed that the percentage of carbon and nitrogen content remains same at all depths for the control specimen. CBAT and NBAT specimens registered maximum carbon and nitrogen content at all depths. The carbon and nitrogen content in CBST and NBST specimens was maximum in the upper depths (0–20 mm) followed by almost same at all depths (Fig. 3). However, overall carbon and nitrogen content in NBAT and NBST specimens was observed to be much higher than CBAT and CBST specimens at all depths. Similar trend of overall carbon and nitrogen content was observed to be higher in NT specimen on comparison with CT specimen at all depths (Fig. 3). The carbon content in NB medium (800 mg/L) was estimated to be fourfold higher than that in the CSL medium (200 mg/L). The pH value in all specimens was found to be

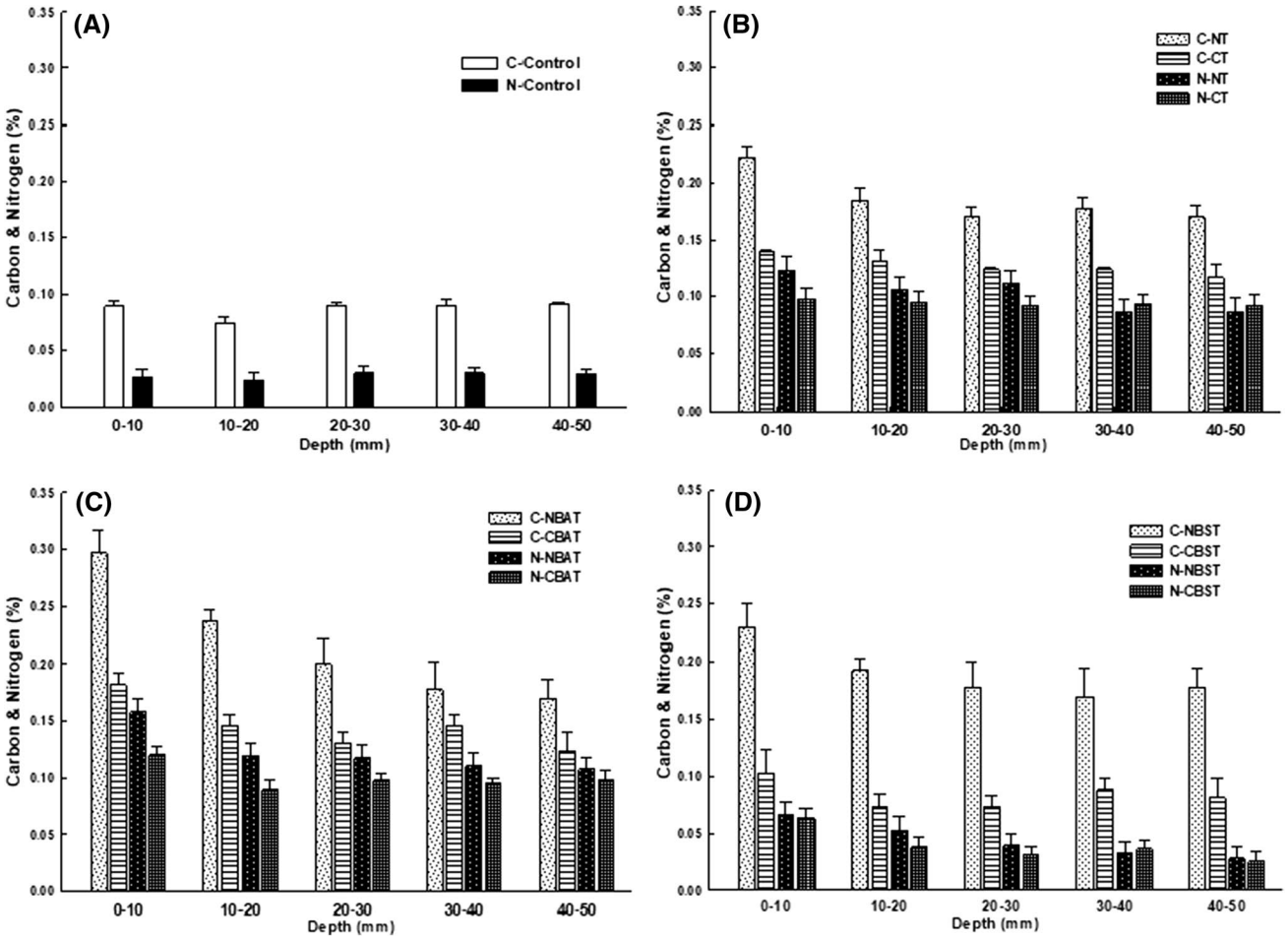

Fig. 3 Carbon and nitrogen content (% by mass) of concrete specimens at different depths in various treatments. *C* carbon content; *N* nitrogen content. **a** Control specimen; **b** NT and CT specimen; **c** NBAT and CBAT specimen; **d** NBST and CBST specimen. Error bars represents standard deviation ($n = 3$)

in the range of 12.1–12.5 indicating no significant change due to different treatments (Fig. 4).

Carbon and nitrogen content in concrete matrix was much higher in NB-treated specimens than that in CSL-treated specimens. Addition of nutrient broth and CSL to the concrete increased the carbon and nitrogen content. This might be due to the additional accumulation of curing material and bacterial cells on the outer surface. Joshi et al. [31] also reported the increase in carbon and nitrogen content in bacteria-treated specimens as compared to control specimens. pH is one of the most influential parameters in concrete durability and the alkaline condition of concrete with pH 12–13 keeps the reinforced steel resistant to corrosion [12]. The drop of pH of concrete destabilizes the passive state of steel which results into rebar corrosion and hence leads to premature deterioration of reinforced concrete [29].

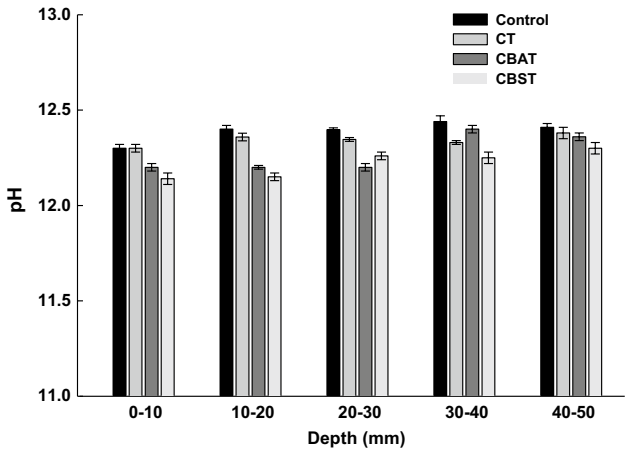

Fig. 4 pH profiles of concrete specimens at different depths in various treatments. Control; CT: CSL treated; CBAT: CSL-bacterial admixed treatment; CBST: CSL-bacterial spray treatment. Error bars represent standard deviation ($n=3$)

Alkaline environment of concrete was not influenced with addition of bacterial cells supplemented with either nutrient broth or CSL in this study. No significant variation in pH was observed in medium-treated specimens as compared to control specimens in this study and the pH was maintained above 12. Similar results were reported when the specimens were treated with bacteria grown in NB medium by Joshi et al. [31].

Permeation properties

Sorptivity coefficient, RCPT and water impermeability of various mixes were measured after 28 days of curing. Among all the tested mixes, control mix has highest sorptivity coefficient. The specimens treated with bacterial cultures grown in CSL and either admixed (CBAT) or sprayed (CBST) registered significantly lowest sorptivity coefficient followed by the specimens treated with bacteria grown in NB (NBAT and NBST) as compared to control or media alone cured specimens (Table 3). In RCPT, resistance to chloride ion penetration by all specimens was evaluated. The charge transfer was significantly reduced in all specimens treated with bacteria and the penetration values fall in low penetration range. In CBAT specimen the total charge passed was 1228 coulombs and in CBST specimen it was 1310 coulombs. While in control and CT specimens, similar charge transfer resistance was registered and both fall in the category of moderate penetration type (Table 3). In water impermeability test, maximum vertical penetration of water was found in control specimen (30.2 mm). The water penetration depth was significantly reduced in all specimens treated with bacteria. In CBAT specimen, minimum penetration depth of 12.5 mm, while in CBST specimen 13.9 mm was recorded. CT specimen prepared by using CSL media had the water penetration depth of 28.2 mm, while for NB medium specimens it was 31.2 mm (Table 3).

Table 3 Permeation properties (sorptivity, RCPT and water impermeability test) of concrete specimens treated with media and bacteria cured for 28 days

Specimen	Sorptivity coefficient[a]	RCPT		Water penetration (mm)[a]
		Mean charge passed (coulombs)[a]	Penetration type[b]	
Control	0.020 ± 0.0^{a}	3180 ± 127^{a}	Moderate	30.2 ± 2.1^{b}
CSL treated (CT)	0.014 ± 0.0^{b}	2838 ± 141^{b}	Moderate	28.2 ± 3.2^{b}
NB treated (NT)	0.014 ± 0.0^{b}	2942 ± 148^{b}	Moderate	31.2 ± 17^{a}
CSL-bacterial admixed treatment (CBAT)	0.005 ± 0.0^{d}	1228 ± 79^{c}	Low	12.5 ± 1.5^{c}
NB-bacterial admixed treatment (NBAT)	0.008 ± 0.0^{c}	1204 ± 95^{c}	Low	14.2 ± 2.1^{c}
CSL-bacterial spray treatment (CBST)	0.005 ± 0.0^{d}	1310 ± 58^{c}	Low	13.9 ± 1.3^{c}
NB-bacterial spray treatment (NBST)	0.007 ± 0.0^{c}	1340 ± 62^{c}	Low	13.6 ± 1.4^{c}

[a]Mean values sharing a common letter within the column are not significant at $P < 0.05$

[b]The range of charge for high (> 4000), moderate (2000–4000), low (1000–2000) and very low (100–1000) as per the ASTM C1202-10 standard

Sorptivity test shows the water ingress into an unsaturated concrete, which is dominated by capillary suction and is an important parameter that can be correlated to the ingress of deteriorating substances (chlorides or sulfates) into concrete [35]. Sorptivity is a good measure of the quality of near surface concrete, which governs durability parameters related to rebar corrosion [24]. The results obtained in sorptivity test indicated that in CBAT and CBST specimens, the transport mechanism of water through capillary rise was altered effectively. On comparison, sorptivity coefficient '*k*' of initial absorption was almost equal in bacterial admixed and bacterial spray-treated specimens. The low '*k*' value of surface-treated specimen indicates that the permeation properties can be significantly improved by bacterial spray. Significant reduction to chloride ion penetration was observed in both curing treatments by RCPT analysis. The movement of aggressive agents like chloride ions in the concrete matrix through capillary pore structures initiates and propagates the corrosion process of steel rebar [11]. Chloride-contaminated water movement in surface layer of concrete depends upon pore diameter, distribution and pore continuity [35]. In aforementioned results of bacterial treated concretes, clearly depict the effective sealant of pore matrix with biogenic calcium carbonate precipitation. In surface treatment, bacterial spray significantly restricts the ingress of water and aggressive agents and blocks the pore with calcium carbonate precipitation.

Micro-structural analysis

SEM and XRD analysis of all concrete specimens was done to characterize the calcium carbonate crystals. SEM–EDX analysis of bacterial treated specimens showed the presence of dense deposition of bacterial mediated precipitation of calcium carbonate (Fig. 5). In case of CBAT specimen, presence of different crystal lattice of calcium carbonate was found. Rhombohedral calcite crystal and spheroid vaterite crystals were observed. The EDX analysis also confirmed the elemental composition of crystals with peaks showing high amount of calcium and carbon (Fig. 5a, b). In CBST specimen, presence of dense biodeposition of closely attached rhombohedral calcite crystals was observed. The high peak of calcium and carbon on EDX analysis further confirmed the presence of calcium carbonate crystals (Fig. 5c, d). However, in case of control and CT specimen, no calcium carbonate crystals were observed in SEM–EDX analysis (Fig. 6). XRD analysis of CBAT and CBST specimen showed that majority of the calcium carbonate deposits were calcite and vaterite (Fig. 7a, b). In case of CT and control specimen, XRD spectrum revealed that the major phases present are quartz, calcium aluminium silicate, coesite and vaterite (Fig. 7c, d).

SEM–EDX analysis of bacterially treated specimens showed the presence of dense deposition of bacterial-mediated precipitation of calcium carbonate. Rhombohedral calcite crystal and spheroid vaterite crystals were observed

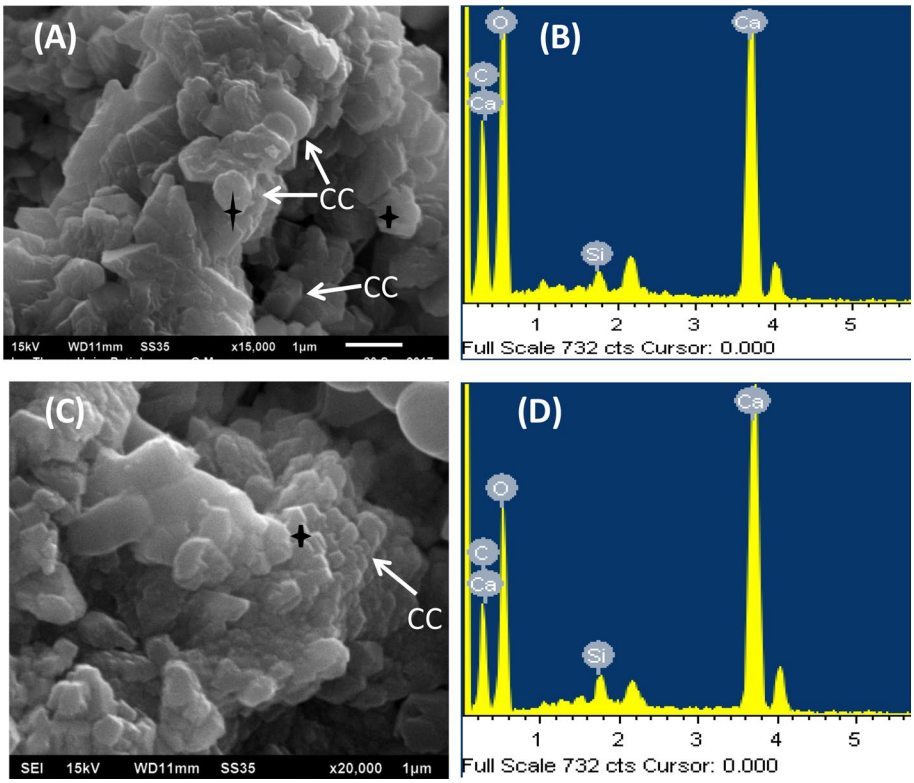

Fig. 5 SEM-EDX images represent the $CaCO_3$ crystals (CC) at upper depth in CBAT (CSL-bacterial admixed treatment) specimen (**a**, **b**) and CBST (CSL-bacterial spray treatment) specimen (**c**, **d**). Star shows the spots of EDX analysis

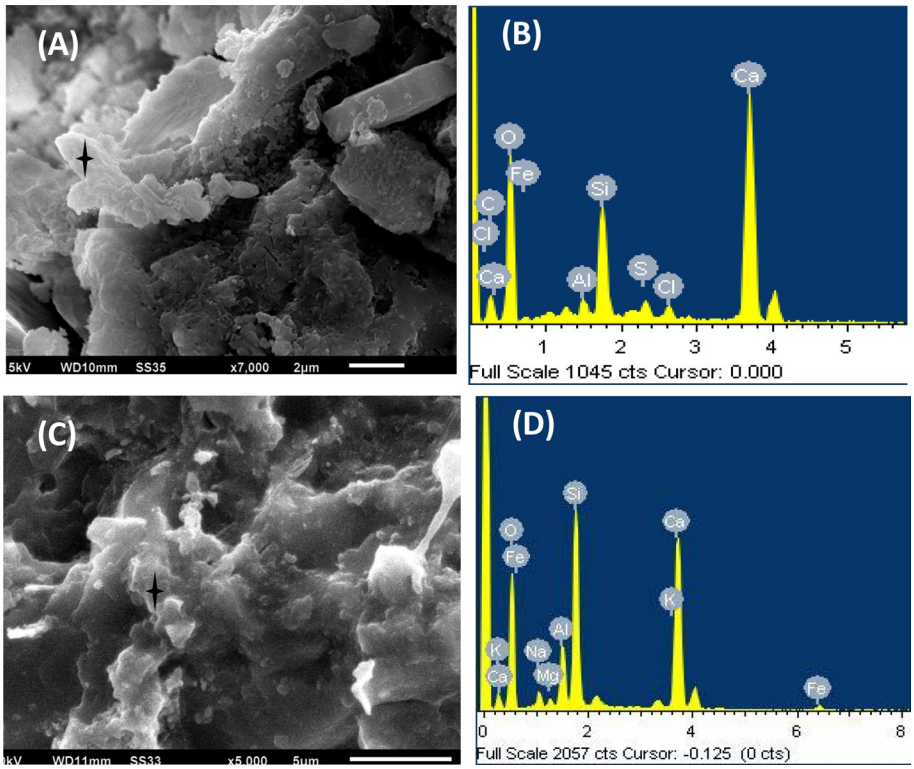

Fig. 6 SEM-EDX images of CSL-treated specimen (**a**, **b**) and control specimen (**c**, **d**) at upper depth. Star shows the spots of EDX analysis

in case of CBAT specimen. In CBST specimen, presence of dense biodeposition of closely attached rhombohedral calcite crystals was observed. Formation of different kinds of morphology of calcium carbonate crystals depends on composition and mineralogy of the substrate. Calcitic substrate promotes the growth of bacterial calcite, while silicate substrate promotes the formation of spherulitic vaterite [39]. XRD analysis of bacterially treated specimens also confirmed the presence of different polymorphs of calcium carbonate like calcite and vaterite.

Conclusions

The present study was aimed to investigate the use of CSL as a low-cost growth substrate for supporting MICP technology and the impact of the growth medium on several key properties of the concrete using the ureolytic bacterial strain, *Bacillus* sp.CT5. Addition of CSL medium had no adverse effect on the setting characteristics of cement paste, while severe retardation was noticed in nutrient medium due to yeast extract. Significant improvement in compressive strength and permeation properties as a result of using CSL in bacterial treatment of concrete was observed. Use of CSL in bacterial admixed and bacterial spray-treated specimen significantly improved the resistance against the ingress of water and aggressive agents. Carbon and nitrogen contents were higher in concrete specimens cured with medium and the maximum contents were observed at the upper layers of the concrete. Both bacterial admixed treatment (that can be used for new structures) and bacterial spray treatment (that can be used as a repair procedure) using CSL were found to be effective in improving the properties of concrete. Use of bacterial admixture, medium only (CSL and NB) and surface treatment with bacterial spray did not affect the alkaline nature of concrete. Bacterial spray treatment of concrete will help in future application of MICP technology at field scale. From these results it was concluded that CSL (an industrial by-product of the starch industry), an inexpensive nutrient medium as compared to yeast extract and peptone, would serve as a potential nutrient source for bacterial cells in microbial treatment of concrete and thus enhance the durability properties of concrete. CSL will also help in developing low-cost and environment-friendly MICP technology in future on a field scale.

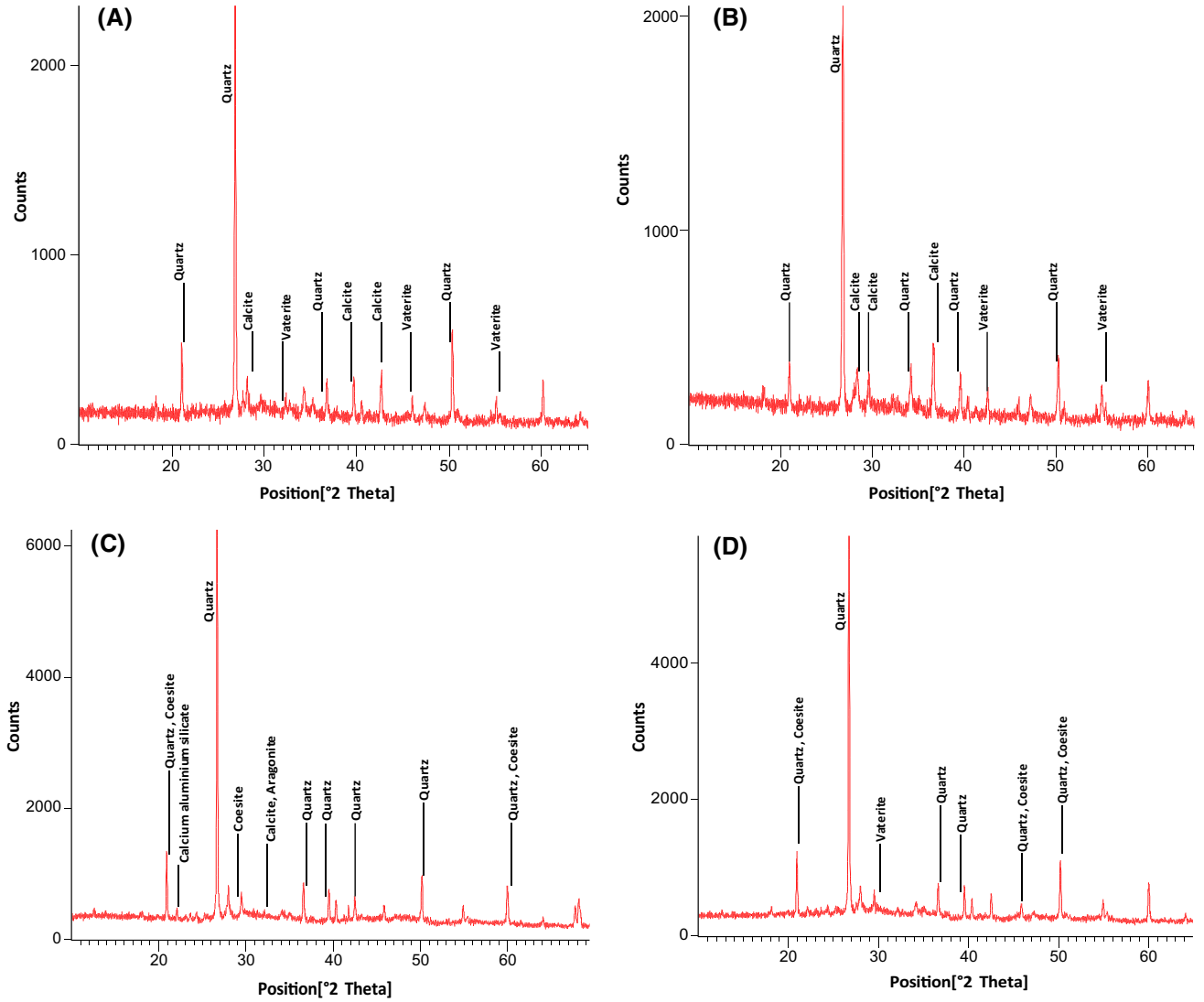

Fig. 7 XRD patterns of $CaCO_3$ crystals obtained: **a** CBAT (CSL-bacterial admixed treatment) specimen; **b** CBST (CSL-bacterial spray treatment) specimen; **c** CSL-treated specimen; and **d** Control specimen

Acknowledgements The authors are thankful to Science and Engineering Research Board (SERB), Department of Science & Technology, Government of India, India, for the financial support under the research Project No. SB/S3/CEE/0063/2013.

References

1. Achal V, Mukherjee A, Basu PC, Reddy MS (2009) Lactose mother liquor as an alternative nutrient source for microbial concrete production by *Sporosarcina pasteurii*. J Ind Microbiol Biotechnol 36:433–438
2. Achal V, Mukherjee A, Goyal S, Reddy MS (2012) Corrosion prevention of reinforced concrete with microbial calcite precipitation. ACI Mater J 109:157–164
3. Achal V, Mukherjee A, Reddy MS (2010) Biocalcification by *Sporosarcina pasteurii* using corn steep liquor as the nutrient source. Ind Biotechnol 6:170–174
4. Achal V, Mukherjee A, Reddy MS (2011) Effect of calcifying bacteria on permeation properties of concrete structures. J Ind Microbiol Biotechnol 38:1229–1234
5. Achal V, Mukherjee A, Reddy MS (2011) Microbial concrete: way to enhance the durability of building structures. J Mater Civil Eng 23:730–734
6. Amiri A, Bundur ZB (2018) Use of corn-steep liquor as an alternative carbon source for biomineralization in cement-based materials and its impact on performance. Constr Build Mater 165:655–662
7. Aprianti SE (2016) A huge number of artificial waste material can be supplementary cementitious material (SCM) for concrete production—a review part II. J Cleaner Prod 142:4178–4194
8. ASTM C1202–97 (1997) Standard test method for electrical indication of concrete's ability to resist chloride ion penetration.

ASTM International, West Conshohocken, PA. http://www.astm.org/
9. ASTM C1585-04 (2004) Standard test method for measurement of rate of absorption of water by hydraulic-cement concretes. ASTM International, West Conshohocken, PA. http://www.astm.org/
10. Basheer L, Kropp J, Cleland DJ (2001) Assessment of the durability of concrete from its permeation properties: a review. Constr Build Mater 15:93–103
11. Basheer PAM, Chidiact SE, Long AE (1996) Predictive models for deterioration of concrete structures. Constr Build Mater 10:27–37
12. Behnood A, Tittelboom KV, De Belie N (2016) Methods for measuring pH in concrete: a review. Constr Build Mater 105:176–188
13. IS: 516-1959 (1959) Indian standard methods of tests for strength of concrete. Bureau of Indian Standards, New Delhi-110002
14. IS: 8112-2013 (2013) Indian standard specification for 43 grade ordinary portland cement. Bureau of Indian Standards, New Delhi-110002
15. IS: 383-1970 (1970) Indian standard specification for coarse and fine aggregates from natural sources for concrete. Bureau of Indian Standards, New Delhi-110002
16. IS: 4031 (Part 4)-1988 (1988) Indian standard methods of physical tests for hydraulic cement. Part 4: Determination of consistency of standard cement paste. Bureau of Indian Standards, New Delhi-110002
17. IS: 4031 (Part 5)-1988 (1988) Indian standard methods of physical tests for hydraulic cement. Part 5: Determination of initial and final setting times. Bureau of Indian Standards, New Delhi-110002
18. IS: 5194-1969 (1969) Indian standard method for determination of nitrogen-Kjeldahl method. Bureau of Indian Standards, New Delhi-110002
19. Bolobova AV, Kondrashchenko VI (2000) Use of yeast fermentation waste as a biomodifier of concrete (review). Appl Biochem Microbiol 36:205–214
20. Bundur ZB, Kirisits MJ, Ferron RD (2015) Biomineralized cement-based materials: impact of inoculating vegetative bacterial cells on hydration and strength. Cem Concr Res 67:237–245
21. De Muynck W, Cox K, De Belie N, Verstraete W (2008) Bacterial carbonate precipitation as an alternative surface treatment for concrete. Constr Build Mater 22:875–885
22. De Muynck W, De Belie N, Verstraete W (2010) Microbial carbonate precipitation in construction materials: a review. Ecol Eng 36:118–136
23. Dhami NK, Reddy MS, Mukherjee A (2013) Bacillus megaterium mediated mineralization of calcium carbonate as biogenic surface treatment of green building materials. World J Microbiol Biotechnol 29:2397–2406
24. Dias WPS (1995) Sorptivity testing for assessing concrete quality, in: Proc. Int. Conf. on Concrete under Severe Exposure Conditions (CONSEC'95), Spon, London, pp 433–442
25. DIN 1048 (1978) Test methods of concrete impermeability to water: part 2. Deutscher Institute Fur Normung, Germany
26. Erşan YC, Da Silva FB, Boon N, Verstraete W, De Belie N (2015) Screening of bacteria and concrete compatible protection materials. Constr Build Mater 88:196–203
27. Eryürük K, Suzuki D, Mizuno SY, Akatsuka T, Tsuchiya T, Yang S, Kitano H, Katayama A (2016) Decrease in hydraulic conductivity of a paddy field using biocalcification *in situ*. Geomicrobiol J 33:690–698
28. Franzoni E, Pigino B, Pistolesi C (2013) Ethyl silicate for surface protection of concrete: performance in comparison with other inorganic surface treatments. Cem Concr Compos 44:69–76
29. Huet B, L'Hostis V, Miserque F, Idrissi H (2005) Electrochemical behavior of mild steel in concrete: influence of pH and carbonate content of concrete pore solution. Electrochim Acta 51:172–180
30. Joshi S, Goyal S, Mukherjee A, Reddy MS (2017) Microbial healing of cracks in concrete: a review. J Ind Microbiol Biotechnol 44:1511–1525
31. Joshi S, Goyal S, Reddy MS (2018) Influence of nutrient components of media on structural properties of concrete during biocementation. Constr Build Mater 158:601–613
32. Kim HK, Park SJ, Han JI, Lee HK (2013) Microbially mediated calcium carbonate precipitation on normal and lightweight concrete. Constr Build Mater 38:1073–1082
33. Kristiansen B (2001) Process economics, basic biotechnology, 2nd edn. Cambridge University Press, Cambridge, pp 239–252
34. Loewus FA (1952) Improvement in anthrone method for determination of carbohydrates. Anal Chem 24:219–219
35. McCarter WJ, Ezirim H, Emerson M (1992) Absorption of water and chloride into concrete. Mag Concr Res 44:31–37
36. Meyer C (2009) The greening of the concrete industry. Cem Concr Compos 31:601–605
37. Montaño-Salazar SM, Lizarazo-Marriaga J, Brandão PFB (2018) Isolation and potential biocementation of calcite precipitation inducing bacteria from colombian buildings. Curr Microbiol 75:256–265
38. Pan X, Shi Z, Shi C, Ling TC, Li N (2017) A review on surface treatment for concrete—part 2: performance. Constr Build Mater 133:81–90
39. Rodriguez-Navarro C, Jroundi F, Schiro M, Ruiz-Agudo E, González –Muñoz MT (2012) Influence of substrate mineralogy on bacterial mineralization of calcium carbonate: implications for stone conservation. Appl Environ Microbiol 78:4017–4029
40. Sharma N, Prasad GS, Choudhury AR (2013) Utilization of corn steep liquor for biosynthesis of pullulan, an important exopolysaccharide. Carbohydr Polym 93:95–101
41. Thomas NL, Birchall JD (1983) The retarding action of sugars on cement hydration. Cem Concr Res 13:830–842
42. Tremblay H, Duchesne J, Locat J, Leroueil S (2002) Influence of the nature of organic compounds on fine soil stabilization with cement. Can Geotech J 39:535–546
43. Walkley A, Black IA (1934) An examination of the Degtjareff method for determining soil organic matter and a proposed modification of the chromic acid titration method. Soil Sci 37:29–38
44. Williams SL, Kirisits MJ, Ferron RD (2016) Optimization of growth medium for *Sporosarcina pasteurii* in bio based cement pastes to mitigate delay in hydration kinetics. J Ind Microbiol Biotechnol 43:567–575
45. Yeo D, Gabbai RD (2011) Sustainable design of reinforced concrete structures through embodied energy optimization. Energy Build 43:2028–2033
46. Young JF (1972) A review of the mechanisms of set-retardation in Portland cement pastes containing organic admixtures. Cem Concr Res 2:415–433

Construction and Building Materials 209 (2019) 156–166

Contents lists available at ScienceDirect

Construction and Building Materials

journal homepage: www.elsevier.com/locate/conbuildmat

Protection of concrete structures under sulfate environments by using calcifying bacteria

Sumit Joshi [a], Shweta Goyal [b], Abhijit Mukherjee [c], M. Sudhakara Reddy [a,*]

[a] Department of Biotechnology, Thapar Institute of Engineering & Technology, Patiala 147004, Punjab, India
[b] Department of Civil Engineering, Thapar Institute of Engineering & Technology, Patiala 147004, Punjab, India
[c] Department of Civil Engineering, Curtin University, Bentley 6102, Australia

HIGHLIGHTS

- Sulfate attack (chemical and physical) causes severe damage to concrete structures.
- Surface deterioration & strength loss of concrete was not found in bacteria treated specimens.
- Mortars showed no surface scaling and salt efflorescence due to bacterial treatment.
- Bacteria improved the lifecycle performance of concrete in sulfate environment.

ARTICLE INFO

Article history:
Received 20 December 2018
Received in revised form 5 March 2019
Accepted 9 March 2019
Available online 14 March 2019

Keywords:
Biomineralization
Concrete
Durability
Sulfate attack
Efflorescence
Expansion

ABSTRACT

Application of microbial induced calcium carbonate precipitation (MICP) via biomineralization process has been considered as a novel method in improving durability properties of concrete. This bio-based treatment had been extensively targeted to improve the overall performance of concrete at lab scale experiments. Durability of microbial treated concrete under aggressive environments is still unexplored. In the current study, the durability properties of microbial treated concrete structures were studied after exposure to chemical and physical sulfate salt solutions (5% Na_2SO_4 and 5% $MgSO_4$). It has been observed that sulfate attack damaged the untreated concrete specimens causing ultimate failure due to expansion under both exposure regimes. Thick salt efflorescence and severe surface scaling was observed in untreated mortar during physical sulfate attack. However, specimens treated with bacteria (*Bacillus* sp. CT5) significantly improved the resistance towards sulfate ingress. The experimental results indicate the extensive reduced expansion rate, salt efflorescence and surface scaling in bacterial treated concrete in sulfate exposure. The present study results indicates the potential of this technology in the overall improved resistance of microbial concrete against sulfate environment.

1. Introduction

Concrete is one of the most widely used construction material and its incomparable and exceptional properties like high compressive strength and durability has made it attractive among other building materials. However, concrete is vulnerable to the ingress of reactive agents like CO_2, SO_4^{2-} and Cl^-, which on chemical interaction with hydration products of concrete causes severe degradation problems. External sulfate attack is one of the most aggressive deterioration factors, which causes irremediable changes in concrete structures. Sulfate salts had a significant impact on the durability of concrete structures constructed on sulfate rich soil or ground water [1]. The phenomena of external sulfate attack on the concrete structures are well documented by several researchers [2–4]. When cement mortars and concrete during their service life comes in contact with the sulfate loaded environments, it causes the ingress of sulfate ions in cementitious matrix [5]. Transportation of the increased sulfate ions concentration from the surface into concrete bulk leads to its chemical interaction with hydrated products of cement [6–8]. Two stage mechanism of distress on concrete matrix in sulfate attack was reported to be the driving cause of deterioration [7]. In the first stage, reaction of sulfate ions with portlandite (CH) forms gypsum, which further reacts with tricalcium aluminate (C_3A) and results into ettringite precipitates in the pores of concrete, which is categorized as chemical sulfate attack [9]. During second stage,

* Corresponding author at: Department of Biotechnology, Thapar Institute of Engineering & Technology, Patiala 147004, Punjab, India.
E-mail address: msreddy@thapar.edu (M.S. Reddy).

https://doi.org/10.1016/j.conbuildmat.2019.03.079
0950-0618/

expansive forces associated with ettringite due to high crystallization pressure leads to swelling, cracking and spalling of concrete [10]. This form of sulfate induced degradation is termed as physical sulfate attack (PSA), in which concrete is vulnerable to damage due to sulfate salt crystallization [11]. Under this condition, process of capillary rise and evaporation of sulfate salts occurs during the contact of concrete surface with sulfate bearing solution [12,13]. Generally, supersaturation of sulfate solution (conversion of anhydrous phase of sodium sulfate salt 'thenardite' into hydrous phase 'mirabilite') in concrete pore distribution results into increase in volume due to salt crystallization [3,14]. The developed crystallization is termed as salt weathering which damage the concrete by surface scaling, salt efflorescence and sub florescence [8,15,16].

Till date different methodologies were adopted by researchers to develop an improved sulfate resistance concrete against chemical as well as physical sulfate attack. Researchers had intensively investigated the effect of different supplementary cementitious materials (SCM), water/binder ratio, pozzolanic minerals, and limestone fillers in improving the performance of concrete under sulfate conditions [17,18]. It was reported that presence of tricalcium aluminate (C_3A) phase in cement clinker promotes the ettringite formation in sulfate environment [3]. Cement with low C_3A content termed as sulfate-resisting cement was reported to have decreased expansion in mortar prism while using high C_3A cement results in increased expansion rate [19]. Partial replacement of cement with metakaolin in concrete was reported to be excellent resistant to both chemical and physical sulfate attack [12,20]. Incorporation of silica fumes, fly ash and blast furnace slag in ordinary portland cement as supplementary cementitious materials resulted in reduced expansion of mortar on exposure to Na_2SO_4 solutions [9]. To protect concrete from physical sulfate attack, surface treatment with commercial available sealants and adhesive chemicals like epoxy, silane, bitumen modified polyurethane and acrylic polymer resin were also reported [21]. Existence of pores and microcracks on the concrete surface provides an ideal path for the ingress of aggressive reactive ions in the concrete bulk [22]. Prevention or retardation of the transportation of harmful agents in the pore matrix of concrete may act as a possible way to isolate the concrete structure from the surrounding environment.

Recently, application of biotechnology in concrete research led to the development of a new domain called "microbial concrete". It is a bio-inspired treatment method in which microbial-induced calcium carbonate precipitation (MICP) by calcifying bacteria is used in construction material via biomineralization process to enhance the mechanical properties and reducing porosity of concrete [23]. MICP technology has emerged as an innovative and promising technique in enhancing durability properties of concrete structures [24]. In a recent study, addition of immobilized bacterial cells with iron oxide nanoparticles showed high potential in $CaCO_3$ precipitation in the concrete pore matrix and improving the durability of concrete [25]. More recently, the potential of MICP in crack remediation of concrete using the self-healing ability of the technology has been explored by researchers [26,27]. The qualitative and quantitative evaluation of MICP in improving mechanical and permeation properties of concrete are still reported under ideal conditions at lab scale. However, the effect of harsh conditions like sulfate attack on the microbial treated concrete is still unexplored. Resistance of microbial concrete against sulfate environment is still in question.

The current study aimed to assess the efficacy of bio-deposition as a barrier in microbial treated concrete against the penetration of sulfate ions in external sulfate attack. The present study explores the performance of microbial treated concrete specimens on exposure to chemical sulfate attack by evaluating change in compressive strength, mass change and length expansion in mortar prism. Further, the microbial treated mortar prisms were subjected to physical sulfate attack conditions to study the deterioration factors like salt efflorescence. Micro-structural analysis was performed in all specimens using scanning electron microscopy/energy dispersive X-ray spectroscopy (SEM-EDX) and X-ray diffraction (XRD).

2. Material and methods

2.1. Bacterial strain and growth conditions

The calcifying bacterial strain, *Bacillus* sp. CT5, isolated from the cement sample was used in this study [28]. The culture was grown in autoclaved Nutrient broth (NB) (Peptone 10 g/L, yeast extract 10 g/L, sodium chloride 5 g/L) procured from Himedia (India) and for experimental purposes culture was supplemented with 2% urea (w/v) and 25 mM $CaCl_2$ solution at 37 °C under shaking condition (120 rpm) [23].

2.2. Materials

An ordinary Portland cement (43 Grade) confirming to IS: 8112-2013 standards was used in the present study [29]. Locally available natural river sand confirming to Zone II as per IS: 383-1970 was used as fine aggregates [30]. The values of specific gravity and water absorption of fine aggregates were 2.70 and 1.8%, respectively. The coarse aggregate used was crushed gravel with nominal particle size of 20 mm and 10 mm. The specific gravity and water absorption of 20 mm aggregates was 2.63 and 1.38% and for 10 mm aggregates, it was 2.65 and 1.4%, respectively. Both fine aggregate and coarse aggregate confirmed to IS: 383–1970 standard [30].

2.3. Sample preparation

Three different sets of concrete cubes of 100 mm dimension were prepared. Control concrete specimen was prepared by using cement: sand: coarse aggregate in the ratio 1:1.82:3.24 (by weight) with water to cement ratio (w/c) of 0.5. For casting of bacterial admixed treated (BAT) specimen, bacterial culture was grown in NB medium supplemented with 2% urea and 25 mM calcium chloride solution (w/v) till the optical density ($O.D_{600}$) reached 0.5 (exponential phase) and used instead of water. Then this culture was admixed with the concrete. The bacterial culture to cement ratio was also maintained at 0.5. For the bacterial spray treated (BST) specimen, control concrete mix was used and cured with bacterial culture grown in NB medium supplemented with 2% urea and 25 mM calcium chloride solution (w/v) till it reached the $O.D_{600}$ of 0.5. Cement, sand and aggregates were thoroughly mixed for 2 min in the concrete mixture before adding water and NB medium. The ingredients were mixed properly and the fresh mix in the plastic stage was immediately transferred to iron moulds (100 mm × 100 mm × 100 mm). Three different sets of mortar prism of 285 mm × 25 mm × 25 mm dimension were also prepared according to ASTM C1012 standard. For each of the set of mortar mixtures, the cement: sand mass ratio was kept constant as 1: 3 (by weight) with water to cement ratio (w/c) of 0.47. Similar procedure for casting of mortar prisms was followed as adopted for concrete specimens. After casting, all the specimens were allowed to remain in the iron moulds and kept in a casting room at room temperature (27 ± 2 °C) for 24 h. Thereafter, the specimens were demoulded and cured till the testing age. Three different curing regimes for the concrete and mortar specimens are specified in Table 1.

2.4. Testing methods

The performance of control and microbial treated specimens under sulfate environment was determined by subjecting to chemical and physical salt exposures. In all the tests, mixture of 5% Na_2SO_4 and 5% $MgSO_4$ were used as sulfate salt solution. The pH value of the produced sulfate salt solution was maintained in the range of 7–8. Two exposure regimes adopted in this experiment are specified below.

Exposure I: Different sets of concrete cubes and mortar prisms specified in Table 1 were subjected to chemical sulfate attack. Concrete and mortar specimens were fully submerged in sulfate solution for 12 months in plastic container and room temperature was maintained at 27 ± 2 °C. Sulfate solution in container was renewed every month. To accelerate the chemical attack, all specimens were exposed to wet-dry cycle in sulfate solution. Wet cycle and dry cycle was kept for 5 days and 2 days respectively throughout experiment of 12 months. Change in compressive strength, mass measurement and visual inspection in concrete cube specimens was monitored throughout the experiment. The change of mass of concrete cube was calculated as follows:

$$\text{Mass change at time(t)} = \frac{Mt - Mi}{Mi} \times 100$$

where *Mi* is the initial mass of cube and *Mt* is the mass of cube at time (t).

Table 1
Fabrication and conditioning of specimens.

Specimens	Material used	Mechanism of curing
Concrete cubes		
Control	Cement: sand: coarse aggregate Water/ cement = 0.5	Water Curing for 28 days
Bacterial admixed treated (BAT)	Cement: sand: coarse aggregate Bacterial culture/ cement = 0.5	Submersion in NB media, urea $CaCl_2$ and bacterial culture for 28 days
Bacterial spray treated (BST)	Cement: sand: coarse aggregate Water/ cement = 0.5	Bacterial spray on specimens twice a day till 28 days
Mortar prisms		
Control	Cement: sand Water/ cement = 0.47	Water Curing for 28 days
Bacterial admixed mortar (BAM)	Cement: sand Bacterial culture/ cement = 0.47	Submersion in NB media, urea $CaCl_2$ and bacterial culture for 28 days
Bacterial spray mortar (BSM)	Cement: sand Water/ cement = 0.47	Bacterial spray on specimens twice a day till 28 days

NB medium, urea and calcium chloride had the following concentrations: NB medium (1.3% w/v), 2% urea (w/v) and 25 mM calcium chloride (w/v).

In mortar prisms, length change due to expansion or shrinkage after chemical sulfate exposure was monitored by using length comparator according to ASTM C1012 standard [31]. The change of length of mortar prism was calculated as follows:

$$\text{Length change at time(t)} = \frac{Lt - Li}{Li} \times 100$$

where *Li* is the initial length of prism and *Lt* is the length of prism at time (t).

SEM-EDX analysis was performed to investigate the presence of reaction products at micro-structural changes after sulfate exposure. For conducting SEM and EDX analyses, small pieces of concrete were collected from different sets of concrete cubes within the range of 5–10 mm depth. XRD spectrum was obtained using Bruker D8 X-ray diffractometer on the powdered samples, obtained by drilling of concrete specimens and sieved through 90 μm sieve.

Exposure II: Three different mortar prismatic specimens specified in Table 1 were subjected to physical sulfate attack. All the prismatic specimens were subjected to partial immersion, in which one third length base of all the specimens was rested against the container of sulfate solution. Similar wet-dry cycle was adopted for the mortar prisms as mentioned in exposure I. Sulfate solution was renewed every month during the experimental period. Appearance of salt efflorescence due to rise of sulfate solution in all the specimens was monitored and recorded throughout the experiment.

3. Results

3.1. Chemical sulfate exposure

3.1.1. Compressive strength variation

Compressive strength results of control and microbial treated concrete specimens during chemical sulfate exposure are presented in Fig. 1. Prior to sulfate exposure, BAT and BST specimens registered significant increase in compressive strength as compare to control specimens due to biocementation at the age of 28 days curing. The BAT and BST specimens showed an increase of 35% and 16% in compressive strength as compared to the control specimen, respectively. The performance of concrete and mortar specimens under exposure of sulfate attack was monitored for 1 year.

Severe strength loss was observed in control specimen after 12 months of sulfate exposure. After the sulfate exposure, compressive strength of control specimen registered a drastic decrease of 30% as compared to its value before exposure. However in BAT and BST specimen, minor variations in compressive strength were observed after sulfate exposure. No major sign of strength loss was registered in BAT and BST specimens throughout the exposure.

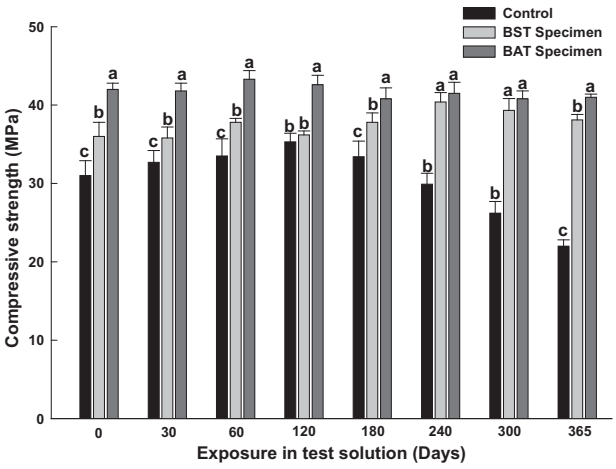

Fig. 1. Influence of sulfate exposure on compressive strength of concrete specimens till the age of 365 days. Bars sharing a common letter within the treatment are not significant at $P < 0.05$. Error bars represent standard deviation (n = 3).

3.1.2. Visual appearance

Visual observations of concrete specimens under exposure I for 12 months are presented in Fig. 2.Clear sign of surface degradation was observed in control specimens during 12 months of immersion in sulfate solution. The first sign of surface cracks in control specimen was visualized at the exposure time of 180 days. The damaging process in control specimen continued with loss of cohesion less particles on the edges due to spalling. Maximum surface deterioration was noted in control specimen during the sulfate exposure. However, no sign of deterioration such as cracking and spalling were visualized in BAT and BST specimens and these microbial treated specimens remained intact (Figs. 3 and 4). Severity of surface scaling in concrete specimens is rated as specified in ASTM C672/C672M – 12 standard [32] and presented in Table 2.

3.1.3. Mass change

The mass variations were monitored for all the concrete specimens under exposure I as shown in Fig. 5. Control concrete specimens gained the higher mass with respect of BAT and BST specimens. Mass gain in concrete specimens was registered till the immersion age of 270 days but thereafter loss in mass was observed. In case of BAT and BST specimens, marginal mass gain was observed.

3.1.4. Mortar length change

The length expansion results for all the mortar prismatic specimens are shown in Fig. 6. After 12 months of full immersion, maximum length expansion was observed in control prismatic specimens. The control prism yielded the maximum expansion of about 0.38% after the complete cycle of exposure I. However, bacterial treated prismatic specimens indicate the higher resistance against sulfate attack towards expansion. In BAM and BSM prisms no evident effect on length was observed as compare to control prism, with maximum expansion reaching 0.18% and 0.15% respectively. Results indicates that BAM and BSM prism showed 52% and 60% lower expansion than control prism, respectively.

3.1.5. Microstructural evaluation

SEM analysis of all concrete specimens was performed at different ages of sulfate exposure I (Fig. 7). In control concrete speci-

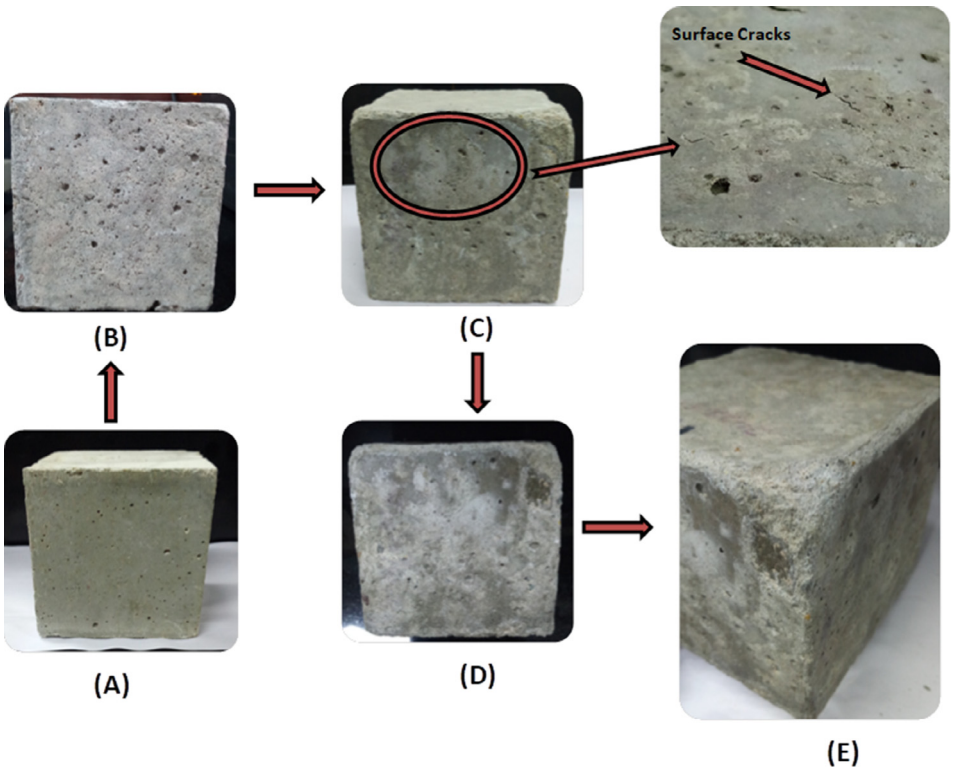

Fig. 2. Visual appearance of control specimen (100 × 100 × 100 mm) after sulfate exposure I at the age of (A) 30 days (B) 90 days (C) 180 days (D) 270 days (E) 365 days.

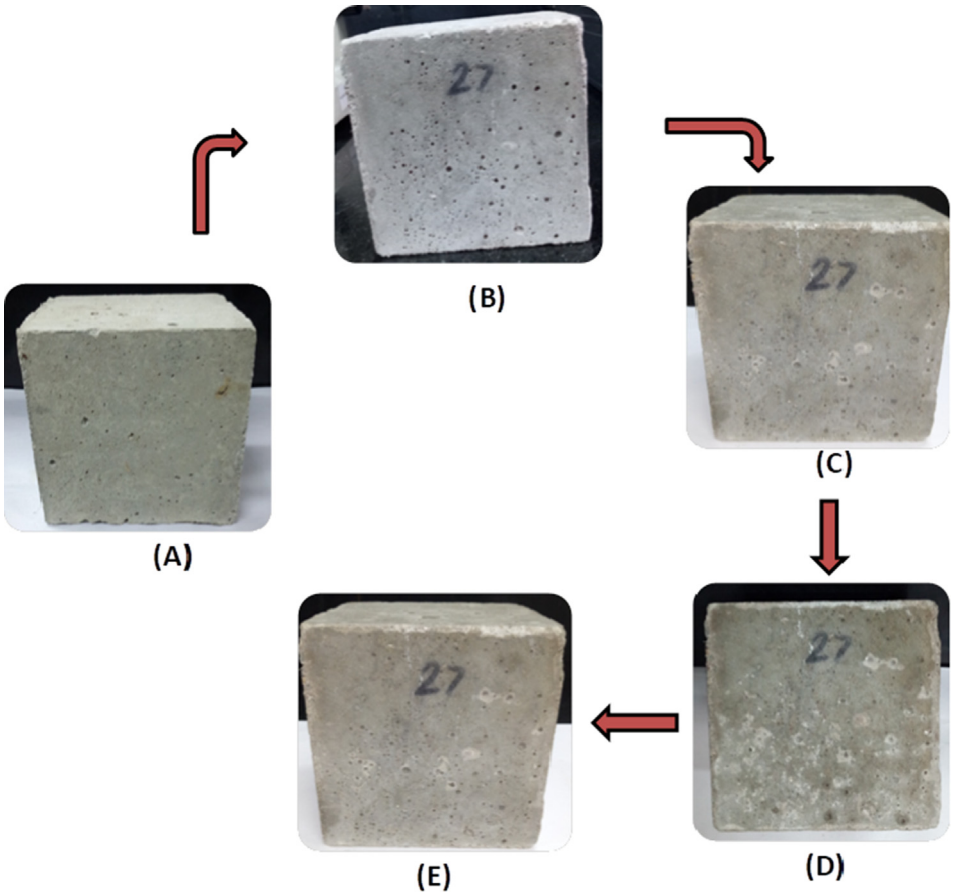

Fig. 3. Visual appearance of BAT specimen (100 × 100 × 100 mm) after sulfate exposure I at the age of (A) 30 days (B) 90 days (C) 180 days (D) 270 days (E) 365 days.

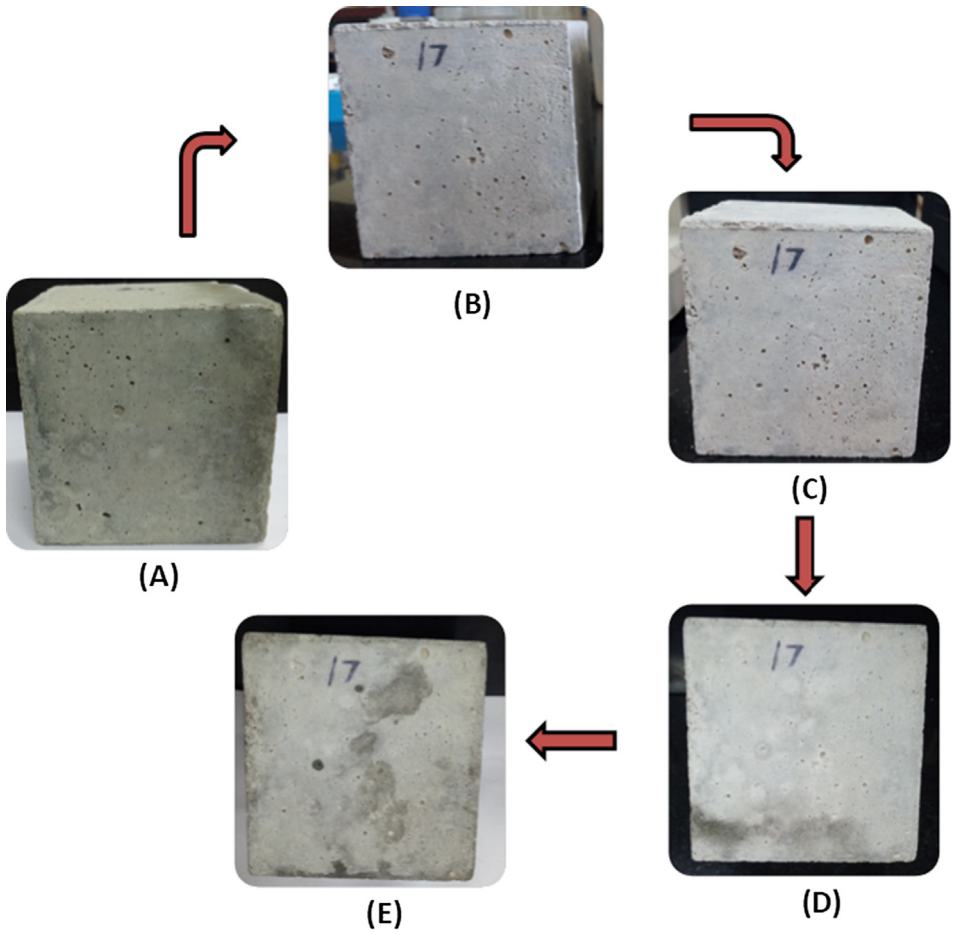

Fig. 4. Visual appearance of BST specimen (100 × 100 × 100 mm) after sulfate exposure I at the age of (A) 30 days (B) 90 days (C) 180 days (D) 270 days (E) 365 days.

Table 2
Surface scaling visual rating adapted from ASTM C672/C672M – 12.

Concrete specimens	Exposure time (months)				
	1	3	6	9	12
Control	0	1	2	3	4
BAT	0	0	0	0	0
BST	0	0	0	0	0

0: No scaling; 1: Very slight scaling; 2: Slight to moderate scaling; 3: Moderate scaling; 4: Moderate to severe scaling; 5: Severe scaling.

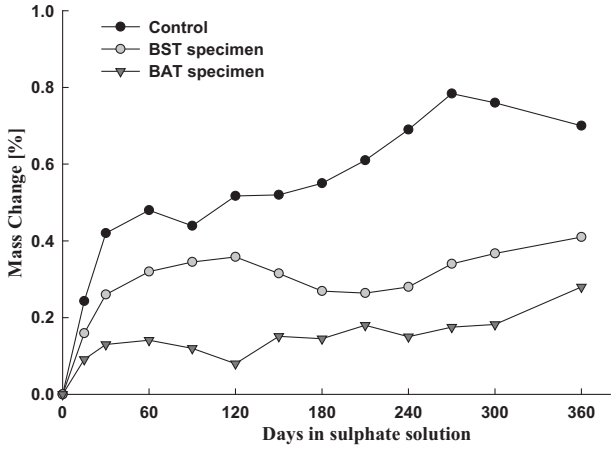

Fig. 5. Mass change of concrete specimens after sulfate exposure I.

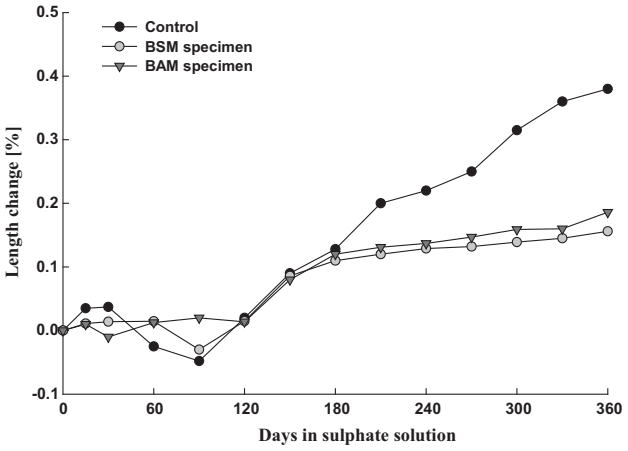

Fig. 6. Length change of mortar specimens after sulfate exposure I.

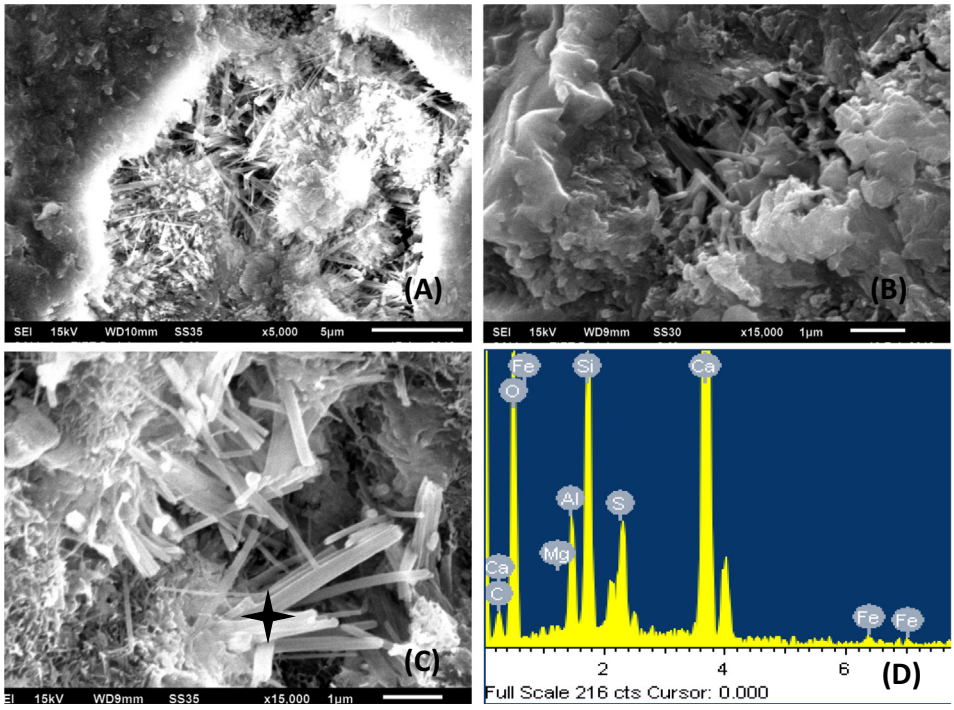

Fig. 7. SEM images of control specimen after (A) 90 days (B) 180 days (C) 365 days of exposure I. (D) EDX analysis represents formation of reaction products. Star shows the spot of EDX analysis.

mens, deposition of different secondary products like gypsum and ettringite crystals were observed. Presence of needle shaped crystals was observed in the pore matrix of control specimen at the immersion age of 90 days (Fig. 7A). With the increasing sulfate immersion age, precipitation rate of ettringite crystals were also escalated. Intense deposition of ettringite crystals with long needle shape and elongated rectangular prism faced column shape in control specimens were observed at the age of 365 days (Fig. 7C).

The EDX analysis also confirmed the elemental composition of crystals with peaks showing high amount of calcium, sulphur and aluminum (Fig. 7D). In contrast, calcium carbonate crystals in BAT and BST specimen were present instead of the formation of ettringite crystals (Figs. 8 and 9). The calcium carbonate crystals have prominent morphologies of calcite and aragonite, as has already been discussed in our previous research article [23]. Till the exposure age of 180 days, secondary products due to sulfate ingress were not observed. However after 365 days of severe sulfate attack, development of micro needle crystals of gypsum and ettringite were observed in BAT and BST specimen. EDX analysis confirmed the formation of gypsum and ettringite crystals showing the peaks of calcium, sulphur, aluminum and oxygen.

XRD analyses of concrete specimens were performed to identify the presence of different crystalline phases during sulfate exposure I (Fig. 10). In control specimen, XRD profile indicates the peak for quartz as well as ettringite and gypsum as the main secondary reaction products (Fig. 10A). In case of BAT and BST specimens, XRD analysis revealed the presence of calcite as the major phase as well as some peaks of gypsum and thaumasite (Fig. 10B–C).

3.2. Physical sulfate exposure

3.2.1. Salt efflorescence

A typical appearance of white efflorescence was developed in the mortar prisms during exposure II. Thick deposition of salt efflorescence was developed in the upper portion of the control prism during immersion period (Fig. 11).

After 30 days of immersion, salt precipitation above the sulfate solution level was developed in control specimens. After 90 days of exposure, crack formation along the edges of control specimen was observed. At a later age, higher surface scaling and increase in longitudinal cracks in submerged portion was observed. XRD analysis performed for the control prism at the end of the sulfate exposure is shown in Fig. 12. XRD patterns from submerged portion revealed the presence of ettringite and gypsum as the major sulfate reaction phases (Fig. 12A). In case of salt efflorescence developed above the sulfate solution level, XRD patterns revealed the formation of thenardite and epsomite as the major phases with minor peaks of mirabilite (Fig. 12B). However, BSM and BAM prism shows better resistance against the physical sulfate attack. No visible deterioration such as surface scaling or crack formation observed in BSM and BAM throughout the exposure (Figs. 13 and 14). Slight formation of salt efflorescence above the sulfate solution level was observed in BSM and BAM at later ages.

4. Discussion

4.1. Effect of chemical sulfate attack

Performance of control as well as microbial treated concrete and mortar specimens under chemical sulfate attack was monitored for 12 months through evaluation of durability factors like compressive strength change, mass change and length expansion. During the first 120 days of exposure, improvement in compressive strength of control specimens was recognized (Fig. 1). This behavior of the initial improvement in mechanical strength reflects the densification of cementitious matrix at microstructural level [33]. It was also reported that due to continuous ingress of sulfate ions into the cementitious matrix progresses the development of expansive products such as gypsum and ettringite was observed. The quantity of expansive products fills the pores and voids causing the microstructure denser during the initial period of sulfate exposure [12]. With the long time exposure, the severity of

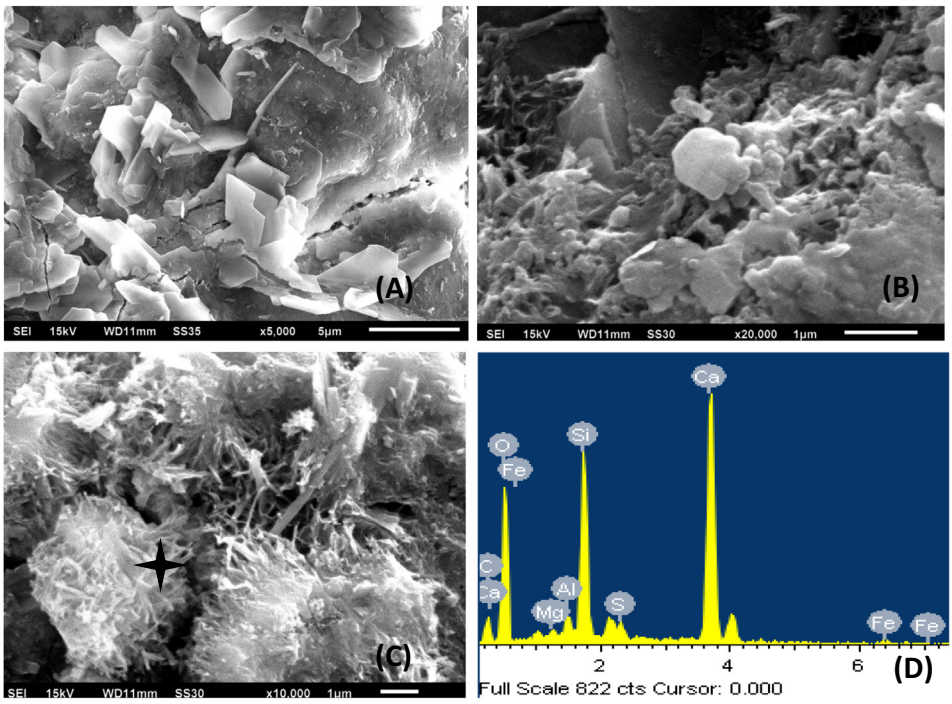

Fig. 8. SEM images of BAT specimen after (A) 90 days (B) 180 days (C) 365 days of exposure I. (D) EDX analysis represents formation of reaction products. Star shows the spot of EDX analysis.

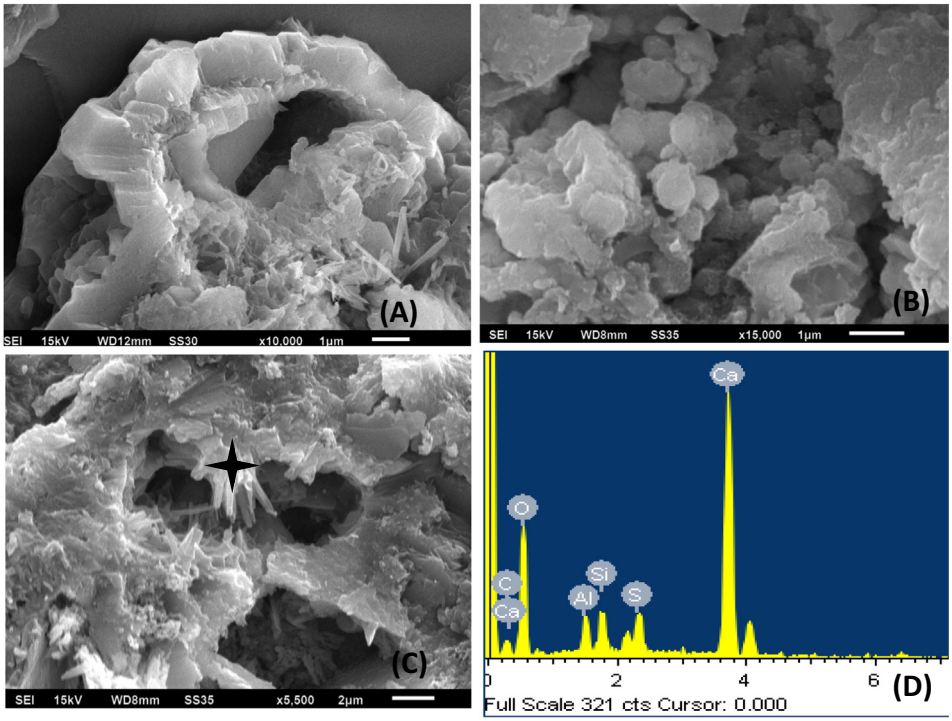

Fig. 9. SEM images of BST specimen after (A) 90 days (B) 180 days (C) 365 days of exposure I. (D) EDX analysis represents formation of reaction products. Star shows the spot of EDX analysis.

chemical sulfate attack intensified and results into significant strength loss in control specimen. Gradual loss in strength observed after 180 days of immersion may be due to increased penetration of sulfate salts causing higher accumulation of expansive products in the pores of control specimens. Formation of ettringite crystals led to the factors like reduction in the quantity of CH and C_3A content of cementitious matrix [15] and salt crystallization pressure within the pores of concrete [34]. It was reported that quantity of CH and C_3A content favored the attack of Na_2SO_4 salt and calcium silicate hydrate (CSH) favored the $MgSO_4$ attack [15]. Deterioration in the form of spalling and cracking on the concrete surface was observed in control specimens. As indicated in

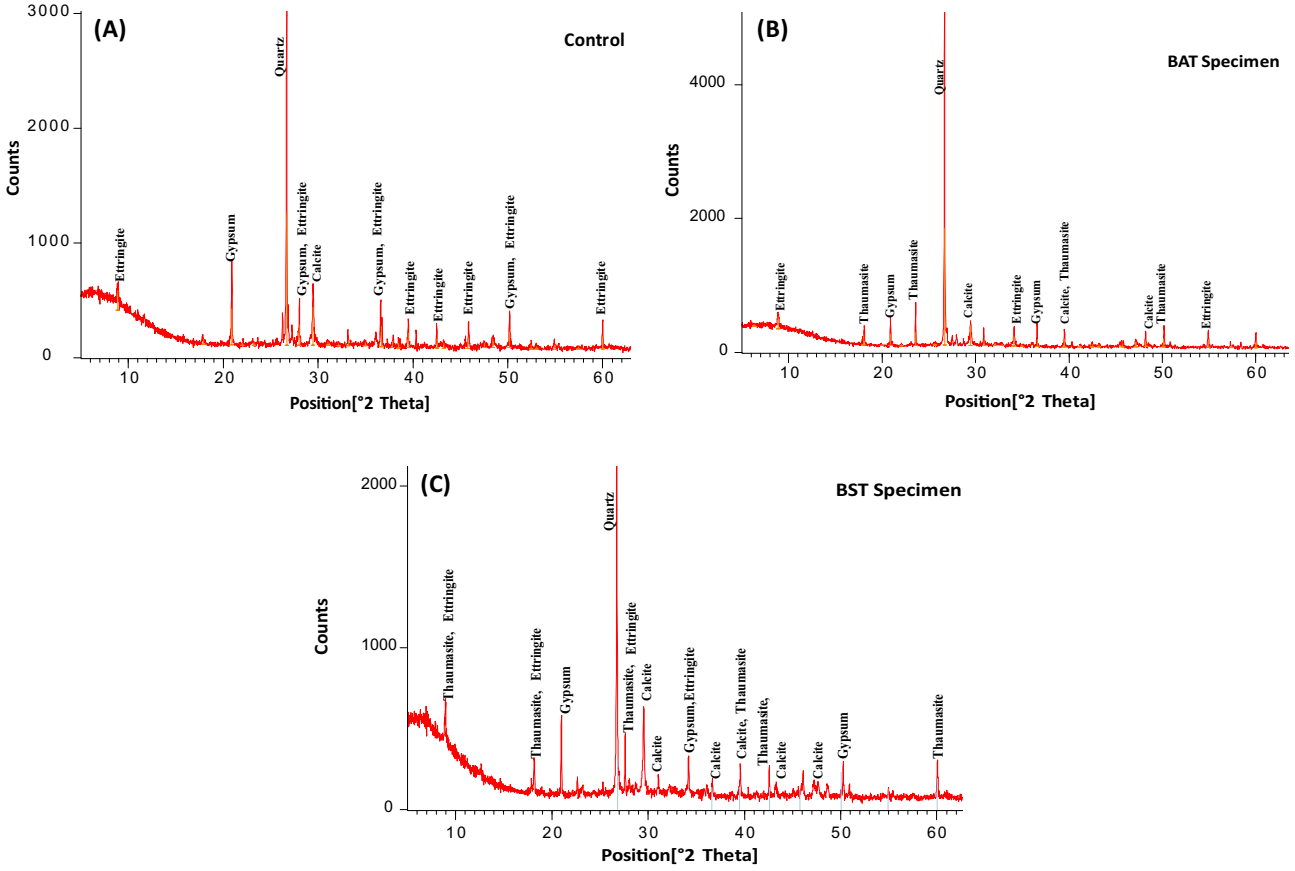

Fig. 10. XRD patterns of (A) Control (B) BAT specimen and (C) BST specimen after sulfate exposure I.

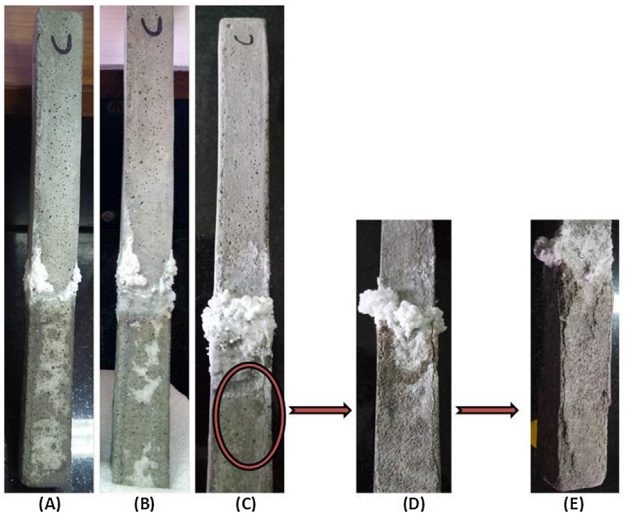

Fig. 11. Typical salt efflorescence development in control prism after sulfate exposure II at the age of (a) 30 days (b) 90 days (c) 180 days (d) 270 days (e) 365 days.

Fig. 2, surface cracks were observed in control specimens at the immersion age of 180 days which further accelerated with the exposure time. Association of gypsum and ettringite crystals accumulation in the pores of concrete supported the possible reason of damage (Fig. 7). Presence of elongated column shaped ettringite crystals generated a significant stress in the pores which causes damage to pore walls resulting into cracking.

On the other hand, influence of sulfate ingress in the pores of control specimen on the mass change was observed. As shown in Fig. 5, it was observed that control specimen undergo mass gain of 0.8% till the immersion age of 270 days. It seems that mass variation may be due to the formation of expansive products during the reaction of hydration products of cement with sulfate ions which leads to compaction of microstructure [35]. Concrete with high porosity was reported to gain mass because of higher ingress of sulfate absorption [13]. Higher pore volume was reported to be the main reason, responsible for the transportation of sulfate ions and consequently filling the concrete pores with expansive products [12]. However, in the later ages of immersion, trend of mass loss was observed in control specimens as the sulfate exposure progressed (Fig. 5). Development of stress due to enhanced growth of expansive products causes surface scaling and loss of cohesion less particles on the edges (Fig. 2). Existence of gypsum and ettringite crystals in concrete pores was claimed to be the deterioration factors [35]. Expansive behavior of reaction products will be the factors responsible for cracking and spalling on the outermost layer of concrete. In SEM and XRD analysis (Figs. 7 and 10A), presence of gypsum and ettringite confirmed the deterioration of control specimens, which is further responsible for mass loss.

In addition, trends of length increase in control prism due to expansive product formation were also observed. As shown in Fig. 6, rate of expansion was much higher in control prism as compared to microbial treated prisms. Length expansion of control mortar prism indicates higher ingress of sulfate ions and filling its pore volume with reaction products. Moreover, during the sulfate exposure a longitudinal crack along the whole length of control prism was observed. Similar observation of crack generation along the length of mortar prism was also reported by Maes and

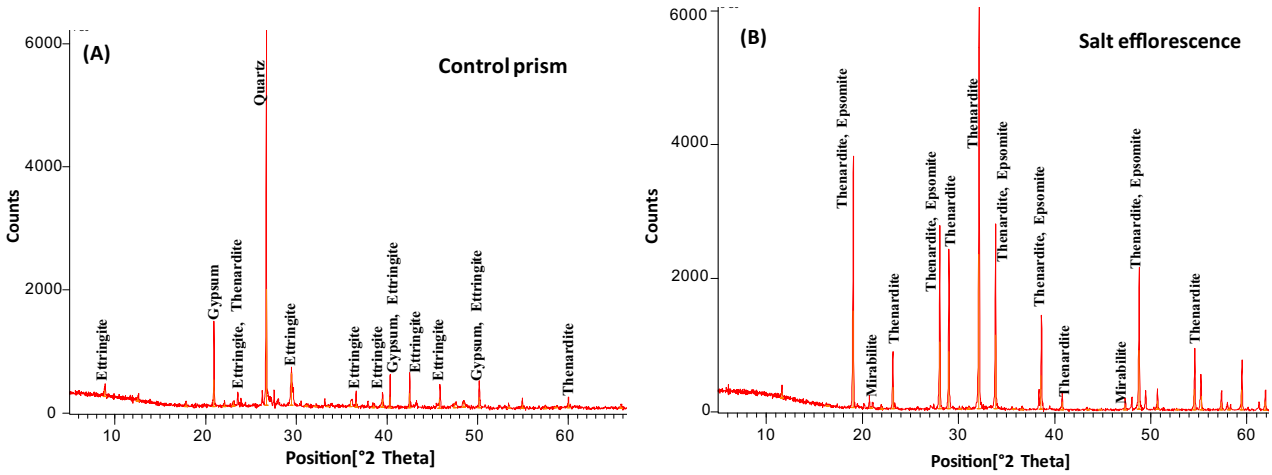

Fig. 12. XRD patterns of (A) submerged portion and (B) salt efflorescence of control prism.

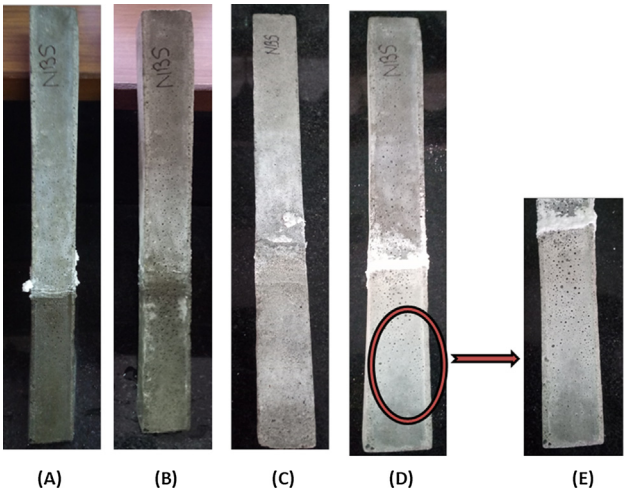

Fig. 13. BSM prism after sulfate exposure II at the age of (a) 30 days (b) 90 days (c) 180 days (d) 270 days (e) 365 days.

De Belie [35]. Appearance of cracks confirms the formation of ettringite and gypsum crystals as a responsible factors for deterioration. Ettringite and gypsum were also reported as the cause of

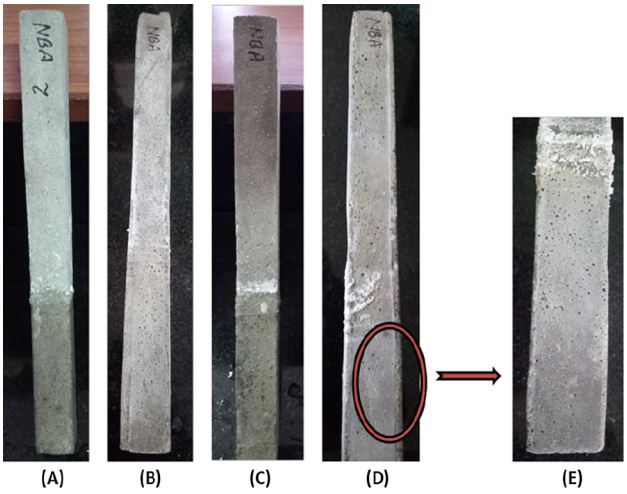

Fig. 14. BAM prism after sulfate exposure II at the age of (a) 30 days (b) 90 days (c) 180 days (d) 270 days (e) 365 days.

expansion in mortar specimens subjected to sulfate environment [7,36]. It has also been reported that leaching of $Ca(OH)_2$ plays an important role in the degradation of mortar specimen immersed in sodium sulfate solution [19]. Dissolution of $Ca(OH)_2$ together with external sulfate attack increased the porosity and making the diffusivity of sulfate ions easier for the formation of gypsum. This mechanism was reported for triggering the overall expansion and cracking of mortar prism.

In contrast, overall performance of microbial treated specimens against sulfate resistance was excellent. Application of both microbial treatments (bacterial admixture and bacterial spray) improved the mechanical and permeation properties of concrete structures (Figs. 1 and 5). Due to biogenic precipitation of $CaCO_3$ crystals, ingress of sulfate ions was extensively reduced inside the cementitious matrix. Low ingress of sulfate ions further reduces the deterioration of concrete leading from the formation of expansive reaction products like ettringite and gypsum (Figs. 8 and 9). However, some researchers also reported that the presence of carbonate in cementitious matrix will favor the thaumasite form of sulfate attack [37]. It was reported that limestone fillers were used as SCM with different replacement levels in concrete mixes [38]. Contrary to the reports of deterioration of concrete structures incorporated with limestone on exposure to sulfate solutions, improvement in resistance against the sulfate attack was reported [33,39]. In XRD analysis, presence of calcite as well as thaumasite phases at the end of exposure was observed (Fig. 10B–C). On the whole, BAT and BST specimens remain unaffected as compared to control specimens and performed well in the chemical sulfate attack.

4.2. Effect of physical sulfate attack

During the exposure II, a thick white efflorescence was developed in control prism on the drying mortar surface which is just above the submerged portion. With the exposure time, thickness of efflorescence continued to increase in control prism (Fig. 11). However, longitudinal crack formation after 90 days of sulfate exposure in submerged portion and severe surface scaling at later ages was observed. This behavior of efflorescence deposition on the upper portion and surface scaling on the submerged portion of mortar prism were reported to be a dual action of physical and chemical sulfate attack respectively [13]. It is reported that in physical sulfate attack, stress development due to salt crystallization pressure in pore structure is the deterioration mechanism. Sulfate ions penetrate from sulfate rich surroundings into concrete

pores by capillary suction and are transported to the evaporation surfaces [4]. At the upper dry surface, rate of evaporation exceeds the rate of capillary rise due to which salt solution becomes supersaturated causing the salt crystallization on the surface [11]. Salt solution uptake into the pores by capillary pressure is dependent on the pore distribution of porous body as well as its wetting behavior [10]. It was also reported that increased porosity and permeability further increases the flux of salt solutions causing more accumulation of salts [34]. In control mortar prism, dual effect of physical sulfate attack on the upper portion and chemical sulfate attack on the submerged portion was observed. However above the efflorescence region no sign of damage like cracking and spalling were observed. It is reported that the growth of mirabilite crystals inside the pore wall generates high crystallization stress developing subflorescence region (above the efflorescence region) where damage occurs [34]. In XRD analysis, presence of anhydrous thenardite deposits on the evaporative surface of control prism shows that the hydrous mirabilite phase dried out on the surface during the exposure (Fig. 12B). This thick efflorescence on upper surface indicates higher concentration of sulfate salt ingress in control specimen. However, in XRD analysis, presence of ettringite and gypsum crystals in the damaged submerged region also mimics the chemical sulfate attack (Fig. 12A). In the submerged portion, instead of salt efflorescence, crack formation along the edges due to expansion was observed. Similar to chemical sulfate attack, this typical crack formation and spalling in the submerged portion causes severe surface damage.

In case of BAM and BSM prisms, resistance to capillary rise of sulfate salts was adequately achieved due to microbial treatment. Throughout the exposure, there was no sign of surface scaling in the submerged portion of BAM and BSM prisms was observed (Figs. 13 and 14). Precipitation of calcium carbonate during microbial treatment might have densify the cementitious pore matrix and acts as a pore blocker. It is reported that permeation properties of concrete structures are significantly improved by bacterial calcium carbonate precipitation. Further, the transport mechanism of salt contaminated water through capillary rise in pore matrix is effectively altered by bacterial treated concrete [40]. BAM and BSM prisms exhibited excellent resistance to sulfate ingress and leading to protection from physical and chemical form of sulfate attacks.

5. Conclusions

In the present study, sulfate resistance of bacterial treated concrete and cement mortars were investigated under two different sulfate exposure regimes and monitored for 12 months. On the basis of experimental outcomes, following conclusions were drawn:

- During the chemical and physical sulfate exposure, significant reduction of sulfate ions ingress was observed in microbial treated concrete and mortars.
- Throughout the chemical sulfate exposure, BAT and BST concrete specimens exhibited no surface deterioration or strength loss. Both specimens were remained intact and no sign of damage due to expansion was observed until the end of experimental study.
- Under physical sulfate exposure, BAM and BSM specimen performed well and no sign of surface scaling and salt efflorescence on the upper drying front was observed.
- During the experiment, untreated concrete specimens performed relatively poor. Deterioration due to expansive products causes surface scaling in both exposure regimes. Thick efflorescence as well as severe surface scaling was observed during physical sulfate attack.
- Overall, the application of MICP treatment improved the lifecycle performance of concrete under harsh sulfate environments.

Acknowledgements

Authors are thankful to Science and Engineering Research Board, Department of Science & Technology, Ministry of Science & Technology, Government of India, India for sponsoring the research project SB/S3/CEE/0063/2013.

Conflicts of interest

None.

References

[1] A. Leemann, R. Loser, Analysis of concrete in a vertical ventilation shaft exposed to sulfate-containing groundwater for 45 years, Cem. Concr. Comp. 33 (2011) 74–83.
[2] M. Santhanam, M.D. Cohen, J. Olek, Sulfate attack research—whither now?, Cem Concr. Res. 31 (2001) 845–851.
[3] A. Neville, The confused world of sulfate attack on concrete, Cem. Concr. Res. 34 (2004) 1275–1296.
[4] Z. Liu, D. Deng, G. De Schutter, Does concrete suffer sulfate salt weathering?, Constr Build. Mater. 66 (2014) 692–701.
[5] G. Massaad, E. Rozière, A. Loukili, L. Izoret, Advanced testing and performance specifications for the cementitious materials under external sulfate attacks, Constr. Build. Mater. 127 (2016) 918–931.
[6] M. Santhanam, M.D. Cohen, J. Olek, Mechanism of sulfate attack: a fresh look: part 1: summary of experimental results, Cem. Concr. Res. 32 (2002) 915–921.
[7] E. Rozière, A. Loukili, R. El Hachem, F. Grondin, Durability of concrete exposed to leaching and external sulphate attacks, Cem. Concr. Res. 39 (2009) 1188–1198.
[8] M. Whittaker, L. Black, Current knowledge of external sulphate attack, Adv. Cem. Res. 27 (2015) 532–545.
[9] M. Nehdi, M. Hayek, Behavior of blended cement mortars exposed to sulfate solutions cycling in relative humidity, Cem. Concr. Res. 35 (2005) 731–742.
[10] G.W. Scherer, Stress from crystallization of salt, Cem. Concr. Res. 34 (2004) 1613–1624.
[11] H. Haynes, M.T. Bassuoni, Physical salt attack on concrete, Concr. Int. 33 (2011) 38–42.
[12] M.F. Najjar, M.L. Nehdi, A.M. Soliman, T.M. Azabi, Damage mechanisms of two-stage concrete exposed to chemical and physical sulfate attack, Constr. Build. Mater. 137 (2017) 141–152.
[13] M.L. Nehdi, A.R. Suleiman, A.M. Soliman, Investigation of concrete exposed to dual sulfate attack, Cem. Concr. Res. 64 (2014) 42–53.
[14] C. Rodriguez-Navarro, E. Doehne, Salt weathering: influence of evaporation rate, supersaturation and crystallization pattern, Earth. Surf. Process. Landforms 24 (1999) 191–209.
[15] T. Aye, C.T. Oguchi, Resistance of plain and blended cement mortars exposed to severe sulfate attacks, Constr. Build. Mater. 25 (2011) 2988–2996.
[16] N. Yoshida, Y. Matsunami, M. Nagayama, E. Sakai, Salt weathering in residential concrete foundations exposed to sulfate-bearing ground, J. Adv. Concr. Technol. 8 (2010) 121–134.
[17] E.F. Irassar, M. Gonzalez, V. Rahhal, Sulphate resistance of type V cements with limestone filler and natural pozzolana, Cem. Concr. Comp. 22 (2000) 361–368.
[18] M. Uysal, M. Sumer, Performance of self-compacting concrete containing different mineral admixtures, Constr. Build. Mater. 25 (2011) 4112–4120.
[19] R. El-Hachem, E. Rozière, F. Grondin, A. Loukili, Multi-criteria analysis of the mechanism of degradation of Portland cement based mortars exposed to external sulphate attack, Cem. Concr. Res. 42 (2012) 1327–1335.
[20] N.M. Al-Akhras, Durability of metakaolin concrete to sulfate attack, Cem. Concr. Res. 36 (2006) 1727–1734.
[21] A.R. Suleiman, A.M. Soliman, M.L. Nehdi, Effect of surface treatment on durability of concrete exposed to physical sulfate attack, Constr. Build. Mater. 73 (2014) 674–681.
[22] J.L. Aguiar, A. Camões, P. Moreira, Performance of concrete in aggressive environment, Int. J. Concr. Struct. Mater. 2 (2008) 21–25.
[23] S. Joshi, S. Goyal, M.S. Reddy, Influence of nutrient components of media on structural properties of concrete during biocementation, Constr. Build. Mater. 158 (2018) 601–613.
[24] N. De Belie, Application of bacteria in concrete: a critical evaluation of the current status, RILEM Tech. Lett. 1 (2016) 56–61.
[25] M. Seifan, A. Ebrahiminezhad, Y. Ghasemi, A. Berenjian, Microbial calcium carbonate precipitation with high affinity to fill the concrete pore space: nanobiotechnological approach, Bioprocess. Biosyst. Eng. 42 (2019) 37–46.
[26] S. Joshi, S. Goyal, A. Mukherjee, M.S. Reddy, Microbial healing of cracks in concrete: a review, J. Ind. Microbiol. Biot. 44 (2017) 1511–1525.

[27] M. Seifan, A. Berenjian, Application of microbially induced calcium carbonate precipitation in designing bio self-healing concrete, World. J. Microbiol. Biotechnol 34 (2018) 1–15.
[28] V. Achal, A. Mukerjee, M.S. Reddy, Microbial concrete: way to enhance the durability of building structures, J. Mater. Civil. Eng. 23 (2011) 730–734.
[29] IS: 8112-2013Indian Standard Specification for 43 Grade Ordinary Portland Cement, Bureau of Indian Standards, New Delhi-110002, 2013.
[30] IS: 383-1970Indian standard specification for coarse and fine aggregates from natural sources for concrete, Bureau of Indian Standards, New Delhi-110002, 1970.
[31] ASTM C1012-04, Standard Test Method for Length Change of Hydraulic-Cement Mortars Exposed to a Sulfate Solution, ASTM International, West Conshohocken, PA, 2004.
[32] ASTM C672/C672M-12, Standard Test Method for Scaling Resistance of Concrete Surfaces Exposed to Deicing Chemicals, ASTM International, West Conshohocken, PA, 2012.
[33] F. Mittermayr, M. Rezvani, A. Baldermann, S. Hainer, P. Breitenbücher, J. Juhart, C.A. Graubner, T. Proske, Sulfate resistance of cement-reduced eco-friendly concretes, Cemt. Concr. Comp. 55 (2015) 364–373.
[34] B.Y. Lee, K.E. Kurtis, Effect of pore structure on salt crystallization damage of cement-based materials: Consideration of w/b and nanoparticle use, Cem. Concr. Res. 98 (2017) 61–70.
[35] M. Maes, N. De Belie, Resistance of concrete and mortar against combined attack of chloride and sodium sulphate, Cem. Concr. Comp. 53 (2014) 59–72.
[36] B. Tian, M.D. Cohen, Does gypsum formation during sulfate attack on concrete lead to expansion?, Cem Concr. Res. 30 (2000) 117–123.
[37] E.F. Irassar, Sulfate attack on cementitious materials containing limestone filler—A review, Cem. Concr. Res. 39 (2009) 241–254.
[38] M.M. Rahman, M.T. Bassuoni, Thaumasite sulfate attack on concrete: Mechanisms, influential factors and mitigation, Constr. Build. Mater. 73 (2014) 652–662.
[39] A. Skaropoulou, K. Sotiriadis, G. Kakali, S. Tsivilis, Use of mineral admixtures to improve the resistance of limestone cement concrete against thaumasite form of sulfate attack, Cem. Concr. Comp. 37 (2013) 267–275.
[40] S. Joshi, S. Goyal, M.S. Reddy, Corn steep liquor as a nutritional source for biocementation and its impact on concrete structural properties, J. Ind. Microbiol. Biot. 45 (2018) 657–667.

J Ind Microbiol Biotechnol (2017) 44:1511–1525
DOI 10.1007/s10295-017-1978-0

ENVIRONMENTAL MICROBIOLOGY - REVIEW

Microbial healing of cracks in concrete: a review

Sumit Joshi[1] · Shweta Goyal[2] · Abhijit Mukherjee[3] · M. Sudhakara Reddy[1]

Received: 20 April 2017 / Accepted: 5 September 2017 / Published online: 12 September 2017

Abstract Concrete is the most widely used construction material of the world and maintaining concrete structures from premature deterioration is proving to be a great challenge. Early age formation of micro-cracking in concrete structure severely affects the serviceability leading to high cost of maintenance. Apart from conventional methods of repairing cracks with sealants or treating the concrete with adhesive chemicals to prevent the cracks from widening, a microbial crack-healing approach has shown promising results. The unique feature of the microbial system is that it enables self-healing of concrete. The effectiveness of microbially induced calcium carbonate precipitation (MICCP) in improving durability of cementitious building materials, restoration of stone monuments and soil bioclogging is discussed. Main emphasis has been laid on the potential of bacteria-based crack repair in concrete structure and the applications of different bacterial treatments to self-healing cracks. Furthermore, recommendations to employ the MICCP technology at commercial scale and reduction in the cost of application are provided in this review.

Keywords Microbial concrete · Autogenous healing · Self-healing · Crack healing · Urea hydrolysis · *Bacillus*

✉ M. Sudhakara Reddy
msreddy@thapar.edu

[1] Department of Biotechnology, Thapar University, Patiala, Punjab 147004, India

[2] Department of Civil Engineering, Thapar University, Patiala, Punjab 147004, India

[3] Department of Civil Engineering, Curtin University, Bentley 6102, Australia

Introduction

Concrete and steel are the two most commonly used structural materials. Among them, reinforced concrete is the most versatile and potentially one of the most durable materials for almost any types of building structures. The factors that affect the lifecycle performance of concrete include climate change, higher temperature and extreme weather events which lead to its premature deterioration. Most of these threatening factors involve chemical attack on concrete or on the rebar embedded in it. The interconnected pore system and presence of micro-cracks also allow penetration of harmful agents like CO_2, SO_4^{2-} and Cl^- to cause corrosion of steel rebar [13]. The rate of deterioration of concrete structures mainly depends on two important factors: permeability of concrete matrix and development of micro-cracks [14]. As nearly 80% of world's infrastructure is built in reinforced concrete, their maintenance needs a huge recurring investment that few countries in the world can afford. There is a worldwide effort for sustainable technologies for maintenance of infrastructures that would offer economy without undue environmental or social costs.

To minimize the cost of repair and rehabilitation of large-scale civil infrastructure facing the deterioration from the cracks, different strategies for the repair of cracks has been studied. Intensive research to heal the concrete structures suffering from cracks has been done by using organic and inorganic filling materials [90]. More recently, introduction of applied biotechnology in the field of concrete has led to the development of a new domain called "microbial concrete" or "bio-concrete". It is a microbial-based strategy in which concrete structures are treated with bacteria to induce calcium carbonate precipitation [4]. A positive benefit of biomineralization activity of various bacterial strains to enhance the durability and crack healing of concrete has

become an important research topic during the last decade. Many reviews have been published addressing the applications of microbial concrete in various fields including the durability enhancement of building material [5, 10, 24, 26, 28, 60, 68, 82, 87, 94]. The ecological benefits of MICCP in urban development have been highlighted [5]. Different applications of the technology have been explored [10, 26, 60]. Different microbial pathways and their applicability in construction have been analyzed [28, 94]. The sustainability of this technology has been examined [82]. More recently, the self-healing ability of the technology has been compared with the existing abiotic processes [87]. Self-healing is essentially autogenous filling of cracks that develop in concrete. Its potential to make concrete sustainable has been explored [67]. However, there has been a rapid development in the understanding of causes of concrete cracking and microbial techniques for healing the cracks. These are the precursors for the development of self-healing concrete. This paper presents a comprehensive review of the concrete cracking problems, different techniques for healing them and finally, autogenous healing of concrete by the microbial means. The mechanisms for microbially induced $CaCO_3$ precipitation and its applications in concrete structures are discussed. The efficacy of microbial techniques of healing them has been examined. Finally, a future direction for the development of self-healing concrete is indicated.

Approach in crack healing

In the context of civil engineering research, healing is the phenomenon of restoration of concrete structure from a state of damage. In case of crack healing, chemical and physical processes result in the introduction of secondary products that block or seal the cracks. To some extent, concrete is capable of healing cracks autogenously, which is called self-healing or autogenous healing [39]. Engineered healing is warranted when autogenous healing is not adequate. Engineered self-healing is a process in which new substitute is incorporated into the cement material which is stimulated on crack propagation resulting in sealing of crack [54, 87].

Autogenous healing in concrete

Autogenous healing is a natural process of crack repair that occur in concrete in the presence of moisture and the absence of tensile stress. The repair is by a combination of mechanical blocking by particles carried into the crack with the water and the deposition of calcium carbonate from the cementitious material. Autogenous healing of cracks was reported due to the formation of calcium carbonate precipitation as consequence of water leakage through cracks [21]. Formation of calcite under wet conditions in cracks of concrete was also cited as a probable healing mechanism. Swelling and hydration of cement paste, blocking of flow path by water impurities or by concrete particles broken from crack surface, and precipitation of calcium carbonate crystals were suggested as possible chemical and physical mechanisms contributing to the autogenous healing [37]. Formation of calcite in the crack seems to be the sole cause for the autogenous healing and the crystal growth rate is dependent on the width of crack and water pressure, whereas concrete composition and water hardness have no influence on autogenous healing [32]. The water entering the cracks exhibits the pH value (5.5–7.5), CO_2 content and certain amount of Ca^{2+}. As the CO_2-containing water penetrates the hardened cement, it dissolves additional Ca^{2+} ions from $Ca(OH)_2$ and calcium silicate hydrate phase of cement resulting in a rise in the pH of water. At pH >8 conversion of in-water bicarbonates into carbonates and Ca^{2+} ion concentration favor precipitation of calcite. Reinhardt and Joss [63] reported that higher temperature favors a faster self-healing while cracks ≤0.10 mm can be closed by self-healing. The main limitation of autogenous healing is the maximum crack width that can be healed is rather limited (~0.1 mm). Concrete structures suffer from cracks that are much wider than that. Thus, engineered self-healing is essential.

Engineered self-healing in concrete

Supplementation of concrete with healing agents to stimulate the healing action to repair cracks is known as engineered self-healing. Many researchers used different healing agents and proposed their mechanisms on cementitious materials (Table 1). Three different approaches are used to incorporate self-healing material in concrete matrix and which activates its healing property when the crack appears in the structure. Based on the mechanisms, engineered self-healing concrete are classified as vascular based, capsule based and intrinsic based [15]. In vascular-based self-healing mechanism, healing material filled in hollow channels or fibers embedded in concrete matrix are released when damage ruptures the hollow channels or fibers (Fig. 1a). The healing agent stored in capsules is triggered through the release of healing material in concrete matrix when capsules are ruptured by damage (Fig. 1b). Intrinsic self-healing materials embedded directly in concrete matrix possess a latent self-healing functionality which is triggered by damage or by external stimulus (Fig. 1c) These materials rely on polymerizations, melting of thermoplastic phases or ionic interactions to initiate self-healing. In the domain of engineered self-healing concrete, incorporation of hollow glass tubes filled with adhesive chemicals in cement matrices was reported in earlier studies [31]. Use of polymer-based admixture was also reported to develop polymer modifying concrete or polymer modifying mortar [57]. Application of different polymer modifiers

Table 1 Overview of different healing agents and mechanism of healing action in cementitious matrix used by researchers

Agent	Mechanism of application	Crack-healing outcomes	References
Methyl methacrylate	Incorporation of hollow porous polypropylene fibers filled with healing agent in concrete structure	Reduction in permeability and enhancement in flexural toughening in active and passive mode, respectively	[31]
Polymer latex-modified mortar or concrete	Polymer latexes are used as admixtures in mortar and concrete or as grout repairing material	Micro-cracks under stress in modified concrete are bridged by polymer films and prevent crack propagation	[57]
Sikadur-52 (epoxy adhesive)	Artificial cracks installed during casting in concrete cube were repaired with epoxy resin by gravity filling method	Increase in tensile and compressive strength across a crack in epoxy repair was observed	[40]
Low-lime fly ash	Fly ash in ratios of 35 and 55% by mass of binder was added Load-induced micro-cracks created in specimens were stored in lime water for 30 days	Mechanical and permeation properties of cracked specimens recovered on self-healing action of fly ash	[66]
Expansive agent (C_4A_3S, $CaSO_4$, CaO) Chemical agent ($NaHCO_3$, Na_2CO_3) Geo-materials (montmorillonite)	Healing agents were used as admixture substitute in concrete specimens with cracks created artificially	Crack width of 0.2 mm was completely healed at 33-day curing due to swelling effect, expansion effect and re-crystallization	[9]
Expansive additive (calcium sulfoaluminate)	10% additive by mass of total cementitious material was admixed	Surface crack introduced in specimen was submerged in water. $CaCO_3$ precipitation healed the surface crack in specimen	[71]

like acrylic, styrene- butadiene latex, polyvinyl acetate and ethylene vinyl acetate in concrete crack sealing was reported by Fowler [34]. Studies based on engineered self-healing concrete investigated by researchers were epoxy repairing of cracks by injection method and gravity filling method [40], incorporation of high volume fly ash [66], expansive healing material, i.e., sodium aluminum silicate hydroxide containing swelling agent montmorillonite [9], crystalline additive and calcium sulfoaluminate-based expansive additive [71]. In aforementioned investigations, promising results in crack closure based on self-healing action were observed. This technology has some limitations depending on the healing agents and strategies applied. In order to select effective and reliable self-healing, care should be taken in choosing a healing agent and a suitable strategy for application [87]. Application of microbially induced carbonate precipitation (MICCP) in civil engineering has become a topic of research worldwide and this technology has been studied mainly for application in the fields of surface protection of building materials, crack remediation in concrete and soil improvement [28]. Adopting MICCP to fill the cracks is very innovative and is pollution free and natural.

Microbially induced calcium carbonate precipitation (MICCP)

MICCP is the capability of microbes to form calcium carbonate extracellularly through a metabolic activity. The phenomenon of mineral formation by living organism due to reaction of its metabolic products with the surrounding environment is called biomineralization. The property of mineral formation by different bacterial species like sulfate-reducing bacteria (SRB), silicate associated bacteria, unicellular cyanobacteria and urea degrading bacteria has been reported [30]. Hammes and Verstraete [38] reported four key factors such as (1) the calcium concentration; (2) the concentration of dissolved inorganic carbon (DIC); (3) the pH and (4) the availability of nucleation sites which influence the precipitation of $CaCO_3$. Sufficient calcium and carbonate ions are required for the $CaCO_3$ precipitation so that the ion activity product (IAP) exceeds the solubility constant (*K*so) as in Eqs. 1 and 2. From the comparison of the IAP with the *K*so the saturation state (Ω) of the system can be defined; if $\Omega > 1$ the system is oversaturated and precipitation is likely as [55]:

$$Ca^{2+} + CO_3^{2-} \leftrightarrow CaCO_3 \tag{1}$$

$$\Omega = \alpha(Ca^{2+})\alpha(CO_3^{2-})/K_{so} \quad \text{with} \quad K_{\text{so calcite},25^\circ} = 4.8 \times 10^{-9}. \tag{2}$$

The concentration of carbonate ions is related to the concentration of DIC and the pH of a given aquatic system. Also the concentration of DIC depends on several environmental

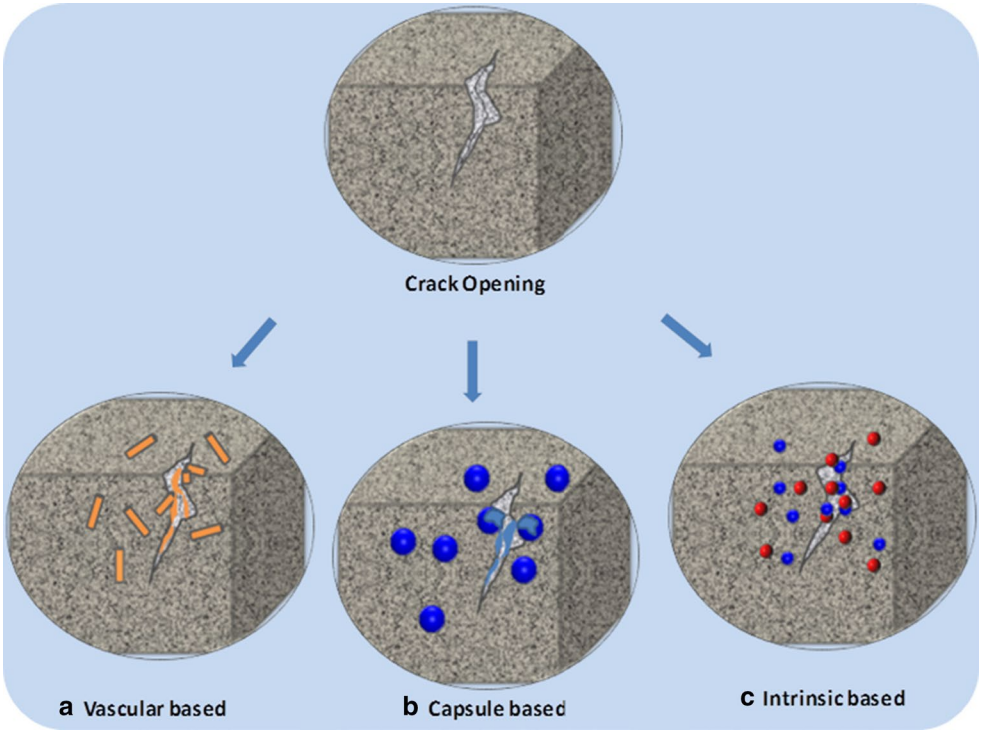

Fig. 1 Different approaches in engineered self-healing concrete. **a** In vascular-based self-healing, hollow channels filled with healing agent ruptures on damage and releases healing material. **b** In capsule-based self-healing, healing agent is released from ruptured capsules on damage. **c** In intrinsic based approach, healing agent possess latent self-healing functionality which is triggered on damage or by external stimulus

parameters such as temperature and the partial pressure of carbon dioxide (for systems exposed to atmosphere). The equilibrium reactions and the constants governing the dissolution of CO_2 in aqueous media (25 °C and 1 atm) are given in Eqs. 3, 4, 5 and 6 [73]:

$$CO_{2(g)} \leftrightarrow CO_{2(aq.)} \quad (pK_H = 1.468), \tag{3}$$

$$CO_{2(aq.)} + H_2O \leftrightarrow H_2CO_3^* \quad (pK = 2.84), \tag{4}$$

$$H_2CO_3^* \leftrightarrow H^+ + HCO_3^- \quad (pK_1 = 6.352), \tag{5}$$

$$HCO_3^- \leftrightarrow CO_3^{2-} + H^+ \quad (pK_2 = 10.329), \tag{6}$$

with $H_2CO_3^* = CO_{2(aq.)} + H_2CO_3$ Broadly two different metabolic pathways are involved in the process of biomineralization associated with the microorganisms: (1) autotrophic pathway and (2) heterotrophic pathway.

Autotrophic-mediated pathways

In autotrophic-mediated pathways, calcium carbonate precipitation is induced by microbes with the conversion of carbon dioxide in the presence of calcium ions in its immediate environment. Autotrophic precipitation of carbonates includes non-methylotrophic methanogenesis, anoxygenic photosynthesis and oxygenic photosynthesis [17, 18, 36, 68]. All of the three autotrophic pathways use carbon dioxide as a carbon source.

Heterotrophic-mediated pathway

In heterotrophic-mediated pathway, carbonate precipitation occurs either by sulphur cycle or by nitrogen cycle [18]. Sulphur cycle is carried out by sulphate reducing bacteria (SRB) via dissimilatory reduction of sulphate. In this process, environment must be anoxic and rich in organic matter, calcium and sulphate. As the organic matter is degraded by SRB, bicarbonate ions and hydrogen sulphide are produced by bacterial action using SO_4^{2-} as a terminal electron acceptor as shown in Eq. 7 [38, 56]. Elevation of pH in the surrounding environment due to degasification of hydrogen sulphide in the presence of Ca^{2+} induces the precipitation of calcium carbonate. In natural environment if anoxygenic sulphide-phototrophic bacteria are present, hydrogen sulphide is used by bacteria and anaerobically oxidized to sulphur. Uptake of hydrogen sulphide results in pH elevation and favors calcium carbonate precipitation. Peckmann et al. [58] reported the precipitation of aragonite crystals on dissolution of gypsum by the action of sulphate reducing bacteria. They reported that gypsum present in cavities provides the calcium ions for aragonite precipitation and sulfate ions for the metabolic processes of sulphate reducing bacteria as shown in Eq. 8. Degradation of organic matter in anaerobic conditions provides the increased alkaline condition and facilitates the formation of aragonite crystals.

$$2CH_2O + SO_4^{2-} \rightarrow H_2S + 2HCO_3^- \tag{7}$$

$$CaSO_4.2H_2O \rightarrow Ca^{2+} + SO_4^{2-} + 2H_2O. \tag{8}$$

Calcium carbonate precipitation by nitrogen cycle is further categorized into three different mechanisms: (1) ammonification of amino acids (presence of organic matter and calcium in aerobic conditions); (2) dissimilatory reduction of nitrate (presence of organic matter, calcium and nitrate in anaerobic conditions) and (3) urea degradation (presence of organic matter, calcium and urea in aerobic conditions) [17]. In all these mechanisms, carbonate and bicarbonate ions as well as ammonia (NH_3) are produced as a metabolic end product. Generation of ammonia creates high alkaline pH in the microenvironment of the bacterial cell and decreased H^+ concentration, affecting the carbonate–bicarbonate equilibria shift towards the production of CO_3^{2-} ions. Presence of calcium ions in the surrounding of bacterial cell results in the precipitation of calcium carbonate. Among the aforementioned mechanisms in heterotrophic pathway, microbially induced calcium carbonate precipitation via urea hydrolysis is widely used in various applications.

MICCP via urea hydrolysis

Microbially induced calcium carbonate precipitation via urea hydrolysis is an easily controlled mechanism in which high amounts of carbonates are produced by the ureolytic bacteria in short time period. In this mechanism, degradation of urea is catalyzed by microbial urease enzyme into carbonate and ammonium [72]. One mole of urea is hydrolyzed intracellularly to 1 mol of ammonia and 1 mol of carbamate which spontaneously hydrolyses to form 1 mol of ammonia and carbonic acid as shown in Eqs. 9 and 10:

$$CO(NH_2)_2 + H_2ONH_2 \xrightarrow{\text{Bacteria}} COOH + NH_3 \quad (9)$$

$$NH_2COOH + H_2O \longrightarrow NH_3 + H_2CO_3. \quad (10)$$

These products further equilibrate in water to form bicarbonate and 2 mol of ammonium and hydroxide ions (Eqs. 11, 12).

$$2NH_3 + 2H_2O \longleftrightarrow 2NH_4^+ + 2OH^- \quad (11)$$

$$2OH^- + H_2CO_3 \longleftrightarrow CO_3^{2-} + 2H_2O. \quad (12)$$

Generation of ammonia on the hydrolysis of urea results in pH increase creating an alkaline condition in the microenvironment around the bacterial cell [72]. Presence of calcium ions in the surroundings of bacterial cell wall results in the precipitation of calcium carbonate as the super-saturation is reached as shown in Eq. 13:

$$CO_3^{2-} + Ca^{2+} \longleftrightarrow CaCO_3. \quad (13)$$

The heterogeneous electronegatively charged bacterial cell wall acts as a nucleating site favoring the adsorption of positively charged cations (e.g., Ca^{2+}, Mg^{2+}) on the cell surface. In bacteria, negatively charged groups dominate over positively charged ones, giving the cell surface an overall anionic charge resulting the deposition of divalent positively charged metal ions on interaction [30]. Bacterial cell surface plays an important role in precipitation of calcium carbonate as nucleation site as shown in Eqs. 14, 15 and 16:

$$Ca^{2+} + \text{Cell} \longrightarrow \text{Cell}\,Ca^{2+}, \quad (14)$$

$$Cl^- + HCO_3^- + NH_3 \longrightarrow NH_4Cl + CO_3^{2-}, \quad (15)$$

$$\text{Cell} - Ca^{2+} + CO_3^{2-} \longrightarrow \text{Cell}\,CaCO_3. \quad (16)$$

Applications of MICCP in civil engineering

The potential and effectiveness of MICCP technology by using bacteria have been used widely in various fields. Several authors have reported the potential of MICCP property in the application of remediation of heavy metal and radionuclide contaminated ground water [35, 83], soil bioclogging [55, 75], restoration of stone monuments [22, 44, 64, 74] and durability enhancement of concrete structures [4, 6, 16, 25, 27, 47, 62]. To reduce the permeability and increase the shear strength of soil, MICCP was performed by using *Bacillus* sp. with urea and calcium solution by Chu et al. [20]. Martinez et al. [53] optimized the MICCP process for soil improvement by injecting *Sporosarcina pasteurii* in half-meter sand column in one-dimensional flow. Their study confirms that the most important factor for achieving uniform calcium carbonate precipitation is the distribution of microbes. Stocks-Fischer et al. [72] reported the urease activity of alkaliphilic bacteria to hydrolyze urea and high pH being the favorable condition for calcite precipitation in porous sand media.

To prevent the deterioration of monumental stones due to weathering action, application of MICCP as a conservative treatment has been reported by various researchers. Le Metayer-Levrel [51] reported the reduction in water absorption of limestone samples due to effective biocalcin coating by carbonatogenic bacteria. Tiano et al. [74] reported that limestone samples treated with *Micrococcus* sp., and *Bacillus subtilis* by brushing showed a reduction of about 60% in water absorption. Precipitation of calcite and vaterite crystals by *Myxococcus xanthus* resulted in efficient protection and consolidation in porous limestone [64]. Daskalakis et al. [22] reported effective vaterite precipitation on the marble sample treated with *Bacillus pumilus* strain isolated from a cave stone. Improved surface drilling resistance and reduction in water absorption was reported due to effective biocalcification on Globigerina limestone specimen treated with *B. subtilis* by spraying and poulticing [52].

The potential of MICCP application in cementitious materials to enhance the mechanical properties as well as permeability properties has been reported by various researchers as shown in Table 2. Precipitation of calcium carbonate by bacteria inside the cement matrix leads into pore refinement resulting in reduced permeability and increased compressive strength of concrete structure. Ramachandran et al. [62] reported increased compressive strength of cement mortar cubes on direct incorporation of live bacterial cells of *S. pasteurii* strain inside the cement matrix. De Muynck et al. [25] reported the effectiveness of pure and mixed ureolytic cultures in biodeposition on surface treatment of concrete. They observed that the use of pure culture of *B. sphaericus* resulted in more pronounced decrease in uptake of water and gas permeability than the use of mixed ureolytic culture. Achal et al. [6] reported the fly ash-amended mortar and concrete specimens on treatment with ureolytic bacterial strain *B. megaterium* showed improvement in strength and permeability properties. In our earlier reports, we have reported an increase in compressive strength of cement mortar specimen and energy-efficient green building materials by treating with bacteria [4, 27]. Kim et al. [47] investigated the distribution of calcium carbonate precipitation and capillary water absorption of concrete specimens after surface treatment with two bacterial strains, *B. sphaericus* and *S. pasteurii* individually. Denser calcium carbonate crystals and lowest weight increase was reported in specimens treated with *B. sphaericus* strain than the specimens treated with *S. pasteurii* strain. Bundur et al. [16] reported increased compressive strength of mortar specimen prepared with incorporation of vegetative bacterial cells than the control specimen. Application of halophilic bacteria *Exiguobacterium mexicanum* isolated from sea water showed 23.5% increase in compressive strength and 5 times reduction in water absorption on concrete specimens under 5% salt stress condition [12]. Kumari et al. [50] reported 49% increase in compressive strength by using non-ureolytic bacteria *Bacillus cohnii*. Our earlier studies showed that *Bacillus* sp. CT-5-treated reinforced concrete (RC) specimens reduced the corrosion rate, reduction in mass loss and increase in pullout strength than the control specimens [7]. Kalhori and Bagherpour [45] studied the effect of $CaCO_3$ precipitating bacteria *Bacillus subtilis* on healing and mechanical properties of shotcrete. Their results showed 30% increase in the compressive strength of bacteria-exposed shotcrete specimens compared to control specimens. The presence of bacteria in the mix design and curing solution enhanced the tensile strength, decreased the water absorption and porosity of shotcrete.

MICCP via urea hydrolysis by urease enzyme offers unlimited advantages in the field of carbonate precipitation, but limitation to the process include ammonia production, which have environmental concerns as well as risks of damage to concrete materials [26]. To overcome the problems associated with urea-based microbial carbonate precipitation, Zhu et al. [96] proposed an alternative technology using autophototrophic bacteria. Their studies showed that biomineralization of cyanobacteria *Synechococcus* PCC8806 formed a thick calcite-cell aggregate layer adhering to the concrete and decreased the water absorption and resistant to sonication. We proposed utilization of CO_2 as alternative source to urea in biocementation [46]. Urea was replaced with direct influx of CO_2 and studied the precipitation of carbonates by *Bacillus megaterium* SS3. The bacteria was able to grow well and precipitate carbonates with CO_2 influx and the amount of $CaCO_3$ precipitated is comparable with that of urea used for precipitation. Our results showed 117 and 47% improvement in compressive strength with respect to control and with urea-treated specimens and significant reduction in water absorption in concrete specimens [46]. Yeast extract often has been used as a carbon source in microbial induced precipitation of $CaCO_3$. Severe retardation of hydration kinetics has been observed due to the addition of yeast extract in cement. Williams et al. [86] replaced yeast extract with a combination of meat extract and sodium acetate in growth medium for *S. pasteurii*. Their results suggested that the medium reduced 75% retardation compared to yeast extract without compromising the growth, urea hydrolysis, cell zeta potential, and $CaCO_3$ formation. Zhu et al. [95] studied the MICCP by live and UV-killed phototrophic cyanobacteria *Gloeocapsa* PCC73106 in mortar specimens to enhance the durability properties. Their results suggested that treatments with live cells under illumination increased the amount of precipitates, while UV-killed cells increased the compressive strength, reduced water absorption and lowest porosity.

Bio-inspired applications in crack healing

Formation of crack is a commonly observed phenomenon in concrete structures. Though micro-crack formation may hardly affect the structural properties of constructions, increased permeability due to micro-crack networking substantially reduces the durability of concrete structures due to risk of ingress of aggressive substances particularly in moist environments. In order to increase the often observed autogenous crack-healing potential of concrete, specific healing agents are incorporated into the concrete matrix. Apart from the surface application and incorporation of live bacterial cells inside the cement matrix, use of bacteria as a self-healing agent is also evolved as new approach. Different methodologies have been adopted by researchers to test the compatibility of calcifying bacterial strains to heal the cracks autonomously (Table 3). Initially, the application of bacteria to remediate the cracks in cement mortar specimens

Table 2 Overview of applications of different microorganisms and nutrient media to prevent deterioration of monumental stones and cementitious materials with microbial $CaCO_3$ precipitation

Microorganism	Nutrient	Application	Mechanism of treatment	Evaluation of specimens	References
Micrococcus sp. *Bacillus subtilis.*	B_4 nutrient medium (calcium acetate, yeast extract, dextrose)	Monumental limestone conservation	Samples were brushed with bacteria and kept wet with B_4 medium for 15 days to feed the bacteria	Water absorption, colorimetric analysis, stone cohesion, SEM, XRD and FTIR of crystals	[74]
Myxococcus xanthus	Pancreatic digest of casein, calcium acetate, potassium carbonate	Porous ornamental limestone	Immersion of samples (shaking and stationary conditions) in bacterial culture with nutrient medium for 30 days	Weight increase, MIP, XRD, SEM analysis, sonication analysis.	[64]
M. xanthus	M-3P nutrient solution (pancreatic digest of casein, calcium acetate, potassium carbonate)	Archaeological gypsum plasters	Bacterial solution was sprayed till 6 days (twice a day) on the upper surface of sample	Drilling resistance analysis, TGA, XRD, SEM, MIP, TEM and colorimetric analysis	[44]
B. pumilus	Basic growth medium (bacteriological peptone, calcium acetate)	Marble substrate	Marble samples were sprayed every 12 h with bacterial culture for 15 days	Chromatic analysis, weight loss with ultrasonic treatment, XRD, SEM and FTIR	[22]
Sporosarcina pasteurii	Urea and calcium chloride medium	Porous sand column	Sand slurry mixed with bacterial cells and urea–$CaCl_2$ medium was fed with nutrient medium for 10 days	XRD, SEM, $CaCO_3$ estimation	[72]
S. pasteurii *Pseudomonas aeruginosa*	Urea and calcium chloride medium	Cement mortar	Casting of mortar cubes with bacterial cells and cured in urea–$CaCl_2$ medium	Compressive strength, XRD and SEM analysis	[62]
B. sphaericus	Urea, nutrient broth, calcium chloride and calcium acetate	Mortar and concrete specimens	Specimens were immersed in bacterial culture for 1 day prior to submersion in nutrient medium for 6 days	Compressive strength, sorptivity test, SEM, gas permeability, XRD, chromatic analysis of specimens	[25]
B. megaterium	Nutrient broth, urea and calcium chloride	Mortar and concrete specimens	NBU-bacteria and fly ash admixed specimens were prepared and cured with respective medium for 28 days	Compressive strength, water impermeability test, water absorption test and SEM analysis	[6]
Bacillus sp. CT-5	Nutrient broth, urea and calcium chloride	Cement mortar	Mortar mixture was admixed with NBU medium-bacterial cells and cured with respective medium for 28 days	Compressive strength, water absorption test and SEM analysis	[4]
B. megaterium SS3	Nutrient broth, urea and calcium chloride	Cement mortar blocks and cylinders	Bacterial-admixed specimens were cured by spraying with respective medium for 28 days	Water absorption test, SEM–EDX, XRD, MIP and $CaCO_3$ estimation of treated samples	[27]
S. pasteurii *B. sphaericus*	Nutrient broth, urea and calcium acetate	Concrete specimens	Specimen's top surface was wetted with nutrient medium containing *S. pasteurii* and *B. sphaericus* cells separately for 28 days	Water absorption test, SEM–EDX and XRD analysis	[47]
S. pasteurii	Urea, yeast extract medium	Cement mortar	Vegetative cells with UYE medium were added in mortar mixture while casting and cured by submersion in UYE medium with lime till 56 days	Hydration kinetics, compressive strength, TGA and XRD analysis	[17]

was investigated by Ramachandran et al. [62]. Cracks in cement mortar beams and cubes were simulated artificially with constant width 3.175 mm and different depths. Their results suggested that calcite precipitated during microbial growth enhanced the compressive strength of cracked mortar cubes. The mineralization process was effective in shallow cracks than in deeper ones because the bacteria grow more actively in presence of oxygen. To enhance the effectiveness of MICCP in remediation of deep cracks, polyurethane-immobilized *S. pasteurii* cells were used in cement matrices [11]. In cement mortar cubes (50.8 × 50.8 × 50.8 mm) with simulated cracks of width 3.18 and 25.4 mm crack depth, polyurethane strip encapsulating bacterial cells was placed in the cracks. Precipitation of calcite throughout of the crack matrices was reported as the polyurethane matrix provides protection to bacterial cells from the extreme alkaline nature of concrete. Jonkers et al. [42] used the spores of *Bacillus pseudofirmus* than vegetative cells as self-healing agent in concrete matrix to seal the cracks. The healing effect in freshly formed cracks appears on revival of immobilized spores by entering water and growth nutrients. To augment the potential of bacteria as a self-healing agent in crack filling, immobilization of bacterial cells with different carriers had been studied. The biochemical healing agent, consisting a mixture of viable but dormant bacteria and organic compounds packed in porous expanded clay particles to heal the cracks was proposed by Jonkers [41]. A two-dimensional mathematical model of bacterial crack healing was developed by Zemskov et al. [91] to estimate the influence of different parameters involved on the rate and quality of the crack healing. To protect the bacteria from strong alkaline environment of concrete, bacteria (*B. sphaericus*) immobilized in silica gel was investigated by Tittelboom et al. [75]. Standard cracks of width 0.3 mm with two depths of 10 and 20 mm were prepared in concrete samples by introducing thin copper plate in cement paste while casting. Realistic cracks with width range from 0.05 to 0.87 mm were also created in concrete cylinders of diameter 80 mm and height 75 mm by subjecting to splitting test and used for water permeability test. Specimens treated with silica gel-immobilized bacteria showed promising results in crack filling and low water permeability similar to epoxy-treated specimens.

Tziviloglou et al. [76] incorporated the bacteria-based healing agent into lightweight aggregates and mixed with fresh mortar and evaluated the recovery of liquid tightness after cracking and exposure to two different healing regimes (water immersion and wet–dry cycles) through water permeability tests. Their results revealed that the recovery of water tightness does not differ substantially for specimens with or without healing agent when immersed continuously in water. However, the recovery of water tightness increases significantly for specimens containing the healing agent compared to specimens without it, when subjected to wet–dry cycles. Sharma et al. [69] demonstrated the potential application of alkaliphilic *Bacillus pseudofirmus* in concrete crack repair by rapid spore production and germination, calcium carbonate formation in vitro and in situ.

The combination of non-ureolytic bacteria with organic calcium source as a two-component self-healing system was proposed by Jonkers et al. [43]. The organic calcium compounds are converted to calcium carbonate due to respiration effect of bacteria. They reported that by this method true self-healing can be achieved because all the components are added to the concrete mixture prior to casting and become an integral part of the concrete. Wiktor and Jonkers [84] incorporated a mixture of bacterial spores (*Bacillus alkalinitrilicus*) and calcium lactate embedded in expanded clay particles as self-healing agent in concrete. Multiple cracks of widths ranging from 0.05 to 1.0 mm were created in specimen on stretching embedded steel by applying tensile force. Cracked bacterial embedded specimens and control specimens were immersed in water to investigate the self-healing properties. It was reported that after 100 days of immersion in water, bacterial-based specimen showed crack-healing of up to 0.46 mm while in control it was only up to 0.18 mm (Fig. 2). Xu and Yao [88] investigated non-ureolytic bacterially induced $CaCO_3$ precipitation as a self-healing strategy for concrete cracking by using *Bacillus cohnii* spores. They suggested that incorporation of bacteria and calcium source nutrients as a two-component healing agent in concrete matrix induces $CaCO_3$ precipitation upon crack formation. Crack width in range of 0.1–0.4 mm was sealed completely as well as a layer of precipitates on the surface of specimen was reported in externally applied healing. They also reported that self-healing efficiency in specimens with incorporated bacterial spores and nutritional agents was higher than the control specimens. Higher efficiency of calcium carbonate precipitation in crack healing on external treatment and self-healing application was observed in calcium glutamate precursor than calcium lactate. However, Xu et al. [89] reported a higher rate of $CaCO_3$ precipitation with calcium lactate than calcium nitrate in case of ureolytic bacteria *Sporosarcina pasteurii*. Zhang et al. [92] reported that presence of excessive Ca^{2+} used in biomineralization not only inhibits the $CaCO_3$ precipitation, but also results in waste of the Ca^{2+} resource. They suggested that Ca^{2+} concentration lower than 30 mM is a good strategy for biomineralization process. A binary self-healing system consisting of oxygen releasing tablet (ORT) and bacteria (*Bacillus* H4) was developed to heal the cracks [93]. The ORT contains CaO_2 and lactic acid (9:1) which provides a stable oxygen supply and maintains pH (9.5–11.0) for effective metabolic activity.

We earlier reported the remediation of simulated cracks in mortar specimens (width 3 mm and depths of 13.4, 18.8, and 27.2 mm) by using bacterial strain *Bacillus* sp. CT-5 [8]. Our results showed an increase of 40 and 37% in compressive

strength in bacterial-treated specimen with crack depth of 13.4 and 27.2 mm, respectively, as compared to control. Successful healing of deepest crack of depth 27.2 mm was reported in bacterial-treated specimen (Fig. 3). Qian et al. [61] reported the healing of early age cracks in cement-based materials by carbonic anhydrase-producing bacteria *Bacillus mucilaginosus* L3. Their experimental results showed that the cracks formed at early ages were completely healed (up to 0.4 mm) due to bacterial treatment and the healing effect reduced with the increasing of cracking age. To protect bacteria from high pH environment of concrete, Wang et al. [78] used diatomaceous earth to immobilize the bacteria.

The immobilized bacteria healed the cracks with a width ranging from 0.15 to 0.17 mm compared to control specimens. Wang et al. [80] encapsulated bacterial spores into hydrogel and then incorporated into specimens to investigate their healing efficiency. Hydrogel was used because of its water retention properties and providing favorable microenvironment to bacterial spores with moisture and nutrients for activation. $CaCO_3$ precipitation by hydrogel-encapsulated spores was demonstrated by thermogravimetric analysis (TGA). Their findings suggest that sufficient amount of water is essential for the bacterial spores to achieve the realistic self-healing mechanism to seal the cracks. The mortar specimens with hydrogel-encapsulated spores healed crack width of about 0.5 mm and the water permeability was decreased by 68% compared to control where maximum healed crack width was 0–0.3 mm and the average water permeability was decreased only by 15–55% (Fig. 4).

Application of microcapsules as self-healing agent carrier in crack remediation was investigated by Wang et al. [81]. The spores of *B. sphaericus* were encapsulated in melamine-based microcapsules. They reported that the crack-healing ratio was much higher for specimens treated with bacteria compared to the ones without bacteria where 18–50% of crack area healed in control while it was 48–80% in the bacteria-treated specimens. The maximum crack width healed in the bacterial-treated specimens was 970 µm which was about 4 times wider than control (250 µm). Wang et al. [79] tested modified alginate-based hydrogel as encapsulating agent for application of *B. sphaericus* spores in concrete. Their results indicated efficient protection of the hydrogel for spores in concrete and great potential to be used for crack self-healing in concrete applications.

To reduce the operational cost of bio-based self-healing action in concrete, a new powderous material containing an efficient ureolytic microbial community (Cyclic EnRiched Ureolytic Powder or CERUP) has been developed [23]. CERUP was produced from a sub-stream of a vegetable treatment plant containing non-axenic bacterial culture with the ability to sporulate. After drying, it was ground to a particle size below 500 µm in diameter. Highest capacity of crack healing was observed in CERUP admixed specimen with complete crack closing up to 0.45 mm crack width after 4 weeks. In specimen without CERUP, autogenous crack healing was observed with closing of crack with 0.25 mm crack width (Fig. 5). Effective crack healing was performed by directly pooling the *S. pasteurii* culture supplemented with $CaCl_2$ and urea around the cracked area of fiber concrete beam [65]. They reported about 100% consolidation of the micro-cracks to a depth of approximately 20 mm. Silva et al. [70] analyzed the costs involved in biological self-healing in concrete and emphasized to develop the bio-additive at much lower costs to make the biological self-healing industrially applicable.

Apart from ureolytic pathway in MICCP, self-protected nitrate (NO_3^-) reducing bacteria was used for repair of concrete cracks [33]. Nitrate reducing bacteria was grown in enrichment culture by using concrete admixtures such as $Ca(NO_3)_2$ and $Ca(HCOO)_2$ as nutrients. The culture grown as granules (0.5–2.0 mm) consisting of 70% biomass and 30% inorganic salts was added into mortar without any additional protection. They reported that, more than 90% of the crack with 500 µm crack width was closed and 68% less water was absorbed by microbial specimen than the reference specimen upon 28-day immersion in water. In specimens cured for 6 months, in microbial specimen 90% crack closure was observed in cracks with crack width up to 400 µm and in reference specimen crack closure was 86% for 135 µm crack width. Their results suggested that enriched mixed denitrifying cultures structured in self-protecting granules are very promising strategies to enhance microbial self-healing.

The field-based potential of MICCP in sealing of sandstone fractures below the ground surface in wellbore using ureolytic bacteria was demonstrated by Phillips et al. [59]. Horizontally fractured sandstone 340.8 m below the ground surface was sealed with ureolytic bacterial strain *S. pasteurii* using conventional oil field delivery technology. In the field test, bacterial culture was injected into the fracture by using an 11.4 l wireline dump bailer for 4 days. Microbial suspensions after injection in fracture was allowed to attach for 1 h and later on the inoculum was amended with calcium containing growth solution (urea and nutrient broth) to promote the growth. In this treatment, 24 urea/calcium solution and 6 microbial suspensions were injected into the fracture zone for 4 days. They reported that the flow rate decreased from 1.9 to 0.47 L/min and in-well pressure falloff from >30% before to 7% after treatment. Their findings suggest that MICCP is a promising tool for sealing subsurface fractures in the near wellbore environment. To monitor the applications of MICCP nondestructively in time and space, Krikland et al. [48] used a low-field nuclear magnetic resonance (NMR) well-logging probe in a sand-filled bioreactor by inoculating *S. pasteurii* and pulsed injections of urea and calcium substrate. NMR signal amplitude and T_2 relaxation

Table 3 Overview of crack remediation in concrete using bacteria as crack-healing agent

Microorganism	Carrier material	Incubation treatment	Crack healing	References
Bacillus pasteurii	Cells mixed with sand	After microbial plugging mortar cubes were immersed in urea–$CaCl_2$ medium for 28 days	Crack with depth of 3.175 mm	[62]
Bacillus pasteurii	Polyurethane-immobilized cells	Incubated in urea–$CaCl_2$ medium for 28 days	Crack width of 3.18 mm and depth of 25.4 mm	[11]
Bacillus sphaericus	Cells immobilized in silica gel	Immersed in solution of urea and calcium source for 3 days	Crack width of 0.3 mm and depths of 10.0 and 20.0 mm	[75]
Bacillus alkalinitrilicus	Spores embedded in expanded clay with calcium lactate	Immersed in water for 100 days	Crack width ranging from 0.05 to 1.0 mm	[84]
Bacillus sp. CT-5	Cells mixed with sand	Immersed in urea and $CaCl_2$ medium for 28 days	Crack width of 3.0 mm and depths of 13.4, 18.8 and 27.2 mm	[8]
Bacillus sphaericus	Hydrogel-encapsulated spores with nutrient and calcium source	Submerged in water for 4 weeks with wet–dry cycle	Crack width of 0.5 mm	[80]
Bacillus cohnii	Treated externally	Submerged in medium containing bacterial spores, yeast extract and calcium source	Crack width ranging 0.1–0.4 mm	[88]
Bacillus sphaericus	Spores encapsulated in microcapsule	Immersed in water for 8 weeks with wet–dry cycle	Maximum crack width healed is 0.97 mm	[81]
Non-axenic ureolytic spores	Cyclic enriched ureolytic powder	Immersed in urea and de-mineralized water for 4 weeks	Crack healing of width 0.45 mm	[23]
Bacillus sphaericus	Spores encapsulated in modified alginate hydrogel	Fully immersed in water	NA	[79]

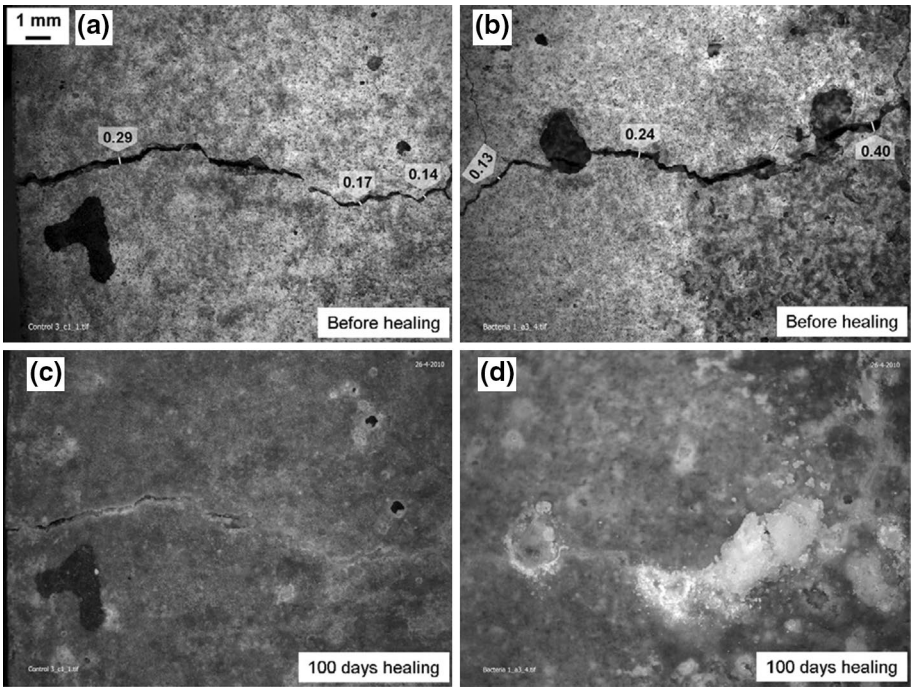

Fig. 2 Stereomicroscopic images of before and after crack-healing process in control (**a**, **c**) and bacterial-treated (**b**, **d**) mortar specimens, respectively Reprinted from Wiktor and Jonkers [84] with permission from Elsevier

were measured after the experiments. They reported that the water content in the reactor decreased to 76% of its initial value and changes in T_2 relaxation distributions due to changes in pore volume and surface mineralogy. Their results indicate the low-field NMR well-logging probe is sensitive to the physical and chemical changes caused by MICCP in a laboratory bioreactor. Wiktor and Jonkers [85] studied field performance of bacteria-based repair system of a two-story parking garage suffering from cracking and damaged concrete pavement due to freeze/thaw. Denitrifying bacteria supplemented with two solutions (1) Solution A (sodium silicate, sodium gluconate) and (2) Solution B (calcium nitrate) were treated by spraying manually until saturation of concrete. Crack-sealing efficiency was evaluated after 2 months of bacteria-based application in treated area of parking garage by means of water permeability test. Concrete pavement was also evaluated in resistance to freeze/thaw conditions and deicing salts by drilling cores from treated area. They reported that cracks that had not been treated with the bacteria-based repair system were still heavily leaking and freeze/thaw resistance of concrete was higher with the bio-based repair system than the untreated concrete. Tziviloglou et al. [77] described the various steps taken towards the outdoor applications of bio-based self-healing, for the laboratory-scale tests which have shown promising results.

The use of genetically modified microbes to heal the cracks is another area of research to improve the durability properties of concrete. The "BacillaFilla" is a genetically modified version of a *Bacillus subtilis* which contains cells that only germinate when they come into contact with the pH of concrete. Upon germination, the cells would descend into cracks in the concrete. The bacteria use quorum sensing to determine when sufficient bacteria have accumulated, triggering production of a mixture of calcium carbonate and a "bacterial glue", which combines with the bacterial cells to fill the crack [29]. Chattopadhyay and Sarkar [19] transformed the gene having silica-leaching attribute to a *Bacillus subtilis* and the transformed bacterial cells are utilized directly for enhancing the strength and durability properties of concrete structures. We earlier reported the development of phenotypic mutant of *Sporosarcina pasteurii* by UV irradiation, which enhanced the urease activity and also calcite production [2].

Conclusion and future perspectives

Bacterial remediation of cracks has shown very promising results. The main advantage of the bacterial system over the conventional systems is the lower viscosity of the bacterial cementation fluid. In case of cement grout or the polymeric resin healing, the ingredients are premixed before pumping into the cracks. As a result, the cementation reaction commences before the ingredients have reached the site of healing. While in case of the bacterial system, the bacteria are pumped in first. The cementation solution is then pumped where the ingredients are dissolved in water. The cementation reaction commences when the ingredients come in

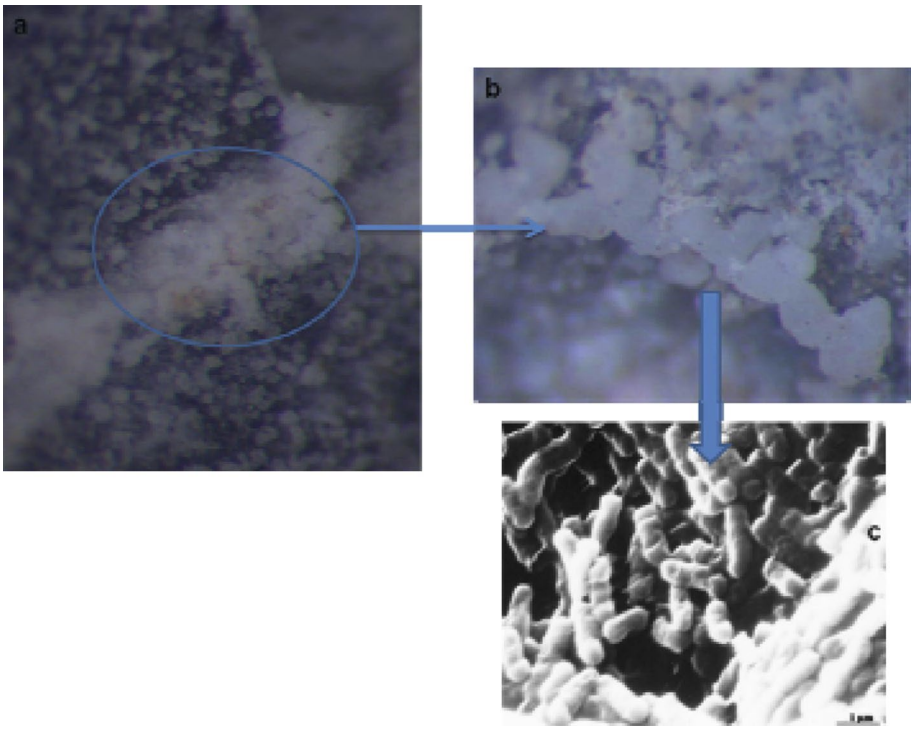

Fig. 3 Microscopic image of **a** remediated crack with **b** enlarged portion of remediated crack showing calcite precipitation and **c** rod-shaped bacteria Reprinted from Achal et al. [8] with permission from Elsevier

contact of the bacterial enzyme. Thus, bacterial healing is able to penetrate deep into the cracks. However, promising results from the microbial-based application in crack healing of concrete at lab scale have been reported. Researchers from all over the world have investigated the potential of biomineralization in crack remediation. The qualitative and quantitative evaluation of microbial application to heal the cracks in concrete are still reported in the lab scale. Some researchers have also reported encouraging results on the application of bacterial-based treatment at field scale. Some limitations which are necessary to be considered for application of this technology at commercial scale have been found. Use of laboratory grade nutrient sources in field applications is one of the economic limitations which restrict the use of this technology in several cases. Successful commercialization of the technique requires economical alternatives of the medium ingredients that cost as high as 60% of the total operating costs [49]. Use of inexpensive materials as nutrients may help to lower the cost of treatment [1, 3]. The other limitation in this application is external treatment of cracks in existing concrete structures. Efficiency of bacteria in $CaCO_3$ precipitation in deeper parts of the crack on external treatment has to be investigated. In field-scale experiments, effective curing method is to be investigated to provide sufficient amount of nutrients and water to the bacterial cells. Further investigations are needed to improve the microbial technology as an innovative crack-healing application for the commercial scale.

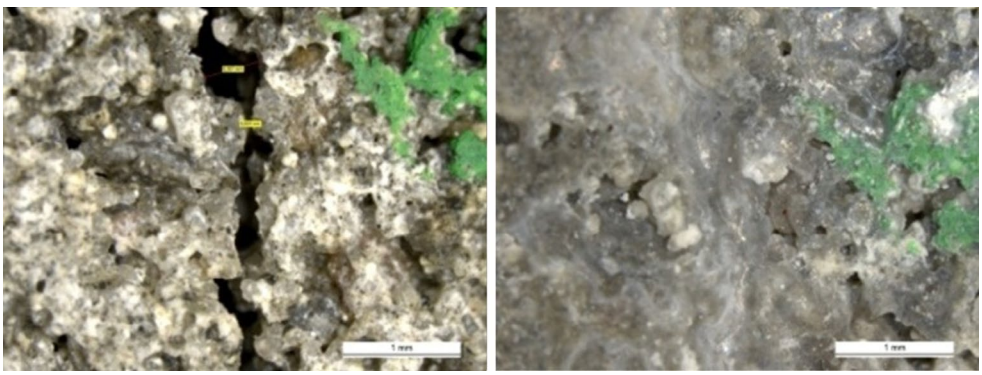

Fig. 4 Maximum crack width of 0.5 mm healed in the specimen treated with hydrogel-encapsulated bacterial spores Reprinted from Wang et al. [80] with permission from Elsevier

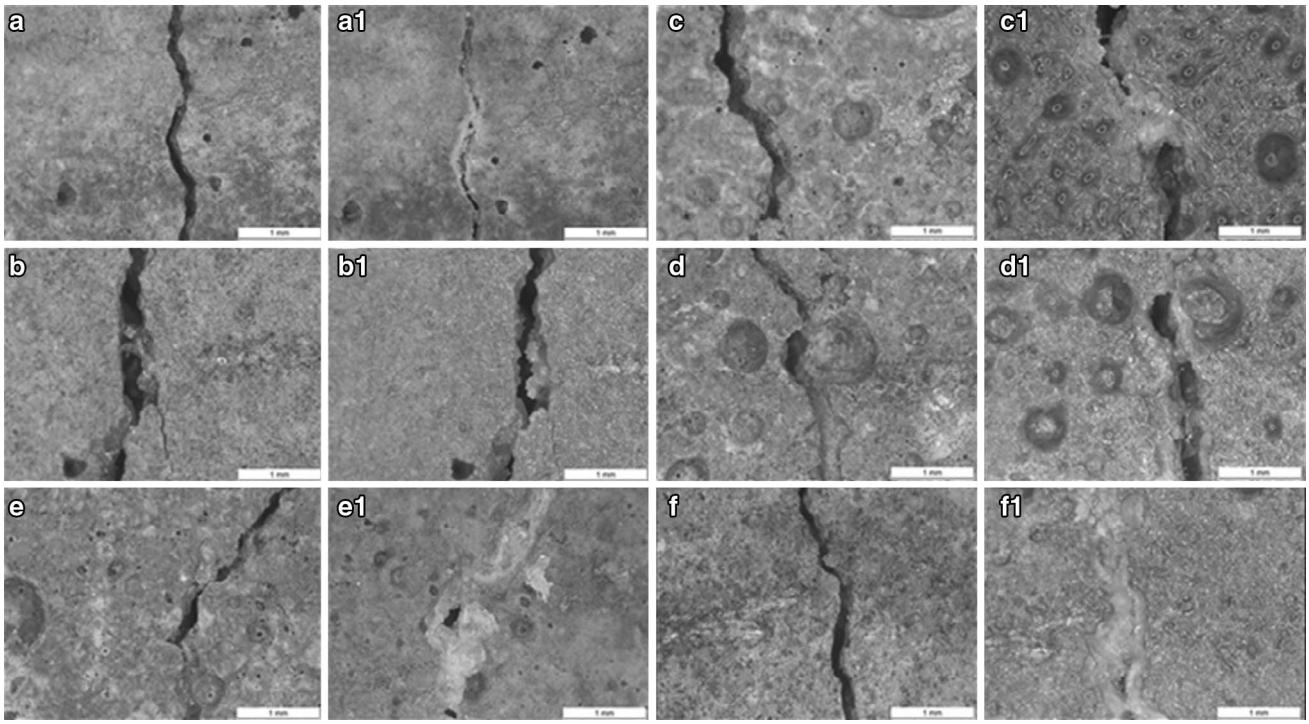

Fig. 5 Photomicrographs of cracked mortar specimens on day 0 and on day 28. **a**, **b** Reference samples on day 0 and **a1**, **b1** on day 28; **c, d** mortar samples containing 1% of autoclaved Cyclic EnRiched Ureolytic Powder (CERUP) on day 0 and **c1**, **d1** on day 28 (1). **e**, **f** Mortar samples containing 1% of CERUP on day 0 and **e1**, **f1** on day 28 Reprinted from Da Silva et al. [23] with permission from Elsevier

Acknowledgements Authors are thankful to Department of Science and Technology, Govt. of India, for providing financial support to carry out research in "Durability enhancement and prevention of damages in reinforced structures using bacteria (DST no: SB/S3/CEE/0063/2013)".

References

1. Achal V, Mukherjee A, Basu PC, Reddy MS (2009) Lactose mother liquor as an alternative nutrient source for microbial concrete production by *Sporosarcina pasteurii*. J Ind Microbiol Biotechnol 36:433–438
2. Achal V, Mukherjee A, Basu PC, Reddy MS (2009) Strain improvement of *Sporosarcina pasteurii* for enhanced urease and calcite production. J Ind Microbiol Biotechnol 36:981–988
3. Achal V, Mukherjee A, Reddy MS (2010) Biocalcification by *Sporosarcina pasteurii* using corn steep liquor as nutrient source. Ind Biotechnol 6:170–174
4. Achal V, Mukherjee A, Reddy MS (2011) Microbial Concrete: way to enhance the durability of building structures. J Mater Civil Eng 23:730–734
5. Achal V, Mukherjee A, Zhang Q (2016) Unearthing ecological wisdom from natural habitats and its ramifications on development of biocement and sustainable cities. Landsc Urban Plan 155:61–68
6. Achal V, Pan X, Özyurt N (2011) Improved strength and durability of fly ash-amended concrete by microbial calcite precipitation. Ecol Eng 37:554–559
7. Achal V, Mukherjee A, Goyal S, Reddy MS (2012) Corrosion prevention of reinforced concrete with microbial calcite precipitation. ACI Mater J 109:157–164
8. Achal V, Mukerjee A, Reddy MS (2013) Biogenic treatment improves the durability and remediates the cracks of concrete structures. Constr Build Mater 48:1–5
9. Ahn TH, Kishi T (2010) Crack self-healing behavior of cementitious composites incorporating various mineral admixtures. J Adv Concr Technol 8:171–186
10. Anbu P, Kang CH, Shin YJ, So JS (2016) Formations of calcium carbonate minerals by bacteria and its multiple applications. Springerplus 5:250
11. Bang SS, Galinat JK, Ramakrishnan V (2001) Calcite precipitation induced by polyurethane-immobilized *Bacillus pasteurii*. Enzyme Microb Technol 28:404–409
12. Bansal R, Dhami NK, Mukherjee A, Reddy MS (2016) Biocalcification by halophilic bacteria for remediation of concrete structures in marine environment. J Ind Microbiol Biotechnol 43:1497–1505
13. Basheer L, Kropp J, Cleland DJ (2001) Assessment of the durability of concrete from its permeation properties: a review. Constr Build Mater 15:93–103
14. Basheer PAM, Chidiac SE, Long AE (1996) Predictive models for deterioration of concrete structures. Constr Build Mater 10:27–37
15. Blaiszik BJ, Kramer SLB, Olugebefola SC, Moore JS, Sottos NR, White SR (2010) Self-healing polymers and composites. Annu Rev Mater Res 40:179–211
16. Bundur ZB, Kirisits MJ, Ferron RD (2015) Biomineralized cement-based materials: impact of inoculating vegetative bacterial cells on hydration and strength. Cem Concr Res 67:237–245
17. Castanier S, Le Me´tayer-Levrel G, Perthuisot JP (2000) Bacterial roles in the precipitation of carbonate minerals. Microbial sediments. Springer, Heidelberg, pp 32–39

18. Castanier S, Le Me´tayer-Levrel G, Perthuisot JP (1999) Ca-carbonates precipitation and limestone genesis—the microbiogeologist point of view. Sediment Geol 126:9–23
19. Chattopadhyay B, Sarkar M (2016) Genetically modified *Bacillus subtilis* bacterial strain for self-healing and sustainable green bioconcrete material. Org Chem Curr Res 5:3
20. Chu J, Stabnikov V, Ivanov V (2012) Microbially induced calcium carbonate precipitation on surface or in the bulk of soil. Geomicrobiol J 29:544–549
21. Clear CA (1985) The effect of autogenous healing upon leakage of water through cracks in concrete. Cem Concr Assoc (Tech Rpt 559)
22. Daskalakis MI, Rigas F, Bakolas A, Magoulas A, Kotoulas G, Katsikis I, Karageorgis AP, Mavridou A (2015) Vaterite bioprecipitation induced by *Bacillus pumilus* isolated from a solutional cave in Paiania, Athens, Greece. Int Biodeterior Biodegrad 99:73–84
23. Da Silva FB, De Belie N, Boon N, Verstraete W (2015) Production of non-axenic ureolytic spores for self-healing concrete applications. Constr Build Mater 93:1034–1041
24. De Belie N (2016) Application of bacteria in concrete: a critical review. RILEM Tech Lett 1:56–61
25. De Muynck W, Cox K, De Belie N, Verstraete W (2008) Bacterial carbonate precipitation as an alternative surface treatment for concrete. Constr Build Mater 22:875–885
26. De Muynck W, De Belie N, Verstraete W (2010) Microbial carbonate precipitation in construction materials: a review. Ecol Eng 36:118–136
27. Dhami NK, Reddy MS, Mukherjee A (2013) Bacillus megaterium mediated mineralization of calcium carbonate as biogenic surface treatment of green building materials. World J Microbiol Biotechnol 29:2397–2406
28. Dhami NK, Reddy MS, Mukherjee A (2013) Biomineralization of calcium carbonates and their engineered applications: a review. Front Microbiol 4:314
29. Dillow C (2010) Engineered bacteria can fill cracks in aging concrete. In: Popular Science. Available via DIALOG. http://www.popsci.com/science/article/2010-11/modified-bacterial-glue-can-shore-cracking-concrete. Accessed 14 Jul 2017
30. Douglas S, Beveridge TJ (1998) Mineral formation by bacteria in natural microbial communities. FEMS Microbiol Ecol 26:79–88
31. Dry C (1994) Matrix cracking repair and filling using active and passive modes for smart timed release of chemicals from fibres into cement matrices. Smart Mater Struct 3:118–123
32. Edvardsen C (1999) Water permeability and autogenous healing of cracks in concrete. ACI Mater J 96:448–455
33. Ersan YC, Gruyaert E, Louis G, Lors C, DeBelie N, Boon N (2015) Self-protected nitrate reducing culture for intrinsic repair of concrete cracks. Front Microbiol 6:1228
34. Fowler DW (1999) Polymers in concrete: a vision for the 21st century. Cem Concr Compos 21:449–452
35. Fujita Y, Redden GD, Ingram JC, Cortez MM, Ferris FG, Smith RW (2004) Strontium incorporation into calcite generated by bacterial ureolysis. Geochim Cosmochim Acta 68:3261–3270
36. Grengg C, Mittermayr F, Baldermann A, Böttcher ME, Leis A, Koraimann G, Grunert P, Dietzel M (2015) Microbiologically induced concrete corrosion: a case study from a combined sewer network. Cem Concr Res 77:16–25
37. Guppy R (1988) Autogenous healing of cracks in concrete and its relevance to radwaste repositories. NSS/R—105. Nirex, United Kingdom
38. Hammes F, Verstraete W (2002) Key roles of pH and calcium metabolism in microbial carbonate precipitation. Rev Environ Sci Biotechnol 1:3–7
39. Hearn N (1998) Self-sealing, autogenous healing and continued hydration: what is the difference? Mater Struct 31:563–567
40. Issa CA, Debs P (2007) Experimental study of epoxy repairing of cracks in concrete. Constr Build Mater 21:157–163
41. Jonkers HM (2011) Bacteria-based self healing concrete. Heron 56:1–12
42. Jonkers HM, Schlangen E (2007) Crack repair by concrete-immobilized bacteria. In: Proceedings of the first international conference on self-healing materials, pp 18–20
43. Jonkers HM, Thijssen A, Muyzer G, Copuroglu O, Schlangen E (2010) Application of bacteria as self-healing agent for the development of sustainable concrete. Ecol Eng 36:230–235
44. Jroundi F, Gonzalez-Muñoz MT, Garcia-Bueno A, Rodriguez-Navarro C (2014) Consolidation of archaeological gypsum plaster by bacterial biomineralization of calcium carbonate. Acta Biomater 10:3844–3854
45. Kalhori H, Bagherpour R (2017) Application of carbonate precipitating bacteria for improving properties and repairing cracks of shotcrete. Constr Build Mater 148:249–260
46. Kaur G, Dhami NK, Goyal S, Mukherjee A, Reddy MS (2016) Utilization of carbon dioxide as an alternative to urea in biocementation. Constr Build Mater 123:527–533
47. Kim HK, Park SJ, Han JI, Lee HK (2013) Microbially mediated calcium carbonate precipitation on normal and lightweight concrete. Constr Build Mater 38:1073–1082
48. Kirkland CM, Zanetti S, Grunewald E, Walsh WO, Codd SL, Phillips AJ (2017) Detecting microbially induced calcite precipitation in a model well-bore using downhole low-field NMR. Environ Sci Technol 51:1537–1543
49. Kristiansen B (2001) Process economics. In: Ratledge C, Kristiansen B (eds) Biotechnology, 2nd edn. Cambridge University Press, Cambridge
50. Kumari C, Das B, Jayabalan R, Davis R, Sarkar P (2017) Effect of nonureolytic bacteria on engineering properties of cement mortar. J Mater Civ Eng 29:06016024
51. Le Metayer-Levrel G, Castanier S, Orial G, Loubiere JF, Perthuisot JP (1999) Applications of bacterial carbonatogenesis to the protection and regeneration of limestones in buildings and historic patrimony. Sediment Geol 126:25–34
52. Micallef R, Vella D, Sinagra E, Zammit G (2016) Biocalcifying *Bacillus subtilis* cells effectively consolidate deteriorated Globigerina limestone. J Ind Microbiol Biotechnol 43:941–952
53. Martinez BC, DeJong JT, Ginn TR, Montoya BM, Barkouki TH, Hunt C, Tanyu B, Major D (2013) Experimental optimization of microbial-induced carbonate precipitation for soil improvement. J Geotech Geoenviron 139:587–598
54. Mihashi H, Nishiwali T (2012) Development of engineered self-healing and self-repairing concrete. J Adv Concr Technol 10:170–184
55. Morse JW (1983) The kinetics of calcium carbonate dissolution and precipitation. Rev Miner Geochem 11:227–264
56. Muyzer G, Stams AJ (2008) The ecology and biotechnology of sulphate-reducing bacteria. Nat Rev Microbiol 6:441–454
57. Ohama Y (1998) Polymer-based admixtures. Cem Concr Compos 20:189–212
58. Peckmann J, Paul J, Thiel V (1999) Bacterially mediated formation of diagenetic aragonite and native sulfur in Zechstein carbonates (Upper Permian, Central Germany). Sediment Geol 126:205–222
59. Phillips AJ, Cunningham AB, Gerlach R, Hiebert R, Hwang C, Lomans BP, Westrich J, Mantilla C, Kirksey J, Esposito R, Spangler L (2016) Fracture sealing with microbially-induced calcium carbonate precipitation: a field study. Environ Sci Technol 50:4111–4117
60. Phillips AJ, Gerlach R, Lauchnor E, Mitchell AC, Cunningham AB, Spangler L (2013) Engineered applications of ureolytic biomineralization: a review. Biofouling 29:715–733

61. Qian C, Chen H, Ren L, Luo M (2015) Self-healing of early age cracks in cement-based materials by mineralization of carbonic anhydrase microorganism. Front Microbiol 6:1225
62. Ramachandran SK, Ramakrishnan V, Bang SS (2001) Remediation of concrete using micro-organisms. ACI Mater J 98:3–9
63. Reinhardt HW, Jooss M (2003) Permeability and self-healing of cracked concrete as a function of temperature and crack width. Cem Concr Res 33:981–985
64. Rodriguez-Navarro C, Rodriguez-Gallego M, Chekroun KB, Gonzalez-Mun˜oz MT (2003) Conservation of ornamental stone by *Myxococcus xanthus*-induced carbonate biomineralization. Appl Env Microbiol 69:2182–2193
65. Richardson A, Coventry K, Pasley J (2016) Bacterial crack sealing and surface finish application to concrete. In: fourth international conference on sustainable construction materials and technologies http://www.claisse.info/Proceedings.htm
66. Sahmaran M, Keskin SB, Ozerkan G, Yaman IO (2008) Self-healing of mechanically-loaded self-consolidating concretes with high volumes of fly ash. Cem Concr Compos 30:872–879
67. Sangadji S (2017) Can self-healing mechanism helps concrete structures sustainable? Procedia Eng 171:238–249
68. Seifan M, Samani AK, Berenjian A (2016) Bioconcrete: next generation of self-healing concrete. Appl Microbiol Biotechnol 100:2591–2602
69. Sharma TK, Alazhari M, Heath A, Paine K, Cooper RM (2017) Alkaliphilic *Bacillus* species show potential application in concrete crack repair by virtue of rapid spore production and germination then extracellular calcite formation. J Appl Microbiol 122:1233–1244
70. Silva FB, Boon N, De Belie N, Verstraete W (2015) Industrial application of biological self-healing concrete: challenges and economical feasibility. J Commer Biotechnol 21:31–38
71. Sisomphon K, Copuroglu O, Koenders EAB (2012) Self-healing of surface cracks in mortars with expansive additive and crystalline additive. Cem Concr Compos 34:566–574
72. Stocks-Fischer S, Galinat JK, Bang SS (1999) Microbiological precipitation of $CaCO_3$. Soil Biol Biochem 31:1563–1571
73. Stumm W, Morgan JJ (1981) Aquatic chemistry. John wiley, NewYork
74. Tiano P, Biagiotti L, Mastromei G (1999) Bacterial bio-mediated calcite precipitation for monumental stones conservation: methods of evaluation. J Microbiol Methods 36:139–145
75. Tittelboom KV, De Belie N, De Muynck W, Verstraete W (2010) Use of bacteria to repair cracks in concrete. Cem Concr Res 40:157–166
76. Tziviloglou E, Wiktor V, Jonkers HM, Schlangen E (2016) Bacteria-based self-healing concrete to increase liquid tightness of cracks. Constr Build Mater 122:118–125
77. Tziviloglou E, Tittelboom KV, Palin D, Wang J, Sierra-Beltran MG, Erşan YC, Mors R, Wiktor V, Jonkers HM, Schlangen E, De Belie N (2016) Bio-based self-healing concrete: from research to field application. In: Hager M, van der Zwaag S, Schubert U (eds) Self-healing materials. Advances in polymer science. Springer, Cham, pp 345–385
78. Wang JY, De Belie N, Verstraete W (2012) Diatomaceous earth as a protective vehicle for bacteria applied for self-healing concrete. J Ind Microbiol Biotechnol 39:567–577
79. Wang J, Mignon A, Snoeck D, Wiktor V, Vliergerghe SV, Boon N, De Belie N (2015) Application of modified alginate encapsulated carbonate producing bacteria in concrete: a promising strategy for crack self-healing. Front Microbiol 6:1088
80. Wang JY, Snoeck D, Vlierberghe SV, Verstraete W, De Belie N (2014) Application of hydrogel encapsulated carbonate precipitating bacteria for approaching a realistic self-healing in concrete. Constr Build Mater 68:110–119
81. Wang JY, Soens H, Verstraete W, De Belie N (2014) Self-healing concrete by use of microencapsulated bacterial spores. Cem Concr Res 56:139–152
82. Wang J, Ersan YC, Boon N, De Belie N (2016) Application of microorganisms in concrete: a promising sustainable strategy to improve concrete durability. Appl Microbiol Biotechnol 100:2993–3007
83. Warren LA, Maurice PA, Parmar N, Ferris FG (2001) Microbially mediated calcium carbonate precipitation: implications for interpreting calcite precipitation and for solid-phase capture of inorganic contaminants. Geomicrobiol J 18:93–115
84. Wiktor V, Jonkers HM (2011) Quantification of crack-healing in novel bacteria-based self-healing concrete. Cem Concr Compos 33:763–770
85. Wiktor V, Jonkers HM (2015) Field performance of bacteria-based repair system: pilot study in a parking garage. Case Stud Constr Mater 2:11–17
86. Williams SL, Kirisits MJ, Ferron RD (2016) Optimization of growth medium for *Sporosarcina pasteurii* in bio-based cement pastes to mitigate delay in hydration kinetics. J Ind Microbiol Biotechnol 43:567–575
87. Wu M, Johannesson B, Geiker M (2012) A review: self-healing in cementitious materials and engineered cementitious composite as a self-healing material. Constr Build Mater 28:571–583
88. Xu J, Yao W (2014) Multiscale mechanical quantification of self-healing concrete incorporating non-ureolytic bacteria-based healing agent. Cem Concr Res 64:1–10
89. Xu J, Du Y, Jiang Z, She A (2015) Effects of calcium source on biochemical properties of microbial $CaCO_3$ precipitation. Front Microbiol 6:1366
90. Yuan YC, Rong MZ, Zhang MQ, Chen J, Yang GC, Li XM (2008) Self-healing polymeric materials using epoxy/mercaptan as the healant. Macromolecules 41:5197–5202
91. Zemskov SV, Jonkers HM, Vermolen FJ (2014) A mathematical model for bacterial self-healing of cracks in concrete. J Intell Mater Syst Struct 25:4–12
92. Zhang JL, Wu RS, Li YM, Zhong JY, Deng X, Liu B, Han NX, Xing F (2016) Screening of bacteria for self-healing of concrete cracks and optimization of the microbial calcium precipitation process. Appl Microbiol Biotechnol 100:6661–6670
93. Zhang JL, Wang CG, Wang QL, Feng JL, Pan W, Zheng XC, Liu B, Han NX, Xing F, Deng X (2016) A binary concrete crack self-healing system containing oxygen-releasing tablet and bacteria and its Ca^{2+}-precipitation performance. Appl Microbiol Biotechnol 100:10295–10306
94. Zhu T, Dittrich M (2016) Carbonate precipitation through microbial activities in natural environment, and their potential in biotechnology: a review. Front Bioeng Biotechnol 4:4
95. Zhu T, Lu X, Dittrich M (2017) Calcification on mortar by live and UV-killed biofilm-forming cyanobacterial *Gloeocapsa* PCC73106. Constr Build Mater 146:43–53
96. Zhu T, Paulo C, Merroun ML, Dittrich M (2015) Potential application of biomineralization by *Synechococcus* PCC8806 for concrete restoration. Ecol Eng 82:459–468

Construction and Building Materials 263 (2020) 120170

Contents lists available at ScienceDirect

Construction and Building Materials

journal homepage: www.elsevier.com/locate/conbuildmat

Review

Influence of biogenic treatment in improving the durability properties of waste amended concrete: A review

Sumit Joshi [a], Shweta Goyal [b], M. Sudhakara Reddy [a,*]

[a] Department of Biotechnology, Thapar Institute of Engineering & Technology, Patiala 147004, Punjab, India
[b] Department of Civil Engineering, Thapar Institute of Engineering & Technology, Patiala 147004, Punjab, India

HIGHLIGHTS

- Utilization of industrial byproducts in construction industry reduces environmental burden.
- Replacement of cement and aggregates with these byproducts substantiate the resources.
- Application of MICP technology to enhance the durability of concrete structures is well documented.
- MICP improves the durability properties of waste amended concrete structures.

ARTICLE INFO

Article history:
Received 11 October 2019
Received in revised form 11 May 2020
Accepted 7 July 2020

Keywords:
Biomineralization
Industrial waste
Ureolytic bacteria
Calcium carbonate
Microbial concrete
Sustainability

ABSTRACT

Bio-precipitation of calcium carbonate through microorganisms has a potential to enhance the durability properties of concrete structures. Microbially induced calcium carbonate precipitation (MICP) has widely been studied and practiced in various applications such as soil consolidation, stone monument restoration and improving the durability properties of concrete. Nowadays use of various industrial by-products or waste materials as a complete or partial replacement of cement and aggregates is practiced to attain sustainable production of concrete. This review article provides the state-of-the-art of recent developments in improving the durability properties of industrial by-product amended concrete combined with the usage of MICP. Recent advances in this review provide insights toward the future developments in introduction of microbial treatment in waste amended concrete.

Contents

* Corresponding author.
E-mail address: msreddy@thapar.edu (M. Sudhakara Reddy).

https://doi.org/10.1016/j.conbuildmat.2020.120170
0950-0618/

1. Introduction

The most frequently used construction material in the world is concrete due to its high durability, ability to mould into different shapes, low production cost and ease of use, which has become attractive than other building materials. Understandably, an overwhelmingly large proportion of infrastructure is built with concrete. With global industrialization and urbanization, demand for infrastructure expansion has increased [1]. Production of concrete has experienced an increased demand to accompany innumerable infrastructure developments [2]. With the ever-growing worldwide demands, yearly consumption of concrete approaches 30 billion tons [3]. Consequently, high levels of concrete production results into high consumption of basic raw materials [2]. Concrete is a mixture of essential constituents like cement, aggregates and water. Ordinary concrete consists of 12% cement and 80% aggregates by weight. To meet the demands of large volumes of concrete making, global cement and aggregate consumption is estimated to be 4 Gt and 17.5 Gt respectively [2]. Globally, production of cement has been escalating to meet the growing need of construction projects. In the database of statisa portal the search of "Major countries in worldwide cement production" shows China and India are top cement producers globally followed by USA [4]. Estimated production of cement in China and India was 2.4 billion metric tons and 290 million metric tons in year 2018 respectively. The cement production and natural aggregate extraction are highly intensive energy consuming as well as a major CO_2 emitting process [5]. Production of conventional concrete contributes approximate 8–9% of the global anthropogenic CO_2 emissions [2]. Carbon dioxide emissions from the cement processing unit play a significant contribution in greenhouse gas (GHG) [6]. In a cement industry, process of calcination of carbonate minerals is one of the potential sources of CO_2 emission [7]. Extraction of aggregates from mining and processing also contribute in environmental impacts including resource depletion, degradation of ground and surface water and global warming [8,9]. Sand used in construction as a major portion is also extracted from rivers and beaches. Extensive sand mining induce erosion, degradation of ecosystem and biological environments of river systems [10,11]. Use of large amounts of fresh water in concrete industry is also a serious environmental concern. Concrete industry being the largest industrial consumer, its global water requirement is 1 trillion Liter per year [12]. Fresh water shortage is one of the significant problems these days. Thus, the embodied energy and emission of conventional concrete is relatively high.

To minimize the development cost and environmental burden contributed by concrete and construction industry, several approaches by researchers have been adopted to develop a sustainable technology [13]. Several studies have been carried out to minimize the consumption of natural resources by utilizing industrial waste and by-products as a supplementary cementitious materials (SCM). Utilization of different SCM in cement industry as replacement of Portland clinkers is already well into the use [14]. Similarly, to reduce the extraction of natural aggregates, utilization of various waste materials as well as recycled concrete waste has been used to improve the durability properties of concrete and to achieve sustainable construction.

With the advancement in concrete research, application of biotechnology in the field of civil engineering led to the development of a new area called "microbial concrete". Microbial concrete is a biobased approach, in which cementitious structures are treated with bacteria capable of $CaCO_3$ precipitation through biomineralization process [15]. This innovative bacterial application has attracted researchers for its positive benefits in enhancing the durability features of concrete structures. Many research articles have reported the effectiveness of this nature inspired technology in quality improvement of building materials [16,17,18].

This paper discusses a comprehensive review on the development of sustainable construction by utilizing waste by-products and eco-friendly microbial treatment. This paper focuses on detailed sections of waste recycling in construction and role of microbial treatment in improving its quality. The schematic representation of waste amended concrete along with MICP treatment is shown in Fig. 1.

2. Waste by-products in construction material

Currently, a considerable quantity of waste materials is generated globally as by-products from different industrial units. Substantial volume of waste materials produced from industry has a problem of accumulation in landfills. Many research articles have been published on the utilization of by-products of industries as cement substitute (e.g. flyash, steel slag, silica fumes, rice husk ash and metakaolin) and aggregate replacement (e.g. copper slag, marble waste, waste foundry sand and concrete demolished waste).

2.1. Substitute to cement

"Portland cement" (PC) is an essential component of conventional concrete which on contact with water form calcium silicate hydrate gels as hydration products. Cement acts as a binder in mortar and concrete. With increasing demand of PC, its environmental impact during manufacturing is a great concern. To reduce the carbon footprints of PC production, use of SCM is increasing worldwide. Two categories of SCM: (i) self-cementing and (ii) pozzolanic are reported according to their hydraulic reactions [19]. A variety of potential SCM generated from industrial wastes has been investigated. Improvement of the durability properties of cementitious structures by utilizing different SCM as replacement of cement is reviewed below. Different approaches adopted by various researchers to utilize different SCM as partial replacement of cement is shown in Table 1.

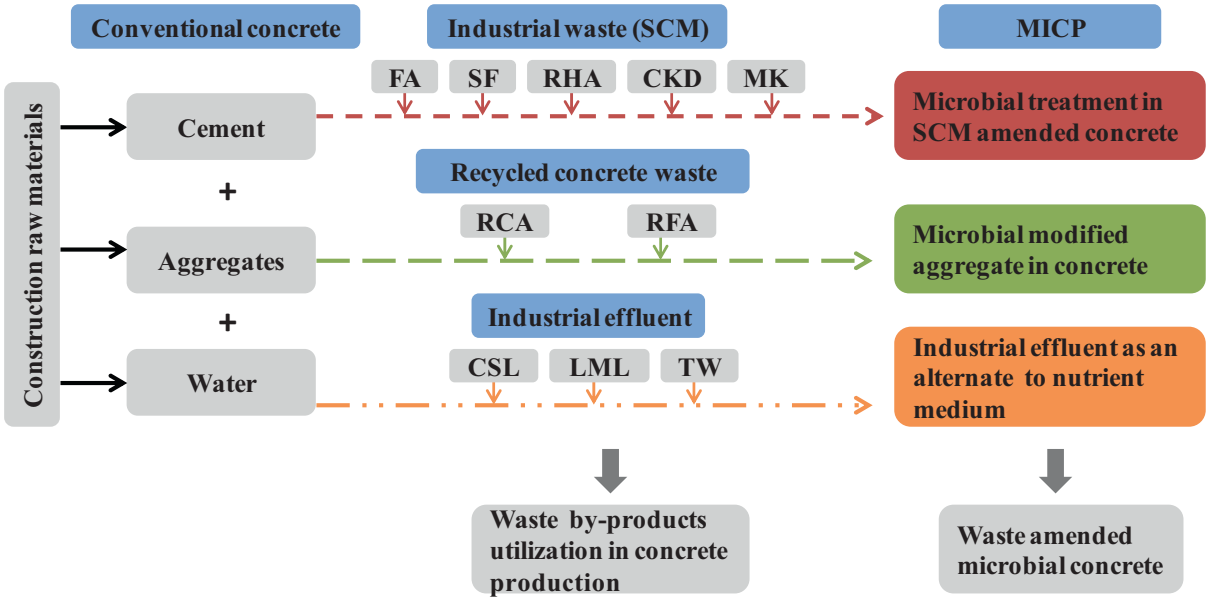

Fig. 1. Schematic illustration of microbial treatment of waste amended concrete.

2.1.1. Flyash

With the beginning of coal power plants, millions of tons of fly-ash (FA) as by-product have been generated every year. Amount of FA released from thermal power plants is increasing throughout the world. Utilization of FA as SCM in cement production by 2050 was estimated to reach the clinker fraction by 71% [20]. Use of FA as a pozzolanic material has been widely applied as a replacement of high volumes of Portland cement for the sustainable construction [21]. Many researchers evaluated the use of FA in concrete with different dosages and proposed different approaches to incorporate it in concrete matrix. Applicable limit of FA according to British standard as well as Indian standard was reported to be a maximum of 35% by mass of cement [21]. Influence of graded fine FA with the dosage of 40% on the strength of mortar was reported [22]. Significant improvement in mechanical properties as well as sulfate resistance was reported with incorporation of very fine FA. In another study, cement was replaced with original fly ash as well as classified fine FA. Their results showed a significant decrease in the pore sizes of fine FA blended cement paste than the coarser FA incorporated cement paste because the finer FA enhanced nucleation effect, pozzolanic reaction and packing [23]. Use of high-volume fly ash (HVFA) with levels up to 45% by mass of cement was also enhanced durability properties in combination with rapid hardening Portland cement [24]. The compressive strength, flexural strength and splitting tensile were improved at 50% cement replacement ratio among the

mixtures, when FA based geopolymer was replaced cement at different ratios (0%, 25%, 50%, 75% and 100%) [25]. The approach of using carbonated flyash (CFA) by utilizing CO_2 to prepare blended cement paste with different replacement levels (10%, 20% and 30%) was investigated [26]. It was reported that the effect of 10% CFA replacement shows better results in enhancing compressive strength than 30% replacement levels. On the whole, utilization of FA in construction industry has improved the performance of concrete with low carbon footprints.

2.1.2. Steel slag

Steel Slag (SS) is a metallurgical waste by-product generated from different sources like iron, steel (categorized as ferrous) and copper (categorized as non-ferrous) extraction units. Environmental impacts of these metallurgical by-products have been associated with their unsystematic dumping in landfills [27]. Recycling and utilization of these industrial wastes as a substitute to cement in construction industry helps in sustainable production of concrete [28,29]. Addition of SS with 10.5% replacement ratio to cement and its effect on the physico-mechanical properties was investigated [30]. It was reported that the values of setting times, water demand and expansion were not affected on the addition of SS and remained similar to reference sample. Compressive strengths of SS amended and reference mortars remained similar. In another study, cement was partially replaced by 50% with low MnO granulated metallurgical slag [31]. The composition of 50:50 blends met the IS 455:1989 standards for Portland slag cements. Beyond 50% replacement, strength loss in mortar specimens was reported. Influence of various replacement ratios along with the fineness of SS was also investigated by researchers. In an investigation, fineness of SS (approx. 4400 cm^2/g) with 30% replacement of cement indicates better compressive strength conforms to ASTM C150 standard [32]. It was also reported that setting time and slag-activity index of fine SS shows strong cementing properties. Significant enhancement of early and the late cementitious properties with the increasing fineness of SS was also reported [33]. The compressive strength and drying shrinkage in SS amended concrete was investigated with different water to binder (W/B) ratio [34]. High W/B ratio (0.5) was reported to have negative impact on strength and shrinkage of concrete. However, low W/B ratio (0.35) in 30% SS amended concrete was reported to have similar compressive strength and shrinkage as that of control concrete. Replacement of cement with three different percentages (10%, 20% and 30%) of variously processed SS showed that cement up to 20% with crushed SS and finer than 125 μm improved the compressive strength [35].

2.1.3. Silica fume

Silica fume (SF) or silica dust is an industrial waste generated through smelting process of silicon and ferrosilicon industry. It contains high content of silicon (75%) and is considered as a very effective pozzolanic material [36]. Utilization of SF as substitute for cement has been reported by many researchers. In an investigation, different dosages of SF (5%, 10%, 15%, 20%, and 25%) were used as replacement to cement [37]. The late significant gains in compressive strength was reported at the age of 56 days on the

Table 1
Summary of effects of partial replacement of cement with different industrial by-products as SCM in mortar and concrete.

SCM type	Evaluation Method					
	Compressive strength	Drying shrinkage	Split tensile strength/Flexural strength	Water absorption/Chloride penetration	Suggested replacement	References
Fly ash	↑	↓	–	–	40% very fine FA in cement mortar	[22]
	↑	↓	–	↓	45% high volume FA in concrete	[24]
	↑	–	↑	–	50% FA based geopolymer in concrete	[25]
	↑	–	–	–	10% carbonated FA	[26]
Steel slag	↑	–	–	–	30% fine SS in cement mortar	[32]
	↑	–	–	–	(20% −45%) fine SS in cement mortar	[33]
	↑	↓	–	↓	30% SS and low W/B ratio (0.35) in concrete	[34]
	↑	↓	↑	–	20% crushed SS finer than 125 μm in cement mortar	[35]
Silica fume	↑	–	↑	–	(15% – 20%) SF in concrete	[37]
	↑	↓	–	–	15% SF in concrete	[38]
	↑	–	–	↓	(5%-7.5%) SF along with 15% SS in concrete	[39]
Rice husk ash	↑	–	↑	↓	30% RHA in concrete	[43]
	↑	–	↑	↓	20% ultra fine RHA in concrete	[44]
	↑	–	–	–	20% ground RHA in concrete	[45]
	↑	–	↑	↓	(20–25%) RHA and 10% micro-silica in concrete	[46]
	↑	↓	–	↓	(10%-15%) Metakaolin in cement mortar	[50]
	–	–	–	↓	(8% −12%) high reactive metakaolin in concrete	[51]
	↑	–	–	↓	10% Metakaolin in cement mortar	[52]
	↑	–	–	↓	(10% – 12.5%) Metakaolin in concrete	[53]

↑ Denotes the "increase" in the observed trend being reported.
↓ Denotes the "decrease" in the observed trend being reported.
- Denotes "no data" being reported.

replacement of cement with up to 15% to 20% of SF. In another study, replacement of cement with various dosages of SF (6%, 10% and 15%) was studied. After 28 days curing, there was an increase of 21% strength 15% SF supplement than the control [38]. However, after 90 days of age, no increment in the compressive strength was reported. Effect of SF (2.5%, 5%, 7.5% and 10%) incorporation along with low reactivity slag (15%, 30% and 50%) in concrete was also reported [39]. SF at the dosage of 5% along with 15% slag in concrete mix was reported to improve the durability properties.

2.1.4. Rice husk ash

Rice husk is an agricultural waste generated in millions of tons per year from rice plant. After milling process of paddy, 22% of its total weight is obtained as rice husk. Rice husk ash (RHA) is obtained after burning of husk, which contains around 85–90% silica with high pozzolanicity property [40]. RHA is used as SCM in cement replacement in concrete production due to its high silica content, [41]. Various research articles are documented in utilization of RHA as partial or complete replacement of cement [42]. It was reported that, 20% of RHA replacement in cement significantly improved compressive strength and at 30% replacement the strength remain equivalent to control concrete specimen [43]. Reduction in water permeability (35%) and chloride permeation (75%) was reported in 30% RHA blended concrete. In other research work, cement was replaced with ultrafine RHA with different dosage percentages (10%, 15%, and 20%) and reported that 20% replacement of cement with ultrafine RHA achieved superior performance compared to control concrete [44]. When concrete mixes were prepared by replacing cement with different doses of RHA such as 10%, 20% and 30% along with 0.35 ratio of W/B, the compressive strength of concrete blended with 20% RHA attained equivalent values as that of control after 28 days of curing [45]. Increase in compressive strength by 20% in concrete specimen blended with combination of (20%-25%) RHA and 10% micro-silica was reported and beyond this percentage decrease in strength was declined [46].

2.1.5. Metakaolin

"Metakaolin" (MK) a pozzolanic material produced by the calcination of kaolinitic clay has become a potential SCM in concrete mix. Many review articles have reported the utilization of MK in mortar as well as concrete and documenting its influence in increasing the mechanical and durability features [47,48,49]. In an investigation, cement was substituted with the different dosages of MK (5%, 10%, 15% and 20%) and resistance to sulfate and chloride diffusion was studied. It was reported that optimum range of dosage of MK was 10% to 15% showing best mechanical performance as well as significant inhibition of chloride diffusion and sulfate attack [50]. Similar results were also reported in another research article, in which the use of 8% to 12% of high reactivity MK in concrete notably reduced the diffusion of chloride ions [51]. Expansion prevention due to alkali-silica reactivity in concrete prism containing 15% MK was also reported. In another research work, addition of 10% MK contributed in enhanced strength development as well as improved corrosion behavior in mortar [52]. Another study reported the usage of different dosages (5%, 12.5% and15%) of MK in concrete and in its findings the incorporation of MK (10%-12.5%) had higher compressive strength [53]. However, addition of 10% of MK was reported into lower water penetration as compare to control concrete.

Table 2
Summary of effects of partial replacement of aggregate with different industrial by-products in mortar and concrete.

Aggregate type	Evaluation Method					
	Compressive strength	Split tensile strength	Flexural strength	Water absorption/Chloride penetration	Suggested replacement	References
Copper slag	↑	↑	–	↓	40% CS in high performance concrete	[58]
	↑	↑	↑	↓	Fine aggregate replaced with (40–50%) CS in concrete	[59]
	↑	–	–	↓	60% CS in self compacting concrete	[60]
	↑	↑	↑	↓	60% CS in ultra high strength concrete	[61]
Waste foundry sand	↑	↑	↑	–	30% WFS in concrete	[63]
	↑	↑	–	↓	15% WFS in concrete	[64]
	↑	↑	↑	–	20% WFS as replacement of sand	[65]
	↑	–	↑	↓	20% WFS as replacement of sand in concrete	[66]
Marble waste	↑	–	–	↓	(20% – 100%) Marble aggregate in concrete	[68]
	↑	–	–	↓	(25%-50%) Marble powder in cement mortar	[69]
	↑	↑	–	↓	40% marble dust as fine aggregates in concrete	[70]
Aggregate type	Evaluation Method					
	Compressive strength	Split tensile strength	Flexural strength	Water absorption/hloride penetration	Suggested replacement	References
Recycled aggregates	↑	–	–	–	50% Recycled crushed brick as fine aggregate in concrete	[75]
	↑	≈	–	–	30% Fine recycled aggregates as sand in concrete	[76]
	↑	↓	↓	–	30% Recycled coarse aggregates in self compacting concrete	[77]
	↑	–	–	–	40% Recycled fine aggregate in self compacting sand concrete	[78]

↑ Denotes the "increase" in the observed trend being reported.
↓ Denotes the "decrease" in the observed trend being reported.
≈ Denotes "almost equal to reference specimen" in the trend being reported.
- Denotes "no data" being reported.

2.2. Substitute to sand

Coarse and fine aggregates are the major components in concrete production making its volume to 70%. Because of the extensive utilization of concrete as construction material in the world, exploitation of natural resources like river beds to extract sands and gravels has caused serious environmental impacts. To reduce the usage of sand in construction materials, researchers are working to introduce alternative material as a substitute to sand. Many review articles have been documented in which industrial by-products has been introduced as a substitute to sand in mortar and concrete production [54,55,56]. Different research studies investigating the potential use of different by-products in sand replacement are discussed below. The outcomes of utilization of different industrial by-products as replacement of aggregates in various studies are shown in Table 2.

2.2.1. Copper slag

Copper slag (CS) is an industrial by-product generated in large quantities during the process of matte smelting and refining of copper [57]. Performance of CS as substitute to sand with different dosages in concrete is investigated by many researchers. Various research articles have documented the partial and full replacement of sand with CS to achieve high performance concrete. In one of the research investigations, fine aggregates were partially and completely replaced with CS at different dosages (10% to 100%) [58]. Incorporation of up to 50% of CS yielded almost equivalent strength gain as that of control mix. However, with increasing dosage (80% to 100%) of CS causes significant decrease in strength. It was recommended that 40% incorporation of CS as fine aggregates was optimum for good durability properties. Similar observation was reported in which substitution of up to 40–50% CS as sand replacement was recommended to obtain good durability requirements [59]. Maximum strength at 20% replacement of fine aggregates and decline after 60% dosage was reported when self-compacting concrete was prepared with different dosages of CS (20% to 100%) [60]. Best performance in electrical resistivity and UPV was reported for concrete mix containing 60% replacement. Overall replacement in this investigation was recommended for 60% substitution of CS over natural sand. In recent research publication, ultra-high strength concrete was designed by using mechanically treated CS for fine size particles ranging from 150 μm to 600 μm [61]. It was reported that 60% replacement of sand with grounded CS enhanced the compressive strength, flexural strength and splitting tensile strength. Sand replaced completely with treated CS in concrete increase in the strength.

2.2.2. Waste foundry sand

Waste foundry sand (WFS), a high quality silica sand is generated as a by-product from ferrous and nonferrous metal casting industries [62]. Large volume of raw sand is used as a moulding casting material. WFS is too fine as 85–90% of its particle size is smaller than 100 μm. Several authors have reported the reuse of WFS as construction material by replacing the conventional sand. In an investigation, foundry sand was incorporated in concrete mix with different dosages (10%, 20% and 30%) as a sand replacement [63]. With increasing dosage of WFS, increase in compressive strength, flexural strength and splitting-tensile strength was reported. In another study, the sand was replaced with WFS at different proportions by weight in concrete mixes (5%, 10%, 15% and 20%). Maximum increase in strength properties was observed with 15% WFS replacement of with sand [64]. Utilization of WFS in concrete was reported to make the concrete matrix denser and impermeable. The optimum dosage of WFS as 20% to substitute fine

aggregates in concrete and beyond this substitution dosage in concrete mixes, reduction in the durability properties was reported [65]. The durability tests (compression strength and flexural strength) were approximately constant with control concrete on the replacement of natural sand with 20% WFS [66].

2.2.3. Marble waste

Marble waste is a waste by-product generated from marble mines and processing units during cutting, grinding and polishing. The processing plants produce huge amount of marble slurry which is disposed off into waste sites. To control air and water pollution caused by the marble dust in the dumping site, some researchers have proposed to use marble dust in ceramic and construction industry as a substitute [67]. In a research work, coarse aggregates were replaced with marble coarse aggregates (MCA) at different ratios (20%, 50% and 100%) and compared with reference concrete mixes made with basalt, granite and limestone coarse aggregates [68]. It was reported that, MCA concrete mix showed similar durability and microstructural characteristics as that were in other reference concrete mixes. Feasibility of incorporation of marble aggregates in concrete was recommended. In another study, sand in mortar was replaced by marble waste with different ratios (25%, 50%, 75% and 100%) [69]. It was reported that, optimum range of replacement of sand with marble waste lies in 25% to 50% under non-aggressive and aggressive exposure. At 50% replacement ratio, water absorption and drying shrinkage characteristics were comparable as that of control mortar mix. Recently it has been reported that 40% replacement fine aggregates with marble dust in concrete enhanced the strength properties [70]. Filler effect of marble waste was reported for the densification of microstructure of concrete mix.

2.2.4. Recycled concrete aggregate (RCA)

With rapid rate of modernization and renovation of existing concrete structures has led to the generation of large quantities of concrete wastes. Demolition of old concrete structures led to the production of sheer amounts of debris which increased its landfill in the dumping sites [71]. To handle the demolished concrete wastes, many researchers had focused on the recycling/reusing of RCA in new concrete as partial or full replacement of natural aggregates. Various research articles have been documented in which recycled aggregates from concrete waste was used as replacement [72]. Utilization of RCA in concrete with replacement of natural aggregates was also reported to have some limitations such as reduced mechanical strength and durability concerns. Factors such as adhered mortar on the surface of RAC and more interfacial transition zone (ITZ) have some weakness over natural aggregate [72]. These factors result into higher porosity and water absorption in RCA when used in concrete. In recent review articles, different treatment methods to remove and strengthen the adhered mortar to improve the properties of RCA are documented [73 74]. The crushed concrete and crushed brick of aggregate size of 5 mm as replacement for natural fine aggregates in different ratios (25%,50%,75% and 100%) was demonstrated and reported that replacing sand with crushed brick at the level of 50% has similar long-term strength as that of control [75]. However, reduction in the strength was more systematic with the sand replaced with crushed concrete. It has been reported that fine aggregates replaced with 30% RCA remain unaffected compared to control mix when tested with various doses of recycled aggregates (10%, 20%, 30%, 50% and 100%). Also, the tensile splitting and modulus of elasticity values remained acceptable at the 30% replacement level [76]. In other study, it was recommended to replace natural coarse aggregate with 30% RCA in self-compacting concrete to attain the required strength as that of control concrete [77]. In another investigation, replacement of aggregates with 40% recycled concrete improved the strength of self-compacting concrete and self-compacting sand concrete. Better performance under sodium sulfate exposure was reported in concrete mixed with recycled aggregates and recycled fine aggregates [78].

In aforementioned approaches, promising results has been reported in sustainable production of concrete by utilizing the wastes generated from industrial units. In order to develop sustainable concrete, a new biotechnological application has emerged in which microbes were used as biogenic agents to induce calcium carbonate deposition. This biobased approach called "Microbial induced calcium carbonate precipitation" (MICP) through biomineralization process has become an attractive topic of research in civil engineering. It has been widely studied in the fields of sand consolidation, bioremediation of heavy metals, restoration of lime stone monuments, durability properties of concrete structures and concrete crack remediation. In this review, metabolic pathways of biomineralization, different bacterial strains and their applications in concrete durability are discussed below. Also, an attempt to reduce the content of cement and aggregates in building materials by utilizing waste by-products along with MICP treatment is reviewed with detailed analysis in the following section.

3. Biomineralization

Biomineralization refers to a biological process of precipitation of mineral phases by living organism through its metabolic activity in the surrounding environment [79]. In nature, biomineralization leads to the formation of more than 60 different biominerals that exists as extracellularly or intracellularly [17]. These could be from biogenic origin involving bacteria, fungi, algae, and metazoan [80]. In prokaryotic systems mineralization takes place either by biologically controlled (BCM) and biologically induced (BIM) [15]. In BCM, biominerals are synthesized at a specific location within the cell or on the cell under certain conditions and mostly happens intracellularly. BCM has been reported to be of three types (i) extracellular (BCMe) (ii) intracellular (BCMin) (iii) intercellular (BCMint) [81] as shown in Fig. 2. In BIM, biominerals are synthesized as a result of metabolic activities and grow extracellularly [81] as shown in Fig. 3.

Precipitation of calcium carbonate by bacteria is also associated with BIM and is the most widely studied branch of biomineralization. The phenomenon of deposition of calcium carbonate crystals by microbes is termed as microbial induced carbonate precipitation (MICP).

3.1. Microbial induced carbonate precipitation (MICP)

MICP is a process in which calcium carbonate crystals are precipitated through the interaction of metabolites produced by microbes (CO_3^{2-}) and in calcium rich environment. In alkaline environments, different bacterial species precipitates carbonates with various mechanisms [82]. Boquet et al. [83] reported that $CaCO_3$ precipitation through biomineralization is a common phenomenon for almost all bacterial species. At neutral pH, the electronegative charge on bacterial cell surface due to carboxyl, phosphoryl and amino groups, act as a nucleation site favors the adsorption of cations such as Ca^{2+} and Mg^{2+} resulting the precipitation of carbonates [84]. Precipitation of carbonates is influenced by the amount of Ca, dissolved inorganic carbon, nucleation sites and pH [85]. The major groups of bacteria involved in biomineralization include unicellular cyanobacteria, sulfate reducing bacteria, organic acids utilizing bacteria and urea hydrolyzing bacteria.

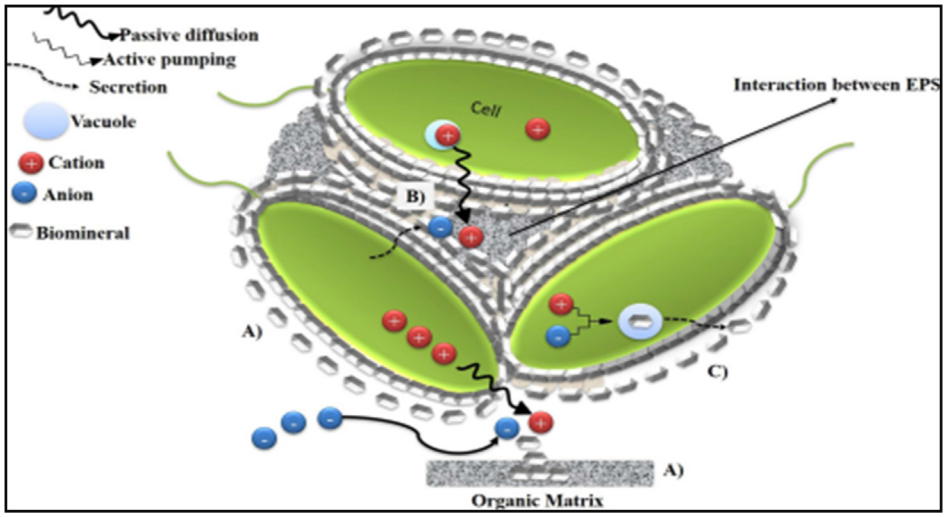

Fig. 2. Graphical representation of biologically controlled mineralization (BCM) (A) BCMe showing mineral nucleation in organic matrix moving cations out of cell by passive diffusion (B) BCMin showing epithelial surface of cell as organic substrate for orientation and precipitation of minerals around the surface. (c) BCMint showing biominerals formed within the specialized vesicle of cell and secreted. [81]

3.2. MICP via urea hydrolysis

Calcium carbonate precipitation via hydrolysis of urea by bacteria is the most predominant and easily controlled mechanism, where high amounts of calcium carbonates are produced in a short time. Urea is hydrolyzed into carbonate and ammonium by microbial urease enzyme [18]. Hydrolysis of one mole of urea results into 1 mol of carbamate and 1 mol of ammonia which subsequently hydrolyses to form 1 mol of carbonic acid and ammonia as shown below (Eq. (1) & Eq. (2)).

$$CO(NH_2)_2 + H_2O \xrightarrow{Bacteria} NH_2COOH + NH_3 \quad (1)$$

$$NH_2COOH + H_2O \rightarrow NH_3 + H_2CO_3 \quad (2)$$

These products further equilibrate in water to form bicarbonate and two moles of ammonium and hydroxide ions Eq. (3) and Eq. (4).

$$2NH_3 + 2H_2O \rightarrow 2NH_4^+ + 2OH^- \quad (3)$$

$$2OH^- + H_2CO_3 \rightarrow CO_3^{2-} + 2H_2O \quad (4)$$

Ammonia increases the pH in the surrounding environment and creates an alkaline condition [84] leading to the precipitation of $CaCO_3$ in presence of Ca^{2+} ions as shown in Eq. (5).

$$CO_3^{2-} + Ca^{2+} \leftrightarrow CaCO_3 \quad (5)$$

To utilize the biomineralization property of ureolytic bacterial strains, different calcium sources of like calcium chloride, calcium acetate and calcium nitrate along with urea has been used by researchers. Urea and calcium chloride medium for the precipitation of calcium carbonate has been preferred by researchers as shown in Eq. (6) – Eq. (8).

$$Ca^{2+} + Cell \rightarrow Cell^- Ca^{2+} \quad (6)$$

$$Cl^- + HCO_3^- + NH_3 \rightarrow NH_4Cl + CO_3^{2-} \quad (7)$$

$$Cell^- Ca^{2+} + CO_3^{2-} \rightarrow Cell^- CaCO_3 \quad (8)$$

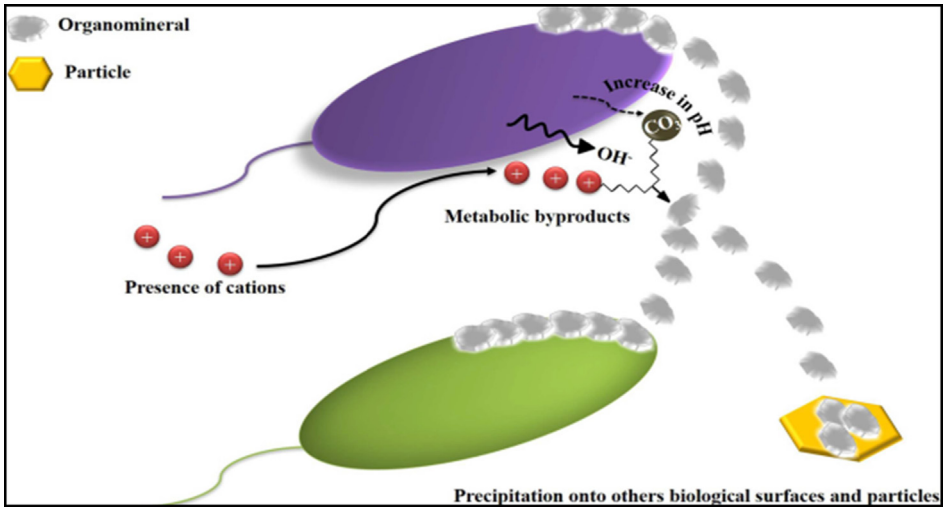

Fig. 3. Graphical representation of BIM showing biomineral precipitation induced because of interaction between microbial metabolic products and inorganic compounds in the environment. [81]

Table 3
Utilization of different industrial waste products as replacement to cement or aggregate along with MICP application.

Type of waste	Replacement	Bacterial strain	Evaluation parameters	Suggested replacement/treatment	References
Fly ash	Cement	*Bacillus megaterium*	Compressive strength ↑ Sorptivity ↓ Water penetration ↓ Higher bacterial cell viability, improved strength of mortar	40% FA dosage	[123]
Fly ash	Cement	*Sporosarcina pasteurii*	Compressive strength ↑ Split tensile strength ↑ Sorptivity ↓ Water absorption ↓ Strength increment and lesser water absorption	30% FA dosage in concrete	[124]
Silica fume	Cement	*S. pasteurii*	Compressive strength ↑ Water absorption ↓ Increased strength and reduced water absorption in SF amended mortar with bacterial treatment	20% SF dosage recommended	[125]
Silica fume	Cement	*Bacillus aerius*	Compressive strength ↑ Water absorption ↓ Chloride permeability ↓ Improved mechanical and permeation properties of in SF amended concrete	10% SF dosage recommended	[126]
Rice husk ash	Cement	*Bacillus aerius*	Compressive strength ↑ Water absorption ↓ Chloride ion penetration ↓ Abrasion resistance ↑ Improved compressive strength and permeability properties of concrete	10% RHA dosage recommended	[127]

Table 3 **Cont.** Utilization of different industrial waste products as replacement to cement or aggregate along with MICP application

Type of waste	Replacement	Bacterial strain	Evaluation parameters	Suggested replacement/treatment	References
Cement kiln dust	Cement	*S. pasteurii*	Grain consolidation ↑ CaO utilized for carbonate precipitation ↑ Formation of biocalcite in presence of CKD, 4 times increased drilling resistance with bacterial treatment	Biostabilization of CKD	[129]
Cement kiln dust	Cement	*Bacillus halodurans*	Compressive strength ↑ Split tensile strength ↑ Sorptivity ↓ Water absorption and chloride permeability ↓ Increased mechanical strength and reduced permeation	10% bacterial treated CKD dosage in concrete	[130]
Metakaolin	Cement	*Bacillus cereus*	Compressive strength ↑ Porosity ↓ Improved compressive strength and reduced porosity in metakaolin modified mortar	50% metakaolin dosage recommended	[131]
Calcareous sand	Sand	*S. pasteurii*	Unconfined compressive strength and stiffness ↑ Permeability of calcareous sand ↓ Extraction of soluble Ca^{2+}, strength and stiffness of calcareous sand increases	Soluble calcium extraction from calcareous sand and MICP	[132]
Recycled concrete aggregate	Natural aggregate	*S. pasteurii*	Water absorption and porosity of treated RCA ↓ Bonding behavior of treated RCA-asphalt mixture ↑ Adhesion behavior of treated RCA-asphalt mixture ↑ Direct tensile strength ↑ Significant reduction in water absorption and porosity, adhesion behavior of treated RCA improved	Surface treatment of RCA with MICP	[136]
Recycled concrete aggregate	Normal Aggregate	*Bacillus sphaericus*	Weight gain in treated RCA ↑ Porosity of treated RCA ↓ Compressive strength of concrete ↑ Water absorption of concrete ↓ Treated aggregates improved the properties of concrete	Immersion bacterial treatment of RCA improved the quality	[137]

Table 3 **Cont.** Utilization of different industrial waste products as replacement to cement or aggregate along with MICP application

Type of waste	Replacement	Bacterial strain	Evaluation parameters	Suggested replacement/treatment	References
MICP modifiedaggregates	Natural aggregate	*S. pasteurii*	Resistance to moisture damage ↑ Indirect tensile strength ↑ Pulse Velocity Ratio and Electrical Resistivity Ratio ↑ Bio modified aggregate significantly improves the properties of cold mix asphalt mixtures	Approach of bacterial spray and submersion in bacterial culture of aggregates were adopted	[138]
Recycled concreteaggregate	Natural aggregate	*Bacillus pseudofirmus*	Water absorption and crushing value of treated RCA ↓ Compressive strength of mortar ↑ Water absorption of mortar ↓ Reduction in water absorption and crushing values, adherence of $CaCO_3$ crystals on to the surface of treated RCA	Aggregates soaked in bacterial culture for 20 days	[139]
Recycled fine aggregates (RFA)	Fine aggregate	*S. pasteurii*	Water absorption and crushing value of treated RFA ↓ Compressive strength of mortar ↑ Water absorption ↓ Improved properties of the treated RFA and corresponding mortars	100% bacterial treated RFA were used in mortar	[140]
Corn steep liquor	Growth medium	*Bacillus* sp. CT5	Compressive strength ↑ Water absorption ↓ Chloride permeability ↓ Improved mechanical and permeation properties, no effect on setting properties of cement	CSL medium (1.5% v/v) as replacement of bacterial growth medium	[143]
Tofu waste water	Growth medium	*Bacillus cereus*	Compressive strength of sandstone ↑ Compressive strength of mortar ↓ Tofu water as preferable growth medium in biocementation	50% replacement of nutrient medium	[144]

↑ Denotes the "increase" in the observed trend being reported.
↓ Denotes the "decrease" in the observed trend being reported.

4. Applications of MICP

The potential and effectiveness of MICP application in various fields such as heavy metal remediation, soil consolidation, restoration of monuments, crack remediation and durability enhancement of concrete structures has been well documented in different review papers [16,18,86–91]. In MICP process, several genera of calcifying bacteria isolated from different environmental conditions has been reported. Isolation of different calcifying bacterial strains from calcareous, marine, karstic caves, hot springs and heavy metal contaminated landfill environments has been reported [92–98]. MICP has been reported with immense potential in bioremediation process of heavy metal contaminated soils by using different ureolytic bacterial and fungal strains by various researchers [99–103]. The potential application of MICP in stabilization of sand and soil through biodeposition has also been reported. Microbial treatment is reported to improve packing of sand grains due to calcite precipitation resulting into increased strength and porosity reduction of soil [104,105]. In some research articles, biostabilization of desert sand with MICP was reported to show high resistant against strong winds and prevents wind erosion during sand storm [106,107]. Concept of ancient monument restoration with the help of calcifying bacterial strains through MICP application has been reported by various researchers [108–112]. Now a days, application of MICP has become a hot topic of research as the positive influence of MICP in strength and durability enhancement of concrete are reported. Improvement in mechanical strength, reduced permeability and resistance to corrosion of reinforcement in concrete structures due to MICP are the significant attributes. Successful application of MICP in improving the durability properties of concrete has been reported by various studies [93,113–116]. To heal the cracks in concrete, various approaches have been practiced by researchers with calcifying bacterial strains [117–122].

5. Waste utilization and MICP

In this section, utilization of industrial wastes in construction material along with the application of MICP as a biotechnological tool in the sustainable production of concrete is discussed. In aforementioned sections, various industrial by-products have been used as a substitute to cement and aggregates. In the current section, similar practice of waste by-product inclusion in concrete along with the application of MICP as shown in Table 3 is discussed.

5.1. Cement substitute and MICP

Different waste materials such as rice husk ash, fly ash, silica fume, cement kiln dust (CKD) and metakaolin as a SCM in mortar and concrete along with bacterial treatment has been proposed by many researchers. Achal et al. [123] proposed the improvement in strength and permeability of fly ash amended cement structures (10%, 20% and 40% dosage) after treatment with bacterial strain (*Bacillus megaterium*). It was reported that bacterial cell viability in FA amended mortar was also higher. Even in mortar and concrete specimens with higher FA dosage (40%), involvement of calcite precipitation improved strength properties. Microstructural analysis of bacterial calcite precipitation in flyash amended mortar specimen is shown in Fig. 4.

Similar study with bacterial (*S. pasteurii*) treated concrete with replacement of cement with FA (10%, 20% and 30%) was conducted [124]. In this research work, use of FA up to 30% as cement replacement was recommended along with bacterial treatment. Biodeposition of calcite precipitates was reported to be involved in strength gain and lesser water absorption (Fig. 5). Sustainable production of green concrete with FA amendment in concrete was reported to lower cement usage as well as production. Bacterial treatment of silica fume amended mortar and concrete was also

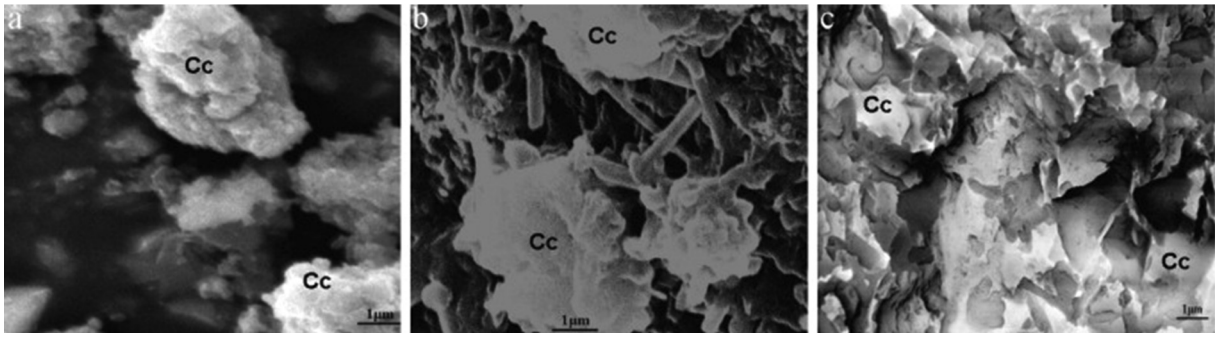

Fig. 4. Scanning electron micrographs depicting bacterially induced calcite precipitation (a) fly ash-supplemented mortar, (b) magnified view of fly ash amended mortar surface (c) fly ash amended concrete (Cc – calcite crystals). [123].

proposed by researchers in which improved durability properties was reported.

Farmani et al. [125] reported increased compressive strength and weight gain in SF amended mortar (20% dosage) due to biodeposition of calcite and aragonite precipitation (Fig. 6). Bacterial treatment of SF amended mortar was reported to significantly reduce the water absorption. Siddique et al. [126] also reported the significant improvement of durability properties of SF amended concrete (5%, 10% and 20% dosage) with bacterial treatment. It was reported that, 12% strength gain in SF concrete (10% dosage) was achieved after treatment with calcifying bacteria. Due to biodeposition of calcite, porosity, water absorption, capillary water rises and chloride permeability was reported to be decreased. In another research work, Siddique et al. [127] proposed the replacement of cement with various concentrations of rice husk ash (5%, 10%, 15% and 20%) in concrete along with bacterial treatment. It was reported that 10% RHA is the optimum dosage and strength gain by 9% and 11.8% was achieved after 28 and 56 days respectively as compare to control. Inclusion of RHA and bacterial treatment reduced chloride ion ingress and calcite precipitation improves the durability of RHA amended concrete. Dhami et al. [128] reported the effectiveness of bacterial treatment of ash bricks with *Bacillus megaterium* strain in improving overall performance of ash amended bricks. In this study, flyash amended bricks (30%) and rice husk ash amended bricks (30%) were immersed in bacterial culture for 4 days and then cured by sprinkling nutrient medium supplemented with urea for 4 weeks. The strength of bricks made with fly ash and rice husk ash was reported to be improved by 24.2% and 21.8% as compared to conventional brick, respectively. Reduction in permeability due to biogenic $CaCO_3$ precipitation on the surface of bricks was reported. Scanning electron microscopy of MICP in fly ash bricks is shown in Fig. 7.

To recycle cement kiln dust, performance of *S. pasteurii* bacterial strain in extreme alkaline condition of CKD was investigated [129]. Stable biocalcite formation was reported in high pH range of 11 and 12 as free calcium ions provided as CaO were present in CKD. Authors also investigated the grain consolidation test with *S. pasteurii* by using CKD as calcium source and granulated blast-furnace slag as pozzolanic additive. In drilling resistance test, resistance increased 4 times for the samples of CKD with bacteria than without bacterial treatment was reported. In another research work, Kunal et al. [130] reported the decrease of alkalinity by 67.3% on treatment of highly alkaline CKD with *Bacillus halodurans* strain. Further, the bacterial treated CKD was used as cement replacement (10%, 20% and 30%). Inclusion of 10% bacterial treated CKD in concrete was reported to increase compressive and tensile strength. Permeation properties were also reported to be decreased by 10% as compare to control. In a recent study, researchers proposed the improved durability properties of bacterial treated metakaolin modified cement mortars [131]. In this study, cement was replaced with 25% and 50% metakaolin in mortar cubes. MK modified mortars were treated with *Bacillus cereus* NS4 strain. It was reported that, biomineralization activity of bacterial strain enhanced the compressive strength of MK modified mortars (Fig. 8). Strength gain 927%) was reported for MK modified mortar with 50% replacement dosage as compared to control. Biogenic precipitation of calcite crystals was reported for strength gain and reduced porosity.

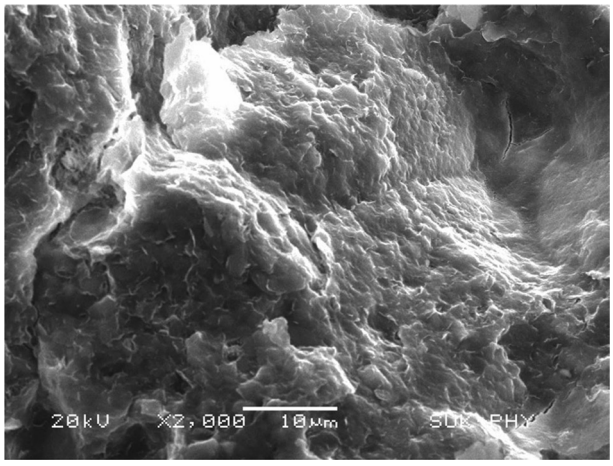

Fig. 5. SEM images of bacterial embedded fly ash concrete. [124]

5.2. Aggregate substitute and MICP

The positive outcome of MICP in enhancing durability properties of mortar and concrete has encouraged the researchers to further make this technique eco-friendlier. To improve this biogenic process, efforts have been made to utilize waste by-products as a replacement for aggregates. Many researchers have proposed the replacement of common aggregates with various industrial by-products in concrete production. Liu et al. [132] suggested the use of calcareous sand as well as the extraction of soluble calcium ions from it to replace $CaCl_2$ in biocementation process. To extract soluble calcium ions from calcareous sand, use of 20% acetic acid for 24 hrs was reported by authors. The extract of calcium ions of 1.0 M adjusted to pH 6.5–7 was used in biocementation application of calcareous sand. The stiffness and strength of the calcareous sand treated increased with *Sporosarcina pasteurii* compared to control. Authors proposed an economically sustainable method of

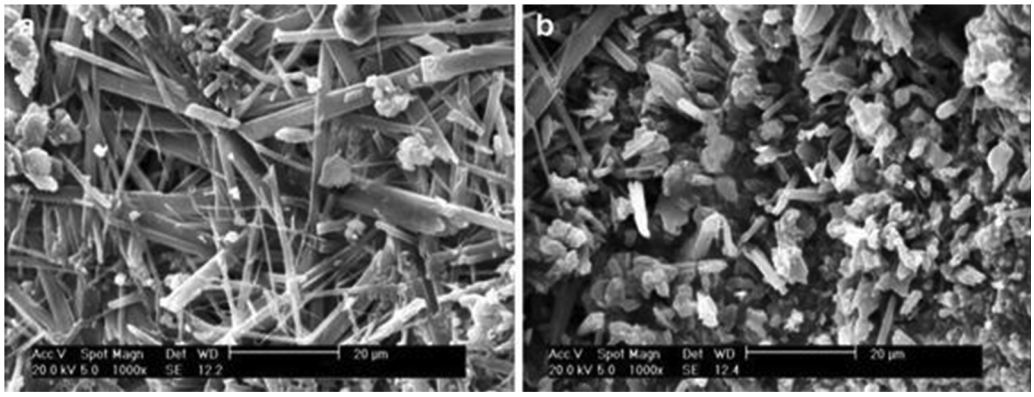

Fig. 6. SEM images of bacterial treated SF amended mortar a) needle shaped aragonite crystals b) rhombohedral calcite crystals. [125]

using calcareous sand in construction. Li et al. [133] reported the use of fly ash as an admixture (10%, 25% and 50%) along with biocementation to enhance the strength of expansive soils. Formulation of FA (25%) blended with *Bacillus megaterium* was reported to significantly improve the unconfined strength of expansive soil by two-times higher than control. Authors recommend 25% dosage of FA and reported that the biocementation reduces the swelling potential of soil. Replacement of sand with fungal treated waste foundry sand in concrete specimen was investigated [134]. Waste

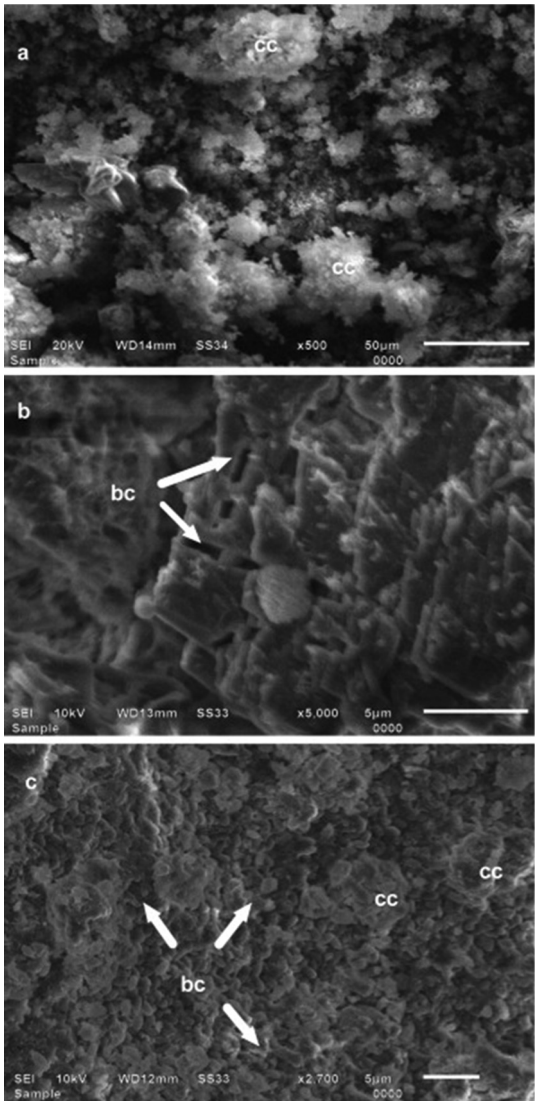

Fig. 7. Scanning electron micrograph of MICP by *B. megaterium* in fly ash bricks. (a) Calcite crystals (cc) deposited over the sand particles in bricks, (b) impressions of rod shaped bacterial cells (bc) spread around the carbonate crystals and (c) carbonate crystals covered by bacteria. [128]

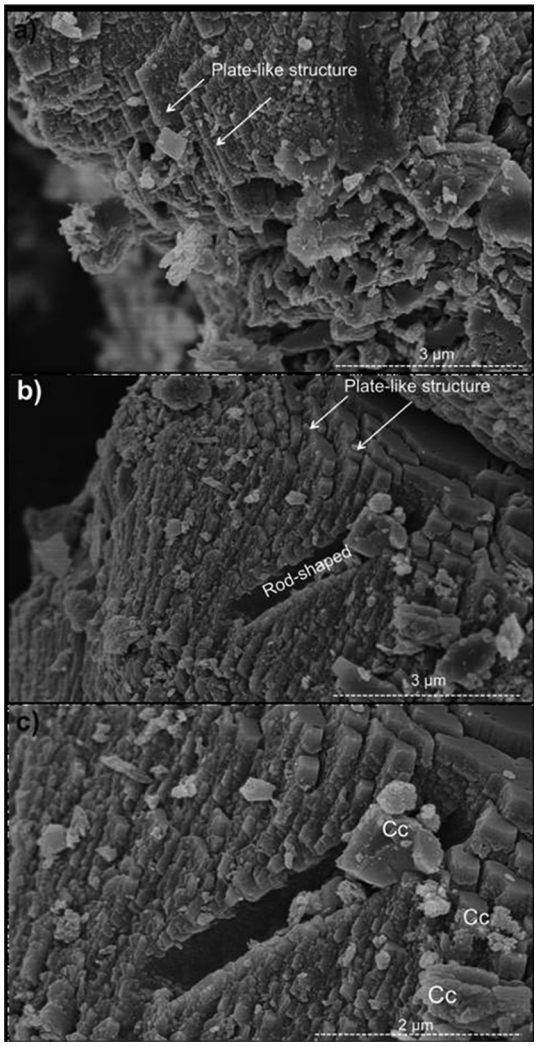

Fig. 8. Scanning electron micrograph of (a) metakaolin treated without bacteria (b, c) metakaolin with treated with bacteria (Cc calcite crystals) [131]

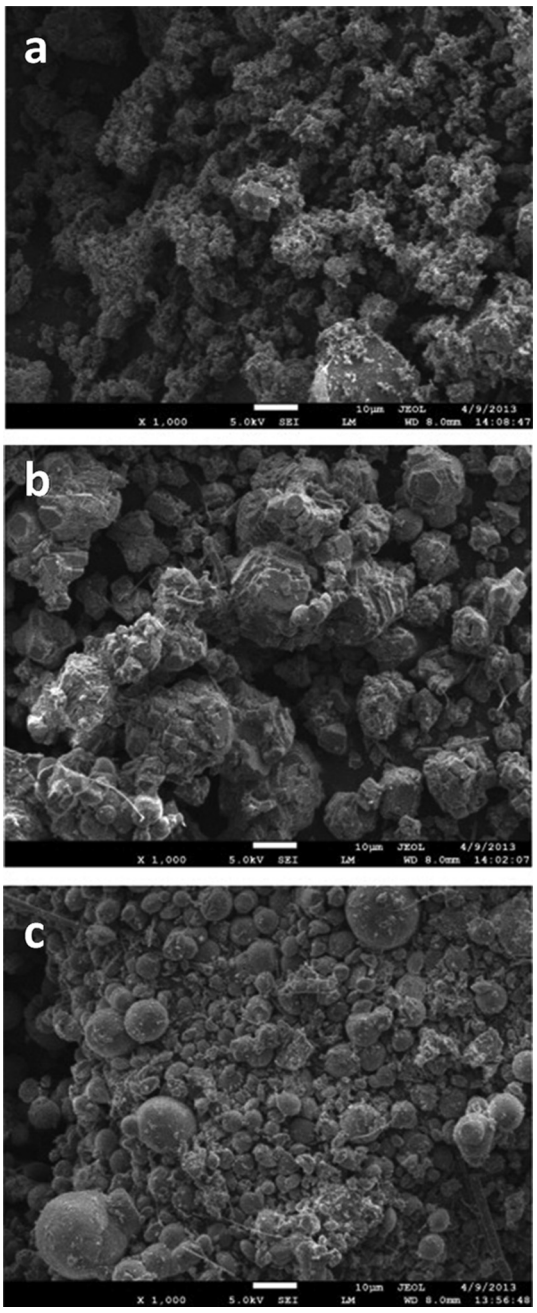

Fig. 9. Scanning electron micrographs of (a) untreated RCA (b,c) microbial treated RCA. Surface modification of RCA with rhombohedral calcite (b) spherical vaterite (c) crystals of $CaCO_3$. [135]

foundry sand of different replacement dosages (10%, 15% and 20%) was treated with fungal strain (*Eupenicillium crustaceum*) for 30 days. Optimum replacement dosage (20%) of fungal treated WFS was recommended to replace natural sand. Increase in compressive strength (24%) with decreased water absorption (44%) of concrete containing treated WFS was reported. Biodeposition of calcium oxalate by *Eupenicillium crustaceum* was reported to decrease the porosity of concrete containing treated WFS. Utilization of recycled concrete aggregates (RCA) along with MICP treatment has been extensively studied by many researchers. Qiu et al. [135] observed the significant reduction of water absorption in MICP treated RCA with *S. pasteurii* strain. After 72 hrs of bacterial surface treatment, weight increase of RCA was reported due to the surface modification through biogenic $CaCO_3$ precipitation. Surface modification of microbial treated RCA was reported due to different calcium carbonate crystals precipitated on it (Fig. 9).

In another research work, surface treated RCA with MICP application was reported to be used in asphalt mixture [136]. Cement mortar particles were removed from RCA and used as bacterial carrier material. *Bacillus pasteurii* cells were mixed with mortar particles and placed on RCA and cementing solution was sprayed for 7 days. It was reported that porosity and capillary water absorption of bacterial treated RCA showed reduction of 86.5% and 32% as compare to control. The bonding strength was improved by 55% in of asphalt mixture with treated RCA over the untreated RCA mixture. The MICP treatment increased the resistance of RCA-asphalt mixture to moisture damage and also increased the adhesive behavior as shown in Fig. 10.

In another research work, RCA was treated with *Bacillus sphaericus* by immersion and spraying method [137]. It was reported that, immersion treatment method was superior to spraying method and results into high weight increase (2%) and decreased water absorption rate due to biogenic $CaCO_3$ precipitation. Increase by 40% of compressive strength and decrease of 27% in water absorption was reported in bacterial treated RCA concrete. Surface strengthening effect after biogenic treatment on the RCA was reported. Dovom et al. [138] reported the improved resistance of cold mix asphalt mixture incorporated with bacterial treated RCA to moisture damage. It was reported that, hydrophobic $CaCO_3$ layer of bacterial treated aggregates facilitates great bonding with the bituminous. The results of boiling water test in the study showed 19% higher bitumen coating ratio in bacterial treated aggregate than the control. Wu et al. [139] proposed a new biodeposition approach based on microbially induced carbonate precipitation through respiration to improve RCA properties. Bio-deposition treatment of RCA was done by pouring *B. pseudofirmus* culture on RCA and soaked it for 20 days. In this process calcium chloride as external calcium source and adhered mortar as internal calcium source was adopted to induce $CaCO_3$ precipitation. Reduction in water absorption (23%) and crushing values (12%) was reported for 5 mm bacterial treated RCA. Biogenic $CaCO_3$ crystals were reported to be adhered on to the surface and pores of bacterial treated RCA (Fig. 11).

Water absorption was significantly reduced (30% reduction) in mortars prepared with treated RCA as compare to untreated RCA. Thick bio-deposition of $CaCO_3$ crystals on the surface of bacterial treated RCA was reported for the improving the density of ITZ between treated RCA and cement paste in mortar. Zhan et al. [140] reported the increment of 32% in compressive strength of mortar containing 100% bacterial treated recycled fine aggregates. Authors also suggested the use of calcium chloride as calcium source for better $CaCO_3$ precipitation in bacterial treated recycled fine aggregates instead of calcium nitrate.

5.3. Industrial effluent as nutrient source in MICP

A new approach of using different industrial by-products as an alternative to nutrient required for bacterial growth in MICP process has been proposed by many researchers [141–144]. Achal et al. [141] reported the use of lactose mother liquor (LML) as an alternate to commercial nutrient medium for the growth of *Sporosarcina pasteurii* bacterial strain. LML is an industrial effluent generated from dairy industry. Use of 10% LML (v/v) as growth medium amended with urea (2%) and $CaCl_2$ (25 mM) was suggested. No significant change in bacterial urease activity and strength of bacterial treated mortar while using LML as source of nutrients. To reduce the cost of cultivation medium in MICP application, use of effluent from chicken manure (CME) gas bio-plant as alternative growth medium was suggested [142]. Use of 25% CME (v/v) amended with 2% urea and 25 mM $CaCl_2$ was suggested as a

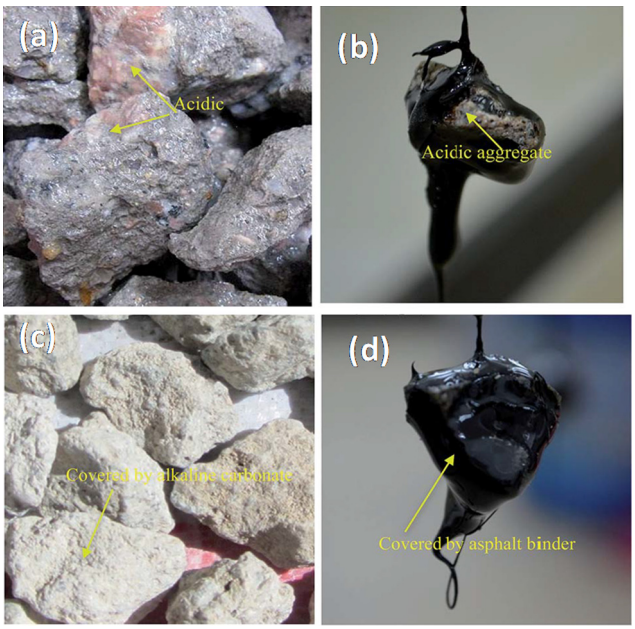

Fig. 10. MICP influence on resistance of asphalt mixture to moisture damage of, a) RCA with acidic surface b) Partial removal of asphalt binder in untreated RCA, c) Bacterial treated RCA d) The surface covered with asphalt for treated RCA. [136]

bacterial growth medium. Compressive strength of bacterial treated cement cubes in CME medium was reported to increase by 30% as compare to control cement cubes. High urease activity and carbonate precipitation by *B. pasteurii* in low cost CME medium was reported. Joshi et al. [143] suggested the use of corn steep liquor (CSL), by-product from starch industry at 1.5% (v/v), as a nutritional source in MICP treatment of concrete. Lower organic carbon in CSL as compare to commercial nutrient medium was reported to have no influence on the cement setting properties. Decreased permeability and enhanced compressive strength were reported for bacterial treated concrete specimens, in which CSL was used. In a recent study, tofu waste water (TW) generated from soybean processing unit was used as a nutritional source for bacterial growth in MICP application [144]. TW as preferable medium for bacterial growth and urease production was proposed. Increased compressive strength of mortars and sandstone was reported when TW was used in biocementation instead of nutrient medium.

6. Challenges and future perspectives

To improve the sustainability and performance of concrete, intense research work has been conducted by researchers. Among the different approaches, MICP application using calcifying bacteria has been widely reported with the positive benefits in the enhancement of mechanical properties of cement-based materials. A novel method of developing eco-friendly microbial concrete along with the addition of industrial by-products as partial or complete replacement of cement and aggregates is presented. Use of different industrial by-products will not only reduce the waste and control the depletion of natural resources but also cut down the embodied energy of concrete. However, the combination of microbial treatment and waste utilization in construction materials is yet a new research approach. In this review, reports on the development of MICP treated waste amended concrete are still at lab scale and limited. Performance of MICP treated waste amended concrete under different environmental conditions such as high chloride concentrations, repeated freeze thaw conditions and cyclic carbonation conditions is still to be reported. In addition, there is a need for more investigations of long-term performance and durability properties of microbial treated waste amended concrete. One of the major concerns is the variability in chemical composition and reactivity of SCM, as it can vary considerably depending on the different sources. Detailed future research focused on the effect of SCM with different chemical composition on the MICP mechanism of bacteria is to be carried out. Appropriate monitoring and additional evaluations of this approach will provide more con-

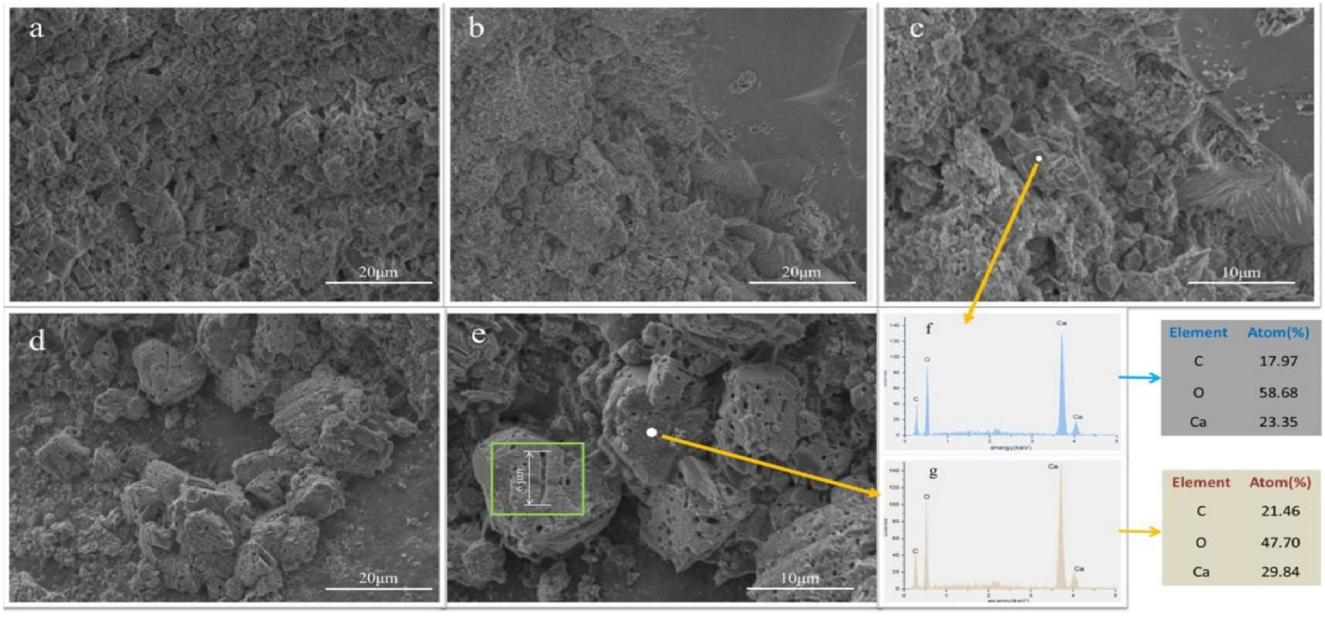

Fig. 11. SEM-EDS images of RCA surface: (a) Untreated-RCA surface; (b,c) RCA surface at high and low magnification without bacterial treatment; (d,e) High and low magnification of bacterial treated-RCA surface; (f) Spectra of EDS showing particles in (c); and (g) EDS spectra of particles in (e). [139]

fidence in producing industrially valuable construction product. This microbial treatment approach could be used for precast products such as waste amended concrete blocks and bricks.

Despite the positive outcomes, upscaling of this microbial approach from lab scale to commercial scale is the first challenge. Economical limitations such as cost of nutrient medium for bacterial growth, optimum bacterial dosage and efficiency of treatment in real-life waste amended concrete structures is still needs to be further proven. Some challenges are associated with microbial treatment of concrete which are necessary to be addressed for the development of this technique for commercial scale applications. In previous studies, it was found that ureolytic pathway for MICP process was predominantly preferred on the performance basis. Production of ammonia as by-product during urea hydrolysis has a disadvantage from an environmental viewpoint [15]. The economic limitations such as use of expensive nutrient medium for bacterial growth, aseptic conditions to produce axenic pure bacterial cultures has been reported for the high production cost of microbial concrete at industrial scale [145]. Some potential alternative nutrients for bacterial growth and economically suitable substitute for urea have been suggested for cheap and affordable implementation of MICP application at field scale [146]. More studies with the consideration of abovementioned concerns will facilitate the practical implementation of microbial treated waste amended concrete in construction sector in the near future.

7. Conclusions

This review is an outcome of the compiled data of utilization of various industrial waste products as partial replacement to either cement or aggregate for the development of sustainable construction materials and enhancement of durability properties of these building materials by biomineralization process. From the data compiled from previous studies, it has been concluded that

- The compressive strength of concrete and mortar specimens increased when cement is partially replaced with fly ash (40–50%), steel slag (20–40%), silica fume (5–15%), rice husk ash (20–30%) and metakaolin (10–15%).
- The permeability and drying shrinkage of concrete and mortar specimens were significantly reduced with partial replacement of cement with different industrial by-products.
- The split tensile strength and flexural strength of cement replaced concrete and mortar specimens increased with industrial by-product replacement.
- Increase in compressive strength of concrete was recorded in partial replacement of aggregate with copper slag (40–60%), waste foundry sand (15–30%), marble waste (25–100%) and recycled aggregates (30–50%).
- Decrease in water absorption and chloride penetration of concrete and mortar specimens was reported with replacement of aggregates with copper slag, waste foundry sand and marble waste.
- Split tensile strength and flexural strength of aggregate replaced concrete and mortar specimens with copper slag, waste foundry sand and marble waste increased while with recycled aggregates they were decreased.
- Biomineralization application in construction materials with the employment of calcifying bacteria offers a sustainable approach to improve durability properties of concrete structures.
- Compressive strength, split tensile strength and other parameters significantly improved in concrete structures when cement is partially replaced with various industrial by-products along with bacterial treatment compared to the by-products alone.
- Water absorption rate significantly decreased due to bacterial treatment in concrete structures amended with these industrial by-products as replacement to cement or aggregate.

Hence, application of MICP combined with alternative industrial by-products has opened a promising path for improving the durability and performance of concrete. This innovative and efficient method of recycling industrial by-products in microbial concrete will pave the way to reduce the carbon footprints of construction industry and promote the sustainable development.

Declaration of Competing Interest

The authors declare that they have no known competing financial interests or personal relationships that could have appeared to influence the work reported in this paper.

Acknowledgment

Authors thank the Science and Engineering Research Board (SERB), Department of Science & Technology, Ministry of Science & Technology, Government of India, India, for the grants under the research project No. SB/S3/CEE/0063/2013.

References

[1] M.W. Doyle, D.G. Havlick, Infrastructure and the Environment, Annu Rev Env Resour. 39 (2009) 349–373.
[2] S.A. Miller, A. Horvath, P.J. Monteiro, Impacts of booming concrete production on water resources worldwide, Nat Sustain. 1 (2018) 69–76.
[3] P.J. Monteiro, S.A. Miller, A. Horvath, Towards sustainable concrete, Nat Mater. 16 (2017) 698–699.
[4] Statista, 2019. Major countries in worldwide cement production 2014-2018. https://www.statista.com/statistics/267364/world-cement-production-by-country/ (accessed 7 September 2019).
[5] A.P. Gursel, E. Masanet, A. Horvath, A. Stadel, Life-cycle inventory analysis of concrete production: A critical review, Cement Concrete Comp. 51 (2014) 38–48.
[6] S.A. Miller, A. Horvath, P.J. Monteiro, Readily implementable techniques can cut annual CO2 emissions from the production of concrete by over 20%, Environ Res Lett. 11 (2016) 074029.
[7] E. Worrell, L. Price, N. Martin, C. Hendriks, L.O. Meida, Carbon dioxide emissions from the global cement industry, Annu Rev Energ Env. 26 (2001) 303–329.
[8] L.J. Drew, W.H. Langer, J.S. Sachs, Environmentalism and natural aggregate mining, Nat Resour Res. 11 (2002) 19–28.
[9] W. Langer, Sustainability of aggregates in construction. In sustainability of construction materials, Woodhead Publishing. (2009) 1–30.
[10] D. Padmalal, K. Maya, S. Sreebha, R. Sreeja, Environmental effects of river sand mining: a case from the river catchments of Vembanad lake Southwest coast of India, Environ Geol. 54 (2008) 879–889.
[11] A. Torres, J. Brandt, K. Lear, J. Liu, A looming tragedy of the sand commons, Science 357 (2017) 970–971.
[12] P.K Mehta, Reducing the environmental impact of concrete, Concr Int. 23 (2001) 61–66.
[13] K. Sakai, T. Noguchi, The sustainable use of concrete, 1st ed., CRC Press, 2012, p. 188p.
[14] R.K.D. Obe, C.Q. Lye, C.J. Lynn, A.A. Elgalhud, Sustainable construction materials for concrete: A question of responsible use, in: In: IOP Conference Series: Materials Science and Engineering, 2018, p. 012001.
[15] N.K. Dhami, M.S. Reddy, A. Mukherjee, Biomineralization of calcium carbonates and their engineered applications: a review, Front Microbiol. 4 (2013) 314.
[16] M. Seifan, A.K. Samani, A. Berenjian, Bioconcrete: next generation of self-healing concrete, Appl. Microbiol. Biot. 100 (2016) 2591–2602.
[17] P. Anbu, C.H. Kang, Y.J. Shin, J.S. So, Formations of calcium carbonate minerals by bacteria and its multiple applications, Springerplus. 5 (2016) 250.
[18] S. Joshi, S. Goyal, A. Mukherjee, M.S. Reddy, Microbial healing of cracks in concrete: a review, J. Ind. Microbiol. Biot. 44 (2017) 1511–1525.
[19] J.M. Paris, J.G. Roessler, C.C. Ferraro, H.D. DeFord, T.G. Townsend, A review of waste products utilized as supplements to Portland cement in concrete, J Clean Prod. 121 (2016) 1–8.
[20] S.A. Miller, V.M. John, S.A. Pacca, A. Horvath, Carbon dioxide reduction potential in the global cement industry by 2050, Cement Concr. Res. 114 (2018) 115–124.
[21] T. Hemalatha, A. Ramaswamy, A review on fly ash characteristics–Towards promoting high volume utilization in developing sustainable concrete, J. Clean Prod. 147 (2017) 546–559.

[22] P. Chindaprasirt, S. Homwuttiwong, V. Sirivivatnanon, Influence of fly ash fineness on strength, drying shrinkage and sulfate resistance of blended cement mortar, Cement Concr. Res. 34 (2004) 1087–1092.
[23] P. Chindaprasirt, C. Jaturapitakkul, T. Sinsiri, Effect of fly ash fineness on microstructure of blended cement paste, Constr. Build. Mater. 21 (2007) 1534–1541.
[24] M.J. McCarthy, R.K. Dhir, Development of high volume fly ash cements for use in concrete construction, Fuel 84 (2005) 1423–1432.
[25] H.K. Shehab, A.S. Eisa, A.M. Wahba, Mechanical properties of fly ash based geopolymer concrete with full and partial cement replacement, Constr. Build Mater. 126 (2016) 560–565.
[26] A. Ebrahimi, M. Saffari, D. Milani, A. Montoya, M. Valix, A. Abbas, Sustainable transformation of fly ash industrial waste into a construction cement blend via CO2 carbonation, J. Clean. Prod. 156 (2017) 660–669.
[27] A. Agrawal, K.K. Sahu, B.D. Pandey, Solid waste management in non-ferrous industries in India, Resour. Conserv. Recy. 42 (2004) 99–120.
[28] E. Özbay, M. Erdemir, H.İ. Durmuş, Utilization and efficiency of ground granulated blast furnace slag on concrete properties–A review, Constr. Build. Mater. 105 (2016) 423–434.
[29] C. Shi, J. Qian, High performance cementing materials from industrial slags—a review, Resour. Conserv. Recy. 29 (2000) 195–207.
[30] P.E. Tsakiridis, G.D. Papadimitriou, S. Tsivilis, C. Koroneos, Utilization of steel slag for Portland cement clinker production, J. Hazard Mater. 152 (2008) 805–811.
[31] A. Rai, J. Prabakar, C.B. Raju, R.K. Morchalle, Metallurgical slag as a component in blended cement, Constr. Build Mater. 16 (2002) 489–494.
[32] Y.N. Sheen, H.Y. Wang, T.H. Sun, A study of engineering properties of cement mortar with stainless steel oxidizing slag and reducing slag resource materials, Constr Build Mater. 40 (2013) 239–245.
[33] S. Liu, L. Li, Influence of fineness on the cementitious properties of steel slag, J. Therm. Anal. Calorim. 117 (2014) 629–634.
[34] W. Qiang, Y. Peiyu, Y. Jianwei, Z. Bo, Influence of steel slag on mechanical properties and durability of concrete, Constr. Build. Mater. 47 (2013) 1414–1420.
[35] J. Rosales, M. Cabrera, F. Agrela, Effect of stainless steel slag waste as a replacement for cement in mortars. Mechanical and statistical study, Constr. Build Mater. 142 (2017) 444–458.
[36] M.I. Khan, R. Siddique, Utilization of silica fume in concrete: Review of durability properties, Resour. Conserv. Recy. 57 (2011) 30–35.
[37] S.A. Khedr, M.N. Abou-Zeid, Characteristics of silica-fume concrete, J Mater. Civil Eng. 6 (1994) 357–375.
[38] M. Mazloom, A.A. Ramezanianpour, J.J. Brooks, Effect of silica fume on mechanical properties of high-strength concrete, Cement Concr. Comp. 26 (2004) 347–357.
[39] A.R. Bagheri, H. Zanganeh, M.M. Moalemi, Mechanical and durability properties of ternary concretes containing silica fume and low reactivity blast furnace slag, Cement Concr. Comp. 34 (2012) 663–670.
[40] A.N. Givi, S.A. Rashid, F.N. Aziz, M.A. Salleh, Contribution of rice husk ash to the properties of mortar and concrete: a review, J. Am. Sci. 6 (2010) 157–165.
[41] M.V. Madurwar, R.V. Ralegaonkar, S.A. Mandavgane, Application of agro-waste for sustainable construction materials: A review, Constr. Build. Mater. 38 (2013) 872–878.
[42] C. Fapohunda, B. Akinbile, A. Shittu, Structure and properties of mortar and concrete with rice husk ash as partial replacement of ordinary Portland cement–A review, Int. J. Sustain. Built. Environ. 6 (2017) 675–692.
[43] K. Ganesan, K. Rajagopal, K. Thangavel, Rice husk ash blended cement: assessment of optimal level of replacement for strength and permeability properties of concrete, Constr. Build. Mater. 22 (2008) 1675–1683.
[44] G.C. Cordeiro, R.D. Toledo Filho, E.D. Fairbairn, Use of ultrafine rice husk ash with high-carbon content as pozzolan in high performance concrete, Mater Struct. 42 (2009) 983–992.
[45] H. Chao-Lung, B. Le Anh-Tuan, C. Chun-Tsun, Effect of rice husk ash on the strength and durability characteristics of concrete, Constr Build Mater. 25 (2011) 3768–3772.
[46] S.A. Zareei, F. Ameri, F. Dorostkar, M. Ahmadi, Rice husk ash as a partial replacement of cement in high strength concrete containing micro silica: Evaluating durability and mechanical properties, Case Stud. Constr. Mater. 7 (2017) 73–81.
[47] B.B. Sabir, S. Wild, J. Bai, Metakaolin and calcined clays as pozzolans for concrete: a review, Cement Concr. Comp. 23 (2001) 441–454.
[48] R. Siddique, J. Klaus, Influence of metakaolin on the properties of mortar and concrete: A review, Appl. Clay Sci. 43 (2009) 392–400.
[49] M.M. Hossain, M.R. Karim, M. Hasan, M.K. Hossain, M.F. Zain, Durability of mortar and concrete made up of pozzolans as a partial replacement of cement: A review, Constr. Build. Mater. 116 (2016) 128–140.
[50] L. Courard, A. Darimont, M. Schouterden, F. Ferauche, X. Willem, R. Degeimbre, Durability of mortars modified with metakaolin, Cement Concr. Res. 33 (2003) 1473–1479.
[51] K.A. Gruber, T. Ramlochan, A. Boddy, R.D. Hooton, M.D. Thomas, Increasing concrete durability with high-reactivity metakaolin, Cement Concr. Comp. 23 (2001) 479–484.
[52] G. Batis, P. Pantazopoulou, S. Tsivilis, E. Badogiannis, The effect of metakaolin on the corrosion behavior of cement mortars, Cement Concr. Comp. 27 (2005) 125–130.
[53] A.A. Ramezanianpour, H.B. Jovein, Influence of metakaolin as supplementary cementing material on strength and durability of concretes, Constr. Build Mater. 30 (2012) 470–479.
[54] M.K. Dash, S.K. Patro, A.K. Rath, Sustainable use of industrial-waste as partial replacement of fine aggregate for preparation of concrete–A review, Int J Sustain. Built Environ. 5 (2016) 484–516.
[55] A. Tiwari, S. Singh, R. Nagar, Feasibility assessment for partial replacement of fine aggregate to attain cleaner production perspective in concrete: a review, J. Clean Prod. 135 (2016) 490–507.
[56] K. Murari, R. Siddique, K.K. Jain, Use of waste copper slag, a sustainable material, J. Mater. Cycles Waste. 17 (2015) 13–26.
[57] C. Shi, C. Meyer, A. Behnood, Utilization of copper slag in cement and concrete, Resour. Conserv. Recy. 52 (2008) 1115–1120.
[58] K.S. Al-Jabri, M. Hisada, S.K. Al-Oraimi, A.H. Al-Saidy, Copper slag as sand replacement for high performance concrete, Cement Concr. Comp. 31 (2009) 483–488.
[59] K.S. Al-Jabri, A.H. Al-Saidy, R. Taha, Effect of copper slag as a fine aggregate on the properties of cement mortars and concrete, Constr Build Mater. 25 (2011) 933–938.
[60] R. Sharma, R.A. Khan, Durability assessment of self compacting concrete incorporating copper slag as fine aggregates, Constr. Build. Mater. 155 (2017) 617–629.
[61] A. Rajasekar, K. Arunachalam, M. Kottaisamy, Assessment of strength and durability characteristics of copper slag incorporated ultra high strength concrete, J. Clean Prod. 208 (2019) 402–414.
[62] B. Bhardwaj, P. Kumar, Waste foundry sand in concrete: A review, Constr. Build. Mater. 156 (2017) 661–674.
[63] R. Siddique, G. De Schutter, A. Noumowe, Effect of used-foundry sand on the mechanical properties of concrete, Constr. Build. Mater. 23 (2009) 976–980.
[64] G. Singh, R. Siddique, Effect of waste foundry sand (WFS) as partial replacement of sand on the strength, ultrasonic pulse velocity and permeability of concrete, Constr. Build. Mater. 2 (2012) 416–422.
[65] G.G. Prabhu, J.H. Hyun, Y.Y. Kim, Effects of foundry sand as a fine aggregate in concrete production, Constr. Build. Mater. 70 (2014) 514–521.
[66] T. Manoharan, D. Laksmanan, K. Mylsamy, P. Sivakumar, A. Sircar, Engineering properties of concrete with partial utilization of used foundry sand, Waste Manage. 71 (2018) 454–460.
[67] M. Singh, K. Choudhary, A. Srivastava, K.S. Sangwan, D. Bhunia, A study on environmental and economic impacts of using waste marble powder in concrete, J. Build. Eng. 13 (2017) 87–95.
[68] A. André, J. de Brito, A. Rosa, D. Pedro, Durability performance of concrete incorporating coarse aggregates from marble industry waste, J. Clean. Prod. 65 (2014) 389–396.
[69] R.K. Khyaliya, K.S. Kabeer, A.K. Vyas, Evaluation of strength and durability of lean mortar mixes containing marble waste, Constr. Build. Mater. 147 (2017) 598–607.
[70] K. Vardhan, R. Siddique, S. Goyal, Strength, permeation and micro-structural characteristics of concrete incorporating waste marble, Constr. Build. Mater. 203 (2019) 45–55.
[71] M. Behera, S.K. Bhattacharyya, A.K. Minocha, R. Deoliya, S. Maiti, Recycled aggregate from C&D waste & its use in concrete–A breakthrough towards sustainability in construction sector: A review, Constr. Build. Mater. 68 (2014) 501–516.
[72] C. Shi, Y. Li, J. Zhang, W. Li, L. Chong, Z. Xie, Performance enhancement of recycled concrete aggregate–a review, J. Clean. Prod. 112 (2016) 466–472.
[73] N. Makul, A review on methods to improve the quality of recycled concrete aggregates, J. Sustainable. Cem. Based Mater. (2020) 1–27.
[74] A. Mistri, S.K. Bhattacharyya, N. Dhami, A. Mukherjee, S.V. Barai, A review on different treatment methods for enhancing the properties of recycled aggregates for sustainable construction materials, Constr. Build. Mater. 233 (2020) 117894.
[75] J.M. Khatib, Properties of concrete incorporating fine recycled aggregate, Cement Concr. Res. 35 (2005) 763–769.
[76] L. Evangelista, J. de Brito, Mechanical behaviour of concrete made with fine recycled concrete aggregates, Cement Concr. Comp. 29 (2007) 397–401.
[77] K.C. Panda, P.K. Bal, Properties of self compacting concrete using recycled coarse aggregate, Procedia Eng. 51 (2013) 159–164.
[78] S. Boudali, D.E. Kerdal, K. Ayed, B. Abdulsalam, A.M. Soliman, Performance of self-compacting concrete incorporating recycled concrete fines and aggregate exposed to sulphate attack, Constr. Build. Mater. 124 (2016) 705–713.
[79] Dhami NK, Reddy SM, Mukherjee A. Biofilm and microbial applications in biomineralized concrete. In: Advanced topics in Biomineralization. IntechOpen Publishers; 2012. p. 137-164..
[80] T. Zhu, M. Dittrich, Carbonate precipitation through microbial activities in natural environment, and their potential in biotechnology: a review, Front.. Bioeng. Biotechnol. 4 (2016) 4.
[81] M.J. Castro Alonso, L.E. Montañez Hernández, M.A. Sanchez Muñoz, M. Franco, M. Rubi, R. Narayanasamy, N. Balagurusamy, Microbially Induced calcium carbonate precipitation (MICP) and its potential in Bioconcrete: Microbiological and molecular concepts, Front. Mater. 6 (2019) 126.
[82] H.L. Ehrlich, Geomicrobiology: its significance for geology, Earth-Sci. Rev. 45 (1998) 45–60.
[83] E. Boquet, A. Boronat, A. Ramos-Cormenzana, Production of calcite (calcium carbonate) crystals by soil bacteria is a general phenomenon, Nature 246 (1973) 527–529.

[84] S. Douglas, T.J. Beveridge, Mineral formation by bacteria in natural microbial communities, FEMS Microbiol. Ecol. 26 (1998) 79–88.
[85] F. Hammes, W. Verstraete, Key roles of pH and calcium metabolism in microbial carbonate precipitation, Rev Environ Sci Bio. 1 (2002) 3–7.
[86] S. Stocks-Fischer, J.K. Galinat, S.S. Bang, Microbiological precipitation of $CaCO_3$, Soil Biol. Biochem. 31 (1999) 1563–1571.
[87] S. Jain, D.N. Arnepalli, Biominerlisation as a remediation technique: A critical review, in: Geotechnical Characterisation and Geoenvironmental Engineering, Springer, 2019, pp. 155–162.
[88] D.P. Tamayo-Figueroa, E. Castillo, P.F. Brandão, Metal and metalloid immobilization by microbiologically induced carbonates precipitation, World J. Microbiol. Biotechnol. 35 (2019) 58.
[89] D. Mujah, M.A. Shahin, L. Cheng, State-of-the-art review of biocementation by microbially induced calcite precipitation (MICP) for soil stabilization, Geomicrobiol. J. 34 (2017) 524–537.
[90] N.K. Dhami, M.S. Reddy, A. Mukherjee, Application of calcifying bacteria for remediation of stones and cultural heritages, Front. Microbiol. 5 (2014) 304.
[91] J.D. Rodrigues, A.P. Pinto, Stone consolidation by biomineralisation. Contribution for a new conceptual and practical approach to consolidate soft decayed limestones. J Cult Herit. proach to consolidate soft decayed limestones, J. Cult. Heritage (2019).
[92] V. Achal, A. Mukherjee, M.S. Reddy, Microbial concrete: way to enhance the durability of building structures, J. Mater. Civil Eng. 23 (2010) 730–734.
[93] R. Bansal, N.K. Dhami, A. Mukherjee, M.S. Reddy, Biocalcification by halophilic bacteria for remediation of concrete structures in marine environment, J. Ind. Microbiol. Biot. 43 (2016) 1497–1505.
[94] N.K. Dhami, A. Mukherjee, E.L. Watkin, Microbial diversity and mineralogical-mechanical properties of calcitic cave speleothems in natural and in vitro biomineralization conditions, Front. Microbiol. 9 (2018) 40.
[95] M. Li, C. Fang, S. Kawasaki, M. Huang, Achal V. Bio-consolidation of cracks in masonry cement mortars by *Acinetobacter* sp. SC4 isolated from a karst cave, Int. Biodeter. Biodegr. 141 (2019) 94–100.
[96] A. Rajasekar, S. Wilkinson, R. Sekar, J. Bridge, E. Medina-Roldán, C.K. Moy, Biomineralisation performance of bacteria isolated from a landfill in China, Can. J. Microbiol. 64 (2018) 945–953.
[97] V.R. Rangamaran, V.K. Shanmugam, Biocalcification by Piezotolerant *Bacillus* sp. NIOTVJ5 Isolated from Deep Sea Sediment and its Influence on the Strength of Concrete Specimens, Mar Biotechnol. 21 (2019) 161–170.
[98] A. Sarkar, A. Chatterjee, S. Mandal, B. Chattopadhyay, An alkaliphilic bacterium BKH 4 of Bakreshwar hot spring pertinent to bio-concrete technology, J Appl Microbiol. 126 (2019) 1742–1750.
[99] V. Achal, X. Pan, D. Zhang, Remediation of copper-contaminated soil by *Kocuria flava* CR1, based on microbially induced calcite precipitation, Ecol Eng. 37 (2011) 1601–1605.
[100] W. Mwandira, K. Nakashima, S. Kawasaki, Bioremediation of lead-contaminated mine waste by *Pararhodobacter* sp. based on the microbially induced calcium carbonate precipitation technique and its effects on strength of coarse and fine grained sand, Ecol. Eng. 109 (2017) 57–64.
[101] N.K. Dhami, M.E. Quirin, A. Mukherjee, Carbonate biomineralization and heavy metal remediation by calcifying fungi isolated from karstic caves, Ecol. Eng. 103 (2017) 106–117.
[102] J. He, X. Chen, Q. Zhang, V. Achal, More effective immobilization of divalent lead than hexavalent chromium through carbonate mineralization by *Staphylococcus epidermidis* HJ2, Int. Biodeter. Biodegr. 140 (2019) 67–71.
[103] A. Bhattacharya, S.N. Naik, S.K. Khare, Harnessing the bio-mineralization ability of urease producing *Serratia marcescens* and *Enterobacter cloacae* EMB19 for remediation of heavy metal cadmium (II), J. Environ. Manage. 215 (2018) 143–152.
[104] V.S. Whiffin, L.A. van Paassen, M.P. Harkes, Microbial carbonate precipitation as a soil improvement technique, Geomicrobiol. J. 24 (2007) 417–423.
[105] S. Al-Thawadi, R. Cord-Ruwisch, M. Bououdina, Consolidation of sand particles by nanoparticles of calcite after concentrating ureolytic bacteria in situ, Int. J. Green Nanotechnol. 4 (2012) 28–36.
[106] F. Chen, C. Deng, W. Song, D. Zhang, F.A. Al-Misned, M.G. Mortuza, G.M. Gadd, X. Pan, Biostabilization of desert sands using bacterially induced calcite precipitation, Geomicrobiol. J. 33 (2016) 243–249.
[107] M. Maleki, S. Ebrahimi, F. Asadzadeh, M.E. Tabrizi, Performance of microbial-induced carbonate precipitation on wind erosion control of sandy soil, Int J Environ Sci Te. 13 (2016) 937–944.
[108] G. Le Metayer-Levrel, S. Castanier, G. Orial, J.F. Loubiere, J.P. Perthuisot, Applications of bacterial carbonatogenesis to the protection and regeneration of limestones in buildings and historic patrimony, Sediment. Geol. 126 (1999) 25–34.
[109] P. Tiano, L. Biagiotti, G. Mastromei, Bacterial bio-mediated calcite precipitation for monumental stones conservation: methods of evaluation, J Microbiol Meth. 36 (1999) 139–145.
[110] M.I. Daskalakis, F. Rigas, A. Bakolas, A. Magoulas, G. Kotoulas, I. Katsikis, A.P. Karageorgis, A. Mavridou, Vaterite bio-precipitation induced by *Bacillus pumilus* isolated from a solutional cave in Paiania, Athens Greece, Int. Biodeter. Biodegr. 99 (2015) 73–84.
[111] R. Micallef, D. Vella, E. Sinagra, G. Zammit, Biocalcifying *Bacillus subtilis* cells effectively consolidate deteriorated Globigerina limestone, J Ind Microbiol Biot. 43 (2016) 941–952.
[112] Q. Li, B. Zhang, Q. Ge, X. Yang, Calcium carbonate precipitation induced by calcifying bacteria in culture experiments: Influence of the medium on morphology and mineralogy, Int. Biodeter. Biodegr. 134 (2018) 83–92.
[113] W. De Muynck, K. Cox, N. De Belie, W. Verstraete, Bacterial carbonate precipitation as an alternative surface treatment for concrete, Constr. Build. Mater. 22 (2008) 875–885.
[114] Z.B. Bundur, M.J. Kirisits, R.D. Ferron, Biomineralized cement-based materials: Impact of inoculating vegetative bacterial cells on hydration and strength, Cement Concr. Res. 67 (2015) 237–245.
[115] H. Kalhori, R. Bagherpour, Application of carbonate precipitating bacteria for improving properties and repairing cracks of shotcrete, Constr. Build Mater. 148 (2017) 249–260.
[116] S. Joshi, S. Goyal, A. Mukherjee, M.S. Reddy, Protection of concrete structures under sulfate environments by using calcifying bacteria, Constr. Build. Mater. 209 (2019) 156–166.
[117] S.K. Ramachandran, V. Ramakrishnan, S.S. Bang, Remediation of concrete using micro-organisms, ACI Mater. J. 98 (2001) 3–9.
[118] V. Achal, A. Mukerjee, M.S. Reddy, Biogenic treatment improves the durability and remediates the cracks of concrete structures, Constr. Build Mater. 48 (2013) 1–5.
[119] J.Y. Wang, D. Snoeck, S. Van Vlierberghe, W. Verstraete, N. De Belie, Application of hydrogel encapsulated carbonate precipitating bacteria for approaching a realistic self-healing in concrete, Constr. Build. Mater. 68 (2014) 110–119.
[120] M. Seifan, A.K. Sarmah, A. Ebrahiminezhad, Y. Ghasemi, A.K. Samani, A. Berenjian, Bio-reinforced self-healing concrete using magnetic iron oxide nanoparticles, Appl. Microbiol. Biot. 102 (2018) 2167–2178.
[121] M. Alazhari, T. Sharma, A. Heath, R. Cooper, K. Paine, Application of expanded perlite encapsulated bacteria and growth media for self-healing concrete, Constr. Build. Mater. 160 (2018) 610–619.
[122] S. Han, E.K. Choi, W. Park, C. Yi, N. Chung, Effectiveness of expanded clay as a bacteria carrier for self-healing concrete, Appl. Biol. Chem. 62 (2019) 19.
[123] V. Achal, X. Pan, N. Özyurt, Improved strength and durability of fly ash-amended concrete by microbial calcite precipitation, Ecolog. Eng. 37 (2011) 554–559.
[124] S.A. Kadapure, G.S. Kulkarni, K.B. Prakash, Study on properties of bacteria-embedded fly ash concrete, Asian J. Civil. Eng. 20 (2019) 627–636.
[125] F. Farmani, B. Bonakdarpour, A.A. Ramezanianpour, pH reduction through amendment of cement mortar with silica fume enhances its biological treatment using bacterial carbonate precipitation, Mater. Struct. 48 (2015) 3205–3215.
[126] R. Siddique, A. Jameel, M. Singh, D. Barnat-Hunek, A. Aït-Mokhtar, R. Belarbi, A. Rajor, Effect of bacteria on strength, permeation characteristics and micro-structure of silica fume concrete, Constr. Build. Mater. 142 (2017) 92–100.
[127] R. Siddique, K. Singh, M. Singh, V. Corinaldesi, A. Rajor, Properties of bacterial rice husk ash concrete, Constr. Build. Mater. 121 (2016) 112–119.
[128] N.K. Dhami, M.S. Reddy, A. Mukherjee, Improvement in strength properties of ash bricks by bacterial calcite, Ecol. Eng. 39 (2012) 31–35.
[129] O.A. Cuzman, S. Rescic, K. Richter, L. Wittig, P. Tiano, *Sporosarcina pasteurii* use in extreme alkaline conditions for recycling solid industrial wastes, J. Biotechnol. 214 (2015) 49–56.
[130] Kunal, Siddique R, Rajor A, Singh M. Influence of bacterial-treated cement kiln dust on strength and permeability of concrete. J Mater Civil Eng. 2016 Apr 20;28(10):04016088..
[131] M. Li, X. Zhu, A. Mukherjee, M. Huang, V. Achal, Biomineralization in metakaolin modified cement mortar to improve its strength with lowered cement content, J Hazard Mater. 329 (2017) 178–184.
[132] L. Liu, H. Liu, Y. Xiao, J. Chu, P. Xiao, Y. Wang, Biocementation of calcareous sand using soluble calcium derived from calcareous sand, B. Eng. Geol. Environ. 77 (2018) 1781–1791.
[133] M. Li, C. Fang, S. Kawasaki, V. Achal, Fly ash incorporated with biocement to improve strength of expansive soil, Sci. Rep. 8 (2018) 2565.
[134] G. Kaur, R. Siddique, A. Rajor, Influence of fungus on properties of concrete made with waste foundry sand, J. Mater. Civil Eng. 25 (2012) 484–490.
[135] J. Qiu, D.Q. Tng, E.H. Yang, Surface treatment of recycled concrete aggregates through microbial carbonate precipitation, Constr. Build. Mater. 57 (2014) 144–150.
[136] Z.Y. Pan, G. Li, C.Y. Hong, H.L. Kuang, Y. Yu, F.X. Feng, D.M. Liu, H. Du, Modified recycled concrete aggregates for asphalt mixture using microbial calcite precipitation, RSC Adv. 5 (2015) 34854–34863.
[137] J. Wang, B. Vandevyvere, S. Vanhessche, J. Schoon, N. Boon, N. De Belie, Microbial carbonate precipitation for the improvement of quality of recycled aggregates, J. Clean. Prod. 156 (2017) 355–366.
[138] H.A. Dovom, A.M. Moghaddam, M. Karrabi, B. Shahnavaz, Improving the resistance to moisture damage of cold mix asphalt modified by eco-friendly Microbial Carbonate Precipitation (MCP), Constr. Build. Mater. 213 (2019) 131–141.
[139] C.R. Wu, Y.G. Zhu, X.T. Zhang, S.C. Kou, Improving the properties of recycled concrete aggregate with bio-deposition approach, Cement Concr. Comp. 94 (2018) 248–254.
[140] M. Zhan, G. Pan, Y. Wang, M. Fu, X. Lu, Recycled aggregate mortar enhanced by microbial calcite precipitation, Mag Concr. Res. 24 (2019) 1–42.
[141] V. Achal, A. Mukherjee, P.C. Basu, M.S. Reddy, Lactose mother liquor as an alternative nutrient source for microbial concrete production by *Sporosarcina pasteurii*, J. Ind. Microbiol. Biot. 36 (2009) 433–438.
[142] S. Yoosathaporn, P. Tiangburanatham, S. Bovonsombut, A. Chaipanich, W. Pathom-Aree, A cost effective cultivation medium for biocalcification of *Bacillus pasteurii* KCTC 3558 and its effect on cement cubes properties, Microbiol. Res. 186 (2016) 132–138.

[143] S. Joshi, S. Goyal, M.S. Reddy, Corn steep liquor as a nutritional source for biocementation and its impact on concrete structural properties, J. Ind. Microbiol. Biot. 45 (2018) 657–667.
[144] C. Fang, J. He, V. Achal, G. Plaza, Tofu Wastewater as efficient nutritional source in biocementation for improved mechanical strength of cement mortars, Geomicrobiol. J. 13 (2019) 1–7.
[145] F.B. Silva, N. Boon, N. De Belie, W. Verstraete, Industrial application of biological self-healing concrete: challenges and economical feasibility, J. Comm. Biotechnol. 21 (2015) 31–38.
[146] O.A. Cuzman, K. Richter, L. Wittig, P. Tiano, Alternative nutrient sources for biotechnological use of *Sporosarcina pasteurii*, World J. Microbiol. Biotechnol. 31 (2015) 897–906.

Carbon dioxide sequestration on biocement-based composites

10

Mondem S. Reddy, Sumit Joshi
Thapar Institute of Engineering & Technology, Patiala, India

10.1 Introduction

Rapid industrial expansion around the world to achieve stable economic growth has led to adverse impact on the global climate system. A large quantity of green house gases (GHG) has accumulated in the earth's atmosphere due to anthropogenic emission. Increased concentrations of GHG in earth's atmosphere mainly consist of carbon dioxide (CO_2), methane (CH_4), nitrous oxide (N_2O), and chlorofluorocarbons (National Research Council's, 2001). The increase in GHG emissions in the global atmosphere led to increased average global temperature. Among the radiative GHG, CO_2 contributes maximum radiative forcing and affects the earth-atmosphere energy balance (Halmann and Steinberg, 1999). According to Intergovernmental Panel on Climate Change (IPCC), a cumulative CO_2 emission since 1970 has tripled because of fossil fuel combustion and cement industry (IPCC, 2014). A human-induced CO_2 emission has severely damaged the climate system, causing irreversible impacts such as thermal expansion of oceans due to warming (Solomon et al., 2008). According to IPCC, the period from 1983 to 2012 in the northern hemisphere was the warmest 30−year period of the last 800 years (IPCC, 2014). Global mean sea level rise of about 75% was reported due to glacier mass loss and ocean thermal expansion from warming. Global warming has led to sensitive change in average global precipitation, which will adversely affect ecosystems, agriculture, and human health (Zhang et al., 2007). However, both land and ocean are the main contributors in the removal of atmospheric CO_2 and act as natural sink. With the increased level of CO_2 concentration, expected decrease in the efficiency of both land and ocean sinks because of CO_2 fertilization limits on land and decrease in carbonate concentration, which buffers CO_2 in the ocean (Le Quéré et al., 2009). Oceanic uptake of atmospheric CO_2 has resulted into gradual acidification of ocean surface water, which further affects coral reefs and marine biota (Kleypas et al., 1999). Carbon sequestration in land sink by terrestrial ecosystem is also effected due to increased level of CO_2 (Bradford, 2017). In order to mitigate the adverse effects of increasing global CO_2 concentration, several approaches are initiated all around the globe.

To counter the alarming increase of CO_2 concentration, approaches such as capture, storage, and utilization of CO_2 were adopted. Different approaches for CO_2 capture and storage have been associated on the basis of combustion processes. CO_2 capture approaches are classified as post-conversion, preconversion, and oxy-fuel

Carbon Dioxide Sequestration in Cementitious Construction Materials
https://doi.org/10.1016/B978-0-08-102444-7.00010-1

combustion (Leung et al., 2014). Post-conversion is a technique in which carbon is captured from flue gas generated after the combustion of fossil fuels. Post-conversion capture method includes absorption in solvents (such as monoethanolamine, diethanolamine, zeolite, and activated carbon) for separation of CO_2 (Aaron and Tsouris, 2005). In preconversion CO_2 capture, the fossil fuel (coal or natural gas) is treated initially before combustion. Coal is treated through gasification process under low O_2 environment, resulting into the formation of syngas ($CO + H_2$) (Olajire, 2010). Post-conversion and preconversion techniques are applied to power plants in which fossil fuels are used as energy source. In the oxy-fuel combustion process fuel is burned in pure oxygen, resulting into high CO_2 concentrations free from NO and NO_2 compounds. This avoids the need for chemicals or other means for the separation of CO_2 from the flue gas (Azapajic et al., 2004). However, the ease and cost economics in the abovementioned carbon separation and capture approaches is a matter of concern (D'Alessandro et al., 2010).

Relocation of captured CO_2 by injection into geologic or oceanic sinks has been an option for disposal methods. Capabilities of CO_2 sequestration into sinks such as ocean, deep saline, oil and gas reservoirs, and coal seams are reported (Leung et al., 2014). At present, geological storage is considered to be the most viable option to store large quantities of CO_2. These geological formations can store collectively hundreds of gigatons of carbon (Herzog et al., 2000). Deep saline aquifers at 700−1000 m below ground level are particularly promising option for the sequestration of large quantities of CO_2. The Sleipner natural gas field in the North Sea off the coast of Norway represents the first time that 1.1 Mt of CO_2/year has been stored underground in the deep saline aquifer (White et al., 2003). CO_2 storage and natural gas recovery in unmineable coal seams were also reported. The concept of enhanced coalbed methane recovery with CO_2 was first developed in 1991 by researchers from the Alberta Research Council. A small CO_2 pilot injection was performed in the Fruitland Coal Formation in southern Colorado to recover CH_4 (White et al., 2003). Deep Ocean has also been reported as largest potential reservoir to store CO_2. Effective ocean sequestration for CO_2 was reported by injecting CO_2 into the sea below thermocline layer of ocean (Herzog et al., 2000). Technical and environmental issues such as leakage of CO_2 in geological storage are also associated. High cost of capture and storage of CO_2 in the abovementioned approaches is also a demerit.

The Paris climate change agreement marks a new era of optimism and action to cater the record levels of high greenhouse gases. Various countries have implemented carbon trading and taxation to tackle increasing carbon emissions (Princiotta, 2007). Boone et al. (2013) reviewed the progress made in developing carbon capture technologies, and IPCC has also published different carbon storage and capture technologies for reducing GHG emissions (IPCC, 2014). Some reviews have also outlined different approaches for carbon capture and also described methods for mitigating global warming (Bose and Satyanarayana, 2017). This review discusses biomimetic carbon sequestration on biocement-based composites through biomineralization process and their applications in civil engineering.

10.2 Biocement

10.2.1 Microbes involved in biocement

Biocementation is an ecological process based on microbial induced carbonate precipitation (MICP) mechanism, which results in the deposition of calcium carbonate. Different bacterial species in natural habitats precipitate carbonates in alkaline environments rich in Ca^{2+} ions with various mechanisms (Ehrlich, 1998). Boquet et al. (1973) reported that calcium carbonate formation under suitable conditions is a common phenomenon for almost all bacteria. At neutral pH, presence of carboxyl, phosphoryl, and amino groups at the bacterial cell surface results in heterogeneous electronegativity charge, which is later responsible for nucleating site favoring the adsorption of positively charged cations (e.g., Ca^{2+}, Mg^{2+}). Presence of calcium ions in the surroundings of bacterial cell wall results into the precipitation of calcium carbonate (Douglas and Beveridge, 1998). Four groups of microorganisms, such as photosynthetic organisms (cyanobacteria and algae), sulfate reducing bacteria (SRB) (dissimilatory reduction of sulfates), organisms utilizing organic acids, and organisms involved in the nitrogen cycle, are reported to be involved in the process of biocementation.

10.2.2 Routes of biomineralization

Broadly two different metabolic pathways are involved in the process of biomineralization associated with the microorganisms: (1) autotrophic pathway; (2) heterotrophic pathway.

10.2.2.1 Autotrophic mediated pathway

This is the conversion of CO_2 into calcium carbonate crystals by microbes in the presence of CO_2 and calcium source. Autotrophic precipitation of carbonates include oxygenic and anoxygenic photosynthesis and nonmethylotropic methanogenesis (Castanier et al., 1999). All of the three autotrophic pathways use CO_2 as a carbon source. Bacterial calcium carbonate precipitations with aforementioned autotrophic pathways with listed mechanism are shown in Table 10.1.

In nonmethylotrophic methanogenesis pathway, methanogenic archaebacteria utilizes CO_2 and H_2 to give methane in the absence of oxygen (Castanier et al., 1999). Anaerobic oxidation of methane results in the formation of bicarbonate by electron acceptor sulfate as shown in Eq. (10.2). Carbonate in the presence of calcium ions results into the precipitation of calcium carbonate as shown in Eq. (10.3). In anoxygenogenic photosynthesis, H_2S acts an electron donor in the formation of methanol carried out by purple and green photosynthetic bacteria as shown in Eq. (10.4) (Castanier et al., 2000). Oxygenogenic photosynthesis is carried out by cyanobacteria using visible light (680−685 nm) as a source of energy leading into the production of oxygen. In this process, water acts as an electron donor as shown in Eq. (10.7) (Ehrlich, 1998). Oxygenic photosynthetic pathway associated with cyanobacteria in marine and

Table 10.1 Different mechanisms of calcium carbonate precipitation by autotrophic bacteria

Metabolic pathway	Mediator	Mechanism	Equation no.	References
Nonmethylotrophic methanogenesis	Methanogenic archaebacteria	$CO_2 + 4H_2 \rightarrow CH_4 + 2H_2O$	(10.1)	Castanier et al. (1999)
		$CH_4 + SO_4^{2-} \rightarrow HCO_3^- + HS^- + H_2O$	(10.2)	
		$Ca^{2+} + 2HCO_3^- \leftrightarrow CaCO_3 + CO_2 + H_2O$	(10.3)	
Anoxygenogenic photosynthesis	Sulfurous or nonsulfurous purple and green photosynthetic bacteria	$CO_2 + 2H_2S + H_2O \rightarrow CH_2O + 2S + 2H_2O$	(10.4)	Castanier et al. (2000)
		$2HCO_3^- \leftrightarrow CO_2 + CO_3^{2-} + H_2O$	(10.5)	
		$CO_3^{2-} + H_2O \leftrightarrow HCO_3^- + OH^-$	(10.6)	
Oxygenogenic photosynthesis	Cyanobacteria	$CO_2 + H_2O \rightarrow CH_2O + O_2$	(10.7)	Ehrlich (1998)
		$2HCO_3^- \leftrightarrow CO_2 + CO_3^{2-} + H_2O$	(10.8)	
		$CO_3^{2-} + H_2O \leftrightarrow HCO_3^- + OH^-$	(10.9)	

fresh water is one of the major contributors of the production of carbonates. Cyanobacterial calcification is an extracellular process and occurs on extrapolysaccharide sheath (EPS) or proteinaceous hydrophobic surface layer (S-layer), which possesses negatively charged sites surrounding the cell (Schultze-Lam and Beveridge, 1994). Generation of alkaline pH at the EPS or S-layer due to carbonic anhydrase (CA) activity promotes the increased CO_3^{2-} concentration at the cell exterior and acts as nucleation site for $CaCO_3$ precipitation (Jansson and Northen, 2010).

10.2.2.2 Heterotrophic mediated pathway

In heterotrophic mediated pathway, two bacterial carbonate precipitation−enhancing processes are reported (Castanier et al., 1999). First metabolic pathway involves sulfur cycle and second involves nitrogen cycle. First heterotrophic pathway involving sulfur cycle is carried out by SRB via dissimilatory reduction of sulfate. In this process, environment must be anoxic and rich in organic matter, calcium, and sulfate. As the organic matter is degraded by SRB, bicarbonate ions and hydrogen sulfide are produced by bacterial action using SO_4^{2-} as a terminal electron acceptor as shown in Eq. (10.10) (Hammes and Verstraete, 2002; Muyzer and Stams, 2008). Elevation of pH in the surrounding environment due to degasification of hydrogen sulfide in the presence of Ca^{2+} induces the precipitation of calcium carbonate. In natural environment anoxygenogenic sulfide-phototrophic bacteria are present, hydrogen sulfide is used by bacteria, and anaerobically oxidized to sulfur. Uptake of hydrogen sulfide results into pH elevation and favor calcium carbonate precipitation. Precipitation of aragonite crystals on dissolution of gypsum by the action of SRB in Zechstein carbonates (upper Permian) located in central Germany was also reported by Peckmann et al. (1999). It was reported that the replacement of gypsum present in cavities provides the calcium ions for aragonite precipitation and sulfate ions for the metabolic processes of SRB as shown in Eq. (10.11). Degradation of organic matter in anaerobic conditions provides the increased alkaline condition and facilitate the formation of aragonite crystals.

$$2CH_2O + SO_4^{2-} \rightarrow H_2S + 2HCO_3^- \tag{10.10}$$

$$CaSO_4 \cdot 2H_2O \rightarrow Ca^{2+} + SO_4^{2-} + 2H_2O \tag{10.11}$$

Second heterotrophic pathway in calcium carbonate precipitation involves nitrogen cycle. This pathway is further categorized into three different mechanisms: (1) ammonification of amino acids (presence of organic matter and calcium in aerobic conditions), (2) dissimilatory reduction of nitrate (presence of organic matter, calcium, and nitrate in anaerobic conditions), and (3) urea degradation (presence of organic matter, calcium, and urea in aerobic conditions) (Castanier et al., 2000). In all these three mechanisms, carbonate and bicarbonate ions as well as ammonia (NH_3) are produced as a metabolic end product. Generation of ammonia creates high alkaline pH in the microenvironment of the bacterial cell and decreased H^+ concentration, affecting the carbonate-bicarbonate equilibria shift towards the production of CO_3^- ions.

Presence of calcium ions in the surrounding of bacterial cell results in the precipitation of calcium carbonate. Among the aforementioned mechanisms in heterotrophic pathway, microbially induced calcium carbonate precipitation via urea hydrolysis is widely used in various applications.

10.3 Biocementation in civil engineering

Concrete production is a highly intensive energy-consuming process and presently facing a number of challenges in reducing the carbon footprint and making it more economic. Sustainable technologies in maintaining concrete structures are proving to be a great challenge. Microbially induced carbonate precipitation (MICP) has developed as a novel and sustainable technique in improving the strength and durability of construction materials. The potential and effectiveness of microbial induced biocementation has been used widely in various fields. A number of authors had reported the potential of biocementation property in the application of soil bioclogging (Martinez et al., 2013; Stocks-Fischer et al., 1999), restoration of stone monuments (Le Metayer-Levrel et al., 1999; Jroundi et al., 2014; Micallef et al., 2016), durability enhancement of concrete structures (De Muynck et al., 2008; Achal et al., 2011; Kim et al., 2013; Dhami et al., 2013; Bundur et al., 2015), and crack remediation (Tittelboom et al., 2010; Wiktor et al., 2011; Achal et al., 2013; Da Silva et al., 2015) (see Table 10.2). Stocks-Fischer et al. (1999) reported the urease activity of alkaliphilic bacteria to hydrolyze urea and high pH being the favorable condition for calcite precipitation in porous sand media. Sand column supplemented with live bacterial cells, nutrient broth, and urea-$CaCl_2$ constituted 30% calcite of total weight of column. Martinez et al. (2013) injected the bacterial cells and subsequent nutrient amendment in half-meter one-dimensional flow sand column. It was reported that change in shear wave velocity from 140 m/s to an average of 600 m/s was observed because of calcium carbonate precipitation resulting into increased shear stiffness of sand. It was suggested that the most important factor to achieve uniform calcium carbonate precipitation is the distribution of bacteria in the column.

Application of MICP technology to prevent the deterioration of monumental stones due to weathering action has been reported by various researchers. Le Metayer-Levrel et al. (1999) reported the reduction in water absorption of limestone samples due to effective biocalcin coating by carbonatogenic bacteria. Tiano et al. (1999) reported the reduction of about 60% in water absorption of limestone samples treated with *Micrococcus* sp. and *Bacillus subtilis* by brushing. Calcite and vaterite crystals precipitated by *Myxococcus xanthus* resulted in efficient protection and consolidation in porous limestone (Rodriguez-Navarro et al., 2003). Jroundi et al. (2014) reported the effective bacterial bioconsolidation produces vaterite ($CaCO_3$) biocement on the treatment of gypsum plaster collected from the archaeological site "Alcázar de Guadalajara" in Guadalajara, Spain. Reduction in the resorption rate of gypsum material was reported. *Bacillus pumilus* strain isolated from a cave stone effectively precipitated vaterite on the marble (Daskalakis et al., 2015). Micallef et al. (2016) reported the

Table 10.2 Overview of different applications of bacteria in biocementation through biomineralization

Microorganism	Application	Mechanism of treatment	Evaluation	References
Sporoscarcina pasteurii	Soil improvement	One-dimensional injection method	Shear wave velocity measurement, $CaCO_3$ content, bulk permeability	Martinez et al. (2013)
Bacillus pasteurii	Microbial sand consolidation	Sand slurry column fed by gravity with urea-$CaCl_2$ medium	$CaCO_3$ content, SEM, XRD	Stocks-Fischer et al. (1999)
Myxococcus xanthus	Archaeological gypsum plasters	Bacterial solution was sprayed till 6 days (twice a day) on the upper surface of sample	Drilling resistance analysis, TGA, XRD, SEM, MIP, TEM, and colorimetric analysis	Jroundi et al. (2014)
Bacillus subtilis	Ancient limestone surface	Brushing or spraying	Drilling resistance analysis, SEM, EDX	Micallef et al. (2016)
Bacillus sphaericus	Mortar and concrete restoration	Specimens were immersed in bacterial culture for 1 day prior to submersion in nutrient medium for 6 days	Compressive strength, sorptivity test, SEM, gas permeability, XRD, chromatic analysis of specimens	De Muynck et al. (2008)
Bacillus sp. CT-5	Cement mortar	Mortar mixture was admixed with NBU medium-bacterial cells and cured with respective medium for 28 days	Compressive strength, water absorption test, and SEM analysis	Achal et al. (2011)
S. pasteurii, *B. sphaericus*	Concrete specimens	Specimen's top surface was wetted with nutrient medium containing *S. pasteurii* and *B. sphaericus* cells separately for 28 days	Water absorption test, SEM-EDX and XRD analysis	Kim et al. (2013)

Continued

Table 10.2 Continued

Microorganism	Application	Mechanism of treatment	Evaluation	References
Bacillus megaterium SS3	Cement mortar blocks and cylinders	Bacterial admixed specimens were cured by spraying with respective medium for 28 days	Water absorption test, SEM-EDX, XRD, MIP, and $CaCO_3$ estimation of treated samples	Dhami et al. (2013)
S. pasteurii	Cement mortar	Vegetative cells with UYE medium were added in mortar mixture while casting and cured by submersion in UYE medium with lime till 56 days	Hydration kinetics, compressive strength, TGA, and XRD analysis	Bundur et al. (2015)
B. sphaericus	Crack remediation	Immersed in solution of urea and calcium source for 3 days	Crack width of 0.3 mm and depths of 10.0 and 20.0 mm	Tittelboom et al. (2010)
Bacillus alkalinitrilicus	Crack remediation	Immersed in water for 100 days	Crack width ranging from 0.05 to 1.0 mm	Wiktor et al. (2011)
Bacillus sp. CT-5	Crack remediation	Immersed in urea and $CaCl_2$ medium for 28 days	Crack width of 3.0 mm and depths of 13.4, 18.8, and 27.2 mm	Achal et al. (2013)
Nonaxenic ureolytic spores	Crack remediation	Immersed in urea and demineralized water for 4 weeks	Crack healing of width 0.45 mm	Da Silva et al. (2015)

effective biocalcification on Globigerina limestone specimen treated with *B. subtilis* strain by spraying and poulticing applications. Uniform bioconsolidation up to 30 mm depth improved surface drilling resistance of limestone, and reduction in water absorption was reported in poultice application.

The potential of MICP technology in cementitious materials to increase the mechanical properties as well as to reduce the permeability properties has been reported by various researchers. Precipitation of $CaCO_3$ by bacteria inside the cement matrix leads into pore refinement, resulting in reduced permeability and increased strength of concrete structure. Ramachandran et al. (2001) reported enhanced compressive strength of cement mortar cubes on direct incorporation of *Sporoscarcina pasteurii* cells inside the cement matrix. De Muynck et al. (2008) reported pronounced decrease in uptake of water and gas permeability in concrete structure because of the use of pure culture of *Bacillus sphaericus* than the use of mixed ureolytic culture. Achal et al. (2011) reported the increase in compressive strength of bacterial treated cement mortar specimen up to 36% in comparison with control specimen. *Bacillus* sp. CT-5 was admixed in the mixture of cement and sand along with nutrient medium and urea-$CaCl_2$ while casting. Bacterial treated specimen showed six times less water absorption than the control specimen. Kim et al. (2013) investigated the distribution of calcium carbonate precipitation and capillary water absorption of concrete specimens after surface treatment with two bacterial strains, *B. sphaericus* and *S. pasteurii* individually. Denser calcium carbonate crystals and lowest weight increase was reported in specimens treated with *B. sphaericus* strain than the specimens treated with *S. pasteurii* strain. The potential of calcifying bacteria to enhance durability of energy-efficient green building materials was reported by Dhami et al. (2013). Blocks of cement and sand were cured by spraying treatment with NBU medium and bacterial strain *Bacillus megaterium* SS3 for 28 days. Reduction of 40% in water absorption and 31% in the porosity was reported in the biogenic surface−treated specimens in comparison with control specimens. Bundur et al. (2015) reported the increased compressive strength of mortar specimen prepared with incorporation of vegetative bacterial cells than the control specimen. Application of halophilic bacteria *Exiguobacterium mexicanum* isolated from sea water showed 23.5% increase in compressive strength and five times reduction in water absorption on concrete specimens under 5% salt stress condition (Bansal et al., 2016). Kumari et al. (2017) reported 49% increase in compressive strength by using nonureolytic bacteria *Bacillus cohnii*. *Bacillus* sp. CT-5−treated reinforced concrete specimens reduced the rate of corrosion, reduced mass loss, and increased pullout strength than the control specimens (Achal et al., 2012). Kalhori and Bagherpour (2017) reported 30% increase in the compressive strength of bacteria-exposed shotcrete specimens compared to control specimens. Apart from soil bioclogging and concrete restoration, different methodologies have been adopted to heal the concrete cracks with the application of bacteria.

Ramachandran et al. (2001) reported that calcite precipitated during microbial growth enhanced the compressive strength of cracked mortar cubes. The mineralization process was effective in shallow cracks than in deeper ones because of the growth of the bacteria more actively in the presence of oxygen. Tittelboom et al. (2010) investigated the crack healing by immobilizing the bacterial cells of *B. sphaericus* strain

LMG 22257 in silica gel. Standard cracks of width 0.3 mm with two depths of 10 and 20 mm and realistic cracks with width ranging from 0.05 to 0.87 mm were also created in concrete samples. In this experiment, promising results in crack filling and silica-immobilized calcifying bacteria as an efficient self-healing agent were reported. The biochemical healing agent consisting of a mixture of viable but dormant bacteria and organic compounds packed in porous expanded clay particles to heal the cracks was also proposed (Jonkers, 2011).

Wiktor et al. (2011) investigated direct incorporation of bacterial spores and calcium lactate embedded in expanded clay as self-healing agent in concrete. Multiple cracks of widths ranging from 0.05 to 1.0 mm were created in specimen, whereas bacterial based specimen showed complete healing of crack of width 0.42 mm after 100 days of immersion in water. Achal et al. (2013) investigated crack healing process with microbial plugging of artificially created cracks of width 3 mm and different depths of 13.4, 18.8, and 27.2 mm. Successful healing of deepest crack of depth 27.2 mm was reported in microbially treated specimen with bacterial strain *Bacillus* sp. CT-5 along with natural sieved sand. Xu and Yao (2014) investigated nonureolytic bacterially induced $CaCO_3$ precipitation as a self-healing strategy for concrete cracking by using *B. cohnii* spores. They suggested that incorporation of bacteria and calcium source nutrients as a two-component healing agent in concrete matrix induces $CaCO_3$ precipitation upon crack formation. Qian et al. (2015) reported the healing of early age cracks in cement-based materials by CA-producing bacteria *Bacillus mucilaginous* L3. Their experimental results showed that the cracks formed at early ages were completely healed (up to 0.4 mm) because of bacterial treatment and the healing effect reduced with the increasing of cracking age. A new biobased powderous material containing nonaxenic ureolytic spores was developed for self-healing (Da Silva et al., 2015). Cyclic EnRiched Ureolytic Powder (CERUP) produced from a substream of a vegetable treatment plant after drying and grinding contains nonaxenic bacterial culture. Mortar prism admixed with 1% (of cement weight) CERUP was subjected to tensile force to create cracks. CERUP admixed specimen with complete crack closing up to 0.45 mm crack width after 4 weeks was reported.

Field performance of bacteria-based repair system of a two-storey parking garage suffering from cracking and damaged concrete pavement due to freeze/thaw was reported by Wiktor and Jonkers (2015). Cracks that had been treated with the bacteria showed higher freeze/thaw resistance of concrete than the untreated concrete. Tziviloglou et al. (2016) showed various steps taken towards the outdoor applications of biobased self-healing, for the laboratory-scale tests that have shown promising results.

10.4 Biocementation based on CO_2 capture

Biomineralization of CO_2 by $CaCO_3$ precipitation is a common phenomenon in marine, freshwater, and terrestrial ecosystems. Photosynthetic microbes, such as cyanobacteria and microalgae, play a prominent role in carbon sequestration by simultaneously capturing CO_2 (Zhu and Dittrich, 2016). Employment of

cyanobacteria in biomineralization offers a novel and self-sustaining strategy in carbon capture and sequestration (CCS). Novel models for point-source CCS based on biomineralization are emerging (Jansson and Northen, 2010). Microalgae have a great potential to be developed as media for biocement production through photosynthetic metabolism (Ariyanti et al., 2012). Some authors had reported the potential of bacteria and microalgae in biocementation of sand stabilization, fugitive dust, and concrete restoration based on CO_2 capture and utilization. Okyay et al. (2016) evaluated the potential of ureolytic consortia in CO_2 sequestration through MICP. In this study, ureolytic consortia were obtained from the "CaveWithout A Name" and "Pamukkale travertines" using 13 different growth media for ureolytic microorganisms. Consortia containing larger abundances of *Sporosarcina*, *Sphingobacterium*, *Stenotrophomonas*, *Acinetobacter*, and *Elizabethkingia* genera were reported for higher CO_2 sequestration and $CaCO_3$ precipitations. It was suggested that combination of CA enzyme activity with MICP in the consortia might have resulted in a greater rate of CO_2 sequestration. Dhami et al. (2014) also reported the synergistic role of urease (UA) and CA enzyme in biomineralization of calcium carbonate. Calcite precipitation was reported to be significantly reduced when both the enzymes were inhibited in comparison with those of the individual enzyme inhibitions. It was suggested that UA and CA enzymes are important for efficient biomineralization in urea-hydrolyzing bacteria. It was reported that CA plays a role in hydrating CO_2 to bicarbonate, whereas UA activity maintained the alkaline pH promoting calcification process. CO_2 sequestering capability of *B. megaterium SS3* in biocementation was also reported (Kaur et al., 2016). In this study, urea was replaced with CO_2 flux and under accelerated carbonation in bacterial treated concrete specimen improved compressive strength by 117% as compare with control specimen. Significant reduction in the water absorption was also reported in bacterial treated carbonated specimens. Calcite as well as aragonite crystals were observed in association with the bacterial cells (Fig. 10.1) CO_2 as an alternate was suggested instead of urea in calcium carbonate precipitation paving a way to develop green building structures. Zhan et al. (2016) reported microbial-induced mineralization and cementation of fugitive dust under the action of *Paenibacillus mucilaginosus*. Cementitious material of biological carbonates was prepared by mixing *P. mucilaginosus* bacterial powder and calcium nitrate with water and sprinkled. It was reported that CO_2 absorbed, transformed, and produced carbonate ions under the enzymatic action of *P. mucilaginosus*, resulting in cementation of fugitive dust due to calcite consolidation layer. Zhan and Qian (2017) investigated the stabilization of sand particles using biocementation process based on CO_2 capture and utilization. Bacteria powder of *Paenibacillus* strain and calcium nitrate dissolved in deionized water was sprayed evenly on the surface of sand particles. It was reported that average porosity of samples was reduced from 18.3% to 13.3%. Calcite precipitation due to the enzymatic activity of bacteria and carbonate ion formation due to CO_2 absorption was also reported. Feasibility of application by using cyanobacteria *Synechococcus* PCC8806 in concrete restoration through biomineralization process was reported by Zhu et al. (2015). In this study, concrete cubes with a size of $3 \times 3 \times 1.5$ cm were immersed in 50 mM calcium chloride solution with

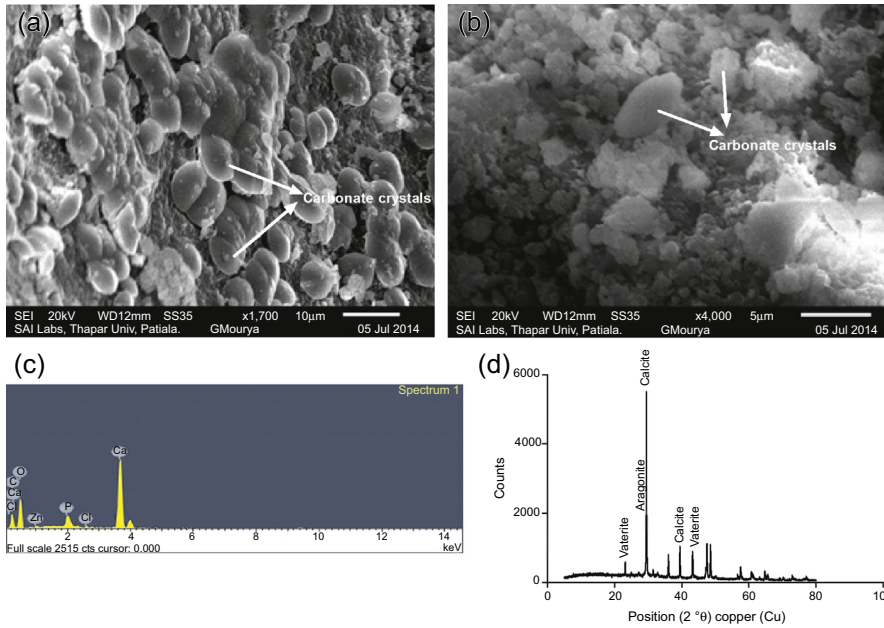

Figure 10.1 Scanning electron microscopic images of carbonate crystals formed by *Bacillus megaterium* through carbonation: (a) carbonate crystals, (b) bacterial cells in association with crystals, (c) energy dispersive X-ray spectrum, (d) X-ray diffraction analysis of carbonate crystals.
Reprinted from Kaur, G., Dhami, N.K., Goyal, S., Mukherjee, A., Reddy, M.S., 2016. Utilization of carbon dioxide as an alternative to urea in biocementation. Construction and Building Materials 123, 527−533 with permission from Elsevier.

1.5×10^8 cells/mL under shaking condition for 45 days. Thick calcite-cell layer adhering to the treated concrete specimen decreased the water absorption twice as compared with control specimen. Zhu et al. (2017) reported the calcification by cyanobacteria *Gloeocapsa* PCC73106 in mortars. Mortar cubes of a size $50 \times 50 \times 50$ mm were treated abiotically, with live *Gloeocapsa* PCC73106 cells under illumination, with live cells under darkness, and with ultraviolet (UV)-killed cells immersed in the cell solution (with a concentration of 3.5×10^7 cells/mL). Largest amount of precipitates was reported in treatment with live cells under illumination, whereas highest compressive strength, the least water absorption, and the lowest porosity were reported in UV-killed cells. In treatment with live cells, a thin layer of EPS around (Fig. 10.2(a)) cells helped in the attachment to the surface of the mortar (Fig. 10.2(b)). After being exposed to UV light, the UV-killed cells produced more EPS, resulting in larger coverage than live cells. It was reported that UV-killed cells were not metabolically active and EPS enhanced biofilm formation triggering calcium carbonate precipitation on the mortar surface (Fig. 10.2(c) and (d)).

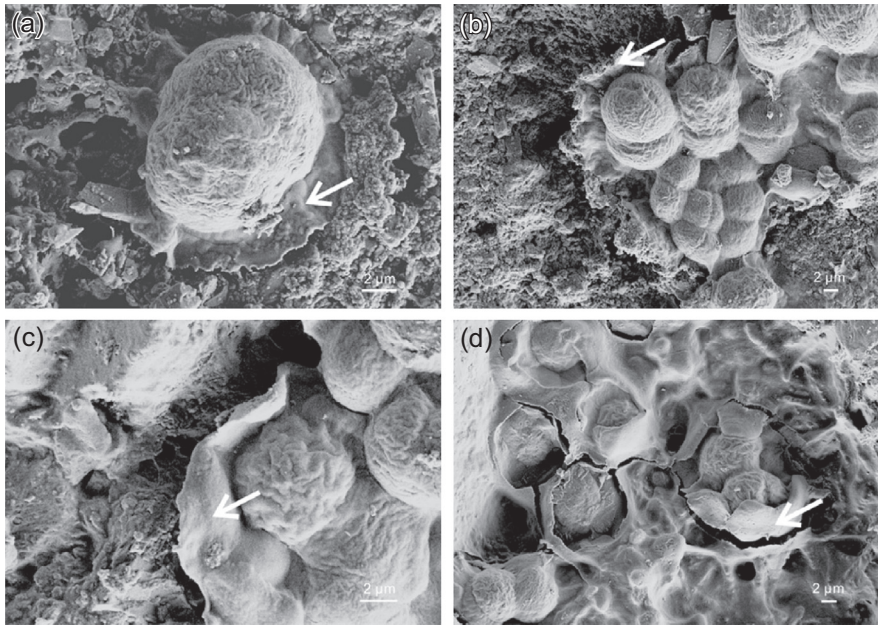

Figure 10.2 Extrapolysaccharide sheath (EPS) of live and ultraviolet (UV)-killed cells. (a and b) A thin layer of EPS resided between the live cells and the mortar surface. (c and d) A thicker layer of EPS around UV-killed cells.
Reprinted from Zhu, T., Lu, X., Dittrich, M., 2017. Calcification on mortar by live and UV-killed biofilm-forming cyanobacterial Gloeocapsa PCC73106. Construction and Building Materials 146, 43−53 with permission from Elsevier.

10.4.1 Role of microbes in CO_2 sequestration

The ubiquitous presence of microorganisms has the potential to utilize and assimilate CO_2 through different metabolic pathways. Diverse naturally occurring prokaryotic taxa are able to utilize CO_2 through several CO_2 assimilation pathways and convert CO_2 into value-added chemicals or induce calcium carbonate ($CaCO_3$) precipitation (Hicks et al., 2017). The oceans are huge carbon sinks, and a large proportion is sequestered in the marine sediments in the deep sea mediated by microbial activity. Evidence from the fossil records, association of laminated stromatolites with microbial fossils of photosynthetic cyanobacteria, was reported (Awramik, 1992). Half of the earth photosynthesis is carried out by phytoplankton, which mostly consists of cyanobacteria, and its 25% is accounted by the two marine cyanobacterial genera, *Prochlorococcus* and *Synechococcus*. In CO_2 capturing, photosynthetic microbes, such as cyanobacteria and microalgae, plays a notable role in carbon sequestration (Zhu and Dittrich, 2016). Beachrock formation of El Hamira bay and biogenic calcification due to carbonate precipitation by photosynthetic CO_2 uptake of cyanobacteria was reported by Krumbein in 1979. The potential of halotolerant sulfate-reducing bacteria for carbonate mineralization in geological carbon sequestration during CO_2 injection in subsurface is also reported (Paul et al., 2017).

10.4.2 Enzyme involved in CO_2 sequestration

Carbonic anhydrase (CA) is the first-discovered zinc-containing metalloenzyme that is widespread in animals, plants, and microorganisms that catalyses the conversion of CO_2 and water into bicarbonate (Smith and Ferry, 1999). The CA is widespread in metabolically diverse species of bacteria indicating that this enzyme plays a significant role in concentrating CO_2 (Dhami et al., 2014). In natural process of photosynthetic assimilation of CO_2, CA enzyme acts as biocatalyst (Jansson and Northen, 2010). Potential role of CA enzyme in addressing environmental issues such as reducing carbon emissions through CO_2 sequestration has gained considerable attention. CA enzyme is reported to be a potential tool to sequester CO_2 from emission sources (Bose and Satyanarayana, 2017). It was reported that partially purified CA from *B. pumilus* immobilized on chitosan beads has improved calcium carbonate precipitation than free CA enzyme in carbonation reaction (Wanjari et al., 2011). Immobilization of CA enzyme into alginate beads showed better operational stability by retaining nearly 67% of its initial activity and entrapped CA hydrates CO_2 to bicarbonate and/or carbonate, which on reaction with Ca^{2+} ions, transform into calcite (Yadav et al., 2012). It was reported as a commercialized development for the onsite scrubber for CO_2 sequestration. Zhang et al. (2011) reported the effective absorption of CO_2 into the potassium carbonate solution with biocatalyst CA immobilized into controlled pore glass material. The immobilized enzyme retained at least 60% of their initial activities and significantly improved resistance to concentrations of sulfate (0.4 M), nitrate (0.05 M), and chloride (0.3 M) conditions in flue gas expected in the Integrated Vacuum Carbonate Absorption Process.

10.5 Challenges and Future trends

Biomineralization of CO_2 with the employment of cyanobacteria offers an innovative and self-sustaining strategy in carbon sequestration. Biocementation provides a cost-effective and environment friendly solution to mitigate the increased level of atmospheric CO_2. Calcium carbonates formed after sequestration using bacteria and microalgae will provide industrially valuable and useful by-products that can be implemented in construction material. Microalgae can be easily cultivated and have a great potential in biocement production. As there is rapid increase in the number of patents related to the use of microbes with ureolytic pathway in the construction biotechnology (Dapurkar and Telang, 2017), the critical research needs to be done in making the use of algae as feasible biocementation producer.

Researchers from all over the world have investigated the potential of biomineralization in improving the durability of building materials. However, the qualitative and quantitative evaluation of microbial application of this technology in concrete are still reported in the laboratory scale. Some researchers have also reported encouraging results on the application of bacterial based treatment at field scale. Some limitations that are necessary to be considered for application of this technology at commercial scale have been found. One of the limitations to apply this technology at field scale is use of

laboratory-grade nutrient sources that restrict the use of this technology in several cases. Successful commercialization of the technique requires economical alternatives of the medium ingredients that cost as high as 60% of the total operating costs (Kristiansen, 2001). Use of inexpensive materials as nutrients may help to lower the cost of treatment (Achal et al., 2009, 2011). In field-scale experiments, effective curing method is to be investigated to provide sufficient amount of nutrients and water to the bacterial cells. Further, investigations are needed to improve the microbial technology as an innovative crack healing application for the commercial scale.

Acknowledgments

Authors are thankful to Science and Engineering Research Board, Department of Science & Technology, Government of India, India for sponsoring the research project SB/S3/CEE/0063/2013.

References

Aaron, D., Tsouris, C., 2005. Separation of CO_2 from flue gas: a review. Separation Science and Technology 40, 321−348.

Achal, V., Mukerjee, A., Reddy, M.S., 2013. Biogenic treatment improves the durability and remediates the cracks of concrete structures. Construction and Building Materials 48, 1−5.

Achal, V., Mukherjee, A., Reddy, M.S., 2011. Microbial Concrete: way to enhance the durability of building structures. Journal of Materials in Civil Engineering 23, 730−734.

Achal, V., Mukherjee, A., Basu, P.C., Reddy, M.S., 2009. Lactose mother liquor as an alternative nutrient source for microbial concrete production by *Sporosarcina pasteurii*. Journal of Industrial Microbiology and Biotechnology 36, 433−438.

Achal, V., Mukherjee, A., Goyal, S., Reddy, M.S., 2012. Corrosion prevention of reinforced concrete with microbial calcite precipitation. ACI Materials Journal 109, 157−164.

Ariyanti, D., Handayani, N.A., Hadiyanto, 2012. Feasibility of using microalgae for biocement production through biocementation. Journal of Bioprocessing & Biotechniques 2, 1−4.

Awramik, S.M., 1992. The oldest records of photosynthesis. Photosynthesis Research 33, 75−89.

Azapajic, A., Perdan, S., Clift, R., 2004. Sustainable Development in Practice. John Wiley & Sons, Chichester.

Bansal, R., Dhami, N.K., Mukherjee, A., Reddy, M.S., 2016. Biocalcification by halophilic bacteria for remediation of concrete structures in marine environment. Journal of Industrial Microbiology and Biotechnology 43, 1497−1505.

Boone, C.D., Gill, S., Habibzadegan, A., McKenna, R., 2013. Carbonic anhydrase: an efficient enzyme with possible global implications. International Journal of Chemical Engineering 2013, 1−7.

Boquet, E., Boronat, A., Ramos-Cormenzana, A., 1973. Production of calcite (calcium carbonate) crystals by soil bacteria is a general phenomenon. Nature 246, 527−529.

Bose, H., Satyanarayana, T., 2017. Microbial carbonic anhydrases in biomimetic carbon sequestration for mitigating global warming: prospects and perspectives. Frontiers in Microbiology 8, 1615.

Bradford, M.A., 2017. Soil carbon: a leaky sink. Nature Climate Change 7, 475−476.
Bundur, Z.B., Kirisits, M.J., Ferron, R.D., 2015. Biomineralized cement-based materials: impact of inoculating vegetative bacterial cells on hydration and strength. Cement and Concrete Research 67, 237−245.
Castanier, S., Le Métayer-Levrel, G., Perthuisot, J.P., 1999. Ca-carbonates precipitation and limestone genesis − the microbiogeologist point of view. Sedimentary Geology 126, 9−23.
Castanier, S., Le Métayer-Levrel, G., Perthuisot, J.P., 2000. Bacterial roles in the precipitation of carbonate minerals. In: Microbial Sediments. Springer-Verlag, Heidelberg, pp. 32−39.
D'Alessandro, D.M., Smit, B., Long, J.R., 2010. Carbon dioxide capture: prospects for new materials. Angewandte Chemie International Edition 49, 6058−6082.
Da Silva, F.B., De Belie, N., Boon, N., Verstraete, W., 2015. Production of non-axenic ureolytic spores for self-healing concrete applications. Construction and Building Materials 93, 1034−1041.
Dapurkar, D., Telang, M., 2017. A patent landscape on application of microorganisms in construction industry. World Journal of Microbiology and Biotechnology 33, 138.
Daskalakis, M.I., Rigas, F., Bakolas, A., Magoulas, A., Kotoulas, G., Katsikis, I., Karageorgis, A.P., Mavridou, A., 2015. Vaterite bio-precipitation induced by *Bacillus pumilus* isolated from a solutional cave in Paiania, Athens, Greece. International Biodeterioration and Biodegradation 99, 73−84.
De Muynck, W., Cox, K., De Belie, N., Verstraete, W., 2008. Bacterial carbonate precipitation as an alternative surface treatment for concrete. Construction and Building Materials 22, 875−885.
Dhami, N.K., Reddy, M.S., Mukherjee, A., 2013. *Bacillus megaterium* mediated mineralization of calcium carbonate as biogenic surface treatment of green building materials. World Journal of Microbiology and Biotechnology 29, 2397−2406.
Dhami, N.K., Reddy, M.S., Mukherjee, A., 2014. Synergistic role of bacterial urease and carbonic anhydrase in carbonate mineralization. Applied Biochemistry and Biotechnology 172, 2552−2561.
Douglas, S., Beveridge, T.J., 1998. Mineral formation by bacteria in natural microbial communities. FEMS Microbiology Ecology 26, 79−88.
Ehrlich, H.L., 1998. Geomicrobiology: its significance for geology. Earth-Science Reviews 45, 45−60.
Halmann, M.M., Steinberg, M., 1999. Greenhouse Gas Carbon Dioxide Mitigation: Science and Technology. CRC Press, Boca Raton, Florida.
Hammes, F., Verstraete, W., 2002. Key roles of pH and calcium metabolism in microbial carbonate precipitation. Reviews in Environmental Science and Biotechnology 1, 3−7.
Herzog, H., Eliasson, B., Kaarstad, O., 2000. Capturing greenhouse gases. Scientific American 282, 72−79.
Hicks, N., Vik, U., Taylor, P., Ladoukakis, E., Park, J., Kolisis, F., Jakobsen, K.S., 2017. Using Prokaryotes for carbon capture storage. Trends in Biotechnology 35, 22−32.
Intergovernmental Panel on Climate Change, 2014. Climate Change 2014−Impacts, Adaptation and Vulnerability: Regional Aspects. Cambridge University Press.
Jansson, C., Northen, T., 2010. Calcifying cyanobacteria—the potential of biomineralization for carbon capture and storage. Current Opinion in Biotechnology 21, 365−371.
Jonkers, H.M., 2011. Bacteria-based self healing concrete. Heron 56, 1−12.
Jroundi, F., Gonzalez-Muñoz, M.T., Garcia-Bueno, A., Rodriguez- Navarro, C., 2014. Consolidation of archaeological gypsum plaster by bacterial biomineralization of calcium carbonate. Acta Biomaterialia 10, 3844−3854.

Kalhori, H., Bagherpour, R., 2017. Application of carbonate precipitating bacteria for improving properties and repairing cracks of shotcrete. Construction and Building Materials 148, 249−260.

Kaur, G., Dhami, N.K., Goyal, S., Mukherjee, A., Reddy, M.S., 2016. Utilization of carbon dioxide as an alternative to urea in biocementation. Construction and Building Materials 123, 527−533.

Kim, H.K., Park, S.J., Han, J.I., Lee, H.K., 2013. Microbially mediated calcium carbonate precipitation on normal and lightweight concrete. Construction and Building Materials 38, 1073−1082.

Kleypas, J.A., Buddemeier, R.W., Archer, D., Gattuso, J.P., Langdon, C., Opdyke, B.N., 1999. Geochemical consequences of increased atmospheric carbon dioxide on coral reefs. Science 284, 118−120.

Kristiansen, B., 2001. Process economics. In: Ratledge, C., Kristiansen, B. (Eds.), Biotechnology, second ed. Cambridge University Press, Cambridge.

Krumbein, W.E., 1979. Photolithotropic and chemoorganotrophic activity of bacteria and algae as related to beachrock formation and degradation (gulf of Aqaba, Sinai). Geomicrobiology Journal 1, 139−203.

Kumari, C., Das, B., Jayabalan, R., Davis, R., Sarkar, P., 2017. Effect of nonureolytic bacteria on engineering properties of cement mortar. Journal of Materials in Civil Engineering 29, 06016024.

Le Metayer-Levrel, G., Castanier, S., Orial, G., Loubiere, J.F., Perthuisot, J.P., 1999. Applications of bacterial carbonatogenesis to the protection and regeneration of limestones in buildings and historic patrimony. Sedimentary Geology 126, 25−34.

Le Quéré, C., Raupach, M.R., Canadell, J.G., Marland, G., 2009. Trends in the sources and sinks of carbon dioxide. Nature Geoscience 2, 831−836.

Leung, D.Y.C., Caramanna, G., Maroto-Valer, M.M., 2014. An overview of current status of carbon dioxide capture and storage technologies. Renewable and Sustainable Energy Reviews 39, 426−443.

Martinez, B.C., DeJong, J.T., Ginn, T.R., Montoya, B.M., Barkouki, T.H., Hunt, C., Tanyu, B., Major, D., 2013. Experimental optimization of microbial induced carbonate precipitation for soil improvement. Journal of Geotechnical and Geoenvironmental Engineering 139, 587−598.

Micallef, R., Vella, D., Sinagra, E., Zammit, G., 2016. Biocalcifying *Bacillus subtilis* cells effectively consolidate deteriorated Globigerina limestone. Journal of Industrial Microbiology and Biotechnology 43, 941−952.

Muyzer, G., Stams, A.J., 2008. The ecology and biotechnology of sulphate-reducing bacteria. Nature Reviews Microbiology 6, 441−454.

National Research Council, 2001. Climate Change Science. National Academy Press, Washington, DC.

Okyay, T.O., Nguyen, H.N., Castro, S.L., Rodrigues, D.F., 2016. CO_2 sequestration by ureolytic microbial consortia through microbially-induced calcite precipitation. The Science of the Total Environment 572, 671−680.

Olajire, A.A., 2010. CO_2 capture and separation technologies for end-of-pipe applications − a review. Energy 35, 2610−2628.

Paul, V.G., Wronkiewicz, D.J., Mormile, M.R., 2017. Impact of elevated CO_2 concentrations on carbonate mineral precipitation ability of sulfate-reducing bacteria and implications for CO_2 sequestration. Applied Geochemistry 78, 250−271.

Peckmann, J., Paul, J., Thiel, V., 1999. Bacterially mediated formation of diagenetic aragonite and native sulfur in Zechstein carbonates (Upper Permian, Central Germany). Sedimentary Geology 126, 205−222.

Princiotta, F., 2007. The role of power generation technology in mitigating global climate change. In: Challenges of Power Engineering and Environment. Springer, Berlin, Heidelberg, pp. 3–13.

Qian, C., Chen, H., Ren, L., Luo, M., 2015. Self-healing of early age cracks in cement-based materials by mineralization of carbonic anhydrase microorganism. Frontiers in Microbiology 6, 1225.

Ramachandran, S.K., Ramakrishnan, V., Bang, S.S., 2001. Remediation of concrete using micro-organisms. ACI Materials Journal 98, 3–9.

Rodriguez-Navarro, C., Rodriguez-Gallego, M., Chekroun, K.B., Gonzalez-Muñoz, M.T., 2003. Conservation of ornamental stone by *Myxococcus xanthus*-induced carbonate biomineralization. Applied and Environmental Microbiology 69, 2182–2193.

Schultze-Lam, S., Beveridge, T.J., 1994. Physicochemical characteristics of the mineral forming S-layer from the cyanobacterium *Synechococcus* strain GL24. Canadian Journal of Microbiology 40, 216–223.

Smith, K.S., Ferry, J.G., 1999. A plant-type (β-class) carbonic anhydrase from the thermophilic methanoarchae on *Methanobacterium thermoautotrophicum*. Journal of Bacteriology 181, 6247–6253.

Solomon, S., Plattner, G.K., Knutti, R., Friedlingstein, P., 2008. Irreversible climate change due to carbon dioxide emissions. Proceedings of the National Academy of Sciences 106, 1704–1709.

Stocks-Fischer, S., Galinat, J.K., Bang, S.S., 1999. Microbiological precipitation of $CaCO_3$. Soil Biology and Biochemistry 31, 1563–1571.

Tiano, P., Biagiotti, L., Mastromei, G., 1999. Bacterial bio-mediated calcite precipitation for monumental stones conservation: methods of evaluation. Journal of Microbiological Methods 36, 139–145.

Tittelboom, K.V., De Belie, N., De Muynck, W., Verstraete, W., 2010. Use of bacteria to repair cracks in concrete. Cement and Concrete Research 40, 157–166.

Tziviloglou, E., Tittelboom, K.V., Palin, D., Wang, J., Sierra-Beltrán, M.G., Erşan, Y.C., Mors, R., Wiktor, V., Jonkers, H.M., Schlangen, E., De Belie, N., 2016. Bio-based self-healing concrete: from research to field application. Self-healing materials. Advances in Polymer Science 273, 345–385.

Wanjari, S., Prabhu, C., Yadav, R., Satyanarayana, T., Labhsetwar, N., Rayalu, S., 2011. Immobilization of carbonic anhydrase on chitosan beads for enhanced carbonation reaction. Process Biochemistry 46, 1010–1018.

White, C.M., Strazisar, B.R., Granite, E.J., Hoffman, J.S., Pennline, H.W., 2003. Separation and capture of CO_2 from large stationary sources and sequestration in geological formations — coalbeds and deep saline aquifers. Journal of the Air and Waste Management Association 53, 645–715.

Wiktor, V., Jonkers, H.M., 2011. Quantification of crack-healing in novel bacteria-based self-healing concrete. Cement and Concrete Composites 33, 763–770.

Wiktor, V., Jonkers, H.M., 2015. Field performance of bacteria-based repair system: pilot study in a parking garage. Case Studies in Construction Materials 2, 11–17.

Xu, J., Yao, W., 2014. Multiscale mechanical quantification of self-healing concrete incorporating non-ureolytic bacteria-based healing agent. Cement and Concrete Research 64, 1–10.

Yadav, R.R., Mudliar, S.N., Shekh, A.Y., Fulke, A.B., Devi, S.S., Krishnamurthi, K., Juwarkar, A., Chakrabarti, T., 2012. Immobilization of carbonic anhydrase in alginate and its influence on transformation of CO_2 to calcite. Process Biochemistry 47, 585–590.

Zhan, Q., Qian, C., 2017. Stabilization of sand particles by bio-cement based on CO_2 capture and utilization: process, mechanical properties and microstructure. Construction and Building Materials 133, 73−80.

Zhan, Q., Qian, C., Yi, H., 2016. Microbial-induced mineralization and cementation of fugitive dust and engineering application. Construction and Building Materials 121, 437−444.

Zhang, S., Zhanga, Z., Lu, Y., Rostam-Abadi, M., Jones, A., 2011. Activity and stability of immobilized carbonic anhydrase for promoting CO_2 absorption into a carbonate solution for post-combustion CO_2 capture. Bioresource Technology 102, 10194−10201.

Zhang, X., Zwiers, F.W., Hegerl, G.C., Lambert, F.H., Gillett, N.P., Solomon, S., Stott, P.A., Nozawa, T., 2007. Detection of human influence on twentieth-century precipitation trends. Nature 448, 461−465.

Zhu, T., Dittrich, M., 2016. Carbonate precipitation through microbial activities in natural environment, and their potential in biotechnology: a review. Frontiers in Bioengineering and Biotechnology 4, 4.

Zhu, T., Lu, X., Dittrich, M., 2017. Calcification on mortar by live and UV-killed biofilm-forming cyanobacterial *Gloeocapsa* PCC73106. Construction and Building Materials 146, 43−53.

Zhu, T., Paulo, C., Merroun, M.L., Dittrich, M., 2015. Potential application of biomineralization by *Synechococcus* PCC8806 for concrete restoration. Ecological Engineering 82, 459−468.